IMMUNE DYSFUNCTION: AN UPDATE OF NEW IMMUNE CELL SUBSETS AND CYTOKINES IN SEPSIS

EDITED BY: Yong Ming Yao, Marcin Filip Osuchowski, Zhixing Kevin Pan and Jiang Huai Wang

PUBLISHED IN: Frontiers in Immunology

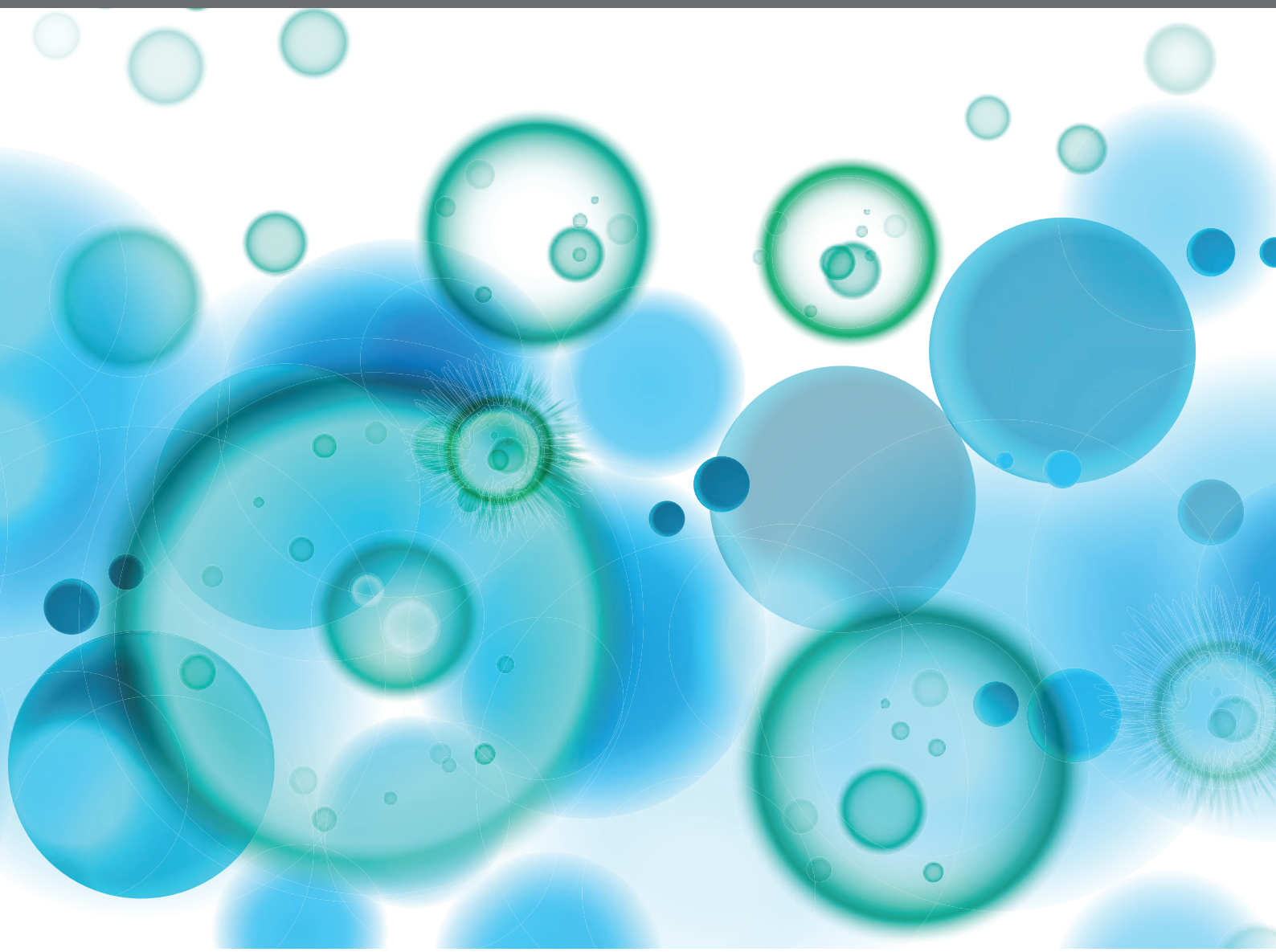

frontiers Research Topics

frontiers

ISSN 1664-8714
ISBN 978-2-88974-248-6
DOI 10.3389/978-2-88974-248-6

About Frontiers

Frontiers is more than just an open-access publisher of scholarly articles: it is a pioneering approach to the world of academia, radically improving the way scholarly research is managed. The grand vision of Frontiers is a world where all people have an equal opportunity to seek, share and generate knowledge. Frontiers provides immediate and permanent online open access to all its publications, but this alone is not enough to realize our grand goals.

Frontiers Journal Series

The Frontiers Journal Series is a multi-tier and interdisciplinary set of open-access, online journals, promising a paradigm shift from the current review, selection and dissemination processes in academic publishing. All Frontiers journals are driven by researchers for researchers; therefore, they constitute a service to the scholarly community. At the same time, the Frontiers Journal Series operates on a revolutionary invention, the tiered publishing system, initially addressing specific communities of scholars, and gradually climbing up to broader public understanding, thus serving the interests of the lay society, too.

Dedication to Quality

Each Frontiers article is a landmark of the highest quality, thanks to genuinely collaborative interactions between authors and review editors, who include some of the world's best academicians. Research must be certified by peers before entering a stream of knowledge that may eventually reach the public - and shape society; therefore, Frontiers only applies the most rigorous and unbiased reviews.
Frontiers revolutionizes research publishing by freely delivering the most outstanding research, evaluated with no bias from both the academic and social point of view. By applying the most advanced information technologies, Frontiers is catapulting scholarly publishing into a new generation.

What are Frontiers Research Topics?

Frontiers Research Topics are very popular trademarks of the Frontiers Journals Series: they are collections of at least ten articles, all centered on a particular subject. With their unique mix of varied contributions from Original Research to Review Articles, Frontiers Research Topics unify the most influential researchers, the latest key findings and historical advances in a hot research area! Find out more on how to host your own Frontiers Research Topic or contribute to one as an author by contacting the Frontiers Editorial Office: frontiersin.org/about/contact

IMMUNE DYSFUNCTION: AN UPDATE OF NEW IMMUNE CELL SUBSETS AND CYTOKINES IN SEPSIS

Topic Editors:
Yong Ming Yao, First Affiliated Hospital of Chinese PLA General Hospital, China
Marcin Filip Osuchowski, Ludwig Boltzmann Institute for Experimental and Clinical Traumatology, Austria
Zhixing Kevin Pan, University of Toledo Medical Center, United States
Jiang Huai Wang, University College Cork, Ireland

Citation: Yao, Y. M., Osuchowski, M. F., Pan, Z. K., Wang, J. H., eds. (2022). Immune Dysfunction: An Update of New Immune Cell Subsets and Cytokines in Sepsis. Lausanne: Frontiers Media SA. doi: 10.3389/978-2-88974-248-6

Table of Contents

frontiers in Immunology

EDITORIAL
published: 16 December 2021
doi: 10.3389/fimmu.2021.822068

Editorial: Immune Dysfunction: An Update of New Immune Cell Subsets and Cytokines in Sepsis

Yong-ming Yao[1], Marcin F. Osuchowski[2], Jiang-huai Wang[3] and Zhixing K. Pan[4]*

[1] Translational Medicine Research Center, Medical Innovation Research Division and Fourth Medical Center of the Chinese People's Liberation Army (PLA) General Hospital, Beijing, China, [2] Trauma, Shock and Sepsis Research Group, Ludwig Boltzmann Institute for Experimental and Clinical Traumatology, Vienna, Austria, [3] Research Lab, Department of Academic Surgery, National University of Ireland, Cork University Hospital, Cork City, Ireland, [4] Department of Medical Microbiology and Immunology, University of Toledo College of Medicine, Toledo, OH, United States

Keywords: sepsis, new immune cell subsets, new cytokines, immune dysfunction, novel single-cell RNA-sequencing analysis

Editorial on the Research Topic

Immune Dysfunction: An Update of New Immune Cell Subsets and Cytokines in Sepsis

The still raging SARS-CoV-2/COVID-19 pandemic has understandably diverted the research attention from other important domains of medical sciences. This Research Topic partly fills the void of the justified neglect and re-focuses the attention on (beyond COVID-19) sepsis – also a globally widespread and burdening problem. Dysregulated host immune response is currently accepted as the major cause of multiple organ dysfunction syndrome (MODS) and subsequent death in septic patients (1, 2). Specifically the dysfunction of innate and adaptive immune systems appears to be responsible for the development of immune deregulation under microbial exposure both regarding the acute sepsis phenotypes as well as their long-term consequences. However, there is currently vague understanding of the pathogenesis of sepsis-induced immune depression, especially of the effects of new immune cell subsets and cytokines.

In recent years, advanced analytical technologies have enabled the discovery of new immune cell subsets and cytokines, which are shown to play various roles in modulating host immune response and initiating MODS secondary to sepsis. This particular Research Topic provides an overview of: i) selected newly discovered immune cell subsets and mediators in the development of sepsis-induced immunosuppression and multiple organ injury, and ii) new functions and modulatory signaling of classical/known immune cells and mediators. The Research Topic features a total of fourteen articles; nine original manuscripts, three review articles, and two mini-reviews. The journal and the Research Topic editors sincerely appreciate all outstanding works and their authors contributing to this collection.

The Sepsis-3 that is defined as life-threatening organ dysfunction caused by a dysregulated host response to infection highlights the importance of immune deregulation in the pathogenesis of sepsis. Darden et al. demonstrated, by using a novel single-cell RNA-sequencing analysis, that the circulating lymphoid cells of late septic patients maintained a transcriptomic profile that was predominantly immunosuppressive with low-grade proinflammatory characteristics. Interestingly, the lymphocyte transcriptomes differed due to various types of infecting organisms, hinting the need for personalized immunotherapy (Darden et al.). While a preliminary report, this analytical direction opens new monitoring frontiers regarding protracted follow-up of chronic sepsis. Using

OPEN ACCESS

Edited and reviewed by:
Pietro Ghezzi,
Brighton and Sussex Medical School, United Kingdom

****Correspondence:***
Yong-ming Yao
c_ff@sina.com

Specialty section:
This article was submitted to Inflammation, a section of the journal Frontiers in Immunology

Received: *25 November 2021*
Accepted: *01 December 2021*
Published: *16 December 2021*

Citation:
Yao Y-m, Osuchowski MF, Wang J-h and Pan ZK (2021) Editorial: Immune Dysfunction: An Update of New Immune Cell Subsets and Cytokines in Sepsis. Front. Immunol. 12:822068. doi: 10.3389/fimmu.2021.822068

an elegant study-design, Skirecki et al. characterized a compartment-and outcome-dependent evolution of myelopoiesis in acute murine sepsis. Mice with cecal ligation and puncture (CLP) were stratified into predicted-to-die (P-DIE) and predicted to-survive (P-SUR) cohorts revealing a varying rate of depletion of the hematopoietic stem and progenitor cells subclasses depending on the analyzed compartment. These findings implicate the early impairment of myelopoiesis in sepsis outcomes and underline an importance of compartment-targeted monitoring.

Dysregulation of innate and adaptive immune system contributes to sepsis-induced immune deregulation. Several markers have been proposed regarding development of immune dysfunction in sepsis, e.g., a suppressed expression of human leukocyte antigen DR (HLA-DR) on monocytes and lymphocytes. Wang et al. observed a heterogeneous immune response in peripheral blood monocytes of septic patients by using high-dimensional flow cytometry. Furthermore, the authors identified two major monocyte subtypes (i.e., hypo- and hyper-responsive) by assessing the production of cytokines and the HLA-DR expression in response to lipopolysaccharide (LPS) stimulation. Such a diagnostic approach aligns well with the notion of the desired personalized therapy tailored based on immune status. The activation and function of neutrophils in sepsis are another noteworthy topic of this Research Topic. Seree-aphinan et al. screened and compared patients with septic shock versus non-septic infection founding that only C-X-C motif chemokine receptor 2 (CXCR2) was closely associated with the onset of sepsis and concentration-dependent relationship with the clinical severity. Platelet activating factor (PAF) plays an important role in rapid depolarization, intracellular alkalization, and increased cell size of neutrophils. Hug et al. reported that an *ex-vivo* LPS stimulation and porcine polymicrobial sepsis resulted in a diminished response of neutrophils to PAF. This abnormality was recorded at the onset of experimental sepsis as it might serve as an early hallmark of an innate immune dysfunction (Hug et al.). In the next original study, Ji and Fan systematically described a phenomenon of neutrophil reverse migration in sepsis – a potentially one of the major causes of organ injury due to an overexposure of neutrophils. Neutrophils that reversely-migrated from the inflammation/infection sites back into the circulation presented with a prolonged lifespan and delayed apoptosis, showing a positive correlation with sepsis-induced acute lung injury (ALI) (Ji and Fan).

Substantially altered innate immune response frequently has grave short-and long-term consequences. Using a novel technique for intracellular cytokine measurement in the whole blood, Fabri et al. reported the suppressed production of tumor necrosis factor-α (TNF-α) but increased interleukin-10 (IL-10) secretion, and the number of IL-10 producing $CD4^+$ T lymphocytes was significantly elevated. An imbalanced responsiveness of both innate and adaptive immune cells undeniably contributes to the overall magnitude of the sepsis-induced immunosuppression. In another mechanistic work, Chen et al. found that activation of group 2 innate lymphoid cells (ILC2s) was able to augment IL-17A-producing γδT cell expansion and secretion of IL-17A by releasing IL-9 in CLP mice. Furthermore, the authors identified the effects of neuromedin U (NMU) on activation of ILC2s by directly binding with NMU receptor 1 (NMUR1), which might be a potential therapeutic target for reversing sepsis-induced ALI. The viability and function of both resident and circulating immune cell subsets are major factors that drive the development of immune dysfunction. Of note, a profound depletion of common myeloid progenitors in P-DIE CLP mice was owing to an increased apoptosis (Skirecki et al.). Other types of cell death, e.g., ferroptosis, could also constitute an essential part of uncontrolled inflammation and immune dysfunction in sepsis (Li et al.). Li et al. systematically reviewed the phenomenon of ferroptosis (characterized by excessive lipid peroxidation and overload ion) and illustrated its close association with a dysregulated immune response. In their pilot study, Lorente-Pozo et al. reported the importance of epigenetic alteration in an impaired immune response in neonatal sepsis. The authors demonstrated that the methylation level in premature septic infants was significant altered in genomic regions functionally associated with multiple inflammatory pathways and innate/adaptive immune responses. These observations suggest that the DNA methylation patterns can be successfully exploited to serve as efficient biomarkers predicting/detecting septic complications.

It is widely accepted that MODS constitutes the ultimate cause of death in septic patients. An excessive inflammation, coagulopathy and/or immune dysregulation are considered as the major mechanisms for the development of multiple organ injury in sepsis. As mentioned above, a delayed withdrawal of neutrophils was critically involved in respiratory tissue damage and the rate of circulating reverse-migrated neutrophils revealed a positive correlation with ALI (Ji and Fan). The IL-17A was observed to be significantly elevated in the lungs of septic mice, urging a further in-depth mechanistic exploration by NMU, ILC2s, and IL-17A-producing γδT cells (Chen et al.). Schulz et al. highlighted the significance of microcirculation and mitochondrial function in the development of gastrointestinal and liver damage during sepsis. The sepsis-induced immune, inflammatory and coagulation fluctuations constitute a complex interwoven network that trigger and drive MODS. Wu et al. discussed the activation of canonical and non-canonical inflammasomes in triggering the release of coagulation factors, such as factor III and tissue factors, from both monocytes and macrophages. This immune-coagulation can be transformed into a vicious cycle for organ damage. Additionally, the authors described a significant role of stimulator of interferon genes (STING) and high mobility group box-1 protein (HMGB1) in modulating the activation of inflammasomes and the immune-to-coagulation interaction (Wu et al.).

An immune suppression does not only contribute to the sepsis onset but it also critically weights upon poor outcomes and protracted post-septic consequences. A timely, efficient and personalized immune-modulation should achieve a high priority in the therapeutic management of sepsis. Bergmann et al.

summarized the pathophysiology of the sepsis-induced immunosuppression and highlighted the importance of anti-inflammatory mediators, such as IL-10, transforming growth factor-β (TGF-β), and thymic stromal lymphopoietin (TSLP), in inducing a persistent immune-depression in sepsis. They concluded that modulation of those cytokines should be considered for reversing sepsis-induced immunosuppression once a precise stratification of septic patients is achievable (Bergmann et al.). Likewise, Royster et al. described the role of sialic acid-binding immunoglobulin-type lectin-G (Siglec-G) in immunomodulation by inhibiting activation of nuclear factor κB and damage associated molecular patterns-mediated inflammation. Though greatly desired, any specific drugs for a successful sepsis-induced immunomodulation remain to be added to the current clinical practice. Future pre-and clinical studies should be therefore prioritized on: i) expanding our understanding of the pathophysiological roles of the old and novel immune cell subsets and mediators by using advanced analytical technologies, ii) constructing personalized immunotherapies based on the patients' immune status, and iii) combined treatments covering both innate and adaptive immunity (rather than any "golden bullet" therapy) as well as re-balancing the pro- and anti-inflammatory dynamics.

AUTHOR CONTRIBUTIONS

All authors contributed to this editorial insight and approved the submitted version.

REFERENCES

1. Singer M, Deutschman CS, Seymour CW, Shankar-Hari M, Annane D, Bauer M, et al. The Third International Consensus Definitions for Sepsis and Septic Shock (Sepsis-3). *JAMA* (2016) 315(8):801–10. doi: 10.1001/jama.2016.0287
2. Lelubre C, Vincent JL. Mechanisms and Treatment of Organ Failure in Sepsis. *Nat Rev Nephrol* (2018) 14(7):417–27. doi: 10.1038/s41581-018-0005-7

Conflict of Interest: The authors declare that the research was conducted in the absence of any commercial or financial relationships that could be construed as a potential conflict of interest.

frontiers in Immunology

ORIGINAL RESEARCH
published: 23 December 2020
doi: 10.3389/fimmu.2020.608696

Distinguishing Sepsis From Infection by Neutrophil Dysfunction: A Promising Role of CXCR2 Surface Level

*Chutima Seree-aphinan[1], Polathep Vichitkunakorn[2], Raphatphorn Navakanitworakul[3] and Bodin Khwannimit[4]**

[1] Department of Internal Medicine, Faculty of Medicine, Prince of Songkla University, Songkhla, Thailand, [2] Department of Family and Preventive Medicine, Faculty of Medicine, Prince of Songkla University, Songkhla, Thailand, [3] Department of Biomedical Sciences, Faculty of Medicine, Prince of Songkla University, Songkhla, Thailand, [4] Division of Critical Care Medicine, Department of Internal Medicine, Faculty of Medicine, Prince of Songkla University, Songkhla, Thailand

Sepsis is one of the well-established diseases with specific patterns of neutrophil dysfunctions. Previous studies demonstrated sepsis-related neutrophil dysfunctions in comparison with subjects without infection. Since sepsis and infection are recently recognized as distinctive processes, whether these neutrophil dysfunctions are associated with sepsis or infection are not known. Therefore, we longitudinally compared neutrophil functions, widely-cited as exhibiting sepsis-related changes, between patients with septic shock and infection. The surface level of cluster of differentiation 64 (CD64), C-C motif chemokine receptor 2 (CCR2), C-X-C motif chemokine receptor 2 (CXCR2); apoptosis; and NETosis were measured from peripheral blood neutrophils for seven consecutive days using flow cytometry. The between-group comparisons of neutrophil functions were made both on a day-by-day basis and as linear regression between time and measured neutrophil functions (sepsis status included as model predictors). Our study found that, among neutrophil functions studied, only CXCR2 surface level is associated with sepsis. At disease onset, CXCR2 level decrease, with a dose-response relationship with clinical severity. Its level reverts to resemble infected patients by the end of the week. The relationship between CD64 surface level, CCR2 surface level, NETosis, and sepsis are mediated through the effect of infection. Apoptosis activity between these groups are similar, hence, not sepsis-related.

Keywords: apoptosis, CCR2, CD64 index on neutrophils, CXCR2, NEtosis, neutrophils, infection, sepsis

OPEN ACCESS

Edited by:
Jiang Huai Wang, University College Cork, Ireland

Reviewed by:
Raffaella Bonecchi, Humanitas University, Italy
Krishna Rajarathnam, University of Texas Medical Branch at Galveston, United States

***Correspondence:**
Bodin Khwannimit
kbordin@medicine.psu.ac.th;
kbordinbodin@gmail.com

Specialty section:
This article was submitted to Inflammation, a section of the journal Frontiers in Immunology

Received: *21 September 2020*
Accepted: *19 November 2020*
Published: *23 December 2020*

Citation:
Seree-aphinan C, Vichitkunakorn P, Navakanitworakul R and Khwannimit B (2020) Distinguishing Sepsis From Infection by Neutrophil Dysfunction: A Promising Role of CXCR2 Surface Level. Front. Immunol. 11:608696. doi: 10.3389/fimmu.2020.608696

INTRODUCTION

Sepsis is a syndrome diagnosed by the presence of life-threatening organ dysfunctions triggered by infection (1); not all patients with infection develop sepsis. At present, physicians rely on clinical tools [e.g., Sequential Organ Failure Assessment (SOFA) score] to distinguish sepsis from infection, even though signs and symptoms of sepsis overlap considerably with other diseases. As part of an updated sepsis definition (1), it was proposed that dysregulated immunological responses could be

the key to distinguish sepsis from an appropriate reaction to infection. Neutrophils could have great potential in this matter since it is considered to have an integral role in sepsis pathobiology; both qualitatively and quantitatively (2). Previous studies consistently identified specific alterations of neutrophil function in sepsis patients (3–5); some of them were linked to poor clinical outcomes (6, 7).

Currently, some knowledge gaps limit a clinical application of these sepsis-related neutrophil dysfunctions. Firstly, most studies demonstrated them in comparison with subjects with good health (8) or pre-existing sterile inflammation (9, 10). In the real clinical setting, however, all sepsis patients are infected. Hence, by using controls without infection, it is impossible to know whether these so-called sepsis-related neutrophil dysfunctions represent a state of infection, infection in conjunction with other inflammatory processes, or sepsis. Secondly, with an update of sepsis definition by the Third International Consensus Definitions for Sepsis and Septic shock (Sepsis-3) (1), neutrophil dysfunctions defined on the background of previous clinical definition may not be relevant to the current practice. Lastly, the paucity of longitudinal studies in this field makes it difficult to generalize the neutrophil dysfunctions demonstrated during one period to another during the clinical course.

Given the knowledge gaps above, our study aims to longitudinally compare neutrophil functions, widely-cited as exhibiting sepsis-related changes, between two groups of patients; clinically defined by Sepsis-3 definition as septic shock or infection. These include the surface level of cluster of differentiation 64 (CD64), C-C motif chemokine receptor 2 (CCR2), C-X-C motif chemokine receptor 2 (CXCR2); apoptosis; and NETosis. The associations between these neutrophil functions and clinical outcomes were also explored.

MATERIALS AND METHODS

Study Design and Participants

This is a longitudinal observational study conducted in a tertiary university teaching hospital in Thailand. Patients who were diagnosed with acute infection and presented within 48 h of their symptom onset were recruited. We used Sepsis-3 definition (1) to classify patients' sepsis status. Based on these clinical definitions, patients with infection, quick SOFA (qSOFA) score ≥ 2, and evidence of organ dysfunction (SOFA score ≥ 2) are diagnosed as sepsis. Sepsis patients are further categorized as septic shock if, despite adequate fluid resuscitation, they require vasopressor support to maintain mean arterial pressure ≥ 65 mmHg and had serum lactate level > 2 mmol/L. Patients with infection and qSOFA score < 2 are categorized as infection. In our study, only ones who could be classified into either septic shock or infection were included. We did not recruit sepsis patients without septic shock because their clinical signs often overlap with other conditions (e.g., acute heart failure precipitated by infection, acute pulmonary embolism); which potentially lead to misclassification. Patients with less than 18 years of age, prior diagnosis of sepsis within three months before the recruitment, autoimmune diseases, the use of immunosuppressive medications, prolonged steroid usage (> 2 weeks), active malignancy, HIV infection, and pregnancy were excluded. All patients with septic shock were admitted to a medical intensive care unit while patients with infection were admitted to general medical wards. qSOFA score was monitored regularly for patients with infection to ensure their non-sepsis status throughout the study period. All patients received appropriate treatment as outlined in the Surviving Sepsis Campaign Bundles (11). The patients or their legal guardians received verbal informed consent initially followed by written informed consent within 48 h of the study recruitment. Ethical clearance was approved by the Human Research Ethics Committee of the Faculty of Medicine, Prince of Songkla University, Thailand (REC. 61-090-14-1).

Sample Size Consideration

Our study employed multilevel analyses to explore the longitudinal trends of neutrophil functions and their associations with sepsis; repeated measurements of neutrophil functions were nested within each patient. Hence, group size for multilevel analysis is the number of patients. In medical research, a consensus method of selecting group size for this type of analysis is lacking, even though bigger group size is traditionally believed to give better estimates than the smaller one. Maas et al. (12) conducted a simulation study to evaluate the performance of two-level models, with one explanatory variable in each level, across different group sizes. They found that, compared to the group sizes of 50 and 100, a group size of 30 gives accurate regression coefficients and variance components with negligible bias and only 1.6% higher non-convergence rate. Therefore, we selected a sample size of 30 for our study. During the analysis, we did not encounter any convergence problem.

Measurement of Neutrophil Functions

For all study participants, two milliliters of fresh whole blood were collected once daily for seven consecutive days (Day 1 to Day 7). Since a clinical course of some septic shock patients may be longer than infected patients, we also collected one additional blood sample at Day 14 in septic shock patients. The surface level of CD64, CCR2, and CXCR2 receptors; apoptosis activity; and NETosis activity were measured from peripheral blood neutrophils using flow cytometry. The degree of CD64, CCR2, and CXCR2 surface level, were quantified by median fluorescent intensity (MFI) of the corresponding molecules in the overall neutrophil population. Additionally, for CD64, CCR2, and CXCR2 receptors, we also quantified the percentages of neutrophils which could be categorized as dysfunctional according to the current literature. Healthy neutrophils have a negligible level of CD64 and CCR2 surface receptors (13, 14) while having abundant CXCR2 surface receptors (15). Compared to normal neutrophils, previous studies have proposed the following neutrophil dysfunctions as sepsis-related: increased phagocytic activity through upregulation of CD64 receptors and transmigration abnormalities due to upregulation of CCR2 receptors or internalization of CXCR2 receptors (3–5).

Therefore, gated using unstained neutrophils as negative control, we quantified the percentages of CD64-positive neutrophils, CCR2-positive neutrophils, and CXCR2-negative neutrophils and referred to them as "dysfunctional neutrophils". Both MFI and the percentages of "dysfunction neutrophils" were used for analyses. Regarding apoptosis and NETosis, the percentages of neutrophils expressing features of apoptosis and NETosis were used to represent apoptosis and NETosis activity.

Specimen Collection and Preparation for Flow Cytometry

The blood samples, stored in ethylenediaminetetraacetic acid-coated tubes at room temperature, were processed within 4 h of collection. Neutrophils were isolated by negative selection immunomagnetic cell separation methods using EasySep™ Direct Human Neutrophil Isolation kit (STEMCELL™ Technologies, BC, CA). Fc receptor blockage was carried out as part of the cell separation process. The cell suspensions were separated for two assays, each resuspended in 50 µl of two different pre-mixed antibody cocktails; one cocktail used in the measurement of CD64, CCR2, and CXCR2 surface level and the other used for apoptosis and NETosis studies. Fluorescent-dye conjugated antibodies used in this study are anti-human CD45-Per-CP antibody (BD Pharmingen, NJ, US); anti-human CD16-PE-Cy™7 antibody (BD Pharmingen, NJ, US); anti-human CD64-PE antibody (BD Pharmingen, NJ, US); anti-human CCR2-Alexa Fluor®647 antibody (BD Pharmingen, NJ, US); anti-human CXCR2-FITC antibody (BD Pharmingen, NJ, US), Annexin V-FITC antibody (BD Pharmingen, NJ, US); Propidium iodide (PI) (BD Pharmingen, NJ, US); and anti-human myeloperoxidase (MPO)-PE antibody (Bio-Rad Laboratories, CA, US). The samples were incubated for 20 min in the dark at room temperature before fixing with 1% paraformaldehyde solution for 4 min. The cells were resuspended in Dulbecco's phosphate-buffered saline and kept in the dark, waiting for data acquisition within 4 h of fixation. The purity of the neutrophil isolates was evaluated in all experimental specimens by CD45/Side scatter gating. All experiments conducted in this study achieved more than 95% of neutrophil purity.

Flow Cytometry Analysis

Data acquisition was performed with the Amnis® ImageStream®X Mk II Imaging Flow Cytometer (Luminex Corporation, TX, US). The fluidics was set at low flow with high sensitivity and 40X magnification objective. In addition, 488- and 642-nm lasers with an output power of 100 and 150 mW were used. We followed Maecker et al. (16) recommendations for the flow cytometry control set-up. We used background fluorescent intensities from unstained cells as negative control. Neutrophils from two septic shock patients were used for positive control experiments. The optimal antibody concentration which gave positivity while minimizing image oversaturation was titrated. The positivity was confirmed both by comparing the fluorescent intensity with unstained samples and the visualization of the surface staining on fluorescent cell images, which were simultaneously collected by the Imaging Flow Cytometer. For positive control of apoptosis, neutrophils were cultured in Roswell Park Memorial Institute 1640 Medium (ThermoFisher Scientific, MA, US), supplemented with 10% heat-inactivated fetal bovine serum (ThermoFisher Scientific, MA, US) and 1× Gibco® Antibiotic-Antimycotic (ThermoFisher Scientific, MA, US) at 37°C, CO2 5%, for 48 h before analysis to allow time for most of the cells to undergo apoptosis. For positive control of NETosis, we used 1× concentration of eBioscience™ Cell Stimulation Cocktail (ThermoFisher Scientific, MA, US), a mixture of phorbol 12-myristate 13-acetate (PMA) and ionomycin, to stimulate NETosis formation. Both PMA and ionomycin are well-known NETosis inducers (17).

Image Data Exploration and Analysis Software (IDEAS®) version 6.2 was used for flow cytometry analysis. Propriety software functions are italicized. Spectral overlap compensation was performed by using single stained controls to create a compensation matrix. Prior to analysis, the collected events underwent camera focusing quality assessment using the software's function called *Gradient RMS* and included only events with good camera focus. For the assay which measured CD64, CCR2, and CXCR2 surface level, dead cell (i.e., PI-positive events) elimination was also performed. The selected events were firstly gated on brightfield (BF) *Area* and side scatter intensity to evaluate their size and granularity, respectively (**Figure 1A**). Single cells were separated from cell aggregates by objects' size quantified by the software's image-based analytic function called *Area*. This function measures the size of the object using image pixels. By applying this function to the BF images, this value represents the cross-sectional area of the object images (i.e., the size of the cell). Utility-wise, it is equivalent to forward scatter geometry in non-imaging flow cytometers. Among single cells, neutrophils were preliminarily identified based on their granularity. Subsequently, CD16 positivity was used to confirm the gated cells as neutrophils (**Figure 1B**); every experimental specimen yielded at least 10,000 neutrophils for further analyses. On CD16-positive neutrophils, we measured the MFI of CD64, CCR2, and CXCR2 receptors, as well as the percentages of CD64-positive cells, CCR2-positive cells, and CXCR2-negative cells (**Figure 1C**). Regarding apoptosis cell count (**Figures 1D, E**), we used a method described by Pietkiewicz et al. (18), which combines an image-based flow cytometry analysis and classical Annexin V/PI staining for apoptosis detection. The method distinguishes cell population into double-negative (healthy) cells, Annexin V-positive/PI-negative (early apoptotic) cells, and double-positive (late apoptotic and necroptotic) cells. Among the double-positive population, the software's image-based analytic functions, namely *Intensity threshold* and *Contrast morphology* for the PI-channel, were employed to discriminate between late apoptotic and necroptotic cells. We collectively counted early and late apoptosis as apoptosis events. NETosis was identified by the presence of cell-appendant neutrophil extracellular traps components, including MPO and extracellular DNA. Extracellular DNA was detected by using the software masking features as previously described (19). These masking features identify cells with DNA contents located extracellularly and help exclude the cells stained by PI intracellularly

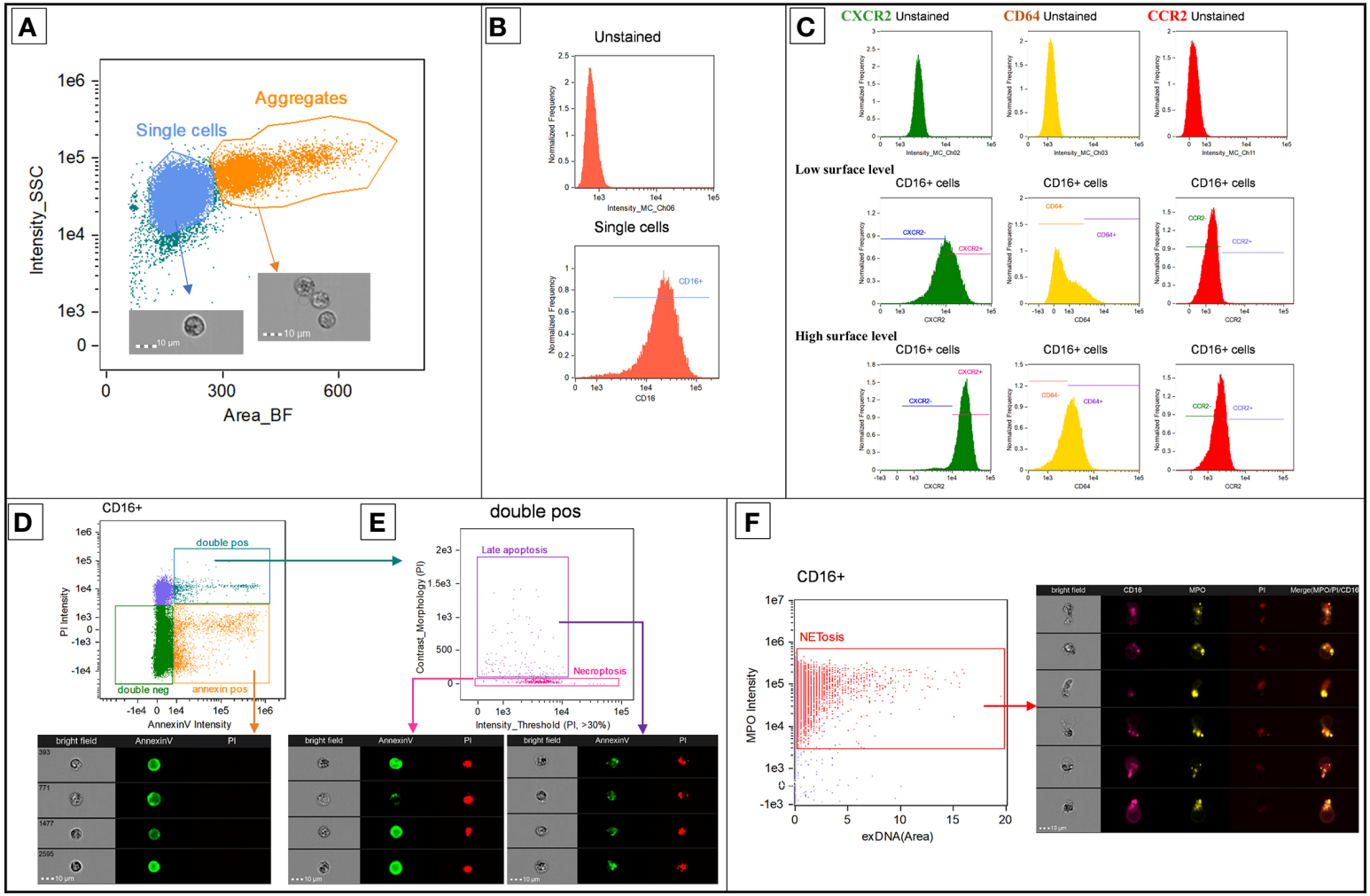

FIGURE 1 | Representative diagrams showing the flow cytometry gating strategy. This analysis was performed on IDEAS® software version 6.2. Propriety software functions are italicized. Prior to analysis, the collected events underwent camera focusing quality assessment using *Gradient RMS* and, for the assay which measured CD64, CCR2, and CXCR2 surface level, dead cells elimination. The selected events were firstly gated on brightfield *Area* and side scatter intensity to evaluate their size and granularity, respectively **(A)**. Single cells were separated from cell aggregates by brightfield *Area* (labeled as Area_BF) and preliminarily identified as neutrophils based on their granularity. CD16 positivity was used to confirm the gated cells as neutrophils **(B)**. The MFI of CD64, CCR2, and CXCR2 surface receptors was measured from neutrophils; which were also gated as positive or negative population using unstained samples as negative control **(C)**. Using Annexin-V and PI intensity, CD16-positive cells were distinguished into double-negative (healthy) cells, Annexin V-positive/PI-negative (early apoptotic) cells and double-positive (late apoptotic and necroptotic) cells **(D)**. *Intensity threshold* and *Contrast morphology* for the PI-channel were employed to discriminate between late apoptotic and necroptotic cells **(E)**. A co-staining of MPO and cell-appendant extracellular DNA was used to identify neutrophils undergoing NETosis **(F)**. The area of extracellular DNA, labeled as exDNA (Area), was established by subtracting BF mask from PI-channel mask; since BF and PI-channel masks delineate cell boundaries and DNA extent, respectively. CCR2, C-C chemokine receptor 2; CD, cluster of differentiation; CXCR2, C-X-C chemokine receptor 2; DNA, Deoxyribonucleic acid; MFI, Median fluorescent intensity; MPO, myeloperoxidase; PI, propidium iodide; SSC, side scatter.

(late apoptotic and necroptotic cells). In brief, a cell-impermeant DNA dye, PI in our experiment, was used to stain extracellular DNA. The software creates masks based on the fluorescent images of the cells stained by PI. The area of extracellular DNA was established by subtracting BF mask from PI-channel mask; since BF and PI-channel masks delineate cell boundaries and DNA extent, respectively. Neutrophils with high extracellular DNA area and MPO positivity were counted as NETosis events (**Figure 1F**).

Data Collection

The following baseline clinical data were collected: age, gender, comorbidities, source of infection, presence or absence of bacteremia, initial absolute neutrophil count, Acute Physiology and Chronic Health Evaluation (APACHE) II score on admission, and patient's status at Days 7, 14, and 28 (i.e., recovered, critically-ill, deceased). Patients were considered critically-ill if they still needed organ support (e.g., mechanical ventilation, vasopressors). Survivors, who did not fall into the critically-ill definition, were classified as recovered. Daily SOFA scores were collected as means to quantify clinical severity in septic shock patients.

Statistical Analysis

Data analysis was performed using STATA 16.1 (StataCorp LLC, TX, US). The graphical illustrations were created with the R program's data visualization package (ggplot2). The baseline characteristics of patients between septic shock and infection groups were compared with Pearson's chi-squared or Fisher's exact tests as appropriate. The following measurements of neutrophil functions were used in the analyses: MFI of CD64, CCR2, and CXCR2 surface receptors; the percentages of "dysfunction neutrophils" (i.e., CD64-positive neutrophils, CCR2-positive neutrophils, and CXCR2-negative neutrophils); the percentages of apoptosis; and the percentages of NETosis. For measurements of CD64, CCR2, and CXCR2 surface receptors, pairwise correlation analyses were performed to determine the degree of correlations between MFI and the percentages of "dysfunction neutrophils". The analyses of associations between each neutrophil function and sepsis status were divided into two parts as described below with $p < 0.05$ defined statistical significance of all tests.

Longitudinal Changes of Neutrophil Functions and Their Associations With Sepsis Status

The comparison of neutrophil functions between septic shock and infected patients was made both on a day-by-day basis and as linear regression between time (i.e., days after admission) and measured neutrophil functions. The measurements of neutrophil functions on specific days were compared with t-tests and Wilcoxon Rank Sum tests for normally and non-normally distributed variables, respectively. Additionally, the measurements of neutrophil functions on Day 7 and Day 14 in the septic shock group were compared using paired t-tests or Wilcoxon matched-pair signed-rank tests as appropriate.

Multilevel regression analyses were performed to examine associations between the longitudinal changes of each neutrophil function and sepsis status while simultaneously explore the degree of interindividual variation in the response patterns. We used two-level mixed linear models with repeated measurements of neutrophil functions (level-1 variable) nested within each patient (level-2 variable). Fixed portion of the models determined the relationship between time (i.e., days after admission) and the measurements of each neutrophil functions. Random portion of the model, also calculated as intraclass correlation coefficients conditioned on a level-2 group effect, represented the degree of interindividual variation of the response patterns. Associations between sepsis status and the longitudinal changes of each neutrophil function were assessed by adding patient's sepsis status (i.e., septic shock, infection) and its interaction with time as model predictors. This model structure aimed to estimate the effect of patient's sepsis status in predicting the changes of neutrophil functions after adjusting for effects of time and interindividual variation. We hypothesized that both infection and septic shock may exert effects on the neutrophil functions, neither one of them should be the base level of the other during regression analyses. Hence, we included both infection status and septic shock status into the model so that their regression coefficients can be compared. The models were executed on the restricted maximum likelihood and the Kenward-Roger degrees of freedom methods, and unstructured covariance between the model's intercept and slope was allowed.

Associations Between Neutrophil Functions and Clinical Outcomes

The clinical outcomes of interest composed of Day 14 clinical status (i.e., recovered, critically-ill, deceased) and, in the subgroup of septic shock patients, SOFA score. Depending on data distribution, either one-way analysis of variance (ANOVA) tests or Kruskal Wallis tests with Dunn's test of multiple comparison was employed to compare the measurements of each neutrophil function on specific days among patients stratified by Day 14 clinical status. Moreover, in septic shock patients, we used the multilevel analysis, structured as described above, to estimate the associations between the measurements of each neutrophil function and SOFA score.

RESULTS

Patient Characteristics

We included 19 septic shock patients and 11 infected patients into the study (**Table 1**). Overall, our study population was elderly patients with many comorbidities. The study participants with septic shock and infection were similar in age, gender, and comorbidities. The difference between them was their clinical status; septic shock patients had a more severe clinical picture as demonstrated by APACHE II score and the percentages of patients who were critically-ill or deceased at Days 7, 14, and 28. Six patients were lost to follow-up toward the end of the specimen collection period resulting in 14 missing observations (6.5% of the expected number of observations). The number of

TABLE 1 | Characteristics of study participants[†] (n = 30).

Characteristics	Septic shock (n = 19)	Infection (n = 11)	p-value
Age (median, 95%CI)	74 (70–83)	78 (70–81)	0.93[1]
Female (%)	42	45	0.58[1]
Co-morbidities (%)			
Cardiovascular disease	47	45	0.92[2]
Diabetes mellitus	42	27	0.34[1]
Neurological disease	32	45	0.35[1]
Respiratory disease	26	18	0.49[1]
Liver disease	21	0	0.14[1]
Renal disease	16	27	0.38[1]
Hematologic disease	11	9	0.70[1]
Source of infection (%)			0.87[1]
Respiratory tract	32	36	
Gastrointestinal tract	26	36	
Urinary tract	21	18	
Others	21	9	
Bacteremia (%)	53	18	0.07[1]
Initial absolute neutrophil count [$\times 10^9$/L] (median, 95%CI)	15,020 (12,994–21,071)	11,011 (10,380–18,403)	0.29[3]
APACHE II score (mean, 95%CI)	29 (25–32)	13 (9–17)	<0.001*[4]
Patient's status 7 days after recruitment (%)			0.004*[1]
Recovered	42	100	
Critically ill	37	0	
Deceased	21	0	
Patient's status 14 days after recruitment (%)			0.008*[1]
Recovered	32	91	
Critically ill	47	9	
Deceased	21	0	
Patient's status 28 days after recruitment (%)			0.008*[1]
Recovered	42	100	
Critically ill	32	0	
Deceased	26	0	

[†]All study participants were diagnosed with acute infection and presented within 48 h of their symptom onset.

**p value < 0.05.*

[1]Fisher's exact test [2]Pearson's chi-squared test [3]Wilcoxon Rank Sum test [4]t-test.

APACHE II, Acute Physiology and Chronic Health Evaluation II; CI, confidence interval.

longitudinal observations per patient ranged from 3 to 8, with a median of 7.

Comparison of Neutrophil Functions Between Septic Shock and Infected Patients

Daily measurements of neutrophil functions stratified by sepsis status were shown in **Tables 2** and **3**. They were also illustrated in graphics (**Figure 2**). Regarding CD64, CCR2, and CXCR2 surface levels, pairwise correlation analyses demonstrated strong correlations between MFI and the percentages of dysfunctional neutrophils, defined by the corresponding molecules (correlation coefficients > 0.7). CD64 and CCR2 MFI positively correlated with the percentages of CD64-positive cells and CCR2-positive cells with correlation coefficients of 0.95 and 0.94, respectively. For CXCR2 receptors, there was a negative correlation between the percentages of CXCR2-negative neutrophils and CXCR2MFI with a correlation coefficient of −0.77.

TABLE 2 | The daily percentages of CD64-positive neutrophils, CCR2-positive neutrophils, CXCR2-negative neutrophils, apoptosis, and NETosis stratified by sepsis status[†] (n = 30: septic shock = 19, infection = 11).

Day	%, Median (95%CI)									
	CD64-positive neutrophils		CCR2-positive neutrophils		CXCR2-negative neutrophils		Apoptosis		NETosis	
	Septic shock	Infection	Septic shock	Infection	Septic shock	Infection	Septic shock	Infection	Septic shock	Infection
1	68.90 (37.91–91.32)	51.10 (26.03–78.33)	2.08 (1.02–7.67)	5.00 (2.00–12.90)	48.60*[2] (8.88–67.53)	2.05 (0.87–6.10)	0.15 (0.10–0.27)	0.15 (0.06–0.20)	0.07 (0.01–0.21)	0.67 (0.06–1.41)
2	71.20*[1] (50.10–90.96)	22.70 (7.58–60.26)	4.13 (2.49–11.73)	12.20 (3.89–20.71)	11.10*[2] (3.45–17.75)	2.14 (1.18–5.19)	0.20 (0.11–0.28)	0.13 (0.03–0.23)	0.09 (0.03–0.34)	0.19 (0.03–1.92)
3	62.25*[1] (48.57–79.17)	36.70 (10.93–63.65)	7.67 (3.29–25.19)	21.80 (7.97–29.73)	3.22 (1.59–28.80)	1.69 (0.88–3.33)	0.17 (0.09–0.25)	0.23 (0.08–0.48)	0.09 (0.02–0.30)	0.32*[2] (0.14–5.47)
4	48.50*[1] (34.50–56.19)	19.90 (3.27–40.09)	10.20 (5.24–15.97)	18.70 (2.93–30.11)	3.35 (2.13–9.81)	1.52 (0.79–3.30)	0.29 (0.12–0.49)	0.43 (0.04–0.78)	0.25 (0.09–1.00)	1.20 (0.16–9.71)
5	23.25*[2] (12.02–39.93)	12.50 (3.91–14.86)	6.28 (4.68–9.82)	8.85 (5.09–16.89)	5.37 (2.25–11.82)	2.39 (1.16–4.25)	0.29 (0.11–0.50)	0.18 (0.09–0.91)	0.41 (0.16–1.36)	0.95 (0.16–5.58)
6	26.50 (17.07–41.28)	12.35 (3.70–33.54)	4.00 (1.73–11.93)	8.54 (3.98–20.97)	5.91 (3.49–25.27)	3.54 (1.20–6.17)	0.24 (0.10–0.57)	0.25 (0.07–0.76)	0.42 (0.05–1.42)	1.76 (0.10–6.27)
7	19.30 (7.62–61.10)	7.44 (3.65–19.43)	2.45 (1.14–10.43)	6.32 (2.27–22.68)	6.69 (3.02–12.36)	4.32 (0.99–8.04)	0.43 (0.15–1.38)	0.24 (0.12–0.27)	0.84 (0.06–2.84)	0.84 (0.03–8.66)
14	17.00 (8.96–86.80)	N/A	2.38 (1.52–17.53)	N/A	4.46 (1.91–14.29)	N/A	0.43 (0.17–0.88)	N/A	2.16*[3] (0.08–4.67)	N/A

[†]Neutrophil functions, including the percentages of "dysfunction neutrophils" (i.e., CD64-positive neutrophils, CCR2-positive neutrophils, and CXCR2-negative neutrophils); the percentages of apoptosis; and the percentages of NETosis, were measured from peripheral blood neutrophils daily for seven consecutive days using flow cytometry. One additional blood sample at Day 14 was collected in septic shock patients to cover their more prolonged clinical courses. T-tests or Wilcoxon Rank Sum tests were applied to compare the measurement of neutrophil functions between septic shock and infection groups, as appropriate. In septic shock groups, Wilcoxon matched-pairs signed-rank tests were used to compare the measurement of neutrophil functions between Day 7 and Day 14.

**1 p-value < 0.05 from t tests, compared with infection group.*

**2 p-value < 0.05 from Wilcoxon Rank Sum tests, compared with infection group.*

**3 p-value < 0.05 from Wilcoxon matched-pairs signed-rank tests, compared with Day 7 in the septic shock group.*

CCR2, C-C chemokine receptor 2; CD64, cluster of differentiation 64; CI, confidence interval; CXCR2, C-X-C chemokine receptor 2; N/A, not applicable.

TABLE 3 | MFI of CD64, CCR2, and CXCR2 surface receptors stratified by sepsis status[†] (n = 30: septic shock = 19, infection = 11).

Day	MFI, Median (95%CI)					
	CD64		CCR2		CXCR2	
	Septic shock	Infection	Septic shock	Infection	Septic shock	Infection
1	3193.94 (2,145.81, 4,242.25)	2492.23 (1,597.89, 3,313.78)	1,337.01 (1,151.99, 1,450.36)	1,433.08 (1,142.61, 1,697.64)	10,196.71*[1] (7,445.314, 2,0940.83)	24,298.33 (20,439.08, 39,750.90)
2	3279.44*[1] (2,435.43, 4,260.54)	1679.51 (618.47, 2,781.14)	1,425.21 (1,302.48, 1,558.88)	1,638.60 (1,483.28, 1,905.19)	2,0549.02*[1] (17,144.55, 25,486.94)	28,013.80 (24,471.31, 28,631.53)
3	2683.48*[1] (2,382.53, 3,638.18)	2049.4 (1,103.699, 3,115.549)	1,465.15 (1,237.06, 2,031.36)	1,774.42 (1,545.59, 2,052.88)	25,155.37 (13,073.41, 31,818.24)	3,0382.27 (26,048.04, 35,935.84)
4	2381.37*[2] (1,657.00, 2,621.17)	1298.55 (529.29, 2,042.85)	1424.52 (1,314.32, 1,686.46)	1,768.58 (1,417.53, 2,085.80)	25,959.55 (23,896.68, 29,663.46)	3,3488.80 (24,209.54, 37,841.40)
5	1677.98*[2] (1,045.90, 2,255.14)	1139.14 (498.70, 1,417.34)	1,411.16 (1,297.23, 1,564.13)	1,645.81 (1,368.05, 1,744.92)	25,675.21 (18,383.27, 28,491.75)	26,454.04 (22,687.25, 29,959.20)
6	1862.86 (1,316.16, 2,202.05)	1242.69 (801.35, 1,833.44)	1,292.21 (1,170.29, 1,591.30)	1,667.09 (1,374.63, 1,854.49)	23,544.83 (17,297.05, 27,167.73)	26,602.44 (22,541.86, 32,232.45)
7	1297.45 (953.56, 2,778.40)	925.66 (186.11, 1,461.47)	1,282.14 (1,070.26, 1,694.45)	1,546.44 (1,360.41,1971.56)	25,100.66 (17,539.61, 29,322.77)	30,463.56 (17,820.35, 31,059.70)
14	1478.60 (635.125, 4,203.85)	N/A	1,420.93 (1,239.58, 1,932.46)	N/A	21,764.50 (17,396.15, 25,409.94)	N/A

[†]*Neutrophil functions, including MFI of CD64, CCR2, and CXCR2 surface receptors, were measured from peripheral blood neutrophils daily for seven consecutive days using flow cytometry. One additional blood sample at Day 14 was collected in septic shock patients to cover their more prolonged clinical courses. T-tests or Wilcoxon Rank Sum tests were applied to compare the measurement of neutrophil functions between septic shock and infection groups, as appropriate. In septic shock groups, paired t-tests or Wilcoxon matched-pairs signed-rank tests were used to compare the measurement of neutrophil functions between Day 7 and Day 14.*

**1 p-value < 0.05 from t-tests, compared with infection group.*

**2 p-value < 0.05 from Wilcoxon Rank Sum tests, compared with infection group.*

CCR2, C-C chemokine receptor 2; CD64, cluster of differentiation 64; CI, confidence interval; CXCR2, C-X-C chemokine receptor 2; MFI, median fluorescent intensity; N/A, not applicable.

Averaged among patients with the same clinical diagnosis, there was a statistically significant difference of CD64 and CXCR2 surface levels as well as NETosis activity between septic shock and infection groups, although the differences could only be demonstrated in some specific days during the clinical course. Neutrophils from septic shock patients had a higher CD64MFI as well as the higher percentages of CD64-positive neutrophils during Day 2 to Day 5. They also showed a lower CXCR2MFI and the higher percentages of CXCR2-negative neutrophils on Day 1 and Day 2. On the contrary, NETosis activity in infected patients was greater than that of septic shock patients on Day 3. In septic shock patients, however, there was a significant increase in NETosis activity from Day 7 to Day 14 in contrast to other neutrophil functions in which the changes in their levels between Day 7 and Day 14 were non-significant. Interestingly, the percentages of NETosis on Day 14 in septic shock patients and Day 3 in infected patients were in a similar range, no statistically significant difference between them can be demonstrated using Wilcoxon Rank Sum tests. Also, no statistically significant difference in CCR2MFI, a percentage of CCR2-positive neutrophils, and apoptosis activity, between septic shock and infection groups was found.

The multilevel regression analyses assessing longitudinal changes of neutrophil functions and their associations with sepsis status were demonstrated in **Table 4**. For CD64, CCR2, and CXCR2 surface levels, since the percentages of dysfunctional neutrophils were highly correlated with MFI and their unit of measurement synchronizes with apoptosis and NETosis, we used the percentages of dysfunctional neutrophils for the regression analysis; so that the coefficients and variances derived from the model of each neutrophil function are comparable. All neutrophil functions studied, except for CCR2 surface level, changed dynamically over time (p-value from Wald's tests for the model coefficient of time < 0.05). The percentages of CD64-positive neutrophils and CXCR2-negative neutrophils declined over time as opposed to apoptosis and NETosis, which increased over time. The percentages of CCR2-positive neutrophils, however, fluctuated throughout the study period. Some degree of interindividual variation of the magnitude of change existed for all neutrophil functions examined as demonstrated by the model variances and level-2 conditional ICCs. The degree of interindividual variation was largest for CCR2 surface level and smallest for apoptosis activity. Adjusting for the effect of time, septic shock status could predict the longitudinal trends of CD64, CCR2, and CXCR2 surface levels. Infection status could also predict CD64 and CCR2 surface levels over time; albeit lack of ability to predict that of CXCR2 receptors. In contrast, our analyses suggested that the changes in apoptosis and NETosis activity during the study period could only be predicted by time. Furthermore, for the longitudinal trends of CXCR2 surface level, there was a significant interaction between time and sepsis status in which an effect of sepsis status diminishes as time passes. In the regression models involving other neutrophil functions, no statistically significant interaction between time and sepsis status was demonstrated.

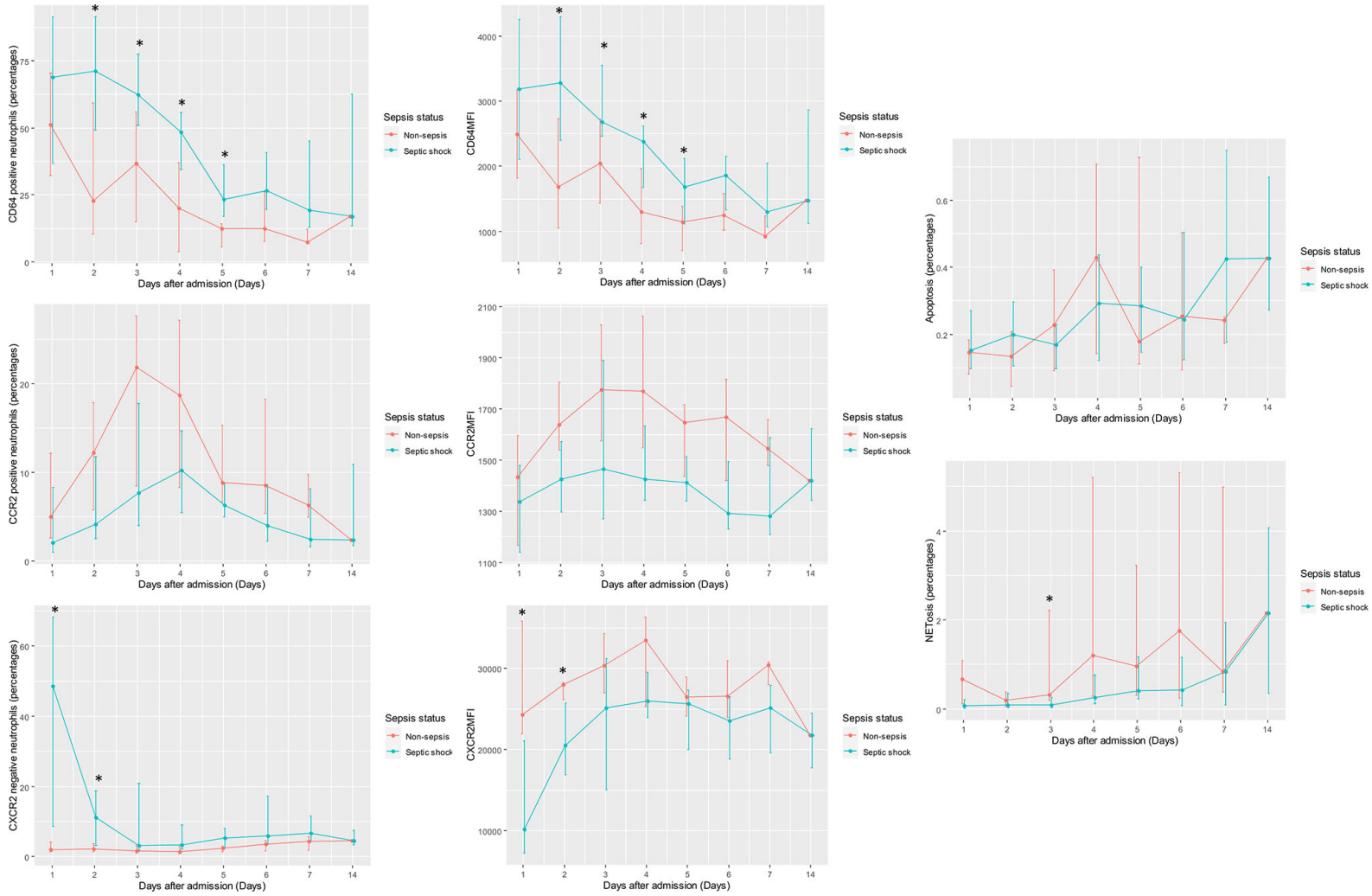

FIGURE 2 | Daily measurements of CD64, CCR2, and CXCR2 surface level; apoptosis; and NETosis stratified by sepsis status (septic shock or infection). MFI of CD64, CCR2, and CXCR2 surface receptors; the percentages of "dysfunction neutrophils" (i.e., CD64-positive neutrophils, CCR2-positive neutrophils, and CXCR2-negative neutrophils); the percentages of apoptosis; and the percentages of NETosis were illustrated in line graphs with error bars grouped by sepsis status. The lines connected median value of the measurements on the specific days. Error bars delineated interquartile ranges. Depending on data distribution, either t-test or Wilcoxon Rank Sum test was employed to compare the measurements of each neutrophil function on specific days between groups. *p-value from t-tests or Wilcoxon Rank Sum tests < 0.05. CCR2, C-C chemokine receptor 2; CD64, cluster of differentiation 64; CXCR2, C-X-C chemokine receptor 2; MFI, median fluorescent intensity.

TABLE 4 | Multilevel mixed model analysis examining the longitudinal correlations between the percentages of CD64-positive neutrophils, CCR2-positive neutrophils, CXCR2-negative neutrophils, apoptotic, and NETosis and sepsis status[†] (n = 30).

Model parameters		Estimate (95%CI)				
		CD64-positive neutrophils	CCR2-positive neutrophils	CXCR2-negative neutrophils	Apoptosis	NETosis
Fixed effects	Coefficient: Time (β_1)	−5.24* (−7.65, −2.83)	−0.62 (−1.91, 0.67)	−3.18* (−4.87, −1.50)	0.09* (0.02, 0.16)	0.28* (0.09, 0.47)
	Coefficient: Infection (β_2)	51.59* (31.70, 71.48)	15.82* (4.15, 27.49)	0.82 (−14.44, 16.09)	0.22 (−0.13, 0.57)	1.40 (−0.13, 2.94)
	Coefficient: Sepsis shock (β_3)	71.20* (56.11–86.28)	12.99* (4.14, 21.83)	32.29* (20.76, 43.82)	0.11 (−0.15, 0.37)	−0.24 (−1.39, 0.92)
	Interaction term:Time x Sepsis status (β_4)	1.03 (−2.96,5.01)	−0.14 (−2.30, 2.02)	−4.05* (−6.90, −1.20)	0.06 (−0.06,0.17)	−0.06 (−0.38,0.25)
Random effects	$\sigma^2_{\mu_0}$	848.59 (448.91, 1604.13)	305.02 (164.16, 566.75)	466.97 (231.45, 942.15)	0.02 (0.001,0.53)	3.82 (1.64, 8.89)
	$\sigma^2_{\mu_1}$	16.18 (7.09, 36.93)	5.08 (2.02, 12.77)	6.26 (1.67, 23.50)	0.01 (0.002, 0.02)	0.04 (0.01, 0.28)
	σ_{01}	−88.98 (−165.51, −12.46)	−37.14 (−64.86, −9.43)	−49.60 (−98.92, −0.28)	−0.01 (−0.04, 0.01)	0.11 (−0.28, 0.50)
	σ^2_e	253.82 (201.50, 319.74)	70.93 (55.71, 90.30)	196.27 (155.57, 247.62)	0.41 (0.34, 0.51)	3.16 (2.51, 3.98)
	Level-2 ICC	0.77 (0.63, 0.87)	0.81 (0.68, 0.90)	0.70 (0.53, 0.84)	0.05 (0.002,0.56)	0.55 (0.33, 0.75)

[†] *Regression equation: $PMN_{ij} = \beta_0 + \beta_1(Time_{ij}) + \beta_2(Infection_j) + \beta_3(Septic\ shock_j) + \beta_4(Time_{ij} \times Sepsis_j) + \mu_{0j} + \mu_{1j}(Time_{ij}) + e_{ij}$;*

i, measurement occasions; j, individual patients; PMN_{ij} repeated measurements of the neutrophil functions; Time, days after admission (days); Sepsis, patient's sepsis status (infection or septic shock); β_0, intercept; β_1, coefficient of time; β_2, coefficient of infection (0 = No, 1 = Yes); β_3, coefficient of septic shock (0 = No, 1 = Yes); β_3, coefficient of an interaction term between Time and Sepsis; μ_{0j}, patient-specific random effects of intercept; μ_{1j}, patient-specific random effects of slope for time; e_{ij}, occasion-specific time-varying residuals; $\sigma^2_{\mu_0}$, between-patient intercept variance; $\sigma^2_{\mu_1}$, between-patient time slope variance; σ_{01}, between-patient intercept-slope covariance; σ^2_e, within-patient variance.

** p-value < 0.05.*

CCR2, C-C chemokine receptor 2; CD64, cluster of differentiation 64; CI, Confidence interval; CXCR2, C-X-C chemokine receptor 2; Level-2 ICC, intraclass correlation coefficient conditioned on the effect of interindividual variation.

Associations Between Neutrophil Functions and Clinical Outcomes

Daily measurements of neutrophil functions stratified by Day 14 clinical status were illustrated in **Figure 3**. The distinction between patients with varying clinical status can be best appreciated in the longitudinal trends of CXCR2MFI and the percentages of CXCR-negative neutrophils. The statistically significant difference in CXCR2MFI and the percentages of CXCR2-negative neutrophils among three groups (recovered, critically-ill, deceased) can be demonstrated on Day 1 and Day 2. During the first two days of admission, CXCR2MFI were lowest and the CXCR2-negative neutrophils were highest in patients who died within 14 days after admission. Also, the multilevel regression analysis assessing associations between the measurements of neutrophil functions and SOFA score found that, after adjusting for the effect of time, the percentages of CXCR2-negative neutrophils could predict SOFA score in patients with septic shock ($p = 0.001$). CD64MFI and the percentages of CD64-positive neutrophils seemed to be highest in deceased patients as opposed to NETosis activity which was highest in patients who recovered. Unfortunately, these trends of CD64 surface level and NETosis activity could not be proved statistically significant; either by between-groups comparisons or multilevel regression analysis assessing its association with SOFA score. The longitudinal trends of CCR2 surface level and apoptosis among patients with different Day 14 clinical status were similar.

DISCUSSION

Numerous physiological and pathological stimuli could trigger changes in neutrophil functions. Various neutrophil phenotypes have been discovered, not only in healthy but also diseased states (20); some with potential for clinical applications (21, 22). Sepsis is one of the well-established diseases resulting in specific patterns of neutrophil dysfunctions; increased CD64 and CCR2 surface levels; decreased CXCR2 surface level; apoptosis delay; and increased NETosis are widely-cited sepsis-related neutrophil dysfunctions. However, the pattern that distinguishes sepsis from infection has not been mentioned; this is partly because sepsis and infection were first recognized and emphasized as distinctive processes in the newest update of sepsis definition (Sepsis-3). Therefore, literature, published before the release of this definition, has been employing non-uniform control settings to establish neutrophil dysfunctions as sepsis-related; none of them used infection as control. Therefore, previously-identified sepsis-related neutrophil dysfunctions are potentially a product of a combined effect between sepsis and infection rather than sepsis itself. However, we hypothesize that, on a background of infection, some of them might be genuinely sepsis-related, if we re-evaluate them in the desirable control setting.

In this study, we compared the neutrophil functions, with reported sepsis-related changes, between patients with septic shock and patients with infection who did not develop sepsis. Since sepsis is a time-dynamic disease, we observed these neutrophil functions longitudinally during the early phase of sepsis. We found that, during this period, each neutrophil function follows differing courses of changes and has a unique

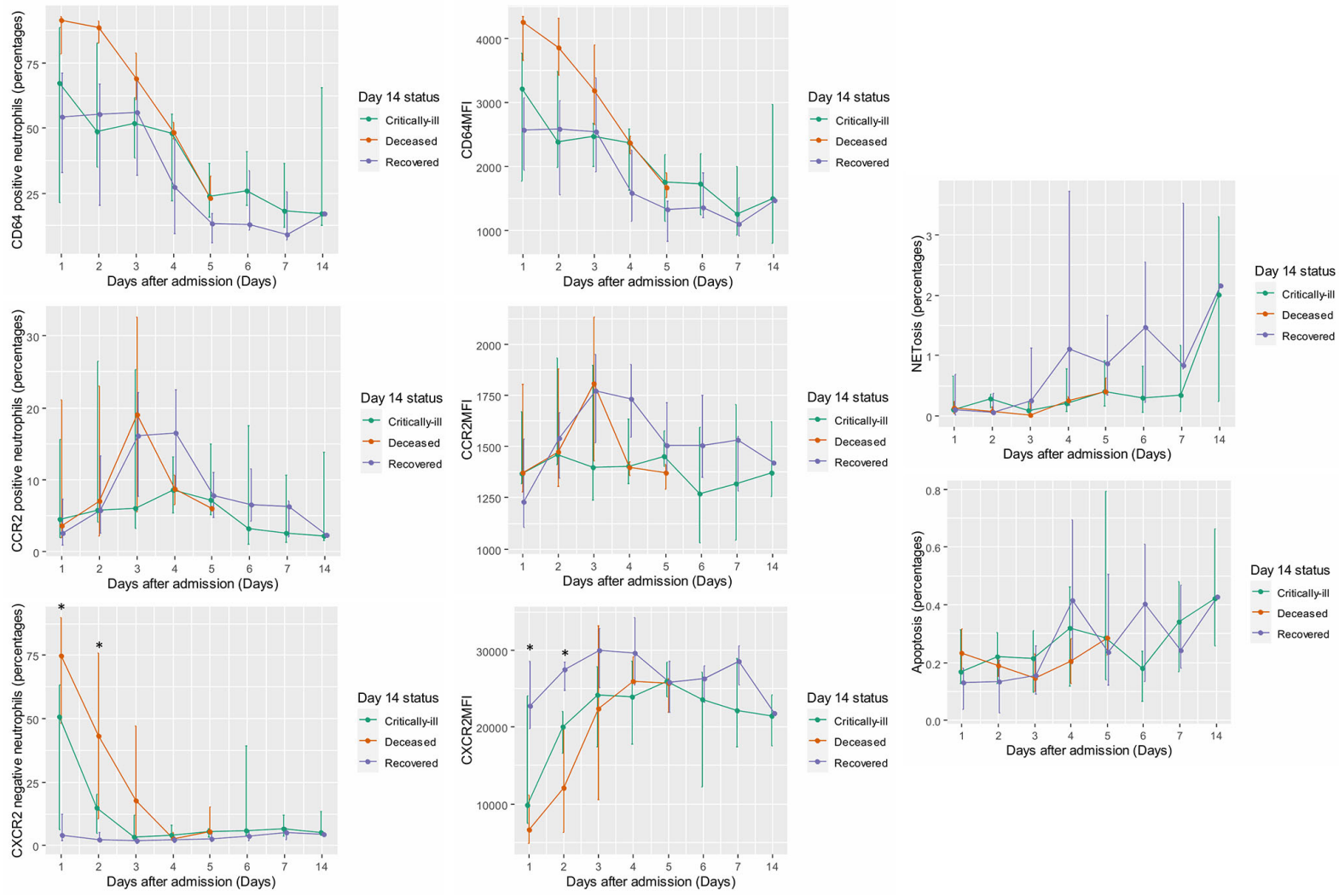

FIGURE 3 | Daily measurements of CD64, CCR2, and CXCR2 surface level; apoptosis; and NETosis stratified by Day 14 clinical status (Recovered, Critically-ill, or Deceased). MFI of CD64, CCR2, and CXCR2 surface receptors; the percentages of "dysfunction neutrophils" (i.e., CD64-positive neutrophils, CCR2-positive neutrophils, and CXCR2-negative neutrophils); the percentages of apoptosis; and the percentages of NETosis were illustrated in line graphs with error bars grouped by Day 14 clinical status. The lines connected median value of the measurements on the specific days. Error bars delineated interquartile ranges. Depending on data distribution, either one-way ANOVA test or Kruskal Wallis test with Dunn's test of multiple comparison was employed to compare the measurements of each neutrophil function on specific days between groups. *p-value from ANOVA or Kruskal Wallis tests < 0.05. ANOVA, analysis of variance; CCR2, C-C chemokine receptor 2; CD64, cluster of differentiation 64; CXCR2, C-X-C chemokine receptor 2, MFI, median fluorescent intensity.

relationship with sepsis. Of all neutrophil functions examined by our study, we can only affirm a reduction of CXCR2 surface level as sepsis-related. CXCR2 receptors play a significant role in the normal regulation of neutrophil recruitment (15). Previous experimental studies have demonstrated reduced CXCR2 surface level due to CXCR2 receptor internalization induced by circulating chemokines (15, 23). The lack of CXCR2 surface receptors was also linked to severe neutrophil hyperplasia in the bone marrow and neutrophilia in sepsis mice model (24). In addition, our study found that a reduction of CXCR2 surface level is related to sepsis, even in the presence of infection. Compared to patients with infection, CXCR2 surface level decreases at the onset of the disease in septic shock patients. As shown by the regression models, septic shock status predicts CXCR2 surface level over time while infection status does not. As patients progress into the less dynamic phase of the disease, CXCR2 surface level increases so that, by the end of the week, the difference of CXCR2 surface level between sepsis and infected patients disappears. Additionally, during early sepsis, patients with more severe disease have a significantly lower CXCR2 surface level than those with milder disease. In fact, in infected patients, CXCR2 surface level is persistently high, closely resembled a response pattern of healthy volunteers (8). These findings suggest that a reduction of CXCR2 surface level occurs synchronously with the peak of disease activity; shows the ability to revert to normal state; and has a dose-response relationship with clinical outcomes. Based on our observation, abnormal neutrophil migration due to decreased CXCR2 surface receptors should be considered the immunopathological feature, which could act as a marker for distinguishing sepsis from infected patients at the onset of the disease. As a consequence of decreased CXCR2 surface level, appropriate neutrophil chemotaxis was disrupted, causing inappropriate extravasation of neutrophils into various organs. Tissue injury inflicted by this process leads to multiorgan failure (15); which is the salient clinical feature that differentiates sepsis from infection by Sepsis-3 definition (1).

In contrast to our findings on CXCR2 surface level, our study fails to demonstrate the changes of CD64 and CCR2 surface levels as sepsis-related. CD64 and CCR2 receptors are not constitutively expressed on neutrophils at resting state (15, 25); however, earlier studies showed that CD64 and CCR2 surface levels were increased during sepsis (3). The amount of CD64 mRNA elevates to a measurable level within 1–3 h of the inciting events leading to a significant increment of CD64 surface level within 4–6 h (13). The emergence of CD64 surface receptors was thought to enhance neutrophil phagocytic activity through its high affinity to Fcγ part of IgG (26). Our study found that, even though a significant difference in CD64 surface level between septic shock and infection groups were observed during Day 2 to Day 5, this is mainly because CD64 surface level in infected patients plummets after Day 1 as opposed to septic shock patients whose CD64 surface level gradually decrease. At the onset of the disease, however, CD64 surface level from septic shock and infected patients are within the same range. Also, as shown by the regression coefficients, both infection and septic shock status could predict the degree of CD64 surface level over time despite the stronger effect exerted by septic shock. These findings suggest that a between-group difference in CD64 surface level likely stems from a more rapid recovery in non-sepsis patients who have milder infection compared to septic shock patients who have a more severe infection. In other words, CD64 surface level is not explicitly altered by sepsis but rather have a dose-response relationship with infection. This hypothesis is also supported by many studies which showed the rise of CD64 surface level as a marker of bacterial infection on a background of various other conditions, such as critically-ill status (27, 28), postoperative period (10, 29), and autoimmune diseases (30). Furthermore, previous studies showed that peripheral blood neutrophils from mice, which developed sepsis from cecal ligation and puncture, express high amount of CCR2 mRNA and CCR2 surface level as well as marked chemotaxis in response to CCL2 (14, 31). Since these mice were also had multiple organ dysfunctions and neutrophil accumulations in heart, lung, and kidney, the presence of CCR2 surface receptors was implicated in driving neutrophil infiltration to distant organs during sepsis (14). Nonetheless, our study found that CCR2 surface levels were similar between septic shock and infection groups and, like CD64 receptors, both infection and septic shock status could predict CCR2 surface levels over time. These findings suggest that elevation of CCR2 surface level is likely to be related to infection rather than sepsis. Organ dysfunction found in the earlier study may be attributable to decreased CXCR2 surface level, which was also demonstrated in these mice (14). Besides, CCR2 surface expression on neutrophil is not specific to sepsis or infection and can be found in other conditions, such as rheumatoid arthritis (32), and ischemic liver injury (33).

With regard to apoptosis and NETosis, although current evidence associates apoptosis delay and increased NETosis activity with sepsis, our study cannot confirm that they are sepsis-related. We found that, even if apoptotic activity starts to rise toward the end of the week, apoptotic activity of neutrophils from septic shock and infected patients was similar throughout the study period. Neither infection nor septic shock status could predict the percentages of apoptosis over time. Hence, within the timeframe of this study, apoptosis is less likely to contribute to the sequelae of sepsis. Similar to apoptosis, NETosis activity increases later during the clinical course. If we compare NETosis activity in septic shock and infected patients on a day-by-day basis, we might have to conclude that NETosis is suppressed in septic shock patients on Day 3. In fact, a few earlier longitudinal studies in sepsis which examined peripherally-measured NETosis for seven days also suggested that NETosis was suppressed throughout the clinical course of sepsis compared to healthy controls (22, 34). Nonetheless, we believe the different between septic shock and infected patients may concern the day NETosis spikes rather than the level of NETosis activity between infected and septic shock patients on the same day. In infection group, NETosis activity peaks on Day 3 and gradually decline thereafter. In septic shock groups, NETosis activity is highest on Day 14. Possibly, we may find a peak-and-fall pattern of NETosis activity in septic shock patients as we observed in infected patients if we follow the patients for a longer period. Despite the absence of statistical significance, patients who recovered at Day 14 seems to have the highest NETosis activity compared to patients who are still critically-ill or deceased at Day 14. Thus, the rise of NETosis in

peripheral blood may signify the recovery of from infection; infected patients who generally recover quicker than sepsis patients, therefore, experience the NETosis spike before sepsis patients.

In summary, by using infection as control, we demonstrated that the relationship between each neutrophil function and sepsis is unique and possibly reflects sepsis processes from different angles. CXCR2 surface level is related to sepsis activity while CD64 and CCR2 surface levels link to sepsis *via* infection. Peripherally-measured NETosis may signify the recovery from infection as it elevates during the less dynamic phase of the disease. Apoptosis during the study period may be equally affected by both sepsis and infection since its activity is indistinguishable between sepsis and infection. The strengths of our study are as follows. Firstly, data from our study can be applied to the current practice since we define septic shock and infection as per the latest clinical definition. Secondly, in contrast to previous studies which focused mainly on the magnitude of neutrophil functions, we provide data in a longitudinal fashion in relation to the clinical progression of the patients. Lastly, we examined the neutrophil functions not only by the group-averaged values but also with multilevel regression model which take into account the interindividual variation of the response pattern during analysis. We believe both methods should be used simultaneously since they serve different but equally important purposes. Group-averaged values give more insight on the neutrophil functions on the specific days in patients stratified by one characteristic (e.g., sepsis status, clinical status) and point out the one with the association which is strong enough to stand out even in the presence of unadjusted interindividual variation. However, multilevel model better highlight associations between neutrophil functions and variable of interest, especially in the neutrophil functions expressing a high degree of interindividual variation in the response pattern such as CCR2 surface level. Limitations of our study concern an inability to apply the result to patients with pre-existing immunological aberrations (e.g., cancer, autoimmune diseases, post-surgery). Further studies in a more immunologically heterogenous patients, especially for CXCR2 surface level, should be done to examine the generalizability of our observation. In addition, we measured these neutrophil functions from circulating pools of neutrophils; whether tissue neutrophils have the same or different phenotype is outside of the scope of our study.

CONCLUSION

With infection as control, a reduction of CXCR2 surface level is associated with sepsis; its level can be used to distinguish sepsis from infection at the onset of the disease. CD64 surface level, CCR2 surface level, and NETosis are not directly sepsis-related; their relationship with sepsis is instead mediated by the effect of infection. Apoptotic activity in septic shock patients does not found to be delayed compared to patients with infection.

DATA AVAILABILITY STATEMENT

The raw data supporting the conclusions of this article will be made available by the authors, without undue reservation.

ETHICS STATEMENT

The studies involving human participants were reviewed and approved by Human Research Ethics Committee of the Faculty of Medicine, Prince of Songkla University, Thailand. The patients/participants provided their written informed consent to participate in this study.

AUTHOR CONTRIBUTIONS

All authors took part in the conceptualization and methodology planning of the study. CS and RN did the validation and conduction of study experiments. CS, PV, and RN were responsible for data curation and formal analysis of the study. The original draft was prepared by CS and reviewed by RN, PV, and BK. All authors have read and agreed to the published version of the manuscript. BK oversaw the project administration as well as funding acquisition. All authors contributed to the article and approved the submitted version.

FUNDING

This study was financially supported by a research grant from the Faculty of Medicine, Prince of Songkla University (Grant No. REC 61-090-14-1).

ACKNOWLEDGMENTS

We deeply appreciate the help from Songklanagarind hospital's medical intensive care unit and general ward nurses during the specimen collection period. We also would like to express our gratitude to RN's laboratory personnel who facilitate us during the experimental set-up and validation.

REFERENCES

1. Singer M, Deutschman CS, Seymour CW, Shankar-Hari M, Annane D, Bauer M, et al. The Third International Consensus Definitions for Sepsis and Septic Shock (Sepsis-3). *JAMA* (2016) 315:801–10. doi: 10.1001/jama.2016.0287
2. Mortaz E, Alipoor SD, Adcock IM, Mumby S, Koenderman L. Update on Neutrophil Function in Severe Inflammation. *Front Immunol* (2018) 9:2171. doi: 10.3389/fimmu.2018.02171
3. Shao S-L, Cong H-Y, Wang M-Y, Liu P. The diagnostic roles of neutrophil in bloodstream infections. *Immunobiology* (2020) 225:151858. doi: 10.1016/j.imbio.2019.10.007
4. Shen X-F, Cao K, Jiang J-P, Guan W-X, Du J-F. Neutrophil dysregulation during sepsis: an overview and update. *J Cell Mol Med* (2017) 21:1687–97. doi: 10.1111/jcmm.13112
5. Sônego F, Castanheira FVES, Ferreira RG, Kanashiro A, Leite CAVG, Nascimento DC, et al. Paradoxical Roles of the Neutrophil in Sepsis:

Protective and Deleterious. *Front Immunol* (2016) 7:155. doi: 10.3389/fimmu.2016.00155
6. Brown KA, Brain SD, Pearson JD, Edgeworth JD, Lewis SM, Treacher DF. Neutrophils in development of multiple organ failure in sepsis. *Lancet* (2006) 368:157–69. doi: 10.1016/S0140-6736(06)69005-3
7. Groeneveld KM, Koenderman L, Warren BL, Jol S, Leenen LPH, Hietbrink F. Early decreased neutrophil responsiveness is related to late onset sepsis in multitrauma patients: An international cohort study. *PloS One* (2017) 12:e0180145. doi: 10.1371/journal.pone.0180145
8. Chishti AD, Shenton BK, Kirby JA, Baudouin SV. Neutrophil chemotaxis and receptor expression in clinical septic shock. *Intensive Care Med* (2004) 30:605–11. doi: 10.1007/s00134-004-2175-y
9. Tarlowe MH, Duffy A, Kannan KB, Itagaki K, Lavery RF, Livingston DH, et al. Prospective study of neutrophil chemokine responses in trauma patients at risk for pneumonia. *Am J Respir Crit Care Med* (2005) 171:753–9. doi: 10.1164/rccm.200307-917OC
10. Fjaertoft G, Håkansson LD, Pauksens K, Sisask G, Venge P. Neutrophil CD64 (FcgammaRI) expression is a specific marker of bacterial infection: a study on the kinetics and the impact of major surgery. *Scand J Infect Dis* (2007) 39:525–35. doi: 10.1080/00365540601113693
11. Rhodes A, Evans LE, Alhazzani W, Levy MM, Antonelli M, Ferrer R, et al. Surviving Sepsis Campaign: International Guidelines for Management of Sepsis and Septic Shock. *Crit Care Med* (2017) 45:486–552. doi: 10.1097/CCM.0000000000002255
12. Maas CJM, Hox JJ. Sufficient Sample Sizes for Multilevel Modeling. *Methodology* (2005) 1:86–92. doi: 10.1027/1614-2241.1.3.86
13. Sack U. CD64 expression by neutrophil granulocytes. *Cytometry B Clin Cytom* (2017) 92:189–91. doi: 10.1002/cyto.b.21216
14. Souto FO, Alves-Filho JC, Turato WM, Auxiliadora-Martins M, Basile-Filho A, Cunha FQ. Essential role of CCR2 in neutrophil tissue infiltration and multiple organ dysfunction in sepsis. *Am J Respir Crit Care Med* (2011) 183:234–42. doi: 10.1164/rccm.201003-0416OC
15. Stadtmann A, Zarbock A. CXCR2: From Bench to Bedside. *Front Immunol* (2012) 3:263. doi: 10.3389/fimmu.2012.00263
16. Maecker HT, Trotter J. Flow cytometry controls, instrument setup, and the determination of positivity. *Cytometry A* (2006) 69:1037–42. doi: 10.1002/cyto.a.20333
17. Hoppenbrouwers T, Autar ASA, Sultan AR, Abraham TE, van Cappellen WA, Houtsmuller AB, et al. In vitro induction of NETosis: Comprehensive live imaging comparison and systematic review. *PloS One* (2017) 12:e0176472. doi: 10.1371/journal.pone.0176472
18. Pietkiewicz S, Schmidt JH, Lavrik IN. Quantification of apoptosis and necroptosis at the single cell level by a combination of Imaging Flow Cytometry with classical Annexin V/propidium iodide staining. *J Immunol Methods* (2015) 423:99–103. doi: 10.1016/j.jim.2015.04.025
19. Lelliott PM, Momota M, Lee MSJ, Kuroda E, Iijima N, Ishii KJ, et al. Rapid Quantification of NETs In Vitro and in Whole Blood Samples by Imaging Flow Cytometry. *Cytometry A* (2019) 95:565–78. doi: 10.1002/cyto.a.23767
20. Hellebrekers P, Vrisekoop N, Koenderman L. Neutrophil phenotypes in health and disease. *Eur J Clin Invest* (2018) 48 Suppl 2:e12943. doi: 10.1111/eci.12943
21. Spijkerman R, Hesselink L, Bongers S, van Wessem KJP, Vrisekoop N, Hietbrink F, et al. Point-of-Care Analysis of Neutrophil Phenotypes: A First Step Toward Immuno-Based Precision Medicine in the Trauma ICU. *Crit Care Explor* (2020) 2:e0158. doi: 10.1097/CCE.0000000000000158
22. Patel JM, Sapey E, Parekh D, Scott A, Dosanjh D, Gao F, et al. Sepsis Induces a Dysregulated Neutrophil Phenotype That Is Associated with Increased Mortality. *Mediators Inflammation* (2018) 2018:4065362. doi: 10.1155/2018/4065362
23. Phillipson M, Kubes P. The neutrophil in vascular inflammation. *Nat Med* (2011) 17:1381–90. doi: 10.1038/nm.2514
24. Shuster D, Kehrli M, Ackermann M. Neutrophilia in mice that lack the murine IL-8 receptor homolog. *Science* (1995) 269:1590–1. doi: 10.1126/science.7667641
25. Capucetti A, Albano F, Bonecchi R. Multiple Roles for Chemokines in Neutrophil Biology. *Front Immunol* (2020) 11:1259. doi: 10.3389/fimmu.2020.01259
26. Hoffmann JJML. Neutrophil CD64 as a sepsis biomarker. *Biochem Med (Zagreb)* (2011) 21:282–90. doi: 10.11613/bm.2011.038
27. Dimoula A, Pradier O, Kassengera Z, Dalcomune D, Turkan H, Vincent J-L. Serial determinations of neutrophil CD64 expression for the diagnosis and monitoring of sepsis in critically ill patients. *Clin Infect Dis* (2014) 58:820–9. doi: 10.1093/cid/cit936
28. Wang X, Li Z-Y, Zeng L, Zhang A-Q, Pan W, Gu W, et al. Neutrophil CD64 expression as a diagnostic marker for sepsis in adult patients: a meta-analysis. *Crit Care* (2015) 19:245. doi: 10.1186/s13054-015-0972-z
29. Perry J, Reed MR, Refaie R, Sprowson AP, Rankin KS, Refaie R. The assessment of neutrophil CD64 count as an early warning marker of joint replacement infection. *Arch Orthop Trauma Surg* (2013) 133:1351–8. doi: 10.1007/s00402-013-1816-4
30. Li S, Huang X, Chen Z, Zhong H, Peng Q, Deng Y, et al. Neutrophil CD64 expression as a biomarker in the early diagnosis of bacterial infection: a meta-analysis. *Int J Infect Dis* (2013) 17:e12–23. doi: 10.1016/j.ijid.2012.07.017
31. Speyer CL, Gao H, Rancilio NJ, Neff TA, Huffnagle GB, Sarma JV, et al. Novel Chemokine Responsiveness and Mobilization of Neutrophils during Sepsis. *Am J Pathol* (2004) 165:2187–96. doi: 10.1016/S0002-9440(10)63268-3
32. Talbot J, Bianchini FJ, Nascimento DC, Oliveira RDR, Souto FO, Pinto LG, et al. CCR2 Expression in Neutrophils Plays a Critical Role in Their Migration Into the Joints in Rheumatoid Arthritis: CCR2 AND NEUTROPHIL MIGRATION INTO RHEUMATOID JOINTS. *Arthritis Rheumatol* (2015) 67:1751–9. doi: 10.1002/art.39117
33. Xu P, Zhang J, Wang H, Wang G, Wang C-Y, Zhang J. CCR2 dependent neutrophil activation and mobilization rely on TLR4-p38 axis during liver ischemia-reperfusion injury. *Am J Transl Res* (2017) 9:2878–90.
34. Delabranche X, Stiel L, Severac F, Galoisy A-C, Mauvieux L, Zobairi F, et al. Evidence of Netosis in Septic Shock-Induced Disseminated Intravascular Coagulation. *Shock* (2017) 47:313–7. doi: 10.1097/SHK.0000000000000719

Conflict of Interest: The authors declare that the research was conducted in the absence of any commercial or financial relationships that could be construed as a potential conflict of interest.

frontiers in Immunology

ORIGINAL RESEARCH
published: 04 February 2021
doi: 10.3389/fimmu.2020.615009

Characterization of Circulating IL-10-Producing Cells in Septic Shock Patients: A Proof of Concept Study

Astrid Fabri[1,2], *Khalil Kandara*[1,2], *Rémy Coudereau*[1,2], *Morgane Gossez*[1,2], *Paul Abraham*[3], *Céline Monard*[2,3], *Martin Cour*[4], *Thomas Rimmelé*[2,3], *Laurent Argaud*[4], *Guillaume Monneret*[1,2] *and Fabienne Venet*[1,2]*

[1] Hospices Civils de Lyon, Edouard Herriot Hospital, Immunology Laboratory, Lyon, France, [2] Hospices Civils de Lyon—bioMérieux, EA 7426 "Pathophysiology of Injury-Induced Immunosuppression", Université Claude Bernard Lyon 1, Villeurbanne, France, [3] Anesthesia and Critical Care Medicine Department, Hospices Civils de Lyon, Edouard Herriot Hospital, Lyon, France, [4] Medical Intensive Care Department, Hospices Civils de Lyon, Edouard Herriot Hospital, Lyon, France

Sepsis is a worldwide health priority characterized by the occurrence of severe immunosuppression associated with increased risk of death and secondary infections. Interleukin 10 (IL-10) is a potent immunosuppressive cytokine which plasma concentration is increased in septic patients in association with deleterious outcomes. Despite studies evaluating IL-10 production in specific subpopulations of purified cells, the concomitant description of IL-10 production in monocytes and lymphocytes in septic patients' whole blood has never been performed. In this pilot study, we characterized IL-10 producing leukocytes in septic shock patients through whole blood intracellular staining by flow cytometry. Twelve adult septic shock patients and 9 healthy volunteers were included. Intracellular tumor necrosis factor-α (TNFα) and IL-10 productions after lipopolysaccharide stimulation by monocytes and IL-10 production after PMA/Ionomycine stimulation by lymphocytes were evaluated. Standard immunomonitoring (HLA-DR expression on monocytes, CD4+ T lymphocyte count) of patients was also performed. TNFα expression by stimulated monocytes was reduced in patients compared with controls while IL-10 production was increased. This was correlated with a reduced monocyte HLA-DR expression. B cells, CD4+, and CD4- T lymphocytes were the three circulating IL-10 producing lymphocyte subsets in both patients and controls. No difference in IL-10 production between patients and controls was observed for B and CD4- T cells. However, IL-10 production by CD4+ T lymphocytes significantly increased in patients in parallel with reduced CD4+ T cells number. Parameters reflecting altered monocyte (increased IL-10 production, decreased HLA-DR expression and decreased TNFα synthesis) and CD4+ T lymphocyte (increased IL-10 production, decreased circulating number) responses were correlated. Using a novel technique for intracellular cytokine measurement in whole blood, our results identify monocytes and CD4+ T cells as the main IL-10 producers in septic patients' whole blood and illustrate the development of a global immunosuppressive profile in septic shock. Overall, these preliminary results add to our understanding of the global increase in IL-10 production induced by septic shock.

OPEN ACCESS

Edited by:
Jiang Huai Wang, University College Cork, Ireland

Reviewed by:
Julie Demaret, Queen Mary University of London, United Kingdom
Marcelo De Carvalho Bittencourt, Université de Lorraine, France

***Correspondence:**
Fabienne Venet
fabienne.venet@chu-lyon.fr

Specialty section:
This article was submitted to Inflammation, a section of the journal Frontiers in Immunology

Received: *07 October 2020*
Accepted: *21 December 2020*
Published: *04 February 2021*

Citation:
Fabri A, Kandara K, Coudereau R, Gossez M, Abraham P, Monard C, Cour M, Rimmelé T, Argaud L, Monneret G and Venet F (2021) Characterization of Circulating IL-10-Producing Cells in Septic Shock Patients: A Proof of Concept Study. Front. Immunol. 11:615009. doi: 10.3389/fimmu.2020.615009

Further research is mandatory to determine the pathophysiological mechanisms leading to such increased IL-10 production in monocytes and CD4+ T cells.

Keywords: sepsis, immunosuppression, flow cytometry, interleukin 10, lymphocytes, monocytes

INTRODUCTION

In 2017, the World Health Assembly and the World Health Organization recognized sepsis as a global health priority (1). Indeed, the incidence of sepsis is high and every year sepsis is responsible for over 10 million deaths worldwide (2). While sepsis and septic shock are caused by an excessive activation of the immune system, current data indicate that after a short pro-inflammatory phase, septic shock patients develop negative regulatory mechanisms aimed at blocking initial hyper-immune activation. In some patients, this may lead to profound immunosuppression involving both innate and adaptive immunity (3).

Sepsis-induced immunosuppression prevents the efficient clearing of the primary infection, is associated with an increased risk of nosocomial infections and favors the reactivation of latent viruses (Cytomegalovirus or Herpes Simplex Virus) (3). In addition, it is reported that over 70% of total mortality after septic shock occurs in the immunosuppressive phase (i.e., after the first 3 days) (4). This is the rationale behind clinical trials based on adjunctive immunostimulation in sepsis (interferon gamma, human granulocyte-macrophage colony-stimulating factor, interleukin 7, anti-PD1/L1 checkpoint inhibitor antibodies) (5). However, a better description of sepsis-induced immune alterations is mandatory in order to improve the understanding of sepsis-induced immunosuppression pathophysiology and to identify innovative therapeutic targets and stratification biomarkers.

Interleukin 10 (IL-10) is a potent immunosuppressive cytokine which concentration is increased in the plasma of septic shock patients. IL-10 blood levels have been shown to correlate with inflammation severity and the development of organ failure in septic shock (6). Increased plasmatic IL-10 concentration has also been associated with an increase in nosocomial infections and mortality (7–9). IL-10 thus likely appears to play a major role in sepsis-induced immunosuppression.

The increased production of IL-10 by some specific cell subpopulations has only partially been described in sepsis (3–5). These data were based on ex vivo experiments with purified cells, which may not necessarily be representative of cytokine production status by circulating leukocytes. In addition, previous studies evaluated IL-10 production by one specific cell subset at a time and thus far, no data are available describing IL-10 production by leukocytes subpopulations simultaneously. In this context, the aim of this exploratory study was to characterize IL-10 producing cells in sepsis through a novel whole blood intracellular staining approach by flow cytometry.

Abbreviations: AB/C, antibodies bound per cell; Abs, antibodies; Breg, regulatory B cell; EFS, Etablissement Français du Sang; HV, healthy volunteer; IL-10, interleukin 10; IQR, interquartile range; LPS, lipopolysaccharide; MFI, mean fluorescence intensity; mHLA-DR, monocyte HLA-DR; SAPS, Simplified Acute Physiology Score; SOFA, Sequential Organ Failure Assessment; TNFα, tumor necrosis factor-α; Treg, regulatory T cell.

MATERIALS AND METHODS

Study Population

This pilot clinical study was conducted on twelve consecutive septic shock patients admitted to the intensive care unit of the Edouard Herriot Hospital (Hospices Civils de Lyon, Lyon, France). This project is part of a global study in sepsis-induced immune dysfunctions (IMMUNOSEPSIS cohort, #NCT04067674). Diagnostic criteria for septic shock was based on the Sepsis-3 definition (10). Exclusion criteria disqualified patients under 18 years of age and subjects with aplasia or pre-existent immunosuppression as defined by preexistent immunosuppressive treatment including corticosteroids at an immunosuppressive dosage (> 10 mg equivalent prednisone/day and cumulative dose >700 mg), ongoing hematological disease or within 5 years preceding inclusion, solid tumor under chemotherapy or in remission, innate immune deficit, extracorporeal circulation within one month before inclusion (cardiac surgery or ECMO). Samples of peripheral blood were collected at day 3–4 after the onset of septic shock in heparin coated tubes. The immunosuppressive state of septic patients was verified by measuring decreased HLA-DR expression on monocytes (mHLA-DR) expressed as a number of antibodies bound per cell (AB/C, see reference for standardized laboratory protocol) and CD4+ T lymphocyte count (11). Clinical parameters were collected during the follow-up period (until 28 days).

This non-interventional study was conducted in accordance with the Declaration of Helsinki, under terms of all relevant local legislation and was approved by our Institutional Review Board for Ethics ["Comité de Protection des Personnes Ouest II - Angers" – n° RCB: 2019-A00210-57, n° CPP: 19.01.23. 71857 (2019/11)], which waived the need for informed consent, as the study was observational and performed on residual blood after the completion of routine follow-up. Patients or next-of-kin were systematically informed of the study and non-opposition to inclusion in the study was systematically obtained and registered for each patient. Residual samples were stored within a blood collection registered at French Ministry of Research and Education (#DC-2008-509) and at the "Commission Nationale de l'Informatique et des Libertés". Peripheral blood from healthy volunteers (HV) was provided by the "Etablissement Français du Sang" (EFS) from Lyon. According to EFS standardized procedures for blood donation and to provisions of the articles R.1243–49 and following ones of

the French public health code, a written non-opposition to the use of donated blood for research purposes was obtained from HV. The blood donors' personal data were anonymized before transfer to our research laboratory.

Intracellular Staining Procedure

Intracellular staining protocol was optimized by Beckman Coulter Immunotech (Marseille, France).

For monocytes, 100 µl of heparin anticoagulated whole blood was directly added to the stimulation tube (DurActive3® tube containing dry coated lipopolysaccharide (LPS) and Brefeldin A, Beckman Coulter, Brea, US) or to an empty control tube. After 3h incubation at 37°C, cells were labeled with cell surface antibodies: FITC-labeled anti-CD16, ECD-labeled anti-HLA-DR, PB-labeled anti-CD14, and KrO-labeled anti-CD45 (all from Beckman Coulter, Brea, US). Thereafter, samples were washed with PBS and treated with the IntraPrep Permeabilization Reagent set (Beckman Coulter, Brea, US) according to the manufacturer's instructions. Samples were then stained for 45min at room temperature in the dark with intracellular antibodies: PE-labeled anti-IL10 (BioLegend, San Diego, US) or Rat IgG2a PE-labeled isotype control antibody (BioLegend, San Diego, US) and AF700-labeled anti-TNFα (Beckman Coulter, Brea, US) or mouse IgG1 AF700-labeled isotype control antibody (BioLegend, San Diego, US). Isotype controls of anti-IL-10 and anti-TNF antibodies were used in order to evaluate non-specific binding both in stimulated and non-stimulated conditions and thus to set-up threshold of positivity when markers were expressed as percentages of positive cells.

For lymphocytes, 100 µl of heparin anticoagulated whole blood was directly added to the stimulation tube (DurActive1® tube containing dry coated Phorbol 12-Myristate13 Acetate (PMA), Ionomycin and Brefeldin A, Beckman Coulter, Brea, US) or to an empty control tube. After 3h incubation at 37°C, cells were labeled with cell surface antibodies: PC7-labeled anti-CD19, KrO-labeled anti-CD45, PB-labeled anti-CD3 and APC-labeled anti-CD4 (all from Beckman Coulter, Brea, US). Thereafter, samples were washed with PBS and treated with the IntraPrep Permeabilization Reagent set (Beckman Coulter, Brea, US) according to the manufacturer's instructions. Samples were then stained for 45min at room temperature in the dark with intracellular antibodies: PE-labeled anti-IL10 (BioLegend, San Diego, US) or Rat IgG2a PE-labeled isotype control antibody (BioLegend, San Diego, US).

Data Acquisition

Data acquisition was performed on a Navios Flow Cytometer (Beckman Coulter, Brea, US). Our instrument was daily calibrated with Flow Check (Beckman Coulter, Brea, US) and Flow Set (Beckman Coulter, Brea, US) calibration beads to control the optical and fluidic stability of the device and for a performance validation throughout the study. To minimize autofluorescence and the improper analysis of cell doublets, cells were first put through a forward scatter area and forward scatter height gate to identify single cells. Leukocytes were then gated out from dead cells and debris on the basis of labeling with CD45. For the monocyte panel, among the CD45+ cell population, monocytes were identified on a CD14/SS dot-plot. Intracellular tumor necrosis factor-α (TNFα) and mHLA-DR results were expressed as mean fluorescence intensity (MFI) of the entire monocyte subpopulation. For the lymphocyte panel, two complementary gating strategies were used. First, in order to phenotype IL-10 producing lymphocytes in stimulated tubes, on a IL-10 (x-axis) and SS (y-axis) dot-plot gated on in CD45+ leukocytes, we selected IL-10 producing lymphocytes (IL-10+ SSClow cells). CD3, CD19, and CD4 expressions were then characterized on these cells based on CD4 (y-axis) and CD3 or CD19 (x-axis) dot-plots. Second, so as to evaluate the impact of sepsis on IL-10 production capacity on beforehand identified lymphocyte subpopulations, B cells were identified on a CD19/SS dot-plot and T cells on a CD3/SS dot-plot among the CD45+ cell population. Finally, CD4- and CD4+ T cells were gated among CD3+ cells on a CD3/CD4 dot-plot. The percentages of IL-10 expressing cells among these three lymphocyte subpopulations were then evaluated. Positivity threshold was defined based on isotype values set up at 1%. A minimum of 5,000 target cells (monocytes or lymphocytes) were systematically acquired to ensure robustness of results. Of note, both in patients and donors, the majority of monocytes were able to produce TNF-α; which was not the case for IL-10. Thus TNF- α results expressed as MFI possessed a better dynamic range compared with percentages which saturated at 100%. In addition, TNF-α results expressed as percentages and MFI were strongly correlated (Data not shown).

Statistical Analysis

Results are expressed as individual values and medians ± IQR (interquartile range). Comparisons between patients and HV were made using the non-parametric Mann-Whitney U test. Comparisons between stimulated and non-stimulated tubes were made using the Wilcoxon paired test. Correlations were made with the Spearman correlation test. Statistical significance was set at $p < 0.05$. Statistical analyses were performed with R Studio software (version 1.2.5001; R studio, Boston, Massachusetts).

RESULTS

Clinical Characteristics of the Cohort

In total, 12 septic shock patients were included in this pilot study. Patients presented with usual demographic and clinical characteristics of septic shock patients (elderly patients and high severity scores, **Table 1**). These septic patients presented with signs of immunosuppression including decreased mHLA-DR and CD4+ T lymphopenia compared with reference values from the lab. In addition, nine healthy volunteers were included (median age = 53, five women - four men).

Intracellular Cytokines in Monocytes

As reported previously, LPS stimulation induced a strong increase in intracellular TNFα expression in monocytes both from healthy volunteers and patients (12). However, this increase was statistically stronger in HV than in patients (MFI 61.6 [IQR:

TABLE 1 | Demographic, clinical, and immunological data for septic shock patients.

Parameters	Septic shock Patients (n=12)
Age at admission (years)	69 [63–73]
Gender - Male, n (%)	7 (58)
Main admission category	
Medical, n (%)	4 (33)
Surgical, n (%)	8 (67)
SAPS II score	53 [50–62]
SOFA score	9 [8-10]
McCabe score	
0, n (%)	6 (50)
1, n (%)	6 (50)
Infection diagnosis, n* (%)	
Microbiology	10 (91)
Surgery	1 (9)
Microbiologicaly documented, n(%)	
Bacilli gram -	6 (40)
Cocci gram +	9 (60)
Other	0 (0)
Site of infection, n* (%)	
Pulmonary	1 (9)
Abdominal	3 (27)
28-day non survivors, n (%)	2 (17)
Secondary nosocomial infections, n (%)	3 (25)
Immunological parameters	
mHLA-DR (AB/C)	4044 [3,246–6,210]
Absolute CD4+ T cell count	317 [248–463]

Continuous data and biological parameters are presented as medians and interquartile ranges [Q1–Q3]. For clinical parameters, categorical data are presented as numbers of cases and percentages among the total population in brackets. SAPS II (Simplified Acute Physiology Score II) and McCabe scores were calculated after admission. SOFA (Sequential Organ Failure Assessment) score was measured after 24h of ICU stay. mHLA-DR was expressed as numbers of anti-HLA-DR antibodies bound per monocyte (AB/C). Reference values for healthy volunteers: mHLA-DR: > 15,000 AB/C, CD4+: 336-1126 cells/µl.

58.0–74.5] vs 23.6 [IQR: 16.8–39.9], p=0.0013) (**Figure 1A**). We observed a good correlation between intracellular TNFα induction after stimulation and monocyte HLA-DR expression both in patients and controls, with individuals with high HLA-DR expression producing more TNFα than individuals with decreased HLA-DR expression (R= 0.79; p<0.001) (**Figure 1B**). This was also observed at the single cell level as, in septic patients, monocytes with high HLA-DR expression also had higher expression of TNFα compared with HLA-DRlow monocytes (MFI 27.5 [IQR: 15.3–45.7] vs 7.3 [IQR: 5.3–16.8], p=0.00049) (**Figures 1C, D**).

LPS challenge also induced IL-10 expression in monocytes in both patients and controls (**Figure 2A**). However, in contrary to TNFα, the proportion of IL-10 positive monocytes was statistically higher in patients than HV (2.4% [IQR: 1.8–3.7] vs 1.2% [IQR: 0.9–1.6], p=0.0093) (**Figure 2B**). The proportion of IL-10 positive monocytes was negatively correlated with HLA-DR (**Figure 2C**) and intracellular TNFα expression (**Figure 2D**) in these cells. Correlation coefficients were -0.61 (p=0.0041) and -0.67 (p=0.0012) respectively.

Intracellular IL-10 Expression in Lymphocytes

In order to identify circulating lymphocyte subsets producing IL-10, we evaluated CD4, CD3 and CD19 expressions on IL-10 expressing cells after stimulation. B lymphocytes, CD4+ T cells and CD4- T cells were the three main subsets of IL-10 producing lymphocytes in both patients and HV (**Figure 3A**). Among the three subsets, CD4+ T cells were the main IL-10 producing lymphocytes representing more than 60% of IL-10+ lymphocytes. No significant difference was found in the relative proportions of IL-10 producing lymphocyte subsets between patients and HV and we did not observe any appearance or disappearance of an IL-10 producing lymphocyte subset after septic shock (**Figure 3B**).

When comparing IL-10 production between patients and controls, in these beforehand identified cells no significant difference was observed in the proportion of B lymphocytes and CD4- T cells expressing IL-10. However, the proportion of CD4+ T cells expressing IL-10 was significantly higher among septic shock patients than HV (median [IQR] 2.8% [1.8–3.4] vs 1.6% [1.3–1.9], p=0.0077) (**Figure 4**).

In addition, intracellular IL-10 expression in CD4+ T cells was inversely correlated to CD4+ T cell counts in patients (R= -0.8, p=002) (**Figure 5A**). The proportion of IL-10 positive CD4+ T cells was also negatively correlated to mHLA-DR and intracellular TNFα expression (R= -0.62, p=0.0026, and -0.46, p=0.034 respectively) and positively correlated to the proportion of IL-10 positive monocytes (R=0.54, p=0.012) (**Figures 5B–D**).

DISCUSSION

Results from this study showed that IL-10 production was induced in circulating monocytes from septic shock patients in parallel with decreased TNFα production and reduced HLA-DR expression. Among circulating lymphocytes, CD4+ T cells were the main IL-10 producers in circulating blood and this cytokine production was increased after septic shock. Such increase was negatively correlated with CD4+ T cell lymphopenia and positively with increased IL-10 production by monocytes. The strong correlations between parameters reflecting altered monocyte (increased IL-10 production, decreased HLA-DR expression and decreased TNFα synthesis) and CD4+ T lymphocyte (increased IL-10 production, decreased circulating number) responses suggest a common regulation mechanism and illustrate the development of a global immunosuppressive profile in septic shock. Overall, these preliminary results add to our understanding of the global increase in IL-10 production induced by septic shock.

Findings in the present study are consistent with sepsis-induced monocyte anergy described in the literature and the concept of leukocyte reprogramming (3–5). We replicated in whole blood results observed on purified or frozen cells showing the decreased TNFα but increased IL-10 productions by monocytes in septic patients characteristic of the phenomenon of endotoxin tolerance (13–15). However, we completed these observations by showing at the single cell level the correlation between decreased HLA-DR expression, decreased TNFα but increased IL-10 productions. Similarly, a negative correlation between mHLA-DR and IL-10 plasmatic concentrations was

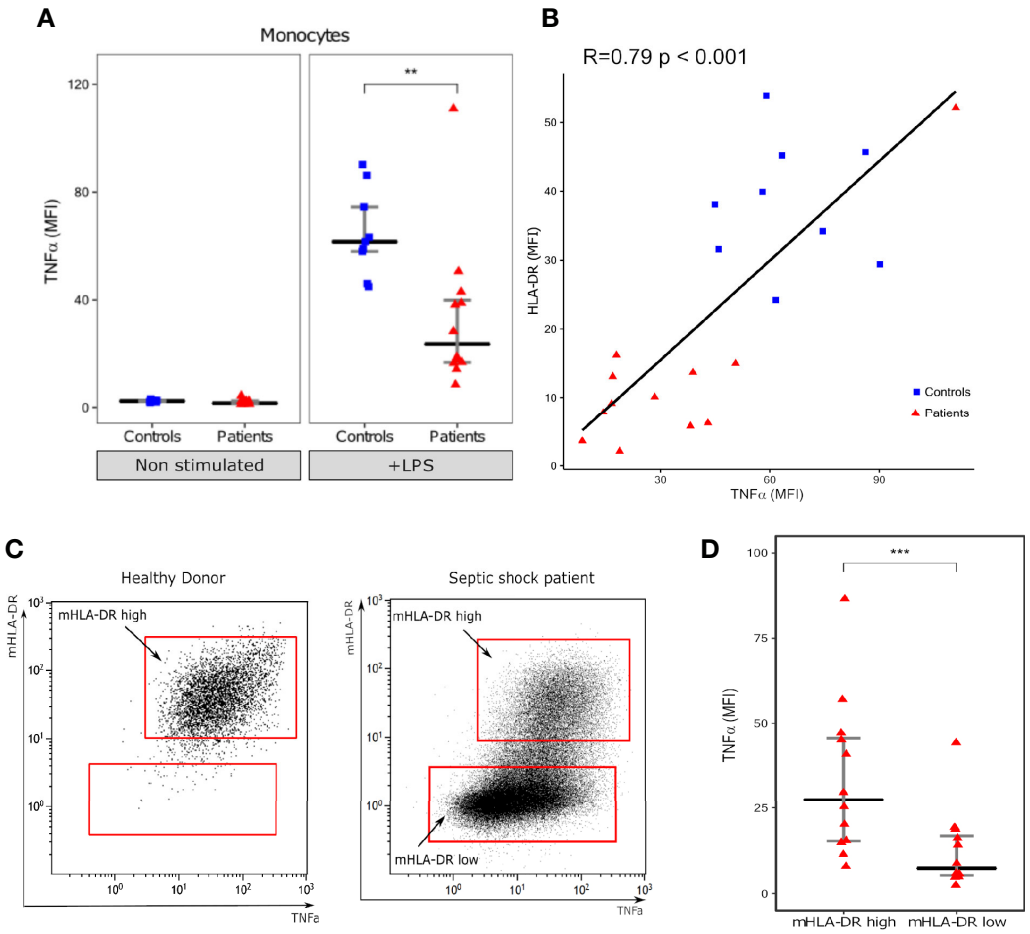

FIGURE 1 | Intracellular TNF-α expression in monocytes. **(A)** Monocyte intracellular TNFα expression (Mean fluorescence intensity – MFI) with (+LPS) and without (Non stimulated) LPS challenge. **(B)** Scatterplot showing the relationship between monocyte intracellular TNFα expression and HLA-DR MFI (measured in LPS stimulated tube). **(C)** One representative flow cytometry image of TNFα (x axis) and mHLA-DR (y axis) in monocytes (gated on CD14+ cells) following LPS challenge in one healthy donor and one septic shock patient. **(D)** Intracellular TNFα expression in mHLA-DR high and mHLA-DR low monocytes. Results are presented as individual values in septic patients (n = 12, red triangles) and healthy donors (n = 9, blue squares) and as medians ± IQR **(A, D)** and **p < 0.01 and ***p < 0.001 with Mann-Whitney U test **(A)** or Wilcoxon paired test. Correlations were analyzed using Spearman correlation coefficient.

described in burned patients with sepsis (16). Together, these results call for further investigation of the theory defended by different groups suggesting that IL-10 plays a role in decreased MHC class II expression in sepsis either through intracellular sequestration of mHLA-DR or *via* inhibition of its transcription (17–19).

Three subsets of IL-10 producing lymphocytes were identified in both patients and HV: a predominant population of CD4+ T cells and two smaller populations of B lymphocytes and CD4- T cells. This was expected as IL-10 production has been reported in the literature for nearly all lymphocyte subsets (including B lymphocytes, CD4+ T cells, and CD8+ T cells) (20). It has also been described that IL-10 produced by CD4+ T cells is critical to limit inflammation in many infections that trigger adaptive immune responses (21). In addition, no new IL-10 producing lymphocyte subset emerged in septic patients. Therefore, any difference in IL-10 production related to septic shock appears to be quantitative and not qualitative.

In other clinical contexts, IL-10 production by lymphocyte subsets such as T or B cells was proposed as a marker of regulatory cell subpopulations (22, 23). In sepsis, the issue of regulatory cells has recently grown in importance and a wide variety of regulatory cell subsets has been identified. Interestingly, different groups have reported an increase in the proportion of regulatory B cells (Breg) in septic shock patients (24, 25). In spite of the absence of consensus on the phenotype of Breg in the literature, there is consensus to attribute their immunosuppressive properties to their secretion of IL-10 (26). Contrary to data from the literature, our current results did not find a significant difference in the proportion of IL-10 positive B cells between septic shock patients and HV. This could be explained by the use of a whole blood approach or different

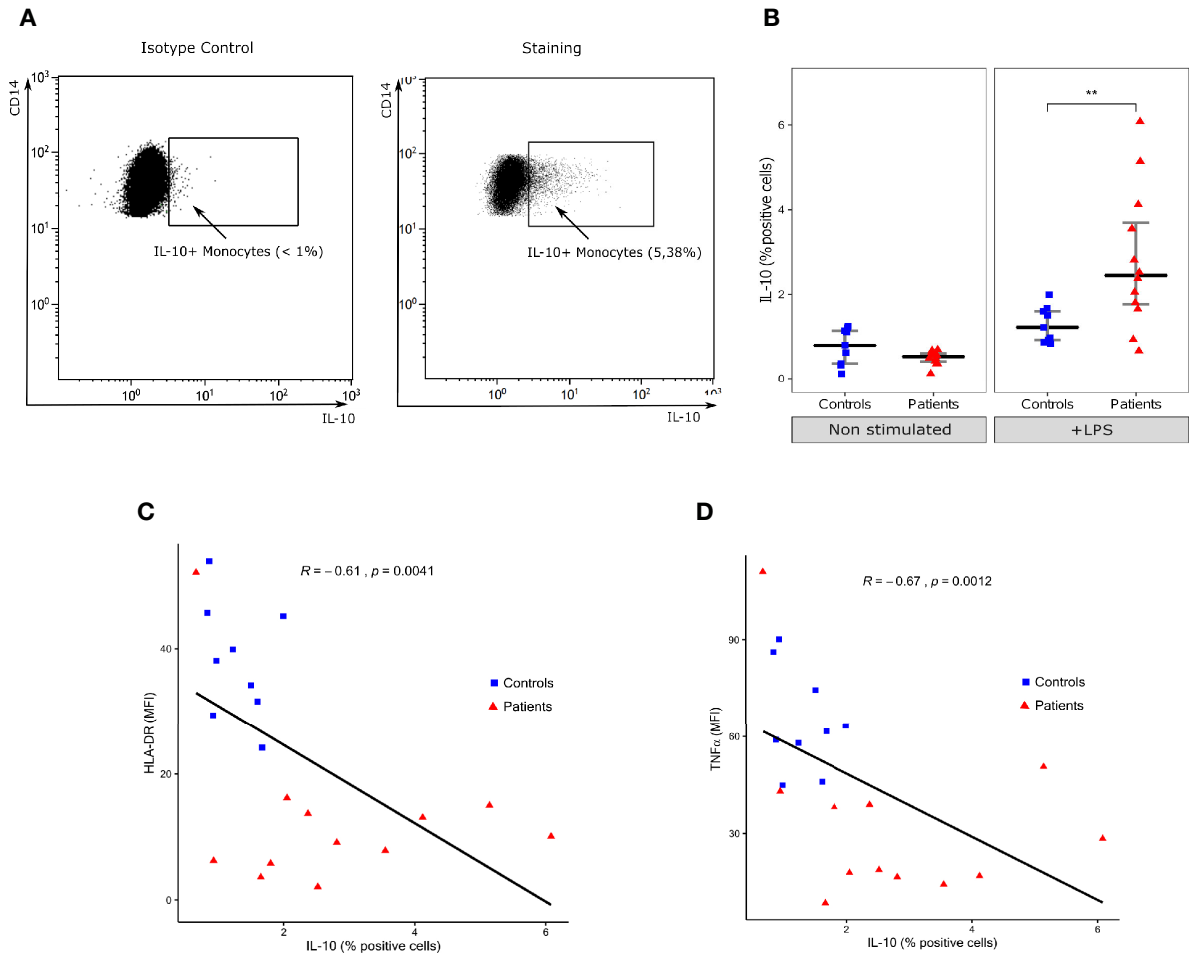

FIGURE 2 | Intracellular IL-10 expression in monocytes. **(A)** One representative flow cytometry dot-plot and its respective isotype control of IL-10 (x-axis) and CD14 (y-axis) in monocytes (gated on CD14+ cells) following LPS challenge in a septic shock patient. Positivity threshold was defined based on isotype value below 1%. **(B)** Proportion of IL-10 positive monocytes among total monocytes with (+LPS) and without (Non stimulated) LPS challenge. Results are presented as individual values in healthy donors (n=9; blue squares) and septic patients (n = 12; red triangles) and medians ± IQR. **p < 0.01 with Mann-Whitney U test. **(C)** Scatterplot showing the relationship between monocyte intracellular IL-10 expression (% of positive monocytes, x-axis) and HLA-DR mean fluorescence intensity (MFI, y-axis). **(D)** Scatterplot showing the relationship between monocyte intracellular IL-10 expression and monocyte intracellular TNFα expression (MFI). Correlations were analyzed using Spearman correlation coefficient.

stimulation conditions compared with previous studies. That said, our results should not contest the importance of Breg in sepsis-induced immunosuppression but encourage further research on IL-10 independent immunoregulatory mechanisms for Breg in sepsis such as IL-35 and adenosine production, checkpoint inhibitors expression, or activation of the Fas/Fas ligand apoptotic pathway (27).

IL-10 synthesis by CD8+ T cells has been described using intracellular flow cytometry protocols in so-called CD8+ T regulatory cells (28). The immunomodulatory role of CD8+ T regulatory cells is well documented in autoimmune diseases, cancer, human transplants and certain infections (Human Immunodeficiency Virus or Epstein-Barr Virus) (29). However, to the best of our knowledge, no study has been conducted on IL-10 production by CD8+ T cells in septic shock patients. Our results did not show a significant difference in the synthesis of IL-10 by CD8+ cells between patients and HV, although we cannot exclude that the possibility that CD4- T cells monitored in this study were double-negative. That said, CD8+ T cell exhaustion remains a hallmark of sepsis, as evidenced by the recently reported decrease in the synthesis of IL-2 and TNFα by CD8+ T cells (30).

Finally, we revealed an increase in IL-10 synthesis by CD4+ T cells in septic shock patients. This finding is consistent with a considerable amount of published literature on regulatory T CD4+ cells (Treg) in sepsis and septic shock (31). Immunosuppressive properties of Treg are mediated by cell-cell contact mechanisms and IL-10 synthesis (32). In sepsis, the percentage of Treg is increased without change in their absolute value due to a selective depletion of other lymphocyte subsets (33, 34). This could imply that the increase in IL-10 production observed in our study is due to CD4+ T regs.

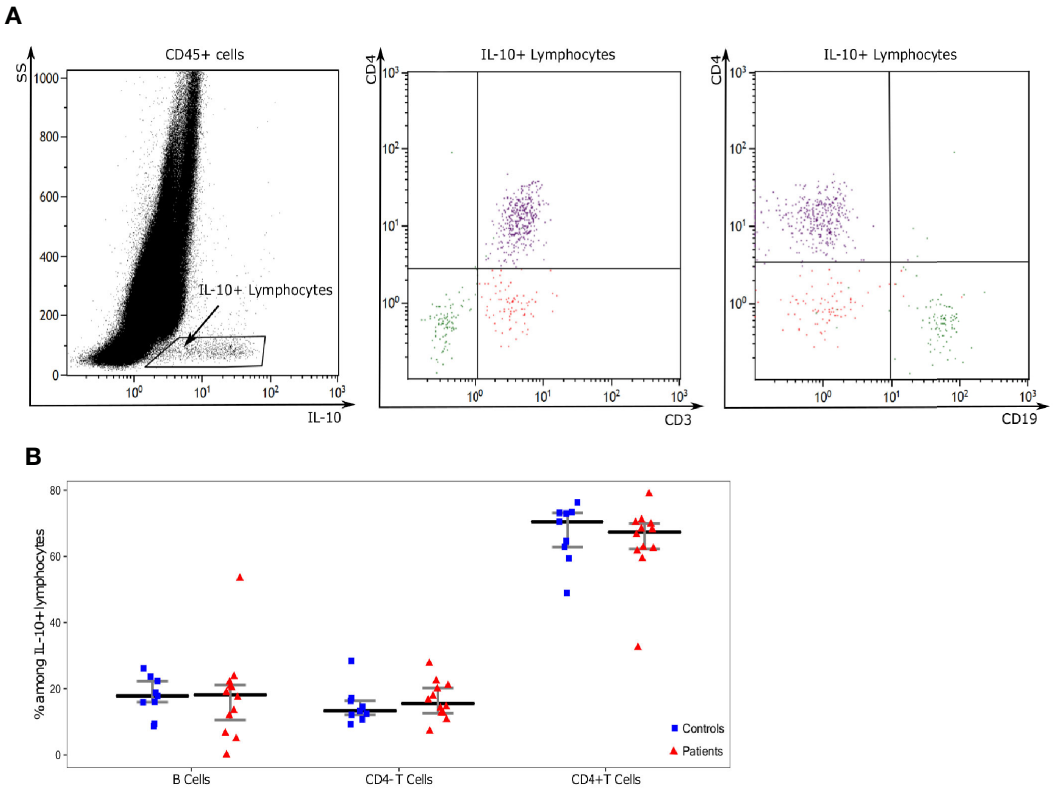

FIGURE 3 | Analysis of IL-10 producing lymphocytes. **(A)** One representative example of flow cytometry staining in a septic patient. First, on a IL-10 (x-axis) and SS (y-axis) dot-plot gated on in CD45+ leukocytes, we selected IL-10 producing lymphocytes (IL-10^{+}SSC^{low} cells). CD3, CD19, and CD4 expressions were then characterized on these cells based on CD4 (y-axis) and CD3 or CD19 (x-axis) dot-plots. Three populations of IL-10 producing cells were identified: CD19+CD3-CD4- cells (Green: B lymphocytes), CD19-CD3+CD4+ cells (purple: CD4+ T cells), CD19-CD3+CD4+ cells (red: CD4- T cells). **(B)** Proportions of lymphocyte subsets among IL-10 positive lymphocytes Results are presented as individual values in healthy donors (n=9; blue squares) and septic patients (n = 12; red triangles) and medians ± IQR.

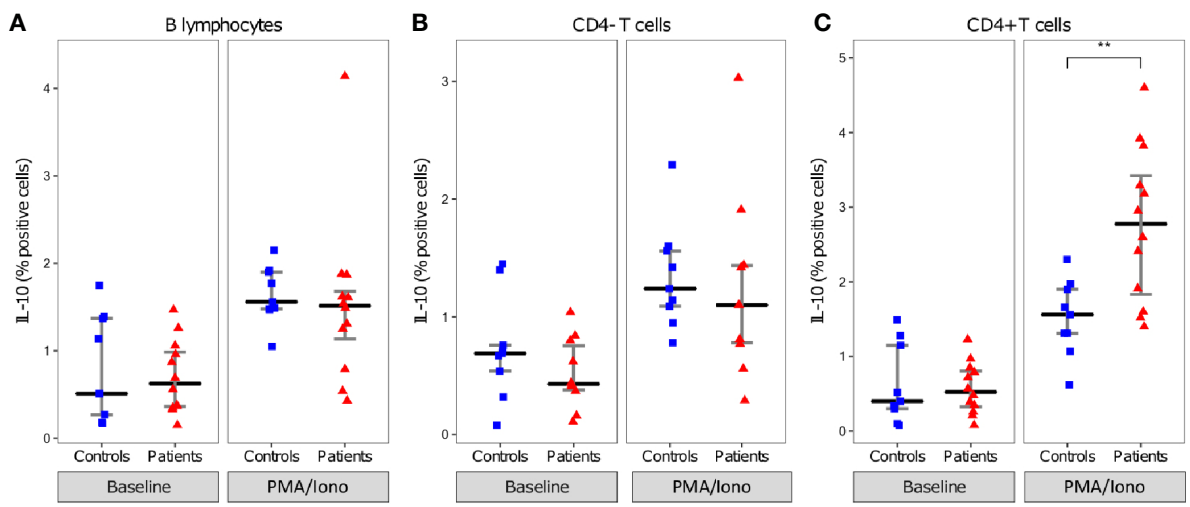

FIGURE 4 | Intracellular IL-10 expression in lymphocytes. Proportion of IL-10 positive B lymphocytes **(A)**, CD4- T cells **(B)**, and CD4+ T cells **(C)**. lymphocytes presented as individual values in healthy donors (n=9; blue squares) and septic patients (n = 12; red triangles) and medians ± IQR, with (PMA/Iono) and without (Non stimulated) PMA/Iononmycin challenge. **p < 0.01 with Mann-Whitney U test.

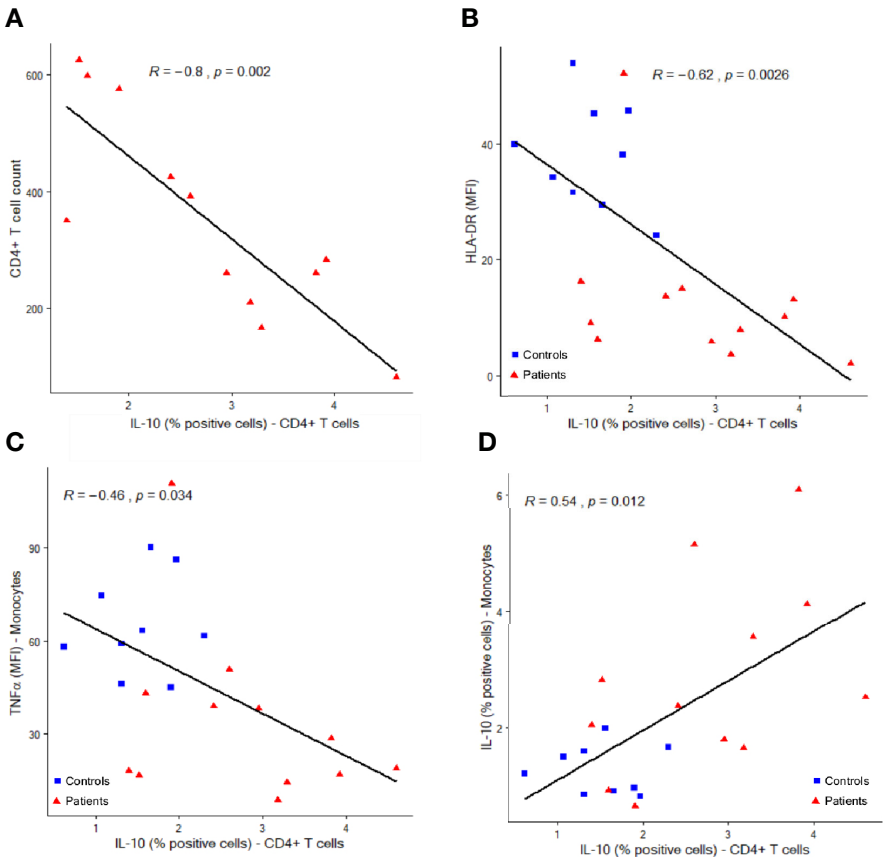

FIGURE 5 | Correlations between IL-10 expressing CD4+ T lymphocytes and other immune parameters. Correlations between IL-10 producing CD4+ T cells (percentages among total CD4+ T cells, x-axis) and CD4+ cell counts (**A**, cells per µl, y-axis), monocyte HLA-DR expression (**B**, mean fluorescence intensity = MFI, y-axis), monocyte intracellular TNFα expression (**C**, MFI, y-axis) and monocyte intracellular IL-10 expression (**D**, percentages of positive cells among total monocytes, y-axis). Correlations were analyzed using Spearman correlation coefficient. Results from n = 9 controls (blue squares) and 12 patients (red triangles) are shown.

We suggest adding an anti-Foxp3 antibody to our panel to explore this hypothesis. In addition, the negative correlation between the absolute count of CD4+ T cells and IL-10 expression in the same cells confirms previous findings by Roth et al. showing that increased IL-10 concentrations in sepsis may be due a susceptibility of Th1 T cells to apoptosis, resulting in a prevalence of Th2 T cells, known for their IL-10 production (35, 36).

To note, some authors rather described a dual role for IL-10 in human endotoxemia (37) and in COVID-19 (38) with both pro and anti-inflammatory properties. This stresses the importance to develop robust and easy to use tools to investigate IL-10 production by leukocytes.

The main limitation of our study was the small sample size and the absence of a kinetic evaluation. As it was a proof-of-concept study, only 12 patients were included, and we could not investigate association with clinical outcomes as our study was not powered for such purposes. In addition, the evaluation of potential confounding factors such as plasma LPS levels could not be performed. Results are thus preliminary and should be assessed and validated in a larger cohort of patients. In addition, in the absence of any extended phenotyping with, for example, no specific marker of regulatory lymphocytes such as Foxp3 or of any functional test, we could not formally qualify IL-10 producing lymphocytes as regulatory cells. This specific aspect should be further confirmed in a dedicated physiopathological study.

CONCLUSION

We demonstrated the feasibility of a novel technique for intracellular cytokine measurement in whole blood to monitor IL-10 production by circulating leukocytes in sepsis. We described sepsis-induced increase in IL-10 production by monocytes and CD4+ T cells but not B cells and CD8+ T lymphocytes. In addition, increased monocyte IL-10 production negatively correlated with mHLA-DR expression and TNFα production and with increased IL-10 production in CD4+ T cells and their absolute count. We therefore described the development of a global immunosuppressive profile affecting monocytes and CD4+ T cells in septic shock. Further research is now required to assess clinical significance of this profile in larger

cohorts of patients and to identify the pathophysiological mechanisms leading to its development in septic shock.

DATA AVAILABILITY STATEMENT

The original contributions presented in the study are included in the article/supplementary materials. Further inquiries can be directed to the corresponding author.

ETHICS STATEMENT

The studies involving human participants were reviewed and approved by CPP Ouest II—Anger. Written informed consent for participation was not required for this study in accordance with the national legislation and the institutional requirements.

AUTHOR CONTRIBUTIONS

AF, KK, RC, MG, GM, and FV designed and performed the experiments. AF performed the statistical analyses. PA, CM, MC, TR, and LA included patients. All authors contributed to the article and approved the submitted version.

FUNDING

This study was funded by the Hospices Civils de Lyon through the IMMUNOSEPSIS cohort. Immunotech (Beckman Coulter, France) provided reagents necessary for this study. However, this diagnostic company had no role in study design or results analysis and publication.

ACKNOWLEDGMENTS

The authors would like to thank Olivier Jaen and Fabrice Malergue (Immunotech, Beckman Coulter) for their help in the technical set-up of the flow cytometry protocol; the technical staff from the Immunology lab of Edouard Herriot Hospital (Anne Portier, Alizée Bègue, Catherine Venard, Laurence Poulat) for their great help in flow cytometry and the research nurses from the Anesthesia and Critical Care Medicine Department (Valérie Cerro, Laurie Bignet) and Medical intensive Care Department (Marion Provent, Sylvie De La Salle) from Edouard Herriot Hospital.

REFERENCES

1. Reinhart K, Daniels R, Kissoon N, Machado FR, Schachter RD, Finfer S. Recognizing Sepsis as a Global Health Priority - A WHO Resolution. *N Engl J Med* (2017) 377:414–7. doi: 10.1056/NEJMp1707170
2. Rudd KE, Johnson SC, Agesa KM, Shackelford KA, Tsoi D, Kievlan DR, et al. Global, regional, and national sepsis incidence and mortality, 1990–2017: analysis for the Global Burden of Disease Study. *Lancet* (2020) 395:200–11. doi: 10.1016/S0140-6736(19)32989-7
3. Hotchkiss RS, Monneret G, Payen D. Sepsis-induced immunosuppression: from cellular dysfunctions to immunotherapy. *Nat Rev Immunol* (2013) 13:862–74. doi: 10.1038/nri3552
4. Venet F, Lukaszewicz A-C, Payen D, Hotchkiss R, Monneret G. Monitoring the immune response in sepsis: a rational approach to administration of immunoadjuvant therapies. *Curr Opin Immunol* (2013) 25:477–83. doi: 10.1016/j.coi.2013.05.006
5. Hotchkiss RS, Monneret G, Payen D. Immunosuppression in sepsis: a novel understanding of the disorder and a new therapeutic approach. *Lancet Infect Dis* (2013) 13:260–8. doi: 10.1016/S1473-3099(13)70001-X
6. Friedman G, Jankowski S, Marchant A, Goldman M, Kahn RJ, Vincent JL. Blood interleukin 10 levels parallel the severity of septic shock. *J Crit Care* (1997) 12:183–7. doi: 10.1016/s0883-9441(97)90030-7
7. van Vught LA, Wiewel MA, Hoogendijk AJ, Frencken JF, Scicluna BP, Klein Klouwenberg PMC, et al. The Host Response in Patients with Sepsis Developing Intensive Care Unit-acquired Secondary Infections. *Am J Respir Crit Care Med* (2017) 196:458–70. doi: 10.1164/rccm.201606-1225OC
8. Abe R, Hirasawa H, Oda S, Sadahiro T, Nakamura M, Watanabe E, et al. Up-regulation of interleukin-10 mRNA expression in peripheral leukocytes predicts poor outcome and diminished human leukocyte antigen-DR expression on monocytes in septic patients. *J Surg Res* (2008) 147:1–8. doi: 10.1016/j.jss.2007.07.009
9. Li X, Xu Z, Pang X, Huang Y, Yang B, Yang Y, et al. Interleukin-10/lymphocyte ratio predicts mortality in severe septic patients. *PLoS One* (2017) 12:e0179050. doi: 10.1371/journal.pone.0179050
10. Singer M, Deutschman CS, Seymour CW, Shankar-Hari M, Annane D, Bauer M, et al. The Third International Consensus Definitions for Sepsis and Septic Shock (Sepsis-3). *JAMA* (2016) 315:801–10. doi: 10.1001/jama.2016.0287
11. Demaret J, Walencik A, Jacob M-C, Timsit J-F, Venet F, Lepape A, et al. Inter-laboratory assessment of flow cytometric monocyte HLA-DR expression in clinical samples. *Cytometry B Clin Cytom* (2013) 84:59–62. doi: 10.1002/cyto.b.21043
12. Monneret G, Demaret J, Gossez M, Reverdiau E, Malergue F, Rimmelé T, et al. Novel Approach in Monocyte Intracellular TNF Measurement: Application to Sepsis-Induced Immune Alterations. *Shock* (2017) 47:318–22. doi: 10.1097/SHK.0000000000000724
13. Sfeir T, Saha DC, Astiz M, Rackow EC. Role of interleukin-10 in monocyte hyporesponsiveness associated with septic shock. *Crit Care Med* (2001) 29:129–33. doi: 10.1097/00003246-200101000-00026
14. Wolk K, Döcke WD, von Baehr V, Volk HD, Sabat R. Impaired antigen presentation by human monocytes during endotoxin tolerance. *Blood* (2000) 96:218–23. doi: 10.1182/blood.V96.1.218.13k04_218_223
15. Wolk K, Döcke W, von Baehr V, Volk H, Sabat R. Comparison of monocyte functions after LPS- or IL-10-induced reorientation: importance in clinical immunoparalysis. *Pathobiology* (1999) 67:253–6. doi: 10.1159/000028104
16. Yang H-M, Yu Y, Chai J-K, Hu S, Sheng Z-Y, Yao Y-M. Low HLA-DR expression on CD14+ monocytes of burn victims with sepsis, and the effect of carbachol in vitro. *Burns* (2008) 34:1158–62. doi: 10.1016/j.burns.2008.01.026
17. Fumeaux T, Pugin J. Role of interleukin-10 in the intracellular sequestration of human leukocyte antigen-DR in monocytes during septic shock. *Am J Respir Crit Care Med* (2002) 166:1475–82. doi: 10.1164/rccm.200203-217OC
18. de Waal Malefyt R, Abrams J, Bennett B, Figdor CG, de Vries JE. Interleukin 10(IL-10) inhibits cytokine synthesis by human monocytes: an autoregulatory role of IL-10 produced by monocytes. *J Exp Med* (1991) 174:1209–20. doi: 10.1084/jem.174.5.1209
19. Chan LLY, Cheung BKW, Li JCB, Lau ASY. A role for STAT3 and cathepsin S in IL-10 down-regulation of IFN-gamma-induced MHC class II molecule on primary human blood macrophages. *J Leukoc Biol* (2010) 88:303–11. doi: 10.1189/jlb.1009659
20. Ouyang W, Rutz S, Crellin NK, Valdez PA, Hymowitz SG. Regulation and functions of the IL-10 family of cytokines in inflammation and disease. *Annu Rev Immunol* (2011) 29:71–109. doi: 10.1146/annurev-immunol-031210-101312

21. Neumann C, Scheffold A, Rutz S. Functions and regulation of T cell-derived interleukin-10. *Semin Immunol* (2019) 44:101344. doi: 10.1016/j.smim.2019.101344
22. Cerqueira C, Manfroi B, Fillatreau S. IL-10-producing regulatory B cells and plasmocytes: Molecular mechanisms and disease relevance. *Semin Immunol* (2019) 44:101323. doi: 10.1016/j.smim.2019.101323
23. Allan SE, Broady R, Gregori S, Himmel ME, Locke N, Roncarolo MG, et al. CD4+ T-regulatory cells: toward therapy for human diseases. *Immunol Rev* (2008) 223:391–421. doi: 10.1111/j.1600-065X.2008.00634.x
24. Gustave C-A, Gossez M, Demaret J, Rimmelé T, Lepape A, Malcus C, et al. Septic Shock Shapes B Cell Response toward an Exhausted-like/Immunoregulatory Profile in Patients. *J Immunol* (2018) 200:2418–25. doi: 10.4049/jimmunol.1700929
25. Pan X, Ji Z, Xue J. Percentage of Peripheral CD19+CD24hiCD38hi Regulatory B Cells in Neonatal Sepsis Patients and Its Functional Implication. *Med Sci Monit* (2016) 22:2374–8. doi: 10.12659/MSM.895421
26. Mauri C, Bosma A. Immune regulatory function of B cells. *Annu Rev Immunol* (2012) 30:221–41. doi: 10.1146/annurev-immunol-020711-074934
27. Valizadeh A, Sanaei R, Rezaei N, Azizi G, Fekrvand S, Aghamohammadi A, et al. Potential role of regulatory B cells in immunological diseases. *Immunol Lett* (2019) 215:48–59. doi: 10.1016/j.imlet.2019.08.004
28. Popescu I, Macedo C, Abu-Elmagd K, Shapiro R, Hua Y, Thomson AW, et al. EBV-specific CD8+ T cell reactivation in transplant patients results in expansion of CD8+ type-1 regulatory T cells. *Am J Transplant* (2007) 7:1215–23. doi: 10.1111/j.1600-6143.2007.01740.x
29. Vieyra-Lobato MR, Vela-Ojeda J, Montiel-Cervantes L, López-Santiago R, Moreno-Lafont MC. Description of CD8+ Regulatory T Lymphocytes and Their Specific Intervention in Graft-versus-Host and Infectious Diseases, Autoimmunity, and Cancer. *J Immunol Res* (2018) 2018:3758713. doi: 10.1155/2018/3758713
30. Letessier W, Demaret J, Gossez M, Allam C, Venet F, Rimmelé T, et al. Decreased intra-lymphocyte cytokines measurement in septic shock patients: A proof of concept study in whole blood. *Cytokine* (2018) 104:78–84. doi: 10.1016/j.cyto.2017.09.029
31. Jiang L-N, Yao Y-M, Sheng Z-Y. The Role of Regulatory T Cells in the Pathogenesis of Sepsis and Its Clinical Implication. *J Interferon Cytokine Res* (2012) 32:341–9. doi: 10.1089/jir.2011.0080
32. Sojka DK, Huang Y-H, Fowell DJ. Mechanisms of regulatory T-cell suppression – a diverse arsenal for a moving target. *Immunology* (2008) 124:13–22. doi: 10.1111/j.1365-2567.2008.02813.x
33. Monneret G, Debard A-L, Venet F, Bohe J, Hequet O, Bienvenu J, et al. Marked elevation of human circulating CD4+CD25+ regulatory T cells in sepsis-induced immunoparalysis. *Crit Care Med* (2003) 31:2068–71. doi: 10.1097/01.CCM.0000069345.78884.0F
34. Venet F, Pachot A, Debard A-L, Bohé J, Bienvenu J, Lepape A, et al. Increased percentage of CD4+CD25+ regulatory T cells during septic shock is due to the decrease of CD4+CD25- lymphocytes. *Crit Care Med* (2004) 32:2329–31. doi: 10.1097/01.ccm.0000145999.42971.4b
35. Roth G, Moser B, Krenn C, Brunner M, Haisjackl M, Almer G, et al. Susceptibility to programmed cell death in T-lymphocytes from septic patients: a mechanism for lymphopenia and Th2 predominance. *Biochem Biophys Res Commun* (2003) 308:840–6. doi: 10.1016/s0006-291x(03)01482-7
36. Moore KW, de Waal Malefyt R, Coffman RL, O'Garra A. Interleukin-10 and the interleukin-10 receptor. *Annu Rev Immunol* (2001) 19:683–765. doi: 10.1146/annurev.immunol.19.1.683
37. Lauw FN, Pajkrt D, Hack CE, Kurimoto M, van Deventer SJ, van der Poll T. Proinflammatory effects of IL-10 during human endotoxemia. *J Immunol* (2000) 165:2783–9. doi: 10.4049/jimmunol.165.5.2783
38. Lu L, Zhang H, Dauphars DJ, He Y-W. A Potential Role of Interleukin 10 in COVID-19 Pathogenesis. *Trends Immunol* (2020) 42(1):3–5. doi: 10.1016/j.it.2020.10.012

Conflict of Interest: The authors declare that the research was conducted in the absence of any commercial or financial relationships that could be construed as a potential conflict of interest.

frontiers in Immunology

ORIGINAL RESEARCH
published: 15 February 2021
doi: 10.3389/fimmu.2021.622599

DNA Methylation Analysis to Unravel Altered Genetic Pathways Underlying Early Onset and Late Onset Neonatal Sepsis. A Pilot Study

Sheila Lorente-Pozo[1,2†], Paula Navarrete[3†], María José Garzón[3], Inmaculada Lara-Cantón[1,2], Jesús Beltrán-García[4,5], Rebeca Osca-Verdegal[4,5], Salvador Mena-Mollá[3,5], Eva García-López[3], Máximo Vento[1,2], Federico V. Pallardó[3,4,5] and José Luis García-Giménez[3,4,5]*

[1] Neonatal Research Group, Health Research Institute La Fe, Valencia, Spain, [2] Division of Neonatology, University and Polytechnic Hospital La Fe, Valencia, Spain, [3] EpiDisease S.L. (Spin-off From the CIBER-ISCIII), Parc Científic de la Universitat de València, Paterna, Spain, [4] Centro de Investigación Biomédica en Red de Enfermedades Raras (CIBERER), Valencia, Spain, [5] Department Fisiología, Facultad de Medicina y Odontología, Universidad de Valencia-INCLIVA, Valencia, Spain

OPEN ACCESS

Edited by:
Jiang Huai Wang,
University College Cork, Ireland

Reviewed by:
Tim Rahmel,
University Hospital Bochum GmbH, Germany
Vishnu Bhat,
Aarupadai Veedu Medical College and Hospital, India

***Correspondence:**
José Luis García-Giménez
j.luis.garcia@uv.es

[†] These authors have contributed equally to this work

Specialty section:
This article was submitted to Inflammation, a section of the journal Frontiers in Immunology

Received: 28 October 2020
Accepted: 25 January 2021
Published: 15 February 2021

Citation:
Lorente-Pozo S, Navarrete P, Garzón MJ, Lara-Cantón I, Beltrán-García J, Osca-Verdegal R, Mena-Mollá S, García-López E, Vento M, Pallardó FV and García-Giménez JL (2021) DNA Methylation Analysis to Unravel Altered Genetic Pathways Underlying Early Onset and Late Onset Neonatal Sepsis. A Pilot Study. Front. Immunol. 12:622599. doi: 10.3389/fimmu.2021.622599

Background: Neonatal sepsis is a systemic condition widely affecting preterm infants and characterized by pro-inflammatory and anti-inflammatory responses. However, its pathophysiology is not yet fully understood. Epigenetics regulates the immune system, and its alteration leads to the impaired immune response underlying sepsis. DNA methylation may contribute to sepsis-induced immunosuppression which, if persistent, will cause long-term adverse effects in neonates.

Objective: To analyze the methylome of preterm infants in order to determine whether there are DNA methylation marks that may shed light on the pathophysiology of neonatal sepsis.

Design: Prospective observational cohort study performed in the neonatal intensive care unit (NICU) of a tertiary care center.

Patients: Eligible infants were premature ≤32 weeks admitted to the NICU with clinical suspicion of sepsis. The methylome analysis was performed in DNA from blood using Infinium Human Methylation EPIC microarrays to uncover methylation marks.

Results: Methylation differential analysis revealed an alteration of methylation levels in genomic regions involved in inflammatory pathways which participate in both the innate and the adaptive immune response. Moreover, differences between early and late onset sepsis as compared to normal controls were assessed.

Conclusions: DNA methylation marks can serve as a biomarker for neonatal sepsis and even contribute to differentiating between early and late onset sepsis.

Keywords: neonatology and pediatric intensive care, DNA methylation, sepsis, inflammation, immunosuppression

INTRODUCTION

Neonatal sepsis is a leading cause of mortality and morbidity in the neonatal period, especially for preterm infants (1). Sepsis is defined as a dysregulated host response caused by infection which can trigger a life-threatening organ failure (2). However, neonatal sepsis lacks a consensus definition (3) and therefore a full understanding of the underlying mechanisms which are functionally distinct in children and adults is needed (3). The neonatal immune response depends mainly on the innate immune system, which is underdeveloped (4, 5); along with a predominant hypo-inflammatory response, this can lead to immunosuppression (6).

Diagnosis and prognosis of neonatal sepsis is a challenge because clinical signs and symptoms are often non-specific. In addition, the result of the blood culture for confirmation of the diagnosis is frequently delayed or provides no results (7). Moreover, given the effects of sepsis in preterm infants on long-term growth and development, efforts to reduce the rates of infection in the neonatal intensive care unit (NICU) are among the most important interventions in neonatal care (8). According to the onset of age, neonatal sepsis is divided into early-onset sepsis (EOS) and late-onset sepsis (LOS). EOS is defined as the onset of features of sepsis that appear within 72 h of life caused by microorganisms acquired from the mother's genital tract during delivery (9–11). In contrast, LOS is defined as onset of features of sepsis appear after 72 h of life due to nosocomial infections acquired during hospitalization (11, 12).

In this context, there is a growing interest in understanding the role of epigenetics in the maturation of the immune system during early life (13) and particularly in sepsis (14, 15). Epigenetics encompasses all the mechanisms that control the gene expression pattern without altering the DNA sequence itself (16–18). Changes in the epigenome can impair immune response to infections (14, 15), suggesting that the study of epigenetic traits through epigenome-wide association studies (EWAS) can improve our understanding of sepsis onset and progression, and even short- and long-term consequences of the disease (19).

In particular, DNA methylation (DNAm) is an important regulator of the immune system (20), maintaining fine-tuned immunological mechanisms needed for an adequate host defense. One of the major consequences of neonatal sepsis is long-term persistence of immunosuppression related to epigenetic dysregulation (6), leading to subsequent infections and increased risk of mortality (15, 21). Importantly, DNAm may drive sepsis-induced immunosuppression through the epigenetic reprogramming of hematopoietic progenitor cells (19). In line with this, although DNAm changes in adult sepsis have been described in some studies (22, 23), information on neonatal sepsis is lacking (24).

We aimed to detect changes in DNAm signatures in preterm neonates that might provide an insight into molecular events driving neonatal sepsis. Consequently, this could contribute to the identification of new biomarkers for the diagnosis and prognosis of neonatal sepsis.

MATERIALS AND METHODS

Experimental Design

The study was performed in the NICU of the Hospital Universitario y Politécnico La Fe (Valencia, Spain). Samples from neonates were obtained from the study approved by the Ethics Committee with registration number 2017/0470. Parents of all the patients signed the informed consent.

This is a prospective cohort study that included preterm neonates born at ≤32 weeks of gestation age. Inclusion and exclusion criteria for the study are shown in **Supplementary Table 1**.

Samples from 23 preterm infants were collected coincident with clinical suspicion of EOS or LOS. Preterm neonates with similar gestational and postnatal ages and perinatal characteristics but free of infection and without suspicion of sepsis acted as controls. EOS and LOS were diagnosed by attending staff neonatologists in the NICU. Patients who met EOS and LOS criteria were included in the study (21, 22). Six patients had confirmed EOS, nine patients confirmed LOS, and two patients suffered both types. Six non-septic preterm neonates were used as controls (**Table 1**). Although a positive blood culture is the golden standard for the diagnosis of sepsis including EOS and LOS, often blood culture renders negative due to the low blood volume available and contamination by peripheral colonizing bacteria. Therefore, in clinical neonatology there is a distinction between "culture positive sepsis" and "clinical sepsis" (**Table 2**). Culture positive sepsis is characterized by a positive bacterial growth in two blood samples taken under stringent aseptic conditions and is treated with specific antibiotics provided by the antibiogram. Clinical sepsis is characterized by the presence of evident of clinical signs that can be or not accompanied by changes in acute phase reactant biomarkers such as CRP, IL-6, or PCT, and or positive peripheral smears and is treated with an empirical combination of antibiotics according to the bacterial eco-system of the NICU. These criteria were not mutually exclusive, and some patients were identified as suffering from both EOS and LOS, being the blood sample taken for analysis after the second sepsis episode.

Blood Sampling and DNA Extraction

Blood (0.5 mL) was sampled from a peripheral vein or central catheter using a heparinized syringe. Blood was centrifuged (1,500 × g for 10 min) at 4°C to separate plasma from the cell pellet. Cell fractions were stored at −80°C until processing. Total DNA was isolated from the cell pellet with All-In-One DNA/RNA Miniprep Kit (BS88203, Bio Basic Canada Inc., Canada) following the manufacturer's instructions. Concentration and purity of DNA was determined with the fluorometric method (Quant-iT PicoGreen dsDNA Assay, Life Technologies, Carlsbad, CA, USA).

DNA Methylation Profiling Using Illumina EPIC 850K Array

The measurement of genome-wide methylation on the 23 samples was performed by means of the Infinium Human DNA

TABLE 1 | Perinatal characteristics of preterm infants ≤32 weeks of gestation with suspicion or confirmed sepsis (EOS, LOS, and EOS+LOS) and neonates without sepsis as controls.

Variables	LOS (*N* = 9)	EOS (*N* = 6)	LOS and EOS (*N* = 2)	CRL (*N* = 6)	*p*-value CRL vs. LOS	*p*-value CRL vs. EOS	*p*-value CRL vs. LOS+EOS	*p*-value EOS vs. LOS
Gestational age (weeks) (median; 5–95% CI)	26 (25–29)	27 (25–30)	25 (25)	29.5 (28–30)	*0.02[a]	0.45[a]	*0.04[a]	0.40[a]
Birth weight (g) (mean ± SD)	797.8 ± 228.7	1082.5 ± 338.2	845 ± 49.5	1253 ± 261	*0.02[a]	0.68[a]	0.26[a]	0.21[a]
Apgar score 1 min (median; 5–95% CI)	7 (4–8)	7 (4–9)	5 (4–6)	8.5 (6–10)	0.27[a]	0.59[a]	0.22[a]	0.97[a]
Apgar score 5 min (median; 5–95% CI)	9 (8, 9)	8.5 (6–10)	7.5 (7, 8)	9 (8–10)	0.69[a]	0.70[a]	0.25[a]	>0.99[a]
Male sex (*n*, %)	7 (77.8)	4 (66.7)	2 (100)	3 (31)	0.33[b]	>0.99[b]	0.46[b]	>0.99[b]
Type of delivery: vaginal/cesarean (*n*, %)	2/7 (22/78)	0/6 (0/100)	2/0 (100/0)	1/5 (17/83)	>0.99 [b]	>0.99[b]	0.11[b]	0.49 [b]
Twin pregnancy (*n*, %)	4 (44.44)	3 (31)	2 (100)	3 (31)	>0.99 [b]	>0.99[b]	0.46 [b]	>0.99 [b]
Antenatal steroids full course[α] (*n*, %)	9 (100)	6 (100)	2 (100)	6 (100)	>0.99 [b]	>0.99[b]	>0.99 [b]	>0.99 [b]
Chorioamnionitis[β] (*n*, %)	1 (11.11)	1 (16.67)	1 (31)	0 (0)	>0.99[b]	>0.99[b]	0.25[b]	>0.99[b]
Antibiotic therapy to mother (*n*, %)	3 (33.33)	6 (100)	6 (100)	0 (0)	0.23[b]	* <0.01[b]	* <0.01[b]	*0.03[b]
Weight at sample collection (g) (mean ± SD)	1087 ± 270.2	1007 ± 266.4	1223 ± 661.1	1205 ± 243.4	0.87[a]	0.66[a]	>0.99[a]	0.95[a]

[α] *Full course of antenatal steroids: 12-mg doses of betamethasone given intramuscularly 24 h apart or four 6-mg doses of dexamethasone administered intramuscularly every 12 h.*
[β] *Chorioamnionitis or intra-amniotic infection was defined as an acute inflammation of the membranes and chorion of the placenta with clinical, histologic, or microbiological findings.*
[a] *Tukey's multiple comparisons test.*
[b] *Fisher's exact test.*
**p-value < 0.05 was considered statistically significant.*

Methylation EPIC 850K arrays (Illumina Inc, San Diego, CAL, USA) following the manufacturer's instructions.

Bioinformatic Analysis

The minfi R-package (27) was used to process and normalize the arrays (28, 29). The identification of differentially methylated CpGs (DMCs) was performed using limma (30) using an FDR cutoff of 0.05, which is the expected proportion of errors and controls for a low proportion of false positives (38). With the aim of discovering differentially methylated regions (DMRs), we employed two complementary bioinformatic tools: DMRcate (34) and mCSEA (39) R-packages. We performed the DNAm differential analysis between the groups of the study. Finally, we performed the overlap of both DMR sets.

DMRs were functionally enriched in both gene ontology (GO) terms and KEGG pathways by means of an over-representation analysis (ORA) using the clusterProfiler R-package (40). The selected FDR threshold was 0.05. Furthermore, the top 1,000 DMCs were analyzed for cell-type enrichment using eFORGE (35), which determines the cell type-specific regulatory component of a set of EWAS-identified differentially methylated positions to identify disease-relevant cell types in a specific disease.

Statistical Analysis

Quantitative variables were analyzed for normality using the Kolmogorov-Smirnov test, and an ordinary one-way ANOVA was performed for multiple comparisons using Tukey's test. Furthermore, qualitative variables were analyzed using Fisher's exact test.

RESULTS

Neonatal Characteristics and Microbiological Data

Twenty-three preterm infants (≤32 weeks of gestation age) were included. Out of these, 17 were diagnosed of neonatal sepsis cases and 6 pre-term neonates were selected as non-septic controls. Subjects' characteristics are shown in **Table 1** and the criteria for "culture positive sepsis" and "clinical sepsis," as well as inflammatory biomarkers, are shown in **Table 2**. Hence, 9 subjects developed LOS, 6 subjects developed EOS, 2 subjects

TABLE 2 | Summary of microbiological, clinical, and analytical results in patients with early and late onset sepsis.

Patient identification	Blood culture results	Clinical signs	Dab suspected sepsis	Lactic acid	CRP	IL6	WBC count (per mm^3)	Neutrophils (per mm^3)
Late onset sepsis								
Patient 1 (5)	*Staphylococcus epidermidis*	Present	7	2.4	75.9	–	41,250	38,130
Patient 2 (7)	*S. epidermidis*	Present	19	1.5	31.9	–	16,840	8,450
Patient 3 (19)	*S. epidermidis*	Present	25	3.6	64.6	–	35,510	19,630
Patient 4 (20)	*S. epidermidis*	Present	26	1.1	13.7	–	16,220	3640
Patient 5 (23)	*S. epidermidis*	Present	11	1.3	8.3	–	28,750	18,470
Patient 6 (14)	*Staphylococcus aureus*	Present	6	2.5	58.8	–	8,440	6,650
Patient 7 (25)	*S. aureus*	Present	>3	1.9	1.3	–	2,630	820
Patient 8 (32)	*S. aureus*	Present	>3	3.7	14.9	–	5,080	2,270
Patient 9 (33)	Negative	Present	11	2.0	36	–	23,590	19,120
Early onset sepsis								
Patient 10 (8)	Negative	Present	<1	1.2	32.2	–	27,170	21,150
Patient 11 (30)	Negative	Present	<1	1.6	2.1	1,180	6,580	1,280
Patient 12 (34)	Negative	Present	<1	2.3	11.7	–	7,950	4,650
Patient 13 (17)	Negative	Present	<1	1.6	15.2	306	14,300	6,120
Patient 14 (35)	Negative	Present	2	1.3	4.2	–	9,580	5,440
Patient 15 (36)	*Staphylococcus haemolyticus*	Present	< 1	1.6	10.8	–	9,150	7,400
Early and Late onset Sepsis								
Patient 16 (4)	*Escherichia coli* *S. epidermidis*	Present Present	<1 5	2.7	37.3	–	35,560	25,420
Patient 17 (37)	*S. epidermidis* *S. epidermidis*	Present Present	<1 17	1.3	111	–	10,500	7,750

Dab: days after birth; CRP, C-reactive protein; WBC, white blood cell count; IL-6, interleukin 6. When clinical signs of sepsis were present, the diagnosis of sepsis was confirmed. Sign (–) indicates no measured parameter. Patient number noted using parentheses corresponds to the patients showed in PCA graph in ***Figure 1****.*

developed EOS+LOS, and 6 subjects were considered healthy controls. In **Table 1**, we found statistical differences in the gestational age when comparing LOS [26 (25–29) weeks] and EOS+LOS [25 (25) weeks] to non-septic pre-term neonates [29.5 (28–30) weeks]. Moreover, we also found statistical differences in birth weight between neonates who developed LOS (797.8 ± 228.7 g) and pre-term neonates (1,253 ± 261 g), and in the antibiotic therapy to mother when comparing EOS to the other clinical groups (See **Table 2**).

The blood culture results are presented in **Table 2** and **Supplementary Figure 1**. In one case of LOS and five cases of EOS, it was not possible to identify the microorganism.

Differential Methylation Profiles Between Neonatal Sepsis Subtypes and Control Subjects

Principal component analysis (PCA) of the processed data showed a slight separation between septic and control samples, with some overlap. Regarding subtypes, LOS samples showed greater separation from controls than did EOS (**Figure 1A**).

The differential methylation analysis between septic and control neonates showed 77,380 differentially methylated CpGs (DMCs). The top 1,000 DMCs were plotted in a heatmap showing a similar methylation pattern in both clinical groups, EOS and LOS (**Figure 1B**). The eFORGE analysis of the top 1,000 DMCs revealed enrichment in blood enhancers, particularly primary hematopoietic stem cells (**Figure 1C**).

To identify DMRs, we used the mCSEA approach, testing 1,051 promoters and 119 genes with differential methylation levels in the neonatal sepsis condition vs. controls. In particular, we found 437 hypomethylated promoters, 26 of which exhibited a beta-value difference >10% (including the promoters for *EGOT*, *IL10*, *CPT1B*, *PILRA*, *ELANE*, *TREM1*, *PRTN3*, *MIR145*, *S100A8*, *CSTA*, *MS4A3*, *ATP8B4*, *CPT1B*, *CMYA5*, *LRG1,* and *CD300LB)* and 614 hypermethylated promoters, 6 of which exhibited a beta-value difference >10% for *CD3G*, *CD3D*, *LTA*, *TXK*, *UBASH3A,*

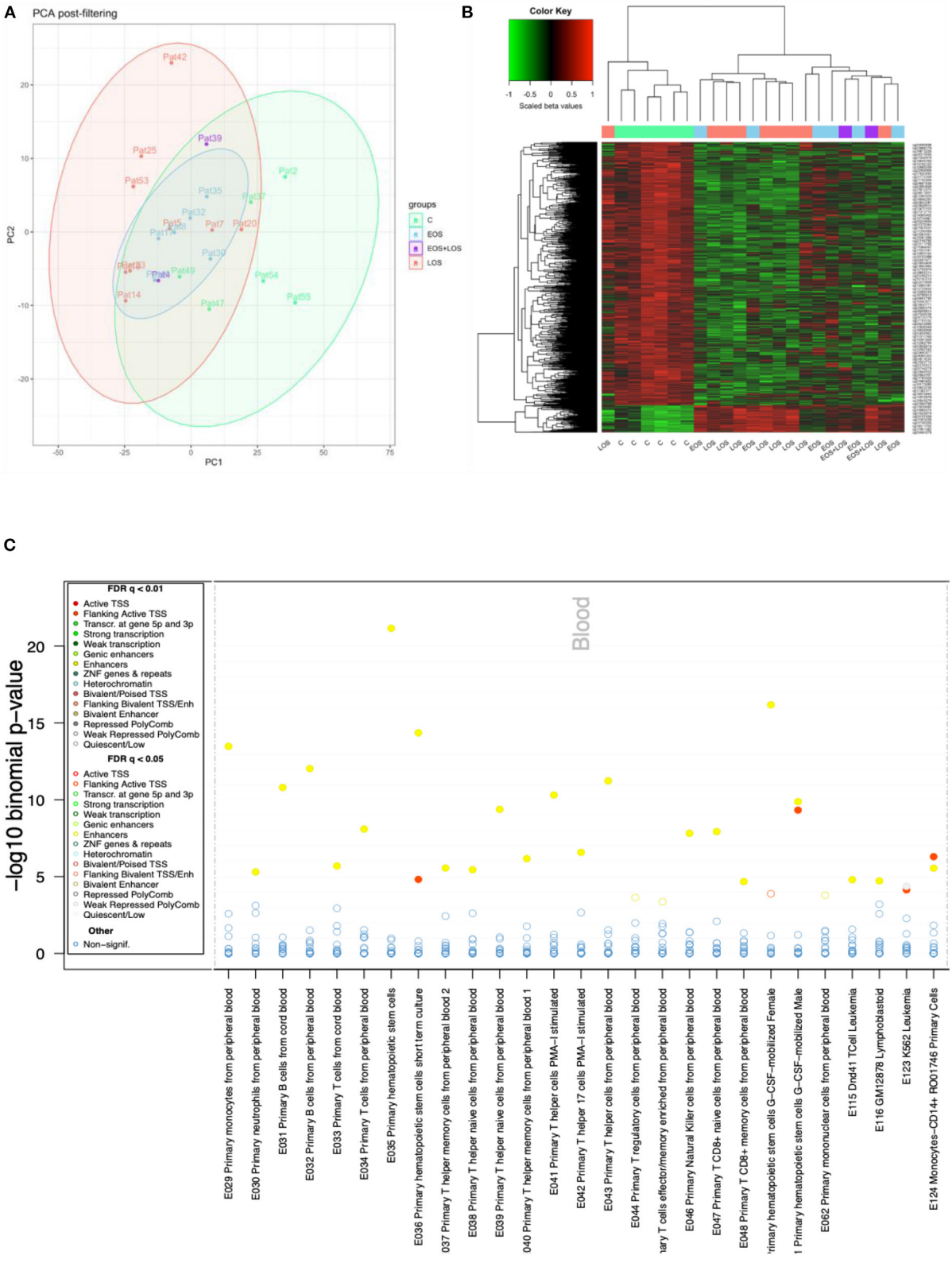

FIGURE 1 | DNAm analysis. **(A)** Principal component analysis (PCA) of methylation data of control (light green), LOS (pink), EOS (light blue), and EOS plus LOS (purple) samples. **(B)** DNAm heatmap showing the significant top 1,000 differentially methylated CpGs between controls and neonates with sepsis, obtained with

(Continued)

FIGURE 1 | limma. The methylation metric used to obtain the heatmap is the beta values scaled by the median, shown at the top left color scale (where red represents higher methylation levels, and green lower methylation levels). This displays the clustering of sepsis samples separated from control samples with the exception of one LOS sample. **(C)** eFORGE analysis. Enrichment analysis of regulatory element classes in different blood cell types for the top 1,000 CpG sites between septic neonates and control neonates. Cell types are shown on the horizontal axis and the significance ($-\log_{10}$ binomial p-values) is shown on the vertical axis. Each dot represents an enrichment q-value for a given cell type, colored according to the enriched regulatory element class, as shown in the legend (where yellow points correspond to enhancers and red points correspond to transcription start sites).

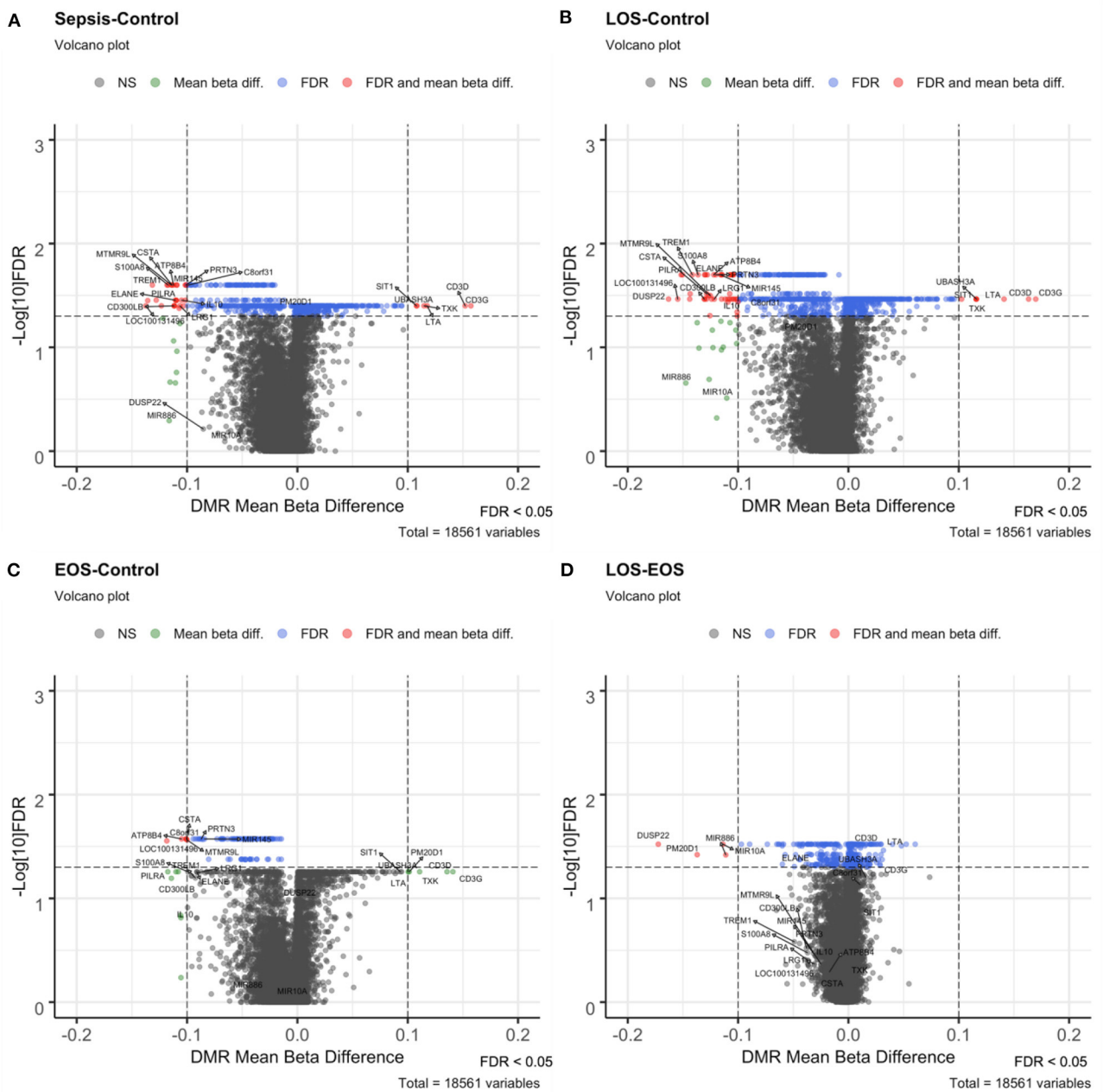

FIGURE 2 | Volcano plots of the different contrasts performed with mCSEA. Volcano plots show the beta-value difference in the x-axis plotted vs. $-\log_{10}$ FDR in the y-axis. Black (not significant) and green (Mean beta diff.) dots were non-significant promoters, while blue (FDR) and red (FDR and mean beta diff.) dots correspond to the significant DMRs, below the selected FDR threshold of significance set at 0.05. Those with a mean beta difference >10% are represented as red and green dots**. (A)** Volcano plot of the sepsis vs. control contrast, **(B)** LOS vs. control contrast, **(C)** EOS vs. control comparison, and **(D)** LOS vs. EOS.

and *SIT1* genes (**Figure 2A**). Conversely, in contrast with the high number of promoters with differential hypomethylation, only 4 genes (*MPO*, *LOC100131496*, *SPI1,* and *PLEK*) showed a beta-value difference above 10%.

In addition, we used the DMRcate method and identified 14,846 genomic regions by fitting DMCs spatially. The vast majority of DMRs were hypomethylated regions, and only 1,577 were hypermethylated. Furthermore, those with a mean beta difference above 10% provided 1,474 DMRs with hypomethylation and 386 DMRs with hypermethylation.

After overlapping the DMR sets obtained with both methods (mCSEA and DMRcate), 302 promoters and 108 genes were found to be hypomethylated and 143 promoters hypermethylated. **Table 3** shows the promoters with the greatest beta differences (>10%) obtained with the two methods for the comparisons between neonatal sepsis and control neonates.

Differential Methylation in EOS and LOS to Identify Distinct Molecular Responses in Both Subtypes of Neonatal Sepsis

As shown in the results above, comparisons between EOS and controls and between LOS and EOS exhibited smaller differences in DNA methylation between conditions. Therefore, we used the mCSEA method which allows discovery of regions with high sensitivity and subtle differences in DNAm but with consistency across a genomic region.

Among the 1,433 promoters obtained with mCSEA, 50 had a difference >10%, and some of them were associated with relevant genes involved in immunological functions (**Figure 2B**). Nevertheless, the comparison between EOS and controls showed differential methylation in only 44 genes and 108 promoters, in which relevant genomic regions that showed significant changes in LOS—such as *S100A8*, *TREM1*, *ELANE*, *CD3D*, and *CD3G*—were not present. Importantly, promoters of *CSTA*, *MIR145*, *PRTN3,* and *ATP8B4* genes were differentially methylated in EOS as well as in LOS when compared to controls (**Figure 2C**).

When we compared LOS with EOS, 803 differentially methylated promoters were obtained, most of them with small differences except for 4 hypomethylated promoters, which displayed large beta differences for gene promoters of *DUSP22*, *PM20D1*, *MIR10A,* and *MIR886* (**Figure 2D**).

Pathways Related With Immune Response Are Altered by DNA Methylation in Neonatal Sepsis

DMR sets obtained using mCSEA and DMRcate methods for sepsis vs. control comparison were enriched to detect

TABLE 3 | General overview of differentially methylated (hypomethylated and hypermethylated) promoters detected by both DMR detection methods (mCSEA and DMRcate) for the comparison between neonatal sepsis and control neonates, including mean beta-value difference, chromosome location, and a brief description.

Methylation status	Gene	Localization	Mean beta difference	Description
Hypo-	S100A8	chr1	−0.11720	Inflammatory mediator participating in the amplification of the immune response. It has also been proposed as a mediator of immunosuppressive states by regulating myeloid-derived suppressor cells (MDSCs)
	CSTA	chr3	−0.11370	Cysteine protease inhibitor (cystatin superfamily) which plays a role in epidermal development and maintenance. It is expressed in tissues participating in the first-line defense against pathogens
	ATP8B4	chr15	−0.11232	Member of type IV P-type ATPases which catalyze the translocation of phospholipids in the cell membrane
	TREM1	chr6	−0.11815	Cell surface receptor that stimulates the release of pro-inflammatory cytokines and chemokines, and cell surface activation molecules in neutrophils and monocytes. TREM1 amplifies inflammation and is a crucial mediator of septic shock
	CD300LB	chr17	−0.11186	Activating receptor of the immunoglobulin superfamily expressed on myeloid cells
	ELANE	chr19	−0.11067	Serine protease involved in the extracellular matrix degradation of microorganisms through the proteolysis of elastin and other components
	CMYA5	chr5	−0.10973	Cardiomyopathy-associated protein 5
	LRG1	chr19	−0.10656	Expressed during neutrophilic granulocyte differentiation, involved in neutrophil degranulation
	IL10	chr1	−0.10504	Anti-inflammatory cytokine involved in immunoregulation and inflammation
	MIR145	chr5	−0.10161	miRNA which plays a role in the growth and division of megakaryocytes
	PRTN3	chr19	−0.10104	Serine protease, paralog of neutrophil elastase (ELANE)
Hyper-	CD3G	chr11	0.15725	Subunit of the TCR-CD3 complex, on the surface of T-cells
	CD3D	chr11	0.15212	Subunit of the TCR-CD3 complex, on the surface of T-cells
	LTA	chr6	0.11763	Cytokine that mediates in inflammatory, immunostimulatory, and antiviral responses
	TXK	chr4	0.11473	Tec family protein tyrosine kinase that regulates T-cell function and differentiation, and participates in Th1 cytokine production
	UBASH3A	chr21	0.10833	Encodes a protein that belongs to the T-cell ubiquitin ligand (TULA) that negatively regulates T-cell signaling
	SIT1	chr9	0.10786	Negatively regulates TCR-mediated signaling in T-cells, and is involved in positive selection of T-cells

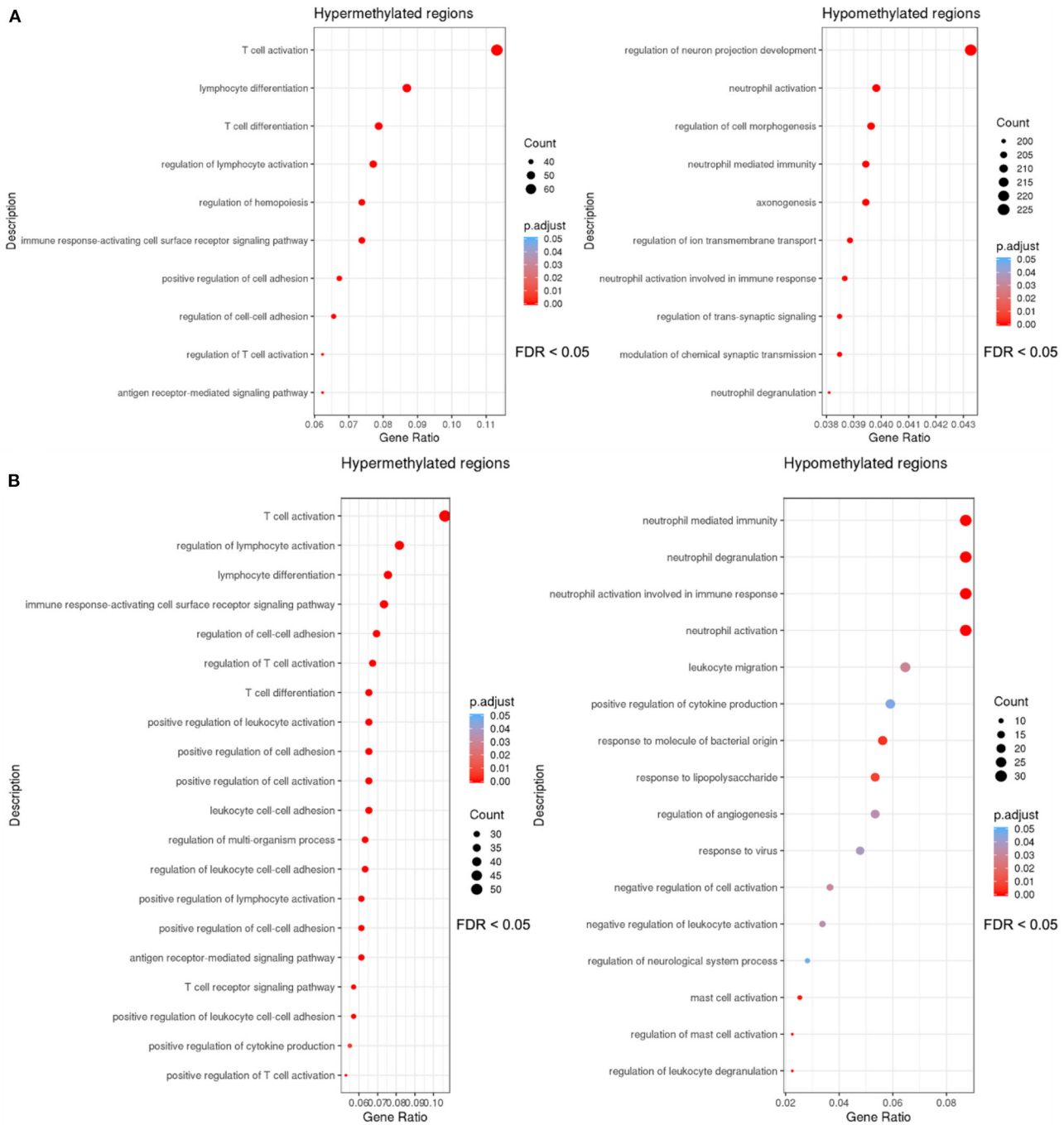

FIGURE 3 | Dotplots of the gene ontology-biological process terms (GO-BP) overrepresented with an FDR threshold of <0.05 in the sets of DMRs. The y axis represents the significant GO terms with the higher proportion of DMRs of the set involved, and the gene ratio in the x-axis represents these proportions (number of DMRs involved in each GO term over the total number of DMRs in the set). The size of each dot or gene cluster depends on the gene count that contributes to the enrichment of that pathway, and the adjusted *p*-value obtained for the terms with the Fisher's exact test in ORA determines the color of the dots. **(A)** Dotplot of the biological processes in which the DMRs (promoters) obtained with mCSEA are enriched. **(B)** Dotplot of the enrichment results of the DMR set (genes and promoters) obtained with DMRcate.

important functions, and as a result similar GO biological processes related with immune response were obtained using both methods (**Figure 3**).

After the overlapping of the DMRs for genes and promoters, obtained with mCSEA and DMRcate approaches, an overrepresentation analysis (ORA) revealed the enrichment

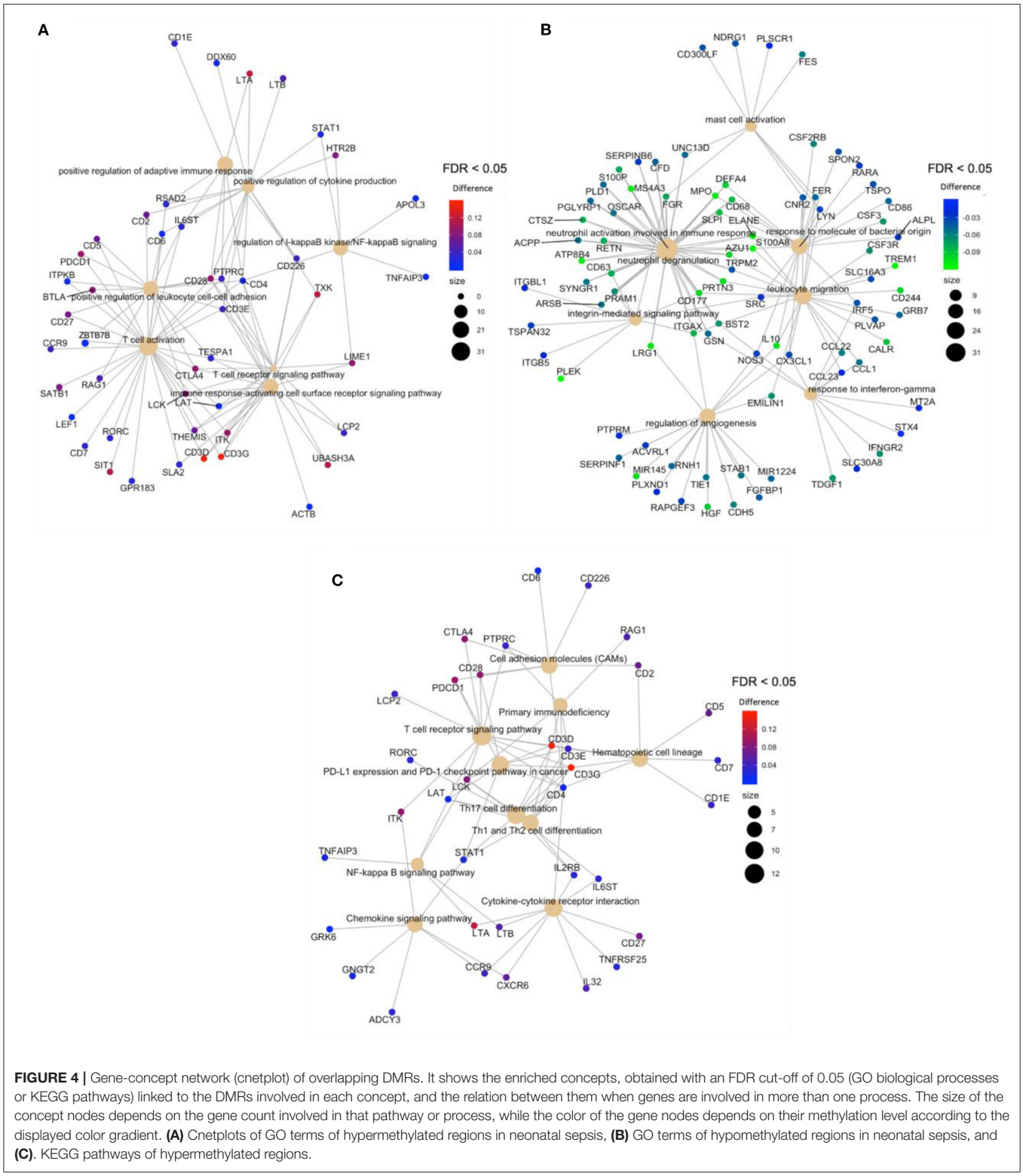

FIGURE 4 | Gene-concept network (cnetplot) of overlapping DMRs. It shows the enriched concepts, obtained with an FDR cut-off of 0.05 (GO biological processes or KEGG pathways) linked to the DMRs involved in each concept, and the relation between them when genes are involved in more than one process. The size of the concept nodes depends on the gene count involved in that pathway or process, while the color of the gene nodes depends on their methylation level according to the displayed color gradient. **(A)** Cnetplots of GO terms of hypermethylated regions in neonatal sepsis, **(B)** GO terms of hypomethylated regions in neonatal sepsis, and **(C)**. KEGG pathways of hypermethylated regions.

of hypermethylated regions in T-cell activation and T-cell differentiation to be the processes with the highest significance, among other relevant GO terms (**Figure 4A**), which demonstrates the scarce immunoreactivity of the cells in septic neonates. Moreover, a high proportion of hypomethylated regions were enriched in neutrophil degranulation and activation involved in immune response processes, as well as in mast cell activation and response to molecules of bacterial origin

(**Figure 4B**). Regarding KEGG pathways, the most relevant pathways enriched in the set of hypermethylated DMRs were T-cell receptor signaling pathway, Th17 cell differentiation, and PD-L1 expression and PD-1 checkpoint pathway, which are related with immunosuppression processes (**Figure 4C**).

DISCUSSION

Sepsis produces high mortality and morbidity and adverse long-term effects in neonates. The pathophysiology of neonatal sepsis is not yet fully understood (3). We propose that epigenetics is involved in the immunopathology of sepsis and can provide biomarkers for clinical management of early onset and late onset sepsis.

Neonatal immune development is complex and incompletely understood. Moreover, neonatal immune development is orchestrated by many factors including intra- and extra-uterine exposure to antigens and commensal organisms (6), which determine the susceptibility of the newborn to sepsis (6). Notably, our results reveal significant changes in the DNA methylation between septic and controls, indicating that sepsis produces epigenetic reprogramming in leukocytes. With sepsis both hyperinflammatory and immunosuppressive responses occur (6, 41). Our results reinforce this idea, since methylation changes occur simultaneously in both pro- and anti-inflammatory mediators.

Upon infection, the immune response relies primarily on the innate immune system, which is not fully mature in preterm infants. Changes in DNAm were greater in LOS than in EOS when compared to controls. Hence, the lower methylation levels observed in the promoters of genes involved in neutrophil activation (i.e., *ATP8B4*, *LRG1*, *TREM1*, *PRTN3*, *S100A8*, *ELANE*, and *CD177*) illustrates the role of DNAm in innate immunity in neonatal sepsis. In addition, TREM-1, which has been proposed as an early biomarker of neonatal sepsis, is involved in the amplification of neutrophil and monocyte inflammatory responses by stimulating pro-inflammatory cytokines (38). Furthermore, the hypomethylation found in the gene coding for neutrophil elastase (*ELANE*) and proteinase 3 (*PRTN3*) may alter the formation of NETs (neutrophil extracellular traps), which is an earlier mechanism used by neutrophils to fight infection (42).

In line with pro-inflammatory responses, previous studies revealed the involvement of CD300b in LPS-induced sepsis (37) as well as apoptotic cell phagocytosis mediated by macrophages (36). As the excessive inflammatory response in sepsis entails apoptosis of lymphocytes and epithelial cells, CD300b contributes to sepsis, so the hypomethylation of the *CD300B* promoter found in our study correlates with previous findings (36, 37). Another relevant pro-inflammatory gene is *LTA* (lymphotoxin alpha), which is a cytokine produced by lymphocytes. This member of the tumor necrosis factor family is associated with increased risk of sepsis in adults (43), so the hypermethylation we found in *LTA* also suggests its use as a predictive marker for risk of sepsis in neonates.

IL-10, together with IL-6 and IL-8, are initial markers with high specificity for neonatal sepsis (32). The upregulation of IL-10 in sepsis is concordant with the lower methylation levels we found in its promoter and may contribute to the immunosuppressive response in neonatal sepsis. In addition, the gene encoding for the inflammatory and immunosuppressive protein S100A8 (S100 calcium binding protein A8) showed low methylation. Interestingly, S100A8 is an alarmin related with immunosuppression, because it prevents the expansion of specific inflammatory monocyte populations in septic neonates (44). Of note, S100A8 participates in neutrophil chemotaxis and adhesion, and it is up-regulated in patients with sepsis (45), which is in agreement with the low methylation levels identified in its promoter found in our study.

Regarding the adaptive immune response, T-cell activation is known to be downregulated during the immunosuppressive state (6). Interestingly, we found that the promoters of genes involved in T-cell regulation (i.e., *CD3D*, *CD3G*, *UBASH3A*, *SIT1,* and *TXK*) were hypermethylated in neonatal sepsis compared to controls, thereby resulting in decreased expression. The CD3D and CD3G proteins are subunits of the TCR-CD3 complex (TCR, T-cell receptor). The TCR-CD3 complex is a multicomponent membrane receptor in mature T cells and in thymocytes, whose under-expression has been described in adult sepsis (46). UBASH3A (part of the T-cell ubiquitin ligand or TULA) and SIT1 participate in the regulation of the TCR-CD3, by negatively regulating TCR signaling (47, 48). The hypermethylation of these genes suggests modulation of the TCR-CD3 complex in neonatal sepsis as well.

Among other significant methylated genes of interest in the context of neonatal sepsis, we also found *CALR,* which codes for calreticulin, an endoplasmic reticulum resident protein, with functions in leukocyte migration and related with the severity of sepsis (49). In addition, our study further revealed the hypomethylation of *MPO* gene, coding for myeloperoxidase, which has previously been described as a potential marker of mortality in sepsis (50).

The overlapping of the DMRs for genes and promoters showed in **Figure 4**, obtained with mCSEA and DMRcate approaches, revealed the scarce immunoreactivity of T-cells in septic neonates. Interestingly, KEGG pathways demonstrate the enrichment of hypermethylated DMRs for T-cell receptor signaling pathway, Th17 cell differentiation, and PD-L1 expression and PD-1 checkpoint pathway, which has been related with immunosuppression processes (31, 51, 52).

Importantly, using mCSEA method we were able to identify 4 gene promoters in *DUSP22*, *PM20D1*, *MIR10A,* and *MIR886* with significant differential DNAm when comparing LOS with EOS. Among these genes, *DUSP22* codes for a JKAP, a JNK pathway-associated phosphatase expressed in various types of human immune cells (e.g., T cells, B cells, and natural killer cells) (33, 53). DUSP22 has been closely related to immune and inflammation response and negatively correlates with APACHE II score, SOFA score, TNF-α, IL-1β, IL-6, and IL-17 (54). It would explain, why IL-6 is found elevated in EOS and considered a clinical criterion to diagnose EOS (55, 56). Interestingly, a work by Khaertynov et al., suggest higher values for TNF-α, IL-1β, IL-6 in LOS than in EOS (57), which is in

agreement with the observation of higher methylation of *DUSP22* in LOS than in EOS. In addition, DUSP22 downregulation correlates with severity, higher level of systemic inflammation, and poor survival in adult septic patients (54). It would be interesting to measure DUSP22 methylation in a cohort of neonatal septic patients in order to evaluate its potential as prognostic biomarkers in neonatal sepsis. Regarding *MIR10A*, it has been shown that miR-10a levels in PBMC at admission were significantly lower in sepsis patients compared with non-septic patients with infection, and with healthy controls (58). Moreover, miR-10a levels were found to predict 28-day mortality and negatively correlate with disease severity as well as levels for C-reactive protein, procalcitonin, and inflammatory cytokines such as IL-6, TNF-α, and MCP-1 (58). Regarding *MIR886*, it has been shown that miR-886-5p is increased in human monocyte-derived macrophages as a response to mycobacterial infection at 48 h (59), and the isoform hsa-miR-886-3p was present at higher levels in PBMCs from critically ill patients infected with H1N1 influenza virus than PBMCs from healthy controls (60). Interestingly, miR-886-5p targets IRAK3, BAX, and TP53 transcripts (59), contributing to inhibiting apoptosis (61). In our study we found the hypomethylation of *MIR886* in LOS compared to EOS, which may contribute to its upregulation, thereby inhibiting apoptosis in immune cells and setting the basis for an adaptive response in more mature immune cells. This is of special relevance because persistence of immunosuppression related to epigenetic dysregulation (6) may increase the susceptibility for future infections and increases the risk of mortality (11, 17).

Our study has some limitations, especially in the small number of newborns included in each group. Nonetheless our results importantly set the basis for further research aimed to validate our findings and provide novel biomarkers for neonatal sepsis based on DNA methylation.

CONCLUSIONS

DNAm profiles with differential methylation were observed between newborns with sepsis and control neonates in relevant genes and promoters involved in immune pathways. Our study demonstrates the potential use of DNAm to reveal relevant mechanisms underlying the inflammatory and immune dysregulation in neonatal sepsis, and particularly in EOS and LOS, which can help to clarify its physiopathology and therefore contribute to prevent life-threatening complications during neonatal sepsis.

DATA AVAILABILITY STATEMENT

The datasets presented in this study can be found in online repositories. The .idat files of the 23 samples were deposited on Gene Expression Omnibus (GEO) with the number GSE155952.

ETHICS STATEMENT

The studies involving human participants were reviewed and approved by Ethics Committee from Hospital Universitario y Politécnico la Fe (Valencia, Spain) with registration number 2017/0470. Written informed consent to participate in this study was provided by the participants' legal guardian/next of kin.

AUTHOR CONTRIBUTIONS

JG-G, MV, SM-M, PN, and FP: conception, study design, and coordination. MV, SL-P, and IL-C: wrote the ethics committee application, present the informed consent, and collect the samples. SL-P, PN, MG, IL-C, JB-G, RO-V, and SM-M: experiment performing and data acquisition. PN, MG, and EG-L: statistical analysis. JG-G, SL-P, SM-M, MV, PN, SL-P, EG-L, and FP: drafting manuscript. All authors approved the final version of the manuscript and agreed to be accountable for all aspects of the work in ensuring that questions related to the accuracy or integrity of any part of the work are appropriately investigated and resolved. All persons designated as authors qualify for authorship, and all those who qualify for authorship are listed.

FUNDING

This work was supported by AES from Spanish Institute of Health Carlos III grant numbers [AES2019, PI19/00994; PFIS grant FI18/0131] co-financed by the European Regional Development Fund (ERDF); by RETICS grant number [PN 2018-2021]; by ISCIII- Sub-Directorate General for Research Assessment and Promotion and the European Regional Development Fund (FEDER) grant number [RD16/0022] and Spanish Institute of Health Carlos III through CIBERer (Biomedical Network Research Center on Rare Diseases) grant number [ACCI2018-09] and Fundación Mútua Madrileña (AP174352020). MG was supported by the Competitiveness Programme for the Promotion of Talent and its Employability in R+D+I Torres Quevedo grant from Spanish Ministerio de Ciencia e Innovación (PTQ2019-010552). RO-V is a fellowship supported by Fundación Mutua Madrileña.

ACKNOWLEDGMENTS

The authors would like to thank Dr. Juan Sandoval and the Epigenomics Unit of the Instituto de Investigación Sanitaria La Fe for their support in performing Infinium Human DNA Methylation EPIC 850K arrays.

SUPPLEMENTARY MATERIAL

The Supplementary Material for this article can be found online at: https://www.frontiersin.org/articles/10.3389/fimmu.2021.622599/full#supplementary-material

REFERENCES

1. Shane AL, Sánchez PJ, Stoll BJ. Neonatal Sepsis. *Lancet.* (2017) 390:1770–80. doi: 10.1016/S0140-6736(17)31002-4
2. Singer M, Deutschman CS, Seymour C, Shankar-Hari M, Annane D, et al. The third international consensus definitions for sepsis and septic shock (sepsis-3). *J Am Med Assoc.* (2016) 315:801–10. doi: 10.1001/jama.2016.0287
3. McGovern M, Giannoni E, Kuester H, Turner MA, van den Hoogen A, Bliss JM, et al. Challenges in developing a consensus definition of neonatal sepsis. *Pediatr Res.* (2020) 88:14–26. doi: 10.1038/s41390-020-0785-x
4. Maddux AB, Douglas IS. Is the developmentally immature immune response in paediatric sepsis a recapitulation of immune tolerance? *Immunology.* (2015) 145:1–10. doi: 10.1111/imm.12454
5. Raymond SL, Stortz JA, Mira JC, Larson SD, Wynn JL, Moldawer LL. Immunological defects in neonatal sepsis and potential therapeutic approaches. *Front Pediatr.* (2017) 5:14. doi: 10.3389/fped.2017.00014
6. Hibbert JE, Currie A, Strunk T. Sepsis-induced immunosuppression in neonates. *Front Pediatr.* (2018) 6:357. doi: 10.3389/fped.2018.00357
7. Cernada M, Serna E, Bauerl C, Collado MC, Pérez-Martínez G, Vento M. Genome-wide expression profiles in very low birth weight infants with neonatal sepsis. *Pediatrics.* (2014) 133:e1203–11. doi: 10.1542/peds.2013-2552
8. Zea-Vera A, Ochoa TJ. Challenges in the diagnosis and management of neonatal sepsis. *J Trop Pediatr.* (2015) 61:1–13. doi: 10.1093/tropej/fmu079
9. Klinger G, Levy I, Sirota L, Boyko V, Reichman B, Lerner-Geva L. Epidemiology and risk factors for early onset sepsis among very-low-birthweight infants. *Am J Obstet Gynecol.* (2009) 201:38.e1-6. doi: 10.1016/j.ajog.2009.03.006
10. Benitz WE, Achten NB. Technical assessment of the neonatal early-onset sepsis risk calculator. *Lancet Infect Dis.* (2020) S1473-3099(20) 30490-4. doi: 10.1016/S1473-3099(20)30490-4
11. Hedegaard SS, Wisborg K, Hvas A-M. Diagnostic utility of biomarkers for neonatal sepsis—a systematic review. *Infect Dis.* (2015) 47:117–24. doi: 10.3109/00365548.2014.971053
12. Dong Y, Speer CP. Late-onset neonatal sepsis: recent developments. *Arch Dis Child Fetal Neonatal Ed.* (2015) 100:F257–63. doi: 10.1136/archdischild-2014-306213
13. Strunk T, Jamieson SE, Burgner D. Genetic and epigenetic susceptibility to early life infection. *Curr Opin Infect Dis.* (2013) 26:241–7. doi: 10.1097/QCO.0b013e32835fb8d9
14. Cross D, Drury R, Hill J, Pollard AJ. Epigenetics in sepsis: understanding Its role in endothelial dysfunction, immunosuppression, and potential therapeutics. *Front Immunol.* (2019) 10:1363. doi: 10.3389/fimmu.2019.01363
15. Carson WF, Cavassani KA, Dou Y, Kunkel SL. Epigenetic regulation of immune cell functions during post-septic immunosuppression. *Epigenetics.* (2011) 6:273–83. doi: 10.4161/epi.6.3.14017
16. Goldberg AD, Allis CD, Bernstein E. Epigenetics: a landscape takes shape. *Cell.* (2007) 128:635–8. doi: 10.1016/j.cell.2007.02.006
17. Berger SL, Kouzarides T, Shiekhattar R, Shilatifard A. An operational definition of epigenetics. *Genes Dev.* (2009) 23:781–3. doi: 10.1101/gad.1787609
18. Bernstein BE, Stamatoyannopoulos JA, Costello JF, Ren B, Milosavljevic A, Meissner A, et al. The NIH roadmap epigenomics mapping consortium. *Nat Biotechnol.* (2010) 28:1045–48. doi: 10.1038/nbt1010-1045
19. Beltrán-García J, Osca-Verdegal R, Romá-Mateo C, Carbonell N, Ferreres J, Rodríguez M,. Epigenetic biomarkers for human sepsis and septic shock: insights from immunosuppression. *Epigenomics.* (2020) 12:617–46. doi: 10.2217/epi-2019-0329
20. Morales-Nebreda L, McLafferty FS, Singer BD. DNA methylation as a transcriptional regulator of the immune system. *Transl Res.* (2019) 204:1–18. doi: 10.1016/j.trsl.2018.08.001
21. Saeed S, Quintin J, Kerstens HHD, Rao NA, Aghajanirefah A, Matarese F, et al. Epigenetic programming of monocyte-to-macrophage differentiation and trained innate immunity. *Science.* (2014) 345:1251086. doi: 10.1126/science.1251086
22. Lorente-Sorolla C, Garcia-Gomez A, Català-Moll F, Toledano V, Ciudad L, Avendaño-Ortiz J, et al. Inflammatory cytokines and organ dysfunction associate with the aberrant DNA methylome of monocytes in sepsis. *Genome Med.* (2019) 11:66. doi: 10.1186/s13073-019-0674-2
23. Binnie A, Walsh CJ, Hu P, Dwivedi DJ, Fox-Robichaud A, Liaw PC, et al. Epigenetic profiling in severe sepsis: a pilot study of DNA methylation profiles in critical illness. *Crit Care Med.* (2020) 48:142–50. doi: 10.1097/CCM.0000000000004097
24. Dhas DBB, Ashmi AH, Bhat BV, Kalaivani S, Parija SC. Comparison of genomic DNA methylation pattern among septic and non-septic newborns—an epigenome wide association study. *Genomics Data.* (2015) 3:36–40. doi: 10.1016/j.gdata.2014.11.004
25. Töllner U. Early diagnosis of septicemia in the newborn—Clinical studies and sepsis score. *Eur J Pediatr.* (1982) 138:331–7. doi: 10.1007/BF00442511
26. Goldstein B, Giroir B, Randolph A. International pediatric sepsis consensus conference: definitions for sepsis and organ dysfunction in pediatrics. *Pediatr Crit Care Med.* (2005) 6:2–8. doi: 10.1097/01.PCC.0000149131.72248.E6
27. Aryee MJ, Jaffe AE, Corrada-Bravo H, Ladd-Acosta C, Feinberg AP, Hansen KD, et al. Minfi: a flexible and comprehensive bioconductor package for the analysis of infinium DNA methylation microarrays. *Bioinformatics.* (2014) 30:1363–69. doi: 10.1093/bioinformatics/btu049
28. Fortin JP, Labbe A, Lemire M, Zanke BW, Hudson TJ, Fertig EJ, et al. Functional normalization of 450k methylation array data improves replication in large cancer studies. *Genome Biol.* (2014) 15:503. doi: 10.1186/s13059-014-0503-2
29. Pidsley R, Zotenko E, Peters TJ, Lawrence MG, Risbridger GP, Molloy P, et al. Critical evaluation of the illumina MethylationEPIC BeadChip microarray for whole-genome DNA methylation profiling. *Genome Biol.* (2016) 17:208. doi: 10.1186/s13059-016-1066-1
30. Ritchie M, Phipson, Wu D, Hu Y, Law CW, Shi W, et al. limma powers differential expression analyses for RNA-sequencing and microarray studies. *Nucleic Acids Res.* (2015) 43:e47. doi: 10.1093/nar/gkv007
31. Chen X, Oppenheim JJ. Th17 cells and Tregs : unlikely allies. *J Leukoc Biol.* (2014) 95:723–31. doi: 10.1189/jlb.1213633
32. Boskabadi Ha, Zakerihamidi M. Evaluate the diagnosis of neonatal sepsis by measuring interleukins: a systematic review. *Pediatr Neonatol.* (2018) 59:329–38. doi: 10.1016/j.pedneo.2017.10.004
33. Zhou R, Chang Y, Liu J, Chen M, Wang H, Huang M, et al. JNK pathway-associated phosphatase/DUSP22 suppresses CD4+ T-cell activation and Th1/Th17-cell differentiation and negatively correlates with clinical activity in inflammatory bowel disease. *Front Immunol.* (2017) 8:781. doi: 10.3389/fimmu.2017.00781
34. Peters TJ, Buckley MJ, Statham AL, Pidsley R, Samaras K, V Lord R, et al. *De novo* identification of differentially methylated regions in the human genome. *Epigenetics Chromatin.* (2015) 8:6. doi: 10.1186/1756-8935-8-6
35. Breeze CE, Reynolds AP, Van Dongen J, Dunham I, Lazar J, Neph S, et al. EFORGE v2.0: updated analysis of cell type-specific signal in epigenomic data. *Bioinformatics.* (2019) 35:4767–69. doi: 10.1093/bioinformatics/btz456
36. Murakami Y, Tian L, Voss OH, Margulies DH, Krzewski K, Coligan JE. CD300b regulates the phagocytosis of apoptotic cells via phosphatidylserine recognition. *Cell Death Differ.* (2014) 21:1746–57. doi: 10.1038/cdd.2014.86
37. Yamanishi Y, Takahashi M, Izawa K, Isobe M, Ito S, Tsuchiya A, et al. A soluble form of LMIR5/CD300b amplifies lipopolysaccharide-induced lethal inflammation in sepsis. *J Immunol.* (2012) 189:1773–79. doi: 10.4049/jimmunol.1201139
38. Benjamini Y, Hochberg Y. Controlling the false discovery rate: a practical and powerful approach to multiple testing. *J R Stat Soc Ser B.* (1995) 57:289–300. doi: 10.1111/j.2517-6161.1995.tb02031.x
39. Martorell-Marugán J, González-Rumayor V, Carmona-Sáez P. mCSEA: detecting subtle differentially methylated regions. *Bioinformatics.* (2019) 35:3257–62. doi: 10.1093/bioinformatics/btz096
40. Yu G, Wang L-G, Han Y, He Q-Y. clusterProfiler: an R package for comparing biological themes among gene clusters. *Omi A J Integr Biol.* (2012) 16:284–7. doi: 10.1089/omi.2011.0118
41. Van Der Poll T, Van De Veerdonk FL, Scicluna BP, Netea MG. The immunopathology of sepsis and potential therapeutic targets. *Nat Rev Immunol.* (2017) 17:407–20. doi: 10.1038/nri.2017.36
42. Delano MJ, Ward PA. The immune system's role in sepsis progression, resolution, and long-term outcome. *Immunol Rev.* (2016) 274:330–53. doi: 10.1111/imr.12499
43. Watanabe E, Buchman TG, Hirasawa H, Zehnbauer BA. Association between lymphotoxin-α (tumor necrosis factor-β) intron polymorphism and

predisposition to severe sepsis is modified by gender and age. *Crit Care Med.* (2010) 38:181–93. doi: 10.1097/CCM.0b013e3181bc805d
44. Heinemann AS, Pirr S, Fehlhaber B, Mellinger L, Burgmann J, Mandy B. In neonates S100A8/S100A9 alarmins prevent the expansion of a specific inflammatory monocyte population promoting septic shock. *FASEB J.* (2017) 31:1153–64. doi: 10.1096/fj.201601083R
45. Lu X, Xue L, Sun W, Ye J, Zhu Z, Mei H. Identification of key pathogenic genes of sepsis based on the gene expression omnibus database. *Mol Med Rep.* (2017) 17:3042–54. doi: 10.3892/mmr.2017.8258
46. Cazalis M-A, Lepape A, Venet F, Frager F, Mougin B, Vallin H, et al. Early and dynamic changes in gene expression in septic shock patients: a genome-wide approach. *Intensive Care Med Exp.* (2014) 2:20. doi: 10.1186/s40635-014-0020-3
47. Ge Y, Paisie TK, Chen S, Concannon P. UBASH3A regulates the synthesis and dynamics of TCR–CD3 complexes. *J Immunol.* (2019) 203:2827–36. doi: 10.4049/jimmunol.1801338
48. Marie-Cardine A, Kirchgessner H, Bruyns E, Shevchenko A, Mann M, Autschbach F, et al. SHP2-interacting transmembrane adaptor protein (SIT), a novel disulfide- linked dimer regulating human T cell activation. *J Exp Med.* (1999) 189:1181–94. doi: 10.1084/jem.189.8.1181
49. Xu Z, Yang Y, Zhou J, Huang Y, Wang Y, Zhang Y, et al. Role of plasma calreticulin in the prediction of severity in septic patients. *Dis Markers.* (2019) 2019:8792640. doi: 10.1155/2019/8792640
50. Schrijver IT, Kemperman H, Roest M, Kesecioglu J, de Lange DW. Myeloperoxidase can differentiate between sepsis and non-infectious SIRS and predicts mortality in intensive care patients with SIRS. *Intensive Care Med Exp.* (2017) 5:43. doi: 10.1186/s40635-017-0157-y
51. Chen G, Huang AC, Zhang W, Zhang G, Wu M, Xu W, et al. Exosomal PD-L1 contributes to immunosuppression and is associated with anti-PD-1 response. *Nature.* (2018) 560:382–6. doi: 10.1038/s41586-018-0392-8
52. Patil N, Guo Y, Luan L, Sherwood E. Targeting immune cell checkpoints during sepsis. *Int J Mol Sci.* (2017) 18:2413. doi: 10.3390/ijms18112413
53. Chuang H-C, Chen Y-M, Hung W-T, Li J-P, Chen D-Y, Lan J-L, et al. Downregulation of the phosphatase JKAP/DUSP22 in T cells as a potential new biomarker of systemic lupus erythematosus nephritis. *Oncotarget.* (2016) 7:57593–605. doi: 10.18632/oncotarget.11419
54. Zhao M, Huang X. Downregulation of JKAP is correlated with elevated disease risk, advanced disease severity, higher inflammation, and poor survival in sepsis. *J Clin Lab Anal.* (2019) 33:e22945. doi: 10.1002/jcla.22945
55. Mirzarahimi M, Barak M, Eslami A, Enteshari-Moghaddam A. The role of interleukin-6 in the early diagnosis of sepsis in premature infants. *Pediatr Rep.* (2017) 9:7305. doi: 10.4081/pr.2017.7305
56. Krueger M, Nauck MS, Sang S, Hentschel R, Wieland H, Berner R. Cord blood levels of interleukin-6 and interleukin-8 for the immediate diagnosis of early-onset infection in premature infants. *Neonatology.* (2001) 80:118–23. doi: 10.1159/000047130
57. Khaertynov KS, Boichuk S V., Khaiboullina SF, Anokhin VA, Andreeva AA, Lombardi VC, et al. Comparative assessment of cytokine pattern in early and late onset of neonatal sepsis. *J Immunol Res.* (2017) 2017:1–8. doi: 10.1155/2017/8601063
58. Zheng G, Qiu G, Ge M, Meng J, Zhang G, Wang J, et al. miR-10a in peripheral blood mononuclear cells is a biomarker for sepsis and has anti-inflammatory function. *Mediat Inflamm.* (2020) 2020:1–10. doi: 10.1155/2020/4370983
59. Sharbati J, Lewin A, Kutz-Lohroff B, Kamal E, Einspanier R, Sharbati S. Integrated MicroRNA-mRNA-analysis of human monocyte derived macrophages upon *Mycobacterium avium* subsp. hominissuis Infection. *PLoS ONE.* (2011) 6:e20258. doi: 10.1371/journal.pone.0020258
60. Song H, Wang Q, Guo Y, Liu S, Song R, Gao X, et al. Microarray analysis of MicroRNA expression in peripheral blood mononuclear cells of critically ill patients with influenza A (H1N1). *BMC Infect Dis.* (2013) 13:257. doi: 10.1186/1471-2334-13-257
61. Li J-H, Xiao X, Zhang Y-N, Wang Y-M, Feng L-M, Wu Y-M, et al. MicroRNA miR-886-5p inhibits apoptosis by down-regulating Bax expression in human cervical carcinoma cells. *Gynecol Oncol.* (2011) 120:145–51. doi: 10.1016/j.ygyno.2010.09.009

Conflict of Interest: JG-G, FP, and SM-M are owners of EpiDisease's shares. JG-G and SM-M are currently the C.E.O. and C.S.O. of 1446 EpiDisease S.L., respectively. EpiDisease is a Spin-Off of the Consortium Centre for Biomedical Network Research on Rare Diseases (Spanish Institute of Health- Instituto de Salud Carlos III), the Biomedical Research Centre INCLIVA and the University of Valencia. There are no patents, products in development or marketed products associated with this research to declare.

The remaining authors declare that the research was conducted in the absence of any commercial or financial relationships that could be construed as a potential conflict of interest.

frontiers in Immunology

REVIEW
published: 23 February 2021
doi: 10.3389/fimmu.2021.621627

The Role of Siglec-G on Immune Cells in Sepsis

William Royster[1,2,3], *Ping Wang*[1,2,3*†] *and Monowar Aziz*[1,2*†]

[1] Center for Immunology and Inflammation, The Feinstein Institutes for Medical Research, Manhasset, NY, United States, [2] Elmezzi Graduate School of Molecular Medicine, Manhasset, NY, United States, [3] Department of Surgery, Donald and Barbara Zucker School of Medicine at Hofstra/Northwell, Manhasset, NY, United States

OPEN ACCESS

Edited by:
Zhixing Kevin Pan,
University of Toledo Medical Center,
United States

Reviewed by:
James Frederick Burrows,
Queen's University Belfast,
United Kingdom
Samithamby Jey Jeyaseelan,
Louisiana State University,
United States

***Correspondence:**
Monowar Aziz
Maziz1@northwell.edu
Ping Wang
pwang@northwell.edu

[†]These authors have contributed equally to this work and share senior authorship

Specialty section:
This article was submitted to Inflammation, a section of the journal Frontiers in Immunology

Received: 26 October 2020
Accepted: 13 January 2021
Published: 23 February 2021

Citation:
Royster W, Wang P and Aziz M (2021) The Role of Siglec-G on Immune Cells in Sepsis. Front. Immunol. 12:621627. doi: 10.3389/fimmu.2021.621627

Sepsis is a life-threatening clinical syndrome that results from an overwhelming immune response to infection. During sepsis, immune cells are activated by sensing pathogen-associated molecular patterns and damage-associated molecular patterns (DAMPs) through pattern recognizing receptors (PRRs). Regulation of the immune response is essential to preventing or managing sepsis. Sialic acid-binding immunoglobulin-type lectin-G (Siglec-G), a CD33 group of Siglec expressed in B-1a cells and other hematopoietic cells, plays an important immunoregulatory role. B-1a cells, a subtype of B lymphocytes, spontaneously produce natural IgM which confers protection against infection. B-1a cells also produce IL-10, GM-CSF, and IL-35 to control inflammation. Sialic acids are present on cell membranes, receptors, and glycoproteins. Siglec-G binds to the sialic acid residues on the B cell receptor (BCR) and controls BCR-mediated signal transduction, thereby maintaining homeostasis of Ca^{++} influx and NFATc1 expression. Siglec-G inhibits NF-κB activation in B-1a cells and regulates B-1a cell proliferation. In myeloid cells, Siglec-G inhibits DAMP-mediated inflammation by forming a ternary complex with DAMP and CD24. Thus, preserving Siglec-G's function could be a novel therapeutic approach in sepsis. Here, we review the immunoregulatory functions of Siglec-G in B-1a cells and myeloid cells in sepsis. A clear understanding of Siglec-G is important to developing novel therapeutics in treating sepsis.

Keywords: sialic acid-binding immunoglobulin-type lectin-G (Siglec-G), B-1a cells, B cell receptor (BCR), TLR, damage-associated molecular patterns (DAMPs), extracellular cold-inducible RNA-binding protein (eCIRP), inflammation, sepsis

Abbreviations: BCR, B cell receptor; DAMPs, damage-associated molecular patterns; eCIRP, extracellular cold-inducible RNA-binding protein; GM-CSF, granulocyte-macrophage colony-stimulating factor; GVHD, graft-versus-host disease; HMGB1, high-mobility group box 1; IFNβ, interferon β; IRF3, interferon regulatory factor 3; ITIM, immunoreceptor tyrosine-based inhibition motif; NFATc1, nuclear factor of activated T-cells, cytoplasmic 1; OxLDL, oxidized low-density lipoprotein; PAMPs, pathogen-associated molecular patterns; PD-1, programmed cell death protein-1; PRRs, pattern recognizing receptors; RANKL, receptor activator of nuclear factor kappa-β ligand; RIG-I, retinoic acid-inducible gene-I; SHP1, Src homology region 2 domain-containing phosphatase 1; Siglec-G, Sialic acid-binding immunoglobulin-type lectin-G; TIGIT, T cell immunoreceptor with Ig and ITIM domains; VAP-1, vascular adhesion protein-1.

INTRODUCTION

Inflammation refers to the body's immune response to foreign particles. Sepsis is characterized as life threatening organ dysfunction caused by a dysregulated host response to infection (1). Sepsis will afflict 1.7 million adults in America, and result in 270,000 each year, attributing a huge economic burden to the US health care system (2). The activation of pattern recognizing receptors (PRRs) of immune cells by pathogen-associated molecular patterns (PAMPs) and damage-associated molecular patterns (DAMPs), results in an immune response to intruders (3, 4). Initiation of inflammation following infection is important to eradicate infection, while excessive inflammation can cause tissue injury, multi-organ dysfunction, and death in sepsis. A clear understanding of this pathophysiology will assist in removing the barriers of developing effective medications to treat sepsis.

Sialic acid-binding immunoglobulin-type lectins (Siglecs) are a group of receptors expressed on multiple types of immune cells. Siglecs are classified into two groups. The first group of Siglecs conserved in human and mouse are Siglec-1, -2, and -4 known as sialoadhesin, CD22, and myelin-associated glycoprotein (MAG) respectively. Siglec-15 is also a member of this group. The second group of Siglecs are known as CD33-related Siglecs. This group is rapidly evolving and comprises 11 members in humans, and 5 members in the mouse (5, 6). The CD33 family of human Siglecs includes CD33 or Siglec-3, -5, -6, -7, -8, -9, -10, -11, -12, -14, and -16. The mouse CD33 orthologs are designated by letters, which include CD33 (Siglec-3), Siglec-E, -F, -G, and -H. The number of extracellular immunoglobulin (Ig) domains in Siglecs varies among different Siglecs, for example Siglec-1 has 17 Ig domains, while Siglec-3 (CD33) and -H, each having only 2 Ig domains (5). Murine Siglec-G's human ortholog is Siglec-10. Here, we focus on the immunoregulatory functions of Siglec-G during sepsis, because of the ubiquitous presence of sialic acid, the ligand of Siglec-G, on cell membranes, membrane receptors, and glycoproteins. Siglec-G is most highly expressed in B-1a cells, but is also present on conventional B-2 cells, where Siglec-2 is predominantly expressed (6, 7). Dendritic cells (DC), macrophages, and T lymphocytes also express Siglec-G (6, 7). It contains five extracellular Ig-like domains. The N-terminal Ig-like domain, which is similar to the variable domain of Ig (V-set domain), contains the sialic acid binding motif. The other parts of Siglec-G include a transmembrane region as well as an intracellular tail with three different tyrosine-based motifs: i) one immunoreceptor tyrosine-based inhibitory motif (ITIM), ii) one ITIM-like domain, and iii) a Grb-2-binding site (6, 8). Siglec-G binds to sialic acid moieties on B cell receptor (BCR), thereby controlling BCR-mediated signal transduction. Deficiency of Siglec-G causes altered BCR signaling which leads to increased Ca^{++} influx, increased nuclear factor of activated T-cells, cytoplasmic 1 (NFATc1) expression, and decreased Src homology region 2 domain-containing phosphatase 1 (SHP1) levels in B-1a cells (7, 8). Siglec-G knockout mice have been found to have expanded populations of B-1a cells in the peritoneal cavity as well as elevated circulatory natural IgM. Overall, a skewed repertoire of secreted natural IgM implicating an altered IgM function has been detected in Siglec-G knockout mice (9, 10). Siglec-G also downregulates NF-κB activation in B-1a cells, which influences B-1a cell proliferation and survival (10, 11). Thus, Siglec-G is a crucial component of B-1a cell signaling and development. In myeloid cells, Siglec-G acts as a negative regulator of DAMPs. CD24 directly binds multiple different DAMPs, which then in turn binds to Siglec-G forming a trimeric assembly, serving to repress the inflammatory responses to DAMPs (12). Thus, preserving Siglec-G's function protects mice from inflammation. The expression of Siglec-G at its mRNA level was increased in LPS-induced sepsis, although the protein level of Siglec-G and its expression in various immune cells during sepsis are unknown (13). By contrast, a recent report has shown that irradiation can cause reduced expression of Siglec-G at its protein level in antigen presenting cells (APCs), which leads to DAMP-mediated inflammatory responses (14). Since irradiation often causes sepsis by disrupting the intestinal barrier resulting in a leak of intestinal flora into the circulation, the findings of deceased expression of Siglec-G in APCs in the irradiation model could be mimicked with a polymicrobial sepsis model. Given the importance of Siglec-G in regulating the immune response, the expression of Siglec-G in various immune cells under inflammatory conditions should be studied.

B-1a cells are a unique subpopulation of B cells with profound immunoregulatory properties. B-1a cells have innate-like functions, playing a critical role in the initial defense against invading pathogens by secreting natural Abs (IgM) that help to protect the host from acute infection as well as lower bacterial load (15). B-1a cells either spontaneously or following infection produce the anti-inflammatory cytokine IL-10 in bulk amounts (16). B-1a cells also release granulocyte-monocyte colony-stimulating factor (GM-CSF) (17), which governs emergency myelopoiesis as well as causing B-1a cells to release more IgM in an both an autocrine and paracrine manner to protect the host against infection (17, 18). Conversely, B-1a cells also produce IL-3, IL-17, and TNF-α, which exhibit pro-inflammatory roles in sepsis (15, 19). B-1a cell-mediated protective outcomes have been reported in bacterial sepsis, pneumonia, and viral infection (15). In this review, we discuss the role of Siglec-G in B-1a cells and other cells to regulate BCR- and PRR-mediated pathways to control inflammation in sepsis. We also discuss the therapeutic interventions by targeting Siglec-G in sepsis. Unveiling the potential role of Siglec-G in B-1a cells and other cells is important for understanding the pathobiology of sepsis and its therapy.

RATIONALE

Siglec-G is expressed in a wide range of immune cells such as B-1a cells, myeloid cells, and T cells (6, 8, 14). B-1a cells have been shown to provide a survival benefit as well as ameliorate end organ damage in sepsis (15, 16). Although the role of Siglec-G in B-1a cells in the context of sepsis has not been studied before, given the evidence of Siglec-G-mediated anti-inflammatory role in CD24 expressing myeloid cells (20), it is speculated that B-1a cells which also express CD24 and Siglec-G could play similar

anti-inflammatory role in sepsis (21). Myeloid cells play a pivotal role in innate-immunity in sepsis. Following infection, these cells respond to PAMPs and become activated to release pro-inflammatory cytokines and DAMPs including high-mobility group box 1 (HMGB1), extracellular cold-inducible RNA-binding protein (eCIRP), and histones (4). The transcription factor NF-κB induces the expression of these pro-inflammatory molecules (22). Given the importance of Siglec-G in controlling DAMP-mediated inflammation by inhibiting NF-κB, the immunoregulatory role of Siglec-G in sepsis is prominent and needs to be further discussed to dissect its mechanism of action in sepsis. Sialic acids are nine-carbon sugars attached to glycopeptides and glycolipids found in the circulation and on cell surfaces. *N*-glycolylneuraminic acid (Neu5Gc) and *N*-acetylneuraminic acid (Neu5Ac) are the two sialic acids most commonly found in mammalian cells. Sialic acids are attached to glycans *via* α2-3, α2-6 or α2-8 linkages (5, 6). The specific orientation of these linkages is often crucial for recognition by the sialic acid binding proteins expressed on mammalian cells. Siglec-G binds sialic acid moieties in a cis (same cell) or trans (adjacent cells) acting manner (9), which widens the scope of Siglec-G's role in sepsis as increased cell to cell interaction is evident in sepsis. Given the increased expression of several glycoproteins which are enriched in sialic acids in inflammatory diseases (23), there seems to be a possibility that sialic acid contents could be increased in sepsis. This in turn may serve to activate Siglec-G to turn on the immunoregulatory mechanism in sepsis. The expression of Siglec-G was shown to be significantly upregulated in immune cells upon stimulation with lipopolysaccharide (LPS) (13), implicating Siglec-G's impact in sepsis. Since the deficiency of Siglec-G could play a beneficial role in sepsis, here the increase of Siglec-G in their model could exhibit detrimental outcomes in sepsis (13). Since the sepsis pathophysiology and etiologies are complex and diverse, relying on a particular study finding may not reflect real clinical scenarios. Collectively, these strong scientific premises led us to focus on Siglec-G's role in B-1a cells and beyond in sepsis.

SIALIC ACID-BINDING IMMUNOGLOBULIN-TYPE LECTIN-G CONTRIBUTES TO HOST PROTECTION IN SEPSIS

Siglec-G is expressed in B-1a cells, as well as in myeloid and lymphoid cells to play immunoregulatory functions (6, 12). Since these cells play a crucial role in sepsis, Siglec-G's role in sepsis is critical. There exists a large body of evidence demonstrating the key role of NF-κB activation in sepsis. Studies have demonstrated that NF-κB inhibitors protect animals from sepsis (24, 25). NF-κB is constitutively activated in Siglec-G$^{-/-}$ B-1a cells (11). In DCs, Siglec-G hinders DAMPs effects on NF-κB activation (12). In myeloid cells, Siglec-G causes SHP2 and Cbl-dependent ubiquitylation and proteasomal degradation of RIG-I resulting in a dampening of the type I IFN response (26). Given the decreased activation of NF-κB and type-I IFN by Siglec-G, sepsis-induced hyperinflammation can be controlled. The direct role of Siglec-G in polymicrobial sepsis was first identified by using Siglec-G$^{-/-}$ mice, which showed increased susceptibility to sepsis-induced death (20). Similarly, the Siglec-G's interacting molecule CD24$^{-/-}$ mice showed increased mortality in sepsis. Corresponding to the increased mortality in the mutant mice, the levels of IL-6, MCP-1, and TNF-α were sharply elevated. Compared to wild-type counterparts, the lung, kidney, and liver of CD24$^{-/-}$ and Siglec-G$^{-/-}$ mice showed severe hemorrhage, venous congestion, and necrosis (20). The CD24-Siglec-G interaction has been shown to be a crucial negative regulator of inflammation in sepsis. Sialidases are a potent virulence factor produced by many different invading pathogens, and sialic acid-based pattern recognition is a cardinal feature of Siglec-G. Therefore, bacterial sialidases may exacerbate sepsis by CD24 desialylation. Treatment of CD24 protein with recombinant sialidases from three different bacteria, *S. pneumoniae*, *C. perfringens*, and *V. cholerae* dramatically reduced Siglec-G's binding with CD24 and therefore exacerbated HMGB1 and HSP70 induced inflammation in sepsis (20). Following sepsis, there is a marked increase in sialidase activity, which disrupts CD24-binding to Siglec-G leading to uncontrolled inflammation (**Figure 1A**). CD24 is not the only molecule that contains sialic acids and also the Siglec-G is not the only receptor that binds to sialic acids to become affected by the bacterial sialidases, there could be a number of molecules which contain sialic acids, binding to other Siglecs, and also become desialylated by bacterial sialidase. As such, the strategy and the findings as made by Chen et al. (20) focuses only on the CD24 and Siglec-G, given the fact that the deficiency of either CD24 or Siglec-G causes detrimental outcomes in sepsis. These findings further shed light on the avenues of identifying other sialic acid containing ligands and Siglecs that become affected by bacterial sialidase to exacerbate sepsis.

Siglec-G$^{-/-}$ B-1a cells possess a constitutively active BCR-mediated intracellular signal transduction pathway, leading to an increase in B-1a cell number as well as elevated levels of natural IgM (7). In context of B-1a cell produced natural IgM's role, the protective outcomes of Siglec-G$^{-/-}$ mice have been demonstrated in atherosclerosis (27). Natural IgM capable of binding OxLDL are significantly increased in the plasma and peritoneal cavities of Siglec-G$^{-/-}$ mice (27). Consistent with the neutralizing functions of OxLDL-specific IgM, Siglec-G$^{-/-}$ mice were shown to have protection from OxLDL-induced sterile inflammation. Despite the increased blood IgM levels, the Siglec-G$^{-/-}$ mice are more susceptible to peritoneal bacterial infections as noticed in CLP-induced sepsis (20). Blood and peritoneal lavage fluid cultures yielded more bacterial colonies in Siglec-G$^{-/-}$ mice than wild-type controls. Although bacterial load in WT and Siglec-G$^{-/-}$ was unaffected, the sialidase activity in the serum of Siglec-G$^{-/-}$ mice after sepsis was increased compared to WT mice in sepsis, which might lead to detrimental outcomes in septic Siglec-G$^{-/-}$ mice (20).

The immunoregulatory function of B-1a cells is altered by the presence of various bacterial proteins. Porin of *Shigella*

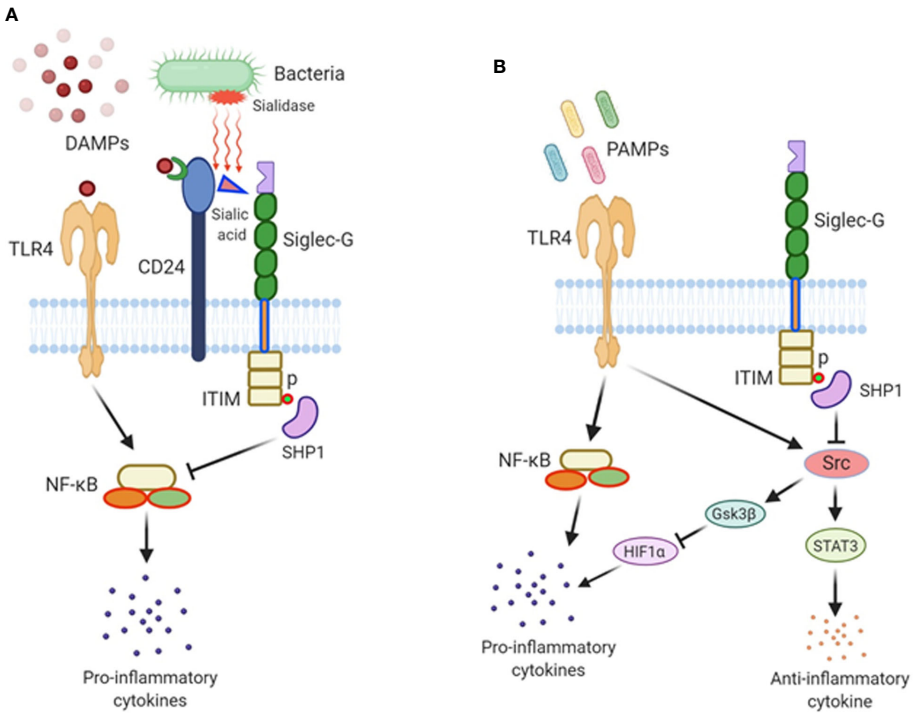

FIGURE 1 | The role of Siglec-G in sepsis. **(A)** Damage-associated molecular patterns (DAMPs) are released from damaged cells during sepsis and recognized by TLR4, fueling inflammation. DAMPs also bind to CD24, and this di-molecular complex further binds to Siglec-G through CD24's sialic acid moiety to form a tri-molecular complex. Siglec-G leads to SHP1 activation which downregulates NF-κB activity and pro-inflammatory cytokine production. In polymicrobial sepsis, bacterial sialidases remove sialic acid residue from CD24, abrogating the CD24-Siglec-G interaction, thus enhancing the inflammatory process. **(B)** Siglec-G regulates PAMPs-TLR4-mediated signaling during sepsis. Siglec-G inhibits Src activation through the activation of SHP1 *via* Siglec-G's ITIM domain. Src inhibits TLR4-induced inflammatory cytokines and increases the expression of IL-10 by activating STAT3. In Siglec-G deficient macrophages due to less recruitment of SHP1, Src is activated at its optimal level possibly through TLR4 pathway. Src then promotes HIF1α degradation through activating GSK3β. HIF1α is critical in inducing LPS-induced inflammatory response. As such, Src-induced degradation of HIF1α results in less pro-inflammatory cytokines production upon LPS stimulation in Siglec-G deficient immune cells. Thus, Siglec-G coordinates TLR4-induced pro- and anti-inflammatory cascades in sepsis.

dysenteriae type 1, an enteric bacteria, induces the proliferation of B-1a cells, but it dramatically reduces Siglec-G on B-1a cells (28). The porin-induced reduction of Siglec-G expression by B-1a cells is characterized by marked elevation of CD69 and CD40 expression, indicating activation of these cells subsequent to the down regulation of Siglec-G. As a result of cell activation, porin skews IL-10 producing/competent B-1a cells toward pro-inflammatory cytokines producing/responsive cells (28). Thus, bacterial infection shifts B-1a cell phenotype towards pro-inflammatory through a decreased expression of Siglec-G.

HUMAN SIALIC ACID-BINDING IMMUNOGLOBULIN-TYPE LECTIN-10 MIMICS THE FUNCTION OF MURINE SIALIC ACID-BINDING IMMUNOGLOBULIN-TYPE LECTIN-G

To describe how the findings of murine Siglec-G can be matched with its human orthologue Siglec-10 during inflammation, at first the interaction of human CD24 and human Siglec-10 was determined. Sialidase treated recombinant human CD24 when combined with recombinant human Siglec-10 did not interact with each other, confirming the importance of sialic acid on CD24 for binding to Siglec-10 to transduce the downstream immunoregulatory signal, controlling DAMP-mediated inflammation (20). This result with human Siglec-10 suggests that the findings on murine Siglec-G to ameliorate inflammation can be transferable to human sepsis. In addition to this study, murine Siglec-G's function was shown to be connected with its human orthologue Siglec-10 in a microbial sepsis model (29). In their study, Stephenson et al. showed that C. jejuni flagella can promote an anti-inflammatory axis *via* glycan-Siglec-10 engagement. They revealed that pseudaminic acid residues on the flagella contributed to IL-10 expression in dendritic cells. They also identified the ability of both viable C. jejuni and purified flagellum to bind to Siglec-10. *In vitro* infection of Siglec-10 overexpressing cells with pseudaminic acid residues containing flagella resulted in increased IL-10 expression in a p38-dependent manner. Detection of Siglec-10 on intestinal dendritic cells added further credence to the notion that this novel interaction may contribute to immune outcome during human infection.

CONTRADICTORY ROLE OF SIALIC ACID-BINDING IMMUNOGLOBULIN-TYPE LECTIN-G IN PAMP-MEDIATED SEPSIS

A recent study explained Siglec-G's role in endotoxemia in a different angle, where they suggested that Siglec-G deficiency attenuated the LPS-TLR4-induction of pro-inflammatory cytokines, and augmented the expression of anti-inflammatory cytokine IL-10 at both acute and immunosuppressive phases of sepsis (13). This study explains the impact of Siglec-G on PAMPs-induced inflammation, as our previous discussion mainly explained Siglec-G's role in DAMPs-mediated inflammation. This non-classical function of Siglec-G was mediated though its regulation of activation of proto-oncogene tyrosine-protein kinase (Src). Src activation is inhibited by Siglec-G through the recruitment and activation of the tyrosine phosphatase SHP1. Src inhibits TLR4-induced inflammatory cytokines and promotes anti-inflammatory cytokine IL-10 production. In Siglec-$G^{-/-}$ macrophages due to less recruitment of SHP1, Src is activated at its optimal level. Src then promotes hypoxia inducible factor 1α (HIF1α) degradation through activating GSK3β. HIF1α is critical in inducing LPS-induced inflammatory response. As such, in Siglec-$G^{-/-}$ macrophages, Src-induced degradation of HIF1α results in less pro-inflammatory cytokines production upon LPS stimulation. Conversely, it has been shown that Src interacts with and phosphorylates STAT3, which leads to increased expression of IL-10, given the fact that STAT3 positively regulates IL-10 expression. Thus, Siglec-G orchestrates TLR-induced inflammation, which leads to the conclusion that the treatment of acute and chronic inflammatory diseases may be achievable through the blockade of Siglec-G or the activation of Src by inhibiting pro-inflammatory cytokines and inducing anti-inflammatory cytokine production (**Figure 1B**). Treatment of septic patients with anti-inflammatory therapy may result in a protracted immunosuppressive phase. However, the blockade of Siglec-G (activation of Src) while the patient is in the hyper-inflammatory phase or the activation of Siglec-G (blockade of Src) while in the hypo-inflammatory phase of sepsis may prove a useful treatment adjunct.

By comparing the findings of two contradictory studies with Siglec-G-deficient mice in sepsis, we found Li et al. showed that Siglec-G deficiency ameliorates hyperinflammation and immune collapse in endotoxemia (13), on the other hand, Chen's study revealed that Siglec-$G^{-/-}$ mice showed detrimental outcomes in CLP-induced sepsis (20). Towards delineating the mechanism, Chen et al. determined the role of Siglec-G in attenuating DAMP-mediated inflammatory responses in sepsis, while Li et al. demonstrated that after LPS challenge, Siglec-$G^{-/-}$ mice produced less IL-6 and TNFα, more IL-10, and had an improved survival rate compared to Siglec-$G^{+/-}$ mice. However, in contrast to Li et al's findings, another study demonstrated Siglec-G's immunomodulatory role in DAMP-mediated, but not PAMP-mediated inflammation (12). They showed that the survival rates between WT and Siglec-$G^{-/-}$ mice in endotoxemia model did not differ between WT and Siglec-$G^{-/-}$ mice (12). Considering these two opposite findings with Siglec-G in DAMP- and PAMP-mediated inflammation, targeting Siglec-G for its activation or modulation may not always be beneficial in sepsis. Thus, additional studies may be required to prove Siglec-G's definitive role in DAMP- and PAMP-mediated inflammation.

SIALIC ACID-BINDING IMMUNOGLOBULIN-TYPE LECTIN-G-MEDIATED SIGNAL TRANSDUCTION IN B-1A CELLS

Mature murine B lymphocytes are broadly categorized into three subsets. Follicular (FO) B cells, marginal zone (MZ) B cells, and B-1 cells. Follicular B cells, which are also called B-2 cells, are the most prevalent subset. B2 cells are found in the lymphoid follicles of the spleen and lymph nodes. FO B cells, upon interaction with $CD4^+$ T helper cells, can differentiate into short lived plasma cells, or can form a germinal center (GC) and become long lived plasma cells or memory B cells (30). MZ B cells possess attributes of both naïve and memory B cells. They are located in the marginal sinus of the spleen where they are exposed to pathogens and particulate antigens (31).

B-1 cells were first described in 1983 by Hayakawa et al. (32). These cells are found in the peritoneal and pleural cavities, as well as the spleen. B-1 cells are characterized as $B220^{lo}$, $CD19^+$, $CD23^-$, $CD43^+$ (15, 33). B-1 cells were first termed Ly-1^+ (murine) or Leu-1^+ (human) due to their expression of the aforementioned surface markers (32). These surface markers have since been renamed CD5. Further research has determined that the presence of CD5 has come to distinguish B-1a ($CD5^+$) cells from B-1b cells ($CD5^-$). B-1 cells originate from distinct hematopoietic progenitor cells. B-1a cells are unique in their ability to release repertoire skewed polyreactive natural antibodies. These natural antibodies serve as a first line of defense by eliminating many different types of pathogens (15, 34). Whereas the B-1b cells exhibit adaptive antibody responses to pneumococcal polysaccharide type 3 (PPS-3) and are essential for long-term protection against *S. pneumoniae* infection (35). B-1a cells are the most prolific producers of IL-10 by B lymphocytes (16, 36). The first phase of B-1 cell development occurs in fetal development and continues into neonatal life. These early B-1 cells largely contributes to the adult B-1 cell compartment, as B-1 cells are capable of self-renew throughout the lifetime of the organism (34).

Siglec-G serves as a negative regulator of BCR (7, 8, 10). Siglec-G is associated, to some extent, with membrane-bound (m)IgM through binding to its sialic acid motif. The binding of antigen to mIgM results in the recruitment of more Siglec-G to the activated receptor. This interaction takes place *via* α2-3 or α2-6-linked sialic acids present on mIgM. The recruitment of Siglec-G to the antigen-activated mIgM, results in tyrosine phosphorylation of ITIMs on Siglec-G, most likely by Lyn. The phosphorylation of ITIMs results in the recruitment of the tyrosine phosphatase SHP1, which inhibits both mIgM-induced Ca^{++} signaling and NFATc1 expression (7, 10). Despite having some disputes, Siglec-G has also been shown to regulate NF-κB activation in B-1a cells through BCR, as Siglec-G deficiency causes activation of this transcription factor (11). Siglec-G-deficient mice have been found to express significantly higher amounts of cytosolic

phosphorylated IκB as well as nuclear accumulation of P65 in peritoneal lavage samples. Since NF-κB governs the expression of a number of pro- and anti-inflammatory cytokines in sepsis (24), Siglec-G's regulation on NF-κB activation may have an impact on these cytokines production by B-1a cells in sepsis. Thus, in B-1a cells Siglec-G works mainly on BCR signaling to regulate NFATc1 and NF-κB pathway (**Figure 2A**).

SIALIC ACID-BINDING IMMUNOGLOBULIN-TYPE LECTIN-G DEFICIENCY ON B-1A CELLS

Signal transduction of the BCR is crucial for initiating B-cell response. Siglec-G knockout mice were found to have extensively enlarged B-1a cell populations (7, 8). Interestingly, the B-1b and B-2 cells were not affected by the loss of Siglec-G in these mice, suggesting the inhibitory role of Siglec-G is much more crucial in B-1a cells. The absence of Siglec-G resulted in higher calcium mobilization by B-1a cells upon BCR stimulation. This increase in calcium signaling has been attributed to the lack of SHP1 recruitment resulting in increased BCR signaling (7). Siglec-G deficient B-1a cells were noted to undergo lower rates of apoptosis and found to have an extended life span (10, 37, 38). This decrease in apoptosis could be a result of greater expression of NFATc1 in Siglec-G-deficient B-1a cells. In addition to NFATc1 activation, studies have also showed that activation of Siglec-G results in the down regulation of NF-κB, which limits the size of B-1a cell lineage (11). Activation of NF-κB is required for the self-renewal of the B-1a cells in the peritoneal cavity and spleen of the Siglec-$G^{-/-}$ mice. Despite the fact that NF-κB plays an important role in B-1a cells and as opposed to this data by Ding et al. (11), Jellusova et al. did not find and difference in the activation of NF-κB in Siglec-G deficient mice (37). The discrepancies between these two studies could be due to the fact that Ding et al. mostly performed experiments with lysates from total unseparated cell populations from peritoneal washouts; whereas Jellusova et al. chose to study purified B-1a cells (11, 37). In addition, the possibility that the genetic background plays a role in these two studies may not be excluded because one group used BALB/c background, while the other group used C57BL/6. In addition to these facts, the Siglec-G's impact on NF-kB in B-1a cells may be not as promising as myeloid cells, as a recent study demonstrate the atypical response of B-1 cells to BCR ligation (39). In this report it is mentioned that peritoneal B-1a cells manifest unusual signaling characteristics that distinguish them from B-2 cells (39). These include the failure of BCR engagement to trigger NF-κB activation and DNA replication given the central role for phosphatase activity. B-1a cells are unable to induce NF-κB or proliferate after BCR cross-linking due to increased phosphatase abundance or activity. This phosphatase abundance and/or activity may be the result of unique B-1a cell characteristics such as increased levels of HSP70 and/or constitutive secretion of IL-10. Furthermore, constitutively active Lyn also plays a negative regulatory role in B-1a cells.

B-1a cells have been shown to secrete natural antibodies in mice. These antibodies are primarily IgM isotype (40, 41). As Siglec-$G^{-/-}$ mice had more B-1a cells, their IgM titers in serum were also higher than WT mice (7, 27). Interestingly, there were no differences in the production of other isotypes of Ig when compared to WT controls. Moreover, the Siglec-$G^{-/-}$ mice had a greater number of IgM-secreting cells both in the bone marrow and in the spleen. The number of IgG-secreting cells was not found to be different. No differences were found in the numbers and structure of B cell follicles in Siglec-$G^{-/-}$ spleen and in WT spleen when stained for sialoadhesin and anti-IgM. Normal B cell numbers were noted in the marginal zone as well. However, Siglec-$G^{-/-}$ sections were noted to show greater extrafollicular IgM-secreting plasma cells compared to WT sections (7, 42, 43).

Intriguingly, the Siglec-$G^{-/-}$ B-1a cells were noted to have an altered BCR repertoire compared with wild-type B-1a cells (37). The BCR repertoire and the VDJ composition of Igs of Siglec-$G^{-/-}$ B-1a cells is similar to the Abs produced by adult bone marrow-derived B cells rather than canonical fetal liver-derived B-1a cells. This suggests that differentiation of precursors into the B-1a cell population is altered in Siglec-G-deficient mice. Holodick et al. showed that B-1a cells from older mice have higher amounts of N-region additions compared to B-1a cells from younger mice (44), which could cause altered naïve B-1a cells- and natural IgM-mediated protective outcomes during infection. Further studies are needed to define the phenotypic and functional aspects of B-1a cells derived from wild-type vs Siglec-G-deficient mice.

Upon BCR stimulation, B-1 cells generally do not have as robust of a response as B-2 cells (45, 46). Anti-IgM antibodies cause weakened Ca^{++} signaling and cellular proliferation in B-1a cells as compared to B-2 cells (8, 46). On the other hand, B-1a cells have a pre-activated phenotype demonstrating increased expression of cell surface activation markers and show pre-activation of signaling pathways such as the ERK and NFATc1 (46, 47). Therefore, besides BCR-mediated signaling as it is weakly responsive in B-1a cells, studying other pathways in B-1a cells needs to be further emphasized. A growing body of literature has elucidated the function of Siglec-G on the regulation of BCR signaling, while the studies on Siglec-G's effects on innate immune sensors like PRRs were mostly overlooked. Since B-1a cells produce both anti- as well as pro-inflammatory mediators (15), studies on the impact of Siglec-G on the expression of pro- and anti-inflammatory mediators in B-1a cells in sepsis would be of great interest.

SIALIC ACID-BINDING IMMUNOGLOBULIN-TYPE LECTIN-G-MEDIATED SIGNAL TRANSDUCTION IN MYELOID CELLS

Siglec-G is expressed in myeloid cells, i.e., DCs and macrophages (6, 48), where it plays an essential role. The first report of the effects of Siglec-G in myeloid cells was determined in DCs, in which it was shown to attenuate DAMPs-, but not PAMPs-mediated inflammation in sterile liver injury (12). This addresses the pivotal question of how our immune system distinguishes between DAMPs and PAMPs signals (49). The glycoprotein

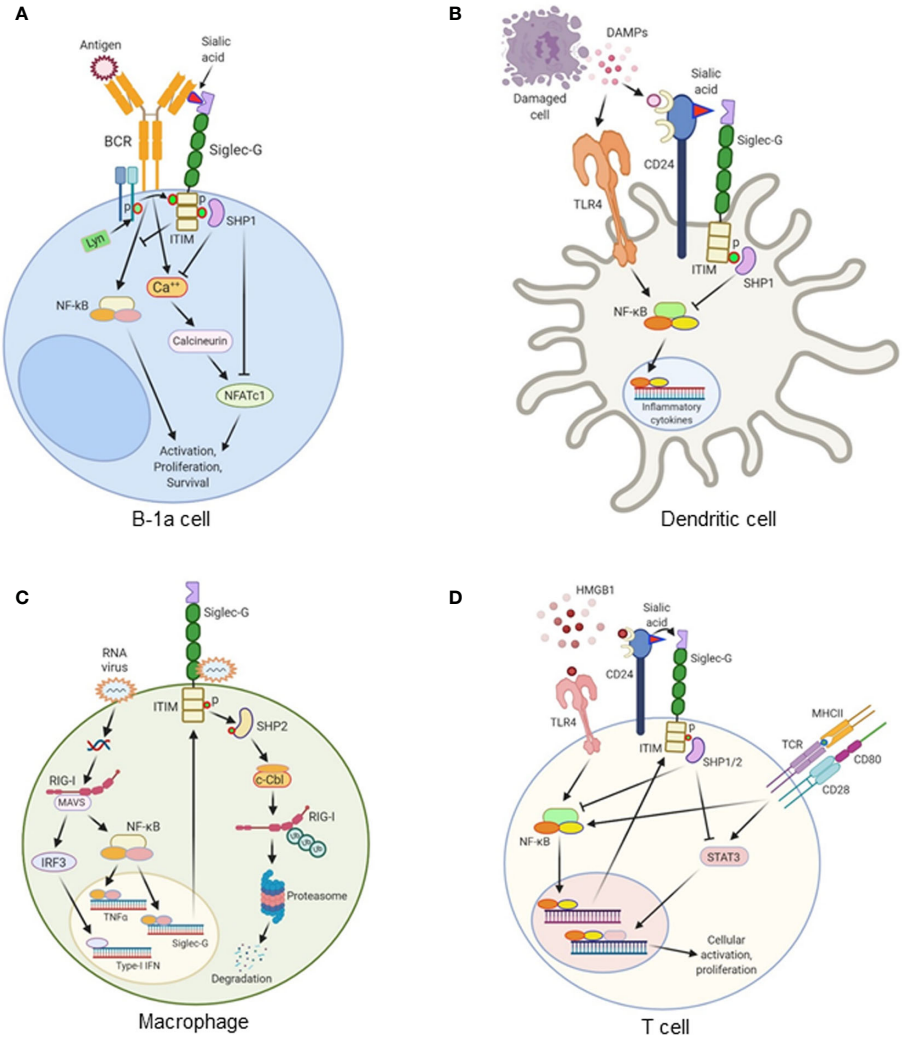

FIGURE 2 | The role of Siglec-G in various immune cells. **(A)** Antigen recognition by the B cell receptor (BCR) on B-1a cells triggers a Ca^{++} influx and activates NFATc1 *via* calcineurin. This leads to the survival, proliferation, and activation of B-1a cells. Siglec-G is recruited to the antigen-activated mIgM, where it binds sialic acid moieties on the mIgM. The ITIM domain of Siglec-G is phosphorylated by Lyn kinase, resulting in the recruitment of the tyrosine phosphatase SHP1, inhibiting both mIgM-induced Ca^{++} signaling and NFATc1 expression. Siglec-G also inhibits NF-κB activation and regulates NF-κB-dependent B-1a cells activation, proliferation, and survival. **(B)** Damage-associated molecular patterns (DAMPs) like HMGB1, HSP70, and HSP90 are released from damaged cells during sterile or infectious inflammation. DAMPs are recognized by TLRs, which subsequently activates NF-κB and increases the expression of proinflammatory cytokines. CD24 expressed on the surface of dendritic cells (DCs) binds DAMPs. CD24 also binds to Siglec-G, thereby forming a tri-molecular complex. This leads to the activation of SHP1 through Siglec-G-mediated signaling. SHP1 inhibits DAMPs-mediated activation of NF-κB, ultimately leading to the decreased production of pro-inflammatory cytokines. **(C)** In macrophages, double-stranded RNA viruses enter into the cells and recognize RIG-1 coupled with MAVS receptors and activate the transcription factors NF-κB and IRF3. NF-κB increases the expression of Siglec-G as a positive feedback loop mechanism, and increases the expression of pro-inflammatory cytokines. IRF3 increases the expression of type I IFNs. RNA viruses also bind to Siglec-G and activates its associated SHP2, which causes Cbl-dependent ubiquitylation and proteasomal degradation of RIG-I, leading to the suppression of IFNβ expression through a negative feedback loop. **(D)** HMGB1 induces TCR-, and CD28-mediated T cell activation, proliferation, and cytokine production through TLR4-NF-κB- and STAT3-dependent pathway. HMGB1 increases Siglec-G expression through TLR4-NF-κB pathway. HMGB1 binds to CD24, and CD24 binds to Siglec-G. This tri-molecular complex activates SHP1 and SHP2 to inhibit NF-κB and STAT3 activation, leading to the decreased cellular activation and proliferation.

receptor CD24 is expressed at high levels in hematopoietic cells and plays a critical role in Siglec-G mediated immunoregulatory function (12). It is unlikely that CD24 and Siglec-G act directly on hepatocytes as there is currently no evidence showing these cells express Siglec-G. DCs respond to HMGB1, a putative DAMP, and express both CD24 and Siglec-G. In sterile liver injury, HMGB1 levels are elevated in the liver to further aggravate inflammation and liver injury. However, HMGB1-mediated liver injury was greatly reduced and the mice were protected from lethal injury by the presence of Siglec-G in hematopoietic cells (12). CD24 has been found to only bind with Siglec-G or -10, but not with other Siglecs. CD24 also binds to the B-box motif of HMGB1. As such,

CD24, Siglec-G and HMGB1 form a tri-molecular complex. This generates a downstream signaling through the ITIM motif of Siglec-G to activate SHP1, a known negative regulator of NF-κB, thereby inhibiting HMGB1-mediated pro-inflammatory cytokine production (12). Both LPS and HMGB1 induce nuclear translocation of NF-κB p65 in wild-type DCs; however, in CD24 or Siglec-G-deficient DCs, HMGB1 can induce higher levels of p65 nuclear translocation compared to LPS. They also provided survival data to mimic clinical outcomes which showed worse outcomes in $CD24^{-/-}$ mice in the liver ischemia model, while the survival rates were not affected between WT and $CD24^{-/-}$ or Siglec-$G^{-/-}$ mice after LPS injection. This reflects the fact that CD24 and Siglec-G negatively regulate immune responses to HMGB1, HSP70, and HSP90, but not to LPS and poly I:C (12). These findings suggest that the CD24-Siglec-G pathway will preferentially dampen the response to DAMPs without having an impact on PAMP signaling by selective repression of NF-κB activation. In addition to a nuclear DAMP like HMGB1, DCs also respond to cytoplasmic DAMPs such as HSP70 and HSP90 through a TLR-dependent pathway (12, 49). CD24 has been found to bind both HSP70 and HSP90. Similar to HMGB1, the association of Siglec-G with HSP70 and HSP90 requires CD24. $CD24^{-/-}$ and Siglec-$G^{-/-}$ DCs have been shown to produce significantly higher amounts of IL-6 and TNF-α in response to recombinant HSP70 and HSP90 compared to wild-type DCs. These data show that CD24 and Siglec-G are crucial surface proteins involved in the negative regulation of DCs response to several different DAMPs (**Figure 2B**).

Besides DCs, the effects of Siglec-G-CD24 pathway in macrophages for inhibiting DAMPs-mediated inflammation is also evident. Siglec-G expression is upregulated on macrophages in an NF-κB- or retinoic acid-inducible gene-I (RIG-1)-dependent manner following infection by RNA viruses such as vesicular stomatitis virus (VSV), but not DNA viruses or bacteria (26). The upregulation of Siglec-G results in SHP2 and Cbl-dependent ubiquitylation and subsequent proteasomal degradation of RIG-I as well as the suppression of the interferon β (IFNβ) response (**Figure 2C**). Due to the detrimental effects of type I IFN in murine polymicrobial sepsis, Siglec-G-mediated inhibition of the production of type I IFN by macrophages in sepsis could be beneficial. Interestingly, the suppression of VSV-triggered IFNβ *via* Siglec-G does not require CD24 nor is it affected by sialidase treatment of the macrophages, suggesting it is sialic acid-independent. Degradation of sialic acid moieties may not be required as the Siglec-G receptors appear to retain phosphorylation of their ITIM domains and subsequently recruit SHP2 after VSV infection (26).

Prior reports reveled that Siglec-G attenuates DAMPs, but not PAMPs induced inflammatory responses. However, a recent study determined the direct interactions between various Siglecs and PRRs (50). Human Siglec-5/9 and mouse Siglec-3/E/F have been shown to bind to some TLRs. Mouse Siglec-G was not shown to interact directly with any TLRs tested. Correspondingly, the deletion of Siglec-E resulted in an augmented dendritic cell response to all microbial TLR ligands tested, while Siglec-G deletion did not show evidence of an altered response. TLR4 activation results in the translocation of neuraminidase 1 (Neu1) to the cell surface, disrupting the interaction between TLR4 and Siglec-E. Conversely, treatment with the sialidase inhibitor Neu5Gc2en resulted in preservation of TLR4-Siglec E/F interactions. Preservation of the sialic acid-TLR-Siglec interaction in mice lacking Neu1 or treated with the sialidase inhibitor Neu5Gc2en resulted in protection from endotoxemia (50). These findings suggest that sialidase mediated de-repression or Siglec mediated repression of TLR function could result in positive feedback of TLR activation. During bacterial infection, both PAMPs and DAMPs fuel inflammation. At first, PAMPs induce tissue damage, causing a release of DAMPs to further exaggerate inflammation. Even though Siglec-G does not exhibit direct interaction with PAMPs, it recognizes DAMPs through a tri-molecular complex with CD24 and inhibits inflammation (12).

THE ROLE OF SIALIC ACID-BINDING IMMUNOGLOBULIN-TYPE LECTIN-G IN T CELLS

T cells express Siglec-G, and its expression is increased upon stimulation with HMGB1 (51). While Siglec-G plays a pivotal role in B cell development and proliferation, it has no influence on T cell development or differentiation at homeostasis. Under normal conditions, Siglec-$G^{-/-}$ mice demonstrate no difference in numbers or distribution of naive, central memory, effector memory, or Treg cells. Nonetheless, Siglec-$G^{-/-}$ T cells demonstrated significantly augmented rates of cellular proliferation in the presence of HMGB1 and anti-CD3/CD28 Abs when compared with Siglec-$G^{-/-}$ T cells lacking stimulation from DAMPs (51). Siglec-G regulates the HMGB1's effects on T cells through ITIM and SHP1 and SHP2 pathways (**Figure 2D**). STAT3 is activated in HMGB1 treated Siglec-$G^{-/-}$ T cells, while the lymphocyte-specific protein tyrosine kinase is not. Interestingly, in the presence of HMGB1, Siglec-$G^{-/-}$ T cells had elevated markers of activation, but had no difference in the expression of exhaustion markers such as programmed cell death protein-1 (PD-1), T cell immunoreceptor with Ig and ITIM domains (TIGIT), or lymphocyte-activation gene 3 (Lag3) when compared with wild-type T cells (51). Therefore, Siglec-G/ITIM signaling is required to control DAMP-mediated increase of the activation signaling or the exhaustion markers. These findings shed light on the pathobiology of graft-versus-host disease (GVHD) in which a T cell-autonomous role is critical for modulating the severity of the T cell-mediated immunopathology (51). GVHD was ameliorated by treatment with the CD24Fc fusion protein, enhancing the Siglec-G signaling in donor T. As such, Siglec-G may serve as a potential therapeutic target in the treatment of GVHD (14, 51, 52).

Siglec-G inhibits antigen-presenting cells (APC) and cytotoxic T lymphocytes (CTL) interaction, thereby inhibiting CTL proliferation by inhibiting the formation of MHC class I peptides (53). In APC such as DCs, phagosome-expressed Siglec-G recruits the phosphatase SHP1, which dephosphorylates the NADPH oxidase component

p47(phox) and inhibits the activation of NOX2 on phagosomes. The inhibition of NOX2 results in reduced cross-presentation to CTLs by hydrolyzing foreign antigens and diminishing antigen presentation *via* MHC class-I peptides (53). Therefore, Siglec-G inhibits DC cross-presentation by impairing such complex formation, and this finding adds insight into the regulation of cross-presentation in adaptive immunity.

THE ROLE OF SIALIC ACID-BINDING IMMUNOGLOBULIN-TYPE LECTIN-G ON LEUKOCYTE MIGRATION DURING INFLAMMATION

During sepsis, leukocytes are recruited to inflamed tissues through their interaction with adhesion molecules present on endothelial cells (3, 54). Vascular adhesion protein-1 (VAP-1) is a glycoprotein expressed on inflamed endothelium with two crucial roles role: it has enzymatic activity resulting in the oxidation of primary amines and also serves as an adhesion molecule that is involved in leukocyte trafficking to sites of inflammation. Siglec-10 (the human homologue of murine Siglec-G) serves as a leukocyte ligand for VAP-1 (55). The interaction between Siglec-10 and VAP-1 results in a greater production of hydrogen peroxide, indicating that Siglec-10 serves as a substrate for VAP-1. Moreover, Siglec-10-VAP-1 interaction seems to mediate lymphocyte adhesion to the endothelium. This interaction may serve to modify the inflammatory microenvironment *via* production of various enzymatic end products (55). Since myeloid cells express Siglec-10 in human or -G in mice, elucidation of its role in enhancing the migration and infiltration of mononuclear cells in the inflamed tissues during sepsis is of interest.

Sepsis often causes acute kidney injury (AKI), which is characterized by excess accumulation of leukocytes (neutrophils and monocytes) into the kidneys to cause inflammation and tissue damage (56). As opposed to the above reports on VAP-1-Siglec-10-mediated lymphocyte migration during inflammation, a recent study demonstrates an indirect effect of Siglec-G as a negative regulator of leukocyte migration into the kidney tissues during AKI (57). After AKI, there is an increase in circulating and kidney B cells, particularly a $B220^{low}$ subset. These $B220^{low}$ B cells, presumably B-1 cells, produce the chemokine CCL7, which promotes infiltration of neutrophils and monocytes into the injured kidney parenchyma. Siglec-$G^{-/-}$ mice, which have increased numbers of $B220^{low}$ innate B cells, had increased levels of CCL7, augmented recruitment of neutrophils and monocytes to the kidney, and more severe AKI. A reduction in myeloid cell infiltration into the was noted after CCL7 blockade in AKI (57). These finding suggest that B cells may play a crucial role in the early sterile inflammation in AKI by producing leukocyte-recruiting chemokines. Siglec-G, by regulating the production of CCL7 by B-1 cells, inhibits leukocyte accumulation in kidneys in sepsis. As a result of the effects of Siglec-G in augmenting or inhibiting leukocyte migration, additional studies should be undertaken to gain a more detailed understanding of the mechanism of leukocyte migration during sepsis.

MODULATING SIALIC ACID-BINDING IMMUNOGLOBULIN-TYPE LECTIN-G FOR THERAPEUTIC APPROACHES IN SEPSIS

It has been shown that bacterial sialidases can remove sialic acid residues from CD24, resulting in an abrogation of the CD24-Siglec-G interaction in mice or CD24-Siglec-10 interaction in humans, leading to an augmentation of the inflammatory process (20). Therefore, inhibition of sialidase will result in a protection in mice from bacterial sepsis in a CD24-Siglec-G-dependent fashion. Studies on bacterial mutants lacking sialidase have confirmed the importance of this enzyme as a virulence factor in sepsis and demonstrate the importance of Siglec-G in controlling the inflammatory responses (20). Siglec-G participates in the attenuation of inflammatory responses for both pathogen and non-pathogen mediated signals. Two sialidase inhibitors, 2,3-dehydro-2-deoxy-N-acetylneuraminic acid (Neu5Ac2en) and 2,3-dehydro-2-deoxy-N-glycolylneuraminic acid (NeuGc2en) have been synthesized and their efficacy in treating polymicrobial sepsis has been tested (20). A combination of the two inhibitors resulted in complete inhibition of the sialidase activity in the sera of septic mice. This ultimately reflected decreased levels of multiple inflammatory cytokines and significantly reduced mortality in sepsis. The dependence on the CD24 and Siglec-G genes demonstrates a specificity of the inhibitors and suggests that the protection is likely achieved by preserving Siglec-G-CD24 interaction. Since septic patients are often treated with antibiotics, sialidase inhibitor therapy was administrated in conjunction with antibiotics. While antibiotic treatment alone had some impact on survival, the addition of sialidase inhibitors resulted in significantly increased survival in septic mice. These results indicate that treatment with sialidase inhibitors in conjunction with antibiotics have cellular implications exceeding potential inhibition of bacterial growth (20).

In light of the above promising finding of the treatment with the sialidase inhibitors in sepsis, a recent study developed a nanoparticle coated with di(α2→8) *N*-acetylneuraminic acid (NANA), which mimics sialic acid, the natural ligand for Siglec-E, which is predominantly expressed in hematopoietic cells such as macrophages and neutrophils (58). Treatment with the nanoparticle resulted in an augmentation of anti-inflammatory activity in culture as well as improving survival in multiple different mouse models, two generalized septic and one pulmonary injury. This nanoparticle has been shown to be effective in human macrophages and in an ex vivo model of human lung injury. In this study, we noticed that these NANA-coated NP provided protection in both LPS- and CLP-driven sepsis models, which was mediated through the Siglec-E pathway (58). However, two prior reports showed opposing outcomes with Siglec-G, in which Siglec-$G^{-/-}$ mice provided protection against CLP (20), but did not in LPS-induced model (13). These contradictory results in Siglec-$G^{-/-}$ mice may raise the possibility that since these NPs blocked both the CLP- and LPS-driven models of sepsis, promoting Siglec-G's function with sialic acid mimics may not be involved in the action of sialic acid mimics as Siglec-G deficiency has opposing impacts upon these two models. Spence et al. identified that IL-10 induced Siglec-E expression and α2,8 NANA-NP further

augmented the expression of IL-10 (58). Indeed, the effectiveness of the nanoparticle depended on IL-10. However, in the report by Li et al. showed that Siglec-G deficient mice or the macrophages had less TNFα and IL-6, but more IL-10 levels in the serum or supernatants compared to WT mice after treatment of mice or cells with LPS (13). Considering IL-10 as the key player in NANA-NP treated and Siglec-G deficient conditions to control LPS induced inflammation, further studies should be performed in mice strains and their age and gender matched conditions, because Li et al's findings on the beneficial outcomes of Siglec-$G^{-/-}$ mice in LPS induced survival did not correlate with the findings of Chen et al. (12), which showed no statistically significant beneficial outcomes in the survival rates between WT and Siglec-$G^{-/-}$ mice following LPS treatment. Moreover, prior studies have shown that HMGB1, CD24 and Siglec-G form a trimolecular complex that induces Siglec-G-mediated Shp1 activation to downregulate TLR4-mediated inflammation (20). Therefore, the treatment with NANA-containing NPs may bind Siglec-G and block the interaction of CD24 with Siglec-G, which may exhibit altered function other than that of Siglec-G-CD24-HMGB-1-mediated regulatory function.

Given the fact that Siglec-G binds to α2,3-linked or α2,6-linked sialic acid (α2,3Sia or α2,6Sia), the α2,8 NANA-NP may not bind to Siglec-G as efficiently as Siglec-E. But, this novel strategy can be further implemented to create α2,3Sia or α2,6Sia NP to specifically target Siglec-G in sepsis. These findings encourage further research to identify sialic acid containing endogenous peptides or glycoproteins to confer protection in microbial sepsis and cell damage-induced sterile inflammation. Potential therapeutic approaches and outcomes by modulating Siglec-G in sepsis are shown in **Table 1**.

CONCLUSION AND FUTURE DIRECTIONS

Siglec-G-mediated immunoregulatory functions in sepsis have been extensively studied in the context of myeloid cells. Given the significance of B-1a cells in sepsis, elucidation of Siglec-G's role in B-1a cells altering its phenotype and function in sepsis is vital. Recently, the phenotype, ontogeny, and function of human B-1a cells have been discovered (21). Therefore, determining the expression and function of Siglec-10, the human orthologue of murine Siglec-G in human B-1a cells in sepsis patients are important. The outbreak of COVID-19 in the US and worldwide has resulted in fatal outcomes for these patients. A recent perspective proposed treating COVID-19 with B-1a cells to mitigate the cytokine storm and eliminate viral loads by B-1a cell-produced IL-10 and natural IgM, respectively (59). Considering Siglec-G's immunomodulatory functions in B-1a cells and myeloid cells, studies on Siglec-G could be a promising area to elucidate the pathophysiology and therapeutic interventions of COVID-19.

Genetic polymorphism studies in humans provide unique opportunities to understand human biology and the mechanisms of diseases. These genetic studies have shown correlations between various human diseases and Siglec genes, for example the CD33 polymorphism is associated with Alzheimer's disease (5). Therefore, studying the genetic polymorphism of human Siglec-10 may benefit reinforcement by independent genetic replication or mechanistic studies in disease pathogenesis. Sialic acid is crucial in maximizing the phagocytic activity of cells (60). Treatment of polymorphonuclear cells with bacterial neuraminidases completely abolishes stimulation of phagocytic activity. Given the importance of membrane sialic acid for stimulation of phagocytosis, Siglec-G's role as a cis- and trans-acting receptor to enhance phagocytosis should be elucidated in sepsis, because impaired efferocytosis is a hallmark of sepsis (3). In chronic inflammatory and autoimmune diseases, B-1a cells are found to be detrimental (61). Studies have shown that peritoneal B-1a cells proliferate and collect in inflamed joint tissue with upregulated receptor activator of nuclear factor kappa-β ligand (RANKL) expression during collagen-induced arthritis development in mice (62). Since Siglec-G regulates BCR signaling and helps maintain a normal B-1a cell pool, its role in B-1a cell mediated chronic inflammatory diseases could be promising. The impact of Siglec-G in immune cells with a wide range of DAMPs stimulation should be assessed. Extracellular CIRP was recently described as a novel DAMP (63). Identification of the role of eCIRP on Siglec-G in B-1a cells and beyond, in terms of the production of pro-inflammatory mediators in sepsis, will help broaden our understanding of the pathophysiology of sepsis. This review demonstrates the immunoregulatory functions of Siglec-G in B-1a cells, myeloid, and lymphoid cells in sepsis, which ultimately

TABLE 1 | Therapeutic outcomes by modulating Siglec-G in sepsis.

Therapeutic approaches	Inflammatory/injury outcomes	Survival outcomes	References
Siglec-$G^{-/-}$ mice in CLP model	Siglec-$G^{-/-}$ mice significantly increased the levels of IL-6, MCP-1, and TNFα in the serum; serum bacterial loads were same in WT vs Siglec-$G^{-/-}$ mice; lungs, liver, and kidney injuries were aggravated in Siglec-$G^{-/-}$ mice.	Survival rates of Siglec-$G^{-/-}$ mice in both with or without antibiotic treated conditions were declined.	(12, 20)
Siglec-$G^{-/-}$ mice in endotoxemia (LPS) model	Siglec-$G^{-/-}$ mice showed decreased levels of IL-6 and TNFα and increased levels of IL-10 in the serum; Siglec-$G^{-/-}$ mice had less severe lung injury.	Siglec-$G^{-/-}$ mice showed improved survival outcomes in endotoxemia model.	(13)
Sialidase inhibitors: Neu5Ac2en (AC) and Neu5Gc2en (GC)	AC + GC treatment decreased serum levels of IL-6, MCP-1, and TNFα, but had no effect on reducing blood bacterial contents.	AC + GC treatment improved survival rates in both with or without antibiotic treated conditions.	(20)
Sialidase inhibitor:Neu5Gc2en	Inhibited IL-6 and TNFα levels in the serum.	Improved survival rates in LPS and *E. Coli* induced sepsis.	(50)
Nanoparticles decorated with Siglec ligand, di(α2→8) *N*-acetylneuraminicacid (α2,8 NANA-NP)	Decreased TNFα and increased IL-10 levels in the serum; decreased neutrophils in the lungs; reduced lung inflammation and injury.	Improved survival rates in both LPS- and CLP-induced sepsis models.	(58)

improves our understanding of the pathophysiology of sepsis for developing novel therapeutics against this deadly disease.

AUTHOR CONTRIBUTIONS

WR and MA wrote the manuscript. WR and PW reviewed and edited the draft. MA and PW conceived the idea and supervised the project. All authors contributed to the article and approved the submitted version.

FUNDING

This study was supported by the National Institutes of Health (NIH) grants R35GM118337 (PW) and R01GM129633 (MA).

REFERENCES

1. Singer M, Deutschman CS, Seymour CW, Shankar-Hari M, Annane D, Bauer M, et al. The Third International Consensus Definitions for Sepsis and Septic Shock (Sepsis-3). *JAMA* (2016) 315(8):801–10. doi: 10.1001/jama.2016.0287
2. Centers for Disease Control and Prevention. *Sepsis: data & reports*. Atlanta: Department of Health and Human Services (2016). Available at: https://www.cdc.gov/sepsis/datareports/index.html.
3. Aziz M, Jacob A, Yang WL, Matsuda A, Wang P. Current trends in inflammatory and immunomodulatory mediators in sepsis. *J Leukoc Biol* (2013) 93(3):329–42. doi: 10.1189/jlb.0912437
4. Denning NL, Aziz M, Gurien SD, Wang P. DAMPs and NETs in Sepsis. *Front Immunol* (2019) 10:2536:2536. doi: 10.3389/fimmu.2019.02536
5. Macauley MS, Crocker PR, Paulson JC. Siglec-mediated regulation of immune cell function in disease. *Nat Rev Immunol* (2014) 14(10):653–66. doi: 10.1038/nri3737
6. Pillai S, Netravali IA, Cariappa A, Mattoo H. Siglecs and immune regulation. *Annu Rev Immunol* (2012) 30:357–92. doi: 10.1146/annurev-immunol-020711-075018
7. Hoffmann A, Kerr S, Jellusova J, Zhang J, Weisel F, Wellmann U, et al. Siglec-G is a B1 cell-inhibitory receptor that controls expansion and calcium signaling of the B1 cell population. *Nat Immunol* (2007) 8(7):695–704. doi: 10.1038/ni1480
8. Nitschke L. Siglec-G is a B-1 cell inhibitory receptor and also controls B cell tolerance. *Ann N Y Acad Sci* (2015) 1362:117–21. doi: 10.1111/nyas.12826
9. Meyer SJ, Linder AT, Brandl C, Nitschke L. B Cell Siglecs-News on Signaling and Its Interplay With Ligand Binding. *Front Immunol* (2018) 9:2820. doi: 10.3389/fimmu.2018.02820
10. Jellusova J, Nitschke L. Regulation of B cell functions by the sialic acid-binding receptors siglec-G and CD22. *Front Immunol* (2011) 2:96. doi: 10.3389/fimmu.2011.00096
11. Ding C, Liu Y, Wang Y, Park BK, Wang CY, Zheng P. Siglecg limits the size of B1a B cell lineage by down-regulating NFkappaB activation. *PloS One* (2007) 2 (10):e997. doi: 10.1371/journal.pone.0000997
12. Chen GY, Tang J, Zheng P, Liu Y. CD24 and Siglec-10 selectively repress tissue damage-induced immune responses. *Science* (2009) 323(5922):1722–5. doi: 10.1126/science.1168988
13. Li W, Li Y, Qin K, Du B, Li T, Yuan H, et al. Siglec-G Deficiency Ameliorates Hyper-Inflammation and Immune Collapse in Sepsis via Regulating Src Activation. *Front Immunol* (2019) 10:2575. doi: 10.3389/fimmu.2019.02575
14. Toubai T, Hou G, Mathewson N, Liu C, Wang Y, Oravecz-Wilson K, et al. Siglec-G-CD24 axis controls the severity of graft-versus-host disease in mice. *Blood* (2014) 123(22):3512–23. doi: 10.1182/blood-2013-12-545335
15. Aziz M, Holodick NE, Rothstein TL, Wang P. The role of B-1 cells in inflammation. *Immunol Res* (2015) 63(1-3):153–66. doi: 10.1007/s12026-015-8708-3
16. Aziz M, Holodick NE, Rothstein TL, Wang P. B-1a Cells Protect Mice from Sepsis: Critical Role of CREB. *J Immunol* (2017) 199(2):750–60. doi: 10.4049/jimmunol.1602056
17. Rauch PJ, Chudnovskiy A, Robbins CS, Weber GF, Etzrodt M, Hilgendorf I, et al. Innate response activator B cells protect against microbial sepsis. *Science* (2012) 335(6068):597–601. doi: 10.1126/science.1215173
18. Weber GF, Chousterman BG, Hilgendorf I, Robbins CS, Theurl I, Gerhardt LM, et al. Pleural innate response activator B cells protect against pneumonia via a GM-CSF-IgM axis. *J Exp Med* (2014) 211(6):1243–56. doi: 10.1084/jem.20131471
19. Weber GF, Chousterman BG, He S, Fenn AM, Nairz M, Anzai A, et al. Interleukin-3 amplifies acute inflammation and is a potential therapeutic target in sepsis. *Science* (2015) 347(6227):1260–5. doi: 10.1126/science.aaa4268
20. Chen GY, Chen X, King S, Cavassani KA, Cheng J, Zheng X, et al. Amelioration of sepsis by inhibiting sialidase-mediated disruption of the CD24-SiglecG interaction. *Nat Biotechnol* (2011) 29(5):428–35. doi: 10.1038/nbt.1846
21. Quách TD, Hopkins TJ, Holodick NE, Vuyyuru R, Manser T, Bayer RL, et al. Human B-1 and B-2 B Cells Develop from Lin-CD34+CD38lo Stem Cells. *J Immunol* (2016) 197(10):3950–8. doi: 10.4049/jimmunol.1600630
22. Lawrence T. The nuclear factor NF-kappaB pathway in inflammation. *Cold Spring Harb Perspect Biol* (2009) 1(6):a001651. doi: 10.1101/cshperspect.a001651
23. Varki A, Gagneux P. Multifarious roles of sialic acids in immunity. *Ann N Y Acad Sci* (2012) 1253:16–36. doi: 10.1111/j.1749-6632.2012.06517.x
24. Liu SF, Malik AB. NF-kappa B activation as a pathological mechanism of septic shock and inflammation. *Am J Physiol Lung Cell Mol Physiol* (2006) 290:(4):L622–45. doi: 10.1152/ajplung.00477.2005
25. Brown MA, Jones WK. NF-kappaB action in sepsis: the innate immune system and the heart. *Front Biosci* (2004) 9:1201–17. doi: 10.2741/1304
26. Chen W, Han C, Xie B, Hu X, Yu Q, Shi L, et al. Induction of Siglec-G by RNA viruses inhibits the innate immune response by promoting RIG-I degradation. *Cell* (2013) 152(3):467–78. doi: 10.1016/j.cell.2013.01.011
27. Gruber S, Hendrikx T, Tsiantoulas D, Ozsvar-Kozma M, Göderle L, Mallat Z, et al. Sialic Acid-Binding Immunoglobulin-like Lectin G Promotes Atherosclerosis and Liver Inflammation by Suppressing the Protective Functions of B-1 Cells. *Cell Rep* (2016) 14(10):2348–61. doi: 10.1016/j.celrep.2016.02.027
28. Ghosh AK, Sinha D, Biswas R, Biswas T. Pathogen-associated porin turns IL-10 competent B-1a cells toward proinflammatory cytokine response. *Immunobiology* (2016) 221(12):1369–73. doi: 10.1016/j.imbio.2016.07.010
29. Stephenson HN, Mills DC, Jones H, Milioris E, Copland A, Dorrell N, et al. Pseudaminic acid on Campylobacter jejuni flagella modulates dendritic cell IL-10 expression via Siglec-10 receptor: a novel flagellin-host interaction. *J Infect Dis* (2014) 210(9):1487–98. doi: 10.1093/infdis/jiu287
30. Pillai S, Cariappa A. The follicular versus marginal zone B lymphocyte cell fate decision. *Nat Rev Immunol* (2009) 9(11):767–77. doi: 10.1038/nri2656
31. Martin F, Kearney JF. Marginal-zone B cells. *Nat Rev Immunol* (2002) 2 (5):323–35. doi: 10.1038/nri799
32. Hayakawa K, Hardy RR, Parks DR, Herzenberg LA. The "Ly-1 B" cell subpopulation in normal immunodefective, and autoimmune mice. *J Exp Med* (1983) 157(1):202–18. doi: 10.1084/jem.157.1.202
33. Montecino-Rodriguez E, Dorshkind K. B-1 B cell development in the fetus and adult. *Immunity* (2012) 36(1):13–21. doi: 10.1016/j.immuni.2011.11.017
34. Hardy RR, Hayakawa K. Developmental origins, specificities and immunoglobulin gene biases of murine Ly-1 B cells. *Int Rev Immunol* (1992) 8(2-3):189–207. doi: 10.3109/08830189209055573
35. Haas KM, Poe JC, Steeber DA, Tedder TF. B-1a and B-1b cells exhibit distinct developmental requirements and have unique functional roles in innate and adaptive immunity to S. pneumoniae. *Immunity* (2005) 23(1):7–18. doi: 10.1016/j.immuni.2005.04.011
36. Wu L, Dalal R, Cao CD, Postoak JL, Yang G, Zhang Q, et al. IL-10-producing B cells are enriched in murine pericardial adipose tissues and ameliorate the

outcome of acute myocardial infarction. *Proc Natl Acad Sci USA* (2019) 116 (43):21673–84. doi: 10.1073/pnas.1911464116
37. Jellusova J, Düber S, Gückel E, Binder CJ, Weiss S, Voll R, et al. Siglec-G regulates B1 cell survival and selection. *J Immunol* (2010) 185(6):3277–84. doi: 10.4049/jimmunol.1001792
38. Hutzler S, Özgör L, Naito-Matsui Y, Kläsener K, Winkler TH, Reth M, et al. The ligand-binding domain of Siglec-G is crucial for its selective inhibitory function on B1 cells. *J Immunol* (2014) 192(11):5406–14. doi: 10.4049/jimmunol.1302875
39. Holodick NE, Rothstein TL. Atypical Response of B-1 Cells to BCR Ligation: A Speculative Model. *Front Immunol* (2013) 4:457. doi: 10.3389/fimmu.2013.00457
40. Baumgarth N. B-1 Cell Heterogeneity and the Regulation of Natural and Antigen-Induced IgM Production. *Front Immunol* (2016) 7:324. doi: 10.3389/fimmu.2016.00324
41. Nguyen TT, Elsner RA, Baumgarth N. Natural IgM prevents autoimmunity by enforcing B cell central tolerance induction. *J Immunol* (2015) 194(4):1489–502. doi: 10.4049/jimmunol.1401880
42. Müller J, Lunz B, Schwab I, Acs A, Nimmerjahn F, Daniel C, et al. Siglec-G Deficiency Leads to Autoimmunity in Aging C57BL/6 Mice. *J Immunol* (2015) 195(1):51–60. doi: 10.4049/jimmunol.1403139
43. Jellusova J, Wellmann U, Amann K, Winkler TH, Nitschke L. CD22 x Siglec-G double-deficient mice have massively increased B1 cell numbers and develop systemic autoimmunity. *J Immunol* (2010) 184(7):3618–27. doi: 10.4049/jimmunol.0902711
44. Holodick NE, Repetny K, Zhong X, Rothstein TL. Adult BM generates CD5+ B1 cells containing abundant N-region additions. *Eur J Immunol* (2009) 39 (9):2383–94. doi: 10.1002/eji.200838920
45. Cyster JG, Allen CDC. B Cell Responses: Cell Interaction Dynamics and Decisions. *Cell* (2019) 177(3):524–40. doi: 10.1016/j.cell.2019.03.016
46. Baumgarth N. A Hard(y) Look at B-1 Cell Development and Function. *J Immunol* (2017) 199(10):3387–94. doi: 10.4049/jimmunol.1700943
47. Rothstein TL, Griffin DO, Holodick NE, Quach TD, Kaku H. Human B-1 cells take the stage. *Ann N Y Acad Sci* (2013) 1285:97–114. doi: 10.1111/nyas.12137
48. Chen GY, Brown NK, Zheng P, Liu Y. Siglec-G/10 in self-nonself discrimination of innate and adaptive immunity. *Glycobiology* (2014) 24 (9):800–6. doi: 10.1093/glycob/cwu068
49. Liu Y, Chen GY, Zheng P. CD24-Siglec G/10 discriminates danger- from pathogen-associated molecular patterns. *Trends Immunol* (2009) 30(12):557–61. doi: 10.1016/j.it.2009.09.006
50. Chen GY, Brown NK, Wu W, Khedri Z, Yu H, Chen X, et al. Broad and direct interaction between TLR and Siglec families of pattern recognition receptors and its regulation by Neu1. *Elife* (2014) 3:e04066. doi: 10.7554/eLife.04066
51. Toubai T, Rossi C, Oravecz-Wilson K, Zajac C, Liu C, Braun T, et al. Siglec-G represses DAMP-mediated effects on T cells. *JCI Insight* (2017) 2(14):e92293. doi: 10.1172/jci.insight.92293
52. Toubai T, Mathewson ND, Magenau J, Reddy P. Danger Signals and Graft-versus-host Disease: Current Understanding and Future Perspectives. *Front Immunol* (2016) 7:539:539. doi: 10.3389/fimmu.2016.00539
53. Ding Y, Guo Z, Liu Y, Li X, Zhang Q, Xu X, et al. The lectin Siglec-G inhibits dendritic cell cross-presentation by impairing MHC class I-peptide complex formation. *Nat Immunol* (2016) 17(10):1167–75. doi: 10.1038/ni.3535
54. Nourshargh S, Alon R. Leukocyte migration into inflamed tissues. *Immunity* (2014) 41(5):694–707. doi: 10.1016/j.immuni.2014.10.008
55. Kivi E, Elima K, Aalto K, Nymalm Y, Auvinen K, Koivunen E, et al. Human Siglec-10 can bind to vascular adhesion protein-1 and serves as its substrate. *Blood* (2009) 114(26):5385–92. doi: 10.1182/blood-2009-04-219253
56. Peerapornratana S, Manrique-Caballero CL, Gómez H, Kellum JA. Acute kidney injury from sepsis: current concepts, epidemiology, pathophysiology, prevention and treatment. *Kidney Int* (2019) 96(5):1083–99. doi: 10.1016/j.kint.2019.05.026
57. Inaba A, Tuong ZK, Riding AM, Mathews RJ, Martin JL, Saeb-Parsy K, et al. B Lymphocyte-Derived CCL7 Augments Neutrophil and Monocyte Recruitment, Exacerbating Acute Kidney Injury. *J Immunol* (2020) 205 (5):1376–84. doi: 10.4049/jimmunol.2000454
58. Spence S, Greene MK, Fay F, Hams E, Saunders SP, Hamid U, et al. Targeting Siglecs with a sialic acid-decorated nanoparticle abrogates inflammation. *Sci Transl Med* (2015) 7(303):303ra140. doi: 10.1126/scitranslmed.aab3459
59. Aziz M, Brenner M, Wang P. Therapeutic Potential of B-1a Cells in COVID-19. *Shock* (2020) 54(5):586–94. doi: 10.1097/SHK.0000000000001610
60. Constantopoulos A, Najjar VA. The requirement of membrane sialic acid in the stimulation of phagocytosis by the natural tetrapeptide, tuftsin. *J Biol Chem* (1973) 248(11):3819–22.
61. Duan B, Morel L. Role of B-1a cells in autoimmunity. *Autoimmun Rev* (2006) 5(6):403–8. doi: 10.1016/j.autrev.2005.10.007
62. Deng J, Wang X, Chen Q, Sun X, Xiao F, Ko KH, et al. B1a cells play a pathogenic role in the development of autoimmune arthritis. *Oncotarget* (2016) 7(15):19299–311. doi: 10.18632/oncotarget.8244
63. Qiang X, Yang WL, Wu R, Zhou M, Jacob A, Dong W, et al. Cold-inducible RNA-binding protein (CIRP) triggers inflammatory responses in hemorrhagic shock and sepsis. *Nat Med* (2013) 19(11):1489–95. doi: 10.1038/nm.3368

Conflict of Interest: The authors declare that the research was conducted in the absence of any commercial or financial relationships that could be construed as a potential conflict of interest.

frontiers in Immunology

SYSTEMATIC REVIEW
published: 25 February 2021
doi: 10.3389/fimmu.2021.622601

Potential Targets to Mitigate Trauma- or Sepsis-Induced Immune Suppression

*Christian B. Bergmann[1], Nadine Beckmann[1], Christen E. Salyer[1], Marc Hanschen[2,3], Peter A. Crisologo[4] and Charles C. Caldwell[1,5]**

[1] Division of Research, Department of Surgery, College of Medicine, University of Cincinnati, Cincinnati, OH, United States, [2] Experimental Trauma Surgery, Klinikum rechts der Isar, Technical University of Munich, Munich, Germany, [3] Department of Trauma Surgery, Klinikum rechts der Isar, Technical University of Munich, Munich, Germany, [4] Division of Podiatric Medicine and Surgery, Critical Care, and Acute Care Surgery, Department of Surgery, College of Medicine, University of Cincinnati, Cincinnati, OH, United States, [5] Division of Research, Shriners Hospital for Children, Cincinnati, OH, United States

In sepsis and trauma, pathogens and injured tissue provoke a systemic inflammatory reaction which can lead to overwhelming inflammation. Concurrent with the innate hyperinflammatory response is adaptive immune suppression that can become chronic. A current key issue today is that patients who undergo intensive medical care after sepsis or trauma have a high mortality rate after being discharged. This high mortality is thought to be associated with persistent immunosuppression. Knowledge about the pathophysiology leading to this state remains fragmented. Immunosuppressive cytokines play an essential role in mediating and upholding immunosuppression in these patients. Specifically, the cytokines Interleukin-10 (IL-10), Transforming Growth Factor-β (TGF-β) and Thymic stromal lymphopoietin (TSLP) are reported to have potent immunosuppressive capacities. Here, we review their ability to suppress inflammation, their dynamics in sepsis and trauma and what drives the pathologic release of these cytokines. They do exert paradoxical effects under certain conditions, which makes it necessary to evaluate their functions in the context of dynamic changes post-sepsis and trauma. Several drugs modulating their functions are currently in clinical trials in the treatment of other pathologies. We provide an overview of the current literature on the effects of IL-10, TGF-β and TSLP in sepsis and trauma and suggest therapeutic approaches for their modulation.

Keywords: IL-10, transforming growth factor β, thymic stromal lymphopoietin, immunosuppression, chronic critical illness

OPEN ACCESS

Edited by:
Marcin Filip Osuchowski, Ludwig Boltzmann Institute for Experimental and Clinical Traumatology, Austria

Reviewed by:
Timothy Paul Moran, University of North Carolina at Chapel Hill, United States
Je-Wook Yu, Yonsei University, South Korea

***Correspondence:**
Charles C. Caldwell
charles.caldwell@uc.edu

Specialty section:
This article was submitted to Inflammation, a section of the journal Frontiers in Immunology

Received: *28 October 2020*
Accepted: *11 January 2021*
Published: *25 February 2021*

Citation:
Bergmann CB, Beckmann N, Salyer CE, Hanschen M, Crisologo PA and Caldwell CC (2021) Potential Targets to Mitigate Trauma- or Sepsis-Induced Immune Suppression. Front. Immunol. 12:622601. doi: 10.3389/fimmu.2021.622601

IMMUNE PERTURBATION IN SEPSIS AND TRAUMA

Infection and injury can lead to an increase of alarm signals that signal the presence of invading pathogens or injured tissue. The so called `danger hypothesis` was developed by Matzinger et al. stating that alarmins are either Pathogen-Associated Molecular Patterns (PAMPs) or Damage-Associated Molecular Patterns (DAMPs) (1). Either may trigger inflammation by recognition through Pattern Recognition Receptors (PPRs) on innate and adaptive immune cells (2). Within

these cells, the nuclear translocation of the transcription factor Nuclear Factor kappa beta (NF-κB) promotes pro-inflammatory cytokine production to include IL-1 and TNF-α (3). These cytokines act upon a variety of target cells (4) that can begin a cascade of increasing pro-inflammatory cytokines, such as IL-6, IL-8, and MIF (5). Increased production of these cytokines can result in the induction of fever (6), the upregulation of adhesion receptors like ICAM-1 on endothelial cells (7), increased L-selectin (CD62L) on lymphocyte cells (8) and neutrophil mobilization. Excessive inflammation can lead to excessive damage tissue and organs, e.g. by the release of radicals by neutrophils (9) to include the lungs, heart, kidney, liver and brain (10). In addition, disseminated intravascular coagulation (DIC) and thrombocytopenia (11) can occur, which are known to contribute to multiple organ dysfunction syndrome (MODS) (12). This cytokine driven initial inflammation can lead to early death if not compensated (13).

Concurrent with the pro-inflammatory response, there is evidence of a number of immune suppressive events occurring. These include the loss of conventional T lymphocytes (14) simultaneous with the lack of regulatory T cell apoptosis (15), the increased number of myeloid suppressor cells (16) coupled with the down regulation of monocyte HLA-Dr (17), and a loss of dendritic cells (18). Additionally, there are increases in immune suppressive cytokines such as IL-10, TGF-ß, and TSLP. Significant immune suppression can impair the proper clearance of pathogens leading to higher bacterial loads both systemically and in tissues. According to a recent clinical observational cohort study, septic patients can develop chronic critical illness, with a 6-month survival of 63%, and continue to demonstrate cytokine profiles of chronic inflammation, as well as biomarker profiles characteristic for persistent immunosuppression (19). Additionally, these patients very often require treatment in long term acute care facilities, and by one year after hospital discharge half of them have died and another quarter remains bedridden (20). Elder patients are more likely to develop these immune disbalances (21). It is therefore key to better understand these pathophysiologies as they become an increasing problem for aging societies (22). It is beyond the scope of this review to detail the entire host response to sepsis and this topic is covered in a number of other reviews (23–25). Here, this review focuses upon release, impact, and potential therapy of a limited number of potent anti-inflammatory cytokines.

MEDIATORS OF IMMUNOSUPPRESSION

The initial upregulation of inflammation after onset of infection or injury results in the activation of the innate immune system, mostly of neutrophils and macrophages *via* Toll like receptors (TLRs) (26, 27). Orchestrated by T cells, they maintain inflammation by the release of pro-inflammatory cytokines such as TNF-α, IL-6, IL-8, MCP-1, MIP-1α (28, 29), among which IL-6 plays a prominent role as it is associated with injury severity (30), MODS and death (31). At the same time, immunosuppression is induced (13), which is strongly driven by anti-inflammatory cytokine release (32). Immunosuppression is characterized by the induction of immunosuppressive functions and partial impairment of pro-inflammatory functions of innate and adaptive immune cells: lymphopenia occurs as the number of circulating lymphocytes decreases due to apoptosis of CD4 and CD8 T cells, B cells, and NK cells (33), Regulatory T cells numbers increase after sepsis or trauma (34, 35), T cells become exhausted and anergic (36, 37), monocytes, macrophages and dendritic cells become impaired in their ability to mount a proinflammatory response (22, 38, 39), neutrophil dysfunction ensues (40) and increased release and activation of immunosuppressive Myeloid Derived Suppressor Cells (MDSCs) is triggered (41). These cells, along with other tissue cells, such as endothelial cells, potently mediate immunosuppression by the release of anti-inflammatory cytokines. The cytokines IL-10, TGF-β and TSLP all exert potent anti-inflammatory functions (42–44). In trauma and sepsis, IL-10 is considered a key immunosuppressive cytokine and correlates with injury severity and outcomes (45) and is widely examined in sepsis and trauma studies. However, it has been demonstrated that all three cytokines also exert pro-inflammatory functions under certain conditions (46–48). This seems contradictory as they are considered key regulators of immunity. In the following chapters, we will review their immunosuppressive mechanisms and dynamics in sepsis and trauma. Finally, the pathological conditions in sepsis and trauma that may drive a detrimental release of these cytokines will be examined.

IMMUNOSUPPRESSIVE CYTOKINES: IL-10, TGF-β, AND TSLP

IL-10

How Does IL-10 Affect Immune Cells?

With its potent anti-inflammatory functions IL-10 is considered an important regulatory cytokine protecting the host from exaggerated inflammation, autoimmunity and allergy (49, 50). It is a V-shaped homodimer and has a molecular weight of 37 kDa (51) and it is a key member of the IL-10 superfamily which consists of IL-19, IL-20, IL-22, IL-24, IL-26 and the type III IFN-γ subfamily (51).

In sepsis and trauma, IL-10 mainly affects immune cells rather than tissue cells, which do not express the IL-10-receptor (IL-10R) to the same extent. Tissue cells are more affected by other member of the IL-10 super family, particularly IL-22 (50). Many variants of the IL-10 gene exist, and an increasing body of literature suggests that IL-10 gene polymorphisms play an important role in different pathological conditions (52). Tumor cells can also produce IL-10 and it is thought that this allows the tumor to mitigate an effective immune response (51).

The IL-10 receptor is a composition of the IL-10R2 and IL-10R1 subunits, with the latter being expressed mainly on immune cells. The expression of the receptor differs from cell type to cell type. For example, some monocytes and macrophages express very high amounts of the receptor, and the expression in

memory T cells is higher than in naïve CD4 T cells (53). The IL-10 cytokine binds to IL-10R1, which subsequently forms a complex with IL-10R2. It is of note that IL-10 can bind to IL-10R1 alone but not to IL-10R2. However, the affinity for the complex is much higher than for IL-10R1 alone (54). The IL-10 receptor complex then phosphorylates STAT3 *via* Jak1 and Tyk2 activation but also STAT1 and STAT5. Among these, STAT3 seems to be most important for modulating the downstream transcription of target genes (42, 51, 54). It is of importance that STAT3 also acts downstream from IL-6, so the resulting modulation depends on A) the cell type, B) the competing stimuli the cell receives and C) the duration of the stimuli (42, 51, 54). Inflammation is potently suppressed by IL-10 through inhibition of NF-κB DNA binding activity (53). IL-10 also hinders TLR signaling through induction of inhibitory miRNAs targeting MyD88-dependent TLR4 signaling and through promoting the ubiquitin-mediated degradation of IRAK1/4 and TRAF6. MyD88-independent attenuation was also reported (55). On a translational level, IL-10 leads to an increase of tristetrapoline, a protein which downregulates mRNA of pro-inflammatory cytokines and can be down-regulated itself in TLR-dependent pathways (55). However, IL-10R binding also limits its own effect by inducing suppressor of cytokine signaling (SOCS)3, which forms a negative feedback loop by inhibiting, amongst others, STAT3 phosphorylation (56). IL-10 also suppresses the production of pro-inflammatory cytokines TNF-α, IL-1, IL-5, IL-8, IL-12, GM-CSF, MIP-1α and MIP-2α in monocytes, macrophages, neutrophils and NK cells (57).

A wide range of immune cells can produce IL-10, such as dendritic cells (DCs), macrophages, mast cells, natural killer cells (NK), eosinophils, neutrophils, B cells, CD8 T cells, type 1 T-helper cells (Th1), Th2, and Th17 CD4 T cells, regulatory T cells, TCRαβ$^+$ double negative (CD4$^-$ CD8$^-$) T cells (DN T cells), and myeloid derived suppressor cells (MDSCs) (49, 50, 58).

The effect of IL-10 on innate and adaptive immune cells differs. Macrophages and monocytes are suppressed by IL-10 through the down regulation of MHC II and costimulatory molecule expression (CD80, CD86, and CD40), both constitutively and in response to IFN-γ (49, 51, 59, 60). This prevents macrophages and monocytes from presenting their respective antigens to Th1 T cells, which in turn do not become activated to orchestrate an immune response. Additionally, the NO production of macrophages is reduced, adhesion to endothelial cells is hindered and the immunosuppressive M2-type is induced (51, 54). Interestingly, IL-10 promotes macrophage phagocytosis of cell debris (54).

Unlike macrophages, neutrophils need to be primed in order to become responsive to IL-10. Neutrophils express IL-10R2 constitutively but can only form the IL-10R complex when IL-10R1 gets upregulated after stimulation. Experimentally, this was determined to take about 4 h (61). Therefore, an immediate response to IL-10 is not possible in non-primed circulating neutrophils. Another important effect that can be seen upon local administration of IL-10 in inflammatory models is that IL-10 prevents the recruitment of neutrophils to the site of injury. Neutrophil migration was not directly hindered by IL-10, but the production of chemoattractants by macrophages or the affected organ tissue was decreased (61, 62). The inhibition of neutrophil apoptosis has been shown to be counter-regulated by IL-10 in severe sepsis (63). Further, it has been demonstrated that IL-10 can inhibit the production of TNF-α and IL-1β in neutrophils when stimulated with LPS or by the phagocytosis of bacteria (64). Further, ROS production seems to be diminished by IL-10 (54). However, further experiments are needed to systematically elucidate the impact of IL-10 on neutrophil functionality. Interestingly, under certain conditions IL-10 induces its own production in neutrophils and macrophages, which is thought to be a positive feedback loop in innate immunosuppression (65). This is of interest as neutrophils themselves are contributing significantly to IL-10 production as shown in a murine model of abdominal sepsis (66).

In dendritic cells, MHC II expression and therefore antigen presentation and activation of naïve CD4 T cells is impaired by IL-10 (54). This potently inhibits CD4 T cell functions. It also diminishes the production of T cell pro-inflammatory cytokines, such as IL-2 and IFN-γ (51). Further, IL-10 blocks proliferation of Th17 cells and inhibits Th2 cells (42, 67). It also promotes the proliferation and function of Regulatory T cell subsets. The generation of Type-1 regulatory T cells (Tr1 T cells) from naïve T cells is induced by IL-10 and it promotes survival and function of CD4$^+$ FoxP3$^+$ Tregs (49, 67). For example, Treg expression of FoxP3 appears to be IL-10 dependent (68). Interestingly, IL-10 suppresses thymic lymphocyte apoptosis in sepsis (69) and has stimulatory effects on CD8 T cells. When stimulated with IL-4 and/or IL-2, CD8 T cells showed increased proliferation (51). Recent murine studies showed increased IFN-γ production by CD8 T cells upon IL-10 administration (53, 70). In clinical trials it could even be shown that modified IL-10 reduces tumor burden in renal cell cancer (71). The application of modified IL-10 enhanced intratumoral CD8 T cell expression of IFN-γ and Granzyme B (42, 71) and thereby promoted anti-tumor cytolysis. However, a final conclusion cannot be drawn yet as IL-10 does also have tumor-supportive functions, i.e., enabling tumor cells to escape an effective immune response (51).

Another pro-inflammatory function of IL-10 can be seen in B cells, as it promotes their survival, proliferation and differentiation into plasma cells (51, 53). Conflicting data exists about the effect of IL-10 on NK cells. It has been shown that IL-10 suppresses TNF-α and IFN-γ production by NK cells, but promotion of IFN-γ production has also been reported in *in vivo* and *in vitro* models (51, 53, 72). Most likely, the predominant conditions, timing and dose in the respective organ or tissue lead to increased or diminished functionality.

Different effects following systemic or local administration of IL-10 could also be utilized therapeutically. Two murine trauma studies showed that IL-10 locally administered *via* inhalation in systemic inflammation attenuated pulmonary inflammation with little or no systemic side effects (62, 73). Altogether, additional research will be needed to elucidate the seemingly paradoxical findings regarding the effect of IL-10 on multiple types of immune cells. The effects of IL-10 depending on the mode of administration are highlighted in **Figure 1**.

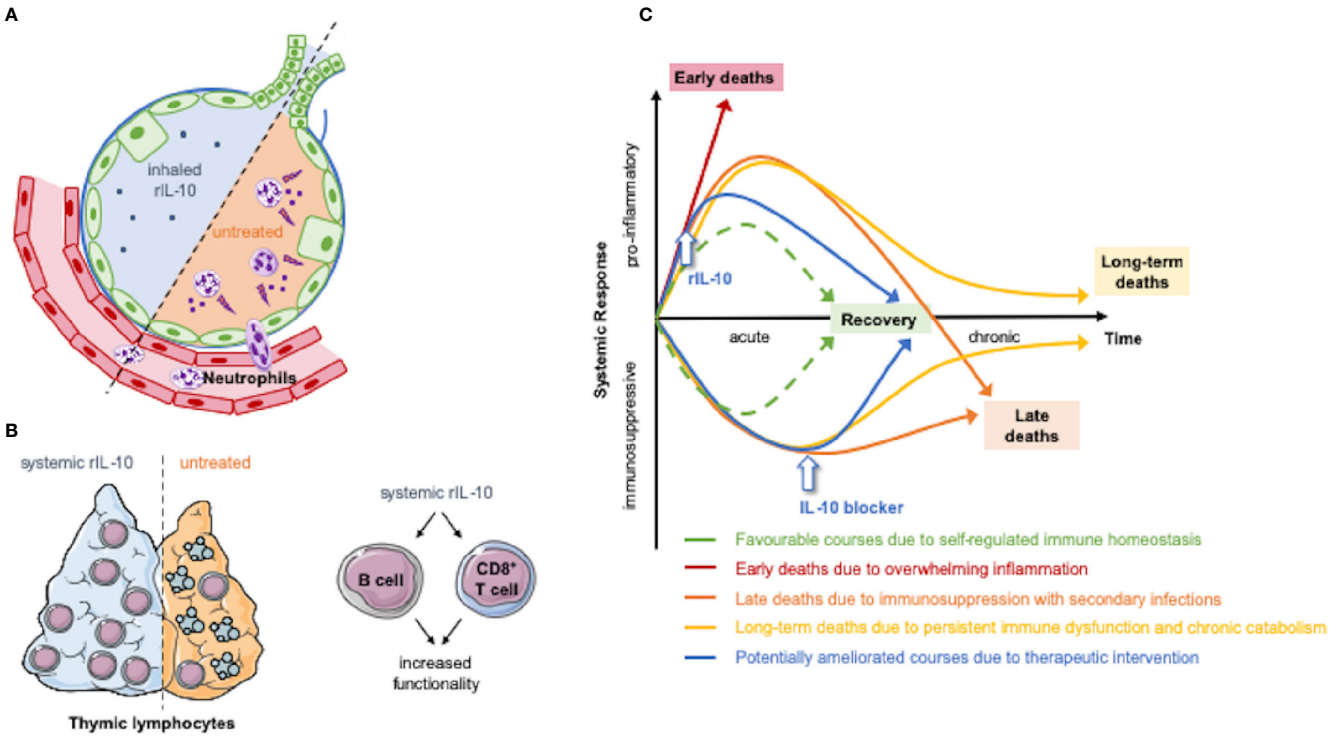

FIGURE 1 | The effect of therapeutic IL-10 modulation depends on the mode of administration and dynamics. The systemic or local application of recombinant IL-10 have experimentally shown beneficial effects. **(A)** Inhaled IL-10 attenuated pulmonary inflammation by preventing detrimental neutrophil recruitment into the lung (61, 62, 73). **(B)** Moreover, IL-10 suppresses thymic lymphocyte apoptosis in sepsis (69) and has stimulatory effects on CD8 T cells (53, 70) and B cells (51, 53). Both modes of application might represent future therapeutic approaches in humans. **(C)** The dynamics of the immune perturbation in trauma and sepsis was modeled in recent literature (74). In general a time dependent modulation of IL-10 levels might restore immune hemostasis (75–77). Animal models suggest a beneficial effect of early IL-10 application (76) and the correlation of elevated IL-10 levels and injury severity suggests beneficial effects by IL-10-blockage in later phases (31, 45, 78). The figure contains adapted graphics from Les Laboratoirs Servier - Medical Art under the terms of the Creative Commons Attribution License (CC BY) for non-commercial use. The use, distribution or reproduction in other forums is permitted: https://creativecommons.org/licenses/by/3.0/legalcode, last accessed July 30th, 2020.

Dynamics in Trauma and Sepsis

The immune perturbation in trauma and sepsis is characterized by the dichotomy of a potent pro-inflammatory upregulation of immunity and immunosuppression (13). During immuno suppression, anti-inflammatory cytokines including IL-10 are released. In search for a marker predicting the severity and outcome of the systemic inflammation, IL-10 has been studied in many animal and clinical studies. There are three broad categories that have been investigated: 1) traumatic injury (mostly burn) 2) sepsis and 3) major surgery, which all lead to a systemic inflammation.

Although studies examining trauma and sepsis do not examine the same clinical conditions leading to systemic inflammation, they share many similarities in the expression of IL-10. Some studies did not show significant differences in IL-10 serum expression between healthy controls, septic patients and patients with septic shock (75, 79). However, the major body of clinical studies examining sepsis does demonstrate this phenomenon.

Huang et al. quantified IL-10 levels in 106 burn patients and showed increased IL-10 levels in septic vs non-septic patients (45). In another study Stensballe et al. examined 265 trauma patients. They found a significant increase of IL-10 levels in patients not surviving 30 days and a positive correlation of IL-10 levels and the injury severity score (ISS) (78). A further multicenter study including 54 polytrauma patients found that elevated IL-10 levels and an elevated IL-6/IL-10 ratio were directly proportional with MODS and mortality (31). In a clinical trial, Chen et al. studied 37 thermally injured patients with a total burn surface area >20% and found increased IL-10 levels in patients who developed sepsis versus those that did not (80).

The team around Gogos et al. included 65 patients with severe sepsis in their trial and found a positive association between serum IL-10 levels, and a high IL-10 to TNF-α ratio and death (81). In another large clinical study of 153 patients with severe sepsis and septic shock, the levels of IL-10 were significantly higher in patients that died within 48h but not for patients that died between 48h and 28 days or after 28 days (82). A separate clinical study by Frencken et al. included 708 patients with severe sepsis or septic shock in the ICU and demonstrated that higher IL-10 levels were positively associated with mortality (83). Another sizable study from Van Vught et al. in 2016 found

overexpression of IL-10 signaling genes in septic patients admitted to the ICU. They did not find differences in the gene expression of IL-10 signaling between patients who later developed ICU-acquired infection compared to those who did not (84). Serum IL-10 levels were not measured, and translational and post-translational regulation of IL-10 expression was observed (85). From these results we extrapolate that sepsis appears to increase IL-10 production and signaling. Whether this indicates adverse outcomes in terms of secondary infection in septic patients has to be examined by assessment of their serum levels.

In cases of sterile trauma associated with major surgery, 28 out of 40 studies found increased systemic IL-10 levels in patients (28). An additional review by Easton and Balogh found a similar conclusion (86).

Together, these studies overwhelmingly suggest that detrimental outcome and elevated IL-10 production are associated. Further, some studies provide interesting additional findings. First, IL-10 levels correlate with the severity of the injury: elevated IL-10 serum levels correlated with the ISS of trauma patients (78), were directly proportional with MODS and mortality in a trauma population (31), showed linear correlation with the increasing percentage of burned total body surface area (45) and the IL-10/lymphocyte ratio was even correlated with the APACHE II score in severe septic patients (87). Secondly, the increase in IL-10 can be seen almost immediately after the onset of trauma, sepsis or surgery. Blood draws of the aforementioned studies were conducted either at admission to the ER or ICU (78, 83) or within 24 h after onset of the trauma, disease or surgery (45, 82, 87). This is of clinical relevance if IL-10 is used to assess the immunological disturbance in a patient at admittance in the ER or the ICU.

Effects and Drivers of Pathological Release in Trauma and Sepsis

The regulatory anti-inflammatory functions are considered a protective counter-regulation to prevent excessive inflammation in the balance of immune hemostasis. However, IL-10 does make the host more susceptible to overwhelming infection if it impairs a proper immune response, and thus has been associated with worse outcomes in infection and cancer (54, 88). It is currently unclear when and how supportive stimulating functions and protective anti-inflammatory regulation deteriorate under pathologic conditions. Therefore, three major questions should be addressed in future studies. A) Which stimuli drive IL-10 expression and how are these signals transmitted in the cells? B) What are the dynamics of IL-10 expression and when does IL-10 become detrimental to an orchestrated clearance of bacteria and cell debris? C) Which cell type drives IL-10 expression in which diseases?

It is known that DAMPs and PAMPs induce IL-10 production by a variety of receptors, that different bacterial pathogens provoke different expression patterns and that IL-10 regulating transcription factors differ in different T cells subsets, macrophages and neutrophils (54). In addition, IL-10 expression is also regulated post-transcriptionally (51). In myeloid cells, TLR-induction, including 2, 4, 5, 7 and 9, drives IL-10 production (54, 89). It is important to differentiate between macrophages and neutrophils in the downstream signaling as they differ. A study conducted by Tamassia et al. found that the MyD88-independent pathway is not mobilized after TLR4 stimulation in human neutrophils (90).

Further, the understanding the dynamics of IL-10 expression is essential. Several studies showed time-dependent effects of IL-10 administration or inhibition in sepsis models (75–77). Given the fact that IL-10 expression is upregulated quickly after trauma and sepsis, as described in the previous section, it seems likely that in the beginning, lower levels of IL-10 may stimulate bacterial clearance but impair functions when the serum levels exceed a certain threshold. A murine study showed increased survival in septic mice when treated with IL-10 up to 6h after the onset of sepsis, which extended the therapeutic window to conduct surgical infectious site control until 30 h after the commencement of sepsis (76).

CD4+FoxP3+Tregs are considered an important source of IL-10 in certain sepsis models (45). It is likely that the dynamic of the apoptosis of T cells in general, and the corresponding proportional changes in the T cell population affect proper IL-10 production and distribution of IL-10 (91). It is important to know which cell type contributes the most to IL-10 production in different diseases. As CD4+FoxP3+Tregs reveal an increase in frequency after trauma it is likely that they significantly contribute to IL-10 production (45). However, T cell apoptosis and murine sepsis models question this assumption. In murine abdominal sepsis, neutrophils are significant producers of IL-10 (66, 92). Of note, in murine burn models, a significant number of IL-10 producing neutrophils were found in the spleen post-injury (54). It has been shown that not only murine- but also human neutrophils can produce IL-10 (65).

Besides CD4+FoxP3+Tregs and neutrophils, also macrophages can produce IL-10 (93) and TGF-β (94) after phagocyting apoptotic antigen presenting cells (APC's), a process coined efferocytosis (95). In this process APC's, such as neutrophils clear bacteria *via* phagocytosis, become apoptotic and then are ingested by macrophages (96). This serves to resolve the inflammation, tissue repair and restores immune homeostasis (94, 97). Efferocytosis has been shown be impaired in sepsis, and if promoted seems to improve outcome in sepsis (98, 99) and trauma (100). In some (98, 101) but not all (99) sepsis and infection models an increase of IL-10 was shown. What remains to elucidate is whether macrophage efferocytosis contributes to chronic immunosuppression by the release of IL-10 and TGF-β. To our knowledge no studies have yet been conducted examining their role in long term (>7 days) immunosuppression after trauma or sepsis.

To assess which cell type contributes the most to IL-10 production is technically difficult. However, this should be addressed when assessing IL-10 mediated effects in the respective pathological condition, as it is necessary for evaluating any potential therapeutic approaches. Modulation of IL-10 has shown promising results in several clinical trials on autoimmune diseases (42). However, the chronic nature of these diseases and

the steadier production of IL-10 varies from the highly dynamic and heterogenous pathology in systemic inflammation due to sepsis or trauma. This may provide some understanding on why past attempts to modulate IL-10 in murine sepsis models did provide conflicting results regarding their outcome (69, 102, 103). Human interventional experimental endotoxemia trials (104, 105) and *in vitro* functional assessment of the innate and adaptive immune system of sepsis patients (46), both modulating IL-10 levels, could not yet provide a clear rationale for IL-10 modulation in a specific inflammatory disease that would allow clinical trials modulating IL-10 production in sepsis and trauma. A better understanding of the dynamics and the producing cell types would significantly improve diagnostics and therapeutic advances.

Potential Therapeutic Modulation of IL-10

Regarding the dynamics and functionality of IL-10, we conclude that two therapeutic modulations of IL-10 in trauma and sepsis seem promising: First, inhalation of IL-10 to treat Acute Respiratory Distress Syndrome (ARDS). This pathology occurs from pulmonary infection or systemic insults such as systemic inflammation in trauma and sepsis (106). Neutrophil infiltration potently contributes to pulmonary inflammation in ARDS and leads to significant pulmonary damage (106). In two different murine trauma models inhaled IL-10 attenuated pulmonary inflammation without systemic immunosuppression by preventing the recruitment of neutrophils to the site of injury through reducing the production of chemoattractants by macrophages or the affected organ tissue (61, 62, 73)

Secondly, systemic administration of recombinant IL-10 for the treatment of sepsis can be considered. However, this approach must be carefully executed as the systemic effects are not yet fully understood. Animal studies show that the effects of IL-10 modulation depend on the injury dynamic in sepsis (75–77, 102). Murine abdominal sepsis studies suggest that the administration of IL-10 within hours after septic onset may have beneficial effects (76, 102). An endotoxemia model in primates seem to support these findings, as early intravenous injection of recombinant human IL-10 significantly decreased TNF-α, IL-6, IL-8 and IL-12 release (107). If this results in a better outcome still has to be examined in further studies, as another murine abdominal sepsis model did not find a beneficial effect of IL-10 administration on mortality (108). In the acute phase IL-10 is suggested to promote protective immunosuppressive effects, whereas in later phases of sepsis increased IL-10 is depicted as a marker for detrimental outcome in many human studies (45, 78, 81, 83). Blockage of IL-10 production or function might constitute a therapeutic approach at this point, as some animal models suggest (102). Pharmaceutic drugs for IL-10 modulation are already in clinical trials. An overview of current IL-10 modulating drugs is provided in **Table 1**. These might be considered to use to augment IL-10 function in very acute sepsis phases (Pegilodecakin: PEGylated recombinant human IL-10 (LY3500518 or AM0010); Phase 3 NCT02923921: pancreatic cancer) or to impair its function in later phases (AS101: tellurium based small compound with immune-modulating characteristics attributed to direct inhibition of IL-10; Phase 2 NCT00926354: treatment of thrombo-cytopenia in solid tumor patients). How a potential dynamic modulation of IL-10 might look like is outlined in **Figure 1**.

Before application of any kind of IL-10 modulation, a very detailed and dynamic assessment of the individual's immune status must be conducted.

TGF-β

How Does TGF-β Affect Immune Cells?

The TGF-β cytokine exits in three isoforms (β1, β2 and β3) and steers multiple immune processes such as immunosuppression and peripheral homeostasis in autoimmunity and infection (109, 110). Leukocytes mainly express the TGF-β1 isoform (48). It regulates a number of different immune cells and importantly T cells. Their function is mediated by the TGF-β receptor complexes type I and II with TGF-β binding first to type II, then I. Signals of these receptors are mediated by the SMAD transcription factors (43).

Many genetic knockout studies in the past have shown that TGF-β has an important influence on T cells. It can impair T cell proliferation and differentiation, except for Tregs whose proliferation is paradoxically stimulated by TGF-β. It inhibits the proliferation and differentiation of Th1, Th2 and cytotoxic T cells by suppressing, amongst others, the transcription factors T-bet, Gata-3 and c-myc. Further, IL-2 expression as a crucial stimulus for T cell proliferation is suppressed by TGF-β as well (48). TGF-β also promotes the development of Th17, Th9 and T follicular helper cells in conjunction with other Interleukins, but

TABLE 1 | Clinical Trials targeting IL-10.

Cytokine	Drug	Sponsor	Description	Indication	Clinical trial
IL-10	Prevascar	Renovo	Recombinant human IL-10	Wound healing	Phase 2 NCT00984646
	AS101	BioMAS Ltd	Tellurium based small compound with immune-modulating characteristics attributed to direct inhibition of IL-10	Treatment of thrombo-cytopenia in solid tumor patients	Phase 2 NCT00926354
	T-allo10	Stanford University	Donor-derived CD4+ T cells which contain a high proportion of host alloantigen specific Tr1 cells	Therapy to prevent GvHD and induce graft tolerance in hematopoietic stem cell transplant	Phase 1 NCT03198234
	Pegilodecakin (LY3500518 or AM0010)	Eli Lilly and Company	PEGylated recombinant human IL-10	Pancreatic cancer	Phase 3 NCT02923921

blocks the development of Th1 and Th2 cells (109). The ability of TGF-β to suppress T cell proliferation depends on the activation status of the T cell, which was demonstrated in a study by Cottrez and Groux (111). The proliferation and cytokine secretion in resting, but not in activated T cells is inhibited by TGF-β1. The latter down regulate TGF-β receptor type II, which interestingly could be upregulated again by IL-10 restoring their responsiveness to TGF-β1 (111). TGF-β regulation of T cell survival appears to be dependent on CD28 co-stimulation. In the presence of CD28 agonist TGF-β inhibits T cell apoptosis and enhances their expansion. In its absence, TGF-β inhibits the TCR-stimulated proliferation of naïve T cells (48). Moreover, TGF-β1 supports survival of T cells with memory and effector functions (48), although this seems to contradict its role in the above-mentioned regulation of T cell differentiation.

The role of TGF-β in the regulation of Tregs cells appears to be less contradictory. TGF-β is necessary for the induction of thymic (109) and peripheral Tregs, which develop by antigen-specific stimulation in the presence of TGF-β (112). TGF-β induces the expression of FoxP3 and the production of IL-10 in Tregs (113, 114). Tregs themselves secrete TGF-β forming a positive feedback-loop (50, 115).

Additionally, dendritic cells mediate the induction of peripheral Tregs *via* TGF-β (116). If dendritic cells themselves are exposed to TGF-β in a pro-inflammatory setting, they show impaired production of pro-inflammatory mediators (117). Similar to dendritic cells, TGF-β strongly influences monocytes and macrophages by downregulating their pro-inflammatory functions when activated (48). However, the effect of TGF-β on monocytes and macrophages strongly depends on their activation. In general, TGF-β promotes monocyte function when resting. For example, adhesion molecules, matrix metalloproteinases and IL-6 production is promoted by TGF-β in monocytes (48). In contrast, when activated monocytes become macrophages, TGF-β can have a dampening effect on their pro-inflammatory functions in that it impairs their ability to produce LPS-induced TNF-α, MIP-1α, MIP-2 and reactive oxygen and nitrogen species (48). Another important contribution to uphold inflammation is the ability of macrophages to present antigens to T cells. TGF-β1 downregulates the IFN-γ-induced expression of MHC II mRNA and antigen presentation in macrophages (118). This might serve to prevent excessive and therefore harmful activation of T cells in inflammation.

The impact of TGF-β on neutrophils is poorly understood. In cancer, TGF-β polarizes neutrophils from an antitumoral N1 type to a pro-tumoral N2 type (119). However, TGF-β can also promote neutrophil oxidant production (120). Of note, TGF-β is a strong chemoattractant for monocytes, eosinophils, mast cells and neutrophils (48). The immunosuppressive effects of TGF-β on immune cells are outlined in **Figure 2**.

Dynamics in Trauma and Sepsis

Given the fact that TGF-β is a potent regulator of immune responses and is considered an important cytokine released by Tregs, the question arises if it is a main regulator in trauma and sepsis and if its dysfunction in these conditions contributes to a disturbed immune response.

Several studies provide contradictory findings. In 2004, Monneret et al. conducted a study examining 38 adult septic

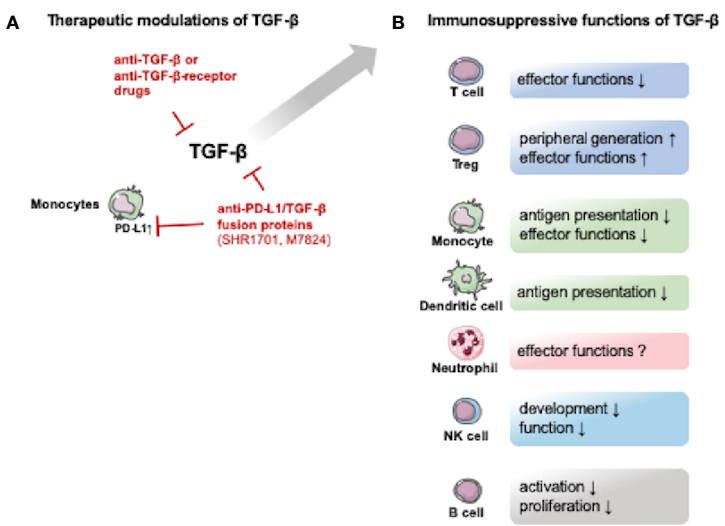

FIGURE 2 | Potential therapeutic TGF-β modulating drugs and the immunosuppressive functions of TGF-β. The figure provides an overview over potential therapeutic approaches and the immunosuppressive effects of TGF-β. **(A)** Several drugs targeting TGF-β or its receptors are currently being tested in non-septic patients. Interestingly an anti- programmed cell death 1 ligand 1 (PD-L1)/TGF-β fusion protein is also being tested. The upregulation of PD-L1 is associated with monocyte dysfunction in post-traumatic and septic immune dysfunction (32). **(B)** TGF-β exerts immunosuppressive effects on both innate and adaptive immune cells. The figure contains adapted graphics from Les Laboratoirs Servier - Medical Art under the terms of the Creative Commons Attribution License (CC BY) for non-commercial use. The use, distribution or reproduction in other forums is permitted: https://creativecommons.org/licenses/by/3.0/legalcode, last accessed July 30th, 2020.

patients with septic shock and found that TGF-β levels were decreased compared to normal values and concluded that the general immunosuppressive state they found the patients in is more likely attributed to increased IL-10 levels (121). In addition, the group suggested that no prognostic information could be obtained from TGF-β levels (121). In further support of this, an additional study did not find any prognostic value of TGF-β2 to determine survival in patients with gram-positive septicemia (122). While TGF-β2 levels were increased in the non-survivor group compared to the survivor group in gram-positive septicemic patients, this difference was not statistically significant (122). Gram-negative septicemic patients showed a trend towards decreased TGF-β levels, but this was also not statistically significant (122). Due to the low numbers of patients within each group (11 or more) the study is potentially underpowered to reveal statistically significant differences (122). Of note, TGF-β1 and not TGF-β2 seems to have the largest impact on T cell function and leukocytes mainly express the TGF-β1 isoform (48). A further trial observing gastrointestinal surgery patients with and without infectious complications could not detect serum TGF-β in most of the samples (103). Burn patients examined for IL-10 and TGF-β1 serum levels showed an initial peak in serum TGF-β1 within one day post-burn and a second peak in which the serum levels of the survivors were higher than in the non-survivor group. No differences were found between patients with burned total body surface area (TBSA) of greater or less than 50% (123). However, a limitation in this study of 15 patients is that the surviving group was younger and suffered less severe burn injury with regard to the TBSA (124).

Other studies found elevated TGF-β levels in septic patients. One study has demonstrated elevated TGF-β1 levels in 26 patients at the time of sepsis diagnosis when compared to healthy controls (125). A more recent study from Huang et al. examined Treg function and IL-10 and TGF-β1 serum levels in 106 burned, septic and non-septic patients with a TBSA of more than 30% (45). They revealed a significant increase in TGF-β1 levels in septic patients compared to non-septic patients and in non-survivors compared to survivors (45). They also stratified the patients in three groups depending on the size of the burn. Serum TGF-β1levels were positively associated increasing TBSA (45). From all these studies, the latter examined the biggest population, therefore making it likely that there is indeed a systemic increase in TGF-β in severely injured and septic patients. This view is supported by studies examining specific organ failures in septic populations. A study from De Pablo et al. revealed that increased TGF-β1 levels were positively associated with sepsis induced ARDS with fatal outcome. The TGF-β1 levels were increased in patients 7 days after ICU admission with sepsis and ARDS compared to patients with sepsis without ARDS. In addition, patients with septic shock associated ARDS showed significantly higher TGF-β1 levels in non-survivors than in survivors (126).

In rodent sepsis models, findings concerning TGF-β serum levels are less contradictory then in human studies. Increased levels of TGF-β were found in peripheral blood of septic mice (127). Nullens et al. conducted a murine sepsis model in which lymphocyte depletion occurred in all tissues examined (spleen, mesenteric lymph node, Ileum, colon) at day seven, coinciding with increased levels of IL-10 and TGF-β (128). In a rat sepsis model, increased levels of TGF-β were observed in the circulation and in adherent splenic cells (129). Additionally, supporting the findings in the human study mentioned above from De Pablo et al., Xu et al. reported a protective role of curcumin, most likely by decreasing the expression of TGF-β1 and the SMAD3-dependent signaling pathway (130). Plasma TGF-β1 levels were significantly increased in the septic group and were downregulated by curcumin treatment. Histology showed curcumin treatment prevented some sepsis-induced lung damage (130). These results suggest that TGF-β plays a detrimental role in sepsis most likely by impairing a proper immune response. Yet TFG-β1 might exert detrimental effects on the host by other cells. A study examining the effect of TGF-β on liver cells when challenged with LPS revealed that it promotes the release of proinflammatory cytokines, e.g. IL-6, by the liver cells, which led to a higher mortality (131). Inducible TGF-β1-transgenic mice that express TGF-β1 under control of the C-reactive protein promoter were used in this study (131). Therefore, future studies will be needed to confirm this mechanism in mice that were not genetically modified.

In contrast, other studies found beneficial effects of TGF-β in sepsis. For example, treatment with TGF-β blocked endotoxin-induced hypotension and improved survival in rat models using *Salmonella typhosa* and *Salmonella enteritidis* to induce septic shock and a murine endotoxic shock model (4). Moreover, cardioprotective effects of TGF-β could be shown, as TGF-β reverses the depression of myocyte contraction *in vitro* (132). Another study found TGF-β1 to decrease neutrophil numbers during the onset of LPS-induced acute lung injury (133). This was due to increased apoptosis rather than reduced migration. TGF-β1 did not directly regulate neutrophil apoptosis but instead promoted IL-6 release from mast cells, which promotes neutrophil clearance (133).

Given the partially contradictory findings in the different human studies, there still lacks a definite answer to the question of whether systemic TGF-β release contributes to a systemic detrimental immune disturbance in sepsis. The unambiguous findings in animal models and the findings of Huang et al. including 106 patients, in which TGF-β serum levels were increased in septic patients (45), suggest that TGF-β does play an important role. Even more so as in the current understanding of sepsis, the action of Tregs is considered important for the outcome. Tregs are considered an important source of TGF-β. Moreover, the association of increased TGF-β levels and impaired lung function seems to be relevant in this context, considering that ARDS is a major clinical challenge in septic patients. The local effect of TGF-β in the different tissues has to be examined in the context of trauma and sepsis. This is of importance, as other diseases like rheumatoid arthritis that TGF-β acts very differently when administered locally or systemically (48). Future studies need to address the dynamic expression of this cytokine during sepsis. Several studies mentioned a peak in

the beginning of sepsis development (4, 123). This might be due to an overwhelming stimulation of TGF-β producing cells in the beginning of inflammation, or an increase in apoptosis of T cells which are known to create an immunosuppressive environment (134). This could lead to a pathologic immunosuppression at the onset of inflammation. Lastly, the role of TGF-β may differ in sepsis and sterile trauma. Therefore, future studies should also address differences in non-sterile and sterile settings to evaluate appropriate therapeutic action in the different diseases.

Effects and Drivers of Pathological Release in Trauma and Sepsis

Assuming an adequate response to an infection, we postulate the role of TGF-β as follows: First, it acts as a chemoattractant for myeloid cells in the very beginning of infection to promote initial innate immune response. This underlying premise is based upon that TGF-β acts in a stimulatory manner on resting monocytes (48). Further, TGF-β impairs the activation of naïve T cells but can be overridden by CD28 co-stimulation in addition to low IL-2 doses (48). The team around Li et al. argues that this circumstance serves as a threshold to divide between self-antigen driven steady state inflammation, which is hindered by TGF-β, and a pathological condition in which the above mentioned stimuli override TGF-β inhibition to guarantee a proper immune response to the infection (48). As stated above, TGF-β curbs macrophages in inflammation which might serve to restore hemostasis and prevent excessive inflammation.

The data suggest that these regulated dynamics are severely impaired in sepsis. In the study from Hiraki et al., a murine abdominal sepsis model was utilized with a TGF-β depleting antibody administered 6 h after the intervention, which lead to improved survival of the mice (103). The group also showed a positive correlation between the percentage of Tregs of all CD4 T cells and the serum TGF-β levels (103). It is known from human clinical studies that an increased percentage of Tregs is correlated with worse outcome (45, 135). The group around Hiraki et al. therefore postulates that the disruption of TGF-β leads to a decrease of Treg abundance which might be harmful in the development of sepsis (103). It is also possible that TGF-β itself plays a detrimental role by depressing T cell functions and disrupting the positive feedback loop that promotes Treg proliferation (50, 115). The study did not examine which cell type provides the major source of TGF-β. It is assumed that the initial release of auto- and or alloantigens released when infection occurs leads to such a massive TGF-β release that homeostasis as described above can no longer be restored. Currently, it is not clear whether this is driven by DAMPs or PAMPs. In the study, the administration of the depleting antibody led to the restoration of this homeostasis. Of note is that a single administration was enough. A current study from Zeng et al. supports these findings (136). An anti-TGF-β antibody was administered, which led to increased IL-2 and IFN-γ levels. This was considered beneficial for the outcome. The authors, however, neglected to provide the timepoint of the anti-TGF-β-antibody administration (136).

Altogether, these studies contribute to the understanding of the role of TGF-β and Tregs in the initial phase of sepsis. However, it is not possible to draw a definite conclusion from what is currently known, given the fact that the effects of TGF-β differ a lot depending on location, timing and the activation status of the cells it affects as described in the section above.

Potential Therapeutic Modulation of TGF-β

Currently, TGF-β dynamics in human sepsis studies need to be expanded before a therapeutic modulation of TGF-β or its receptors should be applied. The focus of studies should be on the dynamics and the origin of sepsis (organ/tissue). In current clinical trials, a number of drugs are tested that might prove useful in the future. An overview of current TGF-β modulating drugs is provided in **Table 2**. These include direct anti-TGF-β antibodies (e.g. Fresolimumab: Human monoclonal anti-TGFβ-antibody (Non-small cell lung carcinoma), Phase 1/2 NCT02581787) and receptor blockage (Galunisertib (LY2157299): small molecule inhibitor of the kinase domain of Type 1 TGFβ receptor (solid tumor, non-small cell lung cancer, hepatocellular carcinoma), Phase 1/2 NCT02423343). Interestingly, an anti- programmed cell death 1 ligand 1 (PD-L1)/TGF-β fusion protein is also being tested (e.g. SHR-1701: anti-PD-L1/TGFβ fusion protein (advanced solid tumors), Phase 1 NCT04324814). If TGF-β blockage proves beneficial in trauma or sepsis, application of this drug would be a very interesting approach as the upregulation of PD-L1 is associated with monocyte dysfunction and upregulation of its ligand programmed cell death protein 1 (PD-1) in lymphoid cells is a detrimental hallmark of post-traumatic and septic immune dysfunction (32). A first anti-PD-1 antibody (nivolumab) has already been tested for safety in septic patients (Phase 1b NCT02960854) (137). The potential therapeutic modulations of TGF-β are outlined in **Figure 2**.

TSLP

How Does TSLP Affect Immune Cells?

Thymic stromal lymphopoietin (TSLP) is a member of the IL-2 cytokine family and is closely related to IL-7 (138). It appears in two variants, a long form of TSLP (lfTSLP) and a short form (sfTSLP). These two forms do not derive from alternative splicing but are promoted by different putative promoter regions (139). Their effects on immune cells differ widely. Of note, many articles do not differentiate between the long and the short form of TSLP (139). In a review of Bjerkan et al., the authors summarized that the in absence of infection the short form is steadily expressed and the long form is absent (139). The short form seems to provide homeostasis especially on healthy barrier tissue like in the skin and gut. However inflammation can induce the expression of the long form and the short form becomes downregulated (139).

The diseases TSLP are best studied in are asthma, inflammatory bowel diseases and cancer, in which a Th2 dominated inflammation occurs or Th2 cells promote cancer cell survival (138). Keratinocytes, epithelial cells, mast cells, smooth muscle cells, fibroblasts and dendritic cells are producers of TSLP (140). However, it can also be produced by mast cells, human monocytes, macrophages and granulocytes, murine basophils and cancer cells (141). Unlike cells producing TSLP, which are comparably few, many more cells become activated by TSLP. Cells known to

TABLE 2 | Clinical Trials targeting TGF-ß or its receptor.

Cytokine	Drug	Sponsor	Description	Indication	Clinical trial
TGF-β	Juvista (Avotermin)	Renovo	TGF-β3	Wound healing	Phase 2 NCT00629811
	TGFβ-resistant LMP-specific cytotoxic T lymphocytes	Baylor College of Medicine	TGFβ-resistant LMP-specific cytotoxic T lymphocytes	Lymphoma	Phase 1 NCT00368082
	LY3200882	The Netherlands Cancer Institute	TGFβRI small molecule inhibitor	Colorectal metastatic cancer	Phase 1/2 NCT04031872
	TGFβ-resistant HER2/EBV-CTLs	Baylor College of Medicine	TGFβ-resistant HER2/EBV-Cytotoxic T cells	Treatment of Her2 positive malignancy	Phase 1 NCT00889954
	AVID200	Formation Biologics	TGFβ-receptor ectodomain-IgG Fc fusion protein inhibitor of TGFβ	Malignant solid tumor	Phase 1 NCT03834662
	TGFβ2 Antisense-GMCSF Gene Modified Autologous Tumor Cell (TAG) Vaccine	Mary Crowley Medical Research Center	TGFβ2 Antisense-GMCSF Gene Modified Autologous Tumor Cell (TAG) Vaccine	Advanced metastatic carcinoma	Phase 1 NCT00684294
	AP 12009	Isarna Therapeutics GmbH	Phosphorothioate antisense oligodeoxynucleotide specific for the mRNA of human TGFβ2	Pancreatic neoplasms, melanoma, colorectal neoplasms	Phase 1 NCT00844064
	GPC3 and/or TGFβ targeting CAR-T cells	Second Affiliated Hospital of Guangzhou Medical University	Third/fourth generation of CAR-T cells that target GPC3 (GPC3-CART cell) and/or soluble TGFβ (GPC3/TGFβ-CART)	Hepatocellular carcinoma, lung cancer	Phase 1 NCT03198546
	P144 cream	ISDIN	TGFβ1-inhibitor, designed to block interaction between TGFβ1 and TGFβ1 type III receptor	Healthy (tolerability and bioavailability)	Phase 1 NCT00656825
	GC 1008	National Cancer Institute (NCI)	Human anti-TGFβ- monoclonal antibody	Renal cell carcinoma	Phase 1 NCT00923169
	M7824	National Cancer Institute (NCI)	Bifunctional anti-PD-L1/TGFβ Trap fusion protein	Head and neck cancer	Phase 1/2 NCT04247282
	Fresolimumab	Maximilian Diehn, Stanford University	Human monoclonal anti-TGFβ-antibody	Non-small cell lung carcinoma	Phase 1/2 NCT02581787
	Galunisertib (LY2157299)	Eli Lilly and Company	Small molecule inhibitor of the kinase domain of Type 1 TGFβ receptor	Solid tumor, non-small cell lung cancer, hepatocellular carcinoma	Phase 1/2 NCT02423343
	Vactosertib (TEW-7197)	MedPacto, Inc.	Inhibitor of the serine/threonine kinase of the TGFBR1	Recurrent advanced urothelial carcinoma	Phase 2 NCT04064190
	GS-1423	Gilead Sciences	Anti-CD73- TGFβ-Trap bifunctional antibody	Advanced solid tumors	Phase 1 NCT03954704
	PF-03446962	Pfizer	Monoclonal antibody against Activin Receptor-Like Kinase-1 (ALK1), a type I subclass of the TGFβ receptor	Advanced solid tumors	Phase 1 NCT00557856
	SHR-1701	Atridia Pty Ltd.	Anti-PD-L1/TGFβ fusion protein	Advanced solid tumor	Phase 1 NCT04324814
	SRK-181	Scholar Rock, Inc.	Inhibitor of the activation of latent TGFβ1	Locally advanced or metastatic solid tumors	Phase 1 NCT04291079
	NIS793	Novartis Pharmaceuticals	Anti-TGFβ-antibody	Breast-, lung-, hepatocellular-, colorectal-, pancreatic-, renal-cancer	Phase 1 NCT02947165

become activated by TSLP, are dendritic cells, innate lymphoid cells 2 (ILC2), CD4 T and Th2 cells, natural killer T cells, CD8 T cells and B cells, regulatory T cells, eosinophils, neutrophils, murine (but not human) basophils, monocytes, mast cells, macrophages, platelets, and sensory neurons (141).

Mouse and human TSLP bind to the combination of the IL-7 receptor α chain (IL-7Rα) and the TSLPR (TSLP receptor) chain, but only rarely to TSLPR alone (142). An extensive review about the intracellular pathways of TSLPR signaling would exceed the scope of this review, but was compiled by Zhong et al. and Yu et al. (143, 144). The lfTSLP receptor is expressed on several immune cells such as dendritic cells, T cells, B cells, natural killer cells, monocytes, basophils, eosinophils, and epithelial cells (139). The TSLPR was also found on tissue in heart, skeletal muscle, kidney, and liver (142). On CD4 T cells the TSLPR is upregulated upon TCR stimulation assuming a regulative role in inflammation (142). It is believed to portray an endothelial reaction to endogenous and exogenic triggers and drive a Th2-dominated inflammatory reaction mediated by dendritic cells. However, these Th2 cells also produce TNF-α, but not IL-10 (145).

It has been demonstrated that TSLP can exert potent antimicrobial effects. It could be shown that TSLP inhibits the growth of *Escherichia coli, Pseudomonas aeruginosa, Staphylococcus aureus, Staphylococcus epidermidis* and fungal species (139). Furthermore, TSLP augments ROS production in neutrophils by triggering the complement C5 system which enhances killing of *S. aureus* in human and mice (146).

Dynamics in Trauma and Sepsis

TSLP has not been studied extensively in sepsis to date. Several studies provide conflicting results concerning the effect of TSLP in animal sepsis models or human studies (44, 47, 147, 148). These findings are summarized in **Table 3** and visualized in **Figure 3**. Undisputed findings of the mentioned murine and human studies are that TSLP serum levels increase within the initial phase of the inflammation. Depending on the injury model or clinical circumstances, this initial peak ranges from 6 (147) to 24 h (44) and seems to decrease with the course of the inflammation.

Up to now, none of the studies included a long-term analysis of TSLP levels and none of the studies conducted in sepsis differentiated between the long and the short TSLP form. As the long form is considered to become upregulated in inflammatory settings (139), it is likely that the long form is what was found to be elevated in the serum and peritoneum. This is of note as it might provide an explanation for the conflicting results found in the TSLP/sepsis studies concerning inflammatory and immunosuppressive actions of TSLP.

The first study that provided an examination of the effect of TSLP in sepsis was performed by Kuethe et al. (147). This group found that TSLP blockade decreased mortality and dampened the production of inflammatory cytokines (147). A similar study was conducted by Piliponsky et al. in 2016 (44). In contrast to the study of Kuethe et al. the administration of anti-TSLP-Ab in a murine abdominal sepsis model lead to an increase in morbidity and did not improve bacterial clearance (44). The authors argue that this may be explained by different injection times and inflammation dynamics. Otherwise, they confirmed the immunosuppressive role of the TSLP-TSLPR interaction as TSLPR-/- mice displayed increased intraperitoneal levels of TNF-a, IL-6, IL-17A and KC after onset of abdominal sepsis (44). However, TSLPR-/- mice had impaired bacterial clearance leading the authors to compare the effect of TSLPR with the effect that can be seen in IL-10 deficient mice succumbing to sepsis due to impaired bacterial clearance (44). Piliponsky et al. depicted that TSLP mainly dampens myeloid cytokine production, which then contributes to reduced morbidity by limiting inflammation (44). Overall, they conclude that the upregulation of TSLP in sepsis aims to restore immune hemostasis by dampening inflammation (44). In contrast, Yu et al. demonstrated a negative correlation between serum TSLP levels in patients with high ratio of neutrophils and increased mortality in a septic patient cohort (47). Moreover, they showed TSLP induces inflammation in neutrophils and T lymphocytes and certain monocyte subtypes (intermediate and non-classical) leading to increased production of e.g. IL-6, TNF-α and IFN-γ (47). They therefore conclude that TSLP has a pro-inflammatory effect on monocytes and lymphocytes but does not improve antibacterial clearance of neutrophils, as phagocytosis and respiratory burst were unchanged (47). In line with these findings is a study by Han et al. They revealed that TSLP-deficient mice show lower levels of IL-6, VEGF, ICAM-1, and MIP2 in serum in LPS challenged mice (148). They also demonstrated TSLP upregulates macrophage-mediated inflammation as TSLP neutralization and TSLP siRNA silencing reduced the production of IL-6, TNF-α and NO after LPS stimulation. Moreover, they showed LPS or *E. coli* stimulated macrophages *via* TLR4 produce TSLP (148). The finding of decreased proinflammatory cytokines in TSLP-deficient mice contradicts the findings of Piliponsky et al. and Kuethe et al., although Han et al. in part used the same experimental approach (Anti-TSLP-Ab) (44, 147, 148). The team of Han et al. argues that the different septic models (LPS vs cecal ligation and puncture (CLP)) may provide an explanation for this. They summarize that TSLP triggers proinflammatory reactions especially of macrophages and might lead to organ dysfunction in sepsis (148).

Taken together, these studies provide surprisingly conflicting data about the effect of TSLP in sepsis. It will be critical to consider the differences between the models to explain these results. The CLP model conducted by Kuethe et al. and Piliponsky et al. constitutes a physiologically more relevant model as it includes pathogen related tissue damage, phagocytic uptake of pathogens by neutrophils and macrophages, as well as the release of other pathogenic antigens compared to the administration of LPS alone, which lacks all these important characteristics. Moreover, Han et al. used relatively low LPS doses (148) which may not induce an inflammatory reaction as strong as in the CLP model. This may indicate a different role of TSLP depending on the injury severity and inflammatory milieu. However, until further direct experimental comparisons, this remains speculative.

The following points should be addressed in further studies to clarify the role of TSLP in sepsis. First, a discrimination between the short and the long form should be conducted in future studies as their effects are considered to differ (139). Secondly, studies should differentiate between the severity of sepsis, as

TABLE 3 | The effect of TSLP in sepsis.

Sepsis Model/ Intervention	Intervention/Mouse model	Murine or human	Mortality	Cytokine expression	Other parameters	Study
CLP	Anti TSLP-Ab	M	↓	TNF-a, IL-17 (ip) ↓	Neutrophil no (ip) ↑ Neutrophil ox. burst ↑ CFU ↓	Kuethe et al. (147)
CLP	Anti TSLP-Ab	M			Drop in body temp ↑ CFU ↔	Piliponsky et al. (44)
CLP	TSLP administration	M		TNF, IL-17A, IL-6, KC (plasma and ip) ↓	Drop in body temp ↓ Neutrophil no (ip) ↓ CFU (ip) ↔ (blood) ↑	
CLP	TLSPR-/-	M	↑	TNF, IL-17A, IL-6, KC (plasma and ip) ↑	Drop in body temp ↑ Neutrophil/Macrophage no (ip) ↑ CFU (ip and blood) ↓	
CLP	Lys-Cre^{+}; Tslpr $^{fl/fl}$ (reduced TSLPR expression)	M	↑	TNF, IL-17A, IL-6, KC (plasma) ↑	Neutrophil/Macrophage no (ip) ↑ CFU (ip and blood) ↓ IL-6 (within Neutrophils and Macrophages) ↑	
LPS stim (*in vitro*: Neutrophils)	TSLP administration	H			IL-6 (within Neutrophils) ↓	
Sepsis	LPS stim (*in vitro*)	H			IL-6, TNF-α, IL-1b (non-classical and intermediate Monocytes) (in patients above av. TSLP serum levels vs lower TSLP Serum levels) ↑	Yu et al. (47)
Sepsis	PMA (*in vitro*)	H			Neutrophil ox burst and phagocytosis ↔ (in patients above av. TSLP serum levels vs lower TSLP Serum levels) ↑	
Sepsis	Cell stim (*in vitro*)	H			TNF-a, IFN-y (CD4 T cells) (in patients above av. TSLP serum levels vs lower TSLP Serum levels) ↑	
LPS injection (ip)	TSLP siRNA injection (reduces TSLP levels) Or TSLP-/-	M		IL-6, VEGF, ICAM-1, and MIP2, TNF-a (serum, liver)↓		Han et al. (148)
LPS injection (ip)	TSLP administration	M		IL-6 (serum) ↑		
LPS stim (*in vitro*: Monocytes (RAW264.7, WT and TSLP-/-))	TSLP siRNA transfection: RAW264.7 cells (reduces TSLP levels). WT: Anti-TSLP-Ab TSLP-/-: no intervention	M			IL-6, ICAM-1, MIP-2, TNF-a, NO production in all types on Monocytes ↓	
CLP	–	M		TSLP (serum) ↑		Kuethe et al. (147)
CLP	–	M		TSLP (plasma, ip) ↑	Neutrophil TSLPR expression ↑	Piliponsky et al. (44)
Severe Sepsis	–	H		TSLP (plasma) ↑		
Sepsis	–	H		TSLP (serum) ↑ (in patients with hyperleukocytosis (HL) and high neutrophil ratio (HNR) vs without HL and HNR)	Mortality ↑ (in patients above average TSLP serum levels vs lower TSLP serum levels)	Yu et al. (47)
Sepsis		H		TSLP (serum) ↑		Han et al. (148)
LPS, E.coli injection (ip)		M		TSLP (plasma, ip) ↑		

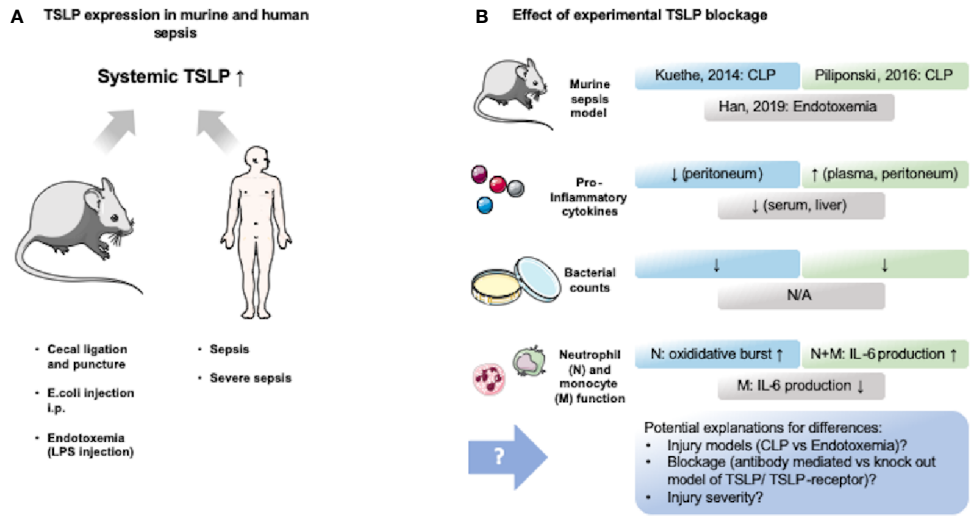

FIGURE 3 | TSLP expression in murine and human sepsis and its experimental modification. Murine and human sepsis acutely lead to increase of systemic TSLP blood levels. Murine studies blocking TSLP provided contradictive results, which might be explained by differing methodology. **(A)** Several murine sepsis (cecal ligation and puncture and intraperitoneal injection of live bacteria) and endotoxemia (intraperitoneal injection of lipopolysaccharide (LPS)) models, as well as human observational trials in sepsis and severe sepsis revealed that TSLP levels are elevated in the blood within 24 h (44, 147, 148). **(B)** Three murine studies (44, 147, 148) assessed the effect of TSLP blockage and provided contradictive results that are highlighted in this figure. An explanation for these differences might be found in the different methods that were used. The figure contains adapted graphics from Les Laboratoirs Servier - Medical Art under the terms of the Creative Commons Attribution License (CC BY) for non-commercial use. The use, distribution or reproduction in other forums is permitted: https://creativecommons.org/licenses/by/3.0/legalcode, last accessed July 30th, 2020.

Piliponsky as well as Yu et al. reported differences in the effect of TSLP regarding the severity of the disease (44, 47). Thirdly, none of the studies so far address the release of TSLP by endothelial cells, which are considered the main producers (140). The effect of TSLP on macrophages and endothelial cells seem most important as they might steer potential pro- or anti-inflammatory effects. Lastly, the dynamics of the septic disease should be examined, as this may also be a potential cause of the current conflicts in the data.

Effects and Drivers of Pathological Release in Trauma and Sepsis

The production of TSLP is triggered by allergens, pro-inflammatory cytokines, viruses, bacteria, fungi and tryptases (141). With respect to a septic setting, the challenge of epithelial cells with bacteria is likely the most relevant. This poses the important question of whether the stimulation occurs directly by microbes or in an indirect manner mediated by consecutively upregulated pro-inflammatory cytokines. In a study performed by Lan et al. it is demonstrated that *Staphylococcus aureus* directly induces epithelial cell-derived TSLP release *via* TLR-2-binding (149). Although not in a septic model, this might explain the upregulation of TSLP in sepsis (149). If TSLP is considered to restore immune hemostasis in sepsis, which still has to be proven due to the conflicting results past studies provided, then overwhelming microbial challenge might lead to detrimentally high release of TSLP. This could provide an explanation for conflicting data as lower levels might restore homeostasis, but by surpassing a certain threshold, TSLP may trigger inflammation and therefore worsen outcome. However, this currently remains a matter of speculation.

Potential Therapeutic Modulation of TSLP

As discussed in the previous section more research is needed to characterize the effect of TSLP in trauma or sepsis. However, antibodies directed against TSLP are currently tested for safety in clinical trials aiming to treat allergic diseases (e.g. MEDI9929: human monoclonal antibody immunoglobulin IgG2λ directed against TSLP (asthma), Phase 2 NCT02698501). An overview of current TSLP modulating drugs is provided in **Table 4**. These might prove useful in clinical trials when dynamics and functions of TSLP in trauma and sepsis have been elucidated.

TABLE 4 | Clinical Trials targeting TSLP.

Cytokine	Drug	Sponsor	Description	Indication	Clinical trial
TSLP	MEDI9929	Celeste Porsbjerg	Human monoclonal antibody immunoglobulin IgG2λ directed against TSLP	Asthma	Phase 2 NCT02698501
	AMG 157 (MEDI9929)	National Institute of Allergy and Infectious Diseases (NIAID)	Anti-TSLP antibody	Cat Allergy	Phase 1/2 NCT02237196

CONCLUSION

Sepsis is responsible for one out of three in-hospital deaths (150) while trauma is still the leading course of death for people under the age of 46 in the United States (151). The following discusses the two most pressing challenges for these pathophysiologies:

1) The development of methods to stratify patients, to evaluate which of three clinical trajectories the respective patient will follow: early death, rapid recovery or chronic critical illness (19). Promising strategies are phenotyping innate and adaptive immune cells, using flow cytometry (32), assessing genetic or transcriptional changes within innate and adaptive immune cells (152), evaluating cytokine levels and their ratio's (31) and most importantly use functional assessment of immune cell behavior (46, 153). The use of functional assays has proven useful to examine the capability of cells to produce cytokines in response to stimuli and thus enables the assessment of the current immune status (46). Moreover, patient endotypes within the sepsis and trauma populations should be defined (10). These endotypes should be studied to determine if they are associated with good or bad clinical outcomes. Knowing the endotype associated with the immune status should allow for a more personalized and effective therapeutic strategy. All of the clinical, phenotypic and functional assays should be analyzed in combination with the standard clinical data on the ICU's. We believe that dynamic immune monitoring prospectively should become a standard in intensive care medicine.

2) If proper stratification of patients is successful the next step would be to therapeutically address immune perturbation. Currently the use of three cytokines is being tested to improve immune function in sepsis and infection: IFN-γ to treat sepsis-induced immunoparalysis (Phase 3, NCT01649921), granulocyte-macrophage colony-stimulating factor (GM-CSF) to decrease ICU acquired infections (Phase 3, NCT02361528), IL-7 to restore lymphocyte counts in sepsis patients (Phase 2, NCT02640807). Beside cytokine modulation the blockage of the programmed cell death protein 1 (PD-1), a checkpoint inhibitor with elevated expressed in sepsis patients (154), might prove beneficial, regarding its ability to hinder T cell apoptosis in murine sepsis model and *in vitro* human sepsis studies (155–157). Moreover, the blockage of cytotoxic T-lymphocyte-associated protein 4 (CTLA-4), another immune checkpoint receptor overexpressed in sepsis patients (155, 158) that improved T cell survival in mice (159), might provide a therapeutic approach.

Other than the above mentioned, there are no current approaches to clinically test modulation of immunosuppressive cytokines, such as IL-10, TGF-β and TSLP in sepsis or trauma. Immunosuppression is responsible for significant numbers of deaths in sepsis and trauma patient populations (13). It is therefore key to further examine how immunosuppressive cytokines affect immune hemostasis and how they can be beneficially modulated.

As highlighted in this review the effect of the potent anti-inflammatory cytokines IL-10, TGF-β, and TSLP depends on dynamics, dose and receptive cell type. Thus, the following prerequisites for these specific cytokines should be met to approach pharmaceutical therapeutic modulation of IL-10, TGF-β, and TSLP: 1) Future pre-clinical or clinical studies should focus on temporal expression of these cytokines. 2) The collective literature shows improved predictive power when a combination of cytokines was assessed to predict outcome (31, 160, 161). Therefore, they should be evaluated relatively to each other and other pro-inflammatory cytokines. 3) Future research should focus on which cells are the main contributors to the systemic release and functionally assess which stimuli drive the release of the respective cytokine, so the specific cell function can be therapeutically modulated.

If these criteria are met and a clear characterization of cytokine behavior emerges, we suggest translating results and immune modulating therapeutics from other pathophysiologies, such as autoimmune diseases and cancer, to sepsis and trauma. These promising treatments that are being tested in these diseases potentially share common mechanisms. Thus, these FDA approved drugs for cancer and autoimmunity could potentially be trialed in the setting of sepsis or trauma to address pathological cytokine release of IL-10, TGF-β, and TSLP leading to disbalanced immunosuppression.

DATA AVAILABILITY STATEMENT

The original contributions presented in the study are included in the article/supplementary material. Further inquiries can be directed to the corresponding author.

AUTHOR CONTRIBUTIONS

CB and CC outlined the review. CB drafted the review, tables, and figures. CB and NB designed the figures. CC, NB, CS, MH, and PC reviewed the drafted review. The latter three especially providing critical clinical input concerning therapeutic approaches. All authors contributed to the article and approved the submitted version.

FUNDING

This work was supported by funding from the Deutsche Forschungsgemeinschaft (German Research Foundation) (BE 7016/1-1) (CB).

REFERENCES

1. Gallucci S, Matzinger P. Danger signals: SOS to the immune system. *Curr Opin Immunol* (2001) 13:114–9. doi: 10.1016/S0952-7915(00)00191-6
2. Raymond SL, Holden DC, Mira JC, Stortz JA, Loftus TJ, Mohr AM, et al. Microbial recognition and danger signals in sepsis and trauma. *Biochim Biophys Acta* (2017) 1863(10):2564–73. doi: 10.1016/j.bbadis.2017.01.013
3. Wajant H, Pfizenmaier K, Scheurich P. Tumor necrosis factor signaling. *Cell Death Differ* (2003) 10:45–65. doi: 10.1038/sj.cdd.4401189

4. Schulte W, Bernhagen J, Bucala R. Cytokines in sepsis: potent immunoregulators and potential therapeutic targets–an updated view. *Mediators Inflammation* (2013) 2013:165974. doi: 10.1155/2013/165974
5. Cohen J. The immunopathogenesis of sepsis. *Nature* (2002) 420:885–91. doi: 10.1038/nature01326
6. Eskilsson A, Mirrasekhian E, Dufour S, Schwaninger M, Engblom D, Blomqvist A. Immune-induced fever is mediated by IL-6 receptors on brain endothelial cells coupled to STAT3-dependent induction of brain endothelial prostaglandin synthesis. *J Neurosci* (2014) 34:15957–61. doi: 10.1523/JNEUROSCI.3520-14.2014
7. Chen Q, Fisher DT, Clancy KA, Gauguet JM, Wang WC, Unger E, et al. Fever-range thermal stress promotes lymphocyte trafficking across high endothelial venules via an interleukin 6 trans-signaling mechanism. *Nat Immunol* (2006) 7:1299–308. doi: 10.1038/ni1406
8. Chen Q, Wang WC, Bruce R, Li H, Schleider DM, Mulbury MJ, et al. Central role of IL-6 receptor signal-transducing chain gp130 in activation of L-selectin adhesion by fever-range thermal stress. *Immunity* (2004) 20:59–70. doi: 10.1016/S1074-7613(03)00358-3
9. Andrades ME, Morina A, Spasic S, Spasojevic I. Bench-to-bedside review: sepsis - from the redox point of view. *Crit Care* (2011) 15:230. doi: 10.1186/cc10334
10. Seymour CW, Kennedy JN, Wang S, Chang CH, Elliott CF, Xu Z, et al. Derivation, Validation, and Potential Treatment Implications of Novel Clinical Phenotypes for Sepsis. *JAMA* (2019) 321:2003–17. doi: 10.1001/jama.2019.5791
11. Semeraro N, Ammollo CT, Semeraro F, Colucci M. Sepsis-associated disseminated intravascular coagulation and thromboembolic disease. *Mediterr J Hematol Infect Dis* (2010) 2:e2010024. doi: 10.4084/mjhid.2010.024
12. Dewar DC, Mackay P, Balogh Z. Epidemiology of post-injury multiple organ failure in an Australian trauma system. *ANZ J Surg* (2009) 79:431–6. doi: 10.1111/j.1445-2197.2009.04968.x
13. Hotchkiss RS, Moldawer LL, Opal SM, Reinhart K, Turnbull IR, Vincent JL. Sepsis and septic shock. *Nat Rev Dis Primers* (2016) 2:16045. doi: 10.1038/nrdp.2016.45
14. Hotchkiss RS, Tinsley KW, Swanson PE, Schmieg REJr., Hui JJ, Chang KC, et al. Sepsis-induced apoptosis causes progressive profound depletion of B and CD4+ T lymphocytes in humans. *J Immunol* (2001) 166:6952–63. doi: 10.4049/jimmunol.166.11.6952
15. Venet F, Pachot A, Debard AL, Bohe J, Bienvenu J, Lepape A, et al. Increased percentage of CD4+CD25+ regulatory T cells during septic shock is due to the decrease of CD4+CD25- lymphocytes. *Crit Care Med* (2004) 32:2329–31. doi: 10.1097/01.CCM.0000145999.42971.4B
16. Hollen MK, Stortz JA, Darden D, Dirain ML, Nacionales DC, Hawkins RB, et al. Myeloid-derived suppressor cell function and epigenetic expression evolves over time after surgical sepsis. *Crit Care* (2019) 23:355. doi: 10.1186/s13054-019-2628-x
17. Drewry AM, Ablordeppey EA, Murray ET, Beiter ER, Walton AH, Hall MW, et al. Comparison of monocyte human leukocyte antigen-DR expression and stimulated tumor necrosis factor alpha production as outcome predictors in severe sepsis: a prospective observational study. *Crit Care* (2016) 20:334. doi: 10.1186/s13054-016-1505-0
18. Hotchkiss RS, Tinsley KW, Swanson PE, Grayson MH, Osborne DF, Wagner TH, et al. Depletion of dendritic cells, but not macrophages, in patients with sepsis. *J Immunol* (2002) 168:2493–500. doi: 10.4049/jimmunol.168.5.2493
19. Stortz JA, Mira JC, Raymond SL, Loftus TJ, Ozrazgat-Baslanti T, Wang Z, et al. Benchmarking clinical outcomes and the immunocatabolic phenotype of chronic critical illness after sepsis in surgical intensive care unit patients. *J Trauma Acute Care Surg* (2018) 84:342–9. doi: 10.1097/TA.0000000000001758
20. Rosenthal MD, Moore FA. Persistent Inflammation, Immunosuppression, and Catabolism: Evolution of Multiple Organ Dysfunction. *Surg Infections* (2016) 17:167–72. doi: 10.1089/sur.2015.184
21. Inoue S, Suzuki K, Komori Y, Morishita Y, Suzuki-Utsunomiya K, Hozumi K, et al. Persistent inflammation and T cell exhaustion in severe sepsis in the elderly. *Crit Care* (2014) 18:R130. doi: 10.1186/cc13941
22. Gentile LF, Cuenca AG, Efron PA, Ang D, Bihorac A, McKinley BA, et al. Persistent inflammation and immunosuppression: a common syndrome and new horizon for surgical intensive care. *J Trauma Acute Care Surg* (2012) 72:1491–501. doi: 10.1097/TA.0b013e318256e000
23. Hawkins RB, Raymond SL, Stortz JA, Horiguchi H, Brakenridge SC, Gardner A, et al. Chronic Critical Illness and the Persistent Inflammation, Immunosuppression, and Catabolism Syndrome. *Front Immunol* (2018) 9:1511. doi: 10.3389/fimmu.2018.01511
24. McBride MA, Owen AM, Stothers CL, Hernandez A, Luan L, Burelbach KR, et al. The Metabolic Basis of Immune Dysfunction Following Sepsis and Trauma. *Front Immunol* (2020) 11:1043. doi: 10.3389/fimmu.2020.01043
25. Rubio I, Osuchowski MF, Shankar-Hari M, Skirecki T, Winkler MS, Lachmann G, et al. Current gaps in sepsis immunology: new opportunities for translational research. *Lancet Infect Dis* (2019) 19:e422–36. doi: 10.1016/S1473-3099(19)30567-5
26. Kawai T, Akira S. The role of pattern-recognition receptors in innate immunity: update on Toll-like receptors. *Nat Immunol* (2010) 11:373–84. doi: 10.1038/ni.1863
27. Robertson CM, Coopersmith CM. The systemic inflammatory response syndrome. *Microbes Infection* (2006) 8:1382–9. doi: 10.1016/j.micinf.2005.12.016
28. Islam MN, Bradley BA, Ceredig R. Sterile post-traumatic immunosuppression. *Clin Trans Immunol* (2016) 5:e77. doi: 10.1038/cti.2016.13
29. Neunaber C, Zeckey C, Andruszkow H, Frink M, Mommsen P, Krettek C, et al. Immunomodulation in polytrauma and polymicrobial sepsis - where do we stand? *Recent Patents Inflammation Allergy Drug Discovery* (2011) 5:17–25. doi: 10.2174/187221311794474892
30. Jawa RS, Anillo S, Huntoon K, Baumann H, Kulaylat M. Interleukin-6 in surgery, trauma, and critical care part II: clinical implications. *J Intensive Care Med* (2011) 26:73–87. doi: 10.1177/0885066610395679
31. Sapan HB, Paturusi I, Jusuf I, Patellongi I, Massi MN, Pusponegoro AD, et al. Pattern of cytokine (IL-6 and IL-10) level as inflammation and anti-inflammation mediator of multiple organ dysfunction syndrome (MODS) in polytrauma. *Int J Burns Trauma* (2016) 6:37–43.
32. Venet F, Monneret G. Advances in the understanding and treatment of sepsis-induced immunosuppression. *Nat Rev Nephrol* (2017) 14:121. doi: 10.1038/nrneph.2017.165
33. Hotchkiss RS, Osmon SB, Chang KC, Wagner TH, Coopersmith CM, Karl IE. Accelerated lymphocyte death in sepsis occurs by both the death receptor and mitochondrial pathways. *J Immunol* (2005) 174:5110–8. doi: 10.4049/jimmunol.174.8.5110
34. Bergmann CB, Hefele F, Unger M, Huber-Wagner S, Biberthaler P, van Griensven M, et al. Platelets modulate the immune response following trauma by interaction with CD4+ T regulatory cells in a mouse model. *Immunol Res* (2016) 64:508–17. doi: 10.1007/s12026-015-8726-1
35. Monneret G, Debard AL, Venet F, Bohe J, Hequet O, Bienvenu J, et al. Marked elevation of human circulating CD4+CD25+ regulatory T cells in sepsis-induced immunoparalysis. *Crit Care Med* (2003) 31:2068–71. doi: 10.1097/01.CCM.0000069345.78884.0F
36. Boomer JS, To K, Chang KC, Takasu O, Osborne DF, Walton AH, et al. Immunosuppression in patients who die of sepsis and multiple organ failure. *Jama* (2011) 306:2594–605. doi: 10.1001/jama.2011.1829
37. Pugh AM, Auteri NJ, Goetzman HS, Caldwell CC, Nomellini V. A Murine Model of Persistent Inflammation, Immune Suppression, and Catabolism Syndrome. *Int J Mol Sci* (2017) 18. doi: 10.3390/ijms18081741
38. Liu YC, Zou XB, Chai YF, Yao YM. Macrophage polarization in inflammatory diseases. *Int J Biol Sci* (2014) 10:520–9. doi: 10.7150/ijbs.8879
39. Venet F, Lepape A, Monneret G. Clinical review: flow cytometry perspectives in the ICU - from diagnosis of infection to monitoring of injury-induced immune dysfunctions. *Crit Care* (2011) 15:231. doi: 10.1186/cc10333
40. Delano MJ, Ward PA. Sepsis-induced immune dysfunction: can immune therapies reduce mortality? *J Clin Invest* (2016) 126:23–31. doi: 10.1172/JCI82224
41. Delano MJ, Scumpia PO, Weinstein JS, Coco D, Nagaraj S, Kelly-Scumpia KM, et al. MyD88-dependent expansion of an immature GR-1(+)CD11b(+) population induces T cell suppression and Th2 polarization in sepsis. *J Exp Med* (2007) 204:1463–74. doi: 10.1084/jem.20062602
42. Ouyang W, O'Garra A. IL-10 Family Cytokines IL-10 and IL-22: from Basic Science to Clinical Translation. *Immunity* (2019) 50:871–91. doi: 10.1016/j.immuni.2019.03.020

43. Chen W, Ten Dijke P. Immunoregulation by members of the TGFbeta superfamily. *Nat Rev Immunol* (2016) 16:723–40. doi: 10.1038/nri.2016.112
44. Piliponsky AM, Lahiri A, Truong P, Clauson M, Shubin NJ, Han H, et al. Thymic Stromal Lymphopoietin Improves Survival and Reduces Inflammation in Sepsis. *Am J Respir Cell Mol Biol* (2016) 55:264–74. doi: 10.1165/rcmb.2015-0380OC
45. Huang LF, Yao YM, Dong N, Yu Y, He LX, Sheng ZY. Association between regulatory T cell activity and sepsis and outcome of severely burned patients: a prospective, observational study. *Crit Care* (2010) 14:R3. doi: 10.1186/cc8232
46. Mazer M, Unsinger J, Drewry A, Walton A, Osborne D, Blood T, et al. IL-10 Has Differential Effects on the Innate and Adaptive Immune Systems of Septic Patients. *J Immunol* (2019) 203:2088–99. doi: 10.4049/jimmunol.1900637
47. Yu Q, Li Y, Wang H, Xiong H. TSLP induces a proinflammatory phenotype in circulating innate cells and predicts prognosis in sepsis patients. *FEBS Open Bio* (2019) 9:2137–48. doi: 10.1002/2211-5463.12746
48. Li MO, Wan YY, Sanjabi S, Robertson AK, Flavell RA. Transforming growth factor-beta regulation of immune responses. *Annu Rev Immunol* (2006) 24:99–146. doi: 10.1146/annurev.immunol.24.021605.090737
49. Ng TH, Britton GJ, Hill EV, Verhagen J, Burton BR, Wraith DC. Regulation of adaptive immunity; the role of interleukin-10. *Front Immunol* (2013) 4:129. doi: 10.3389/fimmu.2013.00129
50. Sabat R, Grutz G, Warszawska K, Kirsch S, Witte E, Wolk K, et al. Biology of interleukin-10. *Cytokine Growth Factor Rev* (2010) 21:331–44. doi: 10.1016/j.cytogfr.2010.09.002
51. Mannino MH, Zhu Z, Xiao H, Bai Q, Wakefield MR, Fang Y. The paradoxical role of IL-10 in immunity and cancer. *Cancer Lett* (2015) 367:103–7. doi: 10.1016/j.canlet.2015.07.009
52. Trifunovic J, Miller L, Debeljak Z, Horvat V. Pathologic patterns of interleukin 10 expression–a review. *Biochem Med (Zagreb)* (2015) 25:36–48. doi: 10.11613/BM.2015.004
53. Saxena A, Khosraviani S, Noel S, Mohan D, Donner T, Hamad AR. Interleukin-10 paradox: A potent immunoregulatory cytokine that has been difficult to harness for immunotherapy. *Cytokine* (2015) 74:27–34. doi: 10.1016/j.cyto.2014.10.031
54. Penaloza HF, Schultz BM, Nieto PA, Salazar GA, Suazo I, Gonzalez PA, et al. Opposing roles of IL-10 in acute bacterial infection. *Cytokine Growth Factor Rev* (2016) 32:17–30. doi: 10.1016/j.cytogfr.2016.07.003
55. Mittal SK, Roche PA. Suppression of antigen presentation by IL-10. *Curr Opin Immunol* (2015) 34:22–7. doi: 10.1016/j.coi.2014.12.009
56. Kany S, Vollrath JT, Relja B. Cytokines in Inflammatory Disease. *Int J Mol Sci* (2019) 20. doi: 10.3390/ijms20236008
57. Opal SM, DePalo VA. Anti-inflammatory cytokines. *Chest* (2000) 117:1162–72. doi: 10.1378/chest.117.4.1162
58. Petitjean G, Chevalier MF, Tibaoui F, Didier C, Manea ME, Liovat AS, et al. Level of double negative T cells, which produce TGF-beta and IL-10, predicts CD8 T-cell activation in primary HIV-1 infection. *AIDS (London England)* (2012) 26:139–48. doi: 10.1097/QAD.0b013e32834e1484
59. de Waal Malefyt R, Haanen J, Spits H, Roncarolo MG, te Velde A, Figdor C, et al. Interleukin 10 (IL-10) and viral IL-10 strongly reduce antigen-specific human T cell proliferation by diminishing the antigen-presenting capacity of monocytes via downregulation of class II major histocompatibility complex expression. *J Exp Med* (1991) 174:915–24. doi: 10.1084/jem.174.4.915
60. Creery WD, Diaz-Mitoma F, Filion L, Kumar A. Differential modulation of B7-1 and B7-2 isoform expression on human monocytes by cytokines which influence the development of T helper cell phenotype. *Eur J Immunol* (1996) 26:1273–7. doi: 10.1002/eji.1830260614
61. Bazzoni F, Tamassia N, Rossato M, Cassatella MA. Understanding the molecular mechanisms of the multifaceted IL-10-mediated anti-inflammatory response: lessons from neutrophils. *Eur J Immunol* (2010) 40:2360–8. doi: 10.1002/eji.200940294
62. Lichte P, Pfeifer R, Kobbe P, Tohidnezhad M, Pufe T, Almahmoud K, et al. Inhalative IL-10 treatment after bilateral femoral fractures affect pulmonary inflammation in mice. *Ann Anat* (2015) 200:73–8. doi: 10.1016/j.aanat.2015.02.005
63. Keel M, Ungethum U, Steckholzer U, Niederer E, Hartung T, Trentz O, et al. Interleukin-10 counterregulates proinflammatory cytokine-induced inhibition of neutrophil apoptosis during severe sepsis. *Blood* (1997) 90:3356–63. doi: 10.1182/blood.V90.9.3356
64. Cassatella MA, Meda L, Bonora S, Ceska M, Constantin G. Interleukin 10 (IL-10) inhibits the release of proinflammatory cytokines from human polymorphonuclear leukocytes. Evidence for an autocrine role of tumor necrosis factor and IL-1 beta in mediating the production of IL-8 triggered by lipopolysaccharide. *J Exp Med* (1993) 178:2207–11. doi: 10.1084/jem.178.6.2207
65. Lewkowicz N, Mycko MP, Przygodzka P, Cwiklinska H, Cichalewska M, Matysiak M, et al. Induction of human IL-10-producing neutrophils by LPS-stimulated Treg cells and IL-10. *Mucosal Immunol* (2016) 9:364–78. doi: 10.1038/mi.2015.66
66. Kasten KR, Muenzer JT, Caldwell CC. Neutrophils are significant producers of IL-10 during sepsis. *Biochem Biophys Res Commun* (2010) 393:28–31. doi: 10.1016/j.bbrc.2010.01.066
67. Zhao HQ, Li WM, Lu ZQ, Sheng ZY, Yao YM. The growing spectrum of anti-inflammatory interleukins and their potential roles in the development of sepsis. *J Interferon Cytokine Res Off J Int Soc Interferon Cytokine Res* (2015) 35:242–51. doi: 10.1089/jir.2014.0119
68. Murai M, Turovskaya O, Kim G, Madan R, Karp CL, Cheroutre H, et al. Interleukin 10 acts on regulatory T cells to maintain expression of the transcription factor Foxp3 and suppressive function in mice with colitis. *Nat Immunol* (2009) 10:1178–84. doi: 10.1038/ni.1791
69. Tschoeke SK, Oberholzer C, LaFace D, Hutchins B, Moldawer LL, Oberholzer A. Endogenous IL-10 regulates sepsis-induced thymic apoptosis and improves survival in septic IL-10 null mice. *Scand J Immunol* (2008) 68:565–71. doi: 10.1111/j.1365-3083.2008.02176.x
70. Mumm JB, Emmerich J, Zhang X, Chan I, Wu L, Mauze S, et al. IL-10 elicits IFNgamma-dependent tumor immune surveillance. *Cancer Cell* (2011) 20:781–96. doi: 10.1016/j.ccr.2011.11.003
71. Naing A, Infante JR, Papadopoulos KP, Chan IH, Shen C, Ratti NP, et al. PEGylated IL-10 (Pegilodecakin) Induces Systemic Immune Activation, CD8(+) T Cell Invigoration and Polyclonal T Cell Expansion in Cancer Patients. *Cancer Cell* (2018) 34:775–791 e3. doi: 10.1016/j.ccell.2018.10.007
72. Yao Y, Simard AR, Shi FD, Hao J. IL-10-producing lymphocytes in inflammatory disease. *Int Rev Immunol* (2013) 32:324–36. doi: 10.3109/08830185.2012.762361
73. Kobbe P, Lichte P, Schreiber H, Reiss LK, Uhlig S, Pape HC, et al. Inhalative IL-10 attenuates pulmonary inflammation following hemorrhagic shock without major alterations of the systemic inflammatory response. *Mediators Inflammation* (2012) 2012:512974. doi: 10.1155/2012/512974
74. Cao C, Yu M, Chai Y. Pathological alteration and therapeutic implications of sepsis-induced immune cell apoptosis. *Cell Death Dis* (2019) 10:782. doi: 10.1038/s41419-019-2015-1
75. Misra AK, Levy MM, Ward NS. Biomarkers of Immunosuppression. *Crit Care Clin* (2020) 36:167–76. doi: 10.1016/j.ccc.2019.08.013
76. Xia BT, Beckmann N, Winer LK, Kim Y, Goetzman HS, Veile RE, et al. Amitriptyline Treatment Mitigates Sepsis-Induced Tumor Necrosis Factor Expression and Coagulopathy. *Shock* (2018) 51(3):356–63. doi: 10.1097/SHK.0000000000001146
77. Latifi SQ, O'Riordan MA, Levine AD. Interleukin-10 controls the onset of irreversible septic shock. *Infection Immun* (2002) 70:4441–6. doi: 10.1128/IAI.70.8.4441-4446.2002
78. Stensballe J, Christiansen M, Tonnesen E, Espersen K, Lippert FK, Rasmussen LS. The early IL-6 and IL-10 response in trauma is correlated with injury severity and mortality. *Acta Anaesthesiol Scand* (2009) 53:515–21. doi: 10.1111/j.1399-6576.2008.01801.x
79. Feng M, Sun T, Zhao Y, Zhang H. Detection of Serum Interleukin-6/10/18 Levels in Sepsis and Its Clinical Significance. *J Clin Lab Anal* (2016) 30:1037–43. doi: 10.1002/jcla.21977
80. Chen P, Stanojcic M, Jeschke MG. Septic predictor index: A novel platform to identify thermally injured patients susceptible to sepsis. *Surgery* (2018) 163:409–14. doi: 10.1016/j.surg.2017.08.010
81. Gogos CA, Drosou E, Bassaris HP, Skoutelis A. Pro- versus anti-inflammatory cytokine profile in patients with severe sepsis: a marker for prognosis and future therapeutic options. *J Infect Dis* (2000) 181:176–80. doi: 10.1086/315214

82. Chuang TY, Chang HT, Chung KP, Cheng HS, Liu CY, Liu YC, et al. High levels of serum macrophage migration inhibitory factor and interleukin 10 are associated with a rapidly fatal outcome in patients with severe sepsis. *Int J Infect Dis* (2014) 20:13–7. doi: 10.1016/j.ijid.2013.12.006
83. Frencken JF, van Vught LA, Peelen LM, Ong DSY, Klein Klouwenberg PMC, Horn J, et al. An Unbalanced Inflammatory Cytokine Response Is Not Associated With Mortality Following Sepsis: A Prospective Cohort Study. *Crit Care Med* (2017) 45:e493–9. doi: 10.1097/CCM.0000000000002292
84. van Vught LA, Klein Klouwenberg PM, Spitoni C, Scicluna BP, Wiewel MA, Horn J, et al. Incidence, Risk Factors, and Attributable Mortality of Secondary Infections in the Intensive Care Unit After Admission for Sepsis. *JAMA* (2016) 315:1469–79. doi: 10.1001/jama.2016.2691
85. Ivanov P, Anderson P. Post-transcriptional regulatory networks in immunity. *Immunol Rev* (2013) 253:253–72. doi: 10.1111/imr.12051
86. Easton R, Balogh ZJ. Peri-operative changes in serum immune markers after trauma: a systematic review. *Injury* (2014) 45:934–41. doi: 10.1016/j.injury.2013.12.002
87. Li X, Xu Z, Pang X, Huang Y, Yang B, Yang Y, et al. Interleukin-10/lymphocyte ratio predicts mortality in severe septic patients. *PloS One* (2017) 12:e0179050. doi: 10.1371/journal.pone.0179050
88. Zhao S, Wu D, Wu P, Wang Z, Huang J. Serum IL-10 Predicts Worse Outcome in Cancer Patients: A Meta-Analysis. *PloS One* (2015) 10: e0139598. doi: 10.1371/journal.pone.0139598
89. Gabrysova L, Howes A, Saraiva M, O'Garra A. The regulation of IL-10 expression. *Curr Top Microbiol Immunol* (2014) 380:157–90. doi: 10.1007/978-3-662-43492-5_8
90. Tamassia N, Le Moigne V, Calzetti F, Donini M, Gasperini S, Ear T, et al. The MyD88-independent pathway is not mobilized in human neutrophils stimulated via TLR4. *J Immunol* (2007) 178:7344–56. doi: 10.4049/jimmunol.178.11.7344
91. Lachmann G, von Haefen C, Kurth J, Yuerek F, Spies C. Innate immunity recovers earlier than acquired immunity during severe postoperative immunosuppression. *Int J Med Sci* (2018) 15:1–9. doi: 10.7150/ijms.21433
92. Ocuin LM, Bamboat ZM, Balachandran VP, Cavnar MJ, Obaid H, Plitas G, et al. Neutrophil IL-10 suppresses peritoneal inflammatory monocytes during polymicrobial sepsis. *J Leukoc Biol* (2011) 89:423–32. doi: 10.1189/jlb.0810479
93. Voll RE, Herrmann M, Roth EA, Stach C, Kalden JR, Girkontaite I. Immunosuppressive effects of apoptotic cells. *Nature* (1997) 390:350–1. doi: 10.1038/37022
94. Huynh ML, Fadok VA, Henson PM. Phosphatidylserine-dependent ingestion of apoptotic cells promotes TGF-beta1 secretion and the resolution of inflammation. *J Clin Invest* (2002) 109:41–50. doi: 10.1172/JCI0211638
95. Ortega-Gomez A, Perretti M, Soehnlein O. Resolution of inflammation: an integrated view. *EMBO Mol Med* (2013) 5:661–74. doi: 10.1002/emmm.201202382
96. Lawrence SM, Corriden R, Nizet V. How Neutrophils Meet Their End. *Trends Immunol* (2020) 41:531–44. doi: 10.1016/j.it.2020.03.008
97. Goren I, Allmann N, Yogev N, Schurmann C, Linke A, Holdener M, et al. A transgenic mouse model of inducible macrophage depletion: effects of diphtheria toxin-driven lysozyme M-specific cell lineage ablation on wound inflammatory, angiogenic, and contractive processes. *Am J Pathol* (2009) 175:132–47. doi: 10.2353/ajpath.2009.081002
98. Korner A, Schlegel M, Theurer J, Frohnmeyer H, Adolph M, Heijink M, et al. Resolution of inflammation and sepsis survival are improved by dietary Omega-3 fatty acids. *Cell Death Differ* (2018) 25:421–31. doi: 10.1038/cdd.2017.177
99. Walker J, Dichter E, Lacorte G, Kerner D, Spur B, Rodriguez A, et al. Lipoxin a4 increases survival by decreasing systemic inflammation and bacterial load in sepsis. *Shock* (2011) 36:410–6. doi: 10.1097/SHK.0b013e31822798c1
100. Kang JW, Lee SM. Resolvin D1 protects the liver from ischemia/reperfusion injury by enhancing M2 macrophage polarization and efferocytosis. *Biochim Biophys Acta* (2016) 1861:1025–35. doi: 10.1016/j.bbalip.2016.06.002
101. Schutters K, Kusters DH, Chatrou ML, Montero-Melendez T, Donners M, Deckers NM, et al. Cell surface-expressed phosphatidylserine as therapeutic target to enhance phagocytosis of apoptotic cells. *Cell Death Differ* (2013) 20:49–56. doi: 10.1038/cdd.2012.107
102. Oberholzer A, Oberholzer C, Moldawer LL. Interleukin-10: A complex role in the pathogenesis of sepsis syndromes and its potential as an anti-inflammatory drug. *Crit Care Med* (2002) 30:S58–63. doi: 10.1097/00003246-200201001-00008
103. Hiraki S, Ono S, Tsujimoto H, Kinoshita M, Takahata R, Miyazaki H, et al. Neutralization of interleukin-10 or transforming growth factor-beta decreases the percentages of CD4+ CD25+ Foxp3+ regulatory T cells in septic mice, thereby leading to an improved survival. *Surgery* (2012) 151:313–22. doi: 10.1016/j.surg.2011.07.019
104. Pajkrt D, van der Poll T, Levi M, Cutler DL, Affrime MB, van den Ende A, et al. Interleukin-10 inhibits activation of coagulation and fibrinolysis during human endotoxemia. *Blood* (1997) 89:2701–5. doi: 10.1182/blood.V89.8.2701
105. Pajkrt D, Camoglio L, Tiel-van Buul MC, de Bruin K, Cutler DL, Affrime MB, et al. Attenuation of proinflammatory response by recombinant human IL-10 in human endotoxemia: effect of timing of recombinant human IL-10 administration. *J Immunol* (1997) 158:3971–7.
106. Wong JJM, Leong JY, Lee JH, Albani S, Yeo JG. Insights into the immuno-pathogenesis of acute respiratory distress syndrome. *Ann Transl Med* (2019) 7:504. doi: 10.21037/atm.2019.09.28
107. van der Poll T, Jansen PM, Montegut WJ, Braxton CC, Calvano SE, Stackpole SA, et al. Effects of IL-10 on systemic inflammatory responses during sublethal primate endotoxemia. *J Immunol* (1997) 158:1971–5.
108. Remick DG, Garg SJ, Newcomb DE, Wollenberg G, Huie TK, Bolgos GL. Exogenous interleukin-10 fails to decrease the mortality or morbidity of sepsis. *Crit Care Med* (1998) 26:895–904. doi: 10.1097/00003246-199805000-00025
109. Sanjabi S, Oh SA, Li MO. Regulation of the Immune Response by TGF-beta: From Conception to Autoimmunity and Infection. *Cold Spring Harb Perspect Biol* (2017) 9. doi: 10.1101/cshperspect.a022236
110. Tran DQ. TGF-beta: the sword, the wand, and the shield of FOXP3(+) regulatory T cells. *J Mol Cell Biol* (2012) 4:29–37. doi: 10.1093/jmcb/mjr033
111. Cottrez F, Groux H. Regulation of TGF-beta response during T cell activation is modulated by IL-10. *J Immunol* (2001) 167:773–8. doi: 10.4049/jimmunol.167.2.773
112. Curotto de Lafaille MA, Lino AC, Kutchukhidze N, Lafaille JJ. CD25- T cells generate CD25+Foxp3+ regulatory T cells by peripheral expansion. *J Immunol* (2004) 173:7259–68. doi: 10.4049/jimmunol.173.12.7259
113. Chen W, Jin W, Hardegen N, Lei KJ, Li L, Marinos N, et al. Conversion of peripheral CD4+CD25- naive T cells to CD4+CD25+ regulatory T cells by TGF-beta induction of transcription factor Foxp3. *J Exp Med* (2003) 198:1875–86. doi: 10.1084/jem.20030152
114. Kitani A, Fuss I, Nakamura K, Kumaki F, Usui T, Strober W. Transforming growth factor (TGF)-beta1-producing regulatory T cells induce Smad-mediated interleukin 10 secretion that facilitates coordinated immunoregulatory activity and amelioration of TGF-beta1-mediated fibrosis. *J Exp Med* (2003) 198:1179–88. doi: 10.1084/jem.20030917
115. Vignali DA, Collison LW, Workman CJ. How regulatory T cells work. *Nat Rev Immunol* (2008) 8:523–32. doi: 10.1038/nri2343
116. Travis MA, Reizis B, Melton AC, Masteller E, Tang Q, Proctor JM, et al. Loss of integrin alpha(v)beta8 on dendritic cells causes autoimmunity and colitis in mice. *Nature* (2007) 449:361–5. doi: 10.1038/nature06110
117. Fogel-Petrovic M, Long JA, Misso NL, Foster PS, Bhoola KD, Thompson PJ. Physiological concentrations of transforming growth factor beta1 selectively inhibit human dendritic cell function. *Int Immunopharmacol* (2007) 7:1924–33. doi: 10.1016/j.intimp.2007.07.003
118. Delvig AA, Lee JJ, Chrzanowska-Lightowlers ZM, Robinson JH. TGF-beta1 and IFN-gamma cross-regulate antigen presentation to CD4 T cells by macrophages. *J Leukoc Biol* (2002) 72:163–6.
119. Fridlender ZG, Sun J, Kim S, Kapoor V, Cheng G, Ling L, et al. Polarization of tumor-associated neutrophil phenotype by TGF-beta: "N1" versus "N2" TAN. *Cancer Cell* (2009) 16:183–94. doi: 10.1016/j.ccr.2009.06.017
120. Balazovich KJ, Fernandez R, Hinkovska-Galcheva V, Suchard SJ, Boxer LA. Transforming growth factor-beta1 stimulates degranulation and oxidant release by adherent human neutrophils. *J Leukoc Biol* (1996) 60:772–7. doi: 10.1002/jlb.60.6.772
121. Monneret G, Finck ME, Venet F, Debard AL, Bohe J, Bienvenu J, et al. The anti-inflammatory response dominates after septic shock: association of low

monocyte HLA-DR expression and high interleukin-10 concentration. *Immunol Lett* (2004) 95:193–8. doi: 10.1016/j.imlet.2004.07.009
122. Knapp S, Thalhammer F, Locker GJ, Laczika K, Hollenstein U, Frass M, et al. Prognostic value of MIP-1 alpha, TGF-beta 2, sELAM-1, and sVCAM-1 in patients with gram-positive sepsis. *Clin Immunol Immunopathol* (1998) 87:139–44. doi: 10.1006/clin.1998.4523
123. Yeh FL, Shen HD, Fang RH. Deficient transforming growth factor beta and interleukin-10 responses contribute to the septic death of burned patients. *Burns J Int Soc Burn Injuries* (2002) 28:631–7. doi: 10.1016/S0305-4179(02)00113-4
124. Gabriel VA. Transforming growth factor-beta and angiotensin in fibrosis and burn injuries. *J Burn Care Res* (2009) 30:471–81. doi: 10.1097/BCR.0b013e3181a28ddb
125. Marie C, Cavaillon JM, Losser MR. Elevated levels of circulating transforming growth factor-beta 1 in patients with the sepsis syndrome. *Ann Intern Med* (1996) 125:520–1. doi: 10.7326/0003-4819-125-6-199609150-00034
126. de Pablo R, Monserrat J, Reyes E, Diaz D, Rodriguez-Zapata M, la Hera A, et al. Sepsis-induced acute respiratory distress syndrome with fatal outcome is associated to increased serum transforming growth factor beta-1 levels. *Eur J Intern Med* (2012) 23:358–62. doi: 10.1016/j.ejim.2011.10.001
127. Ayala A, Knotts JB, Ertel W, Perrin MM, Morrison MH, Chaudry IH. Role of interleukin 6 and transforming growth factor-beta in the induction of depressed splenocyte responses following sepsis. *Arch Surg* (1993) 128:89–94; discussion 94-5. doi: 10.1001/archsurg.1993.01420130101015
128. Nullens S, De Man J, Bridts C, Ebo D, Francque S, De Winter B. Identifying Therapeutic Targets for Sepsis Research: A Characterization Study of the Inflammatory Players in the Cecal Ligation and Puncture Model. *Mediators Inflammation* (2018) 2018:5130463. doi: 10.1155/2018/5130463
129. Ahmad S, Choudhry MA, Shankar R, Sayeed MM. Transforming growth factor-beta negatively modulates T-cell responses in sepsis. *FEBS Lett* (1997) 402:213–8. doi: 10.1016/S0014-5793(96)01535-9
130. Xu F, Lin SH, Yang YZ, Guo R, Cao J, Liu Q. The effect of curcumin on sepsis-induced acute lung injury in a rat model through the inhibition of the TGF-beta1/SMAD3 pathway. *Int Immunopharmacol* (2013) 16:1–6. doi: 10.1016/j.intimp.2013.03.014
131. Garcia-Lazaro JF, Thieringer F, Luth S, Czochra P, Meyer E, Renteria IB, et al. Hepatic over-expression of TGF-beta1 promotes LPS-induced inflammatory cytokine secretion by liver cells and endotoxemic shock. *Immunol Lett* (2005) 101:217–22. doi: 10.1016/j.imlet.2005.06.003
132. Kumar A, Kumar A, Paladugu B, Mensing J, Parrillo JE. Transforming growth factor-beta1 blocks in vitro cardiac myocyte depression induced by tumor necrosis factor-alpha, interleukin-1beta, and human septic shock serum. *Crit Care Med* (2007) 35:358–64. doi: 10.1097/01.CCM.0000254341.87098.A4
133. Ganeshan K, Johnston LK, Bryce PJ. TGF-beta1 limits the onset of innate lung inflammation by promoting mast cell-derived IL-6. *J Immunol* (2013) 190:5731–8. doi: 10.4049/jimmunol.1203362
134. Chen W, Frank ME, Jin W, Wahl SM. TGF-beta released by apoptotic T cells contributes to an immunosuppressive milieu. *Immunity* (2001) 14:715–25. doi: 10.1016/S1074-7613(01)00147-9
135. Conway Morris A, Datta D, Shankar-Hari M, Stephen J, Weir CJ, Rennie J, et al. Cell-surface signatures of immune dysfunction risk-stratify critically ill patients: INFECT study. *Intensive Care Med* (2018) 44:627–35. doi: 10.1007/s00134-018-5247-0
136. Jianqiong Zeng HX, Zhu G, Kuang C, Wu Y. Changes of cytokines levels after decreasing regulatory T cells activity during sepsis. *Int J Clin Exp Pathol* (2017) 10(3):2911–6.
137. Hotchkiss RS, Colston E, Yende S, Crouser ED, Martin GS, Albertson T, et al. Immune checkpoint inhibition in sepsis: a Phase 1b randomized study to evaluate the safety, tolerability, pharmacokinetics, and pharmacodynamics of nivolumab. *Intensive Care Med* (2019) 45:1360–71. doi: 10.1007/s00134-019-05704-z
138. Ziegler SF, Roan F, Bell BD, Stoklasek TA, Kitajima M, Han H. The biology of thymic stromal lymphopoietin (TSLP). *Adv Pharmacol* (2013) 66:129–55. doi: 10.1016/B978-0-12-404717-4.00004-4
139. Bjerkan L, Sonesson A, Schenck K. Multiple Functions of the New Cytokine-Based Antimicrobial Peptide Thymic Stromal Lymphopoietin (TSLP). *Pharm (Basel)* (2016) 9. doi: 10.3390/ph9030041
140. Takai T. TSLP expression: cellular sources, triggers, and regulatory mechanisms. *Allergol Int* (2012) 61:3–17. doi: 10.2332/allergolint.11-RAI-0395
141. Varricchi G, Pecoraro A, Marone G, Criscuolo G, Spadaro G, Genovese A, et al. Thymic Stromal Lymphopoietin Isoforms, Inflammatory Disorders, and Cancer. *Front Immunol* (2018) 9:1595. doi: 10.3389/fimmu.2018.01595
142. He R, Geha RS. Thymic stromal lymphopoietin. *Ann N Y Acad Sci* (2010) 1183:13–24. doi: 10.1111/j.1749-6632.2009.05128.x
143. Zhong J, Sharma J, Raju R, Palapetta SM, Prasad TS, Huang TC, et al. TSLP signaling pathway map: a platform for analysis of TSLP-mediated signaling. *Database (Oxford)* (2014) 2014:bau007. doi: 10.1093/database/bau007
144. Yu X, Li H, Ren X. Signaling cascades initiated by TSLP-mediated signals in different cell types. *Cell Immunol* (2012) 279:174–9. doi: 10.1016/j.cellimm.2012.10.005
145. Soumelis V, Reche PA, Kanzler H, Yuan W, Edward G, Homey B, et al. Human epithelial cells trigger dendritic cell mediated allergic inflammation by producing TSLP. *Nat Immunol* (2002) 3:673–80. doi: 10.1038/ni805
146. West EE, Spolski R, Kazemian M, Yu ZX, Kemper C, Leonard WJ. A TSLP-complement axis mediates neutrophil killing of methicillin-resistant Staphylococcus aureus. *Sci Immunol* (2016) 1. doi: 10.1126/sciimmunol.aaf8471
147. Kuethe JW, Prakash PS, Midura EF, Johnson BL,3, Kasten KR, Caldwell CC. Thymic stromal lymphopoietin mediates the host response and increases mortality during sepsis. *J Surg Res* (2014) 191:19–24. doi: 10.1016/j.jss.2014.05.024
148. Han NR, Moon PD, Kim HM, Jeong HJ. TSLP Exacerbates Septic Inflammation via Murine Double Minute 2 (MDM2) Signaling Pathway. *J Clin Med* (2019) 8. doi: 10.3390/jcm8091350
149. Lan F, Zhang N, Holtappels G, De Ruyck N, Krysko O, Van Crombruggen K, et al. Staphylococcus aureus Induces a Mucosal Type 2 Immune Response via Epithelial Cell-derived Cytokines. *Am J Respir Crit Care Med* (2018) 198:452–63. doi: 10.1164/rccm.201710-2112OC
150. Hajj J, Blaine N, Salavaci J, Jacoby D. The "Centrality of Sepsis": A Review on Incidence, Mortality, and Cost of Care. *Healthc (Basel)* (2018) 6. doi: 10.3390/healthcare6030090
151. Rhee P, Joseph B, Pandit V, Aziz H, Vercruysse G, Kulvatunyou N, et al. Increasing trauma deaths in the United States. *Ann Surg* (2014) 260:13–21. doi: 10.1097/SLA.0000000000000600
152. Mira JC, Szpila BE, Nacionales DC, Lopez MC, Gentile LF, Mathias BJ, et al. Patterns of gene expression among murine models of hemorrhagic shock/trauma and sepsis. *Physiol Genomics* (2016) 48:135–44. doi: 10.1152/physiolgenomics.00072.2015
153. Smedman C, Gardlund B, Nihlmark K, Gille-Johnson P, Andersson J, Paulie S. ELISpot analysis of LPS-stimulated leukocytes: human granulocytes selectively secrete IL-8, MIP-1beta and TNF-alpha. *J Immunol Methods* (2009) 346:1–8. doi: 10.1016/j.jim.2009.04.001
154. Guignant C, Lepape A, Huang X, Kherouf H, Denis L, Poitevin F, et al. Programmed death-1 levels correlate with increased mortality, nosocomial infection and immune dysfunctions in septic shock patients. *Crit Care* (2011) 15:R99. doi: 10.1186/cc10112
155. Hutchins NA, Unsinger J, Hotchkiss RS, Ayala A. The new normal: immunomodulatory agents against sepsis immune suppression. *Trends Mol Med* (2014) 20:224–33. doi: 10.1016/j.molmed.2014.01.002
156. Zhang Y, Li J, Lou J, Zhou Y, Bo L, Zhu J, et al. Upregulation of programmed death-1 on T cells and programmed death ligand-1 on monocytes in septic shock patients. *Crit Care* (2011) 15:R70. doi: 10.1186/cc10059
157. Chang K, Svabek C, Vazquez-Guillamet C, Sato B, Rasche D, Wilson S, et al. Targeting the programmed cell death 1: programmed cell death ligand 1 pathway reverses T cell exhaustion in patients with sepsis. *Crit Care* (2014) 18:R3. doi: 10.1186/cc13176
158. Shipkova M, Wieland E. Surface markers of lymphocyte activation and markers of cell proliferation. *Clin Chim Acta* (2012) 413:1338–49. doi: 10.1016/j.cca.2011.11.006

159. Chang KC, Burnham CA, Compton SM, Rasche DP, Mazuski RJ, McDonough JS, et al. Blockade of the negative co-stimulatory molecules PD-1 and CTLA-4 improves survival in primary and secondary fungal sepsis. *Crit Care* (2013) 17:R85. doi: 10.1186/cc12711
160. Reinhart K, Bauer M, Riedemann NC, Hartog CS. New approaches to sepsis: molecular diagnostics and biomarkers. *Clin Microbiol Rev* (2012) 25:609–34. doi: 10.1128/CMR.00016-12
161. Taneja I, Reddy B, Damhorst G, Dave Zhao S, Hassan U, Price Z, et al. Combining Biomarkers with EMR Data to Identify Patients in Different Phases of Sepsis. *Sci Rep* (2017) 7:10800. doi: 10.1038/s41598-017-09766-1

Conflict of Interest: The authors declare that the research was conducted in the absence of any commercial or financial relationships that could be construed as a potential conflict of interest.

frontiers in Immunology

MINI REVIEW
published: 15 March 2021
doi: 10.3389/fimmu.2021.656039

Neutrophil in Reverse Migration: Role in Sepsis

Jingjing Ji [1,2] *and Jie Fan* [1,3,4]*

[1] Department of Surgery, University of Pittsburgh School of Medicine, Pittsburgh, PA, United States, [2] Department of Critical Care Medicine, General Hospital of Southern Theater Command of PLA, Guangzhou, China, [3] Research and Development, Veterans Affairs Pittsburgh Healthcare System, Pittsburgh, PA, United States, [4] McGowan Institute for Regenerative Medicine, University of Pittsburgh, Pittsburgh, PA, United States

Sepsis is life-threatening organ dysfunction caused by a dysregulated host response to infection. During the development and progression of sepsis, polymorphonuclear neutrophils (PMNs) are the most abundantly recruited innate immune cells at sites of infection, playing critical roles in the elimination of local infection and healing of the injury. PMN reverse migration (rM) describes the phenomenon in which PMNs migrate away from the inflammatory site back into the vasculature following the initial PMN infiltration. The functional role of PMN rM within inflammatory scenarios requires further exploration. Current evidence suggests that depending on the context, PMN rM can be both a protective response, by facilitating an efficient resolution to innate immune reaction, and also a tissue-damaging event. In this review, we provide an overview of current advancements in understanding the mechanism and roles of PMN rM in inflammation and sepsis. A comprehensive understanding of PMN rM may allow for the development of novel prophylactic and therapeutic strategies for sepsis.

Keywords: PMN, sepsis, inflammation, rerverse migration, infection

OPEN ACCESS

Edited by:
Yong Ming Yao,
First Affiliated Hospital of Chinese PLA General Hospital, China

Reviewed by:
Jennifer Catherine Brazil,
University of Michigan, United States
Ronen Sumagin,
Northwestern University, United States

***Correspondence:**
Jie Fan
jif7@pitt.edu

Specialty section:
This article was submitted to Inflammation, a section of the journal Frontiers in Immunology

Received: *20 January 2021*
Accepted: *17 February 2021*
Published: *15 March 2021*

Citation:
Ji J and Fan J (2021) Neutrophil in Reverse Migration: Role in Sepsis. Front. Immunol. 12:656039. doi: 10.3389/fimmu.2021.656039

INTRODUCTION

Polymorphonuclear neutrophils (PMNs) are the first responders in the circulation, playing an important role in defending against invading pathogens (1). Being attracted by a chemokine concentration gradient, PMNs migrate from the bloodstream into the inflamed extravascular tissues (2, 3). In the inflammatory site, PMNs eliminate pathogen through degranulation, phagocytosis, the formation of neutrophil extracellular traps (NETs), and releasing cytokines (3, 4). After PMNs execute their antimicrobial agenda, timely clearance of PMNs is crucial to maintain homeostasis (2, 5, 6). Traditionally, apoptosis or necrosis and subsequent phagocytosis by macrophages were considered as the main ways for PMN clearance (7, 8). However, with the development of imaging technology, it has been found that the recruited PMNs could migrate back to the circulation, which serves as a new way of PMN clearance in inflammatory or injury site (8, 9). In 1997, Hughes et al. using a rat glomerular capillary injury model and radiolabeling of PMN found that over 70% of PMNs that entered inflamed glomerular capillaries were able to return to the main circulation without undergoing apoptosis in the inflammatory site (8, 10). The process of PMN migrating back to circulation has been referred to as "PMN reverse migration (rM)" to describe the general phenomenon of PMN moving in the opposite direction to that expected (11). The *in vivo* visualization of PMN rM was first carried out on zebrafish larvae in 2006 (12). Mathias et al. found that not all recruited PMNs died at the site of injury, and most PMNs left the site and back to circulation (13). In the same year, Buckley et al. observed

in vitro that human PMNs could reverse transmigrate through the tumor necrosis factor-α (TNF-α)-activated endothelial monolayer (14). Further studies showed that reverse migrated PMNs are characterized by high expression of intercellular adhesion molecule-1 (ICAM-1 high) and low expression of C-X-C motif chemokine receptor 1 (CXCR1 low), which are different from the PMN in circulation with ICAM-1 ^{low}/CXCR1 ^{high} or those resident in tissue with ICAM-1 ^{high}/CXCR1 ^{high} (15, 16). The markers of ICAM-1 ^{high}/CXCR1 ^{low} are then found also valid for the reverse migrated PMNs in the peripheral blood of patients with systemic inflammation (14). In 2017, *in vivo* PMN rM in mice was visualized by Wang et al. in a sterile thermal hepatic injury model, in which reverse migrated PMNs from the inflammatory site were imaged in the lungs and bone marrow (17). The published data support the note that PMN rM is an important biological conservative phenomenon existing in from zebrafish to humans (11, 14, 17–21).

CURRENT KNOWLEDGE ON THE MECHANISMS OF PMN rM

The infiltration of PMNs from circulation to an inflammatory site is a regulated multi-stage process, as summarized in several review articles (2, 6, 22). PMNs first recognize inflammatory signs by sensing chemokines, e.g., macrophage-inflammatory protein-2 (MIP-2) and keratinocyte-derived chemokine (KC) (23, 24), followed by several processes, including capture, rolling, firm adhesion, and transendothelial migration, to reach the site of inflammation (25, 26). Corresponding to these steps, PMN rM has been considered as a continuous multi-stage process as well. Sussan et al. proposed terminologies to describe cell reverse migration, including reverse abluminal crawling (rAC), reverse interstitial migration (rIM), reverse luminal crawling (rLC), and reverse transendothelial cell migration (rTEM) (11). These terminologies imply the mechanisms by which PMN rM occurs.

The mechanisms that mediate PMN rM from inflammatory sites remain largely unclear. Many factors, which involve in PMN forward migration, such as chemoattractant and chemotactic repellents, chemokine receptors, the interaction between PMN and endothelia, and alteration of PMN behavior, are also considered as main factors regulating PMN rM (**Figure 1**).

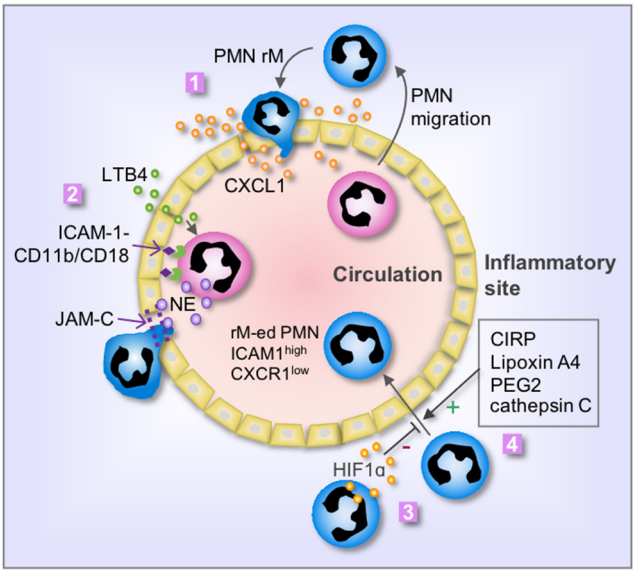

FIGURE 1 | Mechanisms of PMN rM. **1**. Breach of endothelium results in leakage of chemokine, i.e., CXCL1, from the inflammatory site into the vasculature, therefore driving PMN to reenter the circulation; **2**. LTB4 induces PMN release of neutrophil elastase (NE), which in turn cleaves endothelial JAM-C and subsequent damage of endothelial junction and promotes PMN rM. The binding between PMN CD11b/CD18 and endothelial ICAM-1 retains the PMN on the surface of endothelial cells and secures the cleavage of JAM-C by NE; **3**. Activation of HIF1α suppresses PMN rM; and **4**. Many factors, including cold-inducible RNA-binding protein (CIRP), Lipoxin A4, PEG2, and cathepsin C, can promote PMN rM. The phenotype of reverse migrated PMN (rM-ed PMN) is ICAM1^{high} CXCR1^{low}.

During the PMN forward migration, PMNs are chemoattracted by chemokines, and the migration direction is controlled by the concentration gradient of the chemoattractant. Endothelium breach is an important event in the PMN migration from circulation to the inflammatory area (27, 28). Similarly, the alteration of endothelial junction and permeability also play an important role in the mechanism of PMN rM. Owen-Woods et al. revealed the importance of endothelial permeability in regulating PMN trafficking (29). Inflammation usually damages the endothelial junctions and increases endothelial permeability, thereby, resulting in leakage of chemokines from the inflammatory site to circulation. This leakage of chemokines may reverse the directional cues of PMN migration across venular walls (30). For example, the leakage of chemokine and PMN chemoattractant, CXCL1, impairs the chemoattractant gradient and confuses PMNs and droves PMNs reenter the systemic circulation (29, 31). Regarding the mechanism underlying endothelial junction damage, Colom et al. reported that neutrophil elastase (NE) cleaves endothelial junctional adhesion molecule C (JAM-C), therefore, promoting PMN rM (32). This process is mediated by leukotriene B_4 (LTB4). The study showed that LTB_4 exhibits high efficacy in promoting rapid NE release and/or cell-surface expression, which then mediates the cleavage of endothelial JAM-C (32). Decreasing

Abbreviations: CIRP, Cold-inducible RNA-binding protein; CLP, Cecal ligation and puncture; Ctsc, Cathepsin C; CXCL1, C-X-C motif chemokine ligand 1; CXCL8a, Chemokine (C-X-C motif) ligand 8a; CXCR1, C-X-C motif chemokine receptor 1; CXCR2, C-X-C motif chemokine receptor 2; CXCR4, C-X-C motif chemokine receptor 4; DAMPs, Damage associated molecular patterns; HIF1α, Hypoxia inducible factor 1 subunit alpha; ICAM1, Intercellular adhesion molecule-1; iNOS, inducible nitric oxide synthase; JAM-C, Junctional adhesion molecule C; KC, Keratinocyte-derived chemokine; LTB_4, leukotriene B4; LTB4R1, leukotriene B4 receptor 1; LXA4, lipoxin A4; MAPKs, Mitogen activated protein kinases; MIP-2, Macrophage-inflammatory protein-2; NE, Neutrophil elastase; NETs, Neutrophil Extracellular Traps; NF-κB, Nuclear factor kappa B subunit 1; PAMPs, Pathogen-associated molecular patterns; PGE2, Prostaglandin E2; PKC, Phosphorylation of protein kinase C; PMN, Polymorphonuclear neutrophils; rAC, reverse abluminal crawling; rIM, reverse interstitial migration; rLC, reverse luminal crawling; rM, reverse migration; rTEM, reverse transendothelial-cell migration; SFK, Src family kinase; TLR4, Toll-like receptor 4; TNF-α, Tumor necrosis factor-α.

LTB4 concentration or blocking LTB4 receptor could decrease PMN rM in a mouse model of acute pancreatitis (33). Hirano et al. found that inhibition of JAM-C degradation reduces PMN rM in septic mice (34). The study further showed that the soluble JAM-C concentration in circulation is positively correlated with the PMN rM, and thus, increased plasma soluble JAM-C level may serve as an indicator for PMN rM occurring (32).

PMN transepithelial migration is an important event during PMN migration. However, the study on the mechanism of reverse PMN transepithelial migration is lacking in the literature. Future studies are needed to explore the mechanism since reverse PMN transepithelial migration is an indispensable piece of the puzzle for a comprehensive understanding of PMN rM.

Studies have shown that some chemokines and chemokine receptors are critically involved in PMN rM. CXCR1 and CXCR2 are the main receptors on PMNs to sense chemokines during cell migration. The study showed that reverse migrated PMNs exhibit decreased CXCR1 (14). Therefore, it was speculated that those PMNs may lose sensitivity to chemokine cues and move in a reverse direction. However, the direct evidence is still missing. Powell et al. reported that CXCL8a and CXCR2 are required for PMN rM in zebrafish, evidenced by that CXCR2 knockout in zebrafish decreased PMN rM (35). Wang et al. reported that the PMNs that reentered into circulation entailed a sojourn in the lungs, where they up-regulated CXCR4 expression followed by homing back to the bone marrow. The PMNs trafficking back to bone marrow exhibit increased Annexin V in the membrane, suggesting that those PMNs may undergo apoptosis in bone marrow (17).

PMN forward migration to the inflammatory site requires an important step of adhesion to endothelium, which is mediated through the binding between PMN Cd18/Cd11b and endothelial ICAM-1. During PMN rM, Colom et al. found that the binding between Cd18/Cd11b and ICAM-1 secures JAM-C cleavage by neutrophil elastase, which subsequently promotes PMN rM (32).

Some studies revealed negative regulation of PMN rM. For example, the role for hypoxia-inducible factor 1 subunit alpha (HIF1α) in suppressing PMN rM in zebrafish has been reported (36). Activation of HIF1α reduced PMN rM and delayed inflammation resolution in zebrafish; whereas, administration of HIF1α inhibitor enhanced PMN rM (36). Besides, Wang et al. found that reducing serine protease activity by using cathepsin C deficient mice led to a profound reduction in PMN rM (17). Considering that PMNs reenter into circulation followed by migration into the lungs and sequentially homing back to bone marrow, PMN rM is more likely a programmed process, rather than a random event.

Chemotactic repellent in the inflammatory site is another mechanistic hypothesis for PMN rM (8). CXCL8 is an effective chemokine in human. It has been found *in vitro* that CXCL8 functions as a chemoattractant in lower concentrations (at the nM level), whereas, in higher concentrations (at the μM level), CXCL8 plays a role as chemorepellent to promote PMN rM (37). Loynes et al. reported that eicosanoid prostaglandin E_2 (PGE2) can also act as a chemorepellent that drives PMN rM in zebrafish (38). In the late stage of inflammation, pathways of production of pro-inflammatory mediators are usually shifted to the production of pro-resolution mediators, i.e. lipoxin A_4 (LXA4) (39, 40). It has been found in a microfluidic device that LXA4 enhances human PMN rM, suggesting that PMN rM may serve as a partial mechanism of inflammation resolution (41). Macrophages also play a role in regulating PMN rM (42). It has been observed in zebrafish that macrophage depletion decreased PMN rM and resulted in continuous neutrophilic inflammation (38). Redox-Src family kinase (SFK) signaling in macrophages seems important in mediating macrophage-induced PMN rM, although redox-SFK also involves in regulating PMN forward migration (43).

Collectively, published studies underscore the complexity and diversity of mechanisms driving PMN rM, highlighting the need to better understand PMN rM characteristics, prevalence, and downstream implications.

BIOLOGICAL EFFECT OF PMN rM

Both PMN infiltration in tissue and timely clearance are important for maintaining homeostasis, as concluded previously (9, 44). Persistent and excessive PMN infiltration is responsible for many chronic diseases, such as pulmonary fibrosis and rheumatoid arthritis, etc. (45, 46). The functional role of PMN rM in inflammatory scenarios is controversial and requires further exploration. Current evidence suggests that depending on the context, PMN rM can be both a protective response, by facilitating an efficient resolution to innate immune reaction, and also a tissue-damaging event (8, 13, 17, 22, 32, 47–49). Removal of activated PMNs from the inflammatory sites through PMN rM may alleviate the local inflammatory response. On the other aspect, however, activated PMNs that migrate back to circulation may result in dissemination of inflammation (32, 47, 50). The different outcomes may be related to the different disease models, severity, and timing.

Nonetheless, clearance of infiltrated PMNs from the injury or infection sites is essential for inflammation resolution. Most studies in zebrafish found that PMN rM plays a protective role in promoting inflammation resolution. Several interventions aiming to inhibit PMN rM, such as macrophage depletion and activation of HIF1α, aggravated the damage of the wound due to the persistent neutrophilic infiltration (36, 38). Similar results have also been observed in a mouse model of sterile thermal hepatic injury. Using photoactivatable-GFP transgenic mice, Wang et al. visualized the migration of PMNs back into the vasculature in a sterile thermal hepatic injury. They found that reducing serine protease activity by using cathepsin C–deficient mice ($Ctsc^{-/-}$) led to a profound reduction in PMNs reentering healthy patent vessels, and further resulted in delayed revascularization. Though the mechanism was unclear, Ctsc deficiency only decreased PMN rM, but did not affect PMN infiltration, suggesting that Ctsc involved in inflammation resolution (17).

On the other aspect, data from mammal experiments showed that activated PMNs migrating back to circulation contributes to inflammation dissemination and distant organ dysfunction. In a murine model of cremaster muscle ischemia-reperfusion,

inhibition of PMN rM by knockout NE or JAM-C resulted in the alleviation of the remote lung, heart, and liver injury, suggesting that those reverse migrated PMNs may contribute to the distant organ injury (32, 47). The mechanism of how the reverse migrated PMNs lead to distant organ damage remains unclear. This may relate to the interaction between reverse migrated PMNs and circulating cells. Studies have shown that the PMN subsets, which present similar phenotype with reverse migrated PMNs, modulate T cell functions, as summarized by Hirano et al. (51). PMNs with increased cell surface expression of CD11b, CD11c, CD16, and CD54 demonstrate the ability to suppress T cell proliferation in a Cd18/Cd11b dependent manner (51).

It is noticeable that reverse migrated PMNs have an altered phenotype consisting of increased expression of ICAM-1 and effector functions, e.g., increased ROS generation (14, 47). Expression of ICAM-1 on the surface of inactivated PMNs is usually low. PMN expression of ICAM-1 can be induced by chemokines, and thus, infiltrated PMNs in the site of injury or infection present upregulated expression of ICAM-1 (49, 50). Whether the high expressed ICAM-1 involves in the mechanism of PMN rM is under investigation in the authors' laboratory.

PMN rM IN SEPSIS

Sepsis is life-threatening organ dysfunction caused by a dysregulated host response to infection (52). In the progression of sepsis, PMNs are the most abundantly recruited immune cells at sites of infection, playing critical roles in the elimination of local infection and the healing of injury (53–55). Although the mechanisms underlying sepsis development and progression remain to be fully addressed, it is well-accepted that immune imbalance serves as a critical mechanism of the development and progression of sepsis, in which PMNs play important roles (56, 57). PMNs execute their functions to eliminate the pathogen mainly through degranulation, phagocytosis, the formation of neutrophil extracellular traps (NETs), and release of cytokines. These mechanisms, however, may induce tissue damage as well (54, 55).

Theoretically, timely removal of PMNs in a resolution phase from the inflamed site should benefit local inflammation. However, active PMNs that migrate back to systemic circulation may disseminate inflammatory responses to remote organs and tissue. In the development of sepsis, pathogen-associated molecular patterns (PAMPs) and damage-associated molecular patterns (DAMPs) are the early initiators; and PMNs play an important role in further amplifying the inflammation during the progression of sepsis (8, 58). Inflammatory mediators released by PMNs can exaggerate other innate immune cell activation, including PMN itself (8, 59). Reverse migrated PMNs present a pro-inflammatory phenotype, including increased production of superoxide and high membrane expression of ICAM-1 (47, 60). Ode *et al* found that ICAM-1 positive PMNs express higher levels of inducible nitric oxide synthase (iNOS) and NETs, suggesting that reverse migrated PMNs are still highly active (60, 61). In addition, reverse migrated PMNs show prolonged lifespan and delayed apoptosis (62, 63), which might contribute to persistent and amplified inflammation (64). Studies using the mouse abdominal infection model revealed that the ratio of reverse migrated PMNs in circulation shows a positive correlation with acute lung injury (33, 50, 60). A study using the cecal ligation and puncture (CLP) mouse model showed that cold-inducible RNA-binding protein (CIRP) knockout mice exhibited decreased PMN rM and lung injury. After administration of recombinant CIRP, the reverse migrated PMNs significantly increased in the blood in the time- and dose-dependent manner, and NE expression was upregulated, while JAM-C expression was downregulated in the lungs. These results suggest that CIRP promotes PMN rM and subsequent acute lung injury by increasing NE and decreasing JAM-C (50). Interestingly, the CIRP-induced PMN rM occurred in septic mice can be suppressed by neutralizing antibody against TLR4 and inhibitor for NF-κB. In CLP mice, CIRP-TLR4 interaction in PMNs leads to increased PMN rM through the NF-κB pathway. The reverse migrated PMNs produce excessive iNOS and NETs and promote tissue inflammation and injury (60). Li et al. using another sepsis model, the acute pancreatitis model, revealed that LTB4 production promoted PMN rM, and this effect was mediated by substance P. Substance P treatment increase phosphorylation of protein kinase C (PKC) α and mitogen- activated protein kinases (MAPKs), which further promoted LTB4 production. Blocking the leukotriene B4 receptor 1(LTB4R1) resulted in the decreased PMN rM into the circulation and alleviated the severity of acute lung injury (33).

Although the data on the role of PMN rM in sepsis are limited and it is too early to conclude, the published studies tend to suggest a detrimental effect of PMN rM on the development of remote organ injury in sepsis.

SUMMARY

The mechanism of sepsis remains to be fully elucidated, which results in poor therapeutic outcomes for septic patients. PMNs have become an important target for preventive and therapeutic interventions. Despite advances in understanding PMN biology over the last several decades, there remains a significant gap in our knowledge regarding various PMN functions and behavior in sepsis. PMN rM describes the phenomenon in which PMNs migrate away from the inflammatory site back into the vasculature following the initial PMN infiltration. The functional role of PMN rM within inflammatory scenarios, particularly in sepsis, requires further exploration. Current evidence suggests that depending on the context, PMN rM can be both a protective response, by facilitating an efficient resolution to innate immune reaction, and also a tissue-damaging event through the dissemination of inflammation. The investigation on the mechanism of PMN rM is still in a premature stage. Numerous questions are still open in the research of PMN rM. For example, what are the mediators in the circulation that chemoattract the PMNs leaving from the inflammatory sites? Whether the reverse migrated PMNs are a particular subset of PMNs? What are the different functions between the infiltrating PMNs and reverse migrated PMNs? Where is the final

destination and fate of the reverse migrated PMNs? Nonetheless, the potential physiological and pathological roles of PMN rM emphasize the importance of gaining more in-depth insight into these phenomena, since these may serve as novel means of modulating inflammation and treatment of sepsis.

AUTHOR CONTRIBUTIONS

JJ collected the data and drafted the manuscript. JJ and JF conceived and designed the study. JF reviewed and finalized the manuscript. Both authors read and approved the final manuscript.

FUNDING

This work was supported by the USA National Institutes of Health Grant R01-HL-079669 (JF), USA National Institutes of Health Grant R01HL076179 (JF), USA National Institutes of Health Grant R01-HL-139547 (JF), VA Merit Award 1I01BX002729 (JF), and VA BLR&D Award 1IK6BX004211 (JF).

REFERENCES

1. Amulic B, Cazalet C, Hayes GL, Metzler KD, Zychlinsky A. Neutrophil function: from mechanisms to disease. *Annu Rev Immunol.* (2012) 30:459–89. doi: 10.1146/annurev-immunol-020711-074942
2. Langereis JD. Neutrophil integrin affinity regulation in adhesion, migration, and bacterial clearance. *Cell Adh Migr.* (2013) 7:476–81. doi: 10.4161/cam.27293
3. Sadik CD, Kim ND, Luster AD. Neutrophils cascading their way to inflammation. *Trends Immunol.* (2011) 32:452–60. doi: 10.1016/j.it.2011.06.008
4. Kolaczkowska E, Kubes P. Neutrophil recruitment and function in health and inflammation. *Nat Rev Immunol.* (2013) 13:159–75. doi: 10.1038/nri3399
5. Summers C, Rankin SM, Condliffe AM, Singh N, Peters AM, Chilvers ER. Neutrophil kinetics in health and disease. *Trends Immunol.* (2010) 31:318–24. doi: 10.1016/j.it.2010.05.006
6. Injarabian L, Devin A, Ransac S, Marteyn BS. Neutrophil metabolic shift during their lifecycle: impact on their survival and activation. *Int J Mol Sci.* (2019) 21:287. doi: 10.3390/ijms21010287
7. Pittman K, Kubes P. Damage-associated molecular patterns control neutrophil recruitment. *J Innate Immun.* (2013) 5:315–23. doi: 10.1159/000347132
8. de Oliveira S, Rosowski EE, Huttenlocher A. Neutrophil migration in infection and wound repair: going forward in reverse. *Nat Rev Immunol.* (2016) 16:378–91. doi: 10.1038/nri.2016.49
9. Ley K, Laudanna C, Cybulsky MI, Nourshargh S. Getting to the site of inflammation: the leukocyte adhesion cascade updated. *Nat Rev Immunol.* (2007) 7:678–89. doi: 10.1038/nri2156
10. Hughes J, Johnson RJ, Mooney A, Hugo C, Gordon K, Savill J. Neutrophil fate in experimental glomerular capillary injury in the rat. Emigration exceeds in situ clearance by apoptosis. *Am J Pathol.* (1997) 150:223–34.
11. Nourshargh S, Renshaw SA, Imhof BA. Reverse migration of neutrophils: where, when, how, and why? *Trends Immunol.* (2016) 37:273–86. doi: 10.1016/j.it.2016.03.006
12. Starnes TW, Huttenlocher A. Neutrophil reverse migration becomes transparent with zebrafish. *Adv Hematol.* (2012) 2012:398640. doi: 10.1155/2012/398640
13. Mathias JR, Perrin BJ, Liu T-X, Kanki J, Look AT, Huttenlocher A. Resolution of inflammation by retrograde chemotaxis of neutrophils in transgenic zebrafish. *J Leukoc Biol.* (2006) 80:1281–8. doi: 10.1189/jlb.0506346
14. Buckley CD, Ross EA, McGettrick HM, Osborne CE, Haworth O, Schmutz C, et al. Identification of a phenotypically and functionally distinct population of long-lived neutrophils in a model of reverse endothelial migration. *J Leukoc Biol.* (2006) 79:303–11. doi: 10.1189/jlb.0905496
15. Silvestre-Roig C, Hidalgo A, Soehnlein O. Neutrophil heterogeneity: implications for homeostasis and pathogenesis. *Blood.* (2016) 127:2173–81. doi: 10.1182/blood-2016-01-688887
16. Powell DR, Huttenlocher A. Neutrophils in the tumor microenvironment. *Trends Immunol.* (2016) 37:41–52. doi: 10.1016/j.it.2015.11.008
17. Wang J, Hossain M, Thanabalasuriar A, Gunzer M, Meininger C, Kubes P. Visualizing the function and fate of neutrophils in sterile injury and repair. *Science.* (2017) 358:111–6. doi: 10.1126/science.aam9690
18. Yoo SK, Huttenlocher A. Spatiotemporal photolabeling of neutrophil trafficking during inflammation in live zebrafish. *J Leukoc Biol.* (2011) 89:661–7. doi: 10.1189/jlb.1010567
19. Hall C, Flores MV, Chien A, Davidson A, Crosier K, Crosier P. Transgenic zebrafish reporter lines reveal conserved Toll-like receptor signaling potential in embryonic myeloid leukocytes and adult immune cell lineages. *J Leukoc Biol.* (2009) 85:751–65. doi: 10.1189/jlb.0708405
20. Burn T, Alvarez JI. Reverse transendothelial cell migration in inflammation: to help or to hinder? *Cell Mol Life Sci.* (2017) 74:1871–81. doi: 10.1007/s00018-016-2444-2
21. Wu D, Zeng Y, Fan Y, Wu J, Mulatibieke T, Ni J, et al. Reverse-migrated neutrophils regulated by JAM-C are involved in acute pancreatitis-associated lung injury. *Sci Rep.* (2016) 6:20545. doi: 10.1038/srep20545
22. Hind LE, Huttenlocher A. Neutrophil reverse migration and a chemokinetic resolution. *Dev Cell.* (2018) 47:404–5. doi: 10.1016/j.devcel.2018.11.004
23. Zhang Q, Raoof M, Chen Y, Sumi Y, Sursal T, Junger W, et al. Circulating mitochondrial DAMPs cause inflammatory responses to injury. *Nature.* (2010) 464:104–7. doi: 10.1038/nature08780
24. Li L, Chen K, Xiang Y, Yoshimura T, Su S, Zhu J, et al. New development in studies of formyl-peptide receptors: critical roles in host defense. *J Leukoc Biol.* (2016) 99:425–35. doi: 10.1189/jlb.2RI0815-354RR
25. Finger EB, Puri KD, Alon R, Lawrence MB, von Andrian UH, Springer TA. Adhesion through L-selectin requires a threshold hydrodynamic shear. *Nature.* (1996) 379:266–9. doi: 10.1038/379266a0
26. Lawrence MB, Kansas GS, Kunkel EJ, Ley K. Threshold levels of fluid shear promote leukocyte adhesion through selectins (CD62L,P,E). *J Cell Biol.* (1997) 136:717–27. doi: 10.1083/jcb.136.3.717
27. Vestweber D. How leukocytes cross the vascular endothelium. *Nat Rev Immunol.* (2015) 15:692–704. doi: 10.1038/nri3908
28. Weninger W, Biro M, Jain R. Leukocyte migration in the interstitial space of non-lymphoid organs. *Nat Rev Immunol.* (2014) 14:232–46. doi: 10.1038/nri3641
29. Owen-Woods C, Joulia R, Barkaway A, Rolas L, Ma B, Nottebaum AF, et al. Local microvascular leakage promotes trafficking of activated neutrophils to remote organs. *J Clin Invest.* (2020) 130:2301–18. doi: 10.1172/JCI133661
30. Huang AJ, Manning JE, Bandak TM, Ratau MC, Hanser KR, Silverstein SC. Endothelial cell cytosolic free calcium regulates neutrophil migration across monolayers of endothelial cells. *J Cell Biol.* (1993) 120:1371–80. doi: 10.1083/jcb.120.6.1371
31. Marki A, Ley K. Leaking chemokines confuse neutrophils. *J Clin Invest.* (2020) 130:2177–9. doi: 10.1172/JCI136259
32. Colom B, Bodkin JV, Beyrau M, Woodfin A, Ody C, Rourke C, et al. Leukotriene B4-neutrophil elastase axis drives neutrophil reverse transendothelial cell migration *in vivo*. *Immunity.* (2015) 42:1075–86. doi: 10.1016/j.immuni.2015.05.010
33. Li B, Han X, Ye X, Ni J, Wu J, Dai J, et al. Substance P-regulated leukotriene B4 production promotes acute pancreatitis-associated lung injury through neutrophil reverse migration. *Int Immunopharmacol.* (2018) 57:147–56. doi: 10.1016/j.intimp.2018.02.017
34. Hirano Y, Ode Y, Ochani M, Wang P, Aziz M. Targeting junctional adhesion molecule-C ameliorates sepsis-induced acute lung injury by decreasing CXCR4+ aged neutrophils. *J Leukoc Biol.* (2018) 104:1159–71. doi: 10.1002/JLB.3A0218-050R

35. Powell D, Tauzin S, Hind LE, Deng Q, Beebe DJ, Huttenlocher A. Chemokine signaling and the regulation of bidirectional leukocyte migration in interstitial tissues. *Cell Rep.* (2017) 19:1572–85. doi: 10.1016/j.celrep.2017.04.078
36. Elks PM, van Eeden FJ, Dixon G, Wang X, Reyes-Aldasoro CC, Ingham PW, et al. Activation of hypoxia-inducible factor-1α (Hif-1α) delays inflammation resolution by reducing neutrophil apoptosis and reverse migration in a zebrafish inflammation model. *Blood.* (2011) 118:712–22. doi: 10.1182/blood-2010-12-324186
37. Tharp WG, Yadav R, Irimia D, Upadhyaya A, Samadani A, Hurtado O, et al. Neutrophil chemorepulsion in defined interleukin-8 gradients in vitro and *in vivo*. *J Leukoc Biol.* (2006) 79:539–54. doi: 10.1189/jlb.0905516
38. Loynes CA, Lee JA, Robertson AL, Steel MJ, Ellett F, Feng Y, et al. PGE2 production at sites of tissue injury promotes an anti-inflammatory neutrophil phenotype and determines the outcome of inflammation resolution in vivo. *Sci Adv.* (2018) 4:eaar8320. doi: 10.1126/sciadv.aar8320
39. Levy BD, Clish CB, Schmidt B, Gronert K, Serhan CN. Lipid mediator class switching during acute inflammation: signals in resolution. *Nat Immunol.* (2001) 2:612–9. doi: 10.1038/89759
40. Serhan CN, Chiang N, Dalli J, Levy BD. Lipid mediators in the resolution of inflammation. *Cold Spring Harb Perspect Biol.* (2014) 7:a016311. doi: 10.1101/cshperspect.a016311
41. Hamza B, Wong E, Patel S, Cho H, Martel J, Irimia D. Retrotaxis of human neutrophils during mechanical confinement inside microfluidic channels. *Integr Biol (Camb).* (2014) 6:175–83. doi: 10.1039/C3IB40175H
42. Bystrom J, Evans I, Newson J, Stables M, Toor I, van Rooijen N, et al. Resolution-phase macrophages possess a unique inflammatory phenotype that is controlled by cAMP. *Blood.* (2008) 112:4117–27. doi: 10.1182/blood-2007-12-129767
43. Tauzin S, Starnes TW, Becker FB, Lam P, Huttenlocher A. Redox and Src family kinase signaling control leukocyte wound attraction and neutrophil reverse migration. *J Cell Biol.* (2014) 207:589–98. doi: 10.1083/jcb.201408090
44. Serhan CN, Savill J. Resolution of inflammation: the beginning programs the end. *Nat Immunol.* (2005) 6:1191–7. doi: 10.1038/ni1276
45. Wright HL, Moots RJ, Edwards SW. The multifactorial role of neutrophils in rheumatoid arthritis. *Nat Rev Rheumatol.* (2014) 10:593–601. doi: 10.1038/nrrheum.2014.80
46. Cantin AM, Hartl D, Konstan MW, Chmiel JF. Inflammation in cystic fibrosis lung disease: pathogenesis and therapy. *J Cyst Fibros.* (2015) 14:419–30. doi: 10.1016/j.jcf.2015.03.003
47. Woodfin A, Voisin M-B, Beyrau M, Colom B, Caille D, Diapouli F-M, et al. The junctional adhesion molecule JAM-C regulates polarized transendothelial migration of neutrophils *in vivo*. *Nat Immunol.* (2011) 12:761–9. doi: 10.1038/ni.2062
48. Robertson AL, Holmes GR, Bojarczuk AN, Burgon J, Loynes CA, Chimen M, et al. A zebrafish compound screen reveals modulation of neutrophil reverse migration as an anti-inflammatory mechanism. *Sci Transl Med.* (2014) 6:225ra29. doi: 10.1126/scitranslmed.3007672
49. Thompson AAR, Elks PM, Marriott HM, Eamsamarng S, Higgins KR, Lewis A, et al. Hypoxia-inducible factor 2α regulates key neutrophil functions in humans, mice, and zebrafish. *Blood.* (2014) 123:366–76. doi: 10.1182/blood-2013-05-500207
50. Jin H, Aziz M, Ode Y, Wang P. CIRP induces neutrophil reverse transendothelial migration in sepsis. *Shock.* (2019) 51:548–56. doi: 10.1097/SHK.0000000000001257
51. Hirano Y, Aziz M, Wang P. Role of reverse transendothelial migration of neutrophils in inflammation. *Biol Chem.* (2016) 397:497–506. doi: 10.1515/hsz-2015-0309
52. Singer M, Deutschman CS, Seymour CW, Shankar-Hari M, Annane D, Bauer M, et al. The third international consensus definitions for sepsis and septic shock (Sepsis-3). *JAMA.* (2016) 315:801–10. doi: 10.1001/jama.2016.0287
53. Seymour CW, Rosengart MR. Septic shock: advances in diagnosis and treatment. *JAMA.* (2015) 314:708–17. doi: 10.1001/jama.2015.7885
54. Shen X-F, Cao K, Jiang J-P, Guan W-X, Du J-F. Neutrophil dysregulation during sepsis: an overview and update. *J Cell Mol Med.* (2017) 21:1687–97. doi: 10.1111/jcmm.13112
55. Zhang F, Liu A-L, Gao S, Ma S, Guo S-B. Neutrophil dysfunction in sepsis. *Chin Med J.* (2016) 129:2741–4. doi: 10.4103/0366-6999.193447
56. Delano MJ, Ward PA. Sepsis-induced immune dysfunction: can immune therapies reduce mortality? *J Clin Invest.* (2016) 126:23–31. doi: 10.1172/JCI82224
57. Gotts JE, Matthay MA. Sepsis: pathophysiology and clinical management. *BMJ.* (2016) 353:i1585. doi: 10.1136/bmj.i1585
58. Lämmermann T. In the eye of the neutrophil swarm-navigation signals that bring neutrophils together in inflamed and infected tissues. *J Leukoc Biol.* (2016) 100:55–63. doi: 10.1189/jlb.1MR0915-403
59. Sadik CD, Luster AD. Lipid-cytokine-chemokine cascades orchestrate leukocyte recruitment in inflammation. *J Leukoc Biol.* (2012) 91:207–15. doi: 10.1189/jlb.0811402
60. Ode Y, Aziz M, Wang P. CIRP increases ICAM-1+ phenotype of neutrophils exhibiting elevated iNOS and NETs in sepsis. *J Leukoc Biol.* (2018) 103:693–707. doi: 10.1002/JLB.3A0817-327RR
61. Hesse A-K, Dörger M, Kupatt C, Krombach F. Proinflammatory role of inducible nitric oxide synthase in acute hyperoxic lung injury. *Respir Res.* (2004) 5:11. doi: 10.1186/1465-9921-5-11
62. Zhang D, Chen G, Manwani D, Mortha A, Xu C, Faith JJ, et al. Neutrophil ageing is regulated by the microbiome. *Nature.* (2015) 525:528–32. doi: 10.1038/nature15367
63. Ng LG, Ostuni R, Hidalgo A. Heterogeneity of neutrophils. *Nat Rev Immunol.* (2019) 19:255–65. doi: 10.1038/s41577-019-0141-8
64. Woodfin A, Beyrau M, Voisin M-B, Ma B, Whiteford JR, Hordijk PL, et al. ICAM-1-expressing neutrophils exhibit enhanced effector functions in murine models of endotoxemia. *Blood.* (2016) 127:898–907. doi: 10.1182/blood-2015-08-664995

Conflict of Interest: The authors declare that the research was conducted in the absence of any commercial or financial relationships that could be construed as a potential conflict of interest.

frontiers in Immunology

MINI REVIEW
published: 16 March 2021
doi: 10.3389/fimmu.2021.641750

Inflammasome-Dependent Coagulation Activation in Sepsis

Runliu Wu, Nian Wang, Paul B. Comish, Daolin Tang and Rui Kang**

Department of Surgery, University of Texas Southwestern Medical Center, Dallas, TX, United States

Sepsis is a potentially life-threatening, pathological condition caused by a dysregulated host response to infection. Pathologically, systemic inflammation can initiate coagulation activation, leading to organ dysfunction, and ultimately to multiple organ failure and septic death. The inflammasomes are cytosolic multiprotein signaling complexes that control the host response to diverse pathogen-associated molecular patterns (PAMPs) from microorganisms as well as damage-associated molecular patterns (DAMPs) from dead or dying host cells. Recent studies highlight that the activation of canonical and non-canonical inflammasomes not only mediate the maturation and secretion of interleukin-1 (IL1) family cytokines, but also trigger the release of coagulation factor III, tissue factor (F3, best known as TF) in activated macrophages and monocytes. These emerging functions of inflammasomes in immunocoagulation are further positively regulated by stimulator of interferon response cGAMP interactor 1 (STING1, also known as STING or TMEM173, a hub of the innate immune signaling network) and high mobility group box 1 (HMGB1, a nuclear DAMP). This mini-review will discuss the regulation and function of inflammasome-dependent coagulation activation in sepsis.

Keywords: inflammation, inflammasome, sepsis, DIC, coagulation

OPEN ACCESS

Edited by:
Yong Ming Yao,
First Affiliated Hospital of Chinese PLA General Hospital, China

Reviewed by:
Krzysztof Guzik,
Jagiellonian University, Poland
Xu-Lin Chen,
First Affiliated Hospital of Anhui Medical University, China

****Correspondence:***
Daolin Tang
daolin.tang@utsouthwestern.edu
Rui Kang
rui.kang@utsouthwestern.edu

Specialty section:
This article was submitted to Inflammation, a section of the journal Frontiers in Immunology

Received: *14 December 2020*
Accepted: *22 February 2021*
Published: *16 March 2021*

Citation:
Wu R, Wang N, Comish PB, Tang D and Kang R (2021) Inflammasome-Dependent Coagulation Activation in Sepsis. Front. Immunol. 12:641750. doi: 10.3389/fimmu.2021.641750

INTRODUCTION

Sepsis is a challenging clinical syndrome characterized by life-threatening organ dysfunction or failure due to the dysregulated host immune response to pathogen infection, including bacteria, viruses, and fungi (1). The typical pathological process of sepsis involves the early hyperinflammatory state and the late immunosuppressive stage. This dynamic change of the host immune response is closely related to local or systemic coagulation abnormalities (2). Disseminated intravascular coagulation (DIC) is a common complication of sepsis, characterized by systemic activation of the coagulation cascade with microthrombosis, platelet consumption, and subsequent clotting factor exhaustion (3). Clinical studies have shown that the mortality rate of septic shock patients with DIC is twice that of septic patients without DIC (4), highlighting the importance of understanding the pathogenesis, diagnosis, and treatment of DIC in sepsis.

Cells of the innate immune system, such as macrophages, monocytes, neutrophils, and dendritic cells, are the first line of defense against foreign pathogens. However, excessive activation of these professional phagocytes may lead to inflammation, immune dysfunction, and abnormal blood clotting. Inflammasomes are multiprotein intracellular complexes that detect the components of microorganisms [namely pathogen-associated molecular patterns (PAMPs)] and endogenous danger signals released by injured cells [namely damage-associated molecular patterns (DAMPs)] using various pattern recognition receptors (PRRs) (5). Generally, according to whether caspase-1 (CASP1) or caspase-11 (CASP11 in mouse, also known as CASP4 and CASP5 in humans)

is activated, inflammasomes can be divided into canonical and non-canonical subtypes (6, 7). Although they play an important role in host immune defense, the vigorous activation of inflammasomes also cause detrimental consequences, providing the pathogenicity of disease, including septic shock (8). In contrast, genetic depletion of core components of inflammasomes, such as *Nlrp3*, *Casp1*, *Casp11*, and gasdermin D (*Gsdmd*), protects against septic shock (9–15) or lethal endotoxemia (7) in mice, turning them into a promising target for treatment of sepsis.

In this mini-review, we introduce the types and activation of inflammasomes, discuss their roles in coagulation and thrombosis, and highlight their implications in sepsis.

TYPES AND ACTIVATION OF INFLAMMASOMES IN SEPSIS

Inflammasomes typically contain a sensor (cytosolic PRRs), an adaptor [apoptosis-associated speck-like protein containing a caspase recruitment domain (ASC)], and a zymogen (pro-CASP1) (16). Assembly of inflammasome is initiated when PRRs sensing PAMPs, DAMPs, or stress signals. Certain PRRs then recruit ASC, a bipartite protein that bridges the sensors and the effector pro-CASP1 (17). Pro-CASP1 is subsequently cleaved into active caspase, ultimately leading to maturation and secretion of interleukin 1 (IL1) family cytokines (such as IL1B and IL18) or cleaved GSDMD-mediated pyroptosis. Functionally, pyroptosis is a form of pro-inflammatory cell death. Although pyroptosis has been found to occur in various immune and non-immune cells, it was first discovered in macrophages during bacterial infections (18). GSDMD-formed pores not only mediate pyroptosis, but also facilitate the release of IL1B in a pyroptosis-independent manner (19, 20). Below, we summarize the main types of inflammasomes related to sepsis.

Canonical Inflammasome

The NLRP3 Inflammasome

The most extensively studied inflammasome is the NLR family pyrin domain containing 3 (NLRP3) inflammasome, which is activated by a variety of stimuli, including PAMPs, DAMPs, pore-forming toxins, crystals, and nucleic acid (21). Of note, the basic expression of NLRP3 and pro-IL1B in macrophages is very low, and a priming signal (such as TLR ligands or IFN) is required to activate the NF-κB pathway to upregulate the expression of the components for NLRP3 inflammasome in macrophages (22). The second signal triggers NLRP3 activation by multiple mechanisms, including potassium (K^+) efflux, increased calcium (Ca^{2+}) signaling, mitochondrial translocation of NLRP3, excessive mitochondrial reactive oxygen species (ROS) generation, release of mitochondrial DNA and cardiolipin, and lysosomal leakage of cathepsins into cytosol (5, 23). Many studies have found that inhibiting the activation of NLRP3 inflammasome has a protective effect on septic animals (24). In particular, the NLRP3 inhibitor MCC950 attenuates multi-organ injuries in septic rats (25), highlighting the potential of using NLRP3 inhibitors in the treatment of sepsis.

The NLRC4 Inflammasome

The NLRC4 inflammasome responds to more stringent types of stimulation. NLRC4 forms a complex with certain NLR family apoptosis inhibitory protein (NAIP) family proteins, which directly bind to the NLRC4-activating ligands. For example, mouse Naip1 or Naip2 binds to the needle protein or rod component of bacterial type III secretory system (T3SS), respectively (26, 27). Moreover, both mouse Naip5 and Naip6 can recognize bacterial flagellin (27, 28). In humans, only one NAIP homolog has been identified to recognize the needle structure of T3SS. Once bound to their ligands, NAIPs oligomerize with NLRC4 to form the NLRC4 inflammasomes, leading to CASP1 activation. *In vivo*, a severe systemic inflammation is caused by activating NLRC4 inflammasomes with flagellin in monocytes, macrophage and neutrophils (29). Systemic coagulation and massive thrombosis are induced by T3SS infection in mice through the activation of inflammasome, possibly the NLRC4 inflammasome (30). Therefore, inappropriate NLRC4 activation may result in detrimental consequence in sepsis.

Non-canonical Inflammasome

Clinically, septic shock is a multi-step process and mainly related to Gram-negative bacterial infection. Lipopolysaccharides (LPS), the main component of the outer membrane of Gram-negative bacteria, is a prototypical PAMP for studying innate immune response. Historically, the activity of LPS was determined by the membrane receptor toll-like receptor 4 (TLR4). Recent breakthroughs confirmed that CASP11 can act as a receptor for cytoplasmic LPS, which is independent of TLR4 (31, 32). The activation of CASP11 inflammasome also can promote CASP1-dependent IL1B and IL18 production by triggering the activation of NLRP3 inflammasome. CASP11 induces CASP1-independent pyroptosis, which still requires the production of cleaved GSDMD at the N-terminus (termed GSDMD-N) and subsequent translocation of GSDMD-N to the cell membrane (7). Similar function of human non-canonical inflammasome has been identified by the deletion of *CASP4* or *CASP5* in human macrophage, which impairs pyroptosis and NLRP3 inflammasome-mediated cytokine release (33–36). The contribution of non-canonical inflammasome to sepsis has been reported in septic mice model (7, 37–39). The deletion of *CASP11* or using CASP11-targeting inhibitor (e.g., oxPAPC) protects mice against LPS-induced lethality (7, 38). In addition, transgenic expression of *CASP4* in *Casp1*$^{-/-}$/*11*$^{-/-}$ mice renders increased susceptibility to LPS-induced shock (40), indicating the pathogenetic role of human non-canonical inflammasome in sepsis.

MODULATION AND FUNCTION OF INFLAMMASOME IN COAGULATION

Most patients with sepsis show hemostatic changes, while DIC occurs in ∼35% of patients, resulting in organ dysfunction and death (41). The most principal initiator of coagulopathy in sepsis is coagulation factor III (F3). It is a transmembrane single-chain glycoprotein composed of 263 amino acid residues, with

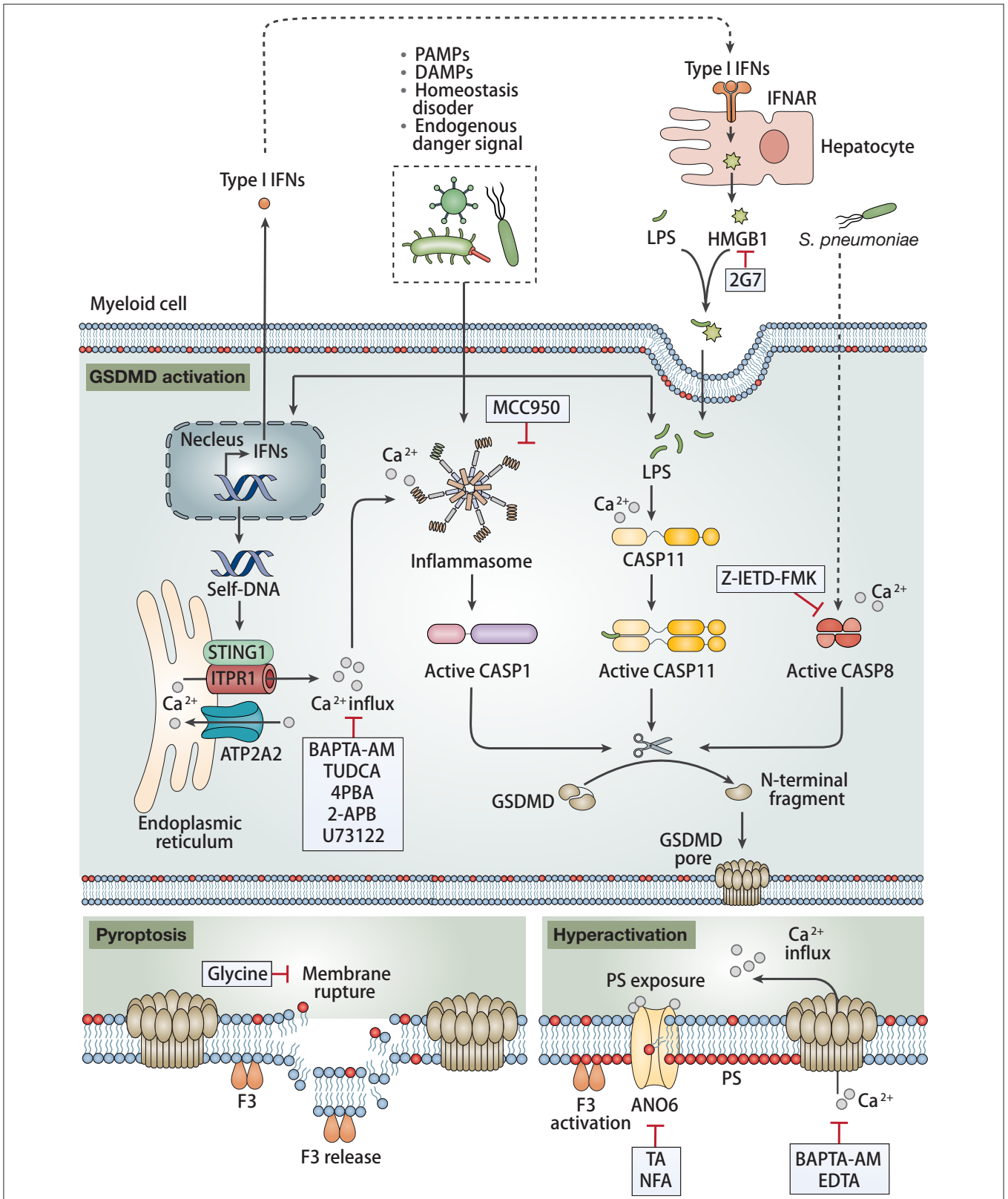

FIGURE 1 | Role of inflammasome in sepsis-induced coagulation. Canonical and non-canonical inflammasome complexes in myeloid cells are assembled when pattern recognition receptors (PRRs) sense pathogen-associated molecular patterns (PAMPs), damage-associated molecular patterns (DAMPs), altered cellular

(Continued)

FIGURE 1 | homeostasis or endogenous danger signals caused by infection during sepsis. Functional inflammasome activates caspase-1 (CASP1), caspase-11 (CASP11) or caspase-8 (CASP8) to cleave gasdermin D (GSDMD) to produce N-terminal fragments (GSDMD-N). GSDMD-N forms pores on the plasma membrane, resulting in cell membrane rupture and pyroptosis or rendering cells into hyperactivation state. Coagulation factor III (F3) released from ruptured membrane promotes blood clotting. Elevated Ca^{2+} influx from extracellular space through GSDMD-N-formed pores in hyperactivation state promotes phosphatidylserine (PS) exposure, thereby enhancing the pro-coagulant activity of F3. Type I interferons (IFNs) mediates release of hepatocyte high mobility group box 1 (HMGB1), which facilitates LPS entering cytosol. Stimulator of interferon response cGAMP interactor 1 (STING1) senses infection-induced DNA damage and mediates CASP1/11/8 activation. Inhibition of inflammasome activation and subsequent pyroptosis prevents sepsis-induced coagulation.

a molecular weight of about 47 kDa (42). F3 initiates the blood coagulation cascade by binding to coagulation factor VII/VIIa (F3:VIIa complex) on the cell surface (42). During sepsis, the host immune response to PAMPs (such as LPS) rapidly triggers the activation of coagulation by inducing the expression of F3 on monocytes, platelets or endothelial cells (43–46). Additionally, the mechanism of regulating F3 activity by transforming F3 from an inactive state to an active state (a process called F3 decryption) also contributes to coagulation activation. Exposure of anionic phospholipids, such as phosphatidylserine (PS), on the outer leaflet of the plasma membrane is considered to be the main cause of F3 decryption (47). This process optimizes the presentation of F3:VIIa complex to provide more efficient binding sites to their substrates factors IX and X. Increased PS exposure on the surface of circulating leukocytes is observed in sepsis (47). Genetic deletion of *F3* or blocking F3 activity using neutralizing antibodies in sepsis animal models prevents activation of coagulation and decreases the mortality (30, 48, 49). The administration of PS-neutralizing binding protein lactadherin markedly ameliorates sepsis-induced coagulation and lethality (50). These evidences suggest that treatment of the altered coagulation would be a reasonable approach to improve the mortality of sepsis. Some DAMPs, such as cell-free DNA, histones, heat shock proteins, and high mobility group box 1 protein (HMGB1) (51, 52), have been reported to induce coagulopathy in sepsis by furtherly augmenting systemic inflammation (53) or impairing the activation of anticoagulants (e.g., protein C) (54). These DAMPs may be released from damaged cells due to apoptosis, necroptosis, or pyroptosis, but the contribution of cell death to coagulation in sepsis is context-dependent. Recently, three independent groups found that both CASP1 and CASP11-dependent inflammasomes trigger systemic coagulation in mice through GSDMD-N-mediated increased F3 release or F3 activity in macrophages and monocytes (**Figure 1**).

Caspase Activation

Either CASP1 or CASP11 can promote the coagulation cascade, depending on the type of bacterial infection. CASP1 is required to release active F3 in mouse bone marrow-derived macrophages (BMDM) challenged or stimulated by bacterial T3SS inner rod protein, including EprJ and EscI from Escherichia coli (E.coli), BsaK of Burkholderia pseudomallei, and PrgJ of Salmonella typhimurium (30). Similarly, T3SS treatment or *E. coli* infection induces CASP1-dependent F3 release in THP1 cells, a human monocytic cell line derived from an acute monocytic leukemia patient (30). *In vivo*, lack of *Casp1* (instead of CASP11) protects mice from EprJ-induced lethality associated with the reduction of DIC biomarkers in blood (30). In polymicrobial sepsis induced by cecal ligation and puncture (CLP), inhibiting the activity of CASP1 with the NLRP3 inhibitor MCC950 also reduces platelet activation in rats (25, 55). These animal studies suggest that CASP1 has a potential role in regulating septic coagulation in mice and rats.

The activation of CASP11-dependent inflammasomes also mediates the release or activation of F3 in sepsis caused by CLP, *E. coli* infection, bacterial outer membrane vesicle (OMV) infection, and LPS stimulation *in vivo* (56, 57). Similar to clinical anticoagulant heparin treatment, in the lethal endotoxemia mouse model, the absence of *Casp11* inhibits the activation of coagulation (56, 57). In *Casp11*-deficient mice, systemic coagulation triggered by the initiation of poly(I:C) and subsequent LPS administration is also blocked (30, 56). Extracellular HMGB1 is not only a DAMP, but also a carrier that brings LPS into the intracellular space (58). In particular, extracellular HMGB1 from liver mediates LPS uptake and promotes the externalization of phosphatidylserine (PS), which is important for F3 activation in macrophages. In contrast, depletion of *Casp11* limits HMGB1/LPS-induced PS exposure and subsequent F3 activation in macrophages (59). Therefore, CASP11-dependent inflammasome is an important regulator of F3 release and activation in macrophages. While TLR4 is essential for LPS-induced gene expression of *Casp11*, TLR4 is considered to be dispensable in most inflammasome-mediated coagulation (30). Injection of LPS primed with poly(I:C) also induces coagulation cascade in *Tlr4*-deficient mice (56). The function of human CASP4 or CASP5 in sepsis-induced coagulopathy remains poorly understood, but it will be enlightened by these investigations of CASP11 in mouse models.

In certain bacterial infections (especially *Y. pestis* and *Y. pseudotuberculosis*), the apoptotic non-inflammatory caspase CASP8 also participates in inducing pyroptosis by activating the NLRP3 inflammasome (60) or acting as a structural component of the inflammasome (61). Consequently, CASP8 (but not CASP1 or CASP11)-mediated GSDMD-N production is required for F3 release in BMDM during *Streptococcus pneumoniae* (*S. pneumoniae*) infection (62). Collectively, these studies indicate that inhibition of caspase activation may have a potential therapeutic effect on fatal coagulopathy during sepsis.

GSDMD Cleavage

The activation of CASP1, CASP11, or CASP8 causes the cleavage of GSDMD, thereby generating a pyroptotic p30 fragment, namely GSDMD-N. GSDMD-N-mediated pore formation has been regarded as the terminal event of pyroptosis or hyperactivation state. Genetic or pharmacological inhibition of GSDMD expression or cleavage prevents F3 release or

activation *in vitro* or systemic activation of coagulation in mice induced by CLP, *E.coli* infection, bacterial rod proteins or OMVs stimulation, as well as LPS challenge in the absence or presence of HMGB1 (30, 56, 57, 59, 62). GSDMD-mediated F3 release is pyroptosis-dependent. Glycine (an osmotic protectant) inhibits the release of F3 in EprJ-infected BMDM by pyroptosis-driven cell membrane rupture instead of GSDMD-mediated pore formation (30). Although the purinergic receptor P2X7 (P2RX7) has been shown to mediate pyroptosis in a GSDMD-independent manner (63), it seems that P2RX7 is not required for the coagulation cascade in endotoxemic mice (30, 56).

It is worth noting that the GSDMD-mediated coagulation cascade may occur in a pyroptosis-independent manner. Glycine is unable to affect F3 activation in mouse peritoneal macrophages (PM) stimulated by cytoplasmic LPS, suggesting another mechanism independent of pyroptosis. Alternatively, the pores formed by GSDMD render cells into a hyperactivation state, which is adequate to permit Ca^{2+} influx, thereby promoting PS exposure through Ca^{2+}-dependent scramblase anoctamin 6 (ANO6). After the externalization of PS is increased, the activity of F3 is enhanced after LPS challenge *in vivo* and *in vitro*, which can be attenuated by using specific PS binding proteins, such as lactadherin and MFG-E8 (56). These studies describe a direct link between GSDMD and coagulopathy, although its mechanism of action is stimulus-dependent.

Cell membrane rupture also occurs in necroptosis, a form of regulated necrosis depending on several kinases, including receptor interacting protein kinase 1 (RIPK1). RIPK1 expressed in epithelial cells favors tumor necrosis factor (TNF)- or TNF/Z-VAD-FMK-induced coagulation with increased plasma F3 in mice (64). These findings indicate that multiple types of necrosis contribute to coagulation through different mechanisms.

STING1 Activation

Stimulator of interferon response cGAMP interactor 1 (STING1) is an ER-associated membrane protein and plays a complex role in innate immune sensing of pathogens. Excessive activation of STING1 pathway is involved in pathogenesis of sepsis and is recently reported to drive lethal coagulation in sepsis through GSDMD-dependent mechanism. STING1, coupled with inositol 1,4,5-trisphosphate receptor type 1 [ITPR1, a calcium release channel of endoplasmic reticulum (ER)] and the ATPase sarcoplasmic/ER Ca^{2+} transporting 2 (ATP2A2, a calcium uptake pump of ER), mediates cytosolic calcium influx to activate CASP1, CASP11, or CASP8 in macrophages/monocytes in response to different infections (62). Therefore, *Sting1* depletion limits the production of GSDMD-N in THP1 cells mediated by CASP1/11/8, resulting in a decrease in F3 release. Reduced coagulation activation and prolonged animal survival are observed in septic mice (CLP, *E.coli* and *S. pneumoniae* infection) with conditional deletion of *Sting1* in myeloid cells (62). Moreover, mRNA expression of *STING1* and *GSDMD* in peripheral blood mononuclear cell (PBMC) closely correlates with DIC severity in patients with sepsis, highlighting the regulatory role of STING1 in DIC during sepsis (62). Notably, STING1-mediated type I interferon (IFN) response does not seem to be important for inflammasome-mediated coagulation response during sepsis, because deletion of type I IFN receptor (*Ifnar*) or interferon regulatory factor 3 (*Irf3*) in mice fails to block infection-induced coagulation activation (62). However, another study suggests that IFNs may contribute to coagulation activation due to its ability to induce hepatocyte HMGB1 release, leading CASP11-dependent GSDMD activation and PS exposure (59). Further animal experiments are needed to understand the role of IFN-dependent HMGB1 release in blood coagulation.

Ca^{2+} Influx

Increased cytosolic Ca^{2+} influx, either released from ER or entered extracellularly through calcium channels, is a critical signal for immune response (65, 66), including modulating inflammasome activation (67–70). Inhibiting cytosolic calcium accumulation by calcium chelator (BAPTA-AM and EDTA) or ER stress inhibitor (TUCDA and 4PBA) leads to reduced F3 release or activity in THP1 or murine macrophages (56, 62). Similarly, decreased Ca^{2+} released by TUCDA or Ca^{2+} channel modulator (2-APB) protects against coagulation activation in CLP mice. (56). In contrast, raising Ca^{2+} influx by ER stress agonist (tunicamycin and thapsigargin) (62) or calcium inophore (A23187) (56) promotes F3 release or activity. These drug studies support the function of cytosolic Ca^{2+} influx in mediating coagulation activation during sepsis. In addition, the production of GSDMD-N in THP1 or BMDM during inflammasome activation is also inhibited by blocking cytosolic Ca^{2+} influx using the knockdown of *ITPR1,* overexpression of *ATP2A2* or inhibition of phospholipase C gamma 1 (PLCG1) (62). Moreover, extracellular Ca^{2+} also enters through GSDMD-N-formed pores to trigger coagulation cascade by promoting PS exposure (56). In general, these findings suggest that during sepsis, Ca^{2+} influx can act as both a regulator and an effector of inflammasome activation during septic coagulation. Approaches that control the Ca^{2+} concentration may improve the therapeutic effect of anticoagulation.

CONCLUSION AND OUTLOOK

The molecular mechanisms of how systemic coagulation is triggered by the inflammasome during lethal sepsis brings a new understanding of the inflammasome function and sets a new stage for immunocoagulation studies. However, some questions have raised and remain unsolved. First, it is not yet clear how different types of inflammasomes coordinate to regulate the coagulation response, because clinical sepsis is usually caused by polymicrobial infection. Second, most studies have focused on the direct effects inflammasomes have on the release and activation of F3. However, whether F3 in turn regulates inflammasome activation is still unknown. Third, how to transform these new understandings into treatment of inflammasome-dependent coagulation during sepsis in human patients? Since the treatment with anticoagulant after onset of sepsis has not resulted in improved clinical outcomes, administration or combination of inflammasome-associated inhibitors may be a favorable approach to fight against sepsis-induced coagulation. Some drugs have displayed a promising effect to protect inflammasome-related coagulation during sepsis

TABLE 1 | Potential inhibitors of inflammasome-dependent coagulation.

Mechanism	Function	Name	Usage	Model	References
Reduce Ca^{2+} influx	Calcium chelator	BAPTA-AM	Up to 10 μM	PMs WT or *ITPR1*-KD BMDMs/THP1	(56, 62)
		Ethylenediaminetetraacetic acid (EDTA)	Up to 600 μM	PMs	(56)
	ER stress inhibitor	Tauroursodeoxycholic acid (TUDCA)	200 mg/kg	WT or *Tmem173*$^{-/-}$ mice	(62)
			50 μM	THP1	(62)
		4-phenyl butyric acid (4PBA)	1 mM	THP1	(62)
	D-myo-inositol 1,4,5-trisphosphate (IP_3) receptor antagonist	2-Aminoethoxydiphenylborane (2-APB)	20 mg/kg	WT or *Tmem173*$^{-/-}$ mice	(62)
	TMEM16F inhibitor	Tannic acid (TA)	NA	PMs	(56)
		Niflumic acid (NFA)	NA	PMs	(56)
	PLCG1 inhibitor	U73122	10 μM	THP1	(62)
			30 mg/kg	WT or *Gsdmd*$^{105N/105N}$ mice	(62)
Inhibit caspase 8 cleavage	Caspase 8 inhibitor	Z-IETD-FMK	20 μM	WT or *Casp1*$^{-/-}$*Casp11*$^{-/-}$ BMDMs	(62)
Prevent NLRP3 oligomerization	NLRP3 inhibitor	MCC950	50 mg/kg	Rat	(25)
Delete *in vivo* macrophage	Macrophage remover	Clodronate liposomes	40 mg/kg	Mice	(30, 56)
Neutralize HMGB1	HMGB1 antibody	2G7	160 μg/mouse	Mice	(56)
Prevent membrane rupture	Osmoprotectant	Glycine	5 mM	BMDMs	(30)

(**Table 1**). The existing small molecules that block inflammasome activation could also be investigated for their potential role in controlling coagulation.

Regulated inflammasome activity is still essential for host defense against pathogens because mounting the immune response with its associated secretory cytokines would further contribute to the adaptive immune response. Thus, treatment of sepsis-induced coagulation by inhibiting inflammasome activity should be strictly monitored to avoid severe side effects caused by a suppressed immune response. Therefore, an in-depth understanding of the mechanism of coagulopathy triggered by inflammasomes is essential for identifying new therapeutic targets and developing more beneficial therapies.

AUTHOR CONTRIBUTIONS

RK and DT conceived of the topic for this review. All authors listed have made a substantial, direct and intellectual contribution to the work, and approved it for publication.

REFERENCES

1. Singer M, Deutschman CS, Seymour CW, Shankar-Hari M, Annane D, Bauer M, et al. The third international consensus definitions for sepsis and septic shock (Sepsis-3). *JAMA*. (2016) 315:801–10. doi: 10.1001/jama.2016.0287
2. Levi M, van der Poll T. Coagulation and sepsis. *Thromb Res.* (2017) 149:38–44. doi: 10.1016/j.thromres.2016.11.007
3. Gando S, Levi M, Toh CH. Disseminated intravascular coagulation. *Nat Rev Dis Primers*. (2016) 2:16037. doi: 10.1038/nrdp.2016.37
4. Gando S, Saitoh D, Ishikura H, Ueyama M, Otomo Y, Oda S, et al. A randomized, controlled, multicenter trial of the effects of antithrombin on disseminated intravascular coagulation in patients with sepsis. *Crit Care.* (2013) 17:R297. doi: 10.1186/cc13163
5. Lamkanfi M, Dixit VM. Mechanisms and functions of inflammasomes. *Cell.* (2014) 157:1013–22. doi: 10.1016/j.cell.2014.04.007
6. Martinon F, Burns K, Tschopp J. The inflammasome: a molecular platform triggering activation of inflammatory caspases and processing of proIL-beta. *Mol Cell.* (2002) 10:417–26. doi: 10.1016/S1097-2765(02)00599-3
7. Kayagaki N, Warming S, Lamkanfi M, Vande Walle L, Louie S, Dong J, et al. Non-canonical inflammasome activation targets caspase-11. *Nature.* (2011) 479:117–21. doi: 10.1038/nature10558
8. Kumar V. Inflammasomes: pandora's box for sepsis. *J Inflamm Res.* (2018) 11:477–502. doi: 10.2147/JIR.S178084
9. Mao K, Chen S, Chen M, Ma Y, Wang Y, Huang B, et al. Nitric oxide suppresses NLRP3 inflammasome activation and protects against LPS-induced septic shock. *Cell Res.* (2013) 23:201–12. doi: 10.1038/cr.2013.6
10. Gong Z, Zhou J, Li H, Gao Y, Xu C, Zhao S, et al. Curcumin suppresses NLRP3 inflammasome activation and protects against LPS-induced septic shock. *Mol Nutr Food Res.* (2015) 59:2132–42. doi: 10.1002/mnfr.201500316
11. Wang P, Huang J, Li Y, Chang R, Wu H, Lin J, et al. Exogenous carbon monoxide decreases sepsis-induced acute kidney injury and inhibits NLRP3 inflammasome activation in rats. *Int J Mol Sci.* (2015) 16:20595–608. doi: 10.3390/ijms160920595
12. Moon JS, Lee S, Park MA, Siempos, II, Haslip M, et al. UCP2-induced fatty acid synthase promotes NLRP3 inflammasome activation during sepsis. *J Clin Invest.* (2015) 125:665–80. doi: 10.1172/JCI78253
13. Luo YP, Jiang L, Kang K, Fei DS, Meng XL, Nan CC, et al. Hemin inhibits NLRP3 inflammasome activation in sepsis-induced acute lung injury, involving heme oxygenase-1. *Int Immunopharmacol.* (2014) 20:24–32. doi: 10.1016/j.intimp.2014.02.017
14. Long H, Xu B, Luo Y, Luo K. Artemisinin protects mice against burn sepsis through inhibiting NLRP3 inflammasome activation.

Am J Emerg Med. (2016) 34:772–7. doi: 10.1016/j.ajem.2015.12.075
15. Kalbitz M, Fattahi F, Grailer JJ, Jajou L, Malan EA, Zetoune FS, et al. Complement-induced activation of the cardiac NLRP3 inflammasome in sepsis. *FASEB J.* (2016) 30:3997–4006. doi: 10.1096/fj.201600728R
16. Rathinam VA, Fitzgerald KA. Inflammasome complexes: emerging mechanisms and effector functions. *Cell.* (2016) 165:792–800. doi: 10.1016/j.cell.2016.03.046
17. Srinivasula SM, Poyet JL, Razmara M, Datta P, Zhang Z, Alnemri ES. The PYRIN-CARD protein ASC is an activating adaptor for caspase-1. *J Biol Chem.* (2002) 277:21119–22. doi: 10.1074/jbc.C200179200
18. Zychlinsky A, Prevost MC, Sansonetti PJ. Shigella flexneri induces apoptosis in infected macrophages. *Nature.* (1992) 358:167–9. doi: 10.1038/358167a0
19. Zanoni I, Tan Y, Di Gioia M, Broggi A, Ruan J, Shi J, et al. An endogenous caspase-11 ligand elicits interleukin-1 release from living dendritic cells. *Science.* (2016) 352:1232–6. doi: 10.1126/science.aaf3036
20. Evavold CL, Ruan J, Tan Y, Xia S, Wu H, Kagan JC. The pore-forming protein gasdermin d regulates interleukin-1 secretion from living macrophages. *Immunity.* (2018) 48:35–44.e6. doi: 10.1016/j.immuni.2017.11.013
21. He Y, Hara H, Nunez G. Mechanism and regulation of NLRP3 inflammasome activation. *Trends Biochem Sci.* (2016) 41:1012–21. doi: 10.1016/j.tibs.2016.09.002
22. Lamkanfi M, Dixit VM. Inflammasomes and their roles in health and disease. *Annu Rev Cell Dev Biol.* (2012) 28:137–61. doi: 10.1146/annurev-cellbio-101011-155745
23. Sutterwala FS, Haasken S, Cassel SL. Mechanism of NLRP3 inflammasome activation. *Ann N Y Acad Sci.* (2014) 1319:82–95. doi: 10.1111/nyas.12458
24. Danielski LG, Giustina AD, Bonfante S, Barichello T, Petronilho F. The NLRP3 inflammasome and its role in sepsis development. *Inflammation.* (2020) 43:24–31. doi: 10.1007/s10753-019-01124-9
25. Cornelius DC, Travis OK, Tramel RW, Borges-Rodriguez M, Baik CH, Greer M, et al. NLRP3 inflammasome inhibition attenuates sepsis-induced platelet activation and prevents multi-organ injury in cecal-ligation puncture. *PLoS ONE.* (2020) 15:e0234039. doi: 10.1371/journal.pone.0234039
26. Miao EA, Mao DP, Yudkovsky N, Bonneau R, Lorang CG, Warren SE, et al. Innate immune detection of the type III secretion apparatus through the NLRC4 inflammasome. *Proc Natl Acad Sci USA.* (2010) 107:3076–80. doi: 10.1073/pnas.0913087107
27. Kofoed EM, Vance RE. Innate immune recognition of bacterial ligands by NAIPs determines inflammasome specificity. *Nature.* (2011) 477:592–5. doi: 10.1038/nature10394
28. Zhao Y, Yang J, Shi J, Gong YN, Lu Q, Xu H, et al. The NLRC4 inflammasome receptors for bacterial flagellin and type III secretion apparatus. *Nature.* (2011) 477:596–600. doi: 10.1038/nature10510
29. Nichols RD, von Moltke J, Vance RE. NAIP/NLRC4 inflammasome activation in MRP8(+) cells is sufficient to cause systemic inflammatory disease. *Nat Commun.* (2017) 8:2209. doi: 10.1038/s41467-017-02266-w
30. Wu C, Lu W, Zhang Y, Zhang G, Shi X, Hisada Y, et al. Inflammasome activation triggers blood clotting and host death through pyroptosis. *Immunity.* (2019) 50:1401–11.e4. doi: 10.1016/j.immuni.2019.04.003
31. Kayagaki N, Wong MT, Stowe IB, Ramani SR, Gonzalez LC, Akashi-Takamura S, et al. Noncanonical inflammasome activation by intracellular LPS independent of TLR4. *Science.* (2013) 341:1246–9. doi: 10.1126/science.1240248
32. Shi J, Zhao Y, Wang Y, Gao W, Ding J, Li P, et al. Inflammatory caspases are innate immune receptors for intracellular LPS. *Nature.* (2014) 514:187–92. doi: 10.1038/nature13683
33. Sollberger G, Strittmatter GE, Kistowska M, French LE, Beer HD. Caspase-4 is required for activation of inflammasomes. *J Immunol.* (2012) 188:1992–2000. doi: 10.4049/jimmunol.1101620
34. Vigano E, Diamond CE, Spreafico R, Balachander A, Sobota RM, Mortellaro A. Human caspase-4 and caspase-5 regulate the one-step non-canonical inflammasome activation in monocytes. *Nat Commun.* (2015) 6:8761. doi: 10.1038/ncomms9761
35. Knodler LA, Crowley SM, Sham HP, Yang H, Wrande M, Ma C, et al. Noncanonical inflammasome activation of caspase-4/caspase-11 mediates epithelial defenses against enteric bacterial pathogens. *Cell Host Microbe.* (2014) 16:249–56. doi: 10.1016/j.chom.2014.07.002
36. Casson CN, Yu J, Reyes VM, Taschuk FO, Yadav A, Copenhaver AM, et al. Human caspase-4 mediates noncanonical inflammasome activation against gram-negative bacterial pathogens. *Proc Natl Acad Sci USA.* (2015) 112:6688–93. doi: 10.1073/pnas.1421699112
37. Hagar JA, Powell DA, Aachoui Y, Ernst RK, Miao EA. Cytoplasmic LPS activates caspase-11: implications in TLR4-independent endotoxic shock. *Science.* (2013) 341:1250–3. doi: 10.1126/science.1240988
38. Chu LH, Indramohan M, Ratsimandresey RA, Gangopadhyay A, Morris EP, Monack DM, et al. The oxidized phospholipid oxPAPC protects from septic shock by targeting the non-canonical inflammasome in macrophages. *Nat Commun.* (2018) 9:996. doi: 10.1038/s41467-018-03409-3
39. Kayagaki N, Stowe IB, Lee BL, O'Rourke K, Anderson K, Warming S, et al. Caspase-11 cleaves gasdermin D for non-canonical inflammasome signalling. *Nature.* (2015) 526:666–71. doi: 10.1038/nature15541
40. Kajiwara Y, Schiff T, Voloudakis G, Gama Sosa MA, Elder G, Bozdagi O, et al. A critical role for human caspase-4 in endotoxin sensitivity. *J Immunol.* (2014) 193:335–43. doi: 10.4049/jimmunol.1303424
41. Levi M, de Jonge E, van der Poll T. Sepsis and disseminated intravascular coagulation. *J Thromb Thrombolysis.* (2003) 16:43–7. doi: 10.1023/B:THRO.0000014592.27892.11
42. Butenas S. Tissue factor structure and function. *Scientifica.* (2012) 2012:964862. doi: 10.6064/2012/964862
43. Pawlinski R, Mackman N. Cellular sources of tissue factor in endotoxemia and sepsis. *Thromb Res.* (2010) 125(Suppl.1):S70–3. doi: 10.1016/j.thromres.2010.01.042
44. Gregory SA, Morrissey JH, Edgington TS. Regulation of tissue factor gene expression in the monocyte procoagulant response to endotoxin. *Mol Cell Biol.* (1989) 9:2752–5. doi: 10.1128/MCB.9.6.2752
45. Brand K, Fowler BJ, Edgington TS, Mackman N. Tissue factor mRNA in THP-1 monocytic cells is regulated at both transcriptional and posttranscriptional levels in response to lipopolysaccharide. *Mol Cell Biol.* (1991) 11:4732–8. doi: 10.1128/MCB.11.9.4732
46. Mackman N, Brand K, Edgington TS. Lipopolysaccharide-mediated transcriptional activation of the human tissue factor gene in THP-1 monocytic cells requires both activator protein 1 and nuclear factor kappa B binding sites. *J Exp Med.* (1991) 174:1517–26. doi: 10.1084/jem.174.6.1517
47. Zhang Y, Meng H, Ma R, He Z, Wu X, Cao M, et al. Circulating microparticles, blood cells, and endothelium induce procoagulant activity in sepsis through phosphatidylserine exposure. *Shock.* (2016) 45:299–307. doi: 10.1097/SHK.0000000000000509
48. Taylor FB Jr, Chang A, Ruf W, Morrissey JH, Hinshaw L, et al. Lethal *E. coli* septic shock is prevented by blocking tissue factor with monoclonal antibody. *Circ Shock.* (1991) 33:127–34.
49. Dackiw AP, McGilvray ID, Woodside M, Nathens AB, Marshall JC, Rotstein OD. Prevention of endotoxin-induced mortality by antitissue factor immunization. *Arch Surg.* (1996) 131:1273–8; discussion 8–9. doi: 10.1001/archsurg.1996.01430240027003
50. Shah KG, Wu R, Jacob A, Molmenti EP, Nicastro J, Coppa GF, et al. Recombinant human milk fat globule-EGF factor 8 produces dose-dependent benefits in sepsis. *Intensive Care Med.* (2012) 38:128–36. doi: 10.1007/s00134-011-2353-7
51. Rittirsch D, Flierl MA, Ward PA. Harmful molecular mechanisms in sepsis. *Nat Rev Immunol.* (2008) 8:776–87. doi: 10.1038/nri2402
52. Gould TJ, Vu TT, Swystun LL, Dwivedi DJ, Mai SH, Weitz JI, et al. Neutrophil extracellular traps promote thrombin generation through platelet-dependent and platelet-independent mechanisms. *Arterioscler Thromb Vasc Biol.* (2014) 34:1977–84. doi: 10.1161/ATVBAHA.114.304114
53. Sunden-Cullberg J, Norrby-Teglund A, Treutiger CJ. The role of high mobility group box-1 protein in severe sepsis. *Curr Opin Infect Dis.* (2006) 19:231–6. doi: 10.1097/01.qco.0000224816.96986.67
54. Ammollo CT, Semeraro F, Xu J, Esmon NL, Esmon CT. Extracellular histones increase plasma thrombin generation by impairing thrombomodulin-dependent protein C activation. *J Thromb Haemost.* (2011) 9:1795–803. doi: 10.1111/j.1538-7836.2011.04422.x
55. Cornelius DC, Baik CH, Travis OK, White DL, Young CM, Austin Pierce W, et al. NLRP3 inflammasome activation in platelets in response to sepsis. *Physiol Rep.* (2019) 7:e14073. doi: 10.14814/phy2.14073

56. Yang X, Cheng X, Tang Y, Qiu X, Wang Y, Kang H, et al. Bacterial endotoxin activates the coagulation cascade through gasdermin D-dependent phosphatidylserine exposure. *Immunity.* (2019) 51:983–96.e6. doi: 10.1016/j.immuni.2019.11.005
57. Peng Y, Gao M, Liu Y, Qiu X, Cheng X, Yang X, et al. Bacterial outer membrane vesicles induce disseminated intravascular coagulation through the caspase-11-gasdermin D pathway. *Thromb Res.* (2020) 196:159–66. doi: 10.1016/j.thromres.2020.08.013
58. Deng M, Tang Y, Li W, Wang X, Zhang R, Zhang X, et al. The endotoxin delivery protein HMGB1 mediates caspase-11-dependent lethality in sepsis. *Immunity.* (2018) 49:740–53.e7. doi: 10.1016/j.immuni.2018.08.016
59. Yang X, Cheng X, Tang Y, Qiu X, Wang Z, Fu G, et al. The role of type 1 interferons in coagulation induced by gram-negative bacteria. *Blood.* (2020) 135:1087–100. doi: 10.1182/blood.2019002282
60. Gurung P, Anand PK, Malireddi RK, Vande Walle L, Van Opdenbosch N, Dillon CP, et al. FADD and caspase-8 mediate priming and activation of the canonical and noncanonical Nlrp3 inflammasomes. *J Immunol.* (2014) 192:1835–46. doi: 10.4049/jimmunol.1302839
61. Sagulenko V, Thygesen SJ, Sester DP, Idris A, Cridland JA, Vajjhala PR, et al. AIM2 and NLRP3 inflammasomes activate both apoptotic and pyroptotic death pathways via ASC. *Cell Death Differ.* (2013) 20:1149–60. doi: 10.1038/cdd.2013.37
62. Zhang H, Zeng L, Xie M, Liu J, Zhou B, Wu R, et al. TMEM173 drives lethal coagulation in sepsis. *Cell Host Microbe.* (2020) 27:556–70 e6. doi: 10.1016/j.chom.2020.02.004
63. Yang D, He Y, Munoz-Planillo R, Liu Q, Nunez G. Caspase-11 requires the pannexin-1 channel and the purinergic P2X7 pore to mediate pyroptosis and endotoxic shock. *Immunity.* (2015) 43:923–32. doi: 10.1016/j.immuni.2015.10.009
64. Zelic M, Roderick JE, O'Donnell JA, Lehman J, Lim SE, Janardhan HP, et al. RIP kinase 1-dependent endothelial necroptosis underlies systemic inflammatory response syndrome. *J Clin Invest.* (2018) 128:2064–75. doi: 10.1172/JCI96147
65. Bettigole SE, Glimcher LH. Endoplasmic reticulum stress in immunity. *Annu Rev Immunol.* (2015) 33:107–38. doi: 10.1146/annurev-immunol-032414-112116
66. Vig M, Kinet JP. Calcium signaling in immune cells. *Nat Immunol.* (2009) 10:21–7. doi: 10.1038/ni.f.220
67. Lee GS, Subramanian N, Kim AI, Aksentijevich I, Goldbach-Mansky R, Sacks DB, et al. The calcium-sensing receptor regulates the NLRP3 inflammasome through Ca2+ and cAMP. *Nature.* (2012) 492:123–7. doi: 10.1038/nature11588
68. Chen R, Zeng L, Zhu S, Liu J, Zeh HJ, Kroemer G, et al. cAMP metabolism controls caspase-11 inflammasome activation and pyroptosis in sepsis. *Sci Adv.* (2019) 5:eaav5562. doi: 10.1126/sciadv.aav5562
69. Zhou B, Liu J, Zeng L, Zhu S, Wang H, Billiar TR, et al. Extracellular SQSTM1 mediates bacterial septic death in mice through insulin receptor signalling. *Nat Microbiol.* (2020) 5:1576–87. doi: 10.1038/s41564-020-00795-7
70. Kang R, Zeng L, Zhu S, Xie Y, Liu J, Wen Q, et al. Lipid peroxidation drives gasdermin d-mediated pyroptosis in lethal polymicrobial sepsis. *Cell Host Microbe.* (2018) 24:97–108.e4. doi: 10.1016/j.chom.2018.05.009

Conflict of Interest: The authors declare that the research was conducted in the absence of any commercial or financial relationships that could be construed as a potential conflict of interest.

frontiers in Immunology

ORIGINAL RESEARCH
published: 16 March 2021
doi: 10.3389/fimmu.2021.642867

Activation of Neutrophil Granulocytes by Platelet-Activating Factor Is Impaired During Experimental Sepsis

*Stefan Hug[1], Stefan Bernhard[1], Alexander Elias Paul Stratmann[1], Maike Erber[1], Lisa Wohlgemuth[1], Christiane Leonie Knapp[1], Jonas Martin Bauer[1], Laura Vidoni[1], Michael Fauler[2], Karl Josef Föhr[3], Peter Radermacher[4], Andrea Hoffmann[4], Markus Huber-Lang[1] and David Alexander Christian Messerer[1,3,4]**

[1] Institute of Clinical and Experimental Trauma Immunology, University Hospital of Ulm, Ulm, Germany, [2] Institute of General Physiology, University of Ulm, Ulm, Germany, [3] Department of Anesthesiology and Intensive Care Medicine, University Hospital of Ulm, Ulm, Germany, [4] Institute of Anesthesiological Pathophysiology and Process Development, University Hospital of Ulm, Ulm, Germany

OPEN ACCESS

Edited by:
Marcin Filip Osuchowski, Ludwig Boltzmann Institute for Experimental and Clinical Traumatology, Austria

Reviewed by:
Matthijs Kox, Radboud University Nijmegen Medical Centre, Netherlands
Matthias Clauss, Indiana University Bloomington, United States

***Correspondence:**
David Alexander Christian Messerer
david.messerer@uni-ulm.de

Specialty section:
This article was submitted to Inflammation, a section of the journal Frontiers in Immunology

Received: 16 December 2020
Accepted: 15 February 2021
Published: 16 March 2021

Citation:
Hug S, Bernhard S, Stratmann AEP, Erber M, Wohlgemuth L, Knapp CL, Bauer JM, Vidoni L, Fauler M, Föhr KJ, Radermacher P, Hoffmann A, Huber-Lang M and Messerer DAC (2021) Activation of Neutrophil Granulocytes by Platelet-Activating Factor Is Impaired During Experimental Sepsis. Front. Immunol. 12:642867. doi: 10.3389/fimmu.2021.642867

Platelet-activating factor (PAF) is an important mediator of the systemic inflammatory response. In the case of sepsis, proper activation and function of neutrophils as the first line of cellular defense are based on a well-balanced physiological response. However, little is known about the role of PAF in cellular changes of neutrophils during sepsis. Therefore, this study investigates the reaction patterns of neutrophils induced by PAF with a focus on membrane potential (MP), intracellular pH, and cellular swelling under physiological and pathophysiological conditions and hypothesizes that the PAF-mediated response of granulocytes is altered during sepsis. The cellular response of granulocytes including MP, intracellular pH, cellular swelling, and other activation markers were analyzed by multiparametric flow cytometry. In addition, the chemotactic activity and the formation of platelet–neutrophil complexes after exposure to PAF were investigated. The changes of the (electro-)physiological response features were translationally verified in a human *ex vivo* whole blood model of endotoxemia as well as during polymicrobial porcine sepsis. In neutrophils from healthy human donors, PAF elicited a rapid depolarization, an intracellular alkalization, and an increase in cell size in a time- and dose-dependent manner. Mechanistically, the alkalization was dependent on sodium-proton exchanger 1 (NHE1) activity, while the change in cellular shape was sodium flux- but only partially NHE1-dependent. In a pathophysiological altered environment, the PAF-induced response of neutrophils was modulated. Acidifying the extracellular pH *in vitro* enhanced PAF-mediated depolarization, whereas the increases in cell size and intracellular pH were largely unaffected. *Ex vivo* exposure of human whole blood to lipopolysaccharide diminished the PAF-induced intracellular alkalization and the change in neutrophil size. During experimental porcine sepsis, depolarization of the MP was significantly impaired. Additionally, there was a trend for increased cellular swelling, whereas intracellular alkalization remained stable. Overall, an impaired

(electro-)physiological response of neutrophils to PAF stimulation represents a cellular hallmark of those cells challenged during systemic inflammation. Furthermore, this altered response may be indicative of and causative for the development of neutrophil dysfunction during sepsis.

Keywords: platelet-activating factor, neutrophil granulocytes, intracellular pH, sepsis, membrane potential, flow cytometry

INTRODUCTION

Platelet-activating factor (PAF) is a phospholipid mediator with well-described proinflammatory properties, among others, by activating thrombocytes and leukocytes (1, 2). The importance of PAF has been investigated in many other diseases, in particular in chronic inflammation including coronary artery disease, asthma, and rheumatoid arthritis, as well as in acute inflammation such as trauma and sepsis (1–4).

Sepsis is defined as life-threatening organ dysfunction caused by a dysregulated host response to infection (5). Upon overwhelming stimulation, the immune system becomes excessively activated, resulting in a dysfunctional immune response, which contributes to multi-organ dysfunction syndrome, and ultimately, lethality (5, 6). In this context, previous studies in cecal ligation and puncture-induced rodent sepsis reported some beneficial effects by inhibiting PAF activity (7). However, despite initial encouraging results in a phase II study (8, 9), PAF degradation (10) or administration of PAF receptor antagonists (11) failed to reduce lethality in patients with severe sepsis.

Neutrophils are the vanguard of innate cellular immunity being crucially involved in the clearance of pathogens. The activity of neutrophils is driven by many proinflammatory mediators including anaphylatoxins such as PAF and the complement cleavage product C5a, interleukins, microbe-associated molecular patterns (MAMPs, e.g., fMLF), and many other factors, activate neutrophils (6, 12–15). On a cellular level, neutrophils respond with membrane potential (MP) depolarization likely generated by NADPH oxidase (NOX) activity (16, 17). Additionally, the intracellular pH (pH_i) of neutrophils increases transiently (15, 18), regulating important cellular functions, for example, interference of apoptosis (19, 20), and modulation of chemotactic activity (21–23). Moreover, neutrophil activation by chemoattractants results in changes in the cellular shape and chemotaxis (14, 24), the generation of reactive oxygen species (ROS) (25, 26), and the expression of surface activation markers. For the last, an upregulation of integrin alpha M (CD11b) was found to facilitate leukocyte adhesion and L-selectin (CD62L) shedding, which both are considered to be hallmarks of neutrophil diapedesis into peripheral tissues (27–29).

The PAF-induced response in various cell types, including neutrophils, was investigated previously. For example, PAF induced a depolarization in rat endothelial cells (30), guinea pig neurons (31), and human neutrophils (32). Moreover, PAF mediated a small increase in pH_i in bovine neutrophils (33, 34), while in human neutrophils an initial acidification and consecutive small rebound alkalization was described (35). During systemic inflammation, cellular parameters of neutrophils have been reported to be altered. For example, in murine sepsis, an increase in neutrophil cell size (14) and pH_i were reported, with the latter verified in patients with sepsis (15). Both alterations have been confirmed in an *ex vivo* model of lipopolysaccharide (LPS)-induced inflammation (36). In this context, it is tempting to speculate that a shift in baseline levels of neutrophil parameters during systemic inflammation affects the response under additional stimulation by inflammatory mediators such as PAF, however, this remains to be further elucidated.

Therefore, in this study, we investigated the cellular response induced by PAF in neutrophils in a multi-step approach: Firstly, under physiological conditions and, secondly mechanistically by identifying the sodium-proton antiport as an important ion transport protein. Finally, we translationally analyzed the response elicited by PAF during inflammation in the setting of *in vitro* acidosis, in an *ex vivo* whole blood model of LPS-driven inflammation, and in a porcine model of polymicrobial sepsis.

MATERIALS AND METHODS

All chemicals were purchased from Merck (Darmstadt, Germany), when not indicated otherwise.

Isolation of Neutrophils

The investigations were approved by the Local Independent Ethics Committee of the University of Ulm (number 459/18; 94/14). After obtaining informed written consent from healthy human volunteers, blood was drawn into syringes containing 3.2% trisodium citrate (Sarstedt, Nürnbrecht, Germany). Neutrophils were isolated by Ficoll-Paque (GE Healthcare, Uppsala, Sweden) density gradient centrifugation and subsequent dextran sedimentation followed by hypotonic lysis of remaining erythrocytes, as described previously (14–16). Polymorphonuclear granulocytes (mainly consisting of neutrophils) were adjusted to a concentration of 2×10^6 cells/ml using Hank's balanced salt solution with calcium and magnesium (HBSS, Thermo Fisher, Darmstadt, Germany), the pH of which was adjusted to 7.3, when not indicated otherwise.

Measurement of Neutrophil Membrane Potential, Intracellular pH, and Cell Size

Isolated neutrophils were incubated in a light-protected water bath at 37°C with the fluorescent dyes bis(1,3-dibutylbarbituric

acid) trimethine oxonol ($DiBAC_4(3)$), 50 nM, or 5-(and-6)-carboxy-SNARF-1 (SNARF), 1 μM (Thermo Fisher) for 20 min or with dihydrorhodamine 123 (D123) (Santa Cruz Biotechnology, Heidelberg, Germany), 1.8 μM, for 30 min to determine MP (16), pH_i, and ROS generation [what is measured by D123 is the byproduct H_2O_2 which is itself derived from $O_2^{\bullet-}$, a product generated by NOX activity (37)], respectively. To determine porcine neutrophil pH_i, the cells were instead incubated with 2′,7′-bis-(2-carboxyethyl)-5-(and-6)-carboxyfluorescein, acetoxymethyl ester (BCECF, Abcam, Cambridge, United Kingdom), 25 nM, for 30 min, because exposure of porcine neutrophils to SNARF resulted in changes in forward scatter area (FSC-A), which was interpreted as possible cellular activation (data not shown). Following incubation, neutrophils were centrifuged for 5 min (340 g) and resuspended in Roswell Park Memorial Institute medium (RPMI) with magnesium and calcium with a pH adjusted to 7.3. $DiBAC_4(3)$ was again added. After a resting period of 10 min in a light-protected water bath at 37°C, neutrophils were stimulated with 1 μM PAF or 100 ng/ml complement factor 5a (C5a, Complement Technology, Tyler, Texas, USA), when not indicated otherwise. Cells were analyzed using a Canto II flow cytometer (BD Biosciences, Heidelberg, Germany). Neutrophils were identified by FSC-A and sideward scatter area. Non-fluorescent reference microspheres (10, 15, and 20 μm diameter; Polybead® Polystyrene Microsphere, Polysciences, Hirschberg, Germany) were used to quantify the shape changes assessed by the FSC-A (14). Differences in absolute FSC-A values between experiments are explained by recalibration of the flow cytometer between different experimental series. The fluorescence of $DiBAC_4(3)$ were converted in changes of the MP as described previously (16) with a small modification: RPMI with varying extracellular concentrations of sodium and potassium were used to calculate the amount of change in $DiBAC_4(3)$ fluorescence per mV.

Near-real time kinetics were measured by acquiring neutrophils for 10 min continuously embedded in a heating unit (TC-1234A Temperature Controller, Warner Instruments LLC, Holliston, Massachusetts, USA), ensuring a steady temperature level of 37°C. Analysis was performed by a specifically designed algorithm using the statistic language R (R Core Team, Vienna, Austria).

Cell Surface Markers

Isolated neutrophils were incubated in a light-protected water bath at 37°C. Following PAF stimulation as indicated above (normally 1 μM) for 10 min, neutrophils were stained with 0.1 μg/ml APC anti-mouse/human CD11b antibody (#101212, Biolegend, San Diego, USA) and 0.5 μg/ml PE anti-human CD62L antibody (#304806, Biolegend) for 5 min at room temperature. Cells were fixed using FACS Lysing Solution (BD, Heidelberg, Germany). Proper isotype controls were used (CD11b: APC Rat IgG2b, κ Isotype Ctrl; CD62L: PE Mouse IgG1, κ Isotype Ctrl; Biolegend).

In vitro Pharmacological Modification

PAF-induced effects on neutrophils were analyzed in the presence of the subsequently listed pharmacological modulators (their proposed targets are given in brackets): Amiloride [200 μM, 10 min, Na^+-channels (15)], BIX [5 μM, 30 min, sodium-proton exchanger 1 (NHE1) (38); Tocris, Wiesbaden, Germany], 5-Nitro-2-(3-phenylpropylamino)benzoic acid [NPPB, 100 μM, 10 min, Cl^- channels (39)], and ebselen [10 nM, 30 min, glutathione peroxidase and peroxiredoxin enzyme mimetic and NOX2 inhibitor (40, 41); Tocris]. Following pre-incubation, samples were divided to obtain paired results and treated as control or stimulated with PAF.

Extracellular Alkalosis and Acidification *in vitro*

Following the described staining and centrifugation, neutrophils were resuspended in RPMI adjusted to a pH of 6.6, 7.0, 7.4, or 7.8 to simulate extracellular alkalosis or acidification. Neutrophils were incubated for 10 min at 37°C and subsequently stimulated with PAF.

Coulter Counter Measurements

Isolated neutrophils were stimulated for 10 min, diluted 1:500 with RPMI adjusted to a pH 7.3 and measured by a cell counter working through electronic current exclusion (Cell Counter CASY, OLS OMNI Life Science, Bremen, Germany).

Chemotaxis

Neutrophil chemotactic activity was assessed using a Neuro Probe A96 chemotaxis chamber (Neuro Probe, Gaithersburg, Maryland, USA). Isolated neutrophils at 5×10^6 cells/ml in HBSS + 0.1% bovine serum albumin (BSA) were stained with the fluorescent dye BCECF (1.6 μg/ml) for 30 min at 37°C, subsequently centrifuged for 5 min (340 g), and resuspended in HBSS + 0.1% BSA. A total of 33 μl chemoattractant PAF (final concentration 1 μM) was added into the wells of the lower plate. Thereafter, a silicone gasket and a framed filter with 3 μm pores were placed upon the lower wells. On top of it, the upper plate was attached, and the dyed neutrophils were pipetted into the corresponding wells. During incubation for 30 min at 37°C, neutrophils migrated from the upper wells toward the lower wells containing PAF, but became adherent to the filter, resulting in increased fluorescence. The fluorescence of the cells in the filter was measured at a wavelength of 485/538 nm using a Fluoroskan Ascent (Thermo Scientific, Rockford, Illinois, USA) with the Ascent Software Version 2.6.

Quantification of Platelet-Neutrophil Complex Formation

Platelet–neutrophil complex (PNC) formation, defined as a neutrophil with at least one platelet in direct proximity, was assessed as described previously by light microscopy and flow cytometry (36, 42). For blood smears, whole blood was diluted 1:1 with phosphate-buffered saline containing calcium and magnesium (PBS) and incubated for 15 min at 37°C with or without 1 μM PAF on a spinning wheel (Snijders Labs, Tilburg, Netherlands) at 3 rpm. Blood smears were created

and stained with Hemacolor® Rapid staining (Merck). In each sample, 50 neutrophils were counted by two independent and blinded individuals. For flow cytometry analysis, whole blood was diluted 1:5 with PBS. Following 15 min of incubation with or without 1 μM PAF, the sample was stained with anti-CD41 APC (125 ng/ml, #303710, Biolegend) and anti-CD61 PerCP (250 ng/ml, # 336412, Biolegend; both monoclonal mouse anti-human antibodies) for 15 min at room temperature followed by 30 min incubation with 1 ml of 1X BD FACS Lysing solution (BD Biosciences, San Jose, California, USA). Samples were centrifuged for 5 min at 340 g and resuspended in 100 μl PBS + 0.1% BSA and stored at 4°C in the dark until further analysis (normally within 1 h).

Ex vivo Human Whole Blood Model of Endotoxemia

An animal-free human whole blood model of endotoxemia was used to investigate the effect of LPS exposure on the PAF-induced response of neutrophils, which was described previously in detail (36). In brief, 0.5 IU/ml heparin (B. Braun Melsungen AG, Melsungen, Germany) and 100 ng/ml LPS (#L2630, Merck) or PBS (control) were added to 9 ml blood, which was transferred into a Cortiva BioActive Surface (Medtronic, Meerbusch, Germany) coated tubing system using a coated connector (Medtronic) to interlink both ends. Following 1 h of rotation (3 rpm) on a spinning wheel (Snijders Labs) at 37°C, the blood was transferred to citrate anti-coagulated monovettes (Sarstedt). Neutrophil activation markers were analyzed directly in whole blood as described previously (36) with or without exposure to PAF (1 μM, 15 min, 37°C). The remaining whole blood was processed to isolate and to analyze neutrophils as described above.

Porcine Polymicrobial Sepsis

The Federal authorities for animal research (#1362, Tuebingen, Germany) as well as the Animal Care Committee of the University of Ulm approved the experiments. The well-described porcine sepsis model was performed in adherence with guidelines on the Use of Laboratory Animals of the National Institutes of Health with anesthesia and surgical instrumentation as described previously (43–45). In brief, nine Bretoncelles-Meishan-Willebrand pigs (5 male-castrated, 4 female, mean weight 65.6 kg ± 8.6) were subjected to polymicrobial sepsis induced by inoculation of autologous feces into the abdominal cavity, followed by intensive care therapy for 60 h after the sepsis initiation. Blood was drawn before inoculation and when the mean arterial pressure was reduced by >10%, indicating cardiocirculatory shock and triggering the beginning of resuscitation. To reduce animal numbers, the analyzed pigs are a subgroup of another currently unpublished trial comparing standard intensive care therapy with or without a pharmacological intervention targeting the calcitonin gene-related peptide receptor. Because intervention started after the fulfillment of the sepsis criteria listed above, animals were included irrespective of their group allocation.

Data Presentation and Statistical Analysis

Results are presented as mean ± standard deviation (SD), when not indicated otherwise. In all experiments, a minimum of 3,000 neutrophils were measured. All data were considered to be paired and non-parametric. Statistical significance is indicated by *, **, and ***, with significance levels of $p < 0.05$, < 0.01, and < 0.001, respectively. Statistical analysis was performed using GraphPad Prism 9 (GraphPad Software Inc., San Diego, California, USA) and Microsoft Excel (Version 16.42, Microsoft Corporation, Redmond, Washington, USA).

RESULTS

PAF Induced Changes in Neutrophil Physiology in a Dose- and Time-Dependent Manner

Neutrophils responded to PAF stimulation with a rapid increase in cell size, peaking after 20 min with a relative increase of 73 ± 19% (**Figures 1A,B**). A near-real time measurement demonstrated that most of the size change occurred within in the first minutes (**Figure 1A**). The increase in the FSC-A induced by PAF was similar to the stimulation with C5a (**Figure 1B**). Using reference microspheres, the calculated diameters of unstimulated cells were 16.9 ± 1.1 μm, and 26.1 ± 0.6 μm for PAF-stimulated cells (after 10 min, $p = 0.06$, $n = 5$, representative measurement in **Figure 1C**). The change in neutrophil size was verified by Coulter counter measurement. Following 10 min of incubation with PAF, neutrophils exhibited an increase of 3.6 ± 1.7% in diameter and 10.5 ± 6.4% in volume in comparison with unstimulated neutrophils (**Figure 1D**).

Next, the response elicited by PAF on the neutrophil MP and pH_i was investigated. PAF rapidly induced a depolarization peaking after 1 min (**Figure 2A**) and an intracellular alkalization attaining a maximum of +0.45 ± 0.07 after 5 min (**Figure 2B**). In addition, PAF induced an increase in ROS production (+26 ± 11% after 10 min, $p < 0.001$ Wilcoxon signed-rank test, $n = 17$, data not shown). Depolarization and intracellular alkalization revealed different kinetics (**Figures 2A–C**). The PAF-induced response was comparable to C5a-stimulation for cell size and pH_i but was more intensive for the MP (1 min: PAF +12 ± 4 mV, C5a: 7 ± 3 mV, **Figures 2A,B**). All PAF-induced effects showed a clear concentration-response relationship (**Supplement 1**). The EC_{50}-values are presented in **Figure 2D** and ranged between 14 and 128 nM.

In accordance with previous findings, neutrophils responded to PAF stimulation with an increased chemotactic activity (15.8 ± 9.7 fold increase after 30 min, $p < 0.05$ Wilcoxon signed-rank test, $n = 6$), CD11b upregulation (+63.3 ± 41.9% after 10 min, $p < 0.01$ Wilcoxon signed-rank test, $n = 8$), and CD62L shedding (−87 ± 10% surface expression after 10 min, $p < 0.01$ Wilcoxon signed-rank test, $n = 8$) (**Supplements 1, 2**). In addition, PAF induced formation of PNCs (**Figure 3**). For all these effects, there was no significant difference when comparing neutrophils from male and female donors (**Supplement 2**).

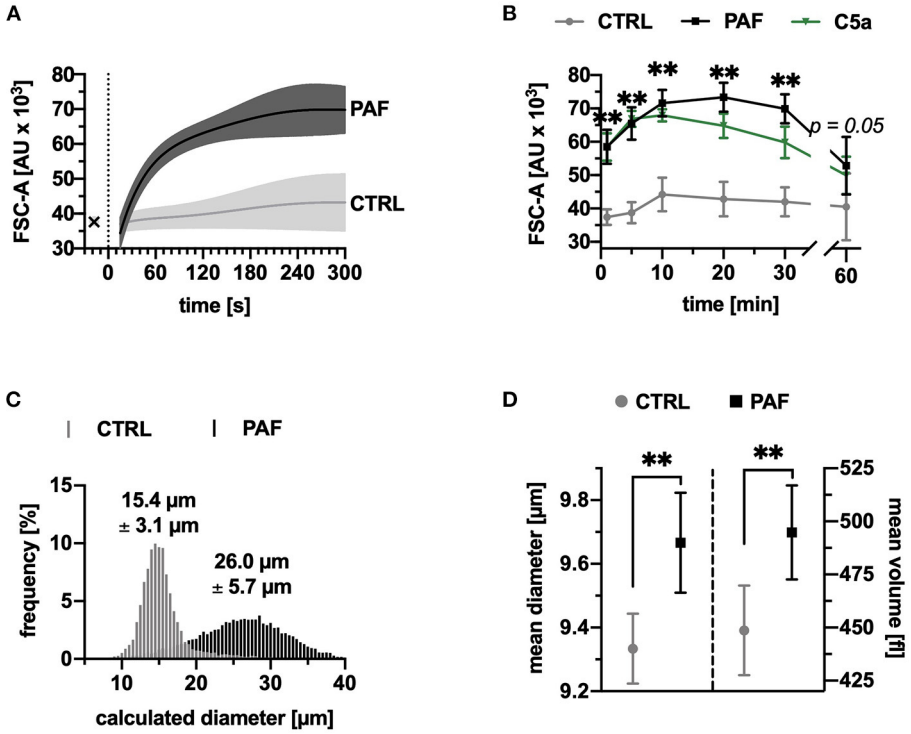

FIGURE 1 | PAF elicited a rapid increase in size of human neutrophils. **(A)** FSC-A (forward scatter area) of neutrophils stimulated by PAF (1 µM, black) or PBS (CTRL, gray), measured by continuous acquisition by flow cytometry for 5 min, x indicating baseline measurement, $n = 5$. **(B)** FSC-A of neutrophils stimulated with PAF or PBS for 60 min, $n = 15$. For comparison, neutrophils exposed to C5a (green) are shown. **(C)** Calculated diameter of neutrophils using counting beads (10, 15, and 20 µm) from one representative donor with or without PAF exposure. **(D)** Mean diameter and volume of neutrophils stimulated by PAF or PBS measured by Coulter counter, $n = 8$. Data are mean ± SD. $^{**}p < 0.01$, Wilcoxon matched-pairs signed rank test comparing PAF-stimulated neutrophils with unstimulated control cells.

Ion Transport Proteins and NOX2 Modulated the PAF-mediated Neutrophil Response

Ion fluxes in stimulated neutrophils are crucially involved in cellular activity. Unspecific inhibition of sodium or chloride flux inhibited most cellular changes induced by PAF (**Figures 4A,C**), however, in parallel also partially altering unstimulated neutrophils (**Supplement 3**).

A more detailed analysis revealed that PAF-induced intracellular alkalization was completely inhibited by targeting NHE1 activity with BIX (+0.30 ± 0.07 vs. −0.02 ± 0.04, $p < 0.01$). Cellular swelling and the ROS generation were also reduced, but to a lesser extent, by targeting NHE1 (**Figure 4B**). PAF-induced depolarization and CD62L shedding displayed no difference during selective NHE1 inhibition. PAF-induced CD11b expression increased during selective NHE1 inhibition, whereas it was fully inhibited by amiloride. However, during incubation with the NHE1 inhibitor BIX, neutrophils expressed less CD11b than cells without an inhibitor (**Supplement 3**).

Mimicking glutathione peroxidase activity and inhibiting NOX2 with ebselen significantly lowered PAF-induced generation of intracellular alkalization, ROS generation and CD62L shedding (**Figure 4D**).

Acidosis Significantly Enhanced PAF-mediated Depolarization

The first step to investigate the above-mentioned PAF-elicited effects under pathologic conditions was to expose neutrophils to buffers of various extracellular pH (pH_e). The pH_e had no influence on the PAF-induced increase in the FSC-A (**Figure 5A**). Depolarization after PAF stimulation was significantly enhanced under acid extracellular conditions (pH_e 6.6 = +23.6 ± 7.5 mV vs. pH_e 7.4 = +10.7 ± 3.1 mV, $p < 0.01$ Kruskal-Wallis test and Dunn's multiple comparison test, $n = 6$, **Figure 5B**). Regarding the pH_i, neutrophils responded with an equal intracellular alkalization when stimulated with PAF under different extracellular conditions. In addition, the pH_i of neutrophils shifted with the pH_e, therefore with rising pH_e, the pH_i increased in parallel (**Figure 5C**).

Endotoxemia Modulated the PAF-induced Response of Neutrophils

To translate the findings to a more clinically relevant setting, an *ex vivo* model of human endotoxemia was used analyzing the modulation of the PAF-induced response in systemic inflammation. As previously reported (36), sole contact with the tubing system of the model did not promote neutrophil activation (data not shown). However, the exposure to LPS

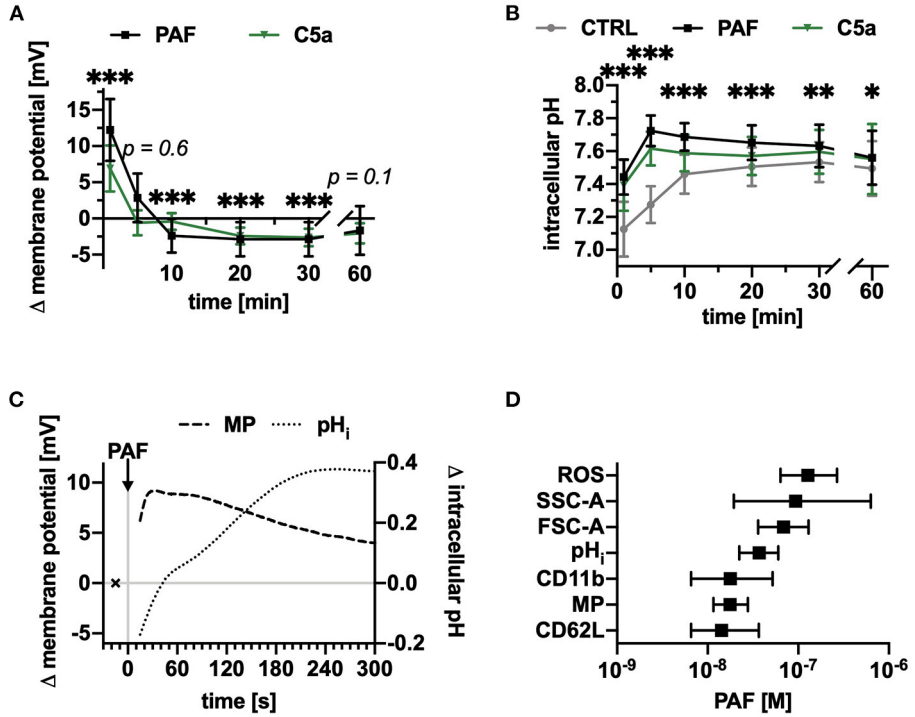

FIGURE 2 | PAF depolarized the membrane potential and increased the intracellular pH of human neutrophils within seconds. **(A)** Changes in membrane potential of neutrophils stimulated with PAF (1 μM) or C5a (green, 10 nM), $n = 15$, unstimulated cells = 0 mV. **(B)** Intracellular pH of neutrophils upon stimulation with PAF, C5a, or PBS (CTRL), $n = 15$. **(C)** Changes in membrane potential and intracellular pH of neutrophils exposed to PAF measured by continuous acquisition on flow cytometry. x represents the baseline measurement prior to stimulation. Depicted is one representative donor out of five independent experiments. **(D)** PAF-induced effects on neutrophils were concentration-dependent (ROS, reactive oxygen species; SSC-A, side scatter area; FSC-A, forward scatter area; pH_i, intracellular pH; CD11b, integrin alpha M; MP, membrane potential; CD62L, L-selectin) and respective EC_{50} ± interquartile range were calculated ($n = 5$–10). **(A,B)** data are mean ± SD. *$p <$ 0.05, **$p < 0.01$, ***$p < 0.001$, Wilcoxon signed-rank test **(A)** and Wilcoxon matched-pairs signed rank test **(B)** comparing PAF-stimulated neutrophils with unstimulated control cells.

(100 ng/ml) resulted in an activated neutrophil phenotype as reflected by of the upregulation of the surface expression of CD11b and downregulation of CD62L. These alterations in baseline expression of these activation markers also modulated the response generated by additional *in vitro* stimulation with PAF (increase in CD62L downregulation, reduction in CD11b upregulation, **Figures 6A,B**).

LPS exposure resulted in increased cellular size, pH_i, and generation of ROS, but not depolarization in neutrophils without further PAF stimulation. The PAF-induced increase in cellular size was significantly reduced after exposure to LPS (CTRL-PAF +64 ± 10% vs. LPS-PAF +8 ± 3%, $p < 0.05$, **Figure 6C**). There was no significant difference in PAF-mediated depolarization after exposure to LPS (**Figure 6D**). Transient intracellular alkalization elicited by PAF was significantly reduced in neutrophils after endotoxemia (CTRL-PAF +0.33 ± 0.05 vs. LPS-PAF +0.02 ± 0.05, $p < 0.05$, **Figure 6E**). The PAF-induced elevation in ROS generation was reduced after LPS exposure (CTRL-PAF +23 ± 12% vs. LPS-PAF −9 ± 15%, **Figure 6F**).

Sepsis Partially Impaired PAF-induced Neutrophil Activation

To validate the *in vitro* and *ex vivo* results, neutrophils isolated from a porcine polymicrobial sepsis model were investigated before and during sepsis. Clinical parameters and electrolytes are summarized in **Table 1**. The baseline FSC-A and pH_i of neutrophils without PAF stimulation remained stable before and during sepsis (data not shown). The PAF-induced change in cellular shape displayed a trend for an increase during sepsis (+0 ± 7% before vs. +12 ± 10% during sepsis, $p = 0.08$, **Figure 7A**). PAF-mediated depolarization was significantly diminished during sepsis (+17.1 ± 5.6 mV before vs. +2.6 ± 2.2 mV during sepsis, $p < 0.05$, **Figure 7B**). There was no difference between neutrophils before and during sepsis regarding the PAF-induced intracellular alkalization (**Figure 7C**).

DISCUSSION

PAF-induced Depolarization, Alkalization, and Cellular Swelling Under Physiological Conditions

The inflammatory mediator PAF induced a rapid sequence of cellular reactions in neutrophils in a concentration- and time-dependent manner as summarized in **Figure 8**. The initial depolarization within seconds can likely be explained by the activation of the NOX activity resulting in excessive electron extrusion (17). This is corroborated by increased ROS generation

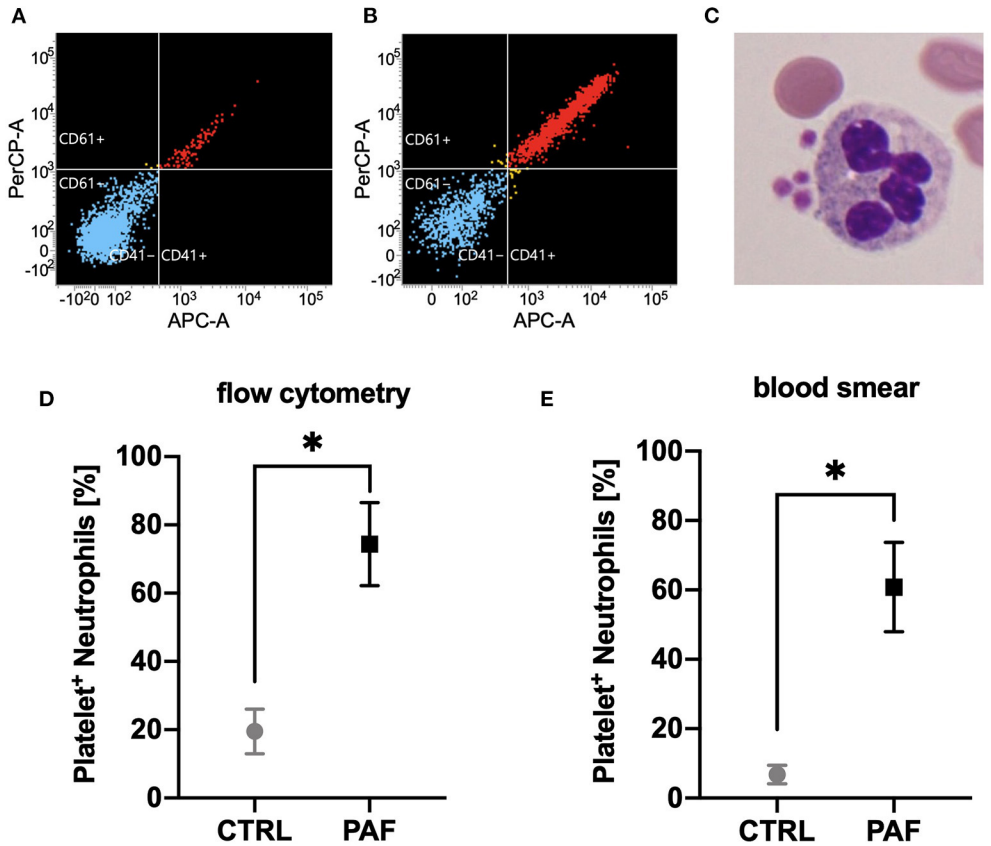

FIGURE 3 | PAF mediated the formation of platelet–neutrophil complexes (PNCs). **(A,B)** Flow cytometric measurements of PNCs using APC-labeled anti-CD41 and PerCP-labeled anti-CD61 antibodies. Shown is one representative donor for blood stimulated with PBS (CTRL, **A**) or PAF 1 μM **(B)**. Blue indicates CD41- and CD61-negative cells, yellow indicates either CD41- or CD61-positive neutrophils, red refers to neutrophils positive for CD41 and CD61. **(C)** Light microscopy of an exemplary PNC. **(D)** Quantification of PAF-induced (1 μM) PNC formation by flow cytometry ($n = 7$). **(E)** PAF mediated PNC formation as detected by blood smear and manual counting ($n = 6$). Data are mean ± SD. *$p < 0.05$, Wilcoxon matched-pairs signed rank test.

and the lack of cellular depolarization in patients with a NOX defect (46). Depolarization was followed by intracellular alkalization within minutes. The time course of the PAF-induced alkalization was in accordance with reports from bovine neutrophils (33). The change in pH_i elicited by PAF was less in the study by Hidalgo et al., however, this might result from the use of different dyes and/or species differences [(33) and the results presented in this work]. In this context, it is noteworthy that shifts in neutrophil pH_i are associated with other cellular functions, for example increasing chemotactic motility (21, 23, 47). Therefore, the impact of PAF-mediated transient alkalization requires further elucidation.

In parallel, neutrophils responded to PAF stimulation with an increase in cellular size as indicated by FSC-A. The rise in cell size was confirmed by analyzing the cell volume by applying the coulter counter principle, although with less pronounced changes. In this context, previous studies with C5a indicated that an increased FSC-A reflects a cellular elongation (14, 48) likely caused by actin polymerization (48). This possibly explains the differences between the PAF-induced changes in cell size reported by different methods. Overall, the PAF-mediated response was similar to that elicited by other chemoattractants, including the complement-derived anaphylatoxin C5a (14–16) and fMLF (18, 35, 46).

The cellular response of neutrophils induced by PAF was also investigated in the absence or presence of pharmacological inhibitors with a special interest in depolarization, intracellular pH, and swelling. In accordance with the results obtained on neutrophil stimulation with other chemokines (14, 15, 33), non-specific inhibition of sodium flux with amiloride and/or chloride flux with NPPB significantly reduced the intracellular alkalization and cellular swelling. Albeit amiloride also reduced depolarization, it should be noted that it also pre-depolarized unstimulated cells. Next, we investigated the role of NHE1 as an important representative ion transporter protein in stimulated granulocytes (15, 38, 49). The pharmacological NHE1 inhibitor BIX (38, 50) also inhibited intracellular alkalization and to a lesser extent, cellular swelling, but not early depolarization. This finding of the PAF-neutrophil interaction is in accordance with previous reports for fMLF and C5a (15, 23), as well as the involvement of NHE1 activity during cellular polarization and migration (49). Lastly,

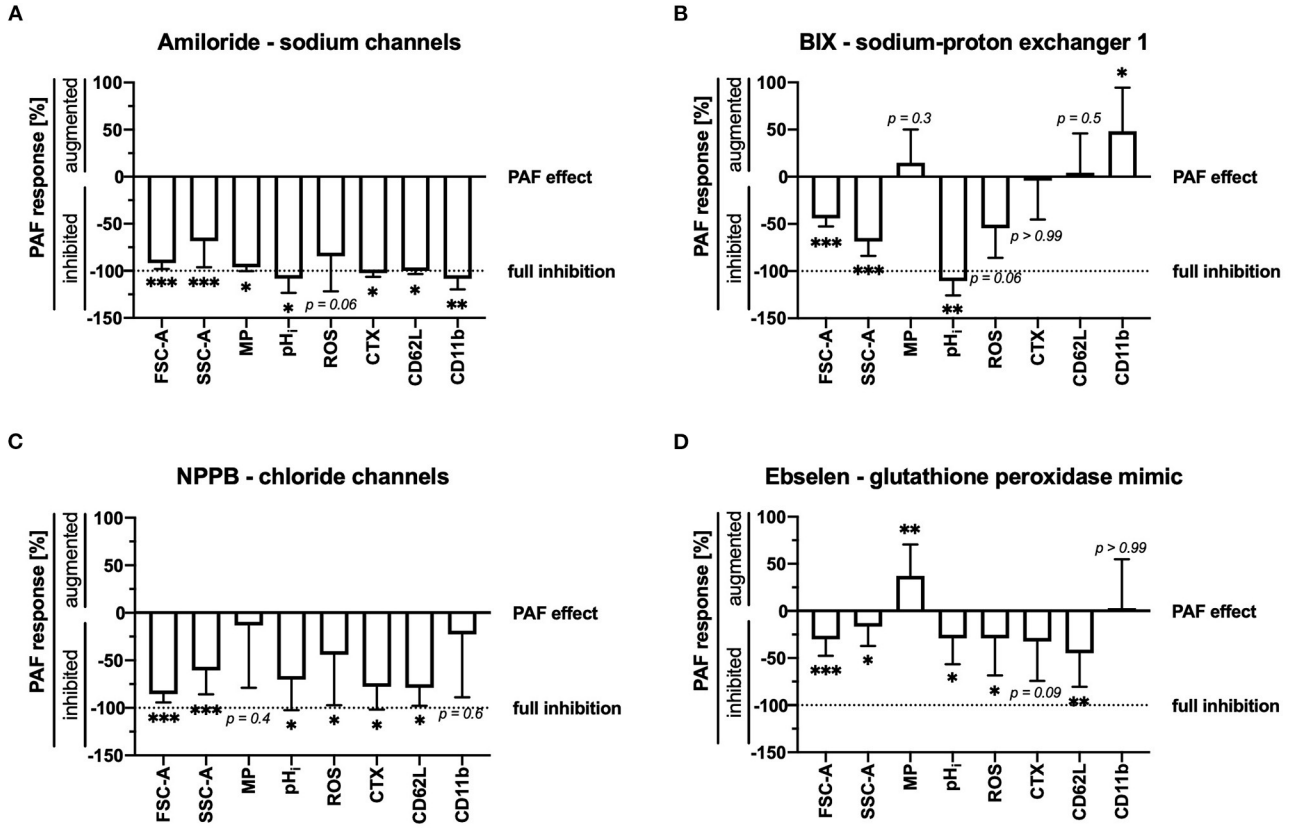

FIGURE 4 | (A) Amiloride (200 μM), **(B)** BIX (5 μM), **(C)** NPPB (100 μM), and **(D)** ebselen (10 nM) modulated the PAF-mediated response of neutrophils. While 0% indicates the regular response induced by 1 μM PAF, −100% indicates full inhibition of the PAF-mediated response = control level. For the calculation, see **Supplement 3**. Data are mean ± SD ($n = 5$–12). *$p < 0.05$, **$p < 0.01$, ***$p < 0.001$, Wilcoxon signed-rank test.

ebselen was used as an inhibitor of NOX2 and peroxide scavenger (40, 41, 51), which also dampened cellular swelling and alkalization but not depolarization. It is noteworthy, that exposure to either BIX or ebselen did not largely alter most cellular functions in unstimulated cells, and, therefore, might be potential targets for clinical evaluations regarding the modulation of the PAF-induced thromboinflammatory response of neutrophils.

In addition to inducing an (electro-)physiological response in neutrophils, PAF elicited chemotactic activity, CD11b upregulation and CD62L downregulation, and PNC formation which is in accordance with previous studies (24, 25, 27, 52). This "platelet satelitism" of neutrophils is also found in several pathologies, including sepsis, augmenting neutrophil activity, including extravasation, neutrophil extracellular trap formation, and bacterial killing (53–56). It is tempting to speculate that inhibition of PNC formation, possibly caused by PAF release during sepsis (57, 58), might be a suitable target to modulate the thromboinflammatory response. For example, the striking relevance of PNC formation has been demonstrated in a murine model of hydrochloric acid-induced acute lung injury, in which blocking PNC formation significantly ameliorated organ dysfunction (59).

PAF-induced (electro-)physiological Response in the Context of Severe Inflammation

During inflammation, neutrophils are required to migrate through various tissues and are exposed to varying levels of extracellular of extracellular proton concentrations. The pH of inflammatory body fluids, for example, abscesses, where neutrophils amass, is acidic (60–64). The experiment involving varying pH_e indicated that even under acidic pH_e, neutrophils remain able to respond with a relative intracellular alkalization and cellular swelling despite a shift in their pH_i in relationship to the pH_e. In addition, PAF-induced depolarization was increased in acidosis, potentially indicating elevated ROS generation, which has been demonstrated in a previous study (65).

Next, the effects of PAF on neutrophils were translationally investigated in two inflammatory environments. The previously described human whole blood model (36) of LPS-driven inflammation allows the investigation of blood physiology and immunity in an animal-free environment in accordance with the 3R principles (66). LPS exposure of whole blood altered the neutrophil phenotype as shown by CD11b and CD62L levels, confirming a sepsis-like phenotype that has been described in

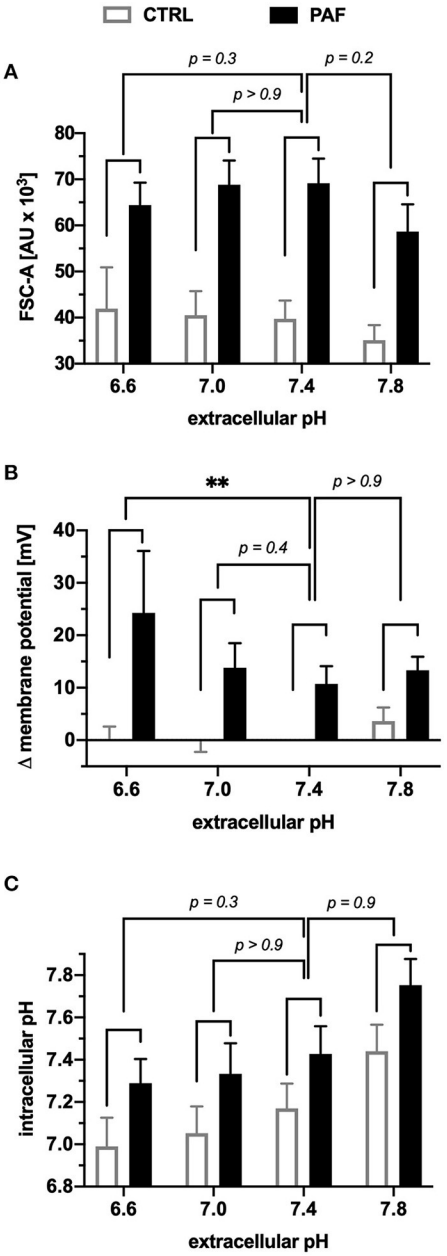

FIGURE 5 | Extracellular acidosis increased the PAF-mediated depolarization in human neutrophils *in vitro*. Neutrophils were incubated in buffers with different extracellular pH and subsequently stimulated by 1 μM PAF. **(A)** The increase in the FSC-A induced by PAF in comparison with unstimulated neutrophils in an acidotic or alkaline environment did not significantly alter the cellular response in comparison to an extracellular pH of 7.4. **(B)** Depolarization of the membrane potential upon PAF stimulation was enhanced in an acidic environment (0 mV = CTRL extracellular pH 7.4). **(C)** Intracellular pH of neutrophils stimulated with PAF (black) or PBS (CTRL, white). Data are mean ± SD ($n = 6$). $^{**}p < 0.01$, Kruskal Wallis and Dunn's *post-hoc* test comparing the PAF-induced response for each extracellular pH.

detail previously (67–71). LPS exposure did not alter the MP in comparison with unstimulated neutrophils and only augmented the PAF-induced response by a small amount. By contrast, a similar *in vitro* experiment comparing the depolarization of neutrophils with or without LPS exposure did report an increase in MP change, however, for fMLF (72). As observed in previous studies with neutrophils from septic humans and/or mice, exposure to LPS prompted an intracellular alkalization and swelling (14, 15, 73). This baseline drift in unstimulated cells was accompanied by a decrease in the PAF-induced response of granulocytes, possibly indicating ceiling effects. In general, the intracellular pH of neutrophils can rise beyond the LPS-induced shift in resting cells and/or the measurement method is capable of detecting larger shifts, arguing against a ceiling effect. Nevertheless, it is possible that neutrophils can only generate a certain alkaline shift, being limited by the pH_e that was not relevantly altered after LPS exposure in the whole blood model as reported earlier (36). LPS exposure in the whole blood model did not significantly change the sodium, potassium, or proton concentration, thus failing to explain the changes in alkalization or depolarization as reported previously (36).

Lastly, we analyzed the PAF-induced (electro-)physiological response in neutrophils before and during a well-characterized porcine model of polymicrobial sepsis (43–45). The clinical data confirmed a cardiocirculatory shock, indicating sepsis, also in corroboration with a significant hemoconcentration, suggesting a blood-organ barrier breakdown and subsequent hypovolemia. In the course of sepsis, the PAF-induced depolarization was significantly impaired, which confirmed findings in C5a-stimulated neutrophils after 3 h of porcine hemorrhagic shock (16). It is noteworthy, that there were no large shifts in extracellular ion concentrations and/or blood pH that could potentially explain this finding. Moreover, the PAF-mediated alkalization remained largely stable during sepsis, whereas cellular swelling was slightly increased. Also, the baseline of neutrophil pH_i and FSC-A did not shift (data not shown), which is in contrast to previous results in murine and/or human sepsis (14, 15, 73). These apparent differences in the findings within the two models might be explained by either species differences (human vs. pig), differences in the time points analyzed (1 h vs. 5.8 h ± 3.5), and/or regarding the pH_i with different fluorescent probes.

STRENGTHS AND LIMITATIONS

Changes in the MP and pH_i of neutrophils were measured by fluorescent dyes *in vitro* yielding indirect results. However, direct measurement of MP by conventional patch-clamp in neutrophils is technically challenging and potentially results in artificial activation of the cells as well as a rapid exchange of the intracellular ion concentration (74, 75). Additionally, the results reported in the present work, including C5a as a positive control, are in agreement with previous studies (14–16). Besides not altering the neutrophil intracellular homeostasis, flow cytometry allows a high throughput of analyzed cells in comparison to the patch-clamp technique when simultaneously analyzing MP, intracellular pH, and cellular size as indicated by FSC-A. However, patch-clamp allows a higher temporal

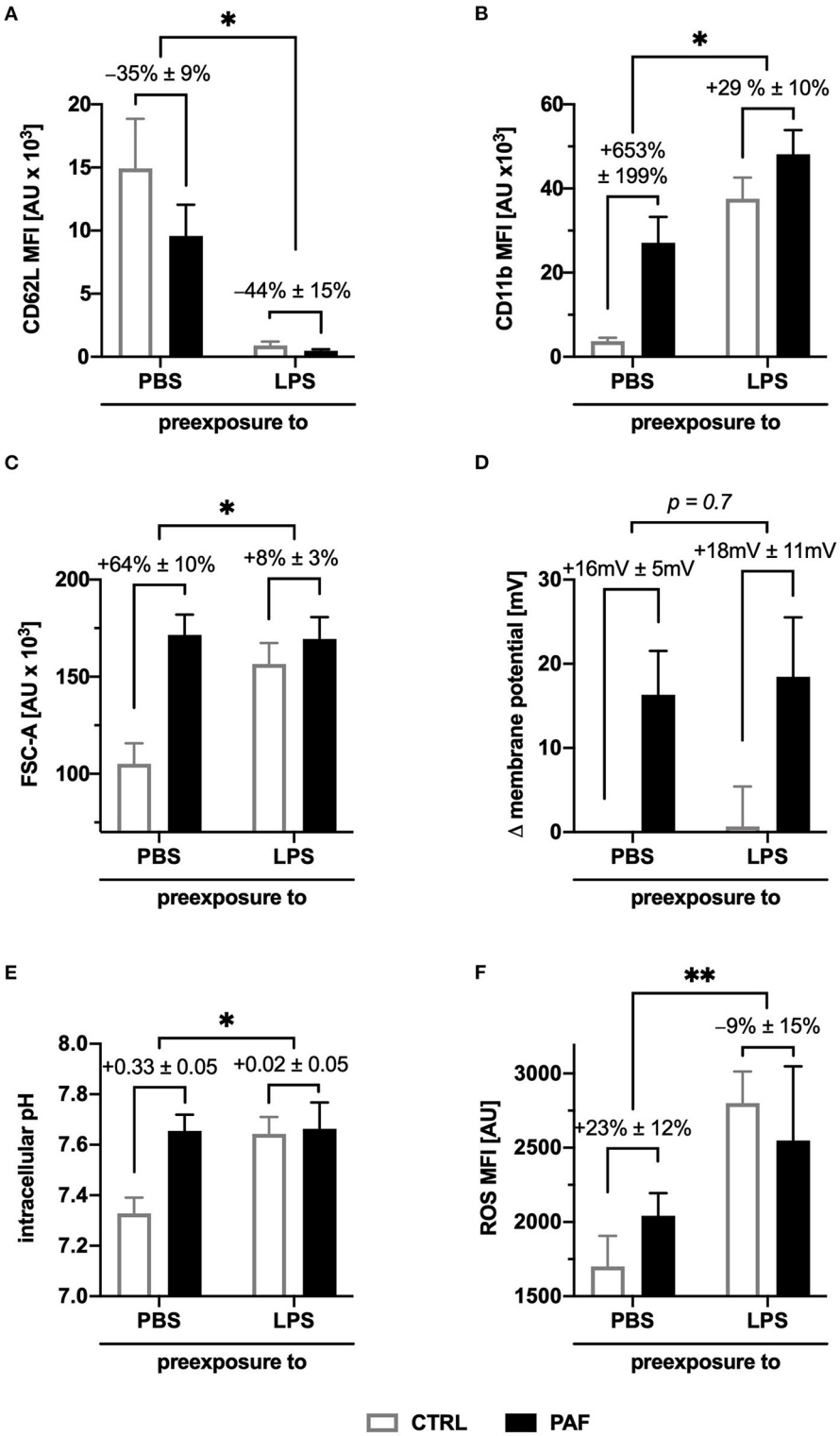

FIGURE 6 | LPS-driven inflammation altered the PAF-induced response pattern of human neutrophils in an *ex vivo* whole blood model. Blood was incubated for 1 h with or without 100 ng/ml LPS. Subsequently, blood **(A,B,F)** or isolated neutrophils **(C–E)** were stimulated with 1 μM PAF *in vitro*. **(A,B)** Surface expression of L-selectin (CD62L, **(A)**) and integrin alpha M (CD11b, **(B)**) on neutrophils. **(C)** Cellular size of neutrophils as indicated by the FSC-A. **(D)** PAF-induced depolarization after exposure to LPS. **(E)** Intracellular pH of neutrophils stimulated with or without PAF. **(F)** PAF-mediated ROS generation. Data are mean ± SD of the PAF-induced response ($n = 6$). *$p < 0.05$, **$p < 0.01$, Wilcoxon matched-pairs signed rank test comparing the response induced by PAF of neutrophils with (LPS) or without (PBS as CTRL) stimulation in the whole blood model. MFI, mean fluorescence intensity.

TABLE 1 | Clinical parameters of the animals before and during experimental polymicrobial sepsis.

Parameter	Unit	Before sepsis	During sepsis	*p*-value
Heart rate	per min	103 ± 19	170 ± 32	*
MAP	mmHg	104 ± 9	82 ± 9	*
Hb	g/dl	8.6 ± 0.6	14.5 ± 3.7	**
pH	$-\log(H^+)$	7.51 ± 0.04	7.48 ± 0.04	0.08
Lactate	mM	1.4 ± 0.5	1.8 ± 1.1	0.30
K^+	mM	3.0 ± 0.2	3.3 ± 0.2	*
Na^+	mM	143.7 ± 2.7	143.8 ± 2.6	>0.99
Ca^{2+}	mM	0.73 ± 0.06	0.69 ± 0.09	0.64
Time	h	–	5.8 ± 3.5	–

*MAP, mean arterial pressure; Hb, hemoglobin concentration; K^+, blood potassium concentration; Na^+, blood sodium concentration; Ca^{2+}, blood calcium concentration; Time, time from initiation to decrease in MAP indicating sepsis. Data are mean ± SD (n = 9). *p < 0.05, **p < 0.01 Wilcoxon matched-pairs signed rank test.*

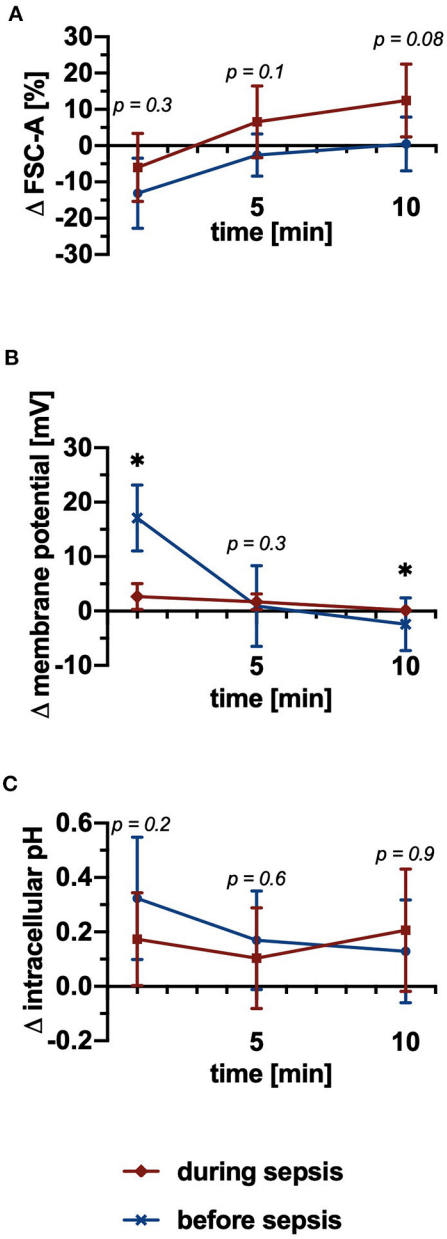

FIGURE 7 | PAF-mediated depolarization was significantly impaired and there was a trend for increased cellular swelling during experimental polymicrobial sepsis, whereas alkalization remained stable. **(A)** Changes of the FSC-A upon stimulation with 1 μM PAF vs. unstimulated cells before (blue) and during (red) sepsis ($n = 9$). **(B)** PAF-induced alteration in membrane potential ($n = 7$). **(C)** Alterations in intracellular pH of PAF-exposed neutrophils ($n = 9$). Data are mean ± SD. *$p < 0.05$, Wilcoxon matched-pairs signed rank test.

resolution in comparison to conventional flow cytometry. In the present work, we used continuous acquisition to partially compensate for the loss of temporal resolution. In addition, the current setup allowed the investigation of the PAF-induced cellular response in a physiologically environment at 37°C in the presence of HCO_3^-, the latter being involved in neutrophil ion channel activity (18, 76) and thereby should be included in measuring depolarization and intracellular alkalization. It is noteworthy that the HCO_3^- containing buffer became slightly alkalotic, thereby likely explaining the alkaline shift in unstimulated neutrophils during the measurement period.

Next, we established a clear concentration-response relationship of the cellular response to PAF. However, we mainly used a concentration of 1 μM PAF (approximately 500 ng/ml). This concentration is higher than found in blood of septic neonates (2.3 ng/ml) (57). Anyhow, one must consider that PAF acts *in vivo* largely as a paracrine signaling molecule and neutrophils encounter PAF via other cells in the immediate vicinity (77). Many other cell types, including platelets and endothelial cells, which are in close proximity to neutrophils (e.g., by forming PNCs), secrete PAF when stimulated, for example, with thrombin, to promote neutrophil adhesion and transmigration (1, 2, 52, 78). In accordance, a study by Mitchell et al. that investigated fluid shear stress on neutrophils and effects of PAF applied a concentration of 1 μM to simulate a concentration neutrophils experience when coming into contact with endothelium (79). Further studies need to develop improved methods to quantify PAF and measure exact PAF levels locally and systemically during sepsis.

Lastly, we transferred the findings generated *in vitro* to the *ex vivo* whole blood model and the porcine sepsis model, which have several advantages and limitations. The whole blood model allowed the investigation of the PAF-induced response with or without LPS-induced inflammation in human blood in a well-defined system (36). In addition, changes of the neutrophil response to PAF were confirmed in an experimental model of polymicrobial sepsis (43–45) with a clinically relevant pathophysiological reaction. Interestingly, the results of both models varied. This might arise because of several reasons: On the one hand, there might be notable interspecies differences. On the other hand, the assay itself differed between the two models regarding the pH_i, because porcine neutrophils had to be analyzed with a different dye. Furthermore, there are

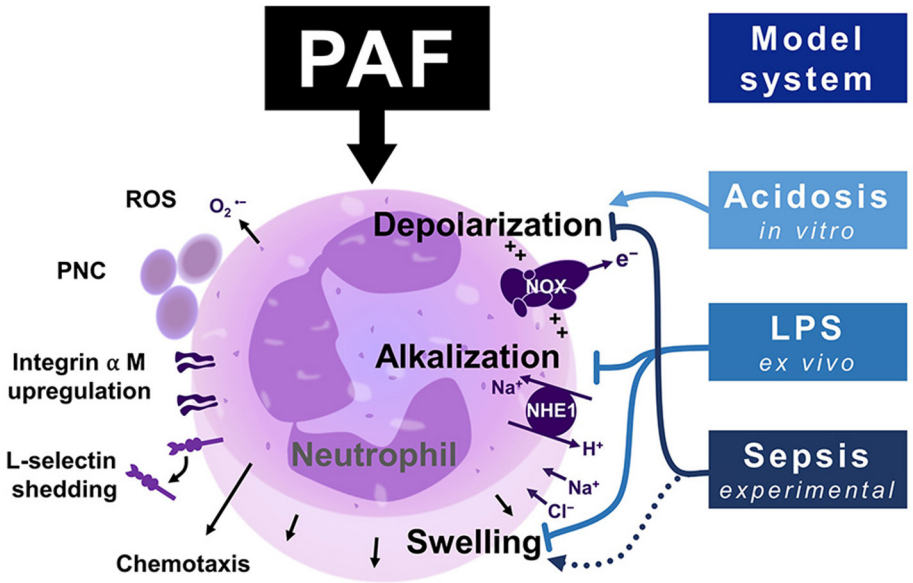

FIGURE 8 | Graphical summary of the neutrophil response upon exposure to platelet-activating factor (PAF), including depolarization, NHE1-dependent alkalization, and cellular swelling and functional thromboinflammatory activity. The (electro-)physiological response mediated by PAF is modulated in inflammatory environments. Endotoxemia increases intracellular pH and cell size of neutrophils while in parallel diminishing an additional change inducible by PAF. Depolarization is enhanced by extracellular acidosis, while being significantly disrupted during experimental sepsis. ROS, reactive oxygen species; PNC, platelet–neutrophil complex; NOX, NADPH oxidase; NHE1, sodium-proton exchanger 1.

different kinetics of the inflammatory response to consider: In the whole blood model of endotoxemia, there was an initial stimulation with LPS resulting in a rapid inflammatory response, while the addition of bacteria in the porcine model triggered a gradually increasing inflammation. In addition, the duration of the period analyzed and/or the inflammatory response elicited by LPS vs. fecal inoculation might explain the different results. In the whole blood model, it is difficult to analyze neutrophils in a long-term investigation, because glucose levels decline while in parallel lactate levels and acidosis increase, resulting in an unphysiological environment beyond 1 h. These issues were circumvented and thus indicated the application of the porcine sepsis model. Moreover, the lack of the presence of the interaction of neutrophils with other organs may play an important role. Another important aspect to consider regarding the porcine sepsis model is that neutrophils were isolated at the onset of sepsis as indicated by a drop of mean arterial blood pressure but prior to severe organ dysfunction. The rationale for this was to increase the sample size, since the current experiments were embedded in an interventional trial, that started after the beginning of sepsis (reduction of animal numbers). Also, the onset of sepsis marked the initiation of a resuscitation therapy, which may have further altered the response of neutrophils and likely ameliorated the degree of the inflammatory response such as lactate acidosis. Taken together, this allowed the investigation of neutrophil dysfunction as an early hallmark of the beginning of sepsis. Further research needs to explore these findings in a non-resuscitated model of sepsis and/or during a more pronounced inflammatory response including systemic acidosis, which may reveal further changes also in pH_i and FSC. Moreover, the findings need to be confirmed in patients with sepsis. Various causes of a potential neutrophil desensitization to stimulation with PAF during sepsis should be investigated, for example, a receptor downregulation of PAF, a previous stimulation by PAF *in vivo*, and/or a defect in PAF-signaling in sepsis. Notably, both models offer a distinct advantage investigating neutrophil pathophysiology during sepsis: Analyzing patients with sepsis does hardly allow firm assumptions regarding the onset of the infection, which was clearly defined in the model systems analyzed in this work.

CONCLUSION

Platelet-activating factor (PAF) is an important activator of neutrophils triggering depolarization, intracellular alkalization, and changes in cellular size. The PAF-induced response was demonstrated to be altered in an *ex vivo* model of endotoxemia and at the onset of porcine experimental sepsis, which might be an early hallmark of innate immune dysfunction during sepsis. Further studies are warranted to elucidate the association between the modulated (electro-)physiological response and cellular effector function. Additionally, translational efforts are needed to explore the therapeutic and diagnostic potential of these findings, for example, by measuring the neutrophil response at the patient's bedside and/or by targeting the involved ion channels, including NHE1, to reduce overwhelming PAF-induced neutrophil activation.

DATA AVAILABILITY STATEMENT

The original contributions presented in the study are included in the article/**Supplementary Material**, further inquiries can be directed to the corresponding author.

ETHICS STATEMENT

The studies involving human volunteers were reviewed and approved by the Local Independent Ethics Committee (number 459/18; 94/14) of the University of Ulm. The participants provided their written informed consent to participate in this study. The animal study was reviewed and approved by the Federal Authorities for Animal Research (#1362, Tuebingen, Germany) as well as the Animal Care Committee of the University of Ulm.

AUTHOR CONTRIBUTIONS

DM and MH-L: conceptualization and supervision. SH, SB, and DM: data curation and formal analysis. SH, SB, PR, AH, and DM: methodology. SH, AS, and DM: validation and visualization. SH and DM: writing—original draft. All authors contributed to the article and approved the submitted version.

FUNDING

The present work was funded by a research grant (Forum Gesundheitsstandort) of the Ministry of Science, Research and Art Baden Wuerttemberg to DACM and MHL, a start-up grant and a Gerok-Rotation (rotation as clinician scientist) to DACM by the Collaborative Research Center 1149 (project number 251293561), German Research Foundation, and a research grant (DFG Ra 396/12-1) to PR (project number 398113988), German Research Foundation. The funders had no role in the design of this study, data collection and interpretation, or decision to submit results.

ACKNOWLEDGMENTS

The authors are indebted to Ms. Carina Kleimaier for outstanding technical assistance.

SUPPLEMENTARY MATERIAL

The Supplementary Material for this article can be found online at: https://www.frontiersin.org/articles/10.3389/fimmu.2021.642867/full#supplementary-material

Supplement 1 | PAF-mediated changes in the response of neutrophils were concentration-dependent. Concentration-response curves were calculated for the following parameters after stimulation with PAF (1 nM−1 μM) at the time point of maximal stimulation as indicated: **(A)** FSC-A (10 min), **(B)** SSC-A (10 min), **(C)** membrane potential (1 min), **(D)** intracellular pH (5 min), **(E)** ROS generation (10 min), **(F)** formation of platelet–neutrophil complexes measured by flow cytometry (15 min), **(G)** L-selectin (CD62L) surface expression (15 min), and **(H)** integrin alpha M (CD11b) surface expression (15 min). Data are mean ± SD ($n = 5$–10).

Supplement 2 | Tabular overview of the relative PAF-induced effects on human neutrophils and gender analysis at the point of a (near-)maximal response during the first hour. FSC-A, forward scatter area; SSC-A, side scatter area; MP, membrane potential; pH_i, intracellular pH; ROS, generation of reactive oxygen species; CTX, chemotaxis; CD62L, L-selectin surface expression downregulation; CD11b, integrin alpha M surface expression upregulation. Data are mean ± standard deviation ($n = 5 - 10$). $^{*}p < 0.05$, $^{**}p < 0.01$, $^{***}p < 0.001$, for comparing PAF vs. CTRL: MP Wilcoxon signed-rank test, for all other parameters Wilcoxon matched-pairs signed rank test. For the comparison of neutrophils from male or female donors: Mann-Whitney test.

Supplement 3 | Modulation of neutrophil parameters by pharmacological inhibitors without further stimulation. The extent of these effects was compared to the response induced by 1 μM PAF. Control = 0%, PAF-mediated effect = 100%. Boxes outside the defined range were colored gray. For calculation see **Supplement 4**. FSC-A, forward scatter area; SSC-A, side scatter area; MP, membrane potential; pH_i, intracellular pH; ROS, generation of reactive oxygen species; CTX, chemotaxis; CD62L, L-selectin surface expression downregulation; CD11b, Integrin alpha M surface expression upregulation. Data are mean ($n = 5$–10).

Supplement 4 | Calculations for **(A)** Figure 4 and **(B)** the Heatmap in Supplement 3; F, mean fluorescence intensity.

REFERENCES

1. Lordan R, Tsoupras A, Zabetakis I, Demopoulos CA. Forty years since the structural elucidation of Platelet-Activating Factor (PAF): historical, current, and future research perspectives. *Molecules.* (2019) 24:4414. doi: 10.3390/molecules24234414
2. Gill P, Jindal NL, Jagdis A, Vadas P. Platelets in the immune response: revisiting platelet-activating factor in anaphylaxis. *J Allergy Clin Immunol.* (2015) 135:1424–32. doi: 10.1016/j.jaci.2015.04.019
3. Ramakrishnan AVKP, Varghese TP, Vanapalli S, Nair NK, Mingate MD. Platelet activating factor: a potential biomarker in acute coronary syndrome? *Cardiovasc Ther.* (2017) 35:64–70. doi: 10.1111/1755-5922.12233
4. Yost CC, Weyrich AS, Zimmerman GA. The platelet activating factor (PAF) signaling cascade in systemic inflammatory responses. *Biochimie.* (2010) 92:692–7. doi: 10.1016/j.biochi.2010.02.011
5. Singer M, Deutschman CS, Seymour CW, Shankar-Hari M, Annane D, Bauer M, et al. The Third International Consensus Definitions for Sepsis and Septic Shock (Sepsis-3). *JAMA.* (2016) 315:801–10. doi: 10.1001/jama.2016.0287
6. Huber-Lang M, Lambris JD, Ward PA. Innate immune responses to trauma. *Nat Immunol.* (2018) 19:327–41. doi: 10.1038/s41590-018-0064-8
7. Tang HM, Teshima DY, Lum BKB. Effects of the PAF antagonists bepafant and L-659, 989 in endotoxic and septic shock. *Drug Dev Res.* (1993) 29:216–21. doi: 10.1002/ddr.430290308
8. Schuster DP, Metzler M, Opal S, Lowry S, Balk R, Abraham E, et al. Recombinant platelet-activating factor acetylhydrolase to prevent acute respiratory distress syndrome and mortality in severe sepsis: phase IIb, multicenter, randomized, placebo-controlled, clinical trial. *Crit Care Med.* (2003) 31:1612–9. doi: 10.1097/01.CCM.0000063267.79824.DB
9. Poeze M, Froon AHM, Ramsay G, Buurman WA, Greve JWM. Decreased organ failure in patients with severe sirs and septic shock treated with the platelet-activating factor antagonist TCV-309: a prospective, multicenter, double-blind, randomized phase II trial. *Shock.* (2000) 14:421–8. doi: 10.1097/00024382-200014040-00001
10. Opal S, Laterre P-F, Abraham E, Francois B, Wittebole X, Lowry S, et al. Recombinant human platelet-activating factor acetylhydrolase for treatment of severe sepsis: results of a phase III, multicenter, randomized, double-blind, placebo-controlled, clinical trial. *Crit Care Med.* (2004) 32:332–41. doi: 10.1097/01.CCM.0000108867.87890.6D
11. Dhainaut JF, Tenaillon A, Hemmer M, Damas P, Le Tulzo Y, Radermacher P, et al. Confirmatory platelet-activating factor receptor antagonist trial

in patients with severe gram-negative bacterial sepsis: a phase III, randomized, double-blind, placebo-controlled, multicenter trial. BN 52021 Sepsis Investigator Group. *Crit Care Med.* (1998) 26:1963–71. doi: 10.1097/00003246-199812000-00021
12. Bosmann M, Ward PA. The inflammatory response in sepsis. *Trends Immunol.* (2013) 34:129–36. doi: 10.1016/j.it.2012.09.004
13. Shen X-F, Cao K, Jiang J-P, Guan W-X, Du J-F. Neutrophil dysregulation during sepsis: an overview and update. *J Cell Mol Med.* (2017) 21:1687–97. doi: 10.1111/jcmm.13112
14. Denk S, Taylor RP, Wiegner R, Cook EM, Lindorfer MA, Pfeiffer K, et al. Complement C5a-induced changes in neutrophil morphology during inflammation. *Scand J Immunol.* (2017) 86:143–55. doi: 10.1111/sji.12580
15. Denk S, Neher MD, Messerer DAC, Wiegner R, Nilsson B, Rittirsch D, et al. Complement C5a functions as a master switch for the pH balance in neutrophils exerting fundamental immunometabolic effects. *J Immunol.* (2017) 198:4846–54. doi: 10.4049/jimmunol.1700393
16. Messerer DAC, Denk S, Föhr KJ, Halbgebauer R, Braun CK, Hönes F, et al. Complement C5a alters the membrane potential of neutrophils during hemorrhagic shock. *Mediat Inflamm.* (2018) 2018:1–12. doi: 10.1155/2018/2052356
17. DeCoursey TE. The intimate and controversial relationship between voltage gated proton channels and the phagocyte NADPH oxidase. *Immunol Rev.* (2016) 273:194–218. doi: 10.1111/imr.12437
18. Giambelluca MS, Gende OA. Cl^-/HCO_3^- exchange activity in fMLP-stimulated human neutrophils. *Biochem Biophys Res Commun.* (2011) 409:567–71. doi: 10.1016/j.bbrc.2011.05.046
19. Coakley RJ, Taggart C, McElvaney NG, O'Neill SJ. Cytosolic pH and the inflammatory microenvironment modulate cell death in human neutrophils after phagocytosis. *Blood.* (2002) 100:3383–91. doi: 10.1182/blood.V100.9.3383
20. Grinstein S, Swallow CJ, Rotstein OD. Regulation of cytoplasmic pH in phagocytic cell function and dysfunction. *Clin Biochem.* (1991) 24:241–7. doi: 10.1016/0009-9120(91)80014-T
21. Simchowitz L, Cragoe EJ. Regulation of human neutrophil chemotaxis by intracellular pH. *J Biol Chem.* (1986) 261:6492–500.
22. Yuo A, Kitagawa S, Kasahara T, Matsushima K, Saito M, Takaku F. Stimulation and priming of human neutrophils by interleukin-8: cooperation with tumor necrosis factor and colony-stimulating factors. *Blood.* (1991) 78:2708–14.
23. Ritter M, Schratzberger P, Rossmann H, Wöll E, Seiler K, Seidler U, et al. Effect of inhibitors of Na^+/H^+-exchange and gastric H^+/K^+ ATPase on cell volume, intracellular pH and migration of human polymorphonuclear leucocytes. *Br J Pharmacol.* (1998) 124:627–38. doi: 10.1038/sj.bjp.0701864
24. Shaw JO, Pinckard RN, Ferrigni KS, McManus LM, Hanahan DJ. Activation of human neutrophils with 1-O-hexadecyl/octadecyl-2-acetyl-sn-glycerol-3-phosphorylcholine (platelet activating factor). *J Immunol.* (1981) 127:1250–5.
25. Zoratti EM, Sedgwick JB, Vrtis RR, Busse WW. The effect of platelet-activating factor on the generation of superoxide anion in human eosinophils and neutrophils. *J Allergy Clin Immunol.* (1991) 88:749–58. doi: 10.1016/0091-6749(91)90182-N
26. Follin P, Johansson A, Dahlgren C. Intracellular production of reactive oxygen species in human neutrophils following activation by the soluble stimuli FMLP, dioctanoylglycerol and ionomycin. *Cell Biochem Funct.* (1991) 9:29–37. doi: 10.1002/cbf.290090106
27. Berends C, Dijkhuizen B, de Monchy J, Dubois A, Gerritsen J, Kauffman H. Inhibition of PAF-induced expression of CD11b and shedding of L-selectin on human neutrophils and eosinophils by the type IV selective PDE inhibitor, rolipram. *Eur Respir J.* (1997) 10:1000.
28. Arnould T, Michiels C, Remacle J. Increased PMN adherence on endothelial cells after hypoxia: involvement of PAF, CD18/CD11b, and ICAM-1. *Amer J Physiol Cell Physiol.* (1993) 264:C1102–C1110. doi: 10.1152/ajpcell.1993.264.5.C1102
29. Condliffe AM, Chilvers ER, Haslett C, Dransfield I. Priming differentially regulates neutrophil adhesion molecule expression/function. *Immunology.* (1996) 89:105–11. doi: 10.1046/j.1365-2567.1996.d01-711.x
30. Brailoiu E, Barlow CL, Ramirez SH, Abood ME, Brailoiu GC. Effects of platelet-activating factor on brain microvascular endothelial cells. *Neuroscience.* (2018) 377:105–13. doi: 10.1016/j.neuroscience.2018.02.039
31. Wang G-D, Wang X-Y, Hu H-Z, Fang X-C, Liu S, Gao N, et al. Platelet-activating factor in the enteric nervous system of the guinea pig small intestine. *Am J Physiol Gastrointest Liver Physiol.* (2006) 291:G928–37. doi: 10.1152/ajpgi.00153.2006
32. Lerner R, Lindström P, Palmblad J. Platelet activating factor and leukotriene B4 induce hyperpolarization of human endothelial cells but depolarization of neutrophils. *Biochem Biophys Res Commun.* (1988) 153:805–10. doi: 10.1016/s0006-291x(88)81167-7
33. Hidalgo MA, Ojeda F, Eyre P, LaBranche TP, Smith C, Hancke JL, et al. Platelet-activating factor increases $pH_{(i)}$ in bovine neutrophils through the PI3K–ERK1/2 pathway. *Br J Pharmacol.* (2004) 141:311–21. doi: 10.1038/sj.bjp.0705590
34. Larrazabal CS, Carretta MD, Hidalgo MA, Burgos RA. Amiloride interferes with platelet-activating factor-induced respiratory burst and MMP-9 release in bovine neutrophils independent of Na^+/H^+ exchanger 1. *Vet Immunol Immunopathol.* (2017) 191:68–73. doi: 10.1016/j.vetimm.2017.08.007
35. Hidalgo MA, Carretta MD, Teuber SE, Zárate C, Cárcamo L, Concha II, et al. fMLP-induced IL-8 release is dependent on NADPH oxidase in human neutrophils. *J Immunol Res.* (2015) 2015:1–14. doi: 10.1155/2015/120348
36. Messerer DAC, Vidoni L, Erber M, Stratmann AEP, Bauer JM, Braun CK, et al. Animal-free human whole blood sepsis model to study changes in innate immunity. *Front Immunol.* (2020) 11:571992. doi: 10.3389/fimmu.2020.571992
37. Elbim C, Lizard G. Flow cytometric investigation of neutrophil oxidative burst and apoptosis in physiological and pathological situations. *Cytometry.* (2009) 75:475–81. doi: 10.1002/cyto.a.20726
38. Huber JD, Bentzien J, Boyer SJ, Burke J, De Lombaert S, Eickmeier C, et al. Identification of a potent sodium hydrogen exchanger isoform 1 (NHE1) inhibitor with a suitable profile for chronic dosing and demonstrated cardioprotective effects in a preclinical model of myocardial infarction in the rat. *J Med Chem.* (2012) 55:7114–40. doi: 10.1021/jm300601d
39. Dreinhöfer J, Gögelein H, Greger R. Blocking kinetics of Cl^- channels in colonic carcinoma cells (HT29) as revealed by 5-nitro-2-(3-phenylpropylamino)benzoic acid (NPPB). *Biochim. Biophys. Acta Biomembr.* (1988) 946:135–42. doi: 10.1016/0005-2736(88)90466-X
40. Masumoto H, Kissner R, Koppenol WH, Sies H. Kinetic study of the reaction of ebselen with peroxynitrite. *FEBS Lett.* (1996) 398:179–82. doi: 10.1016/s0014-5793(96)01237-9
41. Smith SME, Min J, Ganesh T, Diebold B, Kawahara T, Zhu Y, et al. Ebselen and congeners inhibit NADPH oxidase 2-dependent superoxide generation by interrupting the binding of regulatory subunits. *Chem Biol.* (2012) 19:752–63. doi: 10.1016/j.chembiol.2012.04.015
42. Mauler M, Seyfert J, Haenel D, Seeba H, Günther J, Stallmann D, et al. Platelet-neutrophil complex formation–a detailed *in vitro* analysis of murine and human blood samples. *J Leuk Biol.* (2015) 99:781–9. doi: 10.1189/jlb.3TA0315-082R
43. Hauser B, Barth E, Bassi G, Simon F, Gröger M, Oter S, et al. Hemodynamic, metabolic, and organ function effects of pure oxygen ventilation during established fecal peritonitis-induced septic shock. *Crit Care Med.* (2009) 37:2465–9. doi: 10.1097/CCM.0b013e3181aee8ad
44. Nussbaum BL, Stenzel T, Merz T, Scheuerle A, McCook O, Wachter U, et al. Hyperoxia or therapeutic hypothermia during resuscitation from non-lethal hemorrhagic shock in swine. *Shock.* (2017) 48:564–70. doi: 10.1097/SHK.0000000000000884
45. Nußbaum BL, Vogt J, Wachter U, McCook O, Wepler M, Matallo J, et al. Metabolic, cardiac, and renal effects of the slow hydrogen sulfide-releasing molecule GYY4137 during resuscitated septic shock in swine with pre-existing coronary artery disease. *Shock.* (2017) 48:175–84. doi: 10.1097/SHK.0000000000000834
46. Geiszt M, Kapus A, Németh K, Farkas L, Ligeti E. Regulation of capacitative Ca^{2+} influx in human neutrophil granulocytes: alterations in chronic granulomatous disease. *J Biol Chem.* (1997) 272:26471–8. doi: 10.1074/jbc.272.42.26471
47. Hayashi H, Aharonovitz O, Alexander RT, Touret N, Furuya W, Orlowski J, et al. Na^+/H^+ exchange and pH regulation in the control of neutrophil chemokinesis and chemotaxis. *Am J Physiol Cell Physiol.* (2008) 294:C526–34. doi: 10.1152/ajpcell.00219.2007

48. Lepidi H, Zaffran Y, Ansaldi JL, Mege JL, Capo C. Morphological polarization of human polymorphonuclear leucocytes in response to three different chemoattractants: an effector response independent of calcium rise and tyrosine kinases. *J Cell Sci.* (1995) 108 (Pt 4):1771–8.
49. Denker SP, Barber DL. Cell migration requires both ion translocation and cytoskeletal anchoring by the Na-H exchanger NHE1. *J Cell Biol.* (2002) 159:1087–96. doi: 10.1083/jcb.200208050
50. Kilić A, Huang CX, Rajapurohitam V, Madwed JB, Karmazyn M. Early and transient sodium-hydrogen exchanger isoform 1 inhibition attenuates subsequent cardiac hypertrophy and heart failure following coronary artery ligation. *J Pharmacol Exp Ther.* (2014) 351:492–9. doi: 10.1124/jpet.114.217091
51. Bedard K, Krause K-H. The NOX family of ROS-generating NADPH oxidases: physiology and pathophysiology. *Physiol Rev.* (2007) 87:245–313. doi: 10.1152/physrev.00044.2005
52. Sanderson HM, Fox SC, Robbins RA, Losche W, Spangenberg P, Heptinstall S. Role of GPIIb-IIIa in platelet-monocyte and platelet-neutrophil conjugate formation in whole blood. *Platelets.* (1998) 9:245–50. doi: 10.1080/09537109876780
53. Bauer HM. *In-vitro* platelet–neutrophil adherence. *Am J Clin Pathol.* (1975) 63:824–7. doi: 10.1093/ajcp/63.6.824
54. Page C, Pitchford S. Neutrophil and platelet complexes and their relevance to neutrophil recruitment and activation. *Int Immunopharmacol.* (2013) 17:1176–84. doi: 10.1016/j.intimp.2013.06.004
55. Zarbock A, Polanowska-Grabowska RK, Ley K. Platelet-neutrophil-interactions: linking hemostasis and inflammation. *Blood Rev.* (2007) 21:99–111. doi: 10.1016/j.blre.2006.06.001
56. Zucoloto AZ, Jenne CN. Platelet-neutrophil interplay: insights into Neutrophil Extracellular Trap (NET)-driven coagulation in infection. *Front Cardiovasc Med.* (2019) 6:85. doi: 10.3389/fcvm.2019.00085
57. Kültürsay N, Kantar M, Akisü M, Hüseyinov A, Coker I. Platelet-activating factor concentrations in healthy and septic neonates. *Eur J Pediatr.* (1999) 158:740–1. doi: 10.1007/s004310051191
58. Mariano F. Production of platelet-activating factor in patients with sepsis-associated acute renal failure. *Nephrol Dial Transplant.* (1999) 14:1150–7. doi: 10.1093/ndt/14.5.1150
59. Zarbock A, Singbartl K, Ley K. Complete reversal of acid-induced acute lung injury by blocking of platelet-neutrophil aggregation. *J Clin Invest.* (2006) 116:3211–9. doi: 10.1172/JCI29499
60. Hays RC, Mandell GL. pO_2, pH, and redox potential of experimental abscesses. *Exp Biol Med.* (1974) 147:29–30. doi: 10.3181/00379727-147-38275
61. Bryant RE, Rashad AL, Mazza JA, Hammond D. β-Lactamase activity in human pus. *J Infect Dis.* (1980) 142:594–601. doi: 10.1093/infdis/142.4.594
62. Simmen HP, Blaser J. Analysis of pH and pO_2 in abscesses, peritoneal fluid, and drainage fluid in the presence or absence of bacterial infection during and after abdominal surgery. *Am J Surg.* (1993) 166:24–7. doi: 10.1016/s0002-9610(05)80576-8
63. Simmen H-P, Battaglia H, Giovanoli P, Blaser J. Analysis of pH, pO_2 and pCO_2 in drainage fluid allows for rapid detection of infectious complications during the follow-up period after abdominal surgery. *Infection.* (1994) 22:386–9. doi: 10.1007/BF01715494
64. Wagner C, Sauermann R, Joukhadar C. Principles of antibiotic penetration into abscess fluid. *Pharmacology.* (2006) 78:1–10. doi: 10.1159/000094668
65. Riemann A, Schneider B, Ihling A, Nowak M, Sauvant C, Thews O, et al. Acidic environment leads to ROS-induced MAPK signaling in cancer cells. *PLoS ONE.* (2011) 6:e22445. doi: 10.1371/journal.pone.0022445
66. Russell WMS, Burch RL. *The Principles of Humane Experimental Technique*. Wheathampstead: Universities Federation for Animal Welfare (1992).
67. Pillay J, Kamp VM, van Hoffen E, Visser T, Tak T, Lammers J-W, et al. A subset of neutrophils in human systemic inflammation inhibits T cell responses through Mac-1. *J Clin Invest.* (2012) 122:327–36. doi: 10.1172/JCI57990
68. van Wessem KJP, Heeres M, Leliefeld PHC, Koenderman L, Leenen LPH. Lipopolysaccharide and hemorrhagic shock cause systemic inflammation by different mechanisms. *J Trauma Acute Care Surg.* (2013) 74:37–44. doi: 10.1097/TA.0b013e3182789489
69. Demaret J, Venet F, Friggeri A, Cazalis M-A, Plassais J, Jallades L, et al. Marked alterations of neutrophil functions during sepsis-induced immunosuppression. *J Leukoc Biol.* (2015) 98:1081–90. doi: 10.1189/jlb.4A0415-168RR
70. Groeneveld KM, Koenderman L, Warren BL, Jol S, Leenen LPH, Hietbrink F. Early decreased neutrophil responsiveness is related to late onset sepsis in multitrauma patients: an international cohort study. *PLoS ONE.* (2017) 12:e0180145. doi: 10.1371/journal.pone.0180145
71. Maini AA, George MJ, Motwani MP, Day RM, Gilroy DW, O'Brien AJ. A comparison of human neutrophils acquired from four experimental models of inflammation. *PLoS ONE.* (2016) 11:e0165502. doi: 10.1371/journal.pone.0165502
72. Forehand JR, Pabst MJ, Phillips WA, Johnston RB. Lipopolysaccharide priming of human neutrophils for an enhanced respiratory burst. Role of intracellular free calcium. *J Clin Invest.* (1989) 83:74–83. doi: 10.1172/JCI113887
73. Nicholson GC, Tennant RC, Carpenter DC, Sarau HM, Kon OM, Barnes PJ, et al. A novel flow cytometric assay of human whole blood neutrophil and monocyte CD11b levels: upregulation by chemokines is related to receptor expression, comparison with neutrophil shape change, and effects of a chemokine receptor (CXCR2) antagonist. *Pulmon Pharmacol Ther.* (2007) 20:52–9. doi: 10.1016/j.pupt.2005.11.009
74. Jankowski A, Grinstein S. A noninvasive fluorimetric procedure for measurement of membrane potential quantification of the NADPH oxidase-induced depolarization in activated neutrophils. *J Biol Chem.* (1999) 274:26098–104. doi: 10.1074/jbc.274.37.26098
75. DeCoursey TE, Cherny VV, Zhou W, Thomas LL. Simultaneous activation of NADPH oxidase-related proton and electron currents in human neutrophils. *Proc Natl Acad Sci USA.* (2000) 97:6885–9. doi: 10.1073/pnas.100047297
76. Simchowitz L. Chemotactic factor-induced activation of Na^+/H^+ exchange in human neutrophils. II. Intracellular pH changes. *J Biol Chem.* (1985) 260:13248–55.
77. Bussolino F, Camussi G. Platelet-activating factor produced by endothelial cells. *Eur J Biochem.* (1995) 229:327–37. doi: 10.1111/j.1432-1033.1995.0327k.x
78. Prescott SM, Zimmerman GA, McIntyre TM. Human endothelial cells in culture produce platelet-activating factor (1-alkyl-2-acetyl-sn-glycero-3-phosphocholine) when stimulated with thrombin. *Proc Natl Acad Sci USA.* (1984) 81:3534–8. doi: 10.1073/pnas.81.11.3534
79. Mitchell MJ, Lin KS, King MR. Fluid shear stress increases neutrophil activation via platelet-activating factor. *Biophys J.* (2014) 106:2243–53. doi: 10.1016/j.bpj.2014.04.001

Conflict of Interest: The authors declare that the research was conducted in the absence of any commercial or financial relationships that could be construed as a potential conflict of interest.

frontiers in Immunology

ORIGINAL RESEARCH
published: 22 March 2021
doi: 10.3389/fimmu.2021.634127

Immunophenotyping of Peripheral Blood Mononuclear Cells in Septic Shock Patients With High-Dimensional Flow Cytometry Analysis Reveals Two Subgroups With Differential Responses to Immunostimulant Drugs

Ya Wang[1,2†], Brian Gloss[3†], Benjamin Tang[1,2], Suat Dervish[4], Brigitte Santner-Nanan[5], Christina Whitehead[1], Kristy Masters[1], Kristen Skarratt[6], Sally Teoh[1], Stephen Schibeci[2], Nicole Fewings[7], Chrystelle Brignone[8], Frederic Triebel[8], David Booth[2], Anthony McLean[1] and Marek Nalos[1,9]*

[1] Department of Intensive Care Medicine, Nepean Hospital, Penrith, NSW, Australia, [2] Centre for Immunology and Allergy Research, The Westmead Institute for Medical Research, Sydney, NSW, Australia, [3] Westmead Research Hub, Westmead Institute for Medical Research, Sydney, NSW, Australia, [4] Westmead Cytometry, The Westmead Institute for Medical Research, Sydney, NSW, Australia, [5] Charles Perkins Centre Nepean, Sydney Medical School Nepean, The University of Sydney, Kingswood, NSW, Australia, [6] Department of Medicine, Faculty of Medicine and Health, Nepean Clinical School, The University of Sydney, Kingswood, NSW, Australia, [7] Westmead Clinical School, University of Sydney, Sydney, NSW, Australia, [8] Immutep S.A.S., Parc Club Orsay, Orsay, France, [9] 1st Department of Medicine, Medical Faculty in Plzen, Charles University, Prague, Czechia

Sepsis is associated with a dysregulated inflammatory response to infection. Despite the activation of inflammation, an immune suppression is often observed, predisposing patients to secondary infections. Therapies directed at restoration of immunity may be considered but should be guided by the immune status of the patients. In this paper, we described the use of a high-dimensional flow cytometry (HDCyto) panel to assess the immunophenotype of patients with sepsis. We then isolated peripheral blood mononuclear cells (PBMCs) from patients with septic shock and mimicked a secondary infection by stimulating PBMCs for 4 h *in vitro* with lipopolysaccharide (LPS) with or without prior exposure to either IFN-γ, or LAG-3Ig. We evaluated the response by means of flow cytometry and high-resolution clustering cum differential analysis and compared the results to PBMCs from healthy donors. We observed a heterogeneous immune response in septic patients and identified two major subgroups: one characterized by hypo-responsiveness (Hypo) and another one by hyper-responsiveness (Hyper). Hypo and Hyper groups showed significant differences in the production of cytokines/chemokine and surface human leukocyte antigen-DR (HLA-DR) expression in response to LPS stimulation, which were observed across all cell types. When pre-treated with either interferon gamma (IFN-γ) or lymphocyte-activation gene 3 (LAG)-3 recombinant fusion protein (LAG-3Ig) prior to LPS stimulation, cells from the Hypo group were shown to be more responsive to both immunostimulants than cells

OPEN ACCESS

Edited by:
Zhixing Kevin Pan, University of Toledo Medical Center, United States

Reviewed by:
Marcelo De Carvalho Bittencourt, Université de Lorraine, France
Rui Li, University of Pennsylvania, United States

***Correspondence:**
Ya Wang
ya.wang@sydney.edu.au

† These authors share first authorship

Specialty section:
This article was submitted to Inflammation, a section of the journal Frontiers in Immunology

Received: *27 November 2020*
Accepted: *22 February 2021*
Published: *22 March 2021*

Citation:
Wang Y, Gloss B, Tang B, Dervish S, Santner-Nanan B, Whitehead C, Masters K, Skarratt K, Teoh S, Schibeci S, Fewings N, Brignone C, Triebel F, Booth D, McLean A and Nalos M (2021) Immunophenotyping of Peripheral Blood Mononuclear Cells in Septic Shock Patients With High-Dimensional Flow Cytometry Analysis Reveals Two Subgroups With Differential Responses to Immunostimulant Drugs. Front. Immunol. 12:634127. doi: 10.3389/fimmu.2021.634127

from the Hyper group. Our results demonstrate the importance of patient stratification based on their immune status prior to any immune therapies. Once sufficiently scaled, this approach may be useful for prescribing the right immune therapy for the right patient at the right time, the key to the success of any therapy.

Keywords: sepsis, high-dimensional flow cytometry, Lipopolysaccharides, interferon-γ, LAG-3Ig, immunophenotype

INTRODUCTION

Sepsis is a life-threatening condition caused by a dysregulated inflammatory response to infection, which leads to multiple organ dysfunction. Mortality rates of patients suffering severe sepsis are estimated at 26%, and those with septic shock at 40%, contributing to around 5 million deaths a year globally (1, 2). The immune response during sepsis has been described as a biphasic event with an initial cytokine-mediated hyper-inflammatory phase aimed to eradicate the invading pathogens, and a subsequent immunosuppressed phase, as a result of prolonged activation of anti-inflammatory responses counteracting the initial pro-inflammatory responses (3, 4) but there is no clear delineation between the opposing phases (5). Importantly, a majority of septic patients, surviving the hyper-inflammatory phase often die from secondary or opportunistic infections during the immunosuppressed phase (6, 7).

Immune suppression in sepsis is characterized by lymphocyte apoptosis, anergy, a relative increase in T regulatory cells and myeloid derived suppressor cells and deficiencies in MHC class II mediated antigen presentation (8–13). These factors contribute to impaired antigen recognition, reduced antimicrobial effector functions, and poor microbial killing. Immunotherapies aimed at boosting immune responses, by enhancing antigen presentation capacity and lymphocytic functions, have shown some promising results (14–17). Interferon gamma (IFN-γ) has been trialed in sepsis patients and its use was associated with restoration of immune functions with increased HLA-DR expression in monocytes, increased production of cytokines such as tumor necrosis factor alpha (TNF-α), interleukin-1β (IL-1β) and decreased production of interleukin-6 (IL-6) and interleukin-10 (IL-10) (18, 19). The MHC Class II agonist LAG-3Ig is a soluble LAG-3 protein that activates antigen presenting cell (APC) leading to $CD8^+$ T cell activation (20–22). Clinical effectiveness of LAG-3Ig (eftilagimod alpha) has been investigated in several Phase I and Phase II trials in cancer patients (23, 24), but not yet in patients with sepsis due to the presence of significant heterogeneity of patient's immune responses in sepsis and a lack of practical methods to reduce such heterogeneity (25).

In this study, we aimed to develop a method to reduce heterogeneity of patient immune phenotypes prior to the administration of immune therapy. To this end, we evaluated the immune status of patients with septic shock by assessing the proportions of major immune cell subset within PBMCs as well as their ability to produce cytokines/chemokine in response to LPS. Furthermore, we assessed the responses to immunomodulatory agents such as IFN-γ and LAG-3Ig. Our findings suggest immune heterogeneity in septic patients could be identified and quantified by using HDCyto and such quantification may assist subsequent administration of immune therapy.

MATERIALS AND METHODS

Reagents and Antibodies

Fluorochrome-conjugated antibodies (as listed in **Supplementary Table 1**), BD Cytofix/Cytoperm™ Fixation/Permeabilization Solution set, human BD Fc block™, BD GolgiPlug™ and BD Horizon Brilliant Stain Buffer Plus were purchased from BD Biosciences (San Jose, CA). UltraComp eBeads™ Compensation Beads were purchased from ThermoFisher Scientific (Waltham, MA). Recombinant human IFN-γ was purchased from PeproTech (Rocky Hill, NJ). LAG-3Ig was kindly provided by Immutep Pty Ltd. Bovine Serum Albumin solution (35% in D.PBS) and LPS were purchased from Sigma Aldrich (St. Louis, MO).

Study Population

Thirteen patients who were admitted to the intensive care unit (ICU) of the Nepean Hospital (Kingswood, NSW, Australia) between December 2017 and February 2019, were recruited to this study. The inclusion and exclusion criteria are as follows:

Inclusion criteria: (1) age ≥18 years old; (2) presence of shock, likely of infectious origin defined as day 1 Sequential Organ Failure Assessment (SOFA) score cardiovascular > 2; (3) presence of at least 2 organ dysfunctions as defined by aggregate day 1 or day 2 SOFA score >4; (4) no treatment limitations articulated prior to study enrolment.

Exclusion criteria: current or recent use of known immune suppression medication such as steroids (>5 mg prednisone or equivalent) methotrexate, mycophenolate or recent use of immune checkpoint inhibitors.

Ten age-matched healthy volunteers (age ≥18 years old) were also recruited as controls.

Sample Collection and Processing

Venous blood was collected into tubes containing EDTA. For patients with sepsis, blood was collected on days 1–3 post ICU admission. PBMCs were prepared from whole blood by density gradient centrifugation using Ficoll-Paque Plus (Biostrategy Pty Ltd) and cryopreserved. Briefly, whole blood was diluted with an equal volume of Dulbecco's Phosphate-Buffered Saline (D.PBS) (without Ca^{2+} and Mg^{2+}) and layered on top of an equal volume of Ficoll-Paque Plus in a 50 ml Falcon tube. This was followed by centrifugation using a swinging-bucket

rotor at 400× g for 30 min at room temperature (RT) with the brake off. After centrifugation, PBMCs at the interphase between Ficoll-Paque Plus and plasma, was transferred into a new 50 ml Falcon tube and washed twice with D.PBS. Each wash was followed by centrifugation at 300× g for 10 min. For cryopreservation, PBMC cell pellet after the final centrifugation was resuspended in fetal bovine serum (FBS) and then 20% Dimethyl Sulfoxide (DMSO) diluted in FBS was added dropwise to the cell suspension to make the final concentration of DMSO to 10%. One milliliter (ml) of cell suspension was transferred to 2 ml cryovial in a Corning® CoolCell™ Cell Freezing Container (Sigma-Aldrich), which was left at −80°C freezer overnight before transferring to liquid nitrogen for long-term storage. On the day of experiment, cryopreserved PBMCs were thawed and treated with DNase I to prevent cell clumping (26). Briefly, frozen PBMCs were thawed rapidly in a 37°C water bath, followed by washes first with RPMI1640 (Lonza) with 2% FBS and 10 mM HEPES, pH 7.0–7.6 and then with D.PBS. PBMCs were then treated with 100 units/ml DNase I in the presence of 5 mM $MgCl_2$ for 15 min at RT, during which cells were counted with the CytoFLEX Flow Cytometer (Beckman Coulter, Brea, CA). After DNase I treatment, cells were washed once with D.PBS and then resuspended in cell culture medium (RPMI1640 with 10% FBS, 2 mM L-Glutamine, 50 units/ml Penicillin/50 μg/ml Streptomycin at 1×10^6 cells/ml) for culturing in BD Falcon® 5 ml polypropylene round bottom tube (*in vitro* Technologies) at 37°C, 5% CO_2.

Ex vivo Stimulation for Cytokine Detections

PBMCs were cultured under three conditions (two aliquots per condition and up to 1×10^6 per aliquot): untreated, plus IFN-γ (100 ng/ml) (27) or plus LAG-3Ig (1 μg/ml) (22) for 2 h. BD GolgiPlug (1 μg/ml) for detection of intracellular cytokines was added to all the cultures which were then cultured with or without LPS (100 ng/ml) (27) for a further 4 h. Cells were harvested by pipetting at the end of stimulations and subjected to cell count using the CytoFLEX Flow Cytometer before proceeding with flow cytometry staining.

Flow Cytometry Staining

After 6 h of culture, $\sim 1 \times 10^6$ PBMCs were washed twice by resuspending cells in 4 ml D.PBS and centrifugation at 300× g, RT for 5 min. Washed cells were then transferred into a 96-well V-bottom plate for the following staining procedure. Cells were first stained with 100 μl of BD Horizon™ Fixable Viability Stain 440 UV diluted in D.PBS (1:1,000), for 10–15 min at RT in the dark as per manufacturer's instructions. Cells were washed twice with 250 μl of staining buffer (D.PBS with 0.5% Bovine Serum Albumin) with centrifugation as above before surface staining. For surface staining, cells were incubated with 2.5 μg of human Fc Block diluted in staining buffer for 10 min at RT. Fluorochrome-conjugated surface antibodies as listed in **Supplementary Table 1** (amount of antibody used for each test was pre-titrated) was then added along with BD Horizon™ Brilliant Stain Buffer Plus (10 μl per test) in a final staining volume to 100 μl. Samples were incubated for 30 min at 4°C in the dark, then were washed four times with 250 μl staining buffer with centrifugation as above. Washed cell pellets were fixed and permeabilized with 100 μl BD Cytofix/Cytoperm™ Fixation/Permeabilization Solution for 20 min at 4°C in the dark. Fixation/Permeabilizaiton buffer was removed by two washes with 250 μl of freshly prepared 1× BD Perm/Wash buffer. All centrifugation steps after permeabilization were performed at 500× g for 5 min at RT. The cell pellet was resuspended in 200 μl of staining buffer and stored overnight at 4°C in the dark. The following day, cells were pelleted by centrifugation (500× g, 5 min, RT) and fixed/permeabilized again as described above. For intracellular staining, cells were incubated with 100 μl of fluorochrome-conjugated antibody mixture as listed in **Supplementary Table 1** (amount of antibody used for each test was pre-titrated) diluted in 1× BD Perm/Wash buffer with BD Horizon™ Brilliant Stain Buffer Plus (10 μl per test) for 30 min at 4°C in the dark. Cells were then washed four times with 1× BD Perm/Wash buffer by centrifugation (500× g, 5 min, RT), resuspended in 200 μl of staining buffer to be analyzed on a BD FACSymphony™ A5.2 cell analyzer (BD Biosciences). Samples were stained and analyzed in five batches and application settings were applied for each acquisition to ensure consistency in the instrument performance.

Data Analysis Workflow

Flow data were analyzed using CATALYST (28), explored using tidyverse (29) and visualized using ggplot and pheatmap (30) in the R statistical environment (31).

Briefly, flow cytometry files (fcs files) were pre-processed [compensated, gated for single and viable cells and quality control checked using FlowAI (32)]. Data was then scaled and exported for analysis using R (v4.0). FlowSOM (33) is an algorithm for clustering cells with Self-Organizing Maps (SOMs), based on the behavior of chosen markers on all cells. We used FlowSOM to cluster cells (max $k = 50$, using 20×20 SOM grid) by surface markers including CD3, CD4, CD8, CD19, CD25, CD127, CD11c, CD14, CD16, CD56, HLA-DR, which were referred to as "type markers". The type markers are lineage markers that were used to define cell types within PBMCs. Clusters were then manually annotated based on dominant cell frequency. Besides the type markers, we chose eight markers, including IL-2, IL-6, IL-10, IFN-γ, TNF-α, IL-17A, CCL-4, and HLA-DR, to be the "state markers," because expression levels of these state markers give indications on the functional state of the cell. Uniform Manifold Approximation and Projections (UMAPs) were generated based on type or state marker expression, limited to 3,000 cells per sample. We also performed Differential State (DS) analysis using a modified version of diffcyt (34). For DS, cluster medians for state markers were extracted, background corrected (>0 in more than half the number of samples in the smallest group) and then compared using the limma eBayes test (35) with customized contrast matrices and multiple testing (corrected *p*-value cut-off of 0.05). Marker list overlaps were visualized using euler diagrams (36).

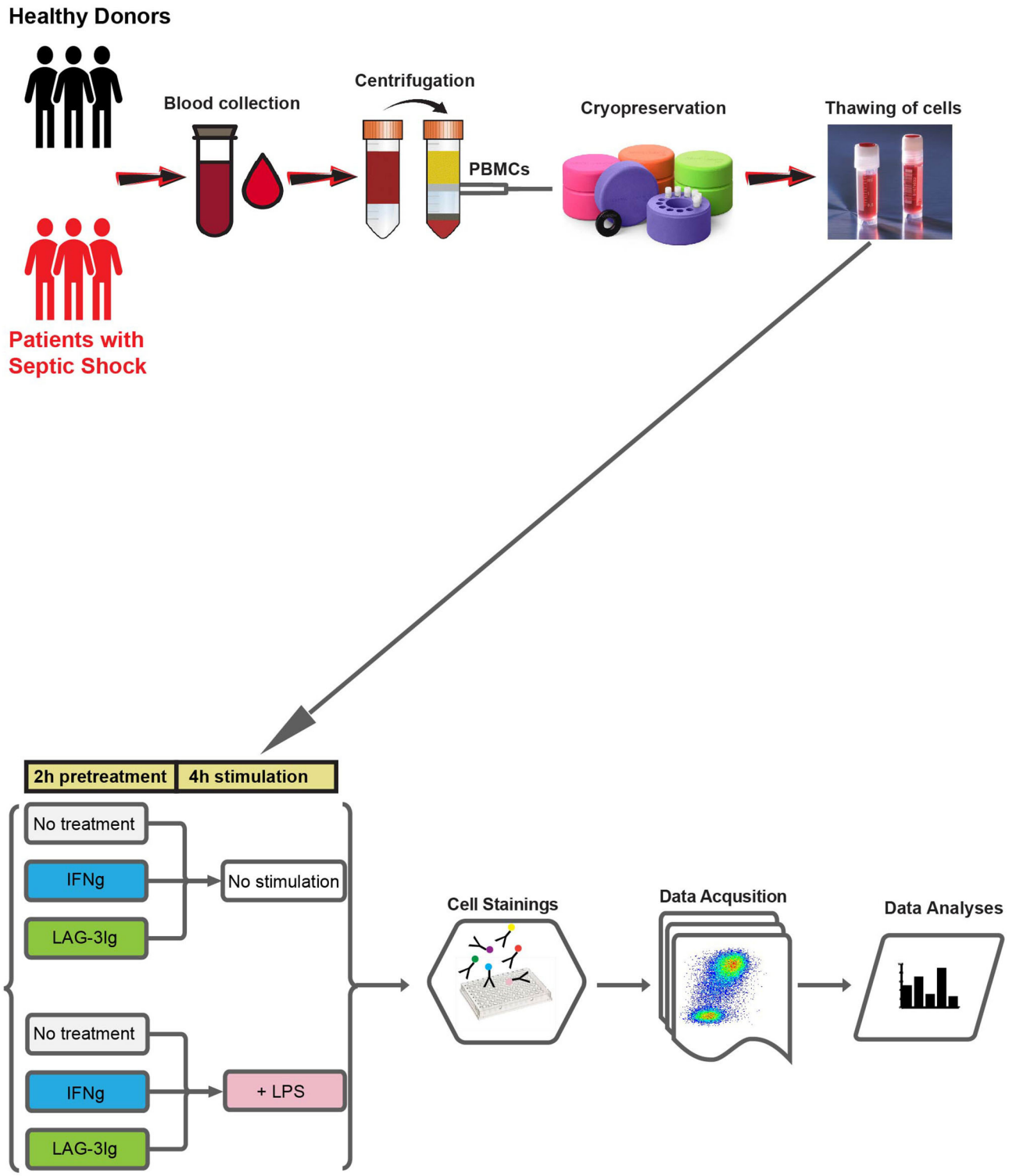

FIGURE 1 | Outline of experimental design and workflow. Whole blood samples are collected from either healthy donors or patients with septic shock. PBMCs are prepared from whole blood using Ficoll gradient centrifugation and cryopreserved. On the day of the experiment, PBMCs are thawed and subjected to six different culture conditions: (1) 2 hours (2 h) "No treatment" followed by 4 hours (4 h) "No stimulation" (No treatment + No stimulation); (2) IFN-γ + No stimulation; (3) LAG-3Ig + No stimulation; (4) LPS stimulation; (5) IFN-γ + LPS stimulation; (6) LAG-3Ig + LPS stimulation. After 6 h of culture, cells are stained with fluorochrome conjugated antibodies, followed by data acquisition using BD FACSymphony™ A5.2 cell analyzer (BD Biosciences). Finally, data is subjected to high-resolution clustering and empirical Bayes moderated tests adapted from transcriptomics.

RESULTS

Experimental Design and Workflow

Figure 1 outlines the experimental design and workflow. PBMCs isolated from the whole blood of either healthy donors or patients with septic shock, underwent six different pre-treatment and/or stimulation conditions before they were stained and subjected to flow cytometry analysis.

Immune Cell Composition Is Significantly Altered in Sepsis

In order to compare immune cell composition of PBMCs between healthy controls (HC, $n = 10$) and sepsis patients (sepsis, $n = 13$), flow cytometric data from untreated PBMCs (no treatment or LPS stimulation) from both HC and sepsis groups, were concatenated and FlowSOM was used to cluster cells by "type markers" as detailed in the materials and methods. Median expression levels of all the type markers in both HC and sepsis groups were shown on the UMAPs (**Figure 2A**). Based on dominant cell frequency, 50 meta-clusters were defined (**Figure 2B**). The meta-clusters were then merged into seven different immune cell subsets: $CD19^+$ B cells, $CD14^+$ monocytes, $CD3^+CD4^+$ T cells, $CD3^+CD8^+$ T cells, $CD11c^+$ mDCs, $CD3^-CD56^+$ NK cells, and lineage negative (lin_neg) cells, based on the presence or absence of specific type markers. Relative proportions of the seven immune cell subsets in PBMCs were compared between HC and sepsis (**Figure 2C**). Our results demonstrate the stark differences between the immune profile of HC and Sepsis subjects. There was a trend toward increased proportion of $CD14^+$ monocytes and decreased proportions of $CD4^+$, $CD8^+$ T cells, and NK cells in sepsis as compared to HC. Proportions of the seven immune cell subsets in individual sample were shown in **Figure 2D**. Heterogeneity within the sepsis patients was observed. Among the seven immune cell subsets investigated, proportions of $CD14^+$ monocytes, $CD4^+$ T cells, $CD8^+$ T cells, mDCs, and NKs were significantly altered in sepsis compared to HC (**Figure 2E**).

Subgroups in Sepsis: Hyper vs. Hypo

Median expression levels of all the "type" and "state markers" (as detailed in the materials and methods) on total PBMCs after 4 h of LPS stimulation without pretreatment with IFN-γ or LAG-3Ig, were compared across all the meta-clusters between HC and sepsis as displayed on UMAPs (**Figure 3A**). We observed an overall trend toward decreased HLA-DR expression on $CD14^+$ monocytes meta-clusters in sepsis as compared to HC, which is one of the hallmarks for sepsis. Median expression levels of all the markers in the seven immune cell subsets were compared between HC and sepsis (**Supplementary Figure 1**). To explore if there was any presence of subgroups in the heterogeneity observed in **Figure 2D**, we performed hierarchical clustering analysis, an algorithm used to group similar objects into clusters with each cluster distinct from each other. Median expression levels of all the type and state markers as in **Figure 3A**, were used for the hierarchical clustering analysis. Eight out of the 10 HC samples formed a tight cluster whereas sepsis samples were segregated into two subgroups which we named "Hyper" and "Hypo" subgroups (**Figure 3B**). The Hyper subgroup displayed an overall upregulation of surface markers CD25, CD11c, CD14, HLA-DR, and intracellular cytokines and chemokine as well as down regulated expression of CD3, CD8, CD127, and CD4 compared to HC. In the Hypo subgroup, expression of CD25, CD11c, CD14, HLA-DR, and intracellular cytokines and chemokines was intermediate between HC and the Hyper subgroup whereas expression of CD3, CD8, CD127, and CD4 was similar to that in the HC.

Commonality and Difference Between the "Hyper" and "Hypo" Subgroups

To further characterize the immune status of the two subgroups of sepsis, we performed differential state (DS) analysis by comparing Hyper and Hypo subgroups to HC in the expression levels of the state markers. Expressions of the state markers on 50 meta-clusters of PBMCs in response to LPS stimulation were analyzed. When compared to HC, both Hyper and Hypo subgroups were shown to have significant changes in the levels of the state markers across the 50 meta-clusters, 155 of which were shared between the two subgroups (**Figure 4A**). Significant differences between Hyper and Hypo subgroups were also observed. There were 59 unique immune alterations for the Hyper subgroup and 57 unique immune alterations for the Hypo subgroup. Differential expression of the state markers in Sepsis compared to HC were expressed as Log2 fold changes (LogFC). Representative meta-clusters from each immune cell subset, which had significant LogFC in either of the eight state markers, were shown in **Figure 4B** comparing the Hypo subgroup to HC (Hypo_vs._HC) and **Figure 4C** comparing the Hyper subgroup to HC (Hyper_vs._HC). An expanded version of **Figures 4B,C** can be found in **Supplementary Figures 2A,B**. Major differences between Hyper and Hypo subgroups were observed in IL-6, TNF-α, IL-17A, HLA-DR, and CCL-4 expression levels. IL-6 production in $CD8^+$ T cells was decreased in the Hyper but was increased in the Hypo subgroup. Monocyte expression of TNF-α production was upregulated in the Hyper but downregulated in the Hypo subgroup. IL-17A production was upregulated in $CD19^+$ B cells and $CD8^+$ T cells from the Hyper but not in the Hypo subgroup. We also observed a more than 2× fold increase in HLA-DR expression on NKs from the Hyper subgroup, which was absent in the Hypo subgroup. CCL-4 upregulation was observed across most of the immune cell subsets in Hyper subgroup. In the Hypo subgroup, however, CCL-4 expression was only increased slightly in $CD4^+$, $CD8^+$ T cells, and NKs. On the other hand, IL-10 and IFN-γ expression levels did not vary too much between these two subgroups. In light of the differences in the immune status between the Hyper and the Hypo subgroups, we sought to determine if the clinical characteristics of these two subgroups also differ. C-reactive protein (CRP), serum lactate, whole blood count (WBC), SOFA score, and Acute Physiology and Chronic Health Evaluation (APACHE) III score were compared between the Hyper and the Hypo subgroups (**Figure 4D**). We did not observe significant differences in these clinical characteristics between the two subgroups. Detailed information on the age and gender of

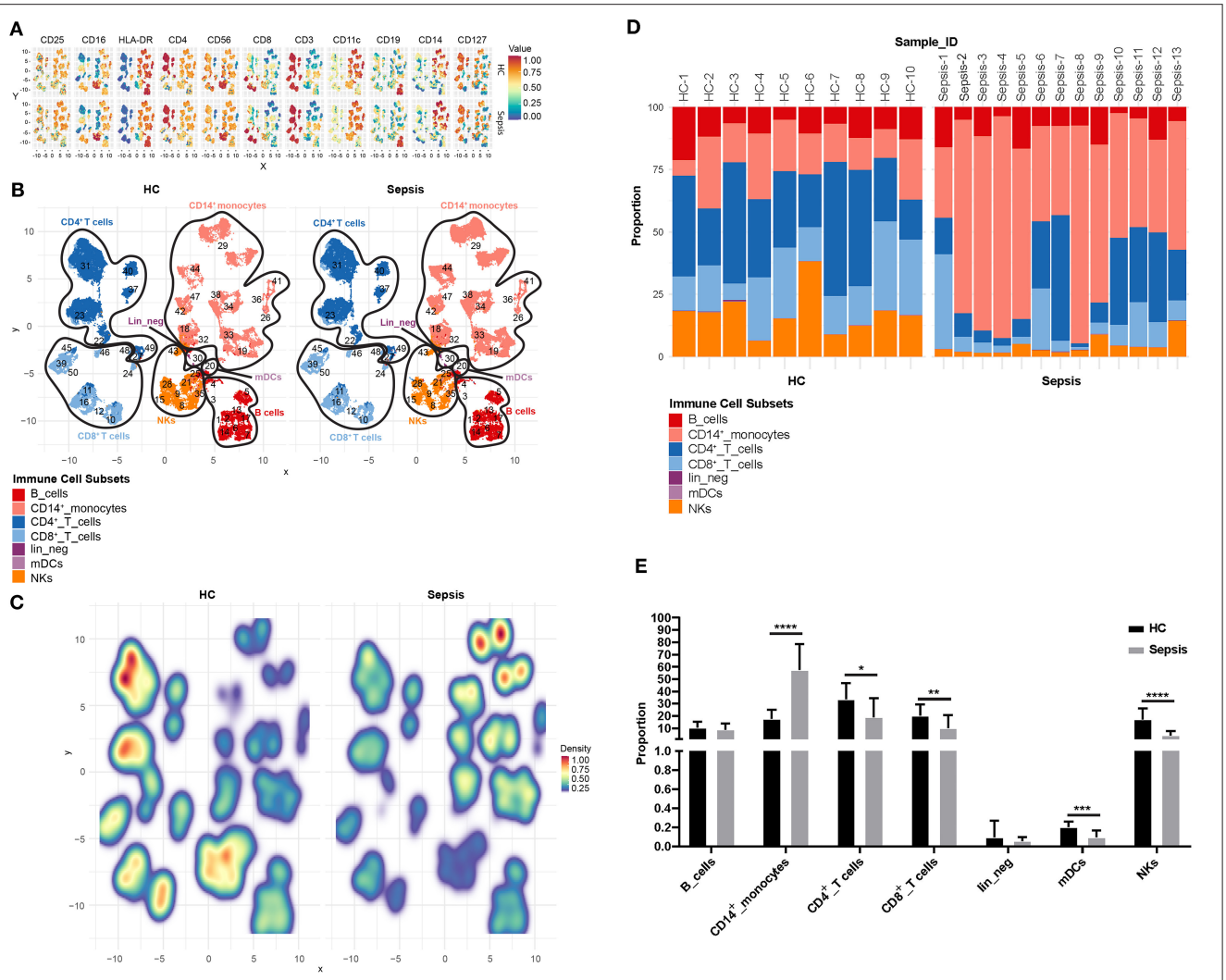

FIGURE 2 | Proportion of immune cell subsets in PBMCs. **(A)** Uniform Manifold Approximation and Projection (UMAP) displays the median expression levels of all the type markers on total untreated PBMCs (no treatment or LPS stimulation) in HC and sepsis. **(B)** 50 meta-clusters, as defined by dominant cell frequency, are shown on UMAP. Based on the presence or absence of specific type markers as shown in **(A)**, the 50 meta-clusters are annotated into seven immune cell subsets. **(C)** Relative proportions of the meta-clusters in PBMCs are compared between HC and sepsis. **(D)** Proportions of the seven immune cell subsets in PBMCs are shown in 10 HC (HC-1 to HC-10) and 13 Sepsis patients (Sepsis-1 to Sepsis-13). Values from each subject were plotted. **(E)** Bar diagram represents mean proportion of each immune cell subset as indicated on the X-axis in HC vs. sepsis. Data represents mean ± SD; $^{*}P < 0.05$, $^{**}P < 0.01$, $^{***}P < 0.001$, $^{****}P < 0.0001$, were determined by Mann-Whitney test.

these patients in addition to the above-mentioned clinical data can be found in **Supplementary Table 2**.

Differential Responses of Hypo and Hyper Subgroup of Sepsis to IFN-γ or LAG-3Ig

To determine if Hyper and Hypo subgroups would respond differently to IFN-γ or LAG-3Ig, we performed DS analysis within each subgroup by comparing median expression of the state markers under "No treatment + LPS" (LPS) to that under either "IFN-γ pretreatment + LPS" (IFN-γ) or "LAG-3Ig pretreatment + LPS" (LAG-3Ig) conditions. As shown in **Figures 5A,B**, immune cell subsets from the Hypo subgroup of sepsis showed significant responses to either IFN-γ or LAG-3Ig. Within each cell subset, the meta-clusters which demonstrated significant responses to either treatment were squared out in red. In response to IFN-γ + LPS, three meta-clusters (#29, 34, and 42) within $CD14^{+}$ monocytes from the Hypo subgroup had higher TNF-α expression and meta-cluster #34 also had higher IL-2 expression as compared to no treatment LPS group (**Figure 5A**). Two meta-clusters (#23 and 31) within $CD4^{+}$ T cells from the Hypo subgroup also responded to IFN-γ by producing more IL-10 as compared to no treatment LPS group. **Figure 5B** showed responses of the Hypo group to LAG-3Ig treatment as compared to no treatment LPS group. All four meta-clusters of $CD4^{+}$ T cells (#22, 23, 31, 37, and 40), two meta-clusters within $CD8^{+}$ T cells (#11 and 45) responded to LAG-3Ig by producing more IL-10.

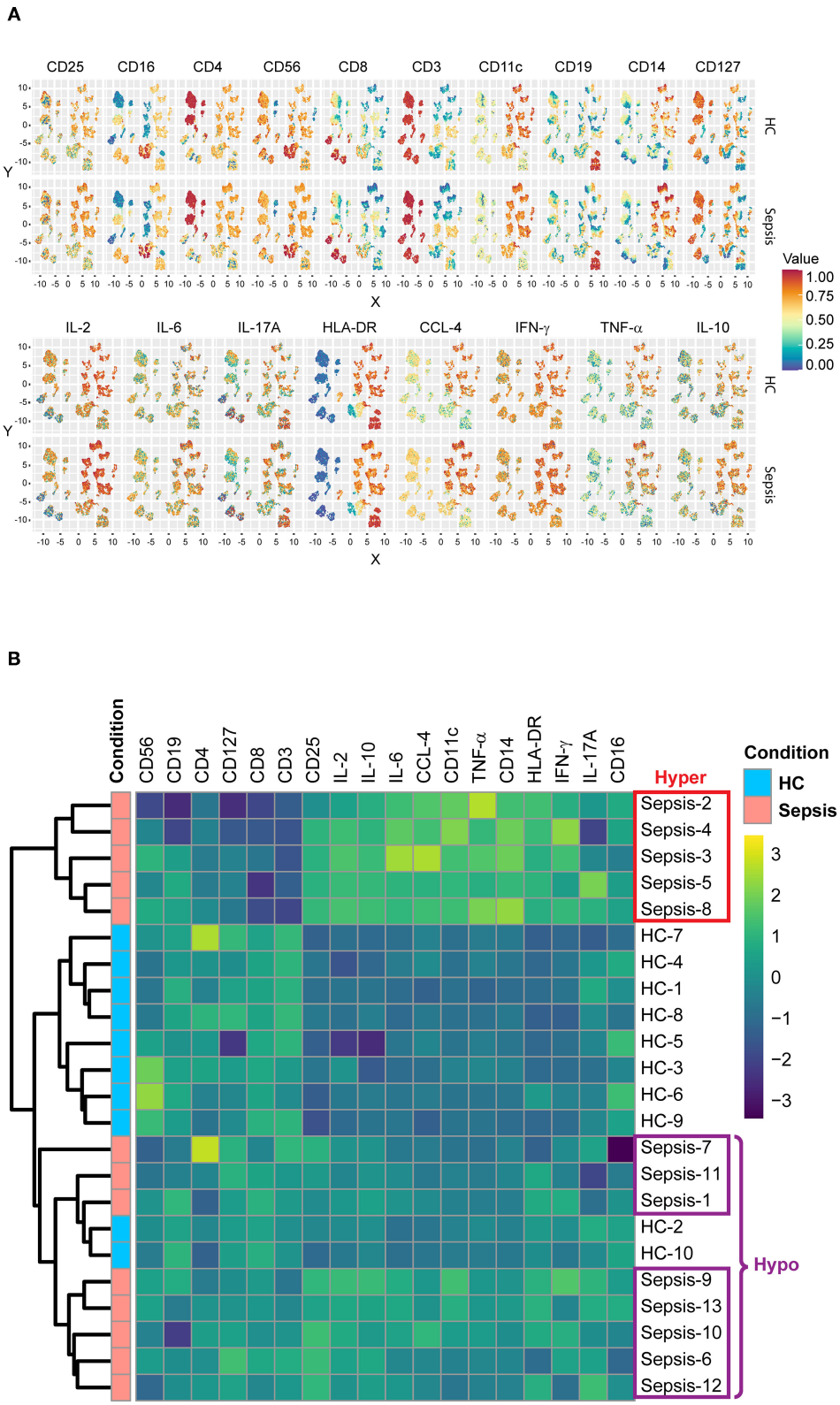

FIGURE 3 | Subgroups in sepsis. **(A)** UMAP displays the median expression levels of all the type and state markers on total PBMCs after 4 h of LPS stimulation without pretreatment in HC and sepsis. **(B)** Heatmap represents the hierarchical clusters based on the median expression levels of all the type and state markers as in **(A)**. Five samples from sepsis group (Sepsis-2, 3, 4, 5, and 8) formed a cluster named as "Hyper" subgroup and the other eight samples (Sepsis-1, 6, 7, 9, 10, 11, 12, and 13) formed a different cluster named as "Hypo" subgroup.

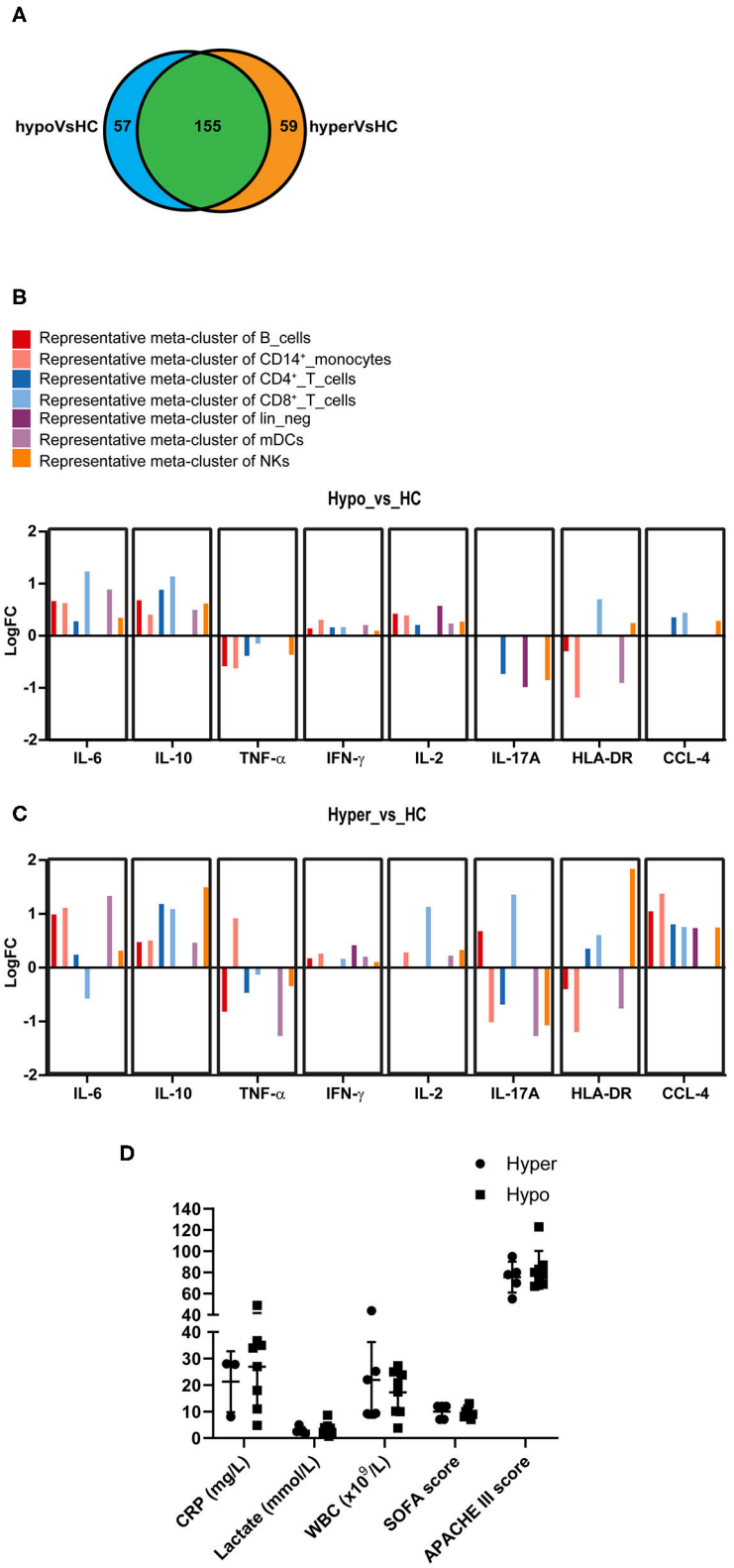

FIGURE 4 | Commonality and difference between the Hyper and the Hypo subgroups. **(A)** Venn diagram represents the number of state markers across 50 meta-clusters of PBMCs that are significantly different between Hyper and HC (in orange) or between Hypo and HC (in blue). The area highlighted in green represents changes that are found in both Hyper and Hypo subgroups compared to HC. **(B)** Bar diagram represents fold changes (logFC) at the expression levels of eight state

(Continued)

FIGURE 4 | markers that are significantly altered in Hypo subgroup compared to HC. A representative cluster is shown. **(C)** Bar diagram represents fold changes (logFC) at the expression levels of eight state markers that are significantly altered in Hyper subgroup compared to HC. A representative cluster is shown. **(D)** C-reactive protein (CRP), serum lactate level, whole blood count (WBC), Sequential Organ Failure Assessment (SOFA) score and Acute Physiology and Chronic Health Evaluation (APACHE) III score are compared between the Hyper and the Hypo subgroups. Data represents mean ± SD and $P < 0.05$ is considered significant as determined by Mann-Whitney test.

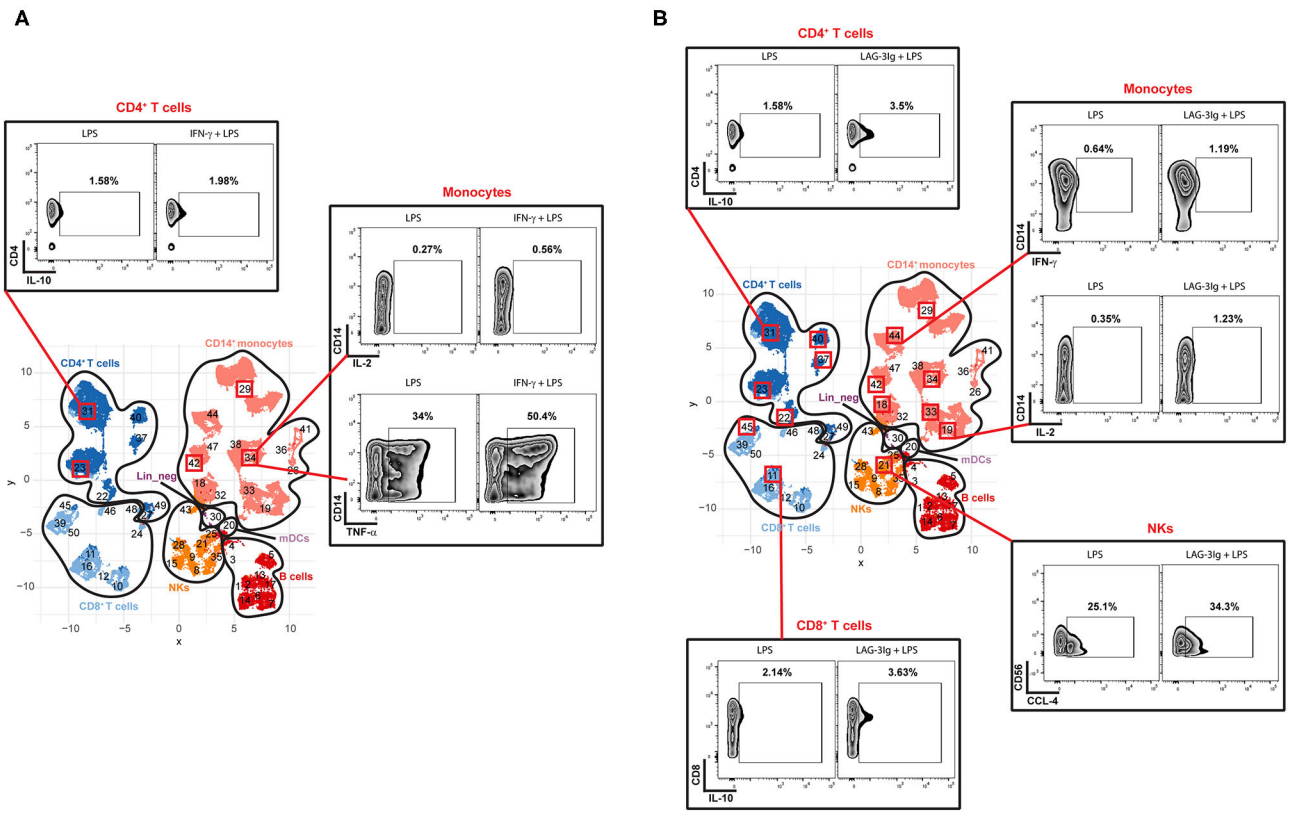

FIGURE 5 | Responses of the Hypo subgroup to IFN-γ or LAG-3Ig pretreatments. UMAP represents the 50 meta-clusters and their corresponding immune cell subsets in sepsis as shown in **Figure 2B**. Meta-clusters that are showing significant responses to either IFN-γ or LAG-3Ig are squared out in red. Representative flow plots of the representative meta-clusters demonstrate responses of the Hypo subgroup to IFN-γ pretreatment **(A)**, the Hypo subgroup to LAG-3Ig pretreatment **(B)**.

Seven meta-clusters within CD14+ monocytes (#18, 19, 29, 33, 34, 42, and 44) produced more IFN-γ and IL-2 in response to LAG-3Ig. An increased CCL-4 expression was observed in meta-cluster #21 within NK cells in response to LAG-3Ig. On the other hand, responses of the Hyper subgroup to either IFN-γ or LAG-3Ig were less prominent compared to the Hypo subgroup. The Hyper subgroup demonstrated no significant responses to IFN-γ treatment (data not shown) and minimal responses to LAG-3Ig as shown in **Supplementary Figure 3**.

DISCUSSION

The immune response during sepsis is variable and often changes as the disease progresses (4). Many factors determine the immune response such as the nature and virulence of the pathogens, site of infection, patient's genetics, physical condition and co-morbidities. It is therefore crucial to assess individual patient's immune status to personalize any immune-modulatory therapy. However, the complex nature of immune response during sepsis requires a comprehensive analysis to capture changes to the important immune cells and their functions, which may allow accurate identification of patients that would benefit from immune modulating treatment. Current markers of sepsis including WBC, CRP, procalcitonin (PCT) or HLA-DR are insufficient for this purpose. CRP and PCT both indicate the acute phase of inflammatory responses but are not helpful in detecting immunosuppression in septic patients (37–39). Decreased expression of HLA-DR on monocytes is so far the best biomarker for detecting immunosuppression in sepsis

(11, 40), but is limited to one cell type and does not provide information on the status of other immune cells. We have also shown in the current study that clinical characteristics such as WBC, CRP, serum lactate, SOFA and APACHE III score, monocytic HLA-DR expression and previous site of infections do not reveal the difference in patient's immune status as demonstrated between the Hyper and the Hypo subgroups (**Figure 4D**, **Supplementary Table 2**, **Supplementary Figure 4**).

In this study, we investigated the potential of HDCyto in revealing and assessing the heterogeneity of immune responses in patients with septic shock. The uniqueness of our HDCyto panel is the incorporation of markers for both enumeration of major immune cell subsets within PBMCs and assessment of functional status of the individual subset. This provided a broad-spectrum clarity on the overall immune status of PBMCs. Importantly, HDCyto analysis tools that were used in this study, including FlowSOM, diffcyt, and CATALYST analysis, provide the means to dissect heterogeneity, and hence identify changes that may be missed if analyzed using 2D approaches, due to the variations within each immune subset. Using this approach, we discovered that immune responses in PBMCs from septic shock patients were significantly altered compared to those from healthy controls, which were observed across all immune cell subsets analyzed. Furthermore, our results revealed, for the first time, two subgroups with distinct immune profiles were present within the sepsis group. The Hyper subgroup was found to have an overall higher production of all state markers in response to *in vitro* LPS stimulation, than the Hypo subgroup. In particular, we observed an increase of HLA-DR expression on NK cells in the Hyper subgroup as compared to the Hypo subgroup. HLA-DR$^+$ NK cells have been associated with a less mature phenotype with antigen-presentation ability (41, 42). This might explain the overall hyper-responsiveness as seen in the Hyper subgroup where NKs, in addition to professional antigen-presenting cells such as DCs, leads to further activation of T-cells. Another interesting finding about the Hyper subgroup is the increased IL-17A production by CD19$^+$ B cells and CD8$^+$ T cells when compared to the Hypo subgroup. Traditionally, IL-17A was thought to be produced mainly by activated Th-17 cells. However, production of IL-17A by other immune cell types such as CD8$^+$ T cells and CD19$^+$ B cells has been reported previously and has been associated with inflammatory disease (43, 44). IL-17A production by CD8$^+$ T cells has also been associated with persistent immune activation in patient with HIV (44). This again explains the hyper-responsiveness as seen in the Hyper subgroup.

We then proceed to assess whether the identification of these two subgroups could help predict responses to immune-modulatory therapy. We evaluated the *ex vivo* effects of immunostimulant agents IFN-γ and LAG-3Ig on PBMCs. Our results showed that the Hyper subgroup did not respond as much as the Hypo subgroup to either IFN-γ or LAG-3Ig in terms of changes in the expression of state markers on different immune cell subsets. Given that the Hyper subgroup already had an elevated basal level of all the state markers compared to the Hypo subgroup, this result is not surprising and suggests that immunostimulant treatment is likely to be ineffective or potentially harmful in the "Hyper" subgroup. We can only speculate whether these patients potentially respond to immune suppressive treatment such as steroids. On the other hand, the PBMCs from the Hypo subgroup, exposed to IFN-γ prior to LPS stimulation, showed increased IL-10 and TNF-α production in CD4$^+$ T cells and monocytes. Similarly, exposure to LAG-3Ig also enhanced the production of IL-10 in CD4$^+$ and CD8$^+$ T cells and CCL-4 production in NKs.

The effects of IFN-γ were seen mainly in monocytes, but not in other cells (**Figure 5A**), which is likely due to the limited 4 h stimulation with a Toll-like Receptor 4 agonist LPS. Further studies may be required to investigate the effect of IFN-γ over longer periods of stimulation with different stimulus. In comparison to IFN-γ, LAG-3Ig seemed to have pleiotropic effects on different immune cells subsets including monocytes, NKs, CD4$^+$ and CD8$^+$ T cells (**Figure 5B**). Whether or not sepsis patients with "Hypo-like" immune status will benefit from immunostimulant therapy such as IFN-γ or LAG-3Ig, remains to be investigated further.

This study using HDCyto provides a deeper understanding of the altered immune phenotype in severe sepsis, providing a window to future therapies. Our small study demonstrated the feasibility and advantage of using HDCyto in assessing immune signature of sepsis patients. It is important to note that many of our findings are in line with previous studies (8, 11, 22, 29, 45), with our panel allowing for assessments in numerous immune cell subsets at the same time. Being able to group patients based on the overall immune status is an important finding. We also demonstrated that the identified groups differed in their response to pretreatment with immune modulatory agents. Further investigations on various *ex vivo* stimulations followed by HDCyto analyses in monitoring patient's immune status and their response to immunomodulatory treatments such as IFN-γ, immune checkpoint inhibitors, tocilizumab and steroids, may allow clinician to tailor sepsis treatments. The protocol for the assessment of intracellular cytokines in this study requires hours of stimulation before measurements. Future studies may aim to find surface markers that could be used as surrogates for immune cell functions, such as CD69, CD80, CD86, PD-1, PD-L1, or LAG-3 among others. This would be critical for timely clinical application of HDCyto in triaging sepsis patients promptly before receiving immunotherapies.

DATA AVAILABILITY STATEMENT

The raw data supporting the conclusions of this article will be made available by the authors, without undue reservation.

ETHICS STATEMENT

The studies involving human participants were reviewed and approved by Nepean Blue Mountains Local Health District Human Research Ethics Committee. The patients/participants provided their written informed consent to participate in this study.

AUTHOR CONTRIBUTIONS

BG was responsible for data analysis and generating figures. BT, DB, and AM were responsible for study concept and manuscript revision. SD was involved in flow panel design and data analysis. CB, FT, and BS-N provided advice on the experiment design. SS and NF provided technical advice on flow cytometry. CW, KM, KS, and ST were responsible for recruiting subjects, sample processing, and ethics application. YW was responsible for flow panel design and optimization, data acquisition, data analysis, and manuscript writing. MN was responsible for study concept, design, ethics application, subject recruitment, data analysis, and interpretation. Final approval for submission was given by all authors.

FUNDING

This study was funded by Nepean Medical Research Foundation Seeding Funding Grant, University of Sydney.

ACKNOWLEDGMENTS

We would like to thank Dr. Andrew Lim (Becton Dickinson) for his continuous help and valuable advice throughout the whole project from panel design to trouble-shooting during panel optimization and data analysis. We would like to thank Dr. Edwin Lau (Westmead Cytometry at the Westmead Institute for Medical Research) for his technical support with BD FACSymphony™ A5.2 cell analyzer throughout this study. We would like to thank Immutep Pty Ltd for kindly donating the LAG-3Ig. We thank all patients and healthy controls who participated in this study. This research made use of the Argus Virtual Research Desktop environment funded by the University of Sydney. Flow cytometry experiments were performed at the Westmead Scientific Platforms, which are supported by the Westmead Research Hub, the Cancer Institute New South Wales, the National Health and Medical Research Council and the Ian Potter Foundation.

SUPPLEMENTARY MATERIAL

The Supplementary Material for this article can be found online at: https://www.frontiersin.org/articles/10.3389/fimmu.2021.634127/full#supplementary-material

Supplementary Figure 1 | Heatmap represents the median expression levels of all the type and state markers in the seven immune cell subsets (as shown in **Figure 2B**) on total PBMCs after 4 h of LPS stimulation without pretreatment in HC and Sepsis.

Supplementary Figure 2 | (A,B) Are the expanded version of **Figures 4B,C**, respectively. The expanded version includes all meta-clusters from each immune subset, which show significant changes in the expression levels of the state marker when comparing the Hypo to HC as in **(A)** or comparing the Hyper to HC as in **(B)**. Meta-cluster with a "*" is the representative meta-cluster of the immune subset as indicated by the color code. The representative meta-cluster was chosen based on its logFC, which is either the median of all included meta-clusters (if more than two meta-clusters) or the average of two meta-clusters.

Supplementary Figure 3 | Responses of the Hyper subgroup to LAG-3Ig pretreatment. UMAP represents the 50 meta-clusters and their corresponding immune cell subsets in sepsis as shown in **Figure 2B**. Meta-clusters that are showing significant responses to either LAG-3Ig are squared out in red. Representative flow plots of the representative meta-clusters demonstrate responses of the Hyper subgroup to LAG-3Ig pretreatment.

Supplementary Figure 4 | Additional clinical characteristics are compared between the Hyper and the Hypo subgroups. **(A)** Whole blood count (WBC) ($\times 10^9$/L) as well as the counts for neutrophils, monocytes and lymphocytes are compared between the Hyper and the Hypo subgroups. *P*-values were determined by Mann-Whitney test. **(B)** Median Fluorescence Intensity (MFI) of HLA-DR on $CD14^+$ monocytes are compared among the three groups: HC, the Hypo and Hyper subgroups. *P*-values were determined by Ordinary One-Way ANOVA—Dunnett's multiple comparison test. **(C)** Table shows details on the site of infections for patients from the Hyper and the Hypo subgroups. Data represents mean ± SD, $^{****}p < 0.0001$.

Supplementary Table 1 | Names of antigens and cell types detected by the HDCyto flow panel are listed. Fluorochrome and clone number of each antibody are also listed.

Supplementary Table 2 | Clinical characteristics of patients from the Hyper and the Hypo subgroups. Age, Male sex%, C-reactive protein (CRP) (mg/L), Serum lactate (mmol/L), SOFA score, whole blood count (WBC) ($\times 10^9$/L), and Acute Physiology and Chronic Health Evaluation (APACHE) III score are compared between the Hyper and the Hypo subgroups. *P*-values were determined by Mann-Whitney test.

REFERENCES

1. Fleischmann C, Scherag A, Adhikari NK, Hartog CS, Tsaganos T, Schlattmann P, et al. Assessment of global incidence and mortality of hospital-treated sepsis. Current estimates and limitations. *Am J Respir Crit Care Med.* (2016) 193:259–72. doi: 10.1164/rccm.201504-0781OC
2. Singer M, Deutschman CS, Seymour CW, Shankar-Hari M, Annane D, Bauer M, et al. The third international consensus definitions for sepsis and septic shock (sepsis-3). *JAMA.* (2016) 315:801–10. doi: 10.1001/jama.2016.0287
3. Hotchkiss RS, Monneret G, Payen D. Immunosuppression in sepsis: a novel understanding of the disorder and a new therapeutic approach. *Lancet Infect Dis.* (2013) 13:260–8. doi: 10.1016/S1473-3099(13)70001-X
4. Boomer JS, Green JM, Hotchkiss RS. The changing immune system in sepsis: is individualized immuno-modulatory therapy the answer? *Virulence.* (2014) 5:45–56. doi: 10.4161/viru.26516
5. Tang BM, Huang SJ, Mclean AS. Genome-wide transcription profiling of human sepsis: a systematic review. *Crit Care.* (2010) 14:R237. doi: 10.1186/cc9392
6. Kalil AC, Florescu DF. Prevalence and mortality associated with cytomegalovirus infection in nonimmunosuppressed patients in the intensive care unit. *Crit Care Med.* (2009) 37:2350–8. doi: 10.1097/CCM.0b013e3181a3aa43
7. Monneret G, Venet F, Kullberg BJ, Netea MG. ICU-acquired immunosuppression and the risk for secondary fungal infections. *Med Mycol.* (2011) 49(Suppl. 1):S17–23. doi: 10.3109/13693786.2010.509744
8. Hotchkiss RS, Swanson PE, Freeman BD, Tinsley KW, Cobb JP, Matuschak GM, et al. Apoptotic cell death in patients with sepsis, shock, and multiple organ dysfunction. *Crit Care Med.* (1999) 27:1230–51. doi: 10.1097/00003246-199907000-00002
9. Oberholzer A, Oberholzer C, Moldawer LL. Sepsis syndromes: understanding the role of innate and acquired immunity. *Shock.* (2001) 16:83–96. doi: 10.1097/00024382-200116020-00001
10. Monneret G, Debard AL, Venet F, Bohe J, Hequet O, Bienvenu J, et al. Marked elevation of human circulating CD4+CD25+ regulatory T cells in sepsis-induced immunoparalysis. *Crit Care Med.* (2003) 31:2068–71. doi: 10.1097/01.CCM.0000069345.78884.0F

11. Lukaszewicz AC, Grienay M, Resche-Rigon M, Pirracchio R, Faivre V, Boval B, et al. Monocytic HLA-DR expression in intensive care patients: interest for prognosis and secondary infection prediction. *Crit Care Med.* (2009) 37:2746–52. doi: 10.1097/00003246-200910000-00011
12. Muenzer JT, Davis CG, Chang K, Schmidt RE, Dunne WM, Coopersmith CM, et al. Characterization and modulation of the immunosuppressive phase of sepsis. *Infect Immun.* (2010) 78:1582–92. doi: 10.1128/IAI.01213-09
13. Schrijver IT, Theroude C, Roger T. Myeloid-derived suppressor cells in sepsis. *Front Immunol.* (2019) 10:327. doi: 10.3389/fimmu.2019.00327
14. Docke WD, Randow F, Syrbe U, Krausch D, Asadullah K, Reinke P, et al. Monocyte deactivation in septic patients: restoration by IFN-gamma treatment. *Nat Med.* (1997) 3:678–81. doi: 10.1038/nm0697-678
15. Nalos M, Santner-Nanan B, Parnell G, Tang B, Mclean AS, Nanan R. Immune effects of interferon gamma in persistent staphylococcal sepsis. *Am J Respir Crit Care Med.* (2012) 185:110–2. doi: 10.1164/ajrccm.185.1.110
16. Ono S, Tsujimoto H, Hiraki S, Aosasa S. Mechanisms of sepsis-induced immunosuppression and immunological modification therapies for sepsis. *Ann Gastroenterol Surg.* (2018) 2:351–8. doi: 10.1002/ags3.12194
17. Peters Van Ton AM, Kox M, Abdo WF, Pickkers P. Precision immunotherapy for sepsis. *Front Immunol.* (2018) 9:1926. doi: 10.3389/fimmu.2018.01926
18. Delsing CE, Gresnigt MS, Leentjens J, Preijers F, Frager FA, Kox M, et al. Interferon-gamma as adjunctive immunotherapy for invasive fungal infections: a case series. *BMC Infect Dis.* (2014) 14:166. doi: 10.1186/1471-2334-14-166
19. Payen D, Faivre V, Miatello J, Leentjens J, Brumpt C, Tissieres P, et al. Multicentric experience with interferon gamma therapy in sepsis induced immunosuppression. A case series. *BMC Infect Dis.* (2019) 19:931. doi: 10.1186/s12879-019-4526-x
20. Andreae S, Piras F, Burdin N, Triebel F. Maturation and activation of dendritic cells induced by lymphocyte activation gene-3 (CD223). *J Immunol.* (2002) 168:3874–80. doi: 10.4049/jimmunol.168.8.3874
21. Andreae S, Buisson S, Triebel F. MHC class II signal transduction in human dendritic cells induced by a natural ligand, the LAG-3 protein (CD223). *Blood.* (2003) 102:2130–7. doi: 10.1182/blood-2003-01-0273
22. Brignone C, Grygar C, Marcu M, Schakel K, Triebel F. A soluble form of lymphocyte activation gene-3 (IMP321) induces activation of a large range of human effector cytotoxic cells. *J Immunol.* (2007) 179:4202–11. doi: 10.4049/jimmunol.179.6.4202
23. Brignone C, Gutierrez M, Mefti F, Brain E, Jarcau R, Cvitkovic F, et al. First-line chemoimmunotherapy in metastatic breast carcinoma: combination of paclitaxel and IMP321 (LAG-3Ig) enhances immune responses and antitumor activity. *J Transl Med.* (2010) 8:71. doi: 10.1186/1479-5876-8-71
24. Atkinson V, Khattak A, Haydon A, Eastgate M, Roy A, Prithviraj P, et al. Eftilagimod alpha, a soluble lymphocyte activation gene-3 (LAG-3) protein plus pembrolizumab in patients with metastatic melanoma. *J Immunother Cancer.* (2020) 8:e001681. doi: 10.1136/jitc-2020-001681
25. Docke WD, Hoflich C, Davis KA, Rottgers K, Meisel C, Kiefer P, et al. Monitoring temporary immunodepression by flow cytometric measurement of monocytic HLA-DR expression: a multicenter standardized study. *Clin Chem.* (2005) 51:2341–7. doi: 10.1373/clinchem.2005.052639
26. Garcia-Pineres AJ, Hildesheim A, Williams M, Trivett M, Strobl S, Pinto LA. DNAse treatment following thawing of cryopreserved PBMC is a procedure suitable for lymphocyte functional studies. *J Immunol Methods.* (2006) 313:209–13. doi: 10.1016/j.jim.2006.04.004
27. Poujol F, Monneret G, Pachot A, Textoris J, Venet F. Altered T lymphocyte proliferation upon lipopolysaccharide challenge *ex vivo*. *PLoS ONE.* (2015) 10:e0144375. doi: 10.1371/journal.pone.0144375
28. Crowell HL, Stéphane Chevrier VRTZ, Robinson MD, Bodenmiller B. *CATALYST: Cytometry dATa anALYSis Tools*. (2020). Available online at: https://github.com/HelenaLC/CATALYST
29. Wickham H, Averick M, Bryan J, Chang W, D'Agostino McGowan L, François R, et al. Welcome to the Tidyverse. *J Open Source Softw.* (2019) 4:1686. doi: 10.21105/joss.01686
30. Kolde R. *pheatmap: Pretty Heatmaps*. (2019). Available online at: https://CRAN.R-project.org/package=pheatmap
31. R Development Core Team. *R: A Language and Environment for Statistical Computing*. Vienna: R Foundation for Statistical Computing (2019).
32. Monaco G, Chen H, Poidinger M, Chen J, De Magalhães JP, Larbi A. flowAI: automatic and interactive anomaly discerning tools for flow cytometry data. *Bioinformatics.* (2016) 32:2473–80. doi: 10.1093/bioinformatics/btw191
33. Van Gassen S, Callebaut B, Van Helden MJ, Lambrecht BN, Demeester P, Dhaene T, et al. FlowSOM: using self-organizing maps for visualization and interpretation of cytometry data. *Cytometry A.* (2015) 87:636–45. doi: 10.1002/cyto.a.22625
34. Weber LM, Nowicka M, Soneson C, Robinson MD. diffcyt: differential discovery in high-dimensional cytometry via high-resolution clustering. *Commun Biol.* (2019) 2:183. doi: 10.1038/s42003-019-0415-5
35. Ritchie ME, Phipson B, Wu D, Hu Y, Law CW, Shi W, et al. limma powers differential expression analyses for RNA-sequencing and microarray studies. *Nucl Acids Res.* (2015) 43:e47. doi: 10.1093/nar/gkv007
36. Larsson J. *eulerr: Area-Proportional Euler and Venn Diagrams With Ellipses*. (2020). Available online at: https://github.com/jolars/eulerr, https://jolars.github.io/eulerr/
37. Pepys MB, Hirschfield GM. C-reactive protein: a critical update. *J Clin Invest.* (2003) 111:1805–12. doi: 10.1172/JCI200318921
38. Castelli GP, Pognani C, Meisner M, Stuani A, Bellomi D, Sgarbi L. Procalcitonin and C-reactive protein during systemic inflammatory response syndrome, sepsis and organ dysfunction. *Crit Care.* (2004) 8:R234–42. doi: 10.1186/cc2877
39. Sridharan P, Chamberlain RS. The efficacy of procalcitonin as a biomarker in the management of sepsis: slaying dragons or tilting at windmills? *Surg Infect.* (2013) 14:489–511. doi: 10.1089/sur.2012.028
40. Cheadle WG, Hershman MJ, Wellhausen SR, Polk HC Jr. HLA-DR antigen expression on peripheral blood monocytes correlates with surgical infection. *Am J Surg.* (1991) 161:639–45. doi: 10.1016/0002-9610(91)91247-G
41. Erokhina SA, Streltsova MA, Kanevskiy LM, Telford WG, Sapozhnikov AM, Kovalenko EI. HLA-DR(+) NK cells are mostly characterized by less mature phenotype and high functional activity. *Immunol Cell Biol.* (2018) 96:212–28. doi: 10.1111/imcb.1032
42. Erokhina SA, Streltsova MA, Kanevskiy LM, Grechikhina MV, Sapozhnikov AM, Kovalenko EI. HLA-DR-expressing NK cells: effective killers suspected for antigen presentation. *J Leukoc Biol.* (2021) 109:327–37. doi: 10.1002/JLB.3RU0420-668RR
43. Vazquez-Tello A, Halwani R, Li R, Nadigel J, Bar-Or A, Mazer BD, et al. IL-17A and IL-17F expression in B lymphocytes. *Int Arch Allergy Immunol.* (2012) 157:406–16. doi: 10.1159/000329527
44. Srenathan U, Steel K, Taams LS. IL-17+ CD8+ T cells: differentiation, phenotype and role in inflammatory disease. *Immunol Lett.* (2016) 178:20–6. doi: 10.1016/j.imlet.2016.05.001
45. Chaudhry H, Zhou J, Zhong Y, Ali MM, Mcguire F, Nagarkatti PS, et al. Role of cytokines as a double-edged sword in sepsis. *In Vivo.* (2013) 27:669–84.

Conflict of Interest: CB and BT were employed by Immutep S.A.S.

The remaining authors declare that the research was conducted in the absence of any commercial or financial relationships that could be construed as a potential conflict of interest.

frontiers in Immunology

ORIGINAL RESEARCH
published: 30 April 2021
doi: 10.3389/fimmu.2021.670676

Neuronal-Activated ILC2s Promote IL-17A Production in Lung γδ T Cells During Sepsis

Weiwei Chen[1,2], Dengming Lai[1], Yuehua Li[2,3], Xueke Wang[1], Yihang Pan[1], Xiangming Fang[4], Jie Fan[2,3,5] and Qiang Shu[1]**

[1] Department of Thoracic and Cardiovascular Surgery, National Clinical Research Center for Child Health, The Children's Hospital, Zhejiang University School of Medicine, Hangzhou, China, [2] Department of Surgery, University of Pittsburgh School of Medicine, Pittsburgh, PA, United States, [3] Research and Development, Veterans Affairs Pittsburgh Healthcare System, Pittsburgh, PA, United States, [4] Department of Anesthesiology and Intensive Care Unit, The First Affiliated Hospital, Zhejiang University School of Medicine, Hangzhou, China, [5] McGowan Institute for Regenerative Medicine, University of Pittsburgh, Pittsburgh, PA, United States

OPEN ACCESS

Edited by:
Yong Ming Yao, First Affiliated Hospital of Chinese PLA General Hospital, China

Reviewed by:
Thomas Griffith, University of Minnesota Twin Cities, United States
Hiroki Yokoo, Tokoha Gakuen University, Japan

***Correspondence:**
Qiang Shu
shuqiang@zju.edu.cn
Xiangming Fang
xmfang@zju.edu.cn

Specialty section:
This article was submitted to Inflammation, a section of the journal Frontiers in Immunology

Received: *22 February 2021*
Accepted: *15 April 2021*
Published: *30 April 2021*

Citation:
Chen W, Lai D, Li Y, Wang X, Pan Y, Fang X, Fan J and Shu Q (2021) Neuronal-Activated ILC2s Promote IL-17A Production in Lung γδ T Cells During Sepsis. Front. Immunol. 12:670676. doi: 10.3389/fimmu.2021.670676

Background: Studies have revealed important roles for IL-17A in the development of acute lung injury (ALI) following sepsis. However, the mechanism underlying the regulation of lung IL-17A remains to be fully addressed. Recent studies suggested the effect of neuromedin U (NMU) on immune cell activation and the role of group 2 innate lymphoid cells (ILC2s) in the modulation of IL-17A production. We aimed to gain in-depth insight into the mechanism underlying sepsis-induced lung IL-17A production, particularly, the role of NMU in mediating neuronal regulation of ILC2s and IL-17A-producing γδ T cells activation in sepsis.

Methods: Wild type mice were subjected to cecal ligation and puncture (CLP) to induce sepsis with or without intraperitoneal injection of NMU. The levels of ILC2s, γδ T cells, IL-17A, NMU and NMU receptor 1 (NMUR1) in the lung were then measured. In order to determine the role of NMU signaling in ILC2 activation and the role of ILC2-released IL-9 in ILC2-γδ T cell interaction, ILC2s were sorted, and the genes of *nmur1* and *il9* in the ILC2s were knocked down using CRISPR/Cas9. The genetically manipulated ILC2s were then co-cultured with lung γδ T cells, and the levels of IL-17A from co-culture systems were measured.

Results: In septic mice, the levels of NMU, IL-17A, ILC2s, and IL-17A-producing γδ T cells in the lung are significantly increased, and the expression of NMUR1 in ILC2s is increased as well. Exogenous NMU further augments these increases. The main source of IL-17A in response to CLP is γδ T cells, and lung *nmur1* is specifically expressed in ILC2s. *In vitro* co-culture of ILC2s and γδ T cells leads to increased number of γδ T cells and higher production of IL-17A from γδ T cells, and these alterations are further augmented by septic treatment and exogenous NMU. Genetic knockdown of *nmur1* or *il9* in ILC2s attenuated the upregulation of γδ T cells and IL-17A production.

Conclusion: In sepsis, NMU acting through NMUR1 in lung ILC2s initiates the ILC2 activation, which, in turn, promote IL-17A-producing γδ T cell expansion and secretion of

IL-17A. ILC2-derived IL-9 plays an important role in mediating γδ T cell expansion and IL-17A production. This study explores a new mechanism underlying neuronal regulation of innate immunity in sepsis.

Keywords: group 2 innate lymphoid cells, neuromedin U, sepsis, γδ T cells, IL-17A

INTRODUCTION

Sepsis is the result of the excessive and dysregulated inflammatory response of the body to infection, which often leads to tissue injury, multiple organ dysfunction syndrome (MODS), and death (1). Sepsis-induced mortality is closely associated with secondary acute lung injury (ALI) (2, 3).

Emerging data have shown that IL-17A is an important predictor and therapeutic target in sepsis and secondary ALI. Circulating levels of IL-17A are elevated in human and experimental sepsis (4–6). The study has shown in cecal ligation and puncture (CLP)-induced sepsis mouse model that IL-17A or IL-17A receptor deficiency significantly increased the mortality, which correlated with reduced neutrophil recruitment and more severe bacteremia (7, 8). A study has also shown that early-activated Vγ4δ T cells are the major resource of IL-17A during sepsis and the secretion of IL-17A decreased the mortality of septic mice (9). Furthermore, a recent study using the mouse CLP model demonstrated that IL-17A promoted IgA production, which coupled with a higher survival rate (10). Several types of cells are found to secrete IL-17A including $CD4^+$ T helper 17 (Th17) cell, $CD8^+$ (Tc17) cell, natural killer T (NKT) cell, γδ T cell, group 3 innate lymphoid cell (ILC3), and "natural" Th17 cell (11, 12). However, in-depth insights into the mechanism underlying the regulation of IL-17A production and secretion in sepsis remains to be fully addressed.

Group 2 innate lymphoid cells (ILC2s) are a special population of cytokine-stimulated and cytokine-producing lymphocytes that exist in mucosal tissues. ILC2s importantly bridge innate and adaptive immunities. Our previous report showed that ILC2s protect lung endothelial cells from pyroptosis in the mouse sepsis model (13). Studies have also found that both $ST2^+$ natural ILC2 (nILC2) and $ST2^-$ inflammatory ILC2 (iILC2) can produce IL-17A (14–17). However, it remains unclear whether lung ILC2s secrete IL-17A or regulate other cells to secret IL-17A in a setting of sepsis.

It has been reported that the nervous system plays dual roles, either stimulating or suppressing, in the regulation of ILC2 activation in different settings (18–21). For example, studies showed that neuropeptide neuromedin U (NMU) regulates ILC2 activation in asthma and the helminth infection model (18, 19, 22). These findings led us to ask how NMU regulates lung ILC2s in a setting of sepsis and what are the subsequent outcomes in the progression of ALI following sepsis.

In this study, using a mouse sepsis model induced by CLP, we show that NMU acting through NMUR1 on lung ILC2s initiates the ILC2 activation, which, in turn, promotes IL-17A-producing γδ T cell expansion and IL-17A secretion. ILC2-derived IL-9 plays an important role in mediating γδ T cell expansion and IL-17A production. This study explores a new mechanism underlying neuronal regulation of innate immunity in sepsis.

METHODS

Mice

Male C57BL/6J wild-type mice were purchased from Jackson Laboratories (Bar Harbor, ME). Mice were bred and maintained under specific pathogen-free condition at the Animal Facility of the University of Pittsburgh School of Medicine, VA Pittsburgh Healthcare System, and the Children's Hospital, Zhejiang University School of Medicine. All mice used in the experiments were 8 weeks old. All mice were performed in compliance with the guidelines of the Institutional Animal Care and Use Committee of the University of Pittsburgh, VA Pittsburgh Healthcare System, and the Children's Hospital, Zhejiang University School of Medicine, respectively.

CLP Model and Survival Analysis

Sepsis was induced by CLP procedure as described previously (23). In short, mice were deeply anesthetized with an intraperitoneal injection of xylazine (5 mg/kg) and ketamine (50 mg/kg). A midline incision (1 cm) on the abdomen was performed to allow exteriorization of the cecum. To obtain a moderate CLP, the cecum was ligated 0.8 cm from the apex with 4-0 silk suture and punctured once with a 22-gauge needle in the ligated segment. To induce a severe CLP, the cecum was ligated 1.2 cm from the apex and punctured twice with an 18-gauge needle. A droplet of cecal contents was then slowly squeezed out of the puncture holes. Then the cecum was placed back into the abdomen. The incision was then sutured in two layers. Sham surgery was identical to CLP without puncture and ligation. Mice were fluid resuscitated immediately after surgery (1 ml/mouse sterile saline, subcutaneously). At the specified time point, mice were sacrificed, and lung tissue samples were obtained under sterile condition. Whole blood was collected by cardiac puncture and spun down, and samples were stored at -80°C for further analysis.

In the survival analysis, the survival of animals (5 mice per group) was monitored each 3 hours for 72 consecutive hours after CLP surgery. To relieve pain, mice with signs of imminent death were overdosed with xylazine/ketamine. The survival rate was evaluated, followed by plotting the survival curve.

Treatment of Mice

In some *in vivo* experiments, mice were injected intraperitoneally (i.p.) with 0.2 μg/g B.W. of NMU-23 peptide (Phoenix Pharmaceuticals, USA) at 6h before and after CLP or with a

single dose of NMU-23 peptide (1 μg/g B.W.) at 6h before CLP. At 24h after CLP, lungs were harvested for further analysis. Control mice were treated with PBS.

Cell Isolation

Cell isolation from lung tissue was performed as described previously (24). Briefly, lungs were perfused with 5 ml cold PBS with 2% heparin through right ventricle of the heart, and then filled with 1 ml HBSS with Liberase ™ (100 μg/ml final concentration) (Roche, USA) and digested in 4 ml HBSS digestion medium for 45 min at 37°C with vortexing every 15 min. The resultant samples were mashed by 70-μm cell strainers, washed with Dulbecco's modified Eagle media [DMEM; supplemented with 10% fetal bovine serum (FBS) and 1% penicillin/streptomycin (Thermo Fisher Scientific, Pittsburgh, PA, USA)], and treated with RBC Lysis Buffer (eBioscience ™) to lyse red blood cells. Cell suspensions were used for subsequent flow cytometry staining.

Western Blot

Western blot was performed using standard methods. In short, protein (30 μg) was electropharesed through 12% SDS polyacrylamide gels and transferred to PVDF membranes (Bio-Rad, USA). The membranes were incubated with primary antibodies at 4°C overnight, followed by secondary antibodies tagged with HRP (Thermo Fisher Scientific, USA) at room temperature for 1 hour. The signals were detected using ECL Kit (Pierce Biotech, Rockford, Illinois, USA). A GAPDH antibody was used as a control for whole-cell lysates.

Flow Cytometry

For flow cytometry analysis, anti-mouse CD16/CD32 antibody (eBioscience, USA) was added to samples at a 1:200 dilution for 20 minutes at 4°C to block nonspecific binding to Fc receptors before cell staining.

LIVE/DEAD Fixable Aqua Dead Cell Stain Kit (eBioscience), Fixable Viability Dye eFluor™ 780 (eBioscience) or 7AAD viability dye (eBioscience) were used to exclude dead cells. Lung cell suspensions were stained with anti-CD45 (30-F11), anti-CD3ϵ (17A2), anti-CD4 (RM4-5), anti-CD5 (53-7.3), anti-CD8α (53-6.7), anti-CD11b (M1/70), anti-CD11c (N418), anti-CD19 (eBio1D3), anti-NK1.1 (PK136), anti-TER119 (TER-119), anti-FceR1α (MAR-1), anti-TCRβ (H57-597), anti-TCRγδ (GL-3), anti-Gr1 (RB6-8C5), anti-Thy1.2 (CD90.2; 53-2.1), anti-CD25 (eBio7D4), anti-CD127 (IL-7Rα; A7R34), anti-IL-17A (eBio17B7) from eBioscience; anti-KLRG1 (2F1), anti-Sca1 (D7) from BD Biosciences, anti-T1/ST2 (DJ8) from MD Biosciences. Lineage was composed by CD3ϵ, CD4, CD5, CD8α, CD11b, CD11c, CD19, NK1.1, TER119, FceR1α, TCRβ, TCR γδ and Gr1; Cell populations were defined as: ILC2s, $CD45^+Lineage^-Thy1.2^+T1/ST2^+CD127^+CD25^+KLRG1^+Sca1^+$; γδ T cells, $CD45^+CD3\epsilon^+$TCR $\gamma\delta^+CD4^-$TCR β^-.

For intracellular cytokine protein analysis *ex vivo*, cells were stimulated using the Cell Stimulation Cocktail (eBioscience), containing PMA/Ionomycin/Brefeldin-A/monensin, for 4 hours at 37°C before staining. Intracellular staining was performed using IC fixation/permeabilization kit (eBioscience).

Flow cytometry analysis and cell sorting were performed using LSR Fortessa, FACS Aria flow cytometers (BD Biosciences) and Cytek Aurora (Cytek Biosciences). The percentage of ILC2s is gated in live $CD45^+Lineage^-$ cells. Data analysis was done using FlowJo software (Tristar).

Sorting and *In Vitro* Culture of Lung ILC2s and γδ T Cells

For flow cytometric sorting, $Lin^-CD45^+CD90.2^+ST2^+$ ILC2s were sorted from the lungs of naive mice by FACSAria (BD Biosciences) or Beckman MoFlo Astrios EQ (Beckman Coulter Life Sciences, Indianapolis, IN, USA). The average purity of ILC2s is > 98%. *In vitro* culture of ILC2s was conducted as previously described (25). Sorted ILC2s were routinely grown in DMEM glutaMAX (Gibco) supplemented with 10% FBS, 100 U/ml penicillin, 100 mg/ml streptomycin, 1% hepes, sodium pyruvate, glutamine at 37°C. Lung ILC2s were plated in 96-well round-bottom plates with two densities (1.5×10^4 or 3.0×10^4 cells/well) in 10 ng/ml rmIL-2 (Biolegend, San Diego, CA, USA), 20 ng/ml rmIL-7 (Biolegend) and 20 ng/ml rmIL-33 (Biolegend) for 6 days. Before use, ILC2s were gently washed twice to remove residual rmIL-2, rmIL-7, and rmIL-33.

Lung γδ T cells were collected after flushing the lungs with 5 ml cold PBS through right ventricle to remove circulating cells. Fresh γδ T cells were enriched from lung by negative and positive selection using the TCRγ/δ^+ T cell isolation Kit (Miltenyi Biotec, Gladbach Bergische, Germany), then $CD45^+CD3\epsilon^+$TCR $\gamma\delta^+$ γδ T cells were sorted by FACSAria (BD Biosciences) or Beckman MoFlo Astrios EQ (Beckman Coulter Life Sciences, Indianapolis, IN, USA). The average purity of γδ T cells is > 98%. *In vitro* culture of γδ T cells was conducted as previously described (26). Sorted γδ T cells were routinely grown in DMEM glutaMAX (Gibco) supplemented with 10% FBS, 100 U/ml penicillin, 100 mg/ml streptomycin, 1% hepes, sodium pyruvate, glutamine at 37°C. Lung γδ T cells were plated in 96-well round-bottom plates with a density of 5.0×10^3 cells/well, in 100 ng/ml rmIL-1β (Biolegend, San Diego, CA, USA) and 100 ng/ml rmIL-23 (Biolegend) to polarize IL-17A-producing γδ T cells (26–28).

For direct co-culture assays, sorted lung ILC2s were cultured with rmIL-2, rmIL-7 and rmIL-33 for 6 days to obtain mature ILC2s, then sorted lung γδ T cells were added to the each ILC2 well, in DMEM glutaMAX (Gibco) supplemented with 10% FBS, 100 U/ml penicillin, 100 mg/ml streptomycin, 1% hepes, sodium pyruvate, glutamine at 37°C. To maintain ILC2 survival, rmIL-7 (20 ng/ml) was included in all assays with ILC2s as well as controls, including when co-culturing with γδ T cells. ILC2s and γδ T cells were co-cultured for 48 hours before the next tests if not otherwise specified.

The following substances were added to cultures as indicated: NMU (1 or 10 μg/ml, Phoenix Pharmaceuticals), rmIL-1β (100 ng/ml; Biolegend), rmIL-23 (100 ng/ml; Biolegend), LPS (1 μg/ml; Sigma-Aldrich) plus TNF-α (20 ng/ml; Biolegend) were added to mimic sepsis stimulation (13).

Quantitative Real-Time PCR

Total RNA from sorted cells or tissues were extracted by RNeasy Plus Mini Kit (Qiagen, Germantown, MD, USA) or Trizol method (Thermo Fisher Scientific, Pittsburgh, PA, USA) and stored at -80°C for further analysis. Total RNA concentration was measured using a Nanodrop One spectrophotometer (Thermo Fisher Scientific, Pittsburgh, PA, USA). Total RNA was reverse transcribed using the High Capacity cDNA Reverse Transcription kit (Thermo Fisher Scientific, Pittsburgh, PA, USA) according to the protocol.

Quantitative PCR was conducted in triplicate on a CFX Connect Real-Time PCR Detection System (Bio-Rad, Hercules, CA, USA) with TaqMan Gene Expression Master Mix (Applied Biosystems) using the following TaqMan Gene Expression Assays (Applied Biosystems): *Nmu* (Mm00479868_m1); *Nmur1* (Mm00515885_m1); *Il5* (Mm00439646_m1); *Il9* (Mm00434305_m1); *Il13* (Mm00434204_m1); *Il17a* (Mm00439618_m1).

Gene expression was normalized as n-fold difference to the gene *Hprt1* (Mm00446968_m1) and *S18* (Mm03928990_g1) for mouse according to the cycling threshold. Calculation of mRNA levels was performed with the CFX Manager Software version 3.1 (Bio-Rad).

Lung Homogenate Assays

For lung homogenate, the whole lung was snap frozen on dry ice homogenized in RIPA buffer (Sigma-Aldrich) containing 0.01% protease and phosphatase inhibitor cocktail (Thermo Scientific). The cell debris and tissue were removed by centrifugation at 19,000 g for 30 min at 4°C. The supernatant was collected for analysis of IL-17A (R&D System) by ELISA according to the manufacturer's instructions.

Cytokine Measurements

Blood samples were collected, and plasma was obtained by centrifugation at 5,000 g for 20 min at 4°C. For determination of mouse IL-1β, IL-9, IL-17A and IL-23, Quantikine ELISA Kits from R&D Systems were used according to manufacturers' instructions.

Gene Knockdown by CRISPR/Cas9 Technology

For CRISPR/Cas9-mediated gene knockdown, the following synthetic guide RNA (sgRNA) sequences were used: 5'-CGATATGCTGGTGCTCCTGG-3' (targeting *nmur1*); 5'-GTGAGCGGACAGCTGTGTCA-3' (targeting *Il5*); 5'-ATTGTACCACACCGTGCTAC-3' (targeting *Il9*); 5'-CTTCGATTTTGGTATCGGGG-3' (targeting *Il13*); 5'-AAUGUGAGAUCAGAGUAAU-3' (non-target control) (ThermoFisher Scientific, USA). *Ex vivo*–expanded ILC2s were transfected with *nmur1/Il5/Il9/Il13* CRISPR/Cas9 plasmid or its non-target control (NTC) in accordance with the manufacturer's instructions. Transfected cells were cultured for 2 days before next step.

Statistical Analysis

Statistical analyses were done using GraphPad Prism 7.00 software (GraphPad Software, Inc., La Jolla, CA, USA). Survival differences were assessed using the Kaplan-Meier analysis followed by a log-rank test. Student's t test or ANOVA was used in all other experiments. Data were expressed as mean ± SEM. A P value < 0.05 was considered statistically significant, and significance is presented as * $P < 0.05$, ** $P < 0.01$, *** $P < 0.001$, or **** $P < 0.0001$.

RESULTS

Sepsis Induces IL-17A-Producing γδ T Cell Expansion and IL-17A Expression in the Lungs

Sepsis induced significant increases in plasma IL-17A levels, lung tissue *Il17a* mRNA expression, and IL-17A protein concentration (**Figures 1A–C**), which were consistent with the previous observations (29). Noteworthy, sepsis also induced a markedly increase in the percentage of lung IL-17A-producing cells (**Figures 1D, E**).

Our previous study has shown that sepsis induces ILC2 expansion in the lungs (13). However, it was unknown whether ILC2s secrete IL-17A during sepsis, although it has been reported that in allergic conditions $ST2^+$ nILC2s secrete IL-17A (17). We found that IL-17A-producing ILC2s were significantly upregulated in the lungs following the CLP procedure (**Figures 1F, G**). However, importantly, IL-17A-producing ILC2s only occupy 1~2% of total IL-17A-producing cells (**Figure 1H**).

Since multiple cell types, including $lineage^-$ ILCs, $CD4^+$ T helper 17 (Th17) cells, $CD8^+$ (Tc17) cells, and γδ T cells can produce and secret IL-17A (30), we then assessed the relative contribution of these cells to the elevated lung IL-17A in sepsis. Using the flow cytometry gating strategy, we found the γδ T cell lineage, but not $lineage^-$ ILCs, $CD4^+$ T cells, and $CD8^+$ T cells, are the major source of IL-17A (**Figures 1D, H**). This finding underscores the important role of γδ T cells in producing IL-17A in the lung in sepsis. We also found that the percentage and numbers of lung γδ T cells were significantly higher in the CLP group than that in the sham group (**Figures 1I–K**). Collectively, these findings suggest an important role for lung γδ T cells in producing and secretion of IL-17A in sepsis.

Sepsis Promotes NMU Expressions in the Lung and NMUR1 Expression in Lung ILC2s

NMU-NMUR1 signaling has been reported to play an important role in the regulation of inflammation in asthma and helminth infection models (19, 22). To determine the role of NMU-NMUR1 signaling in sepsis-induced inflammation, we measured the expression of NMU in the lungs and NMUR1 expression in ILC2s following CLP. The results show that sepsis markedly increased the expressions of *nmu* mRNA by ~2.4-fold and NMU protein by ~2.1-fold in the lungs (**Figures 2A, B**). We then collected ILC2s by flow sorting and treated the ILC2s with LPS + TNF-α to mimic a septic condition *in vitro*. We found that

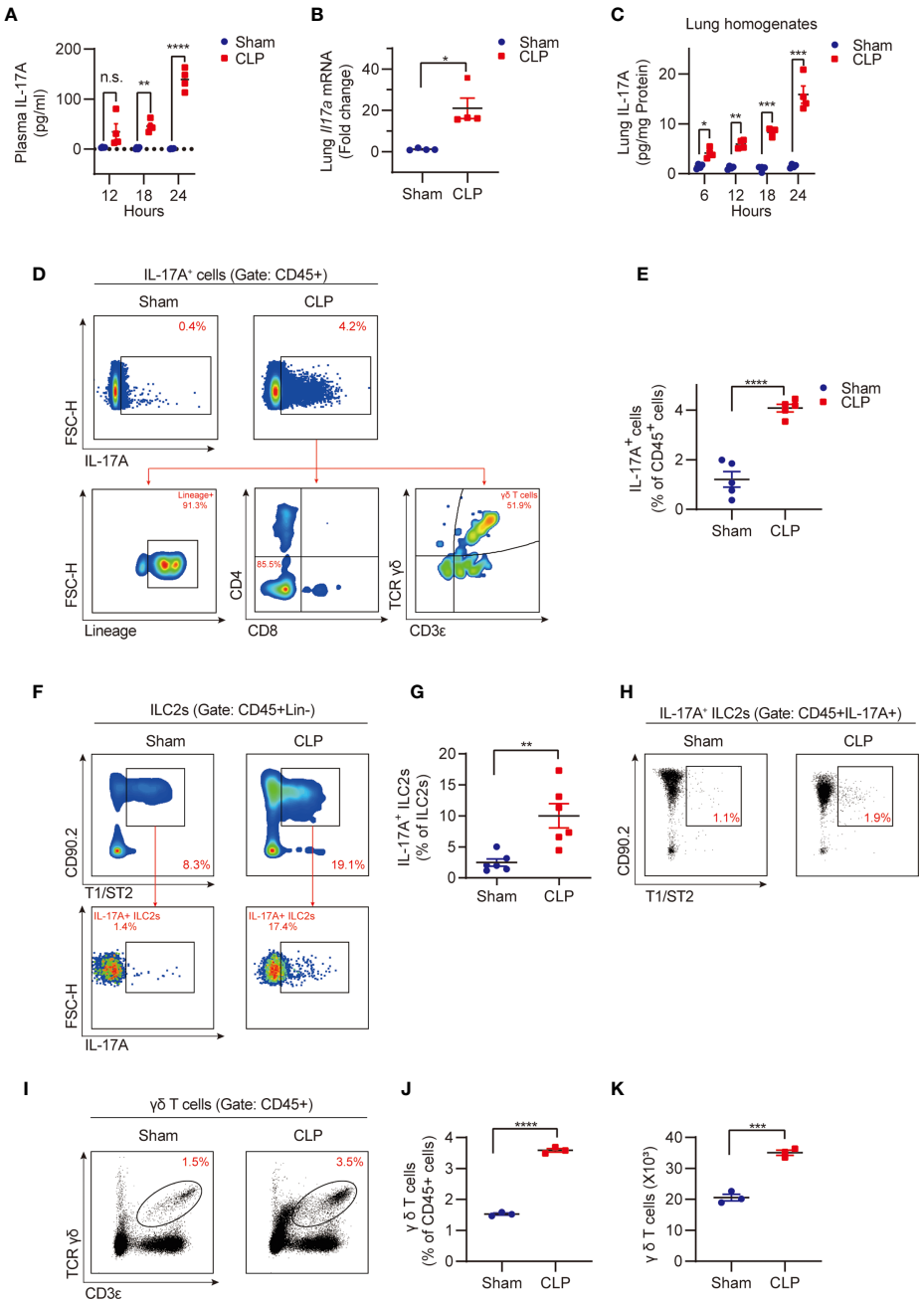

FIGURE 1 | Sepsis induces IL-17A-producing γδ T cell expansion and IL-17A expression in the lungs. Wild type (WT, C57BL/6J) mice were subjected to cecal ligation and puncture (CLP) to induce sepsis or sham surgery, plasma and lung tissue were then collected at different time points as indicated. **(A)** ELISA analysis of plasma IL-17A from CLP or sham mice (n = 4). **(B)** Real-time PCR detection of lung *Il17a* mRNA from mice at 24h after CLP or sham surgery (n = 4). Data were normalized by S18. **(C)** ELISA analysis of IL-17A protein in lung homogenates from CLP or sham mice (n = 4). Data were normalized by protein concentrations. **(D)** Representative flow cytometry plots for IL-17A expression within lung live CD45$^+$ populations at 24h after CLP or sham surgery. The relative contribution of different cells (Lineage$^-$ILCs, CD4$^+$ T cells, CD8$^+$ T cells, and γδ T cells) to lung IL-17A$^+$ cells was determined. **(E)** The percentages of the IL-17A$^+$ cell population within lung live CD45$^+$ populations at 24h after CLP or sham surgery (n = 5). **(F)** Representative flow cytometry plots for ILC2 population within lung live CD45$^+$Lineage$^-$ populations and IL-17A$^+$ ILC2 population within ILC2 population at 24h after CLP or sham surgery. **(G)** The percentages of IL-17A$^+$ ILC2 population within lung ILC2 population at 24h after CLP or sham surgery (n = 6). **(H)** Representative flow cytometry plots for ILC2 population within lung live CD45$^+$IL-17A$^+$ populations at 24h after CLP or sham surgery. **(I–K)** Representative flow cytometry plots **(I)**, percentages **(J)**, and numbers **(K)** of γδ T cells within lung live CD45$^+$ populations at 24h after CLP or sham surgery (n = 3). All data are mean ± SEM, with symbols representing the values of individual mice. *P < 0.05, **P < 0.01, ***P < 0.001, or ****P < 0.0001, n.s., not significant. One-way ANOVA in **(A, C)**; two-tailed Student's t-test in **(B, E, G, J, K)**.

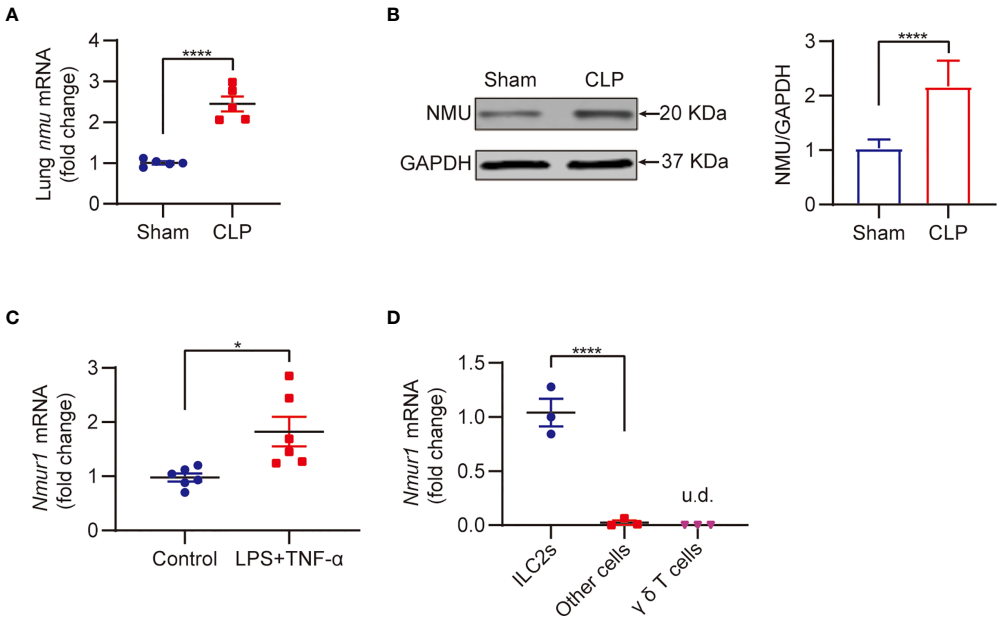

FIGURE 2 | Sepsis promotes NMU expression in the lung and NMUR1 expression in lung ILC2s. **(A, B)** Real-time PCR **(A)** and western blot **(B)** detection of lung NMU expression from CLP or sham mice at 24h (n = 3). **(C)** Real-time PCR detection of nmur1 mRNA in sorted ILC2s under the treatment of LPS + TNF-α for 24h (n = 6). **(D)** Real-time PCR detection of nmur1 mRNA in three cell populations sorted from lung at 24h after CLP surgery (n = 3). All data are mean ± SEM, with symbols representing the values of individual mice. *$P < 0.05$, ****$P < 0.0001$, u.d., undetected. One-way ANOVA in **(D)**; two-tailed Student's t-test in **(A–C)**. Densitometry of western blotting bands was quantified by ImageJ software (gray-scale band analysis) of three independent experiments, non-parametric Mann-Whitney U test.

nmur1 mRNA expression in the ILC2s treated with LPS + TNF-α is significantly increased as compared to that in the PBS treated (control) group (**Figure 2C**).

Previous studies have shown that lung *nmur1* is selectively expressed in ILC2s (22, 31). To determine this is also true in sepsis, we isolated lung cells from CLP mice, then categorized the cells into three populations, including ILC2s, γδ T cells, and other cells, using flow sorting, followed by measurement of *nmur1* expression in these three populations using real-time qPCR. The results showed that *nmur1* was specifically expressed by ILC2s, but not by γδ T cells and other cells (**Figure 2D**) (22, 31). These findings suggest that ILC2s are the major cell population to respond to the increased NMU expression in the lungs in sepsis.

NMU Promotes Lung IL-17A-Producing γδ T Cell Expansion

Based on the data shown above, we hypothesized that NMU might act through ILC2s to upregulate lung IL-17A-producing γδ T cells. To test this hypothesis, we intraperitoneally injected (i.p.) recombinant NMU into the CLP mice at 6 h before and 6 h after the CLP procedure (**Figure 3A**). We found that NMU significantly reduced the mortality of septic mice (**Figure 3A**). Furthermore, exogenous NMU increased the percentage of ILC2s (**Figures 3B, C**), IL-17A-producing cells (**Figures 3D, E**), and γδ T cells (**Figures 3F, G**) in the lungs of septic mice; whereas NMU administration did not alter the percentage of IL-17A$^+$ ILC2s (**Supplemental Figures A, B**). Given that *nmur1* is specifically expressed by ILC2s but not by γδ T cells, the increased γδ T cells in response to NMU is mediated through ILC2s.

ILC2s Mediate NMU-Induced Increase in Lung γδ T Cells

To determine the role of ILC2s in mediating NMU-induced upregulation of lung γδ T cells, we applied an *in vitro* ILC2s and γδ T cells coculture system. IL-17A was undetectable in the culture supernatant of the ILC2 alone group after NMU treatment (**Supplemental Figure C**). However, coculture of ILC2s and γδ T cells with the treatment of NMU resulted in significant increases in the number and percentage of γδ T cells (**Figures 4A–C**) and supernatant IL-17A concentrations (**Figure 4D**). NMU failed to induce γδ T cell expansion and IL-17A release in γδ T cell alone group (**Figures 4A–D**). More importantly, the supernatant IL-17A concentrations were further elevated in the ILC2-γδ T cell coculture group treated with NMU and LPS + TNF-α (**Figure 4D**).

To further establish the role of ILC2s in regulating γδ T cell expansion and IL-17A producing, we cocultured γδ T cells (5.0×10^3 cells) with different numbers of ILC2s (1.5×10^4 and 3.0×10^4 cells/well). After 48-hour coculture, the final numbers of γδ T cells in the group co-cultured with 3.0×10^4 ILC2s/well were

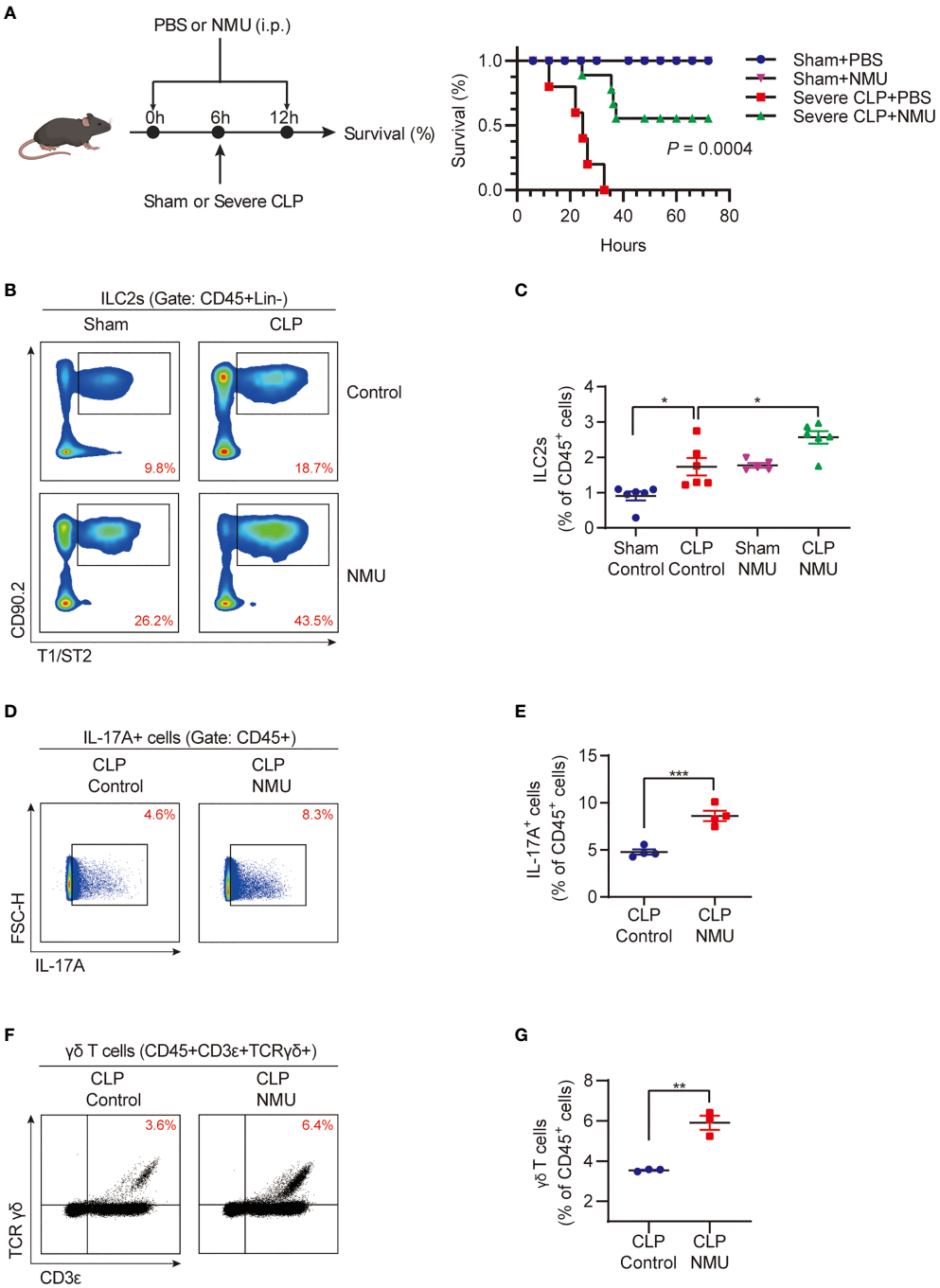

FIGURE 3 | NMU promotes lung IL-17A-producing γδ T cell expansion. **(A)** Survival study of mice monitored for 72h after CLP or sham surgery. Mice received PBS or NMU (0.2 μg/g) at 6h before and after CLP (n = 5). **(B, C) (B)** Representative flow cytometry plots for ILC2 population within lung live CD45$^+$Lineage$^-$ populations; **(C)** The percentages of ILC2s within lung live CD45$^+$ populations at 24h after CLP or sham surgery. Mice received a single dose of NMU (1 μg/g) at 6h before CLP (n = 6). **(D, E)** Representative flow cytometry plots **(D)** and percentages **(E)** of the IL-17A$^+$ cell population within lung live CD45$^+$ populations at 24h after CLP or sham surgery. Mice received a single dose of NMU (1 μg/g) at 6h before CLP (n = 4). **(F, G)** Representative flow cytometry plots **(F)** and percentages **(G)** of γδ T cell population within lung live CD45$^+$ populations at 24h after CLP or sham surgery. Mice received a single dose of NMU (1 μg/g) at 6h before CLP (n = 4). All data are mean ± SEM, with symbols representing the values of individual mice. *P < 0.05, **P < 0.01, ***P < 0.001. Kaplan–Meier analysis in **(A)** One-way ANOVA in **(C)** two-tailed Student's t-test in **(E, G)**.

~3.2-fold higher than that in the group cocultured with 1.5×10^4 ILC2s/well (**Figure 4E**); and the supernatant IL-17A concentrations of 3.0×10^4 ILC2s/well group were also significantly higher than that of 1.5×10^4 ILC2s/well group (**Figure 4F**). In addition, we treated the cocultures with different NMU concentrations (1 μg/ml and 10 μg/ml) but fixed the number of ILC2s (1.5×10^4 cells/well). We found that higher NMU concentration (10 μg/ml) induced higher numbers of γδ T cells and higher IL-17A levels as compared to the group treated with lower NMU concentration (1 μg/ml) (**Figures 4G, H**). These results further suggested that ILC2s mediate NMU-induced γδ T cell expansion and IL-17A production.

To confirm the role of NMUR1 in ILC2s in transducing NMU signaling, we knocked down *nmur1* in ILC2s using the CRISPR/Cas9 approach, which was confirmed by RT-PCR, as shown in **Figure 4I**. Knockdown of *nmur1* significantly attenuated γδ T cell expansion in response to NMU in the co-culture system (**Figures 4J–L**), and decreased IL-17A production (**Figure 4M**).

IL-9 Mediates ILC2 Regulation of γδ T Cell Expansion and IL-17A Production

Next, we wanted to identify the possible mediators that mediate the ILC2 regulation of γδ T cells in the co-culture system. Previous studies have shown that IL-1β and IL-23 can polarize γδ T cells to produce IL-17A (26–28, 32). Thus, we measured the supernatant levels of IL-1β and IL-23 and found that the concentrations of both cytokines were not changed in all groups of ILC2 cultures (**Supplemental Figures D, E**).

Our previous studies have shown that ILC2-derived IL-9 serves as an important mediator in the interaction between ILC2s and lung endothelial cells (13). Reports also showed that NMU can induce ILC2s to secrete IL-9 (18, 22), and IL-9/IL-9R signaling regulates γδ T-cell activation (33). In our current coculture experiments of ILC2 with γδ T cells, we observed a significant increase in supernatant IL-9 in response to treatment with NMU and LPS + TNF-α (**Figure 5A**). We further found that in cocultures of *nmur1* knockdown ILC2s with γδ T cells, supernatant IL-9 levels were remarkably lower than that in cocultures of WT ILC2 with γδ T cells (**Figure 5B**). In order to further determine the role of IL-9 in mediating γδ T cell activation, we knocked down IL-9 in ILC2s using a CRISPR/Cas9 approach. The efficiency of *Il9* knockdown was confirmed by detecting culture supernatant IL-9 using ELISA (**Figure 5C**). Coculture of *Il9* knockdown ILC2s with γδ T cells resulted in lower γδ T cell expansion (**Figures 5D–F**) and lower levels of supernatant IL-17A (**Figure 5G**).

To determine if other ILC2-derived cytokines are also involved in mediating the interaction between ILC2s and γδ T cells, we knocked-down IL-5 and IL-13 in ILC2s using the CRISPR/Cas9 method, respectively. We found that the knockdown of IL-5 and IL-13 in ILC2s did not affect γδ T cell expansion and IL-17A production in the co-culture system (data not shown).

Collectively, the data demonstrate an important role for IL-9 in mediating ILC2 regulation of γδ T cell expansion, activation, and subsequent production of IL-17A.

DISCUSSION

Emerging data suggested the important role of IL-17A in the regulation of inflammation (4–6, 34–36). Although most of the reports have shown that IL-17A plays a beneficial role in improving inflammation (7–10, 35, 36), several studies demonstrated detrimental effects of IL-17A in the development of inflammation (37–40). This ambiguity in the current literature, coupled with the fact that studies on the mechanism of regulation of IL-17A production in sepsis-induced lung injury are lacking, highlights the need for further elucidating how is lung IL-17A regulated and what is the role for IL-17A in the development of ALI and systemic inflammation following sepsis. In this study, we demonstrate that sepsis-induced NMU acting through NMUR1 on lung ILC2s initiates the ILC2 activation, which, in turn, promotes IL-17A-producing γδ T cell expansion and secretion of IL-17A. ILC2-derived IL-9 plays an important role in mediating γδ T cell expansion and IL-17A production.

ILC2s play an important role in bridging innate and adaptive immunities and are functionally similar to polarized Th2 cells (41). ILC2s serve as a potent player in maintaining mucosal homeostasis and host defense against infection in the septic lung (41–43). Regulation of ILC2 activation is multifaceted (44). Recently, the neuronal regulation of ILC2s has been reported (41). Various neuropeptides such as substance P, VIP, CGRP, NMU, and NMB were found to modulate ILC2s. Yet, the mechanism underlying neuronal regulation of ILC2s in sepsis remains unclear. NMU is mainly released by cholinergic sensory neurons originating from the dorsal root ganglion (DRG), but not parasympathetic neurons in the vagal ganglion (41, 45). NMU is also occasionally secreted by some antigen-presenting cells, including monocytes, B cells, and dendritic cells (46). Thus, it is suggested to play an important role in the regulation of adaptive and innate immunity. Recent studies reported that NMU from lamina propria plays a regulatory role in mice type 2 innate immunity through binding to the Nmur1, which is selectively enriched in ILC2s, and NMU-expressing neurons are close vicinity to ILC2s in the lungs (18, 19, 22). In a mice model of worm infection in the lungs and intestine, stimulation of ILC2s with NMU led to strong and immediate production of tissue protection and innate inflammatory cytokines in an NMUR1-dependent manner, thereby alleviating worm burden (18). The report also showed that NMU-activated ILC2s increase the number of lung eosinophils and mast cells, thus alleviating antihelminth responses (18, 19, 22). In this study, we discovered that the lung expression of NMU is elevated during sepsis, and NMU receptor NMUR1 is selectively expressed in the lung ILC2s. This finding suggests an important role for ILC2s as an executive cell population to mediate NMU-regulated downstream events in the lung during sepsis. Indeed, we found in our current study that NMU-induced γδ T cell expansion, activation, and IL-17A production requires ILC2s in the coculture system, and *numr1* deletion in ILC2s disabled NMU-induced γδ T cell activation.

Unlike conventional αβ T cells, γδ T cells are special T cells that exhibit distinctive antigen recognition patterns different from those of αβ T cells and have different functional subsets,

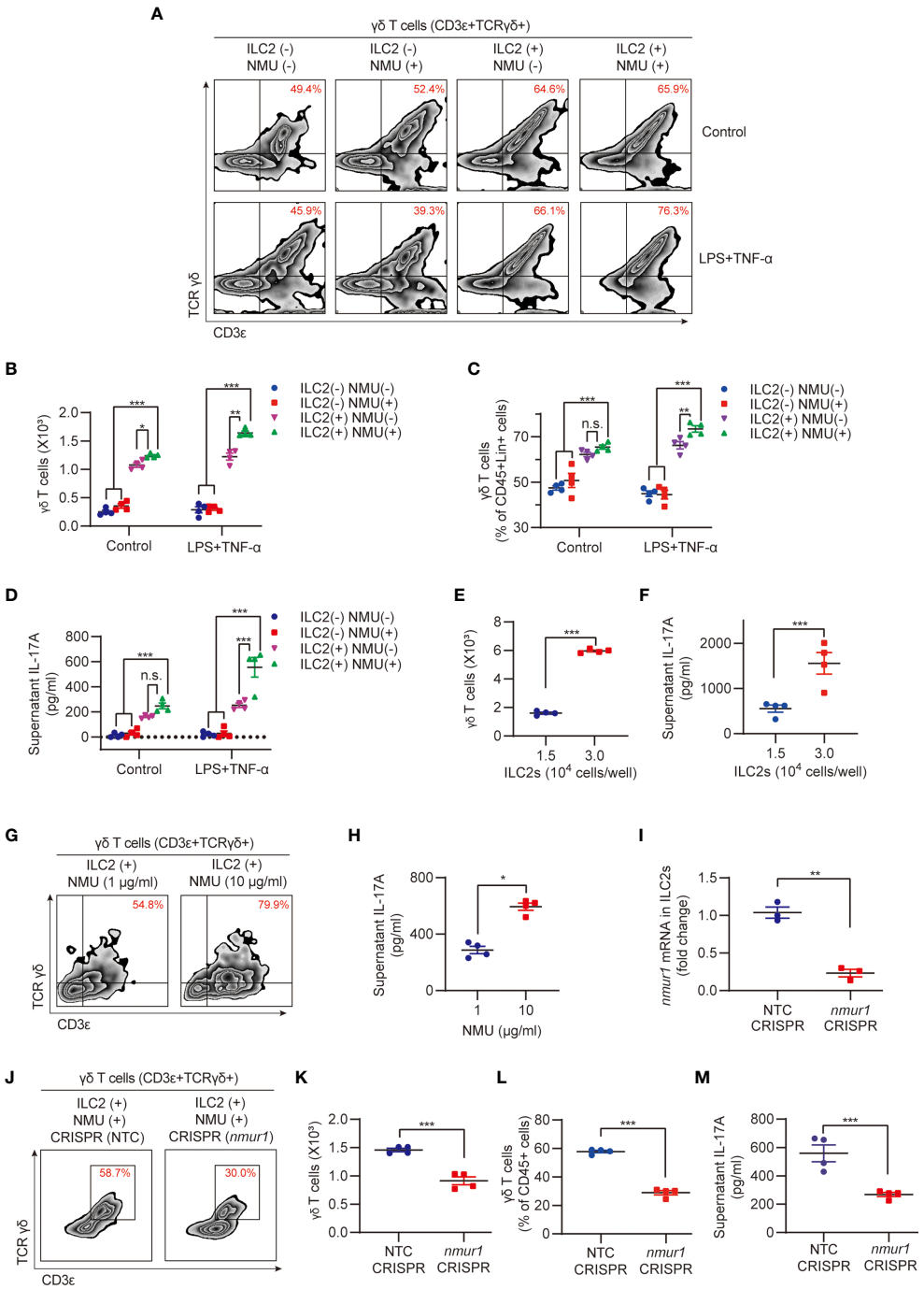

FIGURE 4 | ILC2s mediate NMU-indued increase in lung γδ T cells. **(A–D)** Representative flow cytometry plots **(A)**, numbers **(B)**, percentages **(C)** of γδ T cell population, and ELISA analysis **(D)** of supernatant IL-17A in different groups. ILC2s and γδ T cells were co-cultured for 48h with or without NMU (10 μg/ml). IL-1β (100 ng/ml) and IL-23 (100 ng/ml) were added to polarize IL-17A-producing γδ T cells, LPS (1 μg/ml) plus TNF-α (20 ng/ml) were added to mimic sepsis stimulation (n = 4). **(E, F)** Numbers **(E)** of γδ T cell population and ELISA analysis **(F)** of supernatant IL-17A in groups co-cultured with different numbers of ILC2s. ILC2s and γδ T cells were co-cultured for 48 hours with NMU (10 μg/ml) (n = 4). **(G, H)** Representative flow cytometry plots **(G)** of γδ T cell population and ELISA analysis **(H)** of supernatant IL-17A in co-culture group with different concentrations of NMU (1 or 10 μg/ml). ILC2s and γδ T cells were co-cultured for 48h (n = 4). **(I)** Real-time PCR detection of *nmur1* mRNA in ILC2s after *nmur1* sgRNA transfection using CRISPR/Cas9 approach for 48h (n = 3). **(J–M)** Representative flow cytometry plots **(J)**, numbers **(K)**, percentages **(L)** of γδ T cell population, and ELISA analysis **(M)** of supernatant IL-17A in control and *nmur1* knockdown groups. ILC2s and γδ T cells were co-cultured for 48h (n = 4). All data are mean ± SEM, with symbols representing the values of individual mice. $^{*}P < 0.05$, $^{**}P < 0.01$, $^{***}P < 0.001$, n.s., not significant. One-way ANOVA in **(B–D)**; two-tailed Student's t-test in **(E, F, H, I, K–M)**.

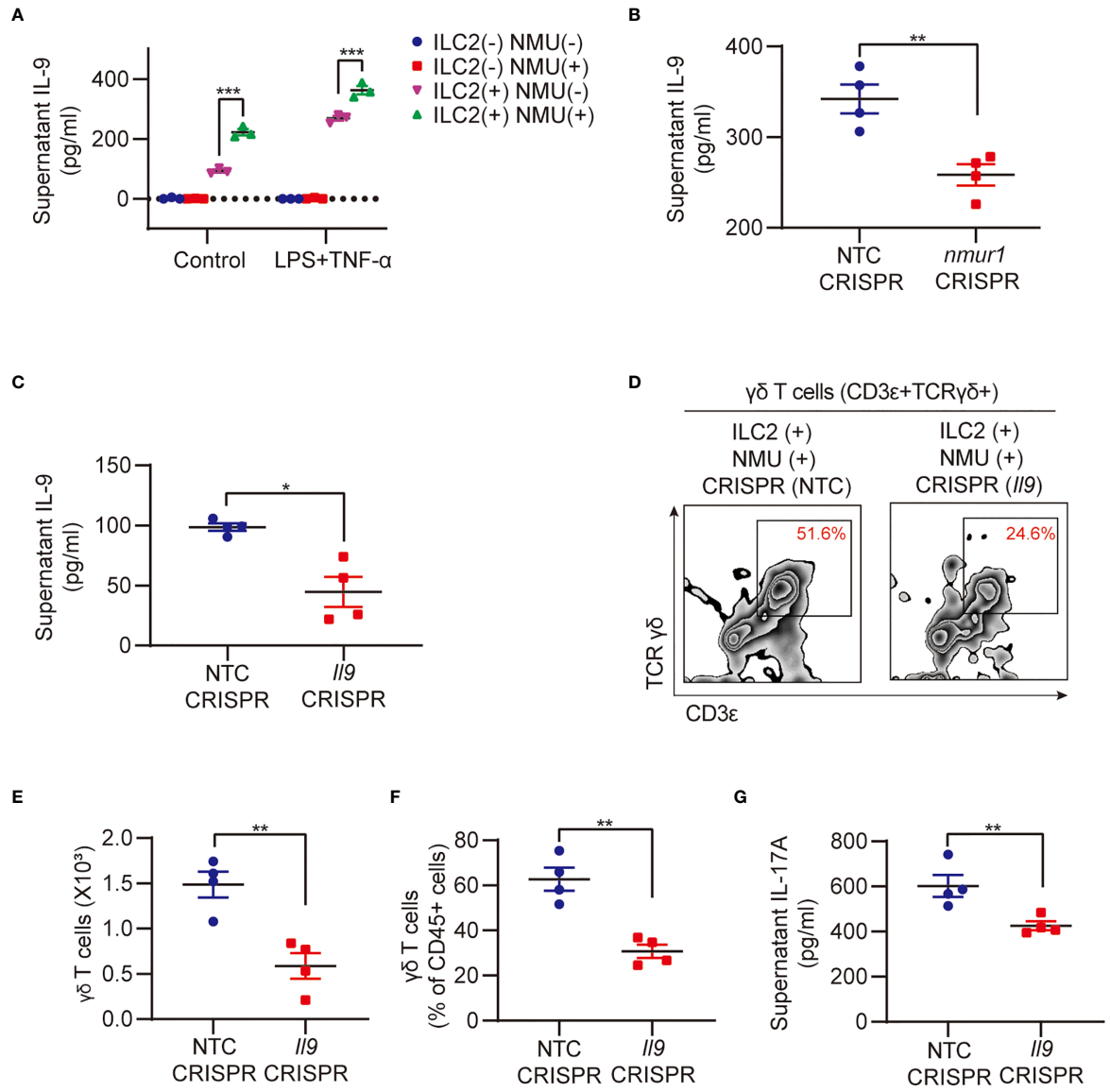

FIGURE 5 | IL-9 mediates ILC2 regulation of γδ T cell expansion and IL-17A production. **(A)** ELISA analysis of supernatant IL-9 in different groups (n = 3). ILC2s and γδ T cells were co-cultured for 48h with or without NMU (10 μg/ml). **(B)** ELISA analysis of supernatant IL-9 in groups after *nmur1* sgRNA transfection using CRISPR/Cas9 approach for 48h and then co-cultured with γδ T cells for 48h (n = 4). **(C)** ELISA analysis of supernatant IL-9 in groups after *Il9* sgRNA transfection using CRISPR/Cas9 approach for 48h (n = 4). **(D–G)** Representative flow cytometry plots **(D)**, numbers **(E)**, percentages **(F)** of γδ T cell population, and ELISA analysis **(G)** of supernatant IL-17A in control and *Il9* knockdown groups. ILC2s and γδ T cells were co-cultured for 48h (n = 4). All data are mean ± SEM, with symbols representing the values of individual mice. $^{*}P < 0.05$, $^{**}P < 0.01$, $^{***}P < 0.001$. One-way ANOVA in **(A)**; two-tailed Student's t-test in **(B, C, E, F, G)**.

defined by the several usages of Vδ and Vγ gene repertoire (47, 48). Antigen processing is not required for γδ T cells to recognize an infection, since γδ T cells can quickly react to various antigens *via* innate surface receptors (49–52) and secret high levels of IL-17A and IFN-γ, both are signature cytokines of γδ T cells (53–57). γδ T cells are a major innate source of IL-17A in the mouse and occupy mostly barrier surfaces, such as the skin and mucosa, as well as secondary lymphoid organs (58, 59). γδ T cells play critical roles in the regulation of inflammation in mouse sepsis model (36, 60–64). The accumulation of γδ T cells in the lungs of CLP mice associates beneficial outcomes of septic mice (60, 61). The protective functions of γδ T cells during experimental sepsis have been attributed to the production of IL-17A, which improves bacterial clearance and triggers neutrophil recruitment (36, 65–67).

ILC2s and γδ T cells share several similarities. γδ T cells are also considered as a bridge linking innate and adaptive immune systems. A recent study showed that tissue-resident lung ILC2s have *TCRγ*

gene rearrangements similar to γδ T cells under steady-state conditions. Rearranged *TCRγ* gene in ILC2s is nonfunctional and aberrant, and thus, it is suggested that ILC2s may arise from failed γδ T cell development (68). Given the similarities between ILC2s and γδ T cells in the immune system, we aimed to gain an insight into the interaction between ILC2s and γδ T cells, particularly, pertaining to the precise regulation of lung IL-17A production in sepsis, as the source of IL-17A is controversial. The data from the current study showed that ILC2s can secret IL-17A. However, IL-17A-producing ILC2s only occupy ~2% of total IL-17A-producing cells. ILC2s are not the major source of IL-17A in the lung in sepsis. Our results then showed that ILC2s increase the number of IL-17A-producing γδ T cells, which associate with increased IL-17A secretion. These ILC2s-induced increases can be further exacerbated by NMU and LPS + TNF-α septic treatment. These results establish a determinate role for ILC2s in upregulation of γδ T cell expansion and production of IL-17A in the lung in sepsis.

Recently, IL-9 has been reported to be involved, either beneficially or deleteriously, in the pathogenesis of some diseases related to inflammation (69, 70). ILC2 is the main source of IL-9 in mouse lung tissue in physiological or inflammatory circumstances (71). Our data showed that the knockdown of *Il9* in ILC2s decreases the number of IL-17A-producing γδ T cells, which associates with decreased IL-17A secretion, in response to NUM and LPS + TNF-α. These findings strongly suggest a role for IL-9 in mediating the ILC2 regulation of IL-17A-producing γδ T cell expansion and secretion of IL-17A.

In summary, this study shows that NMU acting through NMUR1 on lung ILC2s initiates the ILC2 activation, which, in turn, promotes IL-17A-producing γδ T cell expansion and IL-17A secretion. ILC2-derived IL-9 plays an important role in mediating γδ T cell expansion and IL-17A production. This study explores a new mechanism underlying neuronal regulation of innate immunity in sepsis.

DATA AVAILABILITY STATEMENT

The raw data supporting the conclusions of this article will be made available by the authors, without undue reservation.

ETHICS STATEMENT

The animal study was reviewed and approved by Institutional Animal Care and Use Committee of the University of Pittsburgh, VA Pittsburgh Healthcare System Institutional Animal Care and Use Committee of the Children's Hospital, Zhejiang University School of Medicine.

AUTHOR CONTRIBUTIONS

WC conducted the experiments, collected the data, performed the data analysis, and drafted the manuscript. WC, XF, JF, and QS conceived and designed the study. DL, YL, XW, and YP selected and collected the samples. XF, JF, and QS reviewed and finalized the manuscript. All authors contributed to the article and approved the submitted version.

FUNDING

This work was supported by the Zhejiang Provincial Program for the Cultivation of High-level Innovative Health talents 2016-6 (QS), the National Natural Science Foundation of China 81671956 (QS), the National Natural Science Foundation of China 81901989 (DL), China Postdoctoral Science Foundation 2019M652108 (DL), Natural Science Foundation of Zhejiang Province LY21H150005 (DL). This work was supported by the VA Merit Awards 1I01BX002729 (JF) and 1I01 BX004838 (JF), and VA BLR&D Award 1IK6BX004211 (JF). WC was supported in part by a two-year China Scholarship Council scholarship 201806320166. The funders had no role in study design, data collection and analysis, decision to publish, or preparation of the manuscript.

SUPPLEMENTARY MATERIAL

The Supplementary Material for this article can be found online at: https://www.frontiersin.org/articles/10.3389/fimmu.2021.670676/full#supplementary-material

Supplementary Figure | (A) Representative flow cytometry plots for IL-17A$^+$ILC2 population within lung live CD45$^+$Lineage$^-$CD90.2$^+$ populations at 24h after CLP. **(B)** The percentages of IL-17A$^+$ ILC2 population within lung ILC2 population at 24h after CLP (n = 6). **(C)** ELISA analysis of supernatant IL-17A in ILC2 alone group. ILC2s were treated with NMU (10 μg/ml) (n = 3). **(D, E)** ELISA analysis of supernatant IL-1β **(D)** and IL-23 **(E)** in different groups. ILC2s and γδ T cells were co-cultured for 48h with or without NMU (10 μg/ml). IL-1β (100 ng/ml) and IL-23 (100 ng/ml) were added to polarize IL-17A-producing γδ T cells, LPS (1 μg/ml) plus TNF-α (20 ng/ml) were added to mimic sepsis stimulation (n = 3). All data are mean ± SEM. n.s., not significant, u.d., undetected. One-way ANOVA in **(D, E)**; two-tailed Student's t-test in **(B)**.

REFERENCES

1. Cecconi M, Evans L, Levy M, Rhodes A. Sepsis and Septic Shock. *Lancet* (2018) 392(10141):75–87. doi: 10.1016/S0140-6736(18)30696-2
2. Fisher BJ, Kraskauskas D, Martin EJ, Farkas D, Wegelin JA, Brophy D, et al. Mechanisms of Attenuation of Abdominal Sepsis Induced Acute Lung Injury by Ascorbic Acid. *Am J Physiol Lung Cell Mol Physiol* (2012) 303(1):L20–32. doi: 10.1152/ajplung.00300.2011
3. Santacruz CA, Pereira AJ, Celis E, Vincent JL. Which Multicenter Randomized Controlled Trials in Critical Care Medicine Have Shown Reduced Mortality? *A Systematic Review Crit Care Med* (2019) 47 (12):1680–91. doi: 10.1097/CCM.0000000000004000
4. Li Y, Wei C, Xu H, Jia J, Wei Z, Guo R, et al. The Immunoregulation of Th17 in Host Against Intracellular Bacterial Infection. *Mediators Inflammation* (2018) 2018:6587296. doi: 10.1155/2018/6587296

5. Chamoun MN, Blumenthal A, Sullivan MJ, Schembri MA, Ulett GC. Bacterial Pathogenesis and interleukin-17: Interconnecting Mechanisms of Immune Regulation, Host Genetics, and Microbial Virulence That Influence Severity of Infection. *Crit Rev Microbiol* (2018) 44(4):465–86. doi: 10.1080/1040841X.2018.1426556
6. Gouda MM, Bhandary YP. Acute Lung Injury: IL-17A-Mediated Inflammatory Pathway and Its Regulation by Curcumin. *Inflammation* (2019) 42(4):1160–9. doi: 10.1007/s10753-019-01010-4
7. Freitas A, Alves-Filho JC, Victoni T, Secher T, Lemos HP, Sônego F, et al. Il-17 Receptor Signaling is Required to Control Polymicrobial Sepsis. *J Immunol* (2009) 182(12):7846–54. doi: 10.4049/jimmunol.0803039
8. Ogiku M, Kono H, Hara M, Tsuchiya M, Fujii H. Interleukin-17A Plays a Pivotal Role in Polymicrobial Sepsis According to Studies Using IL-17A Knockout Mice. *J Surg Res* (2012) 174(1):142–9. doi: 10.1016/j.jss.2010.11.901
9. Costa MF, de Negreiros CB, Bornstein VU, Valente RH, Mengel J, Henriques M, et al. Murine IL-17+ Vγ4 T Lymphocytes Accumulate in the Lungs and Play a Protective Role During Severe Sepsis. *BMC Immunol* (2015) 16:36. doi: 10.1186/s12865-015-0098-8
10. Ramakrishnan SK, Zhang H, Ma X, Jung I, Schwartz AJ, Triner D, et al. Intestinal non-Canonical Nfκb Signaling Shapes the Local and Systemic Immune Response. *Nat Commun* (2019) 10(1):660. doi: 10.1038/s41467-019-08581-8
11. Cua DJ, Tato CM. Innate IL-17-producing Cells: The Sentinels of the Immune System. *Nat Rev Immunol* (2010) 10(7):479–89. doi: 10.1038/nri2800
12. McGeachy MJ, Cua DJ, Gaffen SL. The IL-17 Family of Cytokines in Health and Disease. *Immunity* (2019) 50(4):892–906. doi: 10.1016/j.immuni.2019.03.021
13. Lai D, Tang J, Chen L, Fan EK, Scott MJ, Li Y, et al. Group 2 Innate Lymphoid Cells Protect Lung Endothelial Cells From Pyroptosis in Sepsis. *Cell Death Dis* (2018) 9(3):369. doi: 10.1038/s41419-018-0412-5
14. Huang Y, Guo L, Qiu J, Chen X, Hu-Li J, Siebenlist U, et al. Il-25-responsive, Lineage-Negative KLRG1(hi) Cells are Multipotential 'Inflammatory' Type 2 Innate Lymphoid Cells. *Nat Immunol* (2015) 16(2):161–9. doi: 10.1038/ni.3078
15. Zhang K, Xu X, Pasha MA, Siebel CW, Costello A, Haczku A, et al. Cutting Edge: Notch Signaling Promotes the Plasticity of Group-2 Innate Lymphoid Cells. *J Immunol* (2017) 198(5):1798–803. doi: 10.4049/jimmunol.1601421
16. Koyasu S. Inflammatory ILC2 Cells: Disguising Themselves as Progenitors? *Nat Immunol* (2015) 16(2):133–4. doi: 10.1038/ni.3080
17. Cai T, Qiu J, Ji Y, Li W, Ding Z, Suo C, et al. IL-17-Producing ST2(+) Group 2 Innate Lymphoid Cells Play a Pathogenic Role in Lung Inflammation. *J Allergy Clin Immunol* (2019) 143(1):229–244 e9. doi: 10.1016/j.jaci.2018.03.007
18. Cardoso V, Chesne J, Ribeiro H, Garcia-Cassani B, Carvalho T, Bouchery T, et al. Neuronal Regulation of Type 2 Innate Lymphoid Cells Via Neuromedin U. *Nature* (2017) 549(7671):277–81. doi: 10.1038/nature23469
19. Wallrapp A, Riesenfeld SJ, Burkett PR, Abdulnour RE, Nyman J, Dionne D, et al. The Neuropeptide NMU Amplifies ILC2-driven Allergic Lung Inflammation. *Nature* (2017) 549(7672):351–6. doi: 10.1038/nature24029
20. Nagashima H, Mahlakõiv T, Shih HY, Davis FP, Meylan F, Huang Y, et al. Neuropeptide CGRP Limits Group 2 Innate Lymphoid Cell Responses and Constrains Type 2 Inflammation. *Immunity* (2019) 51(4):682–95.e6. doi: 10.1016/j.immuni.2019.06.009
21. Galle-Treger L, Suzuki Y, Patel N, Sankaranarayanan I, Aron JL, Maazi H, et al. Nicotinic Acetylcholine Receptor Agonist Attenuates ILC2-dependent Airway Hyperreactivity. *Nat Commun* (2016) 7:13202. doi: 10.1038/ncomms13202
22. Klose CSN, Mahlakoiv T, Moeller JB, Rankin LC, Flamar AL, Kabata H, et al. The Neuropeptide Neuromedin U Stimulates Innate Lymphoid Cells and Type 2 Inflammation. *Nature* (2017) 549(7671):282–6. doi: 10.1038/nature23676
23. Piliponsky AM, Chen CC, Grimbaldeston MA, Burns-Guydish SM, Hardy J, Kalesnikoff J, et al. Mast Cell-Derived TNF can Exacerbate Mortality During Severe Bacterial Infections in C57BL/6-KitW-sh/W-sh Mice. *Am J Pathol* (2010) 176(2):926–38. doi: 10.2353/ajpath.2010.090342
24. Moro K, Ealey KN, Kabata H, Koyasu S. Isolation and Analysis of Group 2 Innate Lymphoid Cells in Mice. *Nat Protoc* (2015) 10(5):792–806. doi: 10.1038/nprot.2015.047
25. von Moltke J, O'Leary CE, Barrett NA, Kanaoka Y, Austen KF, Locksley RM. Leukotrienes Provide an NFAT-dependent Signal That Synergizes With IL-33 to Activate ILC2s. *J Exp Med* (2017) 214(1):27–37. doi: 10.1084/jem.20161274
26. Ribot JC, Serre K, Silva-Santos B. Developmental and Functional Assays to Study Murine and Human γδ T Cells. *Methods Mol Biol* (2017) 1514:257–67. doi: 10.1007/978-1-4939-6548-9_18
27. Sutton CE, Lalor SJ, Sweeney CM, Brereton CF, Lavelle EC, Mills KH. Interleukin-1 and IL-23 Induce Innate IL-17 Production From Gammadelta T Cells, Amplifying Th17 Responses and Autoimmunity. *Immunity* (2009) 31(2):331–41. doi: 10.1016/j.immuni.2009.08.001
28. Lopes N, McIntyre C, Martin S, Raverdeau M, Sumaria N, Kohlgruber AC, et al. Distinct Metabolic Programs Established in the Thymus Control Effector Functions of γδ T Cell Subsets in Tumor Microenvironments. *Nat Immunol* (2021) 22(2):179–92. doi: 10.1038/s41590-020-00848-3
29. de Jong HK, van der Poll T, Wiersinga WJ. The Systemic Pro-Inflammatory Response in Sepsis. *J Innate Immun* (2010) 2(5):422–30. doi: 10.1159/000316286
30. Amatya N, Garg AV, Gaffen SL. Il-17 Signaling: The Yin and the Yang. *Trends Immunol* (2017) 38(5):310–22. doi: 10.1016/j.it.2017.01.006
31. Loser S, Maizels RM. Immunology: The Neuronal Pathway to Mucosal Immunity. *Curr Biol* (2018) 28(1):R33–6. doi: 10.1016/j.cub.2017.11.025
32. Gasse P, Riteau N, Vacher R, Michel ML, Fautrel A, di Padova F, et al. IL-1 and IL-23 Mediate Early IL-17A Production in Pulmonary Inflammation Leading to Late Fibrosis. *PloS One* (2011) 6(8):e23185. doi: 10.1371/journal.pone.0023185
33. Guggino G, Ciccia F, Di Liberto D, Lo Pizzo M, Ruscitti P, Cipriani P, et al. Interleukin (Il)-9/IL-9R Axis Drives γδ T Cells Activation in Psoriatic Arthritis Patients. *Clin Exp Immunol* (2016) 186(3):277–83. doi: 10.1111/cei.12853
34. Iwakura Y, Nakae S, Saijo S, Ishigame H. The Roles of IL-17A in Inflammatory Immune Responses and Host Defense Against Pathogens. *Immunol Rev* (2008) 226:57–79. doi: 10.1111/j.1600-065X.2008.00699.x
35. O'Connor W, Kamanaka M, Booth CJ, Town T, Nakae S, Iwakura Y, et al. A Protective Function for Interleukin 17A in T Cell-Mediated Intestinal Inflammation. *Nat Immunol* (2009) 10(6):603–9. doi: 10.1038/ni.1736
36. Flierl MA, Rittirsch D, Gao H, Hoesel LM, Nadeau BA, Day DE, et al. Adverse Functions of IL-17A in Experimental Sepsis. *FASEB J* (2008) 22(7):2198–205. doi: 10.1096/fj.07-105221
37. Rendon JL, Choudhry MA. Th17 Cells: Critical Mediators of Host Responses to Burn Injury and Sepsis. *J Leukoc Biol* (2012) 92(3):529–38. doi: 10.1189/jlb.0212083
38. Wynn JL, Wilson CS, Hawiger J, Scumpia PO, Marshall AF, Liu JH, et al. Targeting IL-17A Attenuates Neonatal Sepsis Mortality Induced by IL-18. *Proc Natl Acad Sci USA* (2016) 113(19):E2627–35. doi: 10.1073/pnas.1515793113
39. Schüler R, Brand A, Klebow S, Wild J, Veras FP, Ullmann E, et al. Antagonization of IL-17A Attenuates Skin Inflammation and Vascular Dysfunction In Mouse Models of Psoriasis. *J Invest Dermatol* (2019) 139(3):638–47. doi: 10.1016/j.jid.2018.09.021
40. Yadava K, Pattaroni C, Sichelstiel AK, Trompette A, Gollwitzer ES, Salami O, et al. Microbiota Promotes Chronic Pulmonary Inflammation by Enhancing Il-17A and Autoantibodies. *Am J Respir Crit Care Med* (2016) 193(9):975–87. doi: 10.1164/rccm.201504-0779OC
41. Chen W, Shu Q, Fan J. Neural Regulation of Interactions Between Group 2 Innate Lymphoid Cells and Pulmonary Immune Cells. *Front Immunol* (2020) 11:576929. doi: 10.3389/fimmu.2020.576929
42. Branzk N, Gronke K, Diefenbach A. Innate Lymphoid Cells, Mediators of Tissue Homeostasis, Adaptation and Disease Tolerance. *Immunol Rev* (2018) 286(1):86–101. doi: 10.1111/imr.12718
43. Sonnenberg GF, Artis D. Innate Lymphoid Cells in the Initiation, Regulation and Resolution of Inflammation. *Nat Med* (2015) 21(7):698–708. doi: 10.1038/nm.3892
44. Kabata H, Moro K, Koyasu S. The Group 2 Innate Lymphoid Cell (ILC2) Regulatory Network and its Underlying Mechanisms. *Immunol Rev* (2018) 286(1):37–52. doi: 10.1111/imr.12706
45. Moriyama M, Furue H, Katafuchi T, Teranishi H, Sato T, Kano T, et al. Presynaptic Modulation by Neuromedin U of Sensory Synaptic Transmission

in Rat Spinal Dorsal Horn Neurones. *J Physiol* (2004) 559(Pt 3):707–13. doi: 10.1113/jphysiol.2004.070110
46. Hedrick JA, Morse K, Shan L, Qiao X, Pang L, Wang S, et al. Identification of a Human Gastrointestinal Tract and Immune System Receptor for the Peptide Neuromedin U. *Mol Pharmacol* (2000) 58(4):870–5. doi: 10.1124/mol.58.4.870
47. Vantourout P, Hayday A. Six-of-the-Best: Unique Contributions of γδ T Cells to Immunology. *Nat Rev Immunol* (2013) 13(2):88–100. doi: 10.1038/nri3384
48. Carding SR, Egan PJ. Gammadelta T Cells: Functional Plasticity and Heterogeneity. *Nat Rev Immunol* (2002) 2(5):336–45. doi: 10.1038/nri797
49. Hedges JF, Lubick KJ, Jutila MA. Gamma Delta T Cells Respond Directly to Pathogen-Associated Molecular Patterns. *J Immunol* (2005) 174(10):6045–53. doi: 10.4049/jimmunol.174.10.6045
50. Welsh KJ, Risin SA, Actor JK, Hunter RL. Immunopathology of Postprimary Tuberculosis: Increased T-regulatory Cells and DEC-205-positive Foamy Macrophages in Cavitary Lesions. *Clin Dev Immunol* (2011) 2011:307631. doi: 10.1155/2011/307631
51. Uldrich AP, Le Nours J, Pellicci DG, Gherardin NA, McPherson KG, Lim RT, et al. CD1d-Lipid Antigen Recognition by the γδ Tcr. *Nat Immunol* (2013) 14 (11):1137–45. doi: 10.1038/ni.2713
52. Raulet DH, Gasser S, Gowen BG, Deng W, Jung H. Regulation of Ligands for the NKG2D Activating Receptor. *Annu Rev Immunol* (2013) 31:413–41. doi: 10.1146/annurev-immunol-032712-095951
53. Silva-Santos B. γδ Cells Making IL-17. *Blood* (2011) 118(1):3–5. doi: 10.1182/blood-2011-05-351726
54. Ribot JC, deBarros A, Pang DJ, Neves JF, Peperzak V, Roberts SJ, et al. CD27 is a Thymic Determinant of the Balance Between Interferon-Gamma- and Interleukin 17-Producing Gammadelta T Cell Subsets. *Nat Immunol* (2009) 10(4):427–36. doi: 10.1038/ni.1717
55. Wu P, Wu D, Ni C, Ye J, Chen W, Hu G, et al. γδt17 Cells Promote the Accumulation and Expansion of Myeloid-Derived Suppressor Cells in Human Colorectal Cancer. *Immunity* (2014) 40(5):785–800. doi: 10.1016/j.immuni.2014.03.013
56. Haas JD, González FH, Schmitz S, Chennupati V, Föhse L, Kremmer E, et al. CCR6 and NK1.1 Distinguish Between IL-17A and IFN-gamma-producing Gammadelta Effector T Cells. *Eur J Immunol* (2009) 39(12):3488–97. doi: 10.1002/eji.200939922
57. Kong X, Sun R, Chen Y, Wei H, Tian Z. γδt Cells Drive Myeloid-Derived Suppressor Cell-Mediated CD8+ T Cell Exhaustion in Hepatitis B Virus-Induced Immunotolerance. *J Immunol* (2014) 193(4):1645–53. doi: 10.4049/jimmunol.1303432
58. Zheng J, Liu Y, Lau YL, Tu W. γδ-T Cells: An Unpolished Sword in Human Anti-Infection Immunity. *Cell Mol Immunol* (2013) 10(1):50–7. doi: 10.1038/cmi.2012.43
59. Papotto PH, Ribot JC, Silva-Santos B. Il-17+ Gammadelta T Cells as Kick-Starters of Inflammation. *Nat Immunol* (2017) 18(6):604–11. doi: 10.1038/ni.3726
60. Hirsh MI, Hashiguchi N, Chen Y, Yip L, Junger WG. Surface Expression of HSP72 by LPS-stimulated Neutrophils Facilitates Gammadeltat Cell-Mediated Killing. *Eur J Immunol* (2006) 36(3):712–21. doi: 10.1002/eji.200535422
61. Chung CS, Watkins L, Funches A, Lomas-Neira J, Cioffi WG, Ayala A. Deficiency of Gammadelta T Lymphocytes Contributes to Mortality and Immunosuppression in Sepsis. *Am J Physiol Regul Integr Comp Physiol* (2006) 291(5):R1338–43. doi: 10.1152/ajpregu.00283.2006
62. Enoh VT, Lin SH, Lin CY, Toliver-Kinsky T, Murphey ED, Varma TK, et al. Mice Depleted of Alphabeta But Not Gammadelta T Cells are Resistant to Mortality Caused by Cecal Ligation and Puncture. *Shock* (2007) 27(5):507–19. doi: 10.1097/SHK.0b013e31802b5d9f
63. Tschöp J, Martignoni A, Goetzman HS, Choi LG, Wang Q, Noel JG, et al. Gammadelta T Cells Mitigate the Organ Injury and Mortality of Sepsis. *J Leukoc Biol* (2008) 83(3):581–8. doi: 10.1189/jlb.0707507
64. Xu R, Wang R, Han G, Wang J, Chen G, Wang L, et al. Complement C5a Regulates IL-17 by Affecting the Crosstalk Between DC and Gammadelta T Cells in CLP-induced Sepsis. *Eur J Immunol* (2010) 40(4):1079–88. doi: 10.1002/eji.200940015
65. Kasten KR, Prakash PS, Unsinger J, Goetzman HS, England LG, Cave CM, et al. Interleukin-7 (Il-7) Treatment Accelerates Neutrophil Recruitment Through Gamma Delta T-cell Il-17 Production in a Murine Model of Sepsis. *Infect Immun* (2010) 78(11):4714–22. doi: 10.1128/IAI.00456-10
66. Rice L, Orlow D, Ceonzo K, Stahl GL, Tzianabos AO, Wada H, et al. Cpg Oligodeoxynucleotide Protection in Polymicrobial Sepsis is Dependent on Interleukin-17. *J Infect Dis* (2005) 191(8):1368–76. doi: 10.1086/428452
67. Alves-Filho JC, Sônego F, Souto FO, Freitas A, Verri WA, Auxiliadora-Martins M, et al. Interleukin-33 Attenuates Sepsis by Enhancing Neutrophil Influx to the Site of Infection. *Nat Med* (2010) 16(6):708–12. doi: 10.1038/nm.2156
68. Shin SB, Lo BC, Ghaedi M, Scott RW, Li Y, Messing M, et al. Abortive γδtcr Rearrangements Suggest ILC2s are Derived From T-cell Precursors. *Blood Adv* (2020) 4(21):5362–72. doi: 10.1182/bloodadvances.2020002758
69. Zhang W, Tang T, Nie D, Wen S, Jia C, Zhu Z, et al. IL-9 Aggravates the Development of Atherosclerosis in ApoE-/- Mice. *Cardiovasc Res* (2015) 106 (3):453–64. doi: 10.1093/cvr/cvv110
70. Mohapatra A, Van Dyken SJ, Schneider C, Nussbaum JC, Liang HE, Locksley RM. Group 2 Innate Lymphoid Cells Utilize the IRF4-IL-9 Module to Coordinate Epithelial Cell Maintenance of Lung Homeostasis. *Mucosal Immunol* (2016) 9(1):275–86. doi: 10.1038/mi.2015.59
71. Nascimento DC, Melo PH, Piñeros AR, Ferreira RG, Colón DF, Donate PB, et al. Il-33 Contributes to Sepsis-Induced Long-Term Immunosuppression by Expanding the Regulatory T Cell Population. *Nat Commun* (2017) 8:14919. doi: 10.1038/ncomms14919

Conflict of Interest: The authors declare that the research was conducted in the absence of any commercial or financial relationships that could be construed as a potential conflict of interest.

frontiers in Immunology

ORIGINAL RESEARCH
published: 07 June 2021
doi: 10.3389/fimmu.2021.671935

Sodium Thiosulfate Improves Intestinal and Hepatic Microcirculation Without Affecting Mitochondrial Function in Experimental Sepsis

Jan Schulz, Sandra Kramer, Yasin Kanatli, Anne Kuebart, Inge Bauer, Olaf Picker, Christian Vollmer, Richard Truse† and Anna Herminghaus†*

Department of Anesthesiology, University Hospital Duesseldorf, Duesseldorf, Germany

OPEN ACCESS

Edited by:
Marcin Filip Osuchowski, Ludwig Boltzmann Institute for Experimental and Clinical Traumatology, Austria

Reviewed by:
Xiao Wang, Ann & Robert H. Lurie Children's Hospital of Chicago, United States
Christian Lehmann, Dalhousie University, Canada

***Correspondence:**
Jan Schulz
Jan.Schulz@med.uni-duesseldorf.de

†These authors have contributed equally to this work and share last authorship

Specialty section:
This article was submitted to Inflammation, a section of the journal Frontiers in Immunology

Received: *24 February 2021*
Accepted: *18 May 2021*
Published: *07 June 2021*

Citation:
Schulz J, Kramer S, Kanatli Y, Kuebart A, Bauer I, Picker O, Vollmer C, Truse R and Herminghaus A (2021) Sodium Thiosulfate Improves Intestinal and Hepatic Microcirculation Without Affecting Mitochondrial Function in Experimental Sepsis. Front. Immunol. 12:671935. doi: 10.3389/fimmu.2021.671935

Introduction: In the immunology of sepsis microcirculatory and mitochondrial dysfunction in the gastrointestinal system are important contributors to mortality. Hydrogen sulfide (H_2S) optimizes gastrointestinal oxygen supply and mitochondrial respiration predominantly *via* K(ATP)-channels. Therefore, we tested the hypothesis that sodium thiosulfate (STS), an inducer of endogenous H_2S, improves intestinal and hepatic microcirculation and mitochondrial function *via* K(ATP)-channels in sepsis.

Methods: In 40 male Wistar rats colon ascendens stent peritonitis (CASP) surgery was performed to establish sepsis. Animals were randomized into 4 groups (1: STS 1 g • kg^{-1} i.p., 2: glibenclamide (GL) 5 mg • kg^{-1} i.p., 3: STS + GL, 4: vehicle (VE) i.p.). Treatment was given directly after CASP-surgery and 24 hours later. Microcirculatory oxygenation (μHBO_2) and flow (µflow) of the colon and the liver were continuously recorded over 90 min using tissue reflectance spectrophotometry. Mitochondrial oxygen consumption in tissue homogenates was determined with respirometry. Statistic: two-way ANOVA + Dunnett´s and Tukey post - hoc test (microcirculation) and Kruskal-Wallis test + Dunn's multiple comparison test (mitochondria). $p < 0.05$ was considered significant.

Results: STS increased μHbO_2 (colon: 90 min: + 10.4 ± 18.3%; liver: 90 min: + 5.8 ± 9.1%; $p < 0.05$ vs. baseline). Furthermore, STS ameliorated µflow (colon: 60 min: + 51.9 ± 71.1 aU; liver: 90 min: + 22.5 ± 20.0 aU; $p < 0.05$ vs. baseline). In both organs, μHbO_2 and µflow were significantly higher after STS compared to VE. The combination of STS and GL increased colonic μHbO_2 and µflow (μHbO_2 90 min: + 8.7 ± 11.5%; µflow: 90 min: + 41.8 ± 63.3 aU; $p < 0.05$ vs. baseline), with significantly higher values compared to VE. Liver μHbO_2 and µflow did not change after STS and GL. GL alone did not change colonic or hepatic μHbO_2 or µflow. Mitochondrial oxygen consumption and macrohemodynamic remained unaltered.

Conclusion: The beneficial effect of STS on intestinal and hepatic microcirculatory oxygenation in sepsis seems to be mediated by an increased microcirculatory perfusion

and not by mitochondrial respiratory or macrohemodynamic changes. Furthermore, the effect of STS on hepatic but not on intestinal microcirculation seems to be K(ATP)-channel-dependent.

Keywords: sodium thiosulfate, glibenclamide, microcirculation, mitochondria, gut, rat, sepsis

INTRODUCTION

Sepsis and the consecutive multiorgan dysfunction syndrome (MODS) are still a major burden in critical care medicine (1). To prevent MODS, it is of increasing clinical interest to maintain gastrointestinal as well as liver microcirculatory and mitochondrial function and thereby ensure adequate organ performance (2, 3). Insufficient blood supply might lead to gastrointestinal barrier failure with translocation of bacteria and toxins in the blood and lymph system, hypoxic hepatitis and a dysfunctional immune response thereby increasing patients' mortality (4, 5).

In this context, hydrogen sulfide (H_2S), a gaseous mediator, gained growing attraction in the therapy of microcirculatory and mitochondrial organ dysfunction (6). For example, exogenous H_2S increased intestinal blood flow, reduced mesenteric ischemia and preserved LPS-induced organ injury and death in experimental animal models (7, 8). Furthermore, H_2S can maintain mitochondrial function in sepsis as well as in ischemia-reperfusion models and reduce oxygen-consumption to protect cellular integrity (6, 9, 10). Thereby, the vasoactive and the mitochondrial effect of H_2S seems to be K(ATP)-channel-dependent (11–13).

However, administering gaseous H_2S in a clinical setting remains difficult. A simple technique to elevate H_2S-levels is the application of sodium thiosulfate (STS). STS increases endogenic H_2S concentration *via* enzymes, especially under ischemic conditions (14, 15). Thereby, STS can be administered intravenously and in the experimental setting also intraperitoneally and is standardly used in humans to treat calciphylaxis, cyanide intoxication as well as in the prevention of ototoxicity during cisplatin treatment (16–18). However, recent experimental studies have also shown that STS preserves mitochondrial function in ischemic hearts and improves survival in endotoxic mice, mainly mediated due to H_2S (8, 19). Nevertheless, data for the gastrointestinal effect of STS under septic conditions are missing and it remains unclear if this potential effect of STS is also K(ATP)-channel-dependent.

Therefore, we conducted this randomized, placebo-controlled, blinded trial in septic rats to evaluate the effects of STS and glibenclamide on the intestinal as well as hepatic microcirculation and mitochondrial function.

MATERIALS AND METHODS

All parts of this study were performed in accordance with NIH guidelines for animal care and reported in accordance with the ARRIVE guidelines. Experiments started after approval from the local Animal Care and Use Committee (Landesamt für Natur, Umwelt und Verbraucherschutz, Recklinghausen, Germany, Az. Az. 84-02.04.2015.A538).

Surgical Induction of Sepsis

The animals were derived from the breeding facility of the Heinrich-Heine-University Duesseldorf. 48 male Wistar rats (320 - 380 g body weight) were randomly assigned to one of the 4 experimental groups (**Figure 1**). However, 8 animals died within 24 hours after induction of sepsis, so experiments were performed in 40 rats (n = 10). It is of note, that there was no statistically relevant difference between the groups concerning death within the first 24 hours. The experiments started at 8:00 a.m. in the research laboratory of the Heinrich-Heine-University Duesseldorf, Dept. of Anesthesiology. Colon ascendens stent peritonitis (CASP)-surgery was performed with two 16-gauge PVC to develop sepsis using an established protocol as described previously (20) (21). Our previous studies demonstrate this model to be adequate to induce moderate sepsis in contrast to irreversible septic shock models. Anesthesia was induced and maintained by sevoflurane (3.0-3.2 % end-expiratory concentration, F_iO_2 0.5) and buprenorphine (0.05 mg • kg^{-1}, s.c.). A 2 cm-long median laparotomy was performed, the colon was located and penetrated 1 cm distal to the ileocecal valve with two 16-gauge PVC (Vasofix safety, B. Braun Melsungen AG, Melsungen, Germany). The inner needles were withdrawn, allowing constant fecal leakage into the abdominal cavity to develop abdominal sepsis. The intestine was carefully returned and the abdominal wall was closed. Afterwards, animals received vehicle (1.75 ml crystalloid fluid (Jonosteril Fresenius Kabi, Bad Homburg, Germany) and 1 ml DMSO (Dimethyl sulfoxide D8418, Sigma-Aldrich, Taufkirchen, Germany)), sodium thiosulfate (1.0 g • kg^{-1}, i.p., sodium thiosulfate (in Jonosteril) 217263, Sigma-Aldrich, Taufkirchen, Germany) and glibenclamide (5 mg • kg^{-1}, i.p. (in DMSO), glybenclamide G0639, Sigma-Aldrich, Taufkirchen, Germany) or both.

Abbreviations: ATP, Adenosine-triphosphate; ADP, Adenosine-diphospate; ADP/O, Efficacy of oxidative phosphorylation; ANOVA, Analysis of variance; ARRIVE, Animal Research: Reporting In Vivo Experiments; aU, arbitrary perfusion units; BGA, Blood gas analysis; CASP, Colon ascendens stent peritonitis; CoQ, Coenzyme Q; DMSO, Dimethyl sulfoxide; eNOS, endothelial nitric oxide synthase; FiN_2, Inspiratory nitrogen concentration; FiO_2, Inspiratory oxygen concentration; GL, glibenclamide; H_2S, Hydrogen sulfide; HR, Heart rate; IQR, inter quartile range; LPS, Lipopolysaccharide; MAP, Mean arterial blood pressure; MODS, Multiorgan dysfunction syndrome; mU, Milli Units; NIH, National Institutes of Health; O_2C, Oxygen to see; p_aO_2, Arterial oxygen partial pressure; p_aCO_2, Arterial carbon dioxide partial pressure; PAW, Airway pressure; PVC, Peripheral venous catheter; RCI, Respiratory control index; s.c., subcutaneous; SD, Standard deviation; SRSS, Septic rat severity score; STS, sodium thiosulfate; SQR, sulfide quinone reductase; VE, vehicle; VT, Tidal volume; μHBO_2, Microcirculatory oxygenation; µflow, Microcirculatory flow.

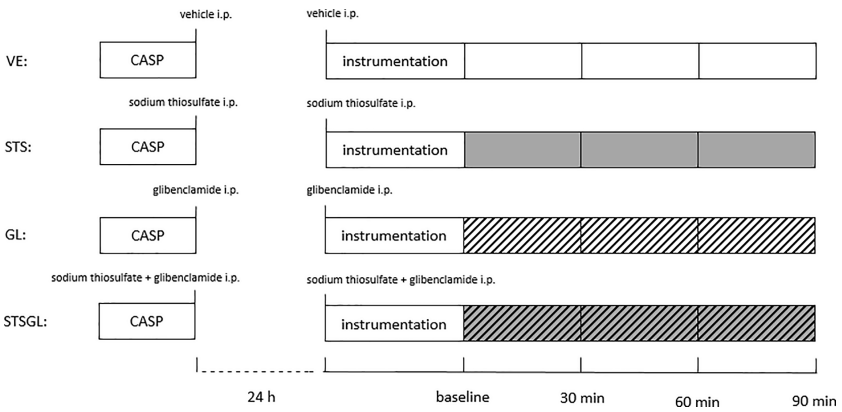

FIGURE 1 | Experimental protocol. Colon ascendens stent peritonitis (CASP)-surgery was carried out 24 h before the experiment. Intraperitoneally treatment with vehicle (VE), sodium thiosulfate (STS), glibenclamide (GL) or sodium thiosulfate + glibenclamide (STSGL) was carried out after CASP surgery and directly before the experiment.

The same treatment was applied 24 h after sepsis induction. The investigator was blinded to the treatment.

After CASP-surgery, animals were kept individually in separate plastic cages at a 12-h light/dark cycle with free access to water and food under controlled temperature (24 ± 2°C) and humidity (50% ± 5%). Buprenorphine (0.05 mg • kg^{-1} s.c.) was applied at 8 h and 16 h after surgery. As described previously, animals were examined and scored every 6 h according to a defined protocol (Septic Rat Severity Score: SRSS) to determine the severity of sepsis and to monitor the animals with respect to their welfare (loss of body weight, appearance, spontaneous behavior, provoked behavior, breathing rate, expiratory breathing sound, abdominal palpation and condition of droppings) (22, 23). Animals with unjustifiable suffering equivalent to a scoring of more than 10 points were euthanized. The scoring of all animals was performed by the same investigator.

Assessment of the Microcirculation

24 h after induction of sepsis, the animals were anesthetized by pentobarbital sodium injection (60 mg • kg^{-1} body weight i.p.) and buprenorphine (0.05 mg • kg^{-1} s.c.). Animals were placed on a heating pad, tracheotomized and mechanically ventilated in a volume-controlled, pressure-limited mode (70 min^{-1}, VT 1.6 – 2.0 ml, PAW < 17 cm • H_2O, FiO_2 = 0.3, Vent Elite, Harvard Apparatus GmbH, March-Hugstetten, Germany). During the experiment 120 µl blood were extracted intermittently (baseline, 45 min, 90 min) for blood gas analysis (BGA) (ABL 800 flex, Radiometer, Copenhagen, Denmark) to check for normocapnic ventilation (p_aCO_2 target value 38 ± 5 mmHg), sufficient oxygenation (p_aO_2 target value 120 – 150 mmHg) and lactate measurement. If the p_aCO_2 or oxygenation target values were not achieved, ventilation or FiO_2 were adjusted. To ensure continuous anesthesia, an external jugular vein catheter was established for continuous pentobarbital infusion (10 mg • kg^{-1} • h^{-1}). Blood pressure and heart rate were measured in the left *arteria carotis communis.* A continuous infusion of crystalloid solution (4 ml • h^{-1}) was applied *via* the arterial access for volume replacement and to prevent blood coagulation.

The animals were re-laparotomized and a flexible light guide probe (O_2C LW 2222, Lea Medizintechnik GmbH, Gießen) was placed on the *tunica serosa* of the colon ascendens, 1 cm distal to the stent and on the left lobe of the rat liver. Microcirculatory oxygenation (µHBO_2) and perfusion (µflow) were measured as previously described *via* reflectance spectrophotometry and laser Doppler flowmetry (20). White light (450-1000 nm) and laser light (820 nm, 30 mW) were transmitted to the tissue (colonic wall and liver parenchyma) *via* a micro-light guide with a penetration depth of 0.7 mm and the reflected light was analyzed. The wavelength-dependent and overall absorption of the applied white light is used to calculate the percentage of oxygenated hemoglobin in the microcirculation (µHbO_2). Due to the Doppler effect, magnitude and frequency distribution of changes in wavelength are proportional to the number of blood cells multiplied by the measured mean velocity (µvelo) of these cells. This product is proportional to flow (µflow) and expressed in arbitrary perfusion units (aU). Hence, this method allows the assessment and comparison of oxygenation and perfusion of the examined region at the same time. Only the microcirculation is measured as light entering vessels bigger than 100 µm is completely absorbed. The biggest fraction of the blood volume is stored in venous vessels (85%), so predominantly postcapillary oxygenation respectively mixed liver blood are measured, which represents the critical partial pressure of oxygen (pO_2) for hypoxia (24). Online evaluation of the signal quality throughout the experiments allows verification of the correct position of the probe tip. The µHbO_2 and the µflow values reported are the means of the last 5 min every 30 min, beginning at baseline (**Figure 1**).

Thus, 4 different groups of septic animals were analyzed: animals with vehicle-infusion (VE), animals with sodium thiosulfate pretreatment (STS), animals with glibenclamide pretreatment (GL), animals with sodium thiosulfate and

glibenclamide pretreatment (STSGL) (**Figure 1**). At the end of the experiments, the animals were euthanized by exsanguination under deep anesthesia and liver and colon tissue samples were harvested.

Preparation of Liver and Colon Homogenates

Liver and colon homogenates were prepared as described previously (23, 25, 26). Briefly, liver tissue was placed in 4°C cold isolation buffer, minced into 2-3 mm^3 pieces, rinsed twice in isolation buffer to remove traces of blood and homogenized (Potter-Elvehjem, 5 strokes, 2000 rpm).

Freshly harvested colon was squeezed out to remove faces, then placed in 4°C cold isolation buffer, quickly longitudinally opened and dried softly with a cotton compress. After treatment with trypsin for 5 minutes on ice, tissue was placed in 4°C isolation buffer containing 20 mg/ml BSA and protease inhibitors (*cOmplete*™ Protease Inhibitor Cocktail, Roche Life Science, Mannheim, Germany), minced into 2-3 mm^3 pieces and homogenized (Potter-Elvehjem, 5 strokes, 2000 rpm).

Protein concentration in the tissue homogenates was determined using the Lowry method with bovine serum albumin as a standard (27).

Measurement of Mitochondrial Respiratory Rates

For measurement of the mitochondrial oxygen consumption, the oxygen uptake rate was measured at 30°C using a Clark-type electrode (model 782, Strathkelvin instruments, Glasgow, Scotland) as described before (22, 25, 26). Tissue homogenates were suspended in respiration medium (130 mM KCl, 5 mM K_2HPO_4, 20 mM MOPS, 2.5 mM EGTA, 1 µM $Na_4P_2O_7$, 0.1% BSA for liver and 2% BSA for colon, pH 7.15) to yield a protein concentration of 4 mg/ml or 6 mg/ml for liver and colon, respectively.

Mitochondrial state 2 respiration was recorded in the presence of either complex I substrates glutamate and malate (both 2.5 mM, G-M) or complex II substrate succinate (10 mM for liver, 5 mM for colon, S).

The maximal mitochondrial respiration in state 3 was measured after addition of ADP (250 µM for liver, 50 µM for colon). The respiratory control index (RCI) was calculated (state 3/state 2) to define the coupling between the electron transport system and oxidative phosphorylation. To reflect the efficacy of oxidative phosphorylation, the ADP/O ratio was calculated from the amount of ADP added and O_2-consumption. The average oxygen consumption was calculated as mean from 3 technical replicates.

The solubility of oxygen was assumed to be 223 µmol $O_2 \bullet l^{-1}$ at 30°C according to the Strathkelvin instruments manual. Respiration rates were expressed as nmol/min/mg protein.

Mitochondria were checked for leakage by addition of 2.5 µM cytochrome c and 0.05 µg/ml oligomycin. Absence of an increase in flux after addition of cytochrome c indicated integrity of the mitochondrial outer membrane. When ATP synthesis was inhibited by oligomycin, the mitochondria were transferred to the state 2, which reflects the respiration rate compensating the proton leak. These results indicate that the inner membrane is intact, and mitochondria were not damaged through the preparation procedure.

Statistical Analysis

To calculate the appropriate sample size an *a priori* power analysis (G*Power Version 3.1.7, University of Dusseldorf, Germany) was performed. With n = 10 animals per group at a given $\alpha \leq 0.05$ (two-tailed) and an expected mean difference in μHbO_2 of at least 20% (percentage points) with an expected standard deviation of 10 – 15% (based on previous studies) a power of 84.5% resulted.

Normal distribution of data was assessed and confirmed in Q-Q- plots (IBM SPSS Statistics, International Business Machine Corp., Armonk, New York, USA) for microcirculatory data and in Kolmogorov/Smirnov test for mitochondrial results. Microcirculatory data were analyzed with a two-way ANOVA for repeated measures, followed by Dunnett´s post - hoc test for differences versus baseline, and Tukey post-hoc test for differences between groups. For mitochondrial data we used a Kruskal-Wallis test for non-parametric data followed by Dunn's multiple comparison test (GraphPad software v 6.0, Int., La Jolla, USA). Data are presented as means ± SD for parametric data and as medians, interquartile range (IQR), minimum and maximum for non-parametric data. $p < 0.05$ was considered significant.

Wherever delta values are presented, the absolute baseline value was subtracted from the absolute value at the respective observation points to individualize the data to each rat's baseline.

RESULTS

Table 1 and **Figures 2**, **3** summarize the effects of intraperitoneal sodium thiosulfate injection as well as glibenclamide on systemic hemodynamics as well as colonic and liver microcirculation in sepsis. Furthermore, **Figures 4**, **5** summarize the effect on mitochondria.

24 h after CASP-surgery, baseline values as well as SRSS scores did not differ significantly between the groups (**Table 1**).

Effect of Intraperitoneal Sodium Thiosulfate on Microcirculation in Septic Animals (STS)

STS increased colonic μHbO_2 compared to baseline (60 min: + 9.6 ± 10.5%, 90 min: + 10.4 ± 18.3%; $p < 0.05$ vs. baseline). Colonic μHbO_2 with STS injection was significantly higher compared to septic animals with vehicle (VE) and glibenclamide (GL) injection (**Figure 2**). Furthermore, sodium thiosulfate ameliorated colonic µflow compared to baseline (60 min: + 51.9 ± 71.1 aU; $p < 0.05$ vs. baseline) and also compared to septic animals with vehicle (VE) and glibenclamide (GL) injection (**Figure 2**).

Sodium thiosulfate enhanced hepatic μHbO_2 compared to baseline (30 min: + 5.5 ± 10.1%, 90 min: + 5.8 ± 9.1%; $p < 0.05$ vs. baseline) as well as compared to septic animals with vehicle (VE)

TABLE 1 | Physiological data and SRSS.

		VE	STS	GL	STSGL
lactate [mmol · l^{-1}]	Baseline	1.4 ± 0.5	1.6 ± 0.8	1.5 ± 0.3	1.4 ± 0.4
	45 min	1.4 ± 0.3	1.3 ± 0.4	1.3 ± 0.3	1.3 ± 0.4
	90 min	1.4 ± 0.5	1.3 ± 0.6	1.2 ± 0.4	1.2 ± 0.7
HR [min^{-1}]	Baseline	439 ± 55	425 ± 59	429 ± 33	397 ± 35
	30 min	432 ± 59	426 ± 65	422 ± 34	404 ± 37
	60 min	433 ± 63	424 ± 68	424 ± 47	405 ± 42
	90 min	435 ± 69	425 ± 66	421 ± 53	409 ± 42
MAP [mmHg]	Baseline	84 ± 16	81 ± 15	82 ± 13	82 ± 17
	30 min	81 ± 14	85 ± 16	82 ± 12	83 ± 17
	60 min	81 ± 11	84 ± 19	80 ± 14	80 ± 15
	90 min	81 ± 11	84 ± 16	81 ± 15	81 ± 15
SRSS	Baseline	4.5 ± 1.1	4.7 ± 1.4	4.4 ± 1.4	4.5 ± 1.3

Lactate levels, heart rate (HR), mean arterial pressure (MAP) and septic rat severity score (SRSS) at baseline. VE, septic animals with vehicle-infusion; STS, septic animals with sodium thiosulfate pretreatment; GL, septic animals with glibenclamide pretreatment; STSGL, septic animals with sodium thiosulfate and glibenclamide. Data are presented as absolute values (means ± SD); n = 10.

and glibenclamide (GL) injection (**Figure 3**). Hepatic μflow was increased due to sodium thiosulfate compared to baseline (60 min: + 17.8 ± 14.1 aU, 90 min: + 22.5 ± 20.0 aU; $p < 0.05$ vs. baseline) and significantly increased compared to all other groups (STS vs. VE; GL; STSGL) (**Figure 3**).

MAP, HR and lactate remained unchanged in septic animals after sodium thiosulfate injection. There was also no significant change between groups (**Table 1**).

Effect of Intraperitoneal Sodium Thiosulfate and Glibenclamide on Microcirculation in Septic Animals (STSGL)

The combination of sodium thiosulfate and glibenclamide increased colonic μHbO$_2$ compared to baseline (60 min: + 7.6 ± 12.0%, 90 min: + 8.7 ± 11.5%; $p < 0.05$ vs. baseline) and μHbO$_2$ was significantly higher compared to septic animals with vehicle (VE) and glibenclamide (GL) injection (**Figure 2**). Besides, sodium thiosulfate in combination with glibenclamide increased colonic μflow compared to baseline (60 min: + 35.2 ± 62.6 aU, 90 min: + 41.8 ± 63.3 aU; $p < 0.05$ vs. baseline) and also compared to septic animals with vehicle (VE) (**Figure 2**).

In contrast to colonic microcirculation, hepatic μHbO and μflow did not change after the combined application of sodium thiosulfate and glibenclamide compared to baseline (**Figure 3**). Likewise, there were no significant changes of hepatic μflow compared to baseline (**Figure 3**).

MAP, HR and lactate remained unchanged in septic animals with sodium thiosulfate and glibenclamide injection. There was also no significant change between groups (**Table 1**).

Effect of Intraperitoneal Glibenclamide on Microcirculation in Septic Animals (GL)

Glibenclamide did not change colonic and hepatic μHbO$_2$ compared to baseline (**Figures 2**, **3**). In addition, there were no significant changes of colonic or hepatic μflow compared to baseline (**Figures 2**, **3**).

MAP, HR and lactate remained unchanged after glibenclamide injection (**Table 1**).

Effect of Vehicle on Microcirculation in Septic Animals (VE)

In septic animals with vehicle injection there were no significant changes of colonic μHbO$_2$ compared to baseline, whereas hepatic μHbO$_2$ declined (60 min: - 8.7 ± 13.5%; 90 min: - 9.1 ± 12.3%; $p < 0.05$ vs. baseline) (**Figures 2**, **3**). Colonic as well as hepatic μflow remained unaltered over the observation period of 90 min (**Figures 2**, **3**).

MAP, HR and lactate remained unchanged in septic animals with vehicle injection (**Table 1**).

Effect of Intraperitoneal Sodium Thiosulfate and Glibenclamide on Mitochondrial Function in Septic Animals

None of the used substances (applied alone or in combination) affected mitochondrial respiration. There were no statistical differences between control and treated groups regarding RCI and ADP/O ratio after stimulation of the respiratory chain through complex I and II in colonic (**Figure 4**) and hepatic (**Figure 5**) mitochondria.

DISCUSSION

This study was carried out to evaluate the effect of STS without and with blockade of K(ATP)-channels using glibenclamide on intestinal as well as hepatic microcirculation and mitochondrial function under septic conditions. The main results are:

i) STS ameliorates intestinal microcirculatory oxygenation in septic animals mainly due to improved microcirculatory blood supply. This effect is independent of K(ATP)-channels.

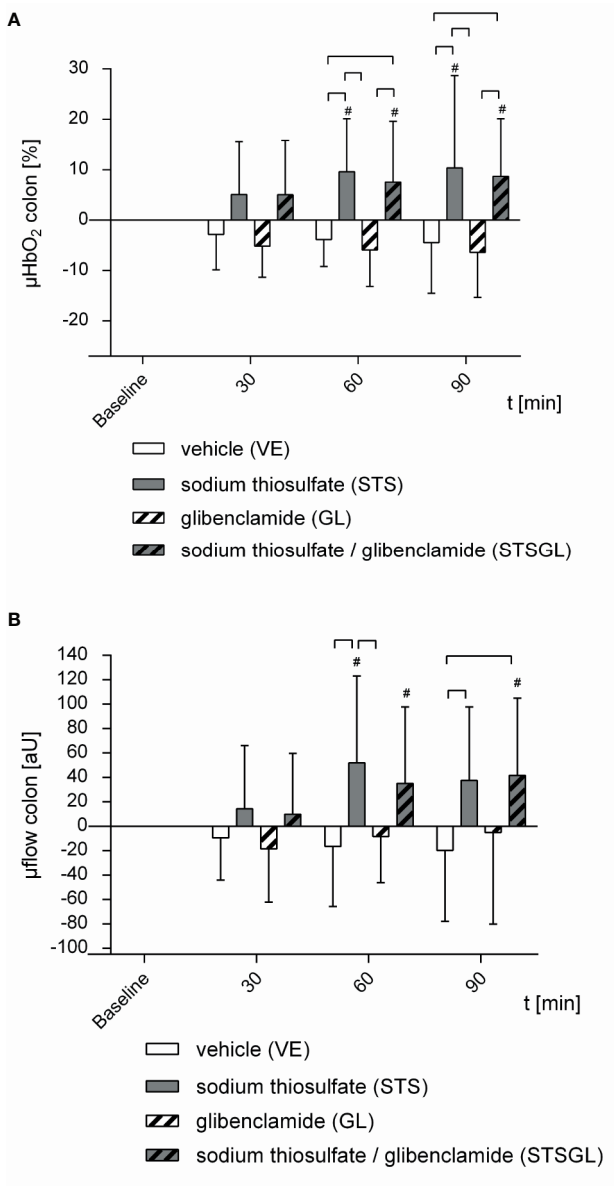

FIGURE 2 | Intestinal microcirculation in septic animals. Effect of sodium thiosulfate (STS), glibenclamide (GL), sodium thiosulfate + glibenclamide (STSGL) or vehicle (VE) on **(A)** colonic microcirculatory oxygenation (μHBO_2) and **(B)** colonic microcirculatory flow (μflow). Δ μHBO_2 [%] and Δ μflow [aU] over time calculated to baseline (means ± SD). # = $p < 0.05$ versus baseline (Two-way ANOVA followed by Dunnett´s *post - hoc* test) ¬ between groups (Two-way ANOVA followed by Tukey *post – hoc* test); n = 10.

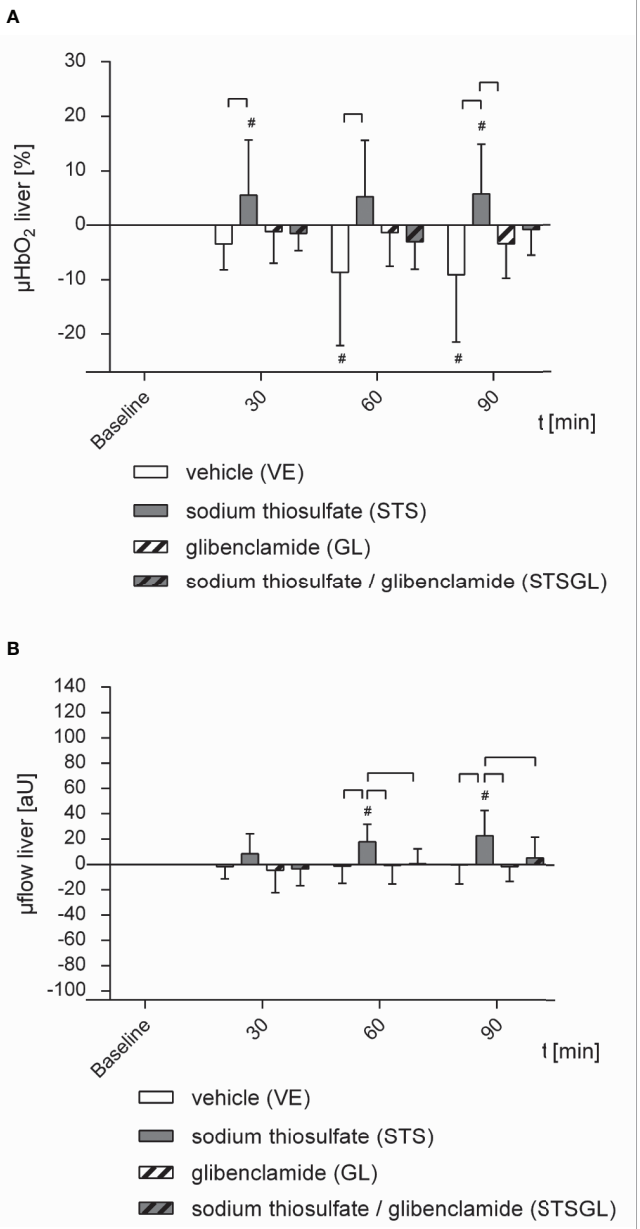

FIGURE 3 | Hepatic microcirculation in septic animals. Effect of sodium thiosulfate (STS), glibenclamide (GL), sodium thiosulfate + glibenclamide (STSGL) or vehicle (VE) on **(A)** hepatic microcirculatory oxygenation (μHBO_2) and **(B)** hepatic microcirculatory flow (μflow). Δ μHBO_2 [%] and Δ μflow [aU] over time calculated to baseline (means ± SD). # = $p < 0.05$ versus baseline (Two-way ANOVA followed by Dunnett´s *post - hoc* test) ¬ between groups (Two-way ANOVA followed by Tukey *post – hoc* test); n = 10.

ii) STS also enhances hepatic microcirculatory oxygenation due to improved microcirculatory blood supply. This enhancement seems to be K(ATP)-channel-dependent.

iii) The impact of STS on the intestinal as well as hepatic microcirculation is not mediated by changes in macrohemodynamic variables.

iv) STS does not change mitochondrial function in the intestine and the liver in septic animals.

To investigate the effect of STS and a possible involvement of K(ATP)-channels in septic animals, we used the CASP-model. This well-established experimental sepsis model is one of the closest models to imitate human sepsis with abdominal focus (21). The observed mortality rate of 17% in this study and the

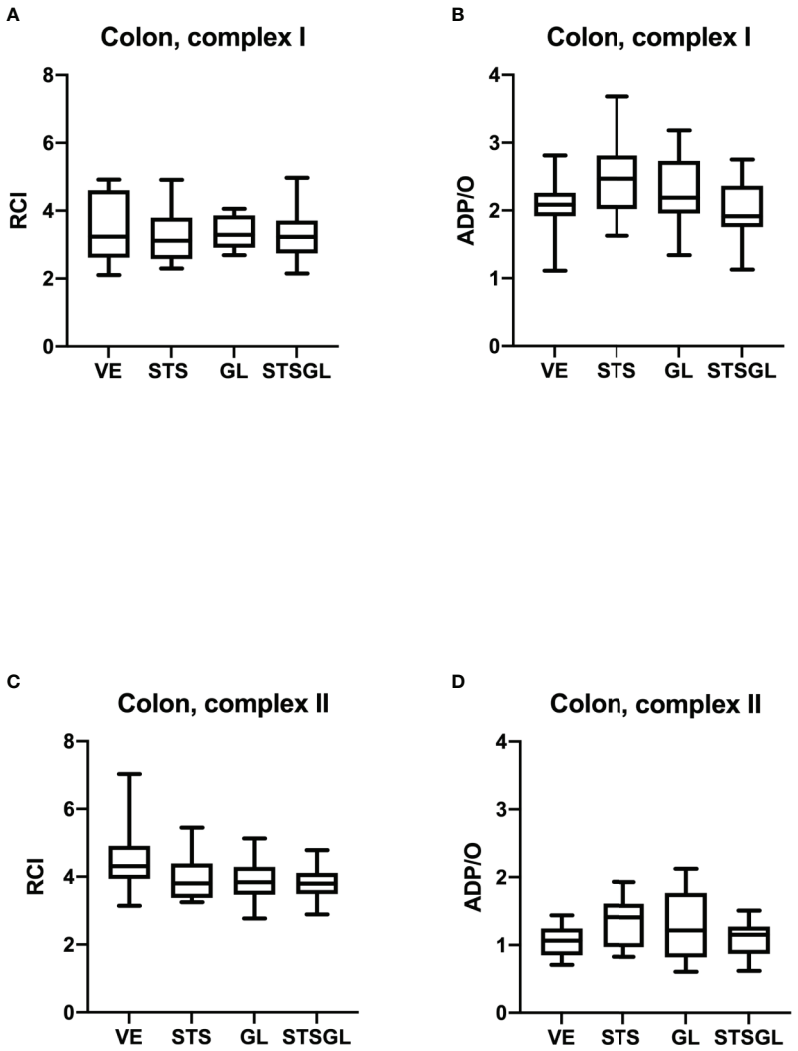

FIGURE 4 | Intestinal mitochondrial function in septic animals. Effect of sodium thiosulfate (STS), glibenclamide (GL) and sodium thiosulfate/glibenclamide (STSGL) compared to control (vehicle: VE) on mitochondrial function of colonic tissue homogenates from septic rats: respiratory control index (RCI) for complex I **(A)** and complex II **(C)** and ADP/ratio for complex I **(B)** and complex II **(D)**. Data are presented as Box-Whisker-Plots presenting median, interquartile range, minimum and maximum value, n=10,.

SRSS scores are similar to own previous reports and reflect the moderate severity of our sepsis model (20, 21). However, it is of note that animals did not suffer from hypotension or elevated lactate levels as one would expect in septic shock. Thereby, the moderate sepsis model allows to start a therapeutic approach before the development of septic shock and in this way to investigate the early sepsis-induced microcirculatory alterations of the gastrointestinal system (21, 28). Besides, it is of note that an important limitation of the current study is that there is no control group to estimate how severe the sepsis-induced microcirculatory changes are compared to sham operated animals. However, as stated above, the animals showed clear signs of infection: visible peritonitis, SRSS, mortality rate, significantly higher cytokine plasma levels and leucocyte counts compared to sham (as shown in previous studies with the same sepsis model (20, 21). Furthermore, we have already shown in a previous study that induction of a milder sepsis (CASP operation with one 18G-stent) led to a significant deterioration of intestinal microcirculatory oxygenation compared to sham operated animals. Thus, factors such as surgical trauma and related inflammation, impact of the anesthetics etc. can be ruled out (20). Therefore and also to be in accordance with the 3 R tenet of the ARRIVE guidelines we have decided against a control group.

Sepsis induced microcirculatory alterations of the colon and the liver were analyzed *via* reflectance spectrophotometry and laser doppler to simultaneously assess oxygenation and flow (20). This method has been validated in various tissues and is used in different experimental and clinical studies (20, 24, 29–32). Especially under septic conditions reflectance spectrophotometry and laser doppler

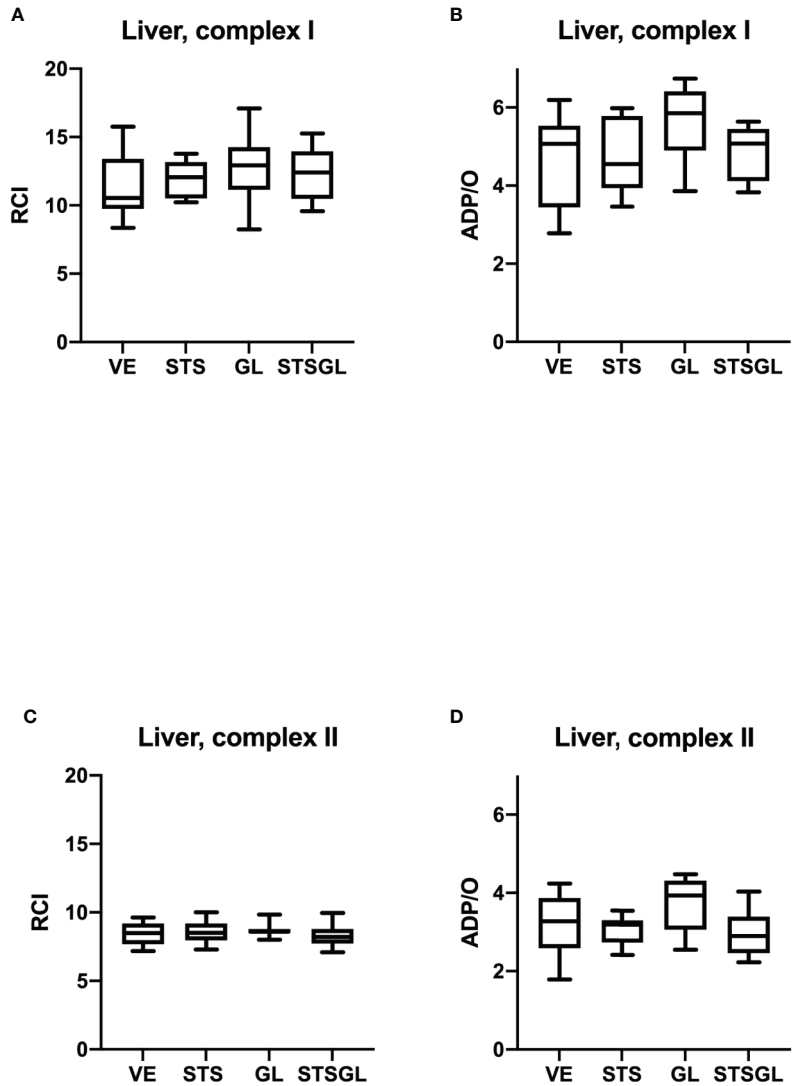

FIGURE 5 | Hepatic mitochondrial function in septic animals. Effect of sodium thiosulfate (STS), glibenclamide (GL) and sodium thiosulfate/glibenclamide(STSGL) compared to control (vehicle: VE) on mitochondrial function of hepatic tissue homogenates from septic rats: respiratory control index (RCI) for complex I **(A)** and complex II **(C)** and ADP/ratio for complex I **(B)** and complex II **(D)**. Data are presented as Box-Whisker-Plots presenting median, interquartile range, minimum and maximum value, n=10,.

are valuable analyzing tools, as they measure mainly the postcapillary area and changes in this area correlate with outcome in septic patients (33, 34). It is important to acknowledge that the O_2C signal averages the whole catchment area and does not provide spatial resolution. This technique is therefore limited in assessment of capillary density or heterogeneity of blood flow. However, an experimental sepsis study could show that amelioration of intestinal oxygenation improves intestinal barrier function and reduces mucosal cell death as indirect outcome parameters, which further underlines the diagnostic relevance of this technique (35).

We decided to assess mitochondrial respiration in tissue homogenates rather than in isolated mitochondria in order to avoid the disadvantages of the isolating procedure (36, 37). Furthermore, to exclude a potential mitochondrial damage due to the preparation procedure, we verified the integrity of the mitochondrial inner and outer membranes.

The dosage of STS used in this study is adapted from the literature (8). Tokuda et al. observed after 2.0 g • kg^{-1} STS i.p. a significantly improved survival rate of septic mice. In their study STS was given after sepsis induction. We applied a dosage of 1.0 g • kg^{-1} STS i.p. at two time points, immediately after sepsis induction and after 24 hours, to include an immediate effect of STS on gastrointestinal microcirculation. Furthermore, we used glibenclamide to investigate if the STS effect is K(ATP)-channel-dependent. Glibenclamide is widely and successfully used as a K (ATP)-channel-blocker in the literature (13, 38–40).

With this study design, we could demonstrate that STS ameliorates intestinal as well as hepatic microcirculatory

oxygenation in sepsis. μHbO_2 in the colon and the liver was significantly higher with STS compared to vehicle treated animals. This improvement of microcirculatory oxygenation seems to be mediated by enhanced microcirculatory perfusion and thereby higher oxygen supply. μflow was also significantly improved in animals treated with STS. Studies concerning the effects of STS on microcirculation are sparse. However, our results are in line with an experimental study of Pihan et al., where STS prevented acute gastrointestinal injury induced by ethanol through maintained microcirculatory flow (41). Furthermore, our results are supported by several studies using H_2S. As stated above, a possible mechanism of action of STS is the elevation of endogenous H_2S-levels, especially under ischemic conditions (14, 15). H_2S improved gastrointestinal microcirculatory perfusion in an ischemia-reperfusion model and furthermore in an experimental sepsis model (7, 42). To date, the microcirculatory mechanism of action of STS, respectively H_2S, remains unclear. We have demonstrated that improved microcirculation by STS does not seem to be mediated through changes in macrohemodynamic variables. Heart rate and global perfusion pressure remained constant in this study. However, we did not examine further perfusion parameters like cardiac output. However, Volpato et al. demonstrated in their echocardiography study that H_2S rather leads to reduced cardiac output. Thus, macrohemodynamic changes do not seem to contribute to the observed protective effect of STS (43). Instead, direct local mechanisms of STS and H_2S might be the reason for increased microcirculatory flow (9, 14, 44).

In this context one main local mechanism of H_2S seems to be the activation of K(ATP)-channels in the microcirculation inducing vasorelaxation (11, 44). We used glibenclamide, a K (ATP)-channel-blocker, to examine a potential role of activation of K(ATP)-channels. We observed tissue-specific effects. Glibenclamide abolished the protective effect of STS in the hepatic microcirculation. In contrast, the effect of STS in the intestinal microcirculation was unaffected by glibenclamide and thus, seems to be independent of K(ATP)-channel activation.

The results in the hepatic microcirculation are in line with the literature regarding H_2S. H_2S induces a vasorelaxant effect in the hepatic vascular bed, predominantly in presinusoidal vessels, *via* K(ATP)-channels, thus, increasing microcirculatory flow (45–47). However, studies relating to the mechanism of action of STS and H_2S in the intestinal microcirculation are sparse. Regarding our results, K(ATP)-channels do not seem to be a major effector for the amelioration of colonic microcirculatory flow and oxygenation in the context of sepsis. Direct vasodilatory effects of STS and H_2S *via* eNOS or local receptors like oxytocin receptors might play a role in this context (48, 49). Therefore, further studies are needed to elucidate the exact mechanisms of the microcirculatory effect of STS in the vascular bed of the gastrointestinal tract.

It remains unclear how long the effect of STS in the gastrointestinal microcirculation persists. We observed a profound microcirculatory effect starting at 30 – 60 min after the second injection and lasting until the end of the experiment. Hence, we could show that the effect of STS is lasting for at least 60 min. Furthermore, it remains unclear if the amelioration of gastrointestinal microcirculation due to STS protects against intestinal barrier dysfunction and liver failure in sepsis, as suspected in the literature (35). Therefore, further studies are needed, to investigate the duration of the STS effect and the impact of the microcirculatory changes on gastrointestinal barrier and overall survival in sepsis.

To investigate if the improved microcirculatory oxygenation is only mediated by enhanced microcirculatory flow or if also an optimized mitochondrial function might play a role, we studied colonic and hepatic mitochondrial respiration. Here, we didn't observe any effect of STS application on colonic and hepatic mitochondrial respiration. Concerning the effect of STS, respectively H_2S, on mitochondrial function it is known, that low concentrations of H_2S (0.1 – 1 μM) stimulate mitochondrial oxygen consumption in most organs, while higher concentrations (3 – 30 μM) show an inhibitory effect (50). High sulfide oxidation flux can limit the pool of oxidized coenzyme Q (CoQ), which accepts electrons from complex I and II and inhibit complex IV (51). Unlike many other tissues, the colonic cells are exposed to high levels of H_2S derived from intestinal microbial metabolism, reaching concentrations of 0.2 – 2.4 mM, depending on the part of the gut (52). In the colon, in *in vitro* experiments with permeabilized cells, concentrations of H_2S up to 20 μM stimulate mitochondrial respiration, while these concentrations are toxic to other tissues (52, 53). The adaptive mechanisms used by the colonic epithelium to compensate for the exposure to potentially harmful luminal H_2S concentrations are largely unknown (53). One of the possible mechanisms could be the sulfide oxidation involving the activity of the sulfide quinone reductase (SQR) activity (10).

In our study, we have not observed any effects of STS on mitochondrial respiration. Our results are in line with those of Datzmann et al., who could not show any changes in mitochondrial respiration in brain, heart, kidney or liver after hemorrhagic shock in swine either (54). The impact of hydrogen sulfide on mitochondrial function is known to be reversible. The reversion characteristics like intensity and kinetics are strongly concentration dependent (10). We have not assessed the tissue concentrations of STS and H_2S. The data from the literature about endogenous tissue concentration of H_2S are discordant, showing micromolar or nanomolar range and great differences between tissues and species (55–57). Moreover, the accumulation of H_2S after exogenous application is also highly tissue specific. The increase in H_2S levels after a subcutaneous application of 60 $\mu g \cdot g^{-1}$ sodium hydrosulfide in mice accounted for about 50% in kidney and brain, but only 18% in liver (57). If tissue concentrations of H_2S after intraperitoneal administration of STS are comparable with those after subcutaneous application of sodium hydrosulfide, is not clear. Thus, it remains speculative if in our experimental setting we reached the effective level of H_2S for affecting the respiratory chain, especially in the colon, where significantly higher concentrations of H_2S are needed to affect the mitochondrial respiration. Concerning the hepatic mitochondria, another mechanism underlying the lack of changes in mitochondrial respiration is conceivable. We could

show that moderate sepsis, as induced by the CASP model, increased mitochondrial respiration in the liver (23). This could depict an adaptative adjustment of the cellular metabolism to preserve the ATP production by impaired oxygen supply under septic conditions. If the adaptive mechanisms are saturated, no further increase in mitochondrial respiration, also under H_2S, is achievable. Therefore, our results show that the ameliorated microcirculatory oxygenation seems only to be caused by increased oxygen supply and not by changes in mitochondrial respiration.

It is important to note that we studied the role of sodium thiosulfate in a rodent model of sepsis and not in human sepsis, so these data and their clinical impact should be interpreted with care. Nevertheless, our CASP model is one of the closest experimental models to imitate anastomosis failure with consecutive abdominal sepsis. Therefore, our results highlight the potential of sodium thiosulfate in sepsis to protect the intestinal as well as hepatic microcirculation and thus even preventing the vicious circle with intestinal ischemia, translocating bacteria (and toxins) and aggravation of sepsis. However, it is of note that this study has not examined if the enhanced intestinal and hepatic microcirculation due to STS leads to histological improvement, e.g. tight junction performance or cell death. The study focuses on microcirculatory and mitochondrial measurements, based on recent data suggesting that even mild changes in regional oxygenation, which most likely do not lead to visible organ damage have an impact on intestinal barrier function, as shown in a canine model (58). In this setting, i.e. in sepsis before visible tissue damage occurs, there is an opportunity for therapy in the clinical setting, whereas once the tissue is obviously damaged, interventional therapy might be too late (33). Nevertheless, further studies have to be performed to elucidate if STS can also protect organ function in sepsis.

CONCLUSION

This randomized, placebo-controlled, blinded animal trial demonstrated that intraperitoneally applied sodium thiosulfate improves intestinal as well as hepatic microcirculatory oxygenation in sepsis. This protective effect seems to be mediated by an increased microcirculatory perfusion and thereby increased oxygen supply and not by changes in mitochondrial respiration or macrohemodynamic variables. We could demonstrate that the intestinal effect of sodium thiosulfate seems to be K(ATP)-channel-independent, whereas the hepatic effect seems to be K(ATP)-channel-dependent. This study reveals a potential new therapy for the compromised gastrointestinal microcirculation during sepsis. Hence, clinical trials have to be performed to investigate the effect of sodium thiosulfate in septic patients.

DATA AVAILABILITY STATEMENT

The raw data supporting the conclusions of this article will be made available by the authors, without undue reservation.

ETHICS STATEMENT

The animal study was reviewed and approved by Landesamt für Natur, Umwelt und Verbraucherschutz, Recklinghausen, Germany, Az. 84-02.04.2015.A538.

AUTHOR CONTRIBUTIONS

JS contributed to the study conception and design, acquisition of data, analysis and interpretation of data and drafting of the article. SK contributed to the acquisition of data, analysis and interpretation of data. YK contributed to the acquisition of data, analysis and interpretation of data. AK contributed to the study conception and design, analysis and interpretation of data and revision of the article. IB contributed to the study conception and design, analysis and interpretation of data and revision of the article. OP contributed to the study conception and design, analysis and interpretation of data and revision of the article. CV contributed to the study conception and design, analysis and interpretation of data and revision of the article. RT contributed to the study conception and design, analysis and interpretation of data and revision of the article. AH contributed to the study conception and design, acquisition of data, analysis and interpretation of data and revision of the article. All authors contributed to the article and approved the submitted version.

REFERENCES

1. Thompson K, Venkatesh B, Finfer S. Sepsis and Septic Shock: Current Approaches to Management. *Internal Med J* (2019) 49(2):160–70. doi: 10.1111/imj.14199
2. Otani S, Coopersmith CM. Gut Integrity in Critical Illness. *J Intensive Care* (2019) 7:17. doi: 10.1186/s40560-019-0372-6
3. De Backer D, Orbegozo Cortes D, Donadello K, Vincent J-L. Pathophysiology of Microcirculatory Dysfunction and the Pathogenesis of Septic Shock. *Virulence* (2014) 5:73–9. doi: 10.4161/viru.26482
4. Sun J, Zhang J, Wang X, Ji F, Ronco C, Tian J, et al. Gut-Liver Crosstalk in Sepsis-Induced Liver Injury. *Crit Care* (2020) 24(1):614. doi: 10.1186/s13054-020-03327-1
5. Meng M, Klingensmith NJ, Coopersmith CM. New Insights Into the Gut as the Driver of Critical Illness and Organ Failure. *Curr Opin Crit Care* (2017) 23 (2):143–8. doi: 10.1097/mcc.0000000000000386
6. Reitsema VA, Star BS, de Jager VD, van Meurs M, Henning RH, Bouma HR. Metabolic Resuscitation Strategies to Prevent Organ Dysfunction in Sepsis. *Antioxidants Redox Signaling* (2019) 31(2):134–52. doi: 10.1089/ars.2018.7537
7. Pavoni V, Nicoletti P, Benemei S, Materazzi S, Perna F, Romagnoli S, et al. Effects of Hydrogen Sulfide (H2S) on Mesenteric Perfusion in Experimental Induced Intestinal Ischemia in a Porcine Model. *Heart Lung vessels* (2015) 7 (3):231–7.
8. Tokuda K, Kida K, Marutani E, Crimi E, Bougaki M, Khatri A, et al. Inhaled Hydrogen Sulfide Prevents Endotoxin-Induced Systemic Inflammation and

Improves Survival by Altering Sulfide Metabolism in Mice. *Antioxidants Redox Signaling* (2012) 17(1):11–21. doi: 10.1089/ars.2011.4363
9. Baumgart K, Radermacher P, Wagner F. Applying Gases for Microcirculatory and Cellular Oxygenation in Sepsis: Effects of Nitric Oxide, Carbon Monoxide, and Hydrogen Sulfide. *Curr Opin Anaesthesiol* (2009) 22 (2):168–76. doi: 10.1097/ACO.0b013e328328d22f
10. Leschelle X, Goubern M, Andriamihaja M, Blottiere HM, Couplan E, Gonzalez-Barroso MD, et al. Adaptative Metabolic Response of Human Colonic Epithelial Cells to the Adverse Effects of the Luminal Compound Sulfide. *Biochim Biophys Acta* (2005) 1725(2):201–12. doi: 10.1016/j.bbagen.2005.06.002
11. Zhao W, Zhang J, Lu Y, Wang R. The Vasorelaxant Effect of H(2)S as a Novel Endogenous Gaseous K(ATP) Channel Opener. *EMBO J* (2001) 20(21):6008–16. doi: 10.1093/emboj/20.21.6008
12. Johansen D, Ytrehus K, Baxter GF. Exogenous Hydrogen Sulfide (H2S) Protects Against Regional Myocardial Ischemia-Reperfusion Injury–Evidence for a Role of K ATP Channels. *Basic Res Cardiol* (2006) 101 (1):53–60. doi: 10.1007/s00395-005-0569-9
13. Spiller F, Orrico MI, Nascimento DC, Czaikoski PG, Souto FO, Alves-Filho JC, et al. Hydrogen Sulfide Improves Neutrophil Migration and Survival in Sepsis Via K+ATP Channel Activation. *Am J Respir Crit Care Med* (2010) 182 (3):360–8. doi: 10.1164/rccm.200907-1145OC
14. Olson KR, Deleon ER, Gao Y, Hurley K, Sadauskas V, Batz C, et al. Thiosulfate: A Readily Accessible Source of Hydrogen Sulfide in Oxygen Sensing. *Am J Physiol Regul Integr Comp Physiol* (2013) 305(6):R592–603. doi: 10.1152/ajpregu.00421.2012
15. Szabo C, Papapetropoulos A. International Union of Basic and Clinical Pharmacology. CII: Pharmacological Modulation of H(2)S Levels: H(2)S Donors and H(2)S Biosynthesis Inhibitors. *Pharmacol Rev* (2017) 69 (4):497–564. doi: 10.1124/pr.117.014050
16. Peng T, Zhuo L, Wang Y, Jun M, Li G, Wang L, et al. A Systematic Review of Sodium Thiosulfate in Treating Calciphylaxis in Chronic Kidney Disease Patients. *Nephrol (Carlton Vic)* (2018) 23(7):669–75. doi: 10.1111/nep.13081
17. Petrikovics I, Budai M, Kovacs K, Thompson DE. Past, Present and Future of Cyanide Antagonism Research: From the Early Remedies to the Current Therapies. *World J Method* (2015) 5(2):88–100. doi: 10.5662/wjm.v5.i2.88
18. Brock PR, Maibach R, Childs M, Rajput K, Roebuck D, Sullivan MJ, et al. Sodium Thiosulfate for Protection From Cisplatin-Induced Hearing Loss. *N Engl J Med* (2018) 378(25):2376–85. doi: 10.1056/NEJMoa1801109
19. Ravindran S, Kurian GA. Preconditioning the Rat Heart With Sodium Thiosulfate Preserved the Mitochondria in Response to Ischemia-Reperfusion Injury. *J Bioenergetics Biomembranes* (2019) 51(3):189–201. doi: 10.1007/s10863-019-09794-8
20. Stübs CCM, Picker O, Schulz J, Obermiller K, Barthel F, Hahn A-M, et al. Acute, Short-Term Hypercapnia Improves Microvascular Oxygenation of the Colon in an Animal Model of Sepsis. *Microvascular Res* (2013) 90:180–6. doi: 10.1016/j.mvr.2013.07.008
21. Schulz J, Schoneborn S, Vollmer C, Truse R, Herminghaus A, Bauer I, et al. Hypercapnia-Induced Amelioration of the Intestinal Microvascular Oxygenation in Sepsis Is Independent of the Endogenous Sympathetic Nervous System. *Shock* (2018) 49(3):326–33. doi: 10.1097/shk.0000000000000920
22. Herminghaus A, Barthel F, Heinen A, Beck C, Vollmer C, Bauer I, et al. Severity of Polymicrobial Sepsis Modulates Mitochondrial Function in Rat Liver. *Mitochondrion* (2015) 24:122–8. doi: 10.1016/j.mito.2015.08.001
23. Herminghaus A, Papenbrock H, Eberhardt R, Vollmer C, Truse R, Schulz J, et al. Time-Related Changes in Hepatic and Colonic Mitochondrial Oxygen Consumption After Abdominal Infection in Rats. *Intensive Care Med Exp* (2019) 7(1):4. doi: 10.1186/s40635-018-0219-9
24. Siegemund M, van Bommel J, Ince C. Assessment of Regional Tissue Oxygenation. *Intensive Care Med* (1999) 25(10):1044–60. doi: 10.1007/s001340051011
25. Herminghaus A, Buitenhuis AJ, Schulz J, Vollmer C, Scheeren TWL, Bauer I, et al. Propofol Improves Colonic But Impairs Hepatic Mitochondrial Function in Tissue Homogenates From Healthy Rats. *Eur J Pharmacol* (2019) 853:364–70. doi: 10.1016/j.ejphar.2019.04.031
26. Herminghaus A, Laser E, Schulz J, Truse R, Vollmer C, Bauer I, et al. Pravastatin and Gemfibrozil Modulate Differently Hepatic and Colonic Mitochondrial Respiration in Tissue Homogenates From Healthy Rats. *Cells* (2019) 8(9):983. doi: 10.3390/cells8090983
27. Lowry OH, Rosebrough NJ, Farr AL, Randall RJ. Protein Measurement With the Folin Phenol Reagent. *J Biol Chem* (1951) 193(1):265–75.
28. Lustig MK, Bac VH, Pavlovic D, Maier S, Gründling M, Grisk O, et al. Colon Ascendens Stent Peritonitis–A Model of Sepsis Adopted to the Rat: Physiological, Microcirculatory and Laboratory Changes. *Shock (Augusta Ga)* (2007) 28:59–64. doi: 10.1097/SHK.0b013e31802e454f
29. Bludau M, Vallbohmer D, Gutschow C, Holscher AH, Schroder W. Quantitative Measurement of Gastric Mucosal Microcirculation Using a Combined Laser Doppler Flowmeter and Spectrophotometer. *Dis Esophagus* (2008) 21(7):668–72. doi: 10.1111/j.1442-2050.2008.00856.x
30. Sturm T, Leiblein J, Schneider-Lindner V, Kirschning T, Thiel M. Association of Microcirculation, Macrocirculation, and Severity of Illness in Septic Shock: A Prospective Observational Study to Identify Microcirculatory Targets Potentially Suitable for Guidance of Hemodynamic Therapy. *J Intensive Care Med* (2018) 33(4):256–66. doi: 10.1177/0885066616671689
31. Klein KU, Schramm P, Glaser M, Reisch R, Tresch A, Werner C, et al. Intraoperative Monitoring of Cerebral Microcirculation and Oxygenation–A Feasibility Study Using a Novel Photo-Spectrometric Laser-Doppler Flowmetry. *J Neurosurg Anesthesiol* (2010) 22(1):38–45. doi: 10.1097/ANA.0b013e3181bea439
32. Forst T, Hohberg C, Tarakci E, Forst S, Kann P, Pfutzner A. Reliability of Lightguide Spectrophotometry (O2C) for the Investigation of Skin Tissue Microvascular Blood Flow and Tissue Oxygen Supply in Diabetic and Nondiabetic Subjects. *J Diabetes Sci Technol* (2008) 2(6):1151–6. doi: 10.1177/193229680800200625
33. De Backer D, Donadello K, Sakr Y, Ospina-Tascon G, Salgado D, Scolletta S, et al. Microcirculatory Alterations in Patients With Severe Sepsis: Impact of Time of Assessment and Relationship With Outcome. *Crit Care Med* (2013) 41:791–9. doi: 10.1097/CCM.0b013e3182742e8b
34. Mayer K, Trzeciak S, Puri NK. Assessment of the Adequacy of Oxygen Delivery. *Curr Opin Crit Care* (2016) 22(5):437–43. doi: 10.1097/mcc.0000000000000336
35. Yeh YC, Wu CY, Cheng YJ, Liu CM, Hsiao JK, Chan WS, et al. Effects of Dexmedetomidine on Intestinal Microcirculation and Intestinal Epithelial Barrier in Endotoxemic Rats. *Anesthesiology* (2016) 125(2):355–67. doi: 10.1097/aln.0000000000001135
36. Pecinová A, Drahota Z, Nůsková H, Pecina P, Houštěk J. Evaluation of Basic Mitochondrial Functions Using Rat Tissue Homogenates. *Mitochondrion* (2011) 11(5):722–8. doi: 10.1016/j.mito.2011.05.006
37. Kozlov AV, Duvigneau JC, Hyatt TC, Raju R, Behling T, Hartl RT, et al. Effect of Estrogen on Mitochondrial Function and Intracellular Stress Markers in Rat Liver and Kidney Following Trauma-Hemorrhagic Shock and Prolonged Hypotension. *Mol Med (Cambridge Mass)* (2010) 16(7-8):254–61. doi: 10.2119/molmed.2009.00184
38. Beck C, Barthel F, Hahn A-M, Vollmer C, Herminghaus A, Schäfer S, et al. The Beneficial Effects of Acute Hypercapnia on Microcirculatory Oxygenation in an Animal Model of Sepsis are Independent of K(+)ATP Channels. *Microvascular Res* (2015) 99:78–85. doi: 10.1016/j.mvr.2015.02.009
39. Hajhashemi V, Amin B. Effect of Glibenclamide on Antinociceptive Effects of Antidepressants of Different Classes. *Clinics (Sao Paulo)* (2011) 66(2):321–5. doi: 10.1590/s1807-59322011000200023
40. Iskit AB, Erkent U, Ertunc M, Guc MO, Ilhan M, Onur R. Glibenclamide Attenuates the Antiarrhythmic Effect of Endotoxin With a Mechanism Not Involving K(ATP) Channels. *Vasc Pharmacol* (2007) 46(2):129–36. doi: 10.1016/j.vph.2006.08.415
41. Pihan G, Majzoubi D, Haudenschild C, Trier JS, Szabo S. Early Microcirculatory Stasis in Acute Gastric Mucosal Injury in the Rat and Prevention by 16,16-Dimethyl Prostaglandin E2 or Sodium Thiosulfate. *Gastroenterology* (1986) 91(6):1415–26. doi: 10.1016/0016-5085(86)90195-2
42. Ahmad A, Druzhyna N, Szabo C. Delayed Treatment With Sodium Hydrosulfide Improves Regional Blood Flow and Alleviates Cecal Ligation and Puncture (Clp)-Induced Septic Shock. *Shock* (2016) 46(2):183–93. doi: 10.1097/shk.0000000000000589
43. Volpato GP, Searles R, Yu B, Scherrer-Crosbie M, Bloch KD, Ichinose F, et al. Inhaled Hydrogen Sulfide: A Rapidly Reversible Inhibitor of Cardiac and

Metabolic Function in the Mouse. *Anesthesiology* (2008) 108(4):659–68. doi: 10.1097/ALN.0b013e318167af0d
44. Guettler C, Kubes P. Hydrogen Sulfide, Another Simple Gas With Complex Biology. *Am J Physiol Gastrointestinal Liver Physiol* (2013) 304(12):G1066–9. doi: 10.1152/ajpgi.00125.2013
45. Fiorucci S, Antonelli E, Mencarelli A, Orlandi S, Renga B, Rizzo G, et al. The Third Gas: H2S Regulates Perfusion Pressure in Both the Isolated and Perfused Normal Rat Liver and in Cirrhosis. *Hepatology (Baltimore Md)* (2005) 42(3):539–48. doi: 10.1002/hep.20817
46. Distrutti E, Mencarelli A, Santucci L, Renga B, Orlandi S, Donini A, et al. The Methionine Connection: Homocysteine and Hydrogen Sulfide Exert Opposite Effects on Hepatic Microcirculation in Rats. *Hepatology (Baltimore Md)* (2008) 47(2):659–67. doi: 10.1002/hep.22037
47. Norris EJ, Larion S, Culberson CR, Clemens MG. Hydrogen Sulfide Differentially Affects the Hepatic Vasculature in Response to Phenylephrine and Endothelin 1 During Endotoxemia. *Shock* (2013) 39(2):168–75. doi: 10.1097/SHK.0b013e3182736688
48. Denoix N, McCook O, Ecker S, Wang R, Waller C, Radermacher P, et al. The Interaction of the Endogenous Hydrogen Sulfide and Oxytocin Systems in Fluid Regulation and the Cardiovascular System. *Antioxidants (Basel Switzerland)* (2020) 9(8):748. doi: 10.3390/antiox9080748
49. Szabo C. Hydrogen Sulfide, an Enhancer of Vascular Nitric Oxide Signaling: Mechanisms and Implications. *Am J Physiol Cell Physiol* (2017) 312(1):C3–c15. doi: 10.1152/ajpcell.00282.2016
50. Módis K, Coletta C, Erdélyi K, Papapetropoulos A, Szabo C. Intramitochondrial Hydrogen Sulfide Production by 3-Mercaptopyruvate Sulfurtransferase Maintains Mitochondrial Electron Flow and Supports Cellular Bioenergetics. *FASEB J* (2013) 27(2):601–11. doi: 10.1096/fj.12-216507
51. Nicholls P, Kim JK. Sulphide as an Inhibitor and Electron Donor for the Cytochrome C Oxidase System. *Can J Biochem* (1982) 60(6):613–23. doi: 10.1139/o82-076
52. Macfarlane GT, Gibson GR, Cummings JH. Comparison of Fermentation Reactions in Different Regions of the Human Colon. *J Appl bacteriology* (1992) 72(1):57–64. doi: 10.1111/j.1365-2672.1992.tb04882.x
53. Libiad M, Vitvitsky V, Bostelaar T, Bak DW, Lee HJ, Sakamoto N, et al. Hydrogen Sulfide Perturbs Mitochondrial Bioenergetics and Triggers Metabolic Reprogramming in Colon Cells. *J Biol Chem* (2019) 294 (32):12077–90. doi: 10.1074/jbc.RA119.009442
54. Datzmann T, Hoffmann A, McCook O, Merz T, Wachter U, Preuss J, et al. Effects of Sodium Thiosulfate (Na(2)s(2)O(3)) During Resuscitation From Hemorrhagic Shock in Swine With Preexisting Atherosclerosis. *Pharmacol Res* (2020) 151:104536. doi: 10.1016/j.phrs.2019.104536
55. Ogasawara Y, Isoda S, Tanabe S. Tissue and Subcellular Distribution of Bound and Acid-Labile Sulfur, and the Enzymic Capacity for Sulfide Production in the Rat. *Biol Pharm Bull* (1994) 17(12):1535–42. doi: 10.1248/bpb.17.1535
56. Furne J, Saeed A, Levitt MD. Whole Tissue Hydrogen Sulfide Concentrations are Orders of Magnitude Lower Than Presently Accepted Values. *Am J Physiol Regul Integr Comp Physiol* (2008) 295(5):R1479–85. doi: 10.1152/ajpregu.90566.2008
57. Mitchell TW, Savage JC, Gould DH. High-Performance Liquid Chromatography Detection of Sulfide in Tissues From Sulfide-Treated Mice. *J Appl Toxicol JAT* (1993) 13(6):389–94. doi: 10.1002/jat.2550130605
58. Truse R, Hinterberg J, Schulz J, Herminghaus A, Weber A, Mettler-Altmann T, et al. Effect of Topical Iloprost and Nitroglycerin on Gastric Microcirculation and Barrier Function During Hemorrhagic Shock in Dogs. *J Vasc Res* (2017) 54(2):109–21. doi: 10.1159/000464262

Conflict of Interest: The authors declare that the research was conducted in the absence of any commercial or financial relationships that could be construed as a potential conflict of interest.

frontiers in Immunology

ORIGINAL RESEARCH
published: 22 July 2021
doi: 10.3389/fimmu.2021.708670

An Early Myelosuppression in the Acute Mouse Sepsis Is Partly Outcome-Dependent

Tomasz Skirecki[1], *Susanne Drechsler*[2], *Aldona Jeznach*[1], *Grażyna Hoser*[1], *Mohammad Jafarmadar*[2], *Jerzy Kawiak*[1] *and Marcin F. Osuchowski*[2]*

[1] Laboratory of Flow Cytometry, Centre of Postgraduate Medical Education, Warsaw, Poland, [2] Ludwig Boltzmann Institute for Experimental and Clinical Traumatology in the Allgemeine Unfallversicherungsanstalt (AUVA) Research Center, Vienna, Austria

Adult hematopoietic stem and progenitor cells (HSPCs) respond to bacterial infections by expansion to myeloid cells. Sepsis impairs this process by suppressing differentiation of stem cells subsequently contributing to an ineffective immune response. Whether the magnitude of HSPCs impairment in sepsis is severity-dependent remains unknown. This study investigated dynamics of the HSPC immune-inflammatory response in the bone marrow, splenic, and blood compartments in moribund and surviving septic mice. The 12-week-old outbred CD-1 female mice (n=65) were subjected to a cecal ligation and puncture (CLP) sepsis, treated with antibiotics and fluid resuscitation, and stratified into predicted-to-die (P-DIE) and predicted-to-survive (P-SUR) cohorts for analysis. CLP strongly reduced the common myeloid and multipotent progenitors, short- and long-term hematopoietic stem cell (HSC) counts in the bone marrow; lineage$^-$ckit$^+$Sca-1$^+$ and short-term HSC suppression was greater in P-DIE *versus* P-SUR mice. A profound depletion of the common myeloid progenitors occurred in the blood (by 75%) and spleen (by 77%) of P-DIE. In P-SUR, most common circulating HSPCs subpopulations recovered to baseline by 72 h post-CLP. Analysis of activated caspase-1/-3/-7 revealed an increased apoptotic (by 30%) but not pyroptotic signaling in the bone marrow HSCs of P-DIE mice. The bone marrow from P-DIE mice revealed spikes of IL-6 (by 5-fold), CXCL1/KC (15-fold), CCL3/MIP-1α (1.7-fold), and CCL2/MCP-1 (2.8-fold) *versus* P-SUR and control (TNF, IFN-γ, IL-1β, -5, -10 remained unaltered). Summarizing, our findings demonstrate that an early sepsis-induced impairment of myelopoiesis is strongly outcome-dependent but varies among compartments. It is suggestive that the HSCPC loss is at least partly due to an increased apoptosis but not pyroptosis.

Keywords: infection, cecal ligation and puncture, hematopoietic stem and progenitor cells, outcome prediction, immunity, caspases

OPEN ACCESS

Edited by:
Christoph Thiemermann, Queen Mary University of London, United Kingdom

Reviewed by:
Jianmin Chen, Queen Mary University of London, United Kingdom
Sina Maren Coldewey, University Hospital Jena, Germany

***Correspondence:**
Marcin F. Osuchowski
marcin.osuchowski@trauma.lbg.ac.at

Specialty section:
This article was submitted to Inflammation, a section of the journal Frontiers in Immunology

Received: *12 May 2021*
Accepted: *05 July 2021*
Published: *22 July 2021*

Citation:
Skirecki T, Drechsler S, Jeznach A, Hoser G, Jafarmadar M, Kawiak J and Osuchowski MF (2021) An Early Myelosuppression in the Acute Mouse Sepsis Is Partly Outcome-Dependent. Front. Immunol. 12:708670. doi: 10.3389/fimmu.2021.708670

INTRODUCTION

Adult mammals constantly produce mature blood cells from the hematopoietic stem cells in the process of hematopoiesis occurring in the bone marrow (BM) (1). In adulthood, the majority of hematopoietic stem and progenitor cells (HSPCs) are located in specialized niches in the BM, which protect them from oxidative injury and tightly control the hematopoiesis *via* multiple molecular

interactions (2). However, even at the steady-state, a small subpopulation of HSCs circulates in the body *via* the blood and lymph in a process orchestrated by the sphingosine-1 phosphate gradient (3). It has been shown that through an expression of the toll-like receptors (TLRs), HSCs can sense microbial infections and locally differentiate to myeloid cells contributing to a local immune response (3, 4). An efficient fight with bacterial infections requires an increased production of short-lived myeloid cells that are constantly consumed from HSPCs in a coordinated process of the so-called emergency myelopoiesis (5). Microbial compounds are sensed by TLRs and nucleotide-binding oligomerization domain containing (NOD)-like receptors located on the endothelial cells of the BM niche, which in turn produce the granulocyte-colony stimulating factor (G-CSF) inducing proliferation and differentiation of HSPCs (6). In mice, G-CSF has been shown to drive mobilization of HSPCs from the BM niche to the blood and subsequently the spleen (7).

It is already well recognized from the murine models that sepsis profoundly affects the HSPCs compartment leading to an impaired myelopoiesis (8). Recognition of lipopolysaccharide (LPS) from gram-negative bacteria (*via* TLR4 receptor expressed by HSPCs) leads to an increased proliferation of HSCs with a concomitant blockage of differentiation into myeloid progenitor cells (9, 10). Importantly, the TLR4 signaling (*via* its adaptor TRIF) mediates a persistent injury to HSC self-renewal and repopulating functions—raising a question regarding the long-term effects of sepsis on hematopoiesis (11). We have reported a dysfunctional expansion of human HSCs following an abdominal sepsis in the humanized mice, demonstrating that this process was partially dependent on an increased Notch signaling (12). The dysfunctional myelopoiesis in the course of sepsis has been shown to especially affect neonatal and old animals (13, 14). Long-lasting epigenetic modifications of murine myeloid progenitor cells were recently shown to impair wound healing by their outgrowth macrophages underscoring negative effects of sepsis on the HSPCs compartment (15).

Currently, little is known about the hematopoiesis dynamics in septic patients, given that the blood serves as the sole source of information. In a previous study, we investigated the changes in circulating HSPCs in septic patients and observed an increased mobilization of primitive $CD34^+CD38^-$ and $Lin^-CD133^+CD45^+$ HSCs early in the course of disease (16). The circulating HSPCs expressed markers of an active cell cycle, which appears to confirm the observations from septic mice. We also demonstrated that patients with a higher number of circulating HSCs are less likely to survive (16). Similarly, a negative correlation between circulating HSPCs and outcome was reported by Tsaganos et al. (17). However, neither the relationship between the BM HSPCs and sepsis severity/outcome nor the mechanistic link between dysfunctional hematopoiesis and sepsis course has been explored.

In this study, we hypothesized that the severity of sepsis is associated with the magnitude of changes in the early hematopoiesis. We analyzed the HSCP compartment in the BM, spleen, and blood harvested from outbred mice subjected to a clinically relevant model of polymicrobial sepsis by cecal ligation and puncture (CLP) and stratified into two homogenous predicted-to-die (P-DIE) and predicted-to-survive (P-SUR) cohorts. Our data provide a missing insight into the disturbances in emergency myelopoiesis that may lead to a potential therapeutic modulation of this process.

MATERIALS AND METHODS

Mice

For the experiments 12-week-old female CD-1 (n=65) mice were purchased from Charles River Laboratories (Sulzfeld, Germany) and allowed to acclimatize to their new environment for at least 1 week prior to the experiment. Groups of five animals were housed in type III cages under standardized conditions (i.e., 12-h light-dark diurnal cycle, controlled temperature of 22–24°C). A standard rodent diet and fresh water were provided *ad libitum* throughout the study. Cages were enriched with carton houses, wooden boards, wood wool, hazel nuts, and wooden sticks for gnawing to facilitate natural behavior.

Ethical Statement

All animal procedures were approved by the Viennese (Austria) legislative committee (Animal Use Proposal Permission No. 0899/2012/05) and conducted according to the National Institutes of Health guidelines.

CLP Sepsis Model

All surgical procedures were executed under inhalation anesthesia with isoflurane (2-3%, Forane®, Baxter, Austria). Mice received analgesia (buprenorphine, bid, 0.05 mg/kg, s.c., Bupaq®, Richter Pharma, Austria), antibiotics (imipenem/cilastatin, Zienam®, bid, 25 mg/kg, s.c.), and fluid resuscitation (1 ml saline, 0,9%, bid) for the first five days after CLP.

Polymicrobial sepsis was induced using the cecal ligation and puncture model following the original protocol by Wichterman et al. (18) with modifications specified elsewhere (19). Shortly, anesthetized mice were placed in a supine position, abdomen was shaved, and skin disinfected. The abdominal cavity was opened, cecum exposed, ligated underneath the ileocecal valve with silk (Silkam® 4.0, B.Braun), and punctured twice with an 18G needle. Abdominal wall was closed with single button sutures (Silkam® 4.0), and skin was closed using skin adhesive (Histoacryl®, B.Braun). Antibiotic treatment was started 2 h after CLP surgery. Control mice did not undergo any surgery nor received treatment to serve as normal healthy mice reference.

Study Design

The study focused on differentiating lethal and surviving phenotypes for the hematopoiesis-related endpoints. To enable that, all CLP mice were stratified into two homogenous cohorts with high and low probability of survival: i.e., predicted-to-die (P-DIE) and predicted-to-survive (P-SUR). Mice identified as P-DIE at approximately 24 and 48 h (± 3 h of each timepoint) were

euthanized and samples harvested. To ensure an appropriate outcome comparison, a limited number of P-SUR mice were simultaneously sacrificed at the same timepoints following the previously used protocol (19, 20). Mice that could not have been stratified into either P-DIE or P-SUR were monitored and sacrificed at later timepoints if they met either of those two criteria. We selected 24 and 48 h timepoints for P-DIE *vs.* P-SUR comparison based on the mortality dynamic of our CLP model: the bulk of CLP deaths occurred within the 48 h of CLP. Extending the P-DIE/P-SUR comparison to further timepoints would have radically increased the number of mice, and it would not have adhered to the 3R tenet. To most judiciously utilize the remaining CLP mice, we created longitudinal P-SUR-only profiles (shown in **Figures 1**–**3B**, **Supplementary Figures 1E–H**, and **Supplementary Figure 4**) by sacrificing P-SUR mice at 72 h and day 9 post-CLP.

The design of our study adheres to the majority of the points described in the Minimum Quality Threshold in Pre-Clinical Sepsis Studies (MQTiPSS) Consensus Recommendations (21); we met 17 points, failed to meet eight, whereas four were not applicable (**Supplementary Table 1**).

Monitoring

All mice were monitored for clinical signs of illness and their status was evaluated using our custom-developed modified mouse clinical assessment scoring system (M-CASS) based on e.g. fur, posture, mobility, alertness, startle, righting reflex (and others) (22) starting 12 h post-CLP. Simultaneously, rectal

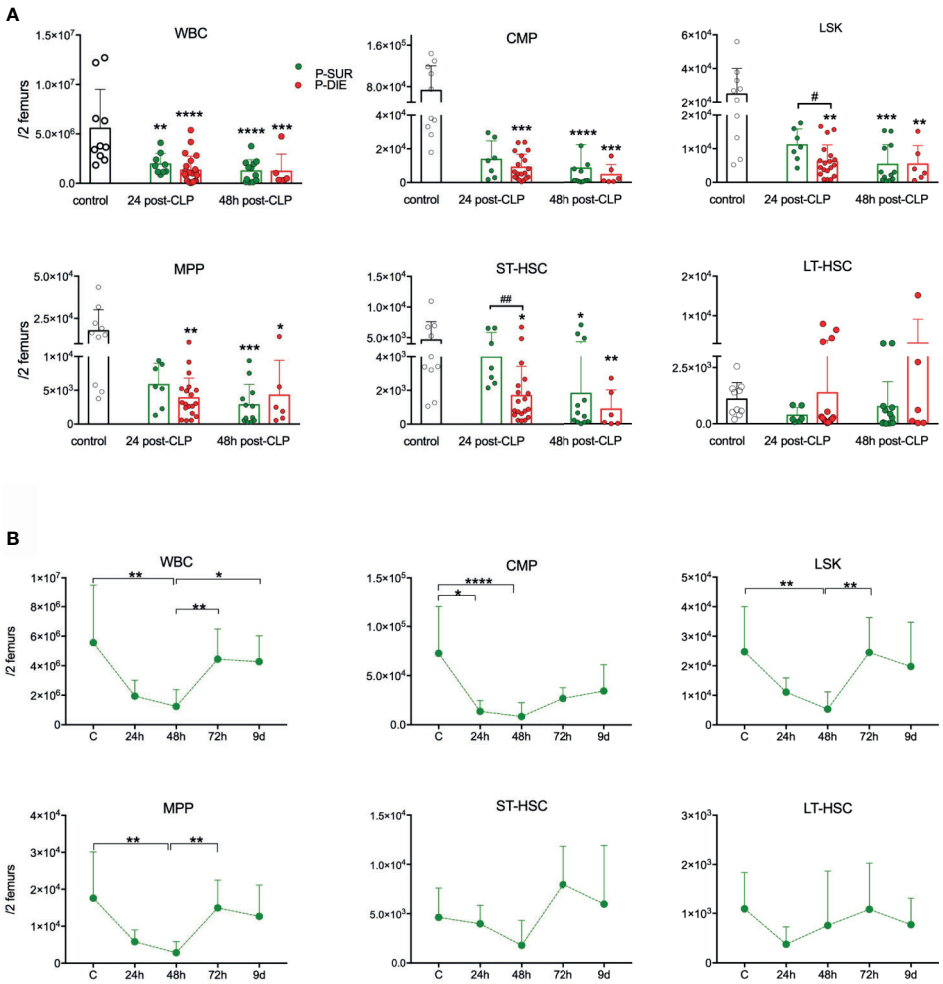

FIGURE 1 | Outcome-related and longitudinal changes in the total cell count of the bone marrow progenitor cells in CD-1 mice subjected to CLP. **(A)** Comparative data for mice assigned as predicted to survive (P-SUR, green) and predicted to die (P-DIE, red) are shown for the white blood count (WBC), common myeloid progenitors (CMP), LSK cells, long-term hematopoietic stem cells (LT-HSC), short-term HSCs (ST-HSC), and multipotent progenitors (MPP). Subgroups were compared using Student t-test with Welch correction whenever required. Hash signs show differences between P-DIE and P-SUR groups; asterisks indicate differences between given subgroups of mice and control (healthy) mice, **(B)** Changes in the cell counts of given populations in the predicted to survive (P-SUR) mice only; dotted connecting lines indicate separate sets of P-SUR sacrificed at a given timepoint. Baseline (BL) n=10, 24 h n=9, 48 h n=12, 72 h n=9, 9 days n=5 Groups were compared using 1-way ANOVA with Tukey's multiple comparison test. *p<0.05, **p<0.01, ***p<0.001, ****p<0.0001. #p<0.05; ##p<0.01.

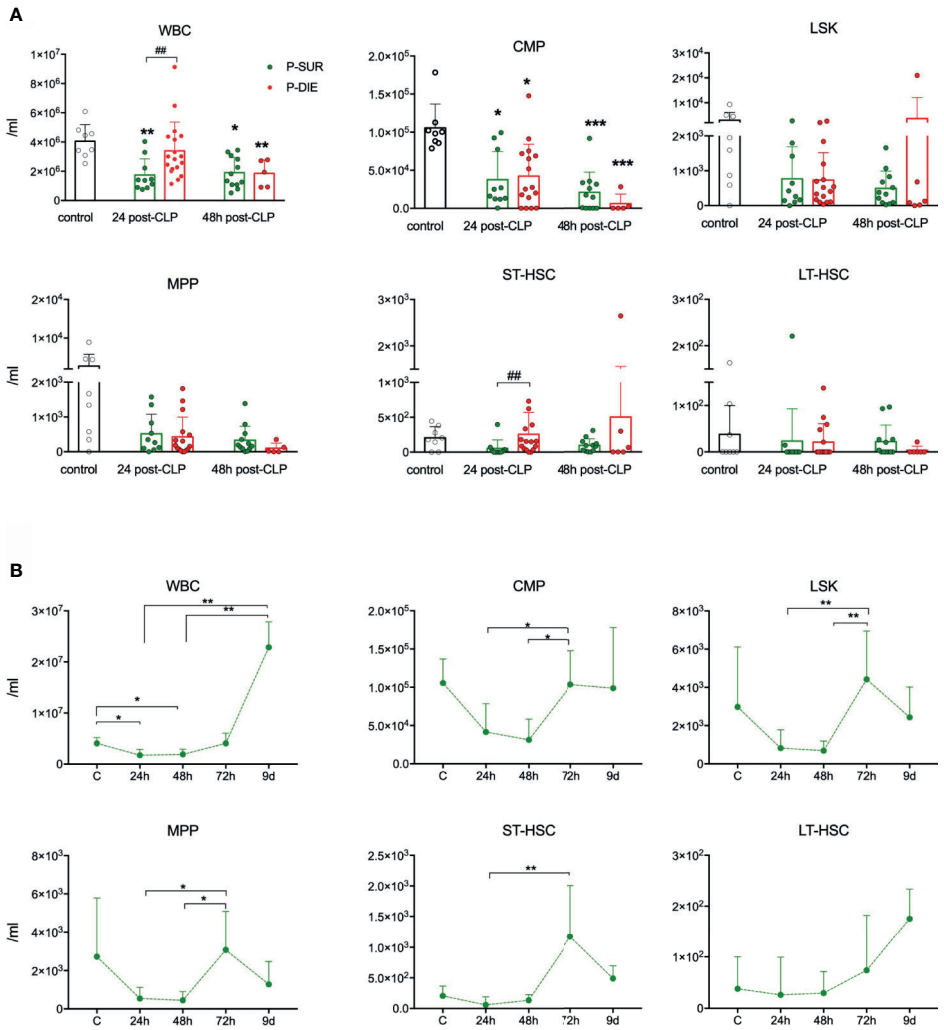

FIGURE 2 | Outcome-related and longitudinal changes in the total cell count of peripheral blood progenitor cells in CD-1 mice subjected to CLP. **(A)** Comparative data for mice assigned as predicted to survive (P-SUR) and predicted to die (P-DIE) are shown for the white blood count (WBC), common myeloid progenitors (CMP), LSK cells, long-term hematopoietic stem cells (LT-HSC), short-term HSCs (ST-HSC), and multipotent progenitors (MPP). Subgroups were compared using Student t-test with Welch correction whenever required. Hash show differences between P-DIE and P-SUR groups; asterisks indicate differences between given subgroups of mice and control (healthy) mice, **(B)** Changes in the cell counts of given populations in P-SUR mice only; dotted connecting lines indicate separate sets of P-SUR sacrificed at a given timepoint. Baseline n=10, 24 h n=10, 48 h n=10, 72 h n=12, 9 days n=5. Groups were compared using 1-way ANOVA test with Tukey's multiple comparison test. *p<0.05, **p<0.01, ***p<0.001. #p<0.05.

temperature was monitored (Fluke Series II thermometer, Fluke, USA) at least twice daily (or more often whenever a mouse deteriorated) to ensure a maximally precise outcome stratification and humane endpoints. Mice were deemed moribund and assigned as P-DIE whenever the righting reflex was absent or/and M-CASS score ≥8 and/or body temperature (BT) < 28°C (recorded in at least two sequential measurements) and immediately euthanized under deep inhalation anesthesia with isoflurane followed by cervical dislocation. The BT-based prediction of outcome we have developed in our laboratory is highly accurate [AUC = 0.94 (19)] and was repeatedly used in previous studies (20, 22, 23).

Blood Sampling and Blood Cell Count

A serial low-volume blood sampling was used to longitudinally monitor the changes in the peripheral blood cell counts (23) shown in **Supplementary Figure 1**. Briefly, 30 µl of blood was drawn by puncturing the facial vein with a 23-G needle, and blood was collected with a pipette. Samples were then immediately diluted 1:10 in PBS with ethylenediaminetetraacetic acid. After centrifugation (1,000*g*, 5 min, 22°C), 270 µl of plasma was removed and the remaining blood pellet was resuspended with 180 µl Cell-Dyn buffer with EDTA and a complete blood count with differential was performed with a Cell-Dyn 3700 counter (Abbott Laboratories, Illinois, USA).

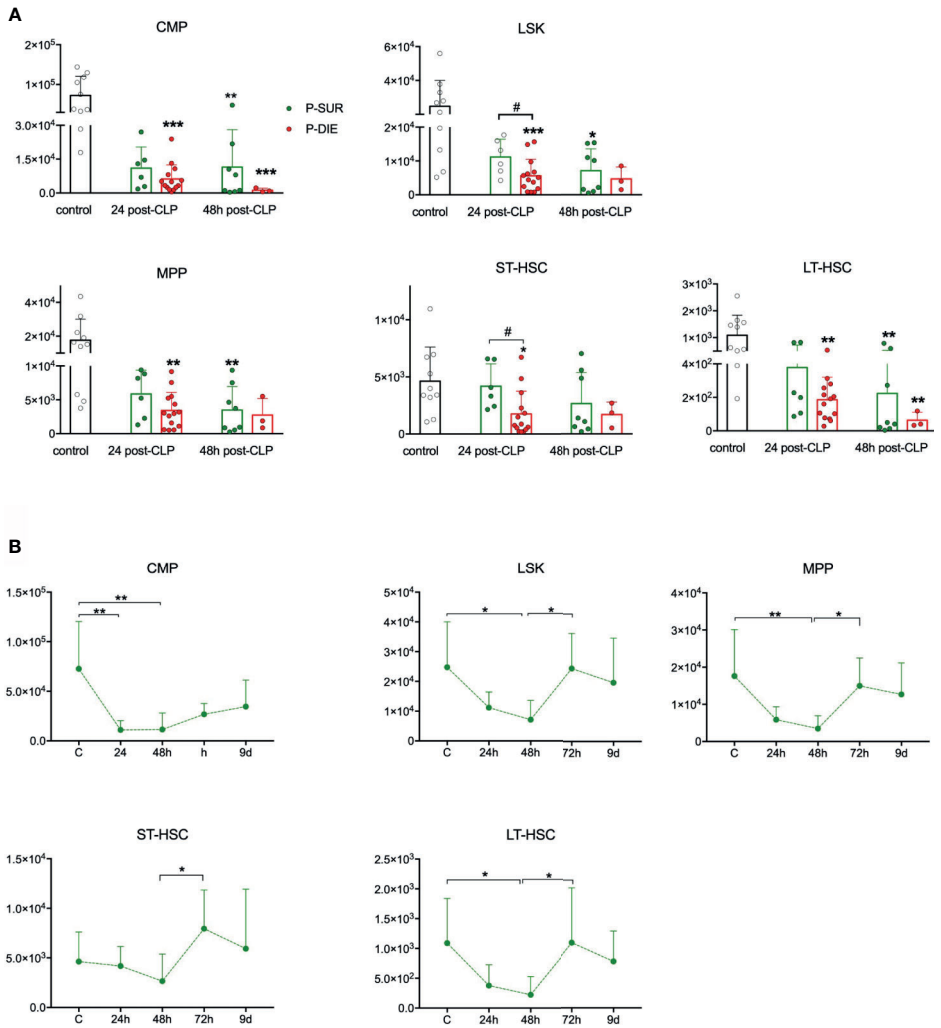

FIGURE 3 | Outcome-related and longitudinal changes in the total cell count of the spleen progenitor cells in CD-1 mice subjected to CLP. **(A)** Comparative data for mice assigned as predicted to survive (P-SUR) and predicted to die (P-DIE) are shown for the common myeloid progenitors (CMP), LSK cells, long-term hematopoietic stem cells (LT-HSC), short-term HSCs (ST-HSC), and multipotent progenitors (MPP). Subgroups were compared using Student t-test with Welch correction whenever required. Hash show differences between P-DIE and P-SUR groups; asterisks indicate differences between given subgroups of mice and control (healthy) mice, **(B)** Changes in the cell counts of given populations in P-SUR animals only; dotted connecting lines indicate separate sets of P-SUR mice sacrificed at a given timepoint; baseline (BL) n=10, 24 h n=8, 48 h n=8, 72 h n=9, 9 days n=5. Groups were compared using one-way ANOVA test with Tukey's multiple comparison test. *p<0.05, **p<0.01, ***p<0.001. #p<0.05.

Immunophenotyping

Peripheral blood was obtained from mice under isoflurane anesthesia from retroorbital venous plexus. After cervical dislocation, the spleen and femurs were dissected. Red blood cells were lysed in all samples with ACK Lysing Buffer (ThermoFisher Scientific). Samples were stained with the following antibodies: anti-lineage cocktail-APC (clones: 145-2C11 (CD3e), M1/70 (CD11b), RA3-6B2 (CD45R/B220), TER-119 (Ly-76), RB6-8C5 (Ly6G/Ly-6C, BD Pharmingen, San Jose, CA, USA), anti-Sca-1 (Ly-6A/E)-PE-Cy7 (D7, BD Pharmingen), anti-ckit (CD117)-PE (2B8, BD Pharmingen), anti-CD48-biotin (clone HM48-1, BioLegend, San Diego, CA, USA), anti-CD150- AlexaFluor 488 (clone TC15-12F12.2, BioLegend). Following 20 min of incubation in room temperature, Streptavidin PE-eFluor610 (eBioscience) was added for next 15 min and cells were washed with 1 ml of PBS and resuspended in 0.5% formaldehyde in PBS. Cells were analyzed FC-500 flow cytometer (Beckman Coulter, Brea, CA, USA). A minimum of 50,000 mononuclear cells were recorded and analyzed in FlowJo software (FlowJo LLC., Ashland, OR, USA).

Cytokine Assay

Both femurs from each mouse were dissected and then flushed with 0.5 ml of PBS each. Next, the bone marrow suspension was spun at 400*g* for 5 min, and supernatants were collected. Samples were stored at −86°C until analysis. The bone marrow concentration cytokines (IL-6, IL-8/KC, IL-10, TNF, MCP-1) was measured using

Luminex Multiplex Immunoassay (Invitrogen, Thermo Fisher Scientific, Vienna, Austria) according to the manufacturer's protocol. Finally, concentration of these mediators was normalized against the albumin concentration (Bradford Protein Assay, Thermofisher) in the BM samples to minimize the potential differences in harvesting BM from femurs.

Apoptosis and Gene Expression Analysis

The bone marrow cells were obtained and subjected to erythrocyte lysis as described above. Next, samples were split for the caspase-1 and caspase-3/7 analysis. For the evaluation of activated caspase-1, BM cells were incubated for 30 min with the FAM-YVAD-FMK FLICA Caspase-1 reagent (ImmunoChemistry Technologies, LLC, MN, USA) according to the manufacturer's protocol and then stained with the anti-Lineage -APC, anti-ckit-PE, and anti-Sca-1-PE-Cy7 antibodies as described. Activated caspases-3/7 were analyzed by staining with the FMK-DEVD FLICA probe (Vybrant FAM caspase-3 and-7 Assay, Thermofisher) and then co-stained with surface antibodies as described above.

For the gene expression flow cytometry analysis, lysed bone marrow cells were stained with the eBioscience Fixable Vability Dye eFluor 506 (Thermofisher) and the following antibodies: anti-lineage eFluor 405 (Thermofisher), anti- Sca-1 (Ly-6A/E)-PE-Cy7, and anti-ckit (CD117)-PE (both BD Pharmingen). Then cells were fixed, permeabilized, and hybridized with probes against TNF, IL6, and IL1β mRNA using the PrimeFlow RNA Assay Kit (Thermofisher) according to the manufacturer's protocol. As a positive controls additional samples were stained against β2-microglobulin. Cells were analyzed with FACSCanto II flow cytometer (BD), and FlowJo software was further used to analyze the results.

Statistical Analysis

Normality of all data sets was assessed using the Shapiro-Wilk test and log-normally transformed whenever necessary to achieve Gaussian distribution and control for existing outliers. Comparisons between P-DIE and P-SUR group were performed by t-test (with Welch correction for unequal variances if needed) and Mann-Whitney (for non-Gaussian data distribution) at each timepoint separately given that the P-DIE group did not meet assumptions (non-random deaths) for a repeated measures testing. The comparison of variables in P-SUR mice at different timepoints was performed using the two-way ANOVA with Tukey's post-hoc test. $p<0.05$ was considered significant. Data are shown on the original scale as scatter plot overlaid over bars and expressed as means and standard deviations (SD), if not otherwise stated. GraphPad Prism 7 (GraphPad, Inc., USA) software was used for evaluating the statistical significance and/or graphical depiction of the data.

RESULTS

A Transient Association of the Peripheral Blood Cell Counts With CLP Outcome

Based on the utilized outcome prediction, CLP resulted in approximately 40% mortality. Using the low-volume blood sampling, we monitored changes in the peripheral blood cell counts without sacrificing mice. Sepsis induced an early generalized peripheral leukopenia (mostly because of the depletion of neutrophils and lymphocytes) and lasted for at least 72 h post-CLP (**Figure S1**). Outcome-related differences were noted at 6 h (platelets lower in P-DIE; **Figure S1D**) and 24 h (lymphocytes higher in P-DIE *vs.* P-SUR; **Figure S1C**) post-CLP. Longitudinal analysis of the blood cell counts in the surviving mice showed a maximal decrease of circulating cells of all lineages at 24 h followed by a slow rebound until day 9 post-CLP (**Figures S1E–H**).

CLP Outcome Is Associated With Depletion of the Hematopoietic Stem and Progenitor Cells (HSPCs) in the Bone Marrow

We utilized flow cytometry staining with a set of validated immunophenotype markers that were previously shown to be stably expressed in inflammatory conditions (7, 10). We used a standard gating strategy to distinguish major populations of murine HSPCs, including common myeloid progenitors (CMP; Lineage$^-$ckit$^+$Sca-1$^-$), LSK (Lineage$^-$ckit$^+$Sca-1$^+$), long-term repopulating stem cells (LT-HSCs; Lin$^-$ckit$^+$Sca-1$^+$CD150$^+$CD48$^-$), short-term repopulating stem cells (ST-HSCs; Lin$^-$ckit$^+$Sca-1$^+$CD150$^+$CD48$^+$), and multipotent progenitors (MPPs; Lin$^-$ckit$^+$Sca-1$^+$CD150$^-$CD48$^-$) (**Figure S2A**) (10, 24, 25).

Although the cellularity of BM in control mice was spread (5.5×10^6 +/−3.9×10^6), CLP mice had a decreased total BM cell count in both P-SUR (1.9×10^6) and P-DIE (1.3×10^6) groups at 24 h; CMP suppression was evident in all groups at both timepoints (**Figure 1A**). The LSK, MPP, and ST-HSC counts were initially reduced in an outcome-dependent fashion: at 24 h, the suppression was more pronounced in P-DIE (*vs.* P-SUR) mice followed by a similar decrease at 48 h post-CLP (**Figure 1A**). In addition, we analyzed the CLP-induced changes in the frequency of given HSPCs subpopulations. Sepsis caused a significant decrease of the myeloid progenitor cell's frequency only in P-SUR (but not P-DIE) mice at 24 h post-CLP (**Figure S2B**). The percentage of LSK and more specified MPP progenitors increased in P-DIE mice, whereas the subpopulations of ST-and LT-HSCs remained unaltered (**Figure S2B**).

We simultaneously monitored hematopoiesis changes in the BM of P-SUR mice until day 9. The strongest reduction in each analyzed cell population (except LT-HSCs) occurred at 48 h and was followed by a rapid recovery (to control values), indicative of their robust proliferation within the 48- to 72-h post-CLP interval (**Figure 1B**). Noteworthy, even at day 9 of observation, the myeloid progenitors count was, on average, two-fold lower compared with healthy mice.

A Limited Effect of CLP Upon the HSPCs Counts in the Blood

As mobilization of HSPCs to circulation from the BM was shown in several infectious conditions in mice (4, 7, 16), we also studied stem cells in the peripheral blood after CLP (**Figure S3A**).

No HSPC subpopulations (except CMP progenitors) were markedly diminished in the blood of septic mice (**Figure 2A**). Regarding outcome-based differences, only the subpopulation of ST-HSCs was 5-fold higher in P-DIE *vs* P-SUR mice 48 h after CLP, albeit not different from control (**Figure 2A**). In surviving mice (similarly to the kinetics observed in the BM), the subpopulations of HSPCs in the circulation were also prone to a robust rebound after 48 h despite the lack of an early post-CLP decrease (**Figure 2B**). Although leukopenia is not a common feature in septic patients, these results adhere to our previous observations showing lack of HSCs mobilization on the first day of ICU admission of septic shock patients (16).

A Profound CLP-Induced Depletion of Splenic HSPCs Is Partly Outcome-Dependent

It was shown in a nonlethal *E. coli* infection that murine LSK cells migrate from the BM and accumulate in the spleen (7). We analyzed the splenic HSPCs to verify whether a similar process occurs in CLP (**Figure S3B**). We observed a profound depletion of CMPs at both post-CLP timepoints, irrespective of the outcome (**Figure 3A**). In LSK and ST-HSC progenitors, the early depletion was markedly outcome-dependent, LSK were 50% and ST-HSCs 60% lower in P-DIE *versus* P-SUR mice at 24 h (**Figure 3A**). In contrast to BM (**Figure 1A**), the rare LT-HSCs subpopulation was depleted in P-DIE mice at both post-CLP timepoints and in P-SUR mice at 48 h (**Figure 3A**).

The kinetic of the splenic HSPCs counts in P-SUR was similar to the one in the BM; both regarding their initial abrupt decrease (nadir at 48 h), as well as a robust numerical recovery of all (except CMP) cell subpopulations (**Figure 3B**). Although on day 9 after CLP, the spleens were enlarged (data not shown), the number of $Lin^{-}ckit^{+}Sca\text{-}1^{-}$ CMPs did not reach the baseline level. Together, these data show that in an early sepsis, splenic HSPCs (including LT-HSCs) are severely depleted in an outcome-dependent manner.

P-DIE Mice Show a Strong Pro-Apoptotic Signaling in the Bone Marrow HSPCs

To gain insight into the mechanisms responsible for the acute depletion of LSK cells in septic mice, we analyzed hallmarks of apoptosis and pyroptosis at 24 h post-CLP (the timepoint preceding the nadir HSPC depletion). Caspase-3 and -7 activity in LSK cells from P-DIE mice was approximately 30% higher than that in P-SUR animals and three-fold higher compared with control (**Figures 4A, B**). Antibody-based analysis suggests increase in the cleavage of caspase-3 in LSK cells from P-DIE mice in comparison to P-SUR counterparts (**Figure S4**). We have utilized the FAM-FLICA probe to detect active caspase-1, which is a hallmark of inflammasome activation leading to pyroptosis. No meaningful inter-group differences for caspase-1 were detected (**Figures 4A, C**). An increased apoptosis appears to be the major mechanism of the HSPCs loss after CLP.

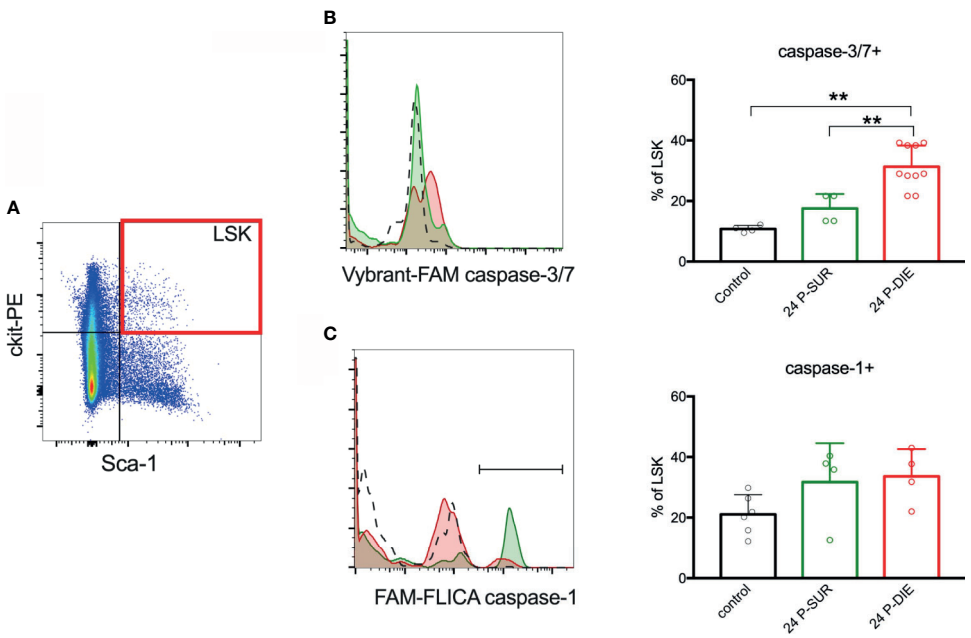

FIGURE 4 | Activation of inflammatory and apoptotic caspases in the bone marrow hematopoietic stem and progenitor cells. **(A)** Lineage-negative mononuclear cells were analyzed for the expression of ckit and Sca-1 and the LSK subpopulation was analyzed for: **(B)** active caspases-3/-7 and **(C)** active caspase-1. Percentage of LSK cells with active caspases were compared between predicted to die (P-DIE) and predicted to survive (P-SUR) mice using 1-way ANOVA test with Tukey's multiple comparison test. **p<0.01.

Outcome-Related Changes in the Bone Marrow Cytokine Milieu After CLP

We have previously shown that the systemic cytokine and chemokine response is strongly outcome-dependent in both early and late sepsis (26). Therefore, we analyzed selected cytokines in the BM supernatant from P-DIE and P-SUR mice 24 h after CLP. Similar to the circulating cytokine dynamics (26), IL-6 measured in the BM of P-DIE mice was approximately five-fold higher compared with P-SUR (2578 *vs* 550 *vs* 364 pg/ml in control mice; **Figure 5A**). In contrast, concentrations of IL-1β, IFN-γ, TNF, IL-5, and IL-10 remained unchanged in all three groups (**Figures 5B–F**). The outcome-dependent chemokine response was very robust: CXCL1/KC was 15-fold, CCL3/MIP-1α 1.7-fold, and CCL2/MCP-1 2.8-fold higher in P-DIE compared with P-SUR mice (**Figures 5G–I**).

We also analyzed the same cytokines/chemokines in P-SUR mice up to day 9 post-CLP. Only CXCL1/KC peaked at 24 h returning to the baseline level 24 h later (**Figure S5G**). Notably, we observed a uniform increase in all other mediators by day 9 after CLP; this change reached significance in IFN-γ (approximately 11-fold) and IL-10 (six-fold *vs* baseline; **Figures S5D, F**).

Hematopoietic stem cells have been shown to produce significant amounts of cytokines in response to the toll-like receptor-mediated stimulation (27). We sought to establish whether HSPCs contribute to an increased production of cytokines in dying septic mice. To analyze the gene expression of IL6, IL1β, and TNF in the infrequent LSK cells, we utilized a flow cytometry-based technique to stain mRNA transcripts with gene-specific probes and branched DNA amplification (28). The LSK cells expressed mRNA for IL6, IL1β, and TNF (**Figure 6**). In cells from P-DIE mice, IL-6 transcripts were upregulated by three-fold in comparison with P-SUR, whereas no differences were present for IL-1β and TNF expression (**Figure 6**). These results indicate that the BM cytokine milieu is selectively altered in dying septic mice and HSPCs also contribute to this differential localized cytokine production.

DISCUSSION

This mouse study addressed a gap in human sepsis by investigating whether the HSPCs in their bone marrow niche are differentially affected with regard to outcome (i.e., dying *versus* surviving). Such a design approach is superior to the most commonly used healthy-*versus*-septic comparison given that it characterizes homogenous phenotypes specific for recovery and death (rather than an unspecific and heterogeneous disease signal). Using a clinically relevant model of polymicrobial sepsis, we demonstrated that the

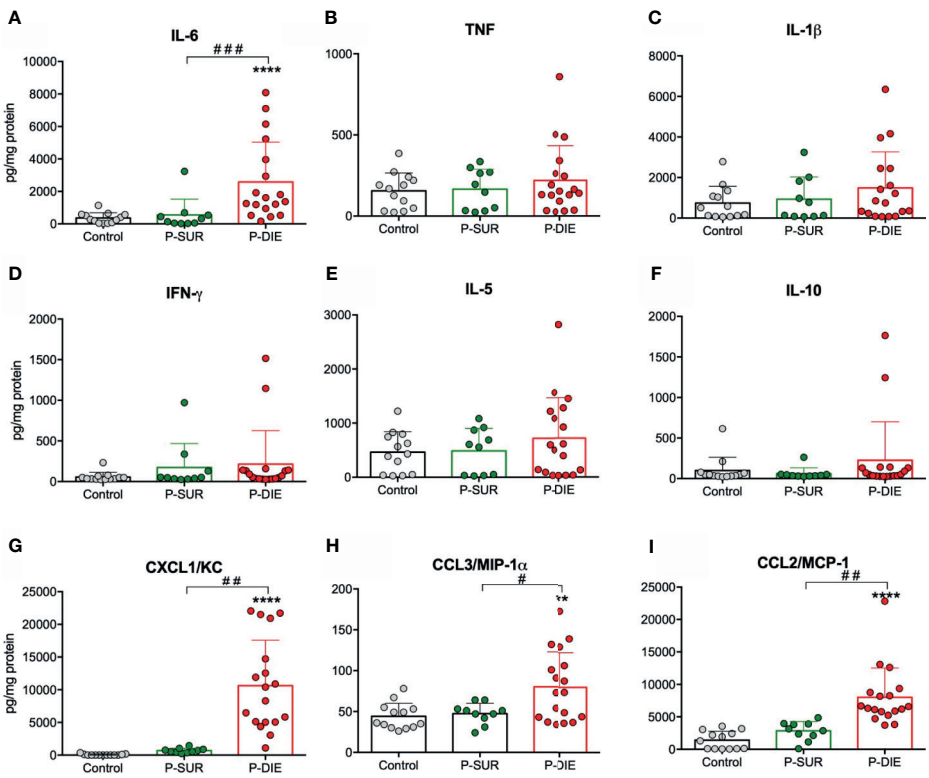

FIGURE 5 | Outcome-related changes in the cytokine's milieu of the bone marrow twenty-four hours after CLP. Total-protein normalized concentrations of **(A)** IL-6. **(B)** TNF. **(C)** IL-1β. **(D)** IFN-γ. **(E)** IL-5. **(F)** IL-10. **(G)** CXCL1/KC. **(H)** CCL3/MIP-1α. **(I)** CCL2/MCP-1 in the bone marrow supernatants of predicted-to survive (P-SUR) and predicted-to die (P-DIE) mice are shown. Concentration of cytokines between groups were compared using Student t-test with Welch correction whenever required. $^{**}p < 0.01$, $^{****}p < 0.0001$ between control and septic mice. $^{\#}p < 0.05$, $^{\#\#}p < 0.01$, $^{\#\#\#}p < 0.001$ between P-DIE and P-SUR groups.

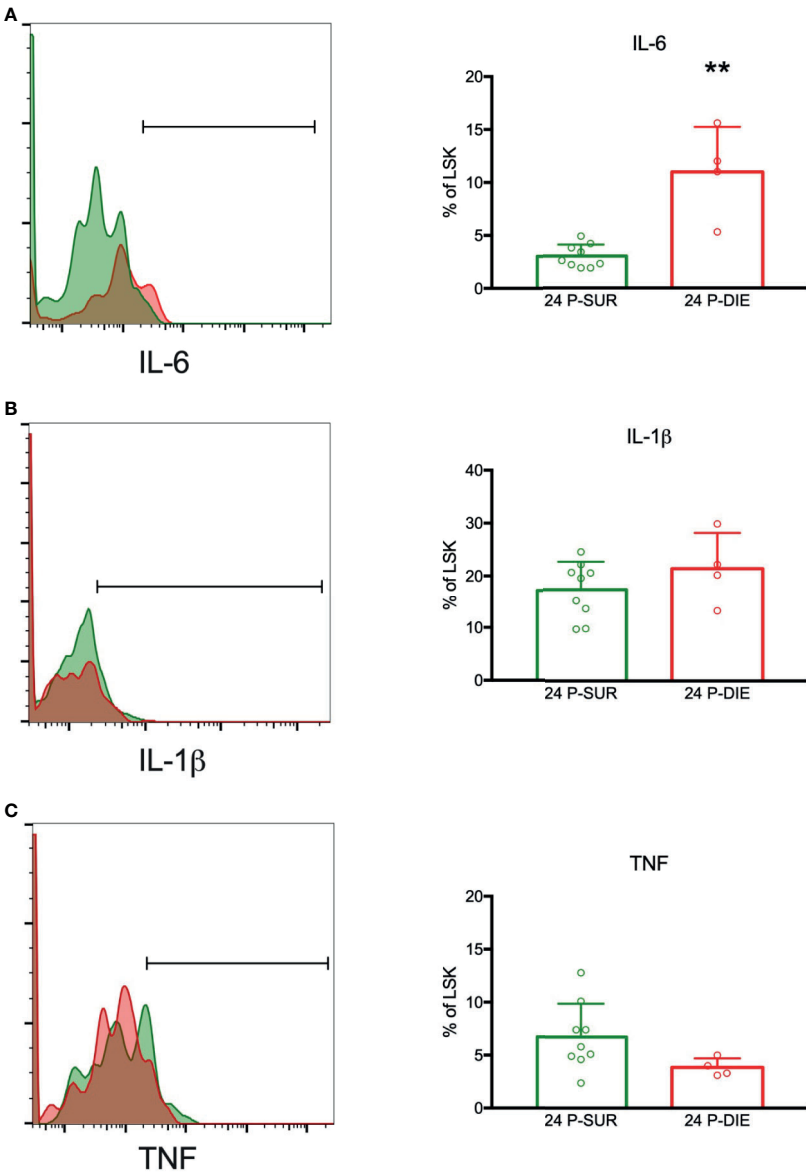

FIGURE 6 | Expression of mRNA for selected cytokines by the bone marrow hematopoietic progenitors in sepsis. The LSK cells were analyzed twenty-four hours after CLP for the expression of mRNA transcripts for: **(A)** IL-6. **(B)** IL-1β. **(C)** TNF by flow cytometry. Groups were compared using Student t-test. **p<0.01.

subpopulations of hematopoietic progenitors are depleted to a higher degree in mice predicted to die. We also identified apoptosis as the primary death pathway contributing to this effect. Simultaneously, the cytokine milieu of the bone marrow was more severely affected in the P-DIE animals and hematopoietic progenitors participated in synthesis of the IL-6.

Dysfunction of the bone marrow hematopoiesis in sepsis has been already shown by us and others and was mainly reported to be related to the block of differentiation of HSCs into myeloid progenitors (9, 12, 29). However, these changes were exclusively studied in pooled septic animals regardless of their clinical severity. In this study, we analyzed changes in several subpopulations of HSPCs in relation to sepsis severity in individual mice. Our results confirmed a depletion of percentage of myeloid progenitor cells in septic mice, which was more profound in mice with favorable prognosis. The frequency of bulk population of LSK cells (containing all hematopoietic stem cells) was expanded in P-DIE mice only. Also, subpopulations of multipotent progenitors and long-term repopulating HSCs expanded only in P-DIE mice. However, a total cell count evaluation of the HSPC subpopulations revealed contrasting dynamics, e.g., P-DIE mice had a markedly reduced number of myeloid progenitors, LSK cells, MPPs, and ST-HSCs. These results oppose some previous works reporting an expansion of LSK cells in sepsis (9, 10). However, others observed an increase in the frequency of LSK cell but without reporting the absolute counts (13, 29). There are several possible

reasons for such discrepancy. First, we used outbred CD-1 mice that better recapitulate the background genetic heterogeneity present in patients and in turn an individual heterogeneity in response to a polymicrobial infection. Most of the above-cited studies used C57BL/6 (9, 10) and BALB/c (29) strains, which were different for various endpoints in response to sepsis compared with outbred mice. Second, mortality of those sepsis models was not defined, and sepsis severity (e.g. mild *vs* lethal) greatly modulates immune-inflammatory responses (30). Importantly, Kobayashi et al. (31), who also showed a CLP-induced LSK expansion, reported no decrease of BM cellularity, which is in striking contrast to severe leukopenia recorded in our study. Sepsis and LPS were shown to induce HSCs impairment by decreasing their self-renewal, repopulating, and myeloid differentiation ability by a direct TLR4 signaling (10, 11). TLR-mediated signaling was shown to induce HSCs proliferation (10, 11); although we did not perform a cell-cycle analysis, it cannot be excluded that our model triggered a similar response despite a numerical HSC loss. In P-SUR mice, the numerical cell recovery was typically present at 72 h post-CLP, suggestive of an enhanced proliferation induction, and the HSPC expansion was evidently halted by day 9. We conclude that physiological mechanisms controlling the HSPC dormancy-renewal balance (24) function properly even in a semi-lethal sepsis phenotype. Importantly, emerging evidence suggests that sepsis induces epigenetic modifications in HSPCs (15), but their exact role remains to be elucidated. Our study expands those earlier findings by exploring an individualized outcome-dependent loss of HSPCs. Yet, the causal relationship between HSCs impairment and its contribution to an early mortality in sepsis remains uncertain. It can be anticipated that in the early phase of sepsis, depletion of HSPCs is one of the many effects of maladaptive inflammatory response but this relationship can be more casual in the chronic phase as suggested by beneficial effects of $CD34^+$ HSPCs transfer after CLP (32).

Depletion of HSPCs in BM can be attributed to either their mobilization to circulation or death. Notwithstanding, analysis of the peripheral blood revealed a decreased number of circulating HSPCs. Interestingly, the P-DIE mice had a five-fold higher number of circulating ST-HSCs in comparison to P-SUR animals. This reproduces our results from septic patients in whom a higher number of $Lin^-CD133^+CD45^+$ HSCs was associated with diminished survival (16). In systemic infections, the spleen can become a site of extramedullary hematopoiesis (33). CLP induced a loss of all the HSPCs subpopulations, and the depletion was more profound in P-DIE mice. Even several days after CLP (with a pronounced splenomegaly present), the total number of any HSPCs subpopulations was not elevated. Although we did not perform analysis of MDSCs, it is conceivable that splenic HSPCs contribute to a local generation of these cells (34, 35). Remick and colleagues showed increased neutrophil and macrophage counts in the peritoneum of P-DIE mice after sepsis (36, 37). It can be speculated that some HSPCs also infiltrate the infection site, contributing locally to the production of those effector cells and cytokines. Particularly, despite failure to control bacterial infection, the P-DIE mice were shown to produce high levels of CXCL1 and CXCL2 in the peritoneum and blood that promoted neutrophil infiltration (36). As both chemokines are also chemoattractant for HSPCs (38), these cells are likely to follow a similar route. Burberry et al. (7) showed that systemic *E. coli* mobilizes HSCs to the spleen from BM in G-CSF-dependent manner, and this effect lasted several days after infection. However, their model was nonlethal and induced by a single pathogen — greatly different from a surgically induced polymicrobial sepsis that we used. It can be hypothesized that in P-DIE mice, the enhanced egress of HSPCs from their professional BM niches to other sites with higher oxygen tension and inflammatory stimulation drives functional impairment of their outgrowth cells [e.g., bactericidal capacities (37)]. As reported by Davis et al. (15), sepsis induces epigenetic modifications of HSPCs that attenuate monocyte functions in a long-term period (15). Evidence supporting this hypothesis were generated by Brudecki et al. (32) who showed that transfer of HSCs from healthy animals improves long-term survival of septic mice (32). However, early HSCs were reported to have also immunoregulatory function *via* TNF secretion (39). Whether such a mechanism contributes to immunosuppression in sepsis remains to be verified. In contrast, in mild, non-lethal infections migratory HSPCs contribute to bacterial clearance (40). Our observations complement the emerging picture of a global depletion of hematopoietic precursors in early days of septic shock.

Our findings also show activation of caspase-3 and -7 in BM HSPCs in P-DIE mice only indicating an activation of HSPC apoptosis in a severity-dependent manner — this is consistent with reports on detrimental role of apoptosis in sepsis (41, 42). Induction of apoptosis in HSPCs subpopulations after CLP was also reported by Zhang et al. (10). Intriguingly, caspase-3 was reported to also play non-apoptotic role in HSCs, e.g., to control their dormancy by limiting ERK signaling in response to some cytokines (43). It can be hypothesized that caspase-3 increase can also contribute to the low HSPCs counts by inhibiting their responsiveness to cytokine signals, but we only assessed the cleaved caspase-3 at 24 h. As HSCs were shown to be able to undergo pyroptosis *via* NLRP1 inflammasome (44), we measured activation of caspase-1 in LSK cells. Although we observed a relatively high activity of caspase-1 in sham mice, sepsis did not increase it further, and there was no significant increase in IL-1β in the BM. It is a rather unexpected finding given that neonatal mice with caspase-1/-11 knock-out showed an increased frequency of LSK cells in septic mice compared to WT littermates (45). The effects of HSPCs-targeted inhibition of caspase-1 and -3 in sepsis await characterization.

To the best of our knowledge, this study characterizes for the first time the changes in the BM cytokine milieu in early sepsis. Importantly, a robust increase in IL-6, CXCL1, MIP-1α (CCL3), and MCP-1 (CCL2) occurred in P-DIE mice only. In contrast to a previously reported steep rise in the blood (26), there was no elevation of TNF, IFN-γ, IL-5, IL-10 in the BM of P-DIE mice at 24 h post-CLP. IL-6 is a known factor inducing proliferation of HSCs (46); recently, its receptor has been shown to be upregulated *via* Notch-dependent manner upon TLR stimulation of HSCs (47). Aside from its proinflammatory profile, MIP-1α inhibits proliferation of HSCs and governs myeloid differentiation (48, 49). However, MIP-1α has been shown to inhibit formation of granulocyte-macrophage colony

forming cells from human BM cells and can, therefore, appear as another factor contributing to a repression of HSPCs in sepsis. Secretion of MCP-1 (CCL2) by BM stromal cells is part of physiological response to infection supporting mobilization of inflammatory monocytes (50) but its local effect on HSPCs in sepsis remains unknown. The net effects of these mediators on HSPCs in sepsis require further studies. Interestingly, in P-SUR mice 9 days after CLP, there was a marked increase in INF-γ and IL-10 in the BM milieu. During a viral infection, INF-γ derived from $CD8^+$ cytotoxic T cells was shown to promote myeloid differentiation by stimulation of IL-6 secretion from the BM niche cells (51), but the CLP mice did not show upregulation of IL-6 at the time of INF-γ peak. Previously, we have shown that BM preserves INF-γ-producing $CD4^+$ memory T cells (52), and it can be speculated that both $CD8^+$ and $CD4^+$ T cells populations contribute to the INF-γ release but its role remains unknown. Using the flow cytometry-based mRNA assay, we confirmed the ability of LSK cells to express IL-6, TNF, and IL-1β (27). In line with the bulk protein analysis, IL-6 transcript was upregulated in P-DIE mice. Although neither the frequency of cytokine-producing LSK cells nor their numbers are high, these cells were shown to be potent IL-6 producers, thereby participating in HSPCs proliferation and differentiation (27). Our results further indicate occurrence of this mechanism during sepsis.

Our study is not limitation-free. We performed the experiments only in female mice and failed to compare our findings in septic males. Moreover, we did not perform functional HSCs assay but relied on the combination of previously validated immunophenotype markers (7, 10, 29). Analysis of HSPCs at the infection site, e.g. peritoneum would be of interest, but we were unable to establish a reliable analysis of LSK cells in probes from the abdominal cavity. Although our model was characterized by the mortality similar to the one reported in septic shock patients (53), most CLP deaths occurred within forty-eight hours (despite fluid resuscitation and antimicrobial treatment). This limited our outcome-related comparative analysis to early sepsis; it is imperative to analyze hematopoiesis in chronic sepsis given that any long-term hematopoietic deficits may contribute to the common post-sepsis sequelae.

Summarizing, we demonstrated that the hematopoietic stem and progenitor cells compartments are more profoundly diminished in P-DIE mice albeit this difference is not all-inclusive but cell population-selective. Depletion of hematopoietic precursors in early CLP sepsis constitutes a systemic feature as we did not observe mobilization nor migration of these cells to extramedullary sites. HSPCs depletion coincided with an increased caspase-3 activation, especially in P-DIE mice. Similarly, the local cytokine milieu in the bone marrow of P-DIE mice was altered to a greater extent compared with P-SUR. Altogether, our study indicates important outcome-related disturbances in hematopoiesis that can inform regarding any future targeted therapies aimed at correcting sepsis-induced myelosuppression.

DATA AVAILABILITY STATEMENT

The raw data supporting the conclusions of this article will be made available by the authors, without undue reservation.

ETHICS STATEMENT

The animal study was reviewed and approved by Viennese (Austria) legislative committee.

AUTHOR CONTRIBUTIONS

TS study design, performing experiments, data analysis/interpretation, and writing manuscript. SD study design, performing experiment, and correction of manuscript. AJ performing experiments. GH study design, performing experiments. MJ sample analysis. JK study design, and writing of the manuscript. MO study design, performing experiments, data analysis/interpretation, and writing manuscript. All authors contributed to the article and approved the submitted version.

FUNDING

Study funded by Polish National Science Centre grant no UMO-2016/23/D/NZ6/02554 and Oesterreichs Agentur für Bildung und Internationalisierung (OaeD) grant #PL07/2014.

SUPPLEMENTARY MATERIAL

The Supplementary Material for this article can be found online at: https://www.frontiersin.org/articles/10.3389/fimmu.2021.708670/full#supplementary-material

REFERENCES

1. Pucella JN, Upadhaya S, Reizis B. The Source and Dynamics of Adult Hematopoiesis: Insights From Lineage Tracing. *Annu Rev Cell Dev Biol* (2020) 36:529–50. doi: 10.1146/annurev-cellbio-020520-114601
2. May M, Slaughter A, Lucas D. Dynamic Regulation of Hematopoietic Stem Cells by Bone Marrow Niches. *Curr Stem Cell Rep* (2018) 4(3):201–8. doi: 10.1007/s40778-018-0132-x
3. Massberg S, Schaerli P, Knezevic-Maramica I, Kollnberger M, Tubo N, Moseman EA, et al. Immunosurveillance by Hematopoietic Progenitor Cells Trafficking Through Blood, Lymph, and Peripheral Tissues. *Cell* (2007) 131(5):994–1008. doi: 10.1016/j.cell.2007.09.047
4. Nagai Y, Garrett KP, Ohta S, Bahrun U, Kouro T, Akira S, et al. Toll-Like Receptors on Hematopoietic Progenitor Cells Stimulate Innate Immune System Replenishment. *Immunity* (2006) 24(6):801–12. doi: 10.1016/j.immuni.2006.04.008

5. Boettcher S, Manz MG. Sensing and Translation of Pathogen Signals Into Demand-Adapted Myelopoiesis. *Curr Opin Hematol* (2016) 23(1):5–10. doi: 10.1097/MOH.0000000000000201
6. Boettcher S, Ziegler P, Schmid MA, Takizawa H, van Rooijen N, Kopf M, et al. Cutting Edge: LPS-Induced Emergency Myelopoiesis Depends on TLR4-expressing Nonhematopoietic Cells. *J Immunol* (2012) 188(12):5824–8. doi: 10.4049/jimmunol.1103253
7. Burberry A, Zeng MY, Ding L, Wicks I, Inohara N, Morrison SJ, et al. Infection Mobilizes Hematopoietic Stem Cells Through Cooperative NOD-Like Receptor and Toll-Like Receptor Signaling. *Cell Host Microbe* (2014) 15 (6):779–91. doi: 10.1016/j.chom.2014.05.004
8. Kelly LS, Darden DB, Fenner BP, Efron PA, Mohr AM. The Hematopoietic Stem/Progenitor Cell Response to Hemorrhage, Injury and Sepsis: A Review of Pathophysiology. *Shock* (2020) 56(1):30–41. doi: 10.1097/SHK.0000000000001699
9. Rodriguez S, Chora A, Goumnerov B, Mumaw C, Goebel WS, Fernandez L, et al. Dysfunctional Expansion of Hematopoietic Stem Cells and Block of Myeloid Differentiation in Lethal Sepsis. *Blood* (2009) 114(19):4064–76. doi: 10.1182/blood-2009-04-214916
10. Zhang H, Rodriguez S, Wang L, Wang S, Serezani H, Kapur R, et al. Sepsis Induces Hematopoietic Stem Cell Exhaustion and Myelosuppression Through Distinct Contributions of TRIF and MYD88. *Stem Cell Rep* (2016) 6(6):940–56. doi: 10.1016/j.stemcr.2016.05.002
11. Takizawa H, Fritsch K, Kovtonyuk LV, Saito Y, Yakkala C, Jacobs K, et al. Pathogen-Induced TLR4-TRIF Innate Immune Signaling in Hematopoietic Stem Cells Promotes Proliferation But Reduces Competitive Fitness. *Cell Stem Cell* (2017) 21(2):225–240 e225. doi: 10.1016/j.stem.2017.06.013
12. Skirecki T, Kawiak J, Machaj E, Pojda Z, Wasilewska D, Czubak J, et al. Early Severe Impairment of Hematopoietic Stem and Progenitor Cells From the Bone Marrow Caused by CLP Sepsis and Endotoxemia in a Humanized Mice Model. *Stem Cell Res Ther* (2015) 6:142. doi: 10.1186/s13287-015-0135-9
13. Cuenca AG, Cuenca AL, Gentile LF, Efron PA, Islam S, Moldawer LL, et al. Delayed Emergency Myelopoiesis Following Polymicrobial Sepsis in Neonates. *Innate Immun* (2015) 21(4):386–91. doi: 10.1177/1753425914542445
14. Nacionales DC, Szpila B, Ungaro R, Lopez MC, Zhang J, Gentile LF, et al. A Detailed Characterization of the Dysfunctional Immunity and Abnormal Myelopoiesis Induced by Severe Shock and Trauma in the Aged. *J Immunol* (2015) 195(5):2396–407. doi: 10.4049/jimmunol.1500984
15. Davis FM, Schaller MA, Dendekker A, Joshi AD, Kimball AS, Evanoff H, et al. Sepsis Induces Prolonged Epigenetic Modifications in Bone Marrow and Peripheral Macrophages Impairing Inflammation and Wound Healing. *Arterioscler Thromb Vasc Biol* (2019) 39(11):2353–66. doi: 10.1161/ATVBAHA.119.312754
16. Skirecki T, Mikaszewska-Sokolewicz M, Godlewska M, Dolegowska B, Czubak J, Hoser G, et al. Mobilization of Stem and Progenitor Cells in Septic Shock Patients. *Sci Rep* (2019) 9(1):3289. doi: 10.1038/s41598-019-39772-4
17. Tsaganos T, Giamarellos-Bourboulis EJ, Kollias S, Zervakis D, Karagianni V, Pelekanou A, et al. Kinetics of Progenitor Hemopoetic Stem Cells in Sepsis: Correlation With Patients Survival? *BMC Infect Dis* (2006) 6:142. doi: 10.1186/1471-2334-6-142
18. Wichterman KA, Baue AE, Chaudry IH. Sepsis and Septic Shock–a Review of Laboratory Models and a Proposal. *J Surg Res* (1980) 29(2):189–201. doi: 10.1016/0022-4804(80)90037-2
19. Drechsler S, Weixelbaumer KM, Weidinger A, Raeven P, Khadem A, Redl H, et al. Why do They Die? Comparison of Selected Aspects of Organ Injury and Dysfunction in Mice Surviving and Dying in Acute Abdominal Sepsis. *Intensive Care Med Exp* (2015) 3(1):48. doi: 10.1186/s40635-015-0048-z
20. Skirecki T, Drechsler S, Hoser G, Jafarmadar M, Siennicka K, Pojda Z, et al. The Fluctuations of Leukocytes and Circulating Cytokines in Septic Humanized Mice Vary With Outcome. *Front Immunol* (2019) 10:1427. doi: 10.3389/fimmu.2019.01427
21. Osuchowski MF, Ayala A, Bahrami S, Bauer M, Boros M, Cavaillon JM, et al. Minimum Quality Threshold in Pre-Clinical Sepsis Studies (Mqtipss): An International Expert Consensus Initiative for Improvement of Animal Modeling in Sepsis. *Shock* (2018) 50(4):377–80. doi: 10.1097/SHK.0000000000001212
22. Rademann P, Weidinger A, Drechsler S, Meszaros A, Zipperle J, Jafarmadar M, et al. Mitochondria-Targeted Antioxidants SkQ1 and MitoTEMPO Failed to Exert a Long-Term Beneficial Effect in Murine Polymicrobial Sepsis. *Oxid Med Cell Longev* (2017) 2017:6412682. doi: 10.1155/2017/6412682
23. Weixelbaumer KM, Raeven P, Redl H, van Griensven M, Bahrami S, Osuchowski MF. Repetitive Low-Volume Blood Sampling Method as a Feasible Monitoring Tool in a Mouse Model of Sepsis. *Shock* (2010) 34 (4):420–6. doi: 10.1097/SHK.0b013e3181dc0918
24. Wilson A, Laurenti E, Oser G, van der Wath RC, Blanco-Bose W, Jaworski M, et al. Hematopoietic Stem Cells Reversibly Switch From Dormancy to Self-Renewal During Homeostasis and Repair. *Cell* (2008) 135(6):1118–29. doi: 10.1016/j.cell.2008.10.048
25. Gu Y, Jones AE, Yang W, Liu S, Dai Q, Liu Y, et al. The Histone H2A Deubiquitinase Usp16 Regulates Hematopoiesis and Hematopoietic Stem Cell Function. *Proc Natl Acad Sci USA* (2016) 113(1):E51–60. doi: 10.1073/pnas.1517041113
26. Osuchowski MF, Welch K, Siddiqui J, Remick DG. Circulating Cytokine/Inhibitor Profiles Reshape the Understanding of the SIRS/CARS Continuum in Sepsis and Predict Mortality. *J Immunol* (2006) 177(3):1967–74. doi: 10.4049/jimmunol.177.3.1967
27. Zhao JL, Ma C, O'Connell RM, Mehta A, DiLoreto R, Heath JR, et al. Conversion of Danger Signals Into Cytokine Signals by Hematopoietic Stem and Progenitor Cells for Regulation of Stress-Induced Hematopoiesis. *Cell Stem Cell* (2014) 14(4):445–59. doi: 10.1016/j.stem.2014.01.007
28. Soh KT, Tario JD Jr, Colligan S, Maguire O, Pan D, Minderman H, et al. Simultaneous, Single-Cell Measurement of Messenger Rna, Cell Surface Proteins, and Intracellular Proteins. *Curr Protoc Cytom* (2016) 75:7 45 41–47 45 33. doi: 10.1002/0471142956.cy0745s75
29. Zhang P, Nelson S, Bagby GJ, Siggins R2nd, Shellito JE, Welsh DA. The lineage-c-Kit+Sca-1+ Cell Response to Escherichia Coli Bacteremia in Balb/c Mice. *Stem Cells* (2008) 26(7):1778–86. doi: 10.1634/stemcells.2007-1027
30. Remick DG, Ayala A, Chaudry IH, Coopersmith CM, Deutschman C, Hellman J, et al. Premise for Standardized Sepsis Models. *Shock* (2019) 51 (1):4–9. doi: 10.1097/SHK.0000000000001164
31. Kobayashi H, Kobayashi CI, Nakamura-Ishizu A, Karigane D, Haeno H, Yamamoto KN, et al. Bacterial c-di-GMP Affects Hematopoietic Stem/Progenitors and Their Niches Through STING. *Cell Rep* (2015) 11(1):71–84. doi: 10.1016/j.celrep.2015.02.066
32. Brudecki L, Ferguson DA, Yin D, Lesage GD, McCall CE, El Gazzar M. Hematopoietic Stem-Progenitor Cells Restore Immunoreactivity and Improve Survival in Late Sepsis. *Infect Immun* (2012) 80(2):602–11. doi: 10.1128/IAI.05480-11
33. Spradling AC, Nystul T, Lighthouse D, Morris L, Fox D, Cox R, et al. Stem Cells and Their Niches: Integrated Units That Maintain Drosophila Tissues. *Cold Spring Harb Symp Quant Biol* (2008) 73:49–57. doi: 10.1101/sqb.2008.73.023
34. Delano MJ, Scumpia PO, Weinstein JS, Coco D, Nagaraj S, Kelly-Scumpia KM, et al. MyD88-dependent Expansion of an Immature GR-1(+)CD11b(+) Population Induces T Cell Suppression and Th2 Polarization in Sepsis. *J Exp Med* (2007) 204(6):1463–74. doi: 10.1084/jem.20062602
35. Cuenca AG, Delano MJ, Kelly-Scumpia KM, Moreno C, Scumpia PO, Laface DM, et al. A Paradoxical Role for Myeloid-Derived Suppressor Cells in Sepsis and Trauma. *Mol Med* (2011) 17(3-4):281–92. doi: 10.2119/molmed.2010.00178
36. Craciun FL, Schuller ER, Remick DG. Early Enhanced Local Neutrophil Recruitment in Peritonitis-Induced Sepsis Improves Bacterial Clearance and Survival. *J Immunol* (2010) 185(11):6930–8. doi: 10.4049/jimmunol.1002300
37. Chiswick EL, Mella JR, Bernardo J, Remick DG. Acute-Phase Deaths From Murine Polymicrobial Sepsis Are Characterized by Innate Immune Suppression Rather Than Exhaustion. *J Immunol* (2015) 195(8):3793–802. doi: 10.4049/jimmunol.1500874
38. Fukuda S, Bian H, King AG, Pelus LM. The Chemokine GRObeta Mobilizes Early Hematopoietic Stem Cells Characterized by Enhanced Homing and Engraftment. *Blood* (2007) 110(3):860–9. doi: 10.1182/blood-2006-06-031401
39. Gur H, Krauthgamer R, Bachar-Lustig E, Katchman H, Arbel-Goren R, Berrebi A, et al. Immune Regulatory Activity of CD34+ Progenitor Cells: Evidence for a Deletion-Based Mechanism Mediated by TNF-Alpha. *Blood* (2005) 105(6):2585–93. doi: 10.1182/blood-2002-11-3463
40. Granick JL, Falahee PC, Dahmubed D, Borjesson DL, Miller LS, Simon SI. Staphylococcus Aureus Recognition by Hematopoietic Stem and Progenitor

Cells *Via* TLR2/MyD88/PGE2 Stimulates Granulopoiesis in Wounds. *Blood* (2013) 122(10):1770–8. doi: 10.1182/blood-2012-11-466268
41. Coopersmith CM, Stromberg PE, Dunne WM, Davis CG, Amiot DM2nd, Buchman TG, et al. Inhibition of Intestinal Epithelial Apoptosis and Survival in a Murine Model of Pneumonia-Induced Sepsis. *JAMA* (2002) 287 (13):1716–21. doi: 10.1001/jama.287.13.1716
42. Hotchkiss RS, Coopersmith CM, Karl IE. Prevention of Lymphocyte Apoptosis–A Potential Treatment of Sepsis? *Clin Infect Dis* (2005) 41 Suppl 7:S465–9. doi: 10.1086/431998
43. Janzen V, Fleming HE, Riedt T, Karlsson G, Riese MJ, Lo Celso C, et al. Hematopoietic Stem Cell Responsiveness to Exogenous Signals Is Limited by Caspase-3. *Cell Stem Cell* (2008) 2(6):584–94. doi: 10.1016/j.stem.2008.03.012
44. Masters SL, Gerlic M, Metcalf D, Preston S, Pellegrini M, O'Donnell JA, et al. NLRP1 Inflammasome Activation Induces Pyroptosis of Hematopoietic Progenitor Cells. *Immunity* (2012) 37(6):1009–23. doi: 10.1016/j.immuni.2012.08.027
45. Gentile LF, Cuenca AL, Cuenca AG, Nacionales DC, Ungaro R, Efron PA, et al. Improved Emergency Myelopoiesis and Survival in Neonatal Sepsis by caspase-1/11 Ablation. *Immunology* (2015) 145(2):300–11. doi: 10.1111/imm.12450
46. Bernad A, Kopf M, Kulbacki R, Weich N, Koehler G, Gutierrez-Ramos JC. Interleukin-6 is Required *In Vivo* for the Regulation of Stem Cells and Committed Progenitors of the Hematopoietic System. *Immunity* (1994) 1 (9):725–31. doi: 10.1016/S1074-7613(94)80014-6
47. Tie R, Li H, Cai S, Liang Z, Shan W, Wang B, et al. Interleukin-6 Signaling Regulates Hematopoietic Stem Cell Emergence. *Exp Mol Med* (2019) 51 (10):1–12. doi: 10.1038/s12276-019-0320-5
48. Cook DN. The Role of MIP-1 Alpha in Inflammation and Hematopoiesis. *J Leukoc Biol* (1996) 59(1):61–6. doi: 10.1002/jlb.59.1.61
49. Staversky RJ, Byun DK, Georger MA, Zaffuto BJ, Goodman A, Becker MW, et al. The Chemokine Ccl3 Regulates Myeloid Differentiation and Hematopoietic Stem Cell Numbers. *Sci Rep* (2018) 8(1):14691. doi: 10.1038/s41598-018-32978-y
50. Shi C, Jia T, Mendez-Ferrer S, Hohl TM, Serbina NV, Lipuma L, et al. Bone Marrow Mesenchymal Stem and Progenitor Cells Induce Monocyte Emigration in Response to Circulating Toll-Like Receptor Ligands. *Immunity* (2011) 34(4):590–601. doi: 10.1016/j.immuni.2011.02.016
51. Schurch CM, Riether C, Ochsenbein AF. Cytotoxic Cd8+ T Cells Stimulate Hematopoietic Progenitors by Promoting Cytokine Release From Bone Marrow Mesenchymal Stromal Cells. *Cell Stem Cell* (2014) 14(4):460–72. doi: 10.1016/j.stem.2014.01.002
52. Skirecki T, Swacha P, Hoser G, Golab J, Nowis D, Kozlowska E. Bone Marrow Is the Preferred Site of Memory CD4+ T Cell Proliferation During Recovery From Sepsis. *JCI Insight* (2020) 5(10):e134475. doi: 10.1172/jci.insight.134475
53. Vincent JL, Jones G, David S, Olariu E, Cadwell KK. Frequency and Mortality of Septic Shock in Europe and North America: A Systematic Review and Meta-Analysis. *Crit Care* (2019) 23(1):196. doi: 10.1186/s13054-019-2478-6

Conflict of Interest: The authors declare that the research was conducted in the absence of any commercial or financial relationships that could be construed as a potential conflict of interest.

frontiers in Immunology

ORIGINAL RESEARCH
published: 16 August 2021
doi: 10.3389/fimmu.2021.696536

A Novel Single Cell RNA-seq Analysis of Non-Myeloid Circulating Cells in Late Sepsis

*Dijoia B. Darden[1], Xiaoru Dong[2], Maigan A. Brusko[3], Lauren Kelly[1], Brittany Fenner[1], Jaimar C. Rincon[1], Marvin L. Dirain[1], Ricardo Ungaro[1], Dina C. Nacionales[1], Marie Gauthier[4], Michael Kladde[4], Todd M. Brusko[3], Azra Bihorac[5], Frederick A. Moore[1], Tyler Loftus[1], Rhonda Bacher[6], Lyle L. Moldawer[1], Alicia M. Mohr[1] and Philip A. Efron[1]**

[1] Department of Surgery, University of Florida College of Medicine, Gainesville, FL, United States, [2] Department of Biomedical Engineering, University of Florida College of Medicine, Gainesville, FL, United States, [3] Department of Pathology, Immunology and Laboratory Medicine, University of Florida College of Medicine, Gainesville, FL, United States, [4] Department of Biochemistry and Molecular Biology, University of Florida College of Medicine, Gainesville, FL, United States, [5] Department of Medicine, University of Florida College of Medicine, Gainesville, FL, United States, [6] Department of Biostatistics, University of Florida, Gainesville, FL, United States

OPEN ACCESS

Edited by:
Jiang Huai Wang,
University College Cork, Ireland

Reviewed by:
Sergio Iván Valdés-Ferrer,
Instituto Nacional de Ciencias Médicas y Nutrición Salvador Zubirán (INCMNSZ), Mexico
Jie Fan,
University of Pittsburgh, United States

***Correspondence:**
Philip A. Efron
philip.efron@surgery.ufl.edu

Specialty section:
This article was submitted to Inflammation, a section of the journal Frontiers in Immunology

Received: *16 April 2021*
Accepted: *30 July 2021*
Published: *16 August 2021*

Citation:
Darden DB, Dong X, Brusko MA, Kelly L, Fenner B, Rincon JC, Dirain ML, Ungaro R, Nacionales DC, Gauthier M, Kladde M, Brusko TM, Bihorac A, Moore FA, Loftus T, Bacher R, Moldawer LL, Mohr AM and Efron PA (2021) A Novel Single Cell RNA-seq Analysis of Non-Myeloid Circulating Cells in Late Sepsis. Front. Immunol. 12:696536. doi: 10.3389/fimmu.2021.696536

Background: With the successful implementation of the Surviving Sepsis Campaign guidelines, post-sepsis in-hospital mortality to sepsis continues to decrease. Those who acutely survive surgical sepsis will either rapidly recover or develop a chronic critical illness (CCI). CCI is associated with adverse long-term outcomes and 1-year mortality. Although the pathobiology of CCI remains undefined, emerging evidence suggests a post-sepsis state of pathologic myeloid activation, inducing suboptimal lymphopoiesis and erythropoiesis, as well as downstream leukocyte dysfunction. Our goal was to use single-cell RNA sequencing (scRNA-seq) to perform a detailed transcriptomic analysis of lymphoid-derived leukocytes to better understand the pathology of late sepsis.

Methods: A mixture of whole blood myeloid-enriched and Ficoll-enriched peripheral blood mononuclear cells from four late septic patients (post-sepsis day 14-21) and five healthy subjects underwent Cellular Indexing of Transcriptomes and Epitopes by Sequencing (CITE-seq).

Results: We identified unique transcriptomic patterns for multiple circulating immune cell subtypes, including B- and $CD4^+$, $CD8^+$, activated $CD4^+$ and activated $CD8^+$ T-lymphocytes, as well as natural killer (NK), NKT, and plasmacytoid dendritic cells in late sepsis patients. Analysis demonstrated that the circulating lymphoid cells maintained a transcriptome reflecting immunosuppression and low-grade inflammation. We also identified transcriptomic differences between patients with bacterial *versus* fungal sepsis, such as greater expression of cytotoxic genes among $CD8^+$ T-lymphocytes in late bacterial sepsis.

Conclusion: Circulating non-myeloid cells display a unique transcriptomic pattern late after sepsis. Non-myeloid leukocytes in particular reveal a host endotype of inflammation,

immunosuppression, and dysfunction, suggesting a role for precision medicine-guided immunomodulatory therapy.

Keywords: lymphocytes, immune cells, sepsis, transcriptome, scRNA-seq, chronic critical illness

INTRODUCTION

Successful implementation of guidelines from the Surviving Sepsis Campaign has led to a significant decrease in early mortality after sepsis (1, 2). Thus, three clinical trajectories or phenotypes are now present subsequent to surgical sepsis: early death (approximately 4%), rapid recovery (approximately 63%) and development of chronic critical illness (CCI; approximately 33%) (3). Specifically, CCI has been defined as patients who have prolonged ICU stays with unresolved organ dysfunction (4–6). CCI patients account for increased hospital costs and use of resources (3). Importantly, approximately 40% of CCI patients have poor 1-year outcomes with a worse 1-year quality of life and mortality after sepsis (3, 4, 7).

Although the underlying pathobiology of the CCI phenotype remains unclear, it is understood that CCI can result from a Persistent Inflammation, Immunosuppression, and Catabolism Syndrome (PICS) endotype (8–12). Previous studies indicate that the dismal long-term outcomes experienced by CCI patients are due in part to a failure of the host to return to their pre-sepsis immune status (5, 6, 9, 11, 13). Understanding the pathobiology of leukocytes in late sepsis, as well as the dysfunctional hematopoiesis that leads to this immune dyscrasia, will be vital to any successful immunomodulation of sepsis survivors. Our laboratory has previously published a pilot study specifically evaluating myeloid-derived suppressor cells in surgical sepsis survivors (14). However, we realized that studies on non-myeloid immune cell subtypes chronically after sepsis are lacking. Using single-cell RNA sequencing (scRNA-seq) in an increased number of samples, we sought to perform a novel transcriptomic analysis of the immune and non-immune subsets of non-myeloid circulating cell types, all of which contribute to the late sepsis survivor patient phenotype.

MATERIALS AND METHODS

Study Design, Patient Enrollment, and Classification

The study was registered with clinicaltrials.gov (NCT02276417) and conducted by the Sepsis and Critical Illness Research Center at the University of Florida College of Medicine. All patients eligible for inclusion in the study were enrolled within 12 hours of initiating sepsis treatment. We used a delayed consent process, as approved by the Institutional Review Board. If written informed consent could not be obtained from the patient or their legally assigned representative within 96 hours of study enrollment, the patient was removed from the study and all collected biologic samples and clinical data were destroyed. Screening for sepsis was performed using the Modified Early Warning Signs-Sepsis Recognition System (MEWS-SRS) (13), which quantifies derangements in vital signs, white blood cell count, and mental status. All patients with sepsis were managed using a standardized, evidence-based protocol that emphasizes early goal-directed fluid resuscitation as well as other time-sensitive interventions such as administration of broad-spectrum antibiotics. Empiric antibiotics were chosen based on hospital antibiograms in conjunction with the suspected source of infection. Antimicrobial therapy was then narrowed based on culture and sensitivity data.

Inclusion criteria consisted of the following: (a) admission to the surgical or trauma ICU; (b) age ≥18 years; (c) clinical diagnosis of sepsis or septic shock as defined by the 2016 SCCM/ESICM International Sepsis Definitions Conference (Sepsis-3) (15) with this being the patient's first septic episode; and, (d) entrance into our sepsis clinical management protocol as previously described (16). Exclusion criteria consisted of: (a) refractory shock (i.e. patients expected to die within the first 24 hours); (b) an inability to achieve source control (i.e. irreversible disease states such as unresectable dead bowel); (c) pre-sepsis expected lifespan <3 months; (d) patient/family not committed to aggressive management; (e) severe CHF (NYHA Class IV); (f) Child-Pugh Class C liver disease or pre-liver transplant; (g) known HIV with $CD4^+$ count <200 cells/mm3; (h) organ transplant recipient or use of chronic corticosteroids or immunosuppressive agents; (i) pregnancy; (j) institutionalized patients; (k) chemotherapy or radiotherapy within 30 days; (l) severe traumatic brain injury (i.e. evidence of neurological injury on CT scan and a GCS <8); (m) spinal cord injury resulting in permanent sensory and/or motor deficits; or, (n) inability to obtain informed consent.

CCI was defined as an ICU length of stay greater than or equal to 14 days with evidence of persistent organ dysfunction, measured using components of the Sequential Organ Failure Assessment (SOFA) score (i.e. cardiovascular SOFA ≥ 1, or score in any other organ system ≥ 2) (3, 5, 12, 17). Patients with an ICU length of stay less than 14 days would also qualify for CCI if they were discharged to another hospital, a long-term acute care facility, or to hospice and demonstrated continuing evidence of organ dysfunction at the time of discharge. Those patients experiencing death within 14 days of sepsis onset were excluded from the analyses. Patients who neither died within 14 days nor developed CCI were defined as having a rapid recovery.

Human Blood Collection and Sample Preparation

Ethylenediaminetetraacetic acid (EDTA)-anticoagulated human whole blood samples were collected by venipuncture from four patients in late sepsis (day 14-21) meeting Sepsis-3 criteria (15) and five healthy control subjects. Samples were stored on ice and

processed within six hours after blood draw. Each sample was divided to undergo two separate enrichment processes. Peripheral blood mononuclear cells (PBMC) from half of each human whole blood sample were collected using Ficoll-Paque™ PLUS (GE Healthcare, Chicago, IL) and density gradient centrifugation. Myeloid cells were collected from the other half of each whole blood sample using RosetteSep™ HLA Myeloid Cell Enrichment Kit (Stemcell Technologies, Cambridge, MA). A 1:3 mixture of enriched PBMCs to myeloid cells from the four sepsis patients and five healthy control subjects underwent further analysis. Although single-cell technology allows for detection of smaller cell populations, the original samples were enriched to ensure our ability to adequately analyze and compare the small target population of MDSCs (especially in healthy controls, who have small populations of MDSCs), while also allowing us to characterize other important circulating immune cells present in late sepsis (e.g. lymphocytes).

scRNA-seq/CITE-seq and Library Construction

Gene expression libraries were prepared from 5,000 cells using the Chromium Single Cell 5' Bead and Library Kit v1 (10x Genomics). Libraries were sequenced on an Illumina HiSeq™ instrument at a target read depth of 50,000 reads per cell. Myeloid cells were labeled with oligo-tagged antibodies to CD33, CD11b, CD14, CD15, CD66b, Lox1 and HLA-DR. Labeled cells (5,000) were encapsulated for droplet-based CITE-seq utilizing the 10x Genomics Chromium Controller™ platform. Granulocytic (G-), Monocytic (M-), and Early (E-) MDSCs were identified as previously described by Bronte et al. (18)): G-MDSCs (Lin^- $CD33^+$ $CD11b^+$ $CD14^-$ and $CD15^+$ or $CD66b^+$); M-MDSCs (Lin^- $HLADR^{low/-}$ $CD33^+$ $CD11b^+$ $CD14^+$ $CD15^-$ $CD66b^-$); and, E-MDSCs (Lin^- $HLADR^{low/-}$ $CD33^+$ $CD11b^+$ $CD14^-$ $CD15^-$ $CD66b^-$). T lymphocytes were identified by known gene markers: $CD4^+$ T (*CD3D, CD4, CCR7*), $CD8^+$ T (*CD3D, CD8A, CCR7*), activated $CD4^+$ T (*CD3D, IL7R, CD4*), activated $CD8^+$ T (*CD3D, CD8A, CCL5*), Treg (*CD3D, FOXP3, IL2RA*), and Th17 (*CD4, IL17*). Activated macrophages, monocytes, dendritic and plasmacytoid cells were labeled using additional oligo-tagged antibodies to CD3, CD127, CD16, CD183, CD4, CD196, CD25, and CD56. B cells were identified using CD19. Natural Killer (NK) and NK T-lymphocytes were identified using CD16 (*FCGR3A*), CD56 (*NCAM1*), and CD3 (*CD3G*). Complementary DNA (cDNA) libraries were constructed to assess gene expression (RNA) and surface phenotype (protein) for subpopulations simultaneously. Cell clusters were manually annotated based on their expression of known marker genes and leveraging both the RNA expression counts and antibody derived tag counts. Details of this analysis are provided in **Supplementary Data Sheet 1**.

Processing of Sequencing Reads and Generation of Gene-Barcode Matrices

Raw sequencing reads were processed using Cell Ranger v3.0.0 to create a raw (unfiltered) gene-barcode matrix. Briefly, Cell Ranger mkfastq was used to make fastq files from bcl files. Next, Cell Ranger count was used for aligning sequencing reads to the hg19 reference genome (refdata-cellranger-hg19-3.0.0), obtained from https://support.10xgenomics.com/single-cell-gene-expression/software/release-notes/build using STAR. For confidently mapped reads, UMI sequences were collapsed and the number of UMI reads per gene were stored in the raw gene-barcode matrix (https://support.10xgenomics.com/single-cell-gene-expression/software/pipelines/latest/algorithms/overview).

Filtering of Barcodes/Quality Control

We distinguished true cells from background droplets using the emptyDrops method implemented in the DropletUtils Bioconductor R package (19). By testing each cell *versus* an ambient RNA distribution, barcodes with a false discovery rate adjusted p-value < 0.01 were retained for further consideration. We performed a second quality control step to identify cells with low RNA content, possible doublets, or dead/damaged cells, in which we filtered cells based on the total number of UMIs per cell, the number of genes expressed, and the percentage of mitochondrial reads per cell. We used the scater R package to identify outlier identify cells in any of these metrics, where outliers were defined as three median absolute deviations (MADs) from the median (20). The scRNA-seq data were normalized using the NormalizeData function in the Seurat R package v 3.1.5 (21) in which the total counts for each cell were scaled to have 10000 total counts. The antibody counts were normalized using the same function with the centered log ratio transformation method.

Dataset Integration and Dimensionality Reduction

The datasets were integrated as detailed by McCarthy et al. (20). Briefly, canonical correlation analysis (CCA) was performed to identify shared sources of variation across the datasets, and mutual nearest neighbors in the CCA space were identified to produce anchors between datasets. Highly variable genes accounting for the majority of the heterogeneity within each sample were identified with the FindVariableFeatures function in the Seurat R package v 3.1.5 (21), which fits a local polynomial regression (loess) model to the mean-variance relationship and selects the top 2000 genes with the greatest standardized deviation from the fitted model. Using these features, anchors between the datasets which correspond to similar cells across datasets were identified using the FindIntegrationAnchors function, and this was used as input into the IntegrateData function to generate an integrated dataset. For dimensionality reduction, expression values for each gene in the integrated dataset were scaled to have a mean of zero and standard deviation of one using the ScaleData function. Principal component analysis (PCA) was run on this matrix using the RunPCA function in Seurat. For visualization Uniform Manifold Approximation and Projection (UMAP), a common dimensionality reduction method in scRNA-seq (21), plots were created based on the top 30 principal components using the RunUMAP function in Seurat.

Cell Cluster Differential Expression Analysis

Cell clusters were manually annotated based on their expression of known marker genes. Marker genes for each cluster were identified by comparing each individual cluster with the remaining pooled clusters for each sample using the Wilcoxon rank sum test implemented in the Seurat R package. Differentially expressed genes across conditions was done by pooling cells across subjects for each cell cluster using the Wilcoxon rank sum test. P-values were adjusted for multiple testing using the Bonferroni method. All analyses were performed using R version 3.6.3.

Pathway Analysis of Non-Myeloid Cells

Differentially expressed genes for each cell of interest were functionally annotated using the R package clusterProfiler (22). The Kyoto Encyclopedia of Genes and Genomes (KEGG) and Gene Ontology (GO) databases were used to determine association with particular diseases and biological processes. For KEGG, the enrichment P-value cutoff was set to pvalueCutoff = 0.05 and for GO we set qvalueCutoff = 0.01.

RESULTS

Three of the four septic patients developed CCI and were sampled during that period. One of the septic patients had recovered sufficiently to be defined as a rapid recovery patient, although the patient was still hospitalized at the time of blood sampling. Two of the four patients with sepsis had fungal sepsis while the other two had bacterial sepsis. The mean age for the septic patients was 65 years; 75% were male and they were all studied post-sepsis day 14-21. Five healthy controls (mean age 42 years; 100% male) were also studied. Patient characteristics are detailed in **Supplementary Table 1**.

Identification of Lymphoid/Non-Myeloid Leukocyte Cell Types

We leveraged CITE-seq data to annotate cell clusters based on known cell markers (**Figure 1A**) as described in the Methods. We successfully identified 11 non-myeloid cell types: six T-lymphocyte subsets (naive $CD4^+$, naive $CD8^+$ activated $CD4^+$, activated $CD8^+$, NK T cells, and regulatory T-lymphocytes) (**Figures 1B, C**), NK cells, B-cells, and plasmacytoid dendritic cells (pDCs). Surprisingly, we were unable to positively identify

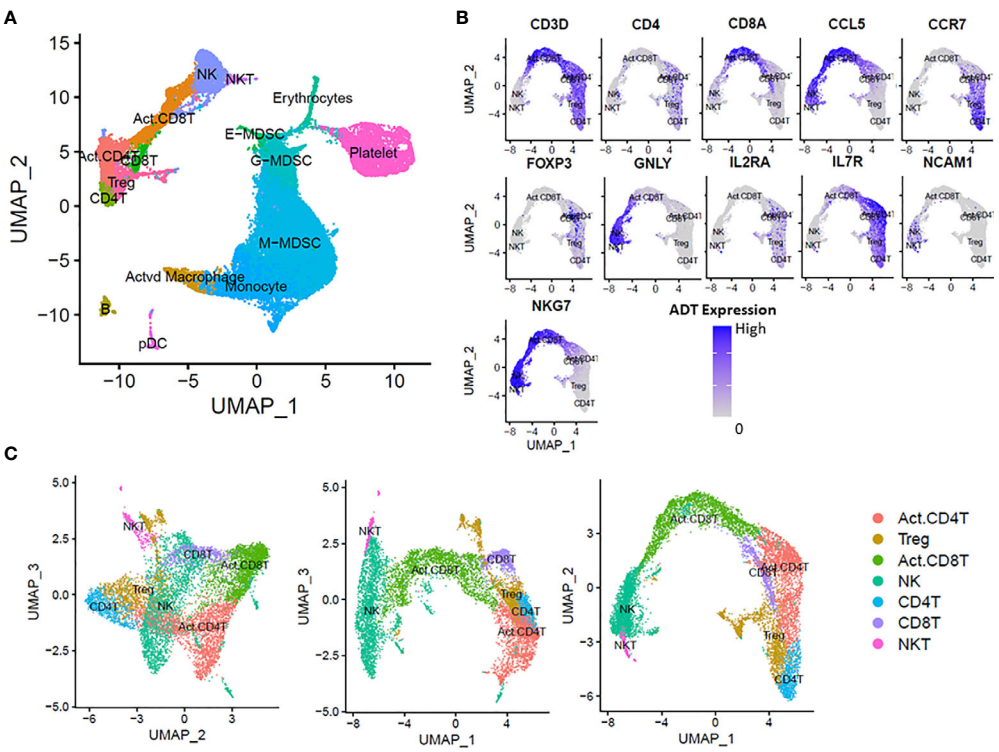

FIGURE 1 | scRNA-seq analysis at 14-21 days post-sepsis *versus* healthy control. Cells depicted are from all subjects in the study, in each corresponding group (sepsis n=4, healthy n=5). Using Seurat's method of integrating data across conditions/batches, the integration allows for joint clustering and to identify shared (or possibly unshared) cell clusters. Cells are visualized on uniform manifold approximation and projection (UMAP) plots colored by cell types. **(A)** UMAP representation of cell clusters identified in healthy patients *versus* late sepsis. **(B)** Annotation of T-lymphocyte subsets was performed manually using expression of *CD3D, CD4, CD8A, CCL5, CCR7, FOXP3, GNLY, IL2RA, IL7R, NCAM1* and *NKG7*. **(C)** UMAP representation of T-cell subset clusters from manual annotation identified in healthy patients *versus* late sepsis in three dimensions. (E-MDSC, early myeloid derived suppressor cell; G-MDSC, granulocytic myeloid derived suppressor cell; M-MDSC, monocytic myeloid derived suppressor cell; pDC, plasmacytoid dendritic cells).

any Th17 cells in our analysis (*via* expression of *IL17*). Th17 cells are known to be important for intact immunity, and their dysfunction can be associated with worse outcomes after sepsis (23, 24).

Non-Myeloid Cells in Healthy *vs* Late Sepsis

T-Lymphocytes

In the analysis of healthy controls (n=5) with all sepsis patients day 14-21 (n=4), scRNA-seq revealed differential expression of 11 genes in $CD4^+$, 30 genes in $CD8^+$, 26 genes in activated $CD4^+$, 50 genes in activated $CD8^+$, and 32 genes in regulatory T (Tregs) lymphocytes (adjusted p-value < 0.01; **Supplementary Data Sheet 2** and **Supplementary Table 2**).

IL32 was significantly upregulated in all T-lymphocyte subsets. The IL-32 family shares no known homology to other cytokines and is a pro-inflammatory cytokine that stimulates the secretion of other proinflammatory cytokines and chemokines *via* nuclear factor kB (NFkB) and p38 mitogen-activated protein kinase (MAPK) pathways (25, 26). In addition, T-lymphocytes and Tregs from septic patients did not have many differentially expressed genes previously reported to be directly immunosuppressive; however, there was upregulation of pro-inflammatory genes such as *STAT1, NEAT1, IL32, PSME1/2, CCL4* (MIP1β), *and LIME1*.

TNFSF10 (TRAIL) and *S100A8/9*, were found to be significantly upregulated in late sepsis $CD4^+$ and $CD8^+$ T-lymphocyte subsets, respectively. *S100A8/A9* encode for proteins that have many pro- *and* anti-inflammatory immune functions (27). *TNFSF10* encodes for a cytokine in the tumor necrosis factor family that mediates cell apoptosis in response to tumor cells and infection (28, 29). *STAT1* and *SETD2* are also both over-expressed in late sepsis $CD4^+$ T-lymphocytes. SETD2 is known to directly mediate methylation of STAT1 and reinforces interferon-α Activated transcription of STAT1 in antiviral immunity (30).

Activated $CD8^+$ T-lymphocytes also showed upregulation of MHC II genes such as *CD74, HLA-DRA, HLA-DRB1, HLA-DRB5, HLA-DQA1*. MHC II gene expression in T-lymphocytes has been described as a late marker of activation, associated with persistent inflammation in many autoimmune disorders (31–33). Not surprisingly, late sepsis $CD4^+$ T-lymphocytes did not have differential expression of any HLA genes. Interestingly, late sepsis activated $CD4^+$ T cells had high expression of *ETS1*, which has been implicated as a negative regulator of Th17 differentiation (34). This could partially explain the lack of Th17 cells seen in this analysis. Activated $CD4^+$ and $CD8^+$ T-lymphocytes also shared upregulation of genes *IRF1*, implicated in T-lymphocyte differentiation (35, 36).

Activated $CD8^+$ T-lymphocytes from late sepsis had the most differentially expressed genes compared to the other T-lymphocyte subsets. *CD27*, which is important in the generation of T-lymphocyte memory and viral immunity, was specifically downregulated in late sepsis activated $CD8^+$ T-lymphocytes (37). Late sepsis activated $CD8^+$ T-lymphocytes also showed upregulation of cytotoxic genes *ITGB1, GZMA, GZMH, NKG7* (38–42). Yet, in late sepsis there was downregulation of other cytotoxic lymphocyte genes *KLRC3* and *KLRC1*. Interestingly, late sepsis activated $CD4^+$ T-lymphocytes also demonstrated upregulation of some cytotoxic genes such as *GZMA, CCL5*, and *CST7* (40, 42, 43).

We utilized functional enrichment analysis to gain greater biological insight into the functional processes activated or inhibited in late sepsis (**Supplementary Table 3**). KEGG enrichment of differentially expressed genes in $CD4^+$ and $CD8^+$ T cells identified only one significant pathway (Ribosome). KEGG enrichment of differentially expressed genes in activated $CD4^+$ T cells and activated $CD8^+$ T cells identified three (ribosome, influenza A, and NOD-like receptor signaling) and 32 pathways, respectively (adjusted p-value < 0.05). Differentially expressed genes from activated $CD8^+$ T cells in late sepsis were enriched for KEGG pathways associated with antigen processing and presentation, many viral diseases and autoimmune disorders.

Most of the differentially expressed genes found in each T-lymphocyte subset are genes important for cell function such as ribosomal, mitochondrial, glycolytic, transcription and binding proteins. The majority of these regulatory genes, especially ribosomal genes, are downregulated in late sepsis T-lymphocytes. This suggests a relative cell "exhaustion or dysfunction" in late sepsis, potentially playing a role in T-lymphocyte exhaustion known to occur after sepsis (44, 45). KEGG enrichment analysis showed significant overlap (adjusted p-value < 0.05) in the Ribosome pathway for all T-lymphocyte subsets. GO analysis of the differentially expressed genes illustrated transcriptome involvement of biological processes related to ribosomal function in all T-lymphocyte subsets, except activated $CD4^+$ T cells, further supporting T-lymphocyte exhaustion in late sepsis (adjusted p-value <0.01; **Supplementary Table 3**).

Cytotoxic Lymphocytes (NK and NKT)

In the comparison between healthy subjects (n=5) and those with late sepsis (n=4), scRNA-seq revealed differential expression of 8 genes in NK T cells and 28 genes in NK cells (adjusted p-value < 0.01; **Supplementary Data Sheet 2** and **Supplementary Table 2**). NK T cells had differential downregulation mainly of cell regulatory genes. However, there was also downregulation of the cytotoxic lymphocyte gene *KLRC3*. Interestingly, NK cells also exhibited downregulation of the cytotoxic gene *KLRC3* along with downregulation of *KLRC1* and *KLRG1*. *KLRC3* encodes for an activating receptor, while *KLRC1* and *KLRG1* encode for inhibitory receptors (46). Downregulation of these genes suggest compromised NK cell and NK T cell function in late sepsis.

Significant terms from KEGG and GO enrichment analyses can be found in **Supplementary Table 3**. KEGG enrichment of the differentially expressed genes in NK cells showed overlap in many immune related pathways including antigen processing and presentation and natural killer cell mediated cytotoxicity. GO analysis of the differentially expressed genes in NK cells revealed overlap with significant biological processes such as antigen processing and presentation, antigen receptor mediated-

signaling pathway, and cytokine signaling. Interestingly, differentially expressed genes in both NK and NKT cells enriched for multiple GO biological process terms related to protein targeting to the membrane. NKT cell genes also enriched for multiple GO biological processes pathways important for proper cellular function (ATP synthesis, ribosome biogenesis, rRNA processing, mitochondrial ATP synthesis. These findings further support NK cell and NK T cell dysfunction in late sepsis.

Plasmacytoid Dendritic Cells

There was differential expression of 16 genes in pDCs in the analysis of healthy controls (n=5) compared with all late sepsis patients (n=4) (adjusted p-value <0.01; **Supplementary Data Sheet 2** and **Supplementary Table 2**). There were only 4 upregulated genes, three of which are proinflammatory markers *S100A8, S100A12* and *FAM26F*. *S100A8* and *S100A12* are danger-associated molecular proteins (DAMPs) which are potent activators of innate immunity (47, 48). *FAM26F* encodes for a membrane glycoprotein which is implicated in immune cell-cell interactions. The synergistic expression of FAM26F is necessary for NK cell activation by dendritic cells (49, 50). Most of the differentially expressed genes downregulated in the late sepsis were important for cell function such as ribosomal, mitochondrial, glycolytic, transcription and binding proteins. One downregulated gene, *DNASE1L3*, which encodes for an endonuclease, has been demonstrated to be necessary for inflammasome-mediated cytokine secretion (51, 52). Enrichment analysis was significant for five KEGG terms (adjusted p-value < 0.05) and 30 GO terms (adjusted p-value <0.01). The significant GO terms include many pathways important for immune cell function, such as protein targeting to the membrane, organelle organization, regulation of inflammatory response and granulocyte chemotaxis (**Supplementary Table 3**). Together these genes highlight immunometabolic dysfunction and suggest pDCs as an important contributor to the persistent inflammation seen in chronic sepsis.

B-Cells

In the analysis of healthy controls (n=5) compared with all late sepsis patients (n=4), there were only 11 differentially expressed genes (adjusted p-value <0.01; **Supplementary Data Sheet 2** and **Supplementary Table 2**). The three downregulated genes encoded for ribosomal and mitochondrial proteins, suggesting immunometabolic dysfunction. Of the upregulated genes, there were 3 pro-inflammatory genes (*FAM26F, IFITM1, and AIM2*) all of which are inducible by interferon and important in the activation of the innate immune response (49, 53, 54). IFITM1 protein has also been reported to play a role in the inhibition of B cell line proliferation (54). AIM2 is an important cytoplasmic sensor that recognizes dsDNA for a wide range of pathogens, as well as host DNA, that triggers the release of many cytokines upon activation (53). This is not reflected in the enrichment analysis (**Supplementary Table 3**). There was significant overlap in only two GO biologic process pathways for protein oligomerization (adjusted p-value <0.01) and no significant KEGG pathways (adjusted p-value <0.05).

Lymphocytes in Chronic Critical Illness

Within our sepsis cohort, three patients were classified as CCI and one patient as rapid recovery. Although our sample size for rapid recovery patients is too low for a direct analysis, there were enough CCI patients to determine if there are differences more specific to CCI patients compared to our previous analysis of all patients. Therefore, further analysis was performed to elucidate transcriptomic patterns in the lymphocytic cell types of late sepsis CCI patients compared to healthy controls. In the analysis of healthy controls (n=5) to late sepsis CCI patients (n=3), scRNA-seq revealed differential expression of 16 genes in $CD4^+$, 30 genes in $CD8^+$, 26 genes in activated $CD4^+$, 52 genes in activated $CD8^+$, and 37 genes in regulatory T (Tregs) lymphocytes. There was differential expression of 8 genes in NKT, 35 genes in NK, 11 genes in B, and 15 genes in pDC (adjusted p-value < 0.01; **Supplementary Data Sheet 3** and **Supplementary Table 4**). The lower number of differentially expressed genes, as well as, the high number of common genes between analyses suggests that the $CD8^+$ T, NK T cells, pDCs, and B cells in late sepsis have begun trending back towards homeostasis, regardless of clinical trajectory. Of note, the $CD8^+$ T-, NKT- and B-lymphocytes differentially expressed genes from the analysis of all late sepsis patients are the same as the differentially expressed genes in the analysis for CCI. The differentially expressed genes for the other non-myeloid cells do not differ wildly between the two analyses, but there are some differences worth mentioning.

As hypothesized, scRNA-seq analysis revealed differentially expressed genes important for both immunosuppression and inflammation in all CCI T-lymphocyte subsets, just as reported for all sepsis patients above. The sub analysis of healthy *versus* CCI $CD4^+$ T-lymphocytes revealed unique differential expression of five genes not seen in the analysis of all late sepsis patients (upregulated: *HBB, ETS1*; downregulated: *SMDT1, RPL41, MTRNR2L12*). There was also unique expression of three genes in CCI activated $CD4^+$ T-lymphocytes (upregulated: *AL592183.1*; downregulated: *PLP2, MTRNR2L12*), five genes in activated $CD8^+$ T-lymphocytes (upregulated: *MT-ND6, THEMIS*; downregulated: *RPL38, RPL41, MTRNR2L12*); ten genes in Tregs (upregulated: *SORL1, ETS1, IRF1, EIF1AX, DDX5, SMCHD1, LINC00657, USP22, tNSF10*; downregulated: *MTRNR2L12*); and eight genes in NK cells (upregulated: *S100A8, CD74, HLA-DPA1, JUNB, MT-ND6, DUSP, AL592183.1*; downregulated: *MTRNR2L12)*. Most of the uniquely expressed genes in CCI lymphocytes encoded for regulatory proteins – mitochondrial, ribosomal and transcriptional However, Tregs also saw an increased expression level of proinflammatory genes *IRF1* and *TNSF10*. While there were no differences noted in this analysis of CCI NKT cells compared to analysis of all sepsis NKT cells, NK cells in CCI had a unique upregulation of inflammatory genes *S100A8, CD74, JUNB*, and *DUSP1*. Although differential regulatory function is reflected in the enrichment terms (**Supplementary Table 5**) which are similar to the previous analysis of all sepsis patients compared to healthy controls, there are no unique pathways to suggest a concerted increase

of inflammation in non-myeloid populations in CCI late sepsis. However, this differential gene expression in conjunction with the lack of significant overlap in related pathways, could represent a dysregulated attempt to increase inflammation in CCI late sepsis when compared to RAP late sepsis and healthy controls. This data also suggests that the persistent inflammation seen in PICS is not driven by non-myeloid cells.

Lymphocytes After Bacteremia *Versus* Fungemia

Finally, we compared scRNA-seq profiles of late sepsis lymphocytes based on initial septic insult (bacterial *vs* fungal). Gene expression analysis between the late sepsis patients with bacteremia (n=2) *versus* fungemia (n=2) revealed differential expression of 25 genes in $CD4^+$ T-lymphocytes, 44 genes in $CD8^+$ T-lymphocytes, 93 genes in activated $CD4^+$ T-lymphocytes, 368 genes in activated $CD8^+$ T-lymphocytes, 24 genes in Tregs, 9 genes in NK T cells, 249 genes in NK cells, 16 genes in B-cells, and ten genes in pDCs (adjusted p-value< 0.01). However, many of these genes differed only modestly in expression; thus, we applied a further cutoff value of log fold-change (FC) > $\left|0.4\right|$ (corresponding to standard FC > $\left|1.5\right|$) to select significant genes. Gene analysis with the more stringent criteria (adjusted p-value < 0.01 and log FC > $\left|0.4\right|$) revealed differential expression of 19 genes in $CD4^+$ T-lymphocytes, 44 genes in $CD8^+$ T-lymphocytes, 41 genes in activated $CD4^+$ T-lymphocytes, 161 genes in activated $CD8^+$ T-lymphocytes, 21 genes in Tregs, 9 genes in NK T-cells, 89 genes in NK cells, 11 genes in B-cells, and six genes in pDCs (**Supplementary Data Sheet 4** and **Supplementary Table 6**).

Interestingly, the naive and activated $CD8^+$ T-lymphocytes in bacterial sepsis demonstrated a more cytotoxic-like pattern with upregulation of cytotoxic genes such as *GZMA, GZMH, GZMK, CCL5, CST7*, and *NKG7* (38, 40–42). Activated T-lymphocytes from late bacterial sepsis showed upregulation of many genes for DAMPs and HLA proteins. B cells and pDCs of late sepsis showed differential expression mainly of genes for ribosomal, mitochondrial, and transcription proteins. Of note, all lymphocytes in late bacterial sepsis showed increased expression of adult hemoglobin genes *HBB* ± *HBA2* when compared to those lymphocytes in fungal sepsis. Although the function of *HBB* and *HBA2* are unknown in lymphocytes, some studies have shown increased expression in non-erythroid cells to be associated with hypoxia (55). Thus, it is possible that the expression of hemoglobin genes may reflect differences in the sepsis phenotype (Skin/Soft Tissue *vs* Vascular/Bloodstream) rather than initial microbial insult.

Enrichment analysis results can be found in **Supplementary Table 7**. Supporting our claim above, activated $CD8^+$ T differential genes enriched for terms that support a more cytotoxic-like pattern natural killer cell mediated cytotoxicity, phagosome, and proteasome pathways. Enrichment of the differential genes in all non-myeloid subsets in late bacterial *versus* late fungal sepsis demonstrated significant overlap in many immune cell related pathways such as antigen processing and presentation, chemokine signaling, NK-kappa B signaling, granulocyte chemotaxis, and immune cell differentiation.

DISCUSSION

Historically, 30-day mortality has been the primary outcome of interest in surgical sepsis populations (56–58). However, many sepsis patients survive thanks to earlier identification and improved subsequent therapy (3, 4). Thus, sepsis research is adapting to evaluate long-term outcomes, such as functional status, cognitive status, and one-year morality, as primary outcomes (3, 4, 57, 59, 60). Ongoing research suggests that the dismal long-term outcomes experienced by CCI patients are due to a dysregulated immune response that fails to return to homeostasis (5, 6, 9, 11, 13), which we have identified as the PICS endotype (12).

This study utilized scRNAseq to reveal novel gene expression patterns in circulating non-myeloid cells of late sepsis. Similar to previous studies, our study supports the hypothesis that immune dysregulation and failure to restore immune homeostasis is associated with the development of CCI among sepsis survivors. As noted in other sepsis cohorts, there is substantial variability in transcriptional changes in inflammatory genes, both early and late after sepsis, for CCI and rapid recovery patients (61–64). Neither early nor late sepsis transcriptomic patterns identify a distinctive pro-inflammatory or immunosuppressive phase (65). Rather, there is an aberrance of both inflammatory and immunosuppressive genes simultaneously, suggesting global immune dysregulation further promoting PICS as the underlying pathobiology of late sepsis.

Our study highlights that lymphoid populations have a transcriptomic profile more suggestive of immune and metabolic dysfunction than inflammation at 14-21 days post-sepsis. T-lymphocytes had some overexpression of both pro-inflammatory and immunosuppressive genes in late sepsis, but not to the levels seen in myeloid populations (12). In contrast, both pDCs and platelets appear to play an important role in the persistent inflammation seen in chronic sepsis with upregulation of genes for pro-inflammatory cytokines and chemokines. Particularly in CCI late sepsis, transcriptomic patterns suggest the potential for persistent inflammation *via* NK cells and Treg lymphocytes. The transcriptomic profiles could represent a compensatory upregulation of these inflammatory genes to combat the relative immunosuppression. Importantly, our analysis also suggests that the transcriptomic profile may be influenced not only by initial microbial insult and clinical trajectory but also by sepsis endotype/initial site of infection.

Surprisingly, we were unable to identify circulating Th17 lymphocytes in our study population. Specifically, we were unable to identify the expression of *IL17* messenger RNA (mRNA) in any of our T-lymphocyte subsets. Th17 lymphocytes are one of the effector cell types differentiated from activated CD4+T-lymphocytes *via* induction from TGF-β, IL-6, IL-21 (24, 66). Th17 cells have been demonstrated to be crucial in neutrophil

recruitment for defense against extracellular pathogens and crucial in mucosal host defense (67). Th17 lymphocytes play an important role in autoimmune diseases, promoting chronic inflammation, but this has not been described in late sepsis. In one study, circulatory Th17 lymphocyte counts were higher in survivors with severe sepsis than in non-survivors and counts were increased after 6 days in severe sepsis, suggesting an association of Th17 with severe sepsis survival (68). To our knowledge, this is the first study to look at T-lymphocytic subsets after 7 days post-sepsis. Our study suggests that there is a significant decrease in circulating Th17 cells at 14 days post sepsis, which could indicate decreased differentiation of Th17 lymphocytes. Importantly, Th17 cells are the major producers of IL17 cytokine, which has been documented to increase extramedullary hematopoiesis and bone marrow granulopoiesis (67, 69–71). Therefore, the lack of Th17 lymphocytes in late sepsis/CCI may play a critical role in the persistent dysfunctional hematopoiesis of PICS.

We also observed that the majority of the downregulated differentially expressed genes in non-myeloid cells of late sepsis encode for glycolytic, ribosomal and mitochondrial proteins. Previous studies report similar alterations in leukocyte transcriptomic profiles in early inflammation (72, 73). However, the perseverance of this transcriptome has not been well delineated in late sepsis. The functional consequences of downregulation of these genes in the T-lymphocyte subsets are consistent with what has been described as "T-lymphocyte exhaustion", which is characterized by dysfunctional differentiation and decreased immune response to a new inflammatory stimulus, usually to chronic viral infections (74, 75). The repression of genes encoding for ribosomal and mitochondrial proteins has been associated with a decrease in T-lymphocyte function and differentiation (76, 77). This could explain our failure to confidently identify Th17-lymphocytes in these late sepsis patients. The lack of definitive Th17 cells could contribute to the increase susceptibility to secondary infections in CCI sepsis patients (78, 79).

The main limitation of this study was that it was performed in a limited number of surgical sepsis patients. Further validation of the differentially expressed genes with more patients, especially those that rapidly recovered, is warranted. Additionally, we were only able to analyze immune cell transcriptome patterns at one time point in late sepsis. Future transcriptomic analysis with more time points is warranted to analyze time-dependent genomic expression patterns of late sepsis in sepsis survivors (14). Finally, this is a descriptive study. It is important to note that mRNA expression does not always correlate with protein expression due to many epigenetic and posttranslational factors. We recognize that the KEGG and GO enrichment analyses did not perfectly align with how we interpret gene interaction within each non-myeloid cell. Yet this does not trivialize the importance of our findings. In fact, this highlights our lack of understanding of the immune cell transcriptomic response and subsequent endotype in late sepsis. Further functional studies to elucidate the specific role of these differentially expressed genes in chronic sepsis are warranted. In addition, the circulating leukocyte transcriptome does not necessarily represent the leukocyte transcriptome within individual tissues. However, the work presented in this manuscript highlights a number of genes and non-myeloid cell subsets that could be targeted for therapy in those sepsis patients that have CCI and adverse outcomes as a consequence of PICS.

CONCLUSIONS

Utilizing scRNA-seq, we identified unique transcriptomic profiles of lymphocytic cell types in late sepsis patients. scRNA-seq analysis demonstrated that circulating lymphocytic cells maintain a transcriptomic profile that is predominantly immunosuppressive with low-grade pro-inflammatory characteristics in late sepsis patients. In addition, the type of infecting organism (e.g. bacterial *vs* fungal) can alter the lymphocyte transcriptome later in sepsis, further highlighting the need for personalized immunotherapy. Importantly, this data highlight that the persistent global immune dysfunction in late sepsis extends to nearly all lymphocytic subsets which are all likely playing a role in the increased secondary infections, increased late mortality, and poorer prognosis seen in CCI. Future studies with particular attention to Th17 lymphocytic dysfunction may reveal this subset as a major target to reflect poor prognosis and adverse outcomes in late sepsis. However, many more studies are warranted to completely understand the PICS endotype in order to devise an effective treatment plan for CCI patients in late sepsis.

DATA AVAILABILITY STATEMENT

The datasets presented in this study can be found in online repositories. The names of the repository/repositories and accession number(s) can be found below: https://www.ncbi.nlm.nih.gov/geo/query/acc.cgi?acc=GSE175453, GSE175453.

ETHICS STATEMENT

The studies involving human participants were reviewed and approved by University of Florida's Institutional Review Board. The patients/participants provided their written informed consent to participate in this study.

AUTHOR CONTRIBUTIONS

Project conception and design: DD, RB, MB, XD, MD, RU, DN, JR, TB, AB, FM, LM, AM, and PE. Data collection: MB, MD, RU, DN, and JR. Data analysis and interpretation: DD, XD, RB, and PE. Original manuscript drafting: DB, RB, XD, and PE. Manuscript review and editing: DD, RB, MB, XD, MD, RU, DN, JR, TB, AB, FM, LM, TJ, AM, and PE. Manuscript final approval: DD, FM, LM, TL, AM, and PE. All authors contributed to the article and approved the submitted version.

FUNDING

This work was supported in part by the following National Institutes of Health grants: NIGMS: R01 GM-104481, R01 GM-113945, P50 GM-111152, RM1 GM-139690-01. T32 GM-008721; and NIA: 1P30AG028740.

SUPPLEMENTARY MATERIAL

The Supplementary Material for this article can be found online at: https://www.frontiersin.org/articles/10.3389/fimmu.2021.696536/full#supplementary-material

Supplementary Data Sheet 1 | Summary of cell cluster annotation.

Supplementary Data Sheet 2 | Volcano plots for each cell cluster of the top up and down regulated genes between healthy subjects *versus* all late sepsis non-myeloid cells. Each dot represents a gene statistically enriched or reduced within the cell cluster. The volcano plot compares natural log fold-change (healthy mean divided by sepsis mean; x-axis) with adjusted p-values (y-axis). Significance of differential gene expression was determined with adjusted p-value (p adj.) < 0.01.

Supplementary Data Sheet 3 | Volcano plots for each cell cluster of the top up and down regulated genes between healthy subjects *versus* late sepsis chronic critical illness non-myeloid cells. Each dot represents a gene statistically enriched or reduced within the cell cluster. The volcano plot compares natural log fold-change (healthy mean divided by sepsis mean; x-axis) with adjusted p-values (y-axis). Significance of differential gene expression was determined with adjusted p-value (p adj.) < 0.01.

Supplementary Data Sheet 4 | Volcano plots for each cell cluster of the top up and down regulated genes between bacterial *versus* fungal late sepsis non-myeloid cells. Each dot represents a gene statistically enriched or reduced within the cell cluster. The volcano plot compares natural log fold-change (healthy mean divided by sepsis mean; x-axis) with adjusted p-values (y-axis). Significance of differential gene expression was determined with adjusted p-value (p adj.) < 0.01 and $|FC|>0.4$.

Supplementary Table 1 | Patient characteristics.

Supplementary Table 2 | Significant differentially expressed genes by cell type in analysis of Healthy controls vs All Sepsis patients. Differentially expressed genes are listed for each cell type (individual tabs). Natural log fold-changes are calculated as healthy mean divided by sepsis mean, i.e. negative value of logFC indicates higher expression in sepsis patients. PCT represents the proportion of cells that the corresponding gene is detected.

Supplementary Table 3 | Kyoto Encyclopedia of Genes and Genomes (KEGG) pathway and Gene Ontology (GO) biological process functions pathway analyses of differentially expressed genes in healthy *versus* all late sepsis non-myeloid cells.

Supplementary Table 4 | Significant differentially expressed genes by cell type in analysis of Healthy controls vs Chronic Critical Illness Sepsis patients. Differentially expressed genes are listed for each cell type (individual tabs). Natural log fold-changes are calculated as healthy mean divided by sepsis mean, i.e. negative value of logFC indicates higher expression in sepsis patients. PCT represents the proportion of cells that the corresponding gene is detected.

Supplementary Table 5 | Kyoto Encyclopedia of Genes and Genomes (KEGG) pathway and Gene Ontology (GO) biological process functions pathway analyses of differentially expressed genes in healthy *versus* chronic critical illness late sepsis non-myeloid cells.

Supplementary Table 6 | Significant differentially expressed genes by cell type in analysis of Bacterial Sepsis vs Fungal Sepsis patients. Differentially expressed genes are listed for each cell type (individual tabs). Natural log fold-changes are calculated as healthy mean divided by sepsis mean, i.e. negative value of logFC indicates higher expression in sepsis patients. PCT represents the proportion of cells that the corresponding gene is detected.

Supplementary Table 7 | Kyoto Encyclopedia of Genes and Genomes (KEGG) pathway and Gene Ontology (GO) biological process functions pathway analyses of differentially expressed genes in bacterial *versus* fungal late sepsis non-myeloid cells.

REFERENCES

1. Prescott HC, Angus DC. Enhancing Recovery From Sepsis: A Review. *JAMA* (2018) 319(1):62–75. doi: 10.1001/jama.2017.17687
2. Rhee C, Dantes R, Epstein L, Murphy DJ, Seymour CW, Iwashyna TJ, et al. Incidence and Trends of Sepsis in US Hospitals Using Clinical vs Claims Data, 2009-2014. *JAMA* (2017) 318(13):1241–9. doi: 10.1001/jama.2017.13836
3. Brakenridge SC, Efron PA, Cox MC, Stortz JA, Hawkins RB, Ghita G, et al. Current Epidemiology of Surgical Sepsis: Discordance Between Inpatient Mortality and 1-Year Outcomes. *Ann Surg* (2019) 270(3):502–10. doi: 10.1097/SLA.0000000000003458
4. Gardner AK, Ghita GL, Wang Z, Ozrazgat-Baslanti T, Raymond SL, Mankowski RT, et al. The Development of Chronic Critical Illness Determines Physical Function, Quality of Life, and Long-Term Survival Among Early Survivors of Sepsis in Surgical ICUs. *Crit Care Med* (2019) 47(4):566–73. doi: 10.1097/CCM.0000000000003655
5. Stortz JA, Mira JC, Raymond SL, Loftus TJ, Ozrazgat-Baslanti T, Wang Z, et al. Benchmarking Clinical Outcomes and the Immunocatabolic Phenotype of Chronic Critical Illness After Sepsis in Surgical Intensive Care Unit Patients. *J Trauma Acute Care Surg* (2018) 84(2):342–9. doi: 10.1097/TA.0000000000001758
6. Mira JC, Gentile LF, Mathias BJ, Efron PA, Brakenridge SC, Mohr AM, et al. Sepsis Pathophysiology, Chronic Critical Illness, and Persistent Inflammation-Immunosuppression and Catabolism Syndrome. *Crit Care Med* (2017) 45(2):253–62. doi: 10.1097/CCM.0000000000002074
7. Mankowski RT, Anton SD, Ghita GL, Brumback B, Cox MC, Mohr AM, et al. Older Sepsis Survivors Suffer Persistent Disability Burden and Poor Long-Term Survival. *J Am Geriatr Soc* (2020) 68(9):1962–9. doi: 10.1111/jgs.16435
8. Stortz JA, Cox MC, Hawkins RB, Ghita GL, Brumback BA, Mohr AM, et al. Phenotypic Heterogeneity by Site of Infection in Surgical Sepsis: A Prospective Longitudinal Study. *Crit Care* (2020) 24(1):203. doi: 10.1186/s13054-020-02917-3
9. Hawkins RB, Raymond SL, Stortz JA, Horiguchi H, Brakenridge SC, Gardner A, et al. Chronic Critical Illness and the Persistent Inflammation, Immunosuppression, and Catabolism Syndrome. *Front Immunol* (2018) 9:1511. doi: 10.3389/fimmu.2018.01511
10. Horiguchi H, Loftus TJ, Hawkins RB, Raymond SL, Stortz JA, Hollen MK, et al. Innate Immunity in the Persistent Inflammation, Immunosuppression, and Catabolism Syndrome and Its Implications for Therapy. *Front Immunol* (2018) 9:595. doi: 10.3389/fimmu.2018.00595
11. Gentile LF, Cuenca AG, Efron PA, Ang D, Bihorac A, McKinley BA, et al. Persistent Inflammation and Immunosuppression: A Common Syndrome and New Horizon for Surgical Intensive Care. *J Trauma Acute Care Surg* (2012) 72(6):1491–501. doi: 10.1097/TA.0b013e318256e000
12. Fenner BP, Darden DB, Kelly LS, Rincon J, Brakenridge SC, Larson SD, et al. Immunological Endotyping of Chronic Critical Illness After Severe Sepsis. *Front Med (Lausanne)* (2020) 7:616694. doi: 10.3389/fmed.2020.616694
13. Efron PA, Mohr AM, Bihorac A, Horiguchi H, Hollen MK, Segal MS, et al. Persistent Inflammation, Immunosuppression, and Catabolism and the Development of Chronic Critical Illness After Surgery. *Surgery* (2018) 164(2):178–84. doi: 10.1016/j.surg.2018.04.011
14. Darden DB, Bacher R, Brusko MA, Knight P, Hawkins RB, Cox MC, et al. Single-Cell RNA-Seq of Human Myeloid-Derived Suppressor Cells in Late Sepsis Reveals Multiple Subsets With Unique Transcriptional Responses: A Pilot Study. *Shock* (2021) 55(5):587–95. doi: 10.1097/SHK.0000000000001671

15. Singer M, Deutschman CS, Seymour CW, Shankar-Hari M, Annane D, Bauer M, et al. The Third International Consensus Definitions for Sepsis and Septic Shock (Sepsis-3). *JAMA* (2016) 315(8):801–10. doi: 10.1001/jama.2016.0287
16. Loftus TJ, Mira JC, Ozrazgat-Baslanti T, Ghita GL, Wang Z, Stortz JA, et al. Sepsis and Critical Illness Research Center Investigators: Protocols and Standard Operating Procedures for a Prospective Cohort Study of Sepsis in Critically Ill Surgical Patients. *BMJ Open* (2017) 7(7):e015136. doi: 10.1136/bmjopen-2016-015136
17. Cox MC, Brakenridge SC, Stortz JA, Hawkins RB, Darden DB, Ghita GL, et al. Abdominal Sepsis Patients Have a High Incidence of Chronic Critical Illness With Dismal Long-Term Outcomes. *Am J Surg* (2020) 220(6):1467–74. doi: 10.1016/j.amjsurg.2020.07.016
18. Bronte V, Brandau S, Chen SH, Colombo MP, Frey AB, Greten TF, et al. Recommendations for Myeloid-Derived Suppressor Cell Nomenclature and Characterization Standards. *Nat Commun* (2016) 7:12150. doi: 10.1038/ncomms12150
19. Lun ATL, Riesenfeld S, Andrews T, Dao TP, Gomes Tparticipants in the 1st Human Cell Atlas J, et al. EmptyDrops: Distinguishing Cells From Empty Droplets in Droplet-Based Single-Cell RNA Sequencing Data. *Genome Biol* (2019) 20(1):63. doi: 10.1186/s13059-019-1662-y
20. McCarthy DJ, Campbell KR, Lun AT, Wills QF. Scater: Pre-Processing, Quality Control, Normalization and Visualization of Single-Cell RNA-Seq Data in R. *Bioinformatics* (2017) 33(8):1179–86. doi: 10.1093/bioinformatics/btw777
21. Stuart T, Butler A, Hoffman P, Hafemeister C, Papalexi E, Mauck WM3rd, et al. Comprehensive Integration of Single-Cell Data. *Cell* (2019) 177(7):1888–902 e21. doi: 10.1016/j.cell.2019.05.031
22. Yu G, Wang LG, Han Y, He QY. Clusterprofiler: An R Package for Comparing Biological Themes Among Gene Clusters. *OMICS* (2012) 16(5):284–7. doi: 10.1089/omi.2011.0118
23. Gupta DL, Bhoi S, Mohan T, Galwnkar S, Rao DN. Coexistence of Th1/Th2 and Th17/Treg Imbalances in Patients With Post Traumatic Sepsis. *Cytokine* (2016) 88:214–21. doi: 10.1016/j.cyto.2016.09.010
24. Rendon JL, Choudhry MA. Th17 Cells: Critical Mediators of Host Responses to Burn Injury and Sepsis. *J Leukoc Biol* (2012) 92(3):529–38. doi: 10.1189/jlb.0212083
25. Netea MG, Azam T, Ferwerda G, Girardin SE, Walsh M, Park JS, et al. IL-32 Synergizes With Nucleotide Oligomerization Domain (NOD) 1 and NOD2 Ligands for IL-1beta and IL-6 Production Through a Caspase 1-Dependent Mechanism. *Proc Natl Acad Sci U S A* (2005) 102(45):16309–14. doi: 10.1073/pnas.0508237102
26. Kim SH, Han SY, Azam T, Yoon DY, Dinarello CA. Interleukin-32: A Cytokine and Inducer of TNFalpha. *Immunity* (2005) 22(1):131–42. doi: 10.1016/j.immuni.2004.12.003
27. Wang S, Song R, Wang Z, Jing Z, Wang S, Ma J. S100A8/A9 in Inflammation. *Front Immunol* (2018) 9:1298. doi: 10.3389/fimmu.2018.01298
28. Schaefer U, Voloshanenko O, Willen D, Walczak H. TRAIL: A Multifunctional Cytokine. *Front Biosci* (2007) 12:3813–24. doi: 10.2741/2354
29. Ishikawa E, Nakazawa M, Yoshinari M, Minami M. Role of Tumor Necrosis Factor-Related Apoptosis-Inducing Ligand in Immune Response to Influenza Virus Infection in Mice. *J Virol* (2005) 79(12):7658–63. doi: 10.1128/JVI.79.12.7658-7663.2005
30. Chen K, Liu J, Liu S, Xia M, Zhang X, Han D, et al. Methyltransferase SETD2-Mediated Methylation of STAT1 Is Critical for Interferon Antiviral Activity. *Cell* (2017) 170(3):492–506.e14. doi: 10.1016/j.cell.2017.06.042
31. Reddy M, Eirikis E, Davis C, Davis HM, Prabhakar U. Comparative Analysis of Lymphocyte Activation Marker Expression and Cytokine Secretion Profile in Stimulated Human Peripheral Blood Mononuclear Cell Cultures: An *In Vitro* Model to Monitor Cellular Immune Function. *J Immunol Methods* (2004) 293(1-2):127–42. doi: 10.1016/j.jim.2004.07.006
32. Ferenczi K, Burack L, Pope M, Krueger JG, Austin LM. CD69, HLA-DR and the IL-2R Identify Persistently Activated T Cells in Psoriasis Vulgaris Lesional Skin: Blood and Skin Comparisons by Flow Cytometry. *J Autoimmun* (2000) 14(1):63–78. doi: 10.1006/jaut.1999.0343
33. Gansbacher B, Zier KS. Regulation of HLA-DR, DP, and DQ Expression in Activated T Cells. *Cell Immunol* (1988) 117(1):22–34. doi: 10.1016/0008-8749(88)90073-1
34. Moisan J, Grenningloh R, Bettelli E, Oukka M, Ho IC. Ets-1 Is a Negative Regulator of Th17 Differentiation. *J Exp Med* (2007) 204(12):2825–35. doi: 10.1084/jem.20070994
35. Kroger A. IRFs as Competing Pioneers in T-Cell Differentiation. *Cell Mol Immunol* (2017) 14(8):649–51. doi: 10.1038/cmi.2017.37
36. Giang S, La Cava A. IRF1 and BATF: Key Drivers of Type 1 Regulatory T-Cell Differentiation. *Cell Mol Immunol* (2017) 14(8):652–4. doi: 10.1038/cmi.2017.38
37. Hendriks J, Gravestein LA, Tesselaar K, van Lier RA, Schumacher TN, Borst J. CD27 Is Required for Generation and Long-Term Maintenance of T Cell Immunity. *Nat Immunol* (2000) 1(5):433–40. doi: 10.1038/80877
38. Ng SS, De Labastida Rivera F, Yan J, Corvino D, Das I, Zhang P, et al. The NK Cell Granule Protein NKG7 Regulates Cytotoxic Granule Exocytosis and Inflammation. *Nat Immunol* (2020) 21(10):1205–18. doi: 10.1038/s41590-020-0758-6
39. Nicolet BP, Guislain A, van Alphen FPJ, Gomez-Eerland R, Schumacher TNM, van den Biggelaar M, et al. CD29 Identifies IFN-Gamma-Producing Human CD8(+) T Cells With an Increased Cytotoxic Potential. *Proc Natl Acad Sci U S A* (2020) 117(12):6686–96. doi: 10.1073/pnas.1913940117
40. Munier CML, van Bockel D, Bailey M, Ip S, Xu Y, Alcantara S, et al. The Primary Immune Response to Vaccinia Virus Vaccination Includes Cells With a Distinct Cytotoxic Effector CD4 T-Cell Phenotype. *Vaccine* (2016) 34(44):5251–61. doi: 10.1016/j.vaccine.2016.09.009
41. Hou Q, Zhao T, Zhang H, Lu H, Zhang Q, Sun L, et al. Granzyme H Induces Apoptosis of Target Tumor Cells Characterized by DNA Fragmentation and Bid-Dependent Mitochondrial Damage. *Mol Immunol* (2008) 45(4):1044–55. doi: 10.1016/j.molimm.2007.07.032
42. Langerholc T, Zavasnik-Bergant V, Turk B, Turk V, Abrahamson M, Kos J. Inhibitory Properties of Cystatin F and its Localization in U937 Promonocyte Cells. *FEBS J* (2005) 272(6):1535–45. doi: 10.1111/j.1742-4658.2005.04594.x
43. Szabo PA, Levitin HM, Miron M, Snyder ME, Senda T, Yuan J, et al. Single-Cell Transcriptomics of Human T Cells Reveals Tissue and Activation Signatures in Health and Disease. *Nat Commun* (2019) 10(1):4706. doi: 10.1038/s41467-019-12464-3
44. Jensen IJ, Sjaastad FV, Griffith TS, Badovinac VP. Sepsis-Induced T Cell Immunoparalysis: The Ins and Outs of Impaired T Cell Immunity. *J Immunol* (2018) 200(5):1543–53. doi: 10.4049/jimmunol.1701618
45. Hotchkiss RS, Monneret G, Payen D. Sepsis-Induced Immunosuppression: From Cellular Dysfunctions to Immunotherapy. *Nat Rev Immunol* (2013) 13(12):862–74. doi: 10.1038/nri3552
46. Pegram HJ, Andrews DM, Smyth MJ, Darcy PK, Kershaw MH. Activating and Inhibitory Receptors of Natural Killer Cells. *Immunol Cell Biol* (2011) 89(2):216–24. doi: 10.1038/icb.2010.78
47. Patel S. Danger-Associated Molecular Patterns (DAMPs): The Derivatives and Triggers of Inflammation. *Curr Allergy Asthma Rep* (2018) 18(11):63. doi: 10.1007/s11882-018-0817-3
48. Roh JS, Sohn DH. Damage-Associated Molecular Patterns in Inflammatory Diseases. *Immune Netw* (2018) 18(4):e27. doi: 10.4110/in.2018.18.e27
49. Malik U, Javed A. FAM26F: An Enigmatic Protein Having a Complex Role in the Immune System. *Int Rev Immunol* (2016) 19:1–11. doi: 10.1080/08830185.2016.1206098
50. Kasamatsu J, Azuma M, Oshiumi H, Morioka Y, Okabe M, Ebihara T, et al. INAM Plays a Critical Role in IFN-Gamma Production by NK Cells Interacting With Polyinosinic-Polycytidylic Acid-Stimulated Accessory Cells. *J Immunol* (2014) 193(10):5199–207. doi: 10.4049/jimmunol.1400924
51. Soni C, Reizis B. Self-DNA at the Epicenter of SLE: Immunogenic Forms, Regulation, and Effects. *Front Immunol* (2019) 10:1601. doi: 10.3389/fimmu.2019.01601
52. Shi G, Abbott KN, Wu W, Salter RD, Keyel PA. Dnase1L3 Regulates Inflammasome-Dependent Cytokine Secretion. *Front Immunol* (2017) 8:522. doi: 10.3389/fimmu.2017.00522
53. Man SM, Karki R, Kanneganti TD. AIM2 Inflammasome in Infection, Cancer, and Autoimmunity: Role in DNA Sensing, Inflammation, and Innate Immunity. *Eur J Immunol* (2016) 46(2):269–80. doi: 10.1002/eji.201545839
54. Bailey CC, Zhong G, Huang IC, Farzan M. IFITM-Family Proteins: The Cell's First Line of Antiviral Defense. *Annu Rev Virol* (2014) 1:261–83. doi: 10.1146/annurev-virology-031413-085537
55. Saha D, Patgaonkar M, Shroff A, Ayyar K, Bashir T, Reddy KV. Hemoglobin Expression in Nonerythroid Cells: Novel or Ubiquitous? *Int J Inflam* (2014) 2014:803237. doi: 10.1155/2014/803237
56. Shukeri W, Ralib AM, Abdulah NZ, Mat-Nor MB. Sepsis Mortality Score for the Prediction of Mortality in Septic Patients. *J Crit Care* (2018) 43:163–8. doi: 10.1016/j.jcrc.2017.09.009

57. Loss SH, Nunes DSL, Franzosi OS, Salazar GS, Teixeira C, Vieira SRR. Chronic Critical Illness: Are We Saving Patients or Creating Victims? *Rev Bras Ter Intensiva* (2017) 29(1):87–95. doi: 10.5935/0103-507X.20170013
58. Stevenson EK, Rubenstein AR, Radin GT, Wiener RS, Walkey AJ. Two Decades of Mortality Trends Among Patients With Severe Sepsis: A Comparative Meta-Analysis*. *Crit Care Med* (2014) 42(3):625–31. doi: 10.1097/CCM.0000000000000026
59. Brakenridge SC, Moore FA, Mercier NR, Cox M, Wu Q, Moldawer LL, et al. Persistently Elevated Glucagon-Like Peptide-1 Levels Among Critically Ill Surgical Patients After Sepsis and Development of Chronic Critical Illness and Dismal Long-Term Outcomes. *J Am Coll Surg* (2019) 229(1):58–67.e1. doi: 10.1016/j.jamcollsurg.2019.04.014
60. McKinley BA, Moore LJ, Sucher JF, Todd SR, Turner KL, Valdivia A, et al. Computer Protocol Facilitates Evidence-Based Care of Sepsis in the Surgical Intensive Care Unit. *J Trauma* (2011) 70(5):1153–66; discussion 66-7. doi: 10.1097/TA.0b013e31821598e9
61. Raymond SL, Hawkins RB, Murphy TJ, Rincon JC, Stortz JA, Lopez MC, et al. Impact of Toll-Like Receptor 4 Stimulation on Human Neonatal Neutrophil Spontaneous Migration, Transcriptomics, and Cytokine Production. *J Mol Med (Berl)* (2018) 96(7):673–84. doi: 10.1007/s00109-018-1646-5
62. Sweeney TE, Azad TD, Donato M, Haynes WA, Perumal TM, Henao R, et al. Unsupervised Analysis of Transcriptomics in Bacterial Sepsis Across Multiple Datasets Reveals Three Robust Clusters. *Crit Care Med* (2018) 46(6):915–25. doi: 10.1097/CCM.0000000000003084
63. Ulas T, Pirr S, Fehlhaber B, Bickes MS, Loof TG, Vogl T, et al. S100-Alarmin-Induced Innate Immune Programming Protects Newborn Infants From Sepsis. *Nat Immunol* (2017) 18(6):622–32. doi: 10.1038/ni.3745
64. Mira JC, Szpila BE, Nacionales DC, Lopez MC, Gentile LF, Mathias BJ, et al. Patterns of Gene Expression Among Murine Models of Hemorrhagic Shock/Trauma and Sepsis. *Physiol Genomics* (2016) 48(2):135–44. doi: 10.1152/physiolgenomics.00072.2015
65. Gentile LF, Nacionales DC, Lopez MC, Vanzant E, Cuenca A, Cuenca AG, et al. Protective Immunity and Defects in the Neonatal and Elderly Immune Response to Sepsis. *J Immunol* (2014) 192(7):3156–65. doi: 10.4049/jimmunol.1301726
66. Zhu J, Paul WE. Peripheral CD4+ T-Cell Differentiation Regulated by Networks of Cytokines and Transcription Factors. *Immunol Rev* (2010) 238 (1):247–62. doi: 10.1111/j.1600-065X.2010.00951.x
67. Ouyang W, Kolls JK, Zheng Y. The Biological Functions of T Helper 17 Cell Effector Cytokines in Inflammation. *Immunity* (2008) 28(4):454–67. doi: 10.1016/j.immuni.2008.03.004
68. Wu HP, Chung K, Lin CY, Jiang BY, Chuang DY, Liu YC. Associations of T Helper 1, 2, 17 and Regulatory T Lymphocytes With Mortality in Severe Sepsis. *Inflamm Res* (2013) 62(8):751–63. doi: 10.1007/s00011-013-0630-3
69. Ye P, Rodriguez FH, Kanaly S, Stocking KL, Schurr J, Schwarzenberger P, et al. Requirement of Interleukin 17 Receptor Signaling for Lung CXC Chemokine and Granulocyte Colony-Stimulating Factor Expression, Neutrophil Recruitment, and Host Defense. *J Exp Med* (2001) 194(4):519–27. doi: 10.1084/jem.194.4.519
70. Schwarzenberger P, Huang W, Ye P, Oliver P, Manuel M, Zhang Z, et al. Requirement of Endogenous Stem Cell Factor and Granulocyte-Colony-Stimulating Factor for IL-17-Mediated Granulopoiesis. *J Immunol* (2000) 164(9):4783–9. doi: 10.4049/jimmunol.164.9.4783
71. Fossiez F, Djossou O, Chomarat P, Flores-Romo L, Ait-Yahia S, Maat C, et al. T Cell Interleukin-17 Induces Stromal Cells to Produce Proinflammatory and Hematopoietic Cytokines. *J Exp Med* (1996) 183(6):2593–603. doi: 10.1084/jem.183.6.2593
72. Reyes M, Filbin MR, Bhattacharyya RP, Billman K, Eisenhaure T, Hung DT, et al. An Immune-Cell Signature of Bacterial Sepsis. *Nat Med* (2020) 26 (3):333–40. doi: 10.1038/s41591-020-0752-4
73. Khan HN, Perlee D, Schoenmaker L, van der Meer AJ, Franitza M, Toliat MR, et al. Leukocyte Transcriptional Signatures Dependent on LPS Dosage in Human Endotoxemia. *J Leukoc Biol* (2019) 106(5):1153–60. doi: 10.1002/JLB.4A0219-050R
74. Saeidi A, Zandi K, Cheok YY, Saeidi H, Wong WF, Lee CYQ, et al. T-Cell Exhaustion in Chronic Infections: Reversing the State of Exhaustion and Reinvigorating Optimal Protective Immune Responses. *Front Immunol* (2018) 9:2569. doi: 10.3389/fimmu.2018.02569
75. Wherry EJ, Ha SJ, Kaech SM, Haining WN, Sarkar S, Kalia V, et al. Molecular Signature of CD8+ T Cell Exhaustion During Chronic Viral Infection. *Immunity* (2007) 27(4):670–84. doi: 10.1016/j.immuni.2007.09.006
76. Angajala A, Lim S, Phillips JB, Kim JH, Yates C, You Z, et al. Diverse Roles of Mitochondria in Immune Responses: Novel Insights Into Immuno-Metabolism. *Front Immunol* (2018) 9:1605. doi: 10.3389/fimmu.2018.01605
77. Talwar S, Munson PJ, Barb J, Fiuza C, Cintron AP, Logun C, et al. Gene Expression Profiles of Peripheral Blood Leukocytes After Endotoxin Challenge in Humans. *Physiol Genomics* (2006) 25(2):203–15. doi: 10.1152/physiolgenomics.00192.2005
78. Ramos-Sevillano E, Ercoli G, Brown JS. Mechanisms of Naturally Acquired Immunity to Streptococcus Pneumoniae. *Front Immunol* (2019) 10:358. doi: 10.3389/fimmu.2019.00358
79. Sehrawat S, Rouse BT. Interplay of Regulatory T Cell and Th17 Cells During Infectious Diseases in Humans and Animals. *Front Immunol* (2017) 8:341. doi: 10.3389/fimmu.2017.00341

Conflict of Interest: The authors declare that the research was conducted in the absence of any commercial or financial relationships that could be construed as a potential conflict of interest.

frontiers in Immunology

REVIEW
published: 18 August 2021
doi: 10.3389/fimmu.2021.701163

Ferroptosis: A Trigger of Proinflammatory State Progression to Immunogenicity in Necroinflammatory Disease

Jing-yan Li[1], *Yong-ming Yao*[1,2*] *and Ying-ping Tian*[1*]

[1] Department of Emergency, The Second Hospital of Hebei Medical University, Shijiazhuang, China, [2] Translational Medicine Research Center, Medical Innovation Research Division and Fourth Medical Center of the Chinese PLA General Hospital, Beijing, China

Until recently, necrosis is generally regarded as traumatic cell death due to mechanical shear stress or other physicochemical factors, while apoptosis is commonly thought to be programmed cell death, which is silent to immunological response. Actually, multiple modalities of cell death are programmed to maintain systematic immunity. Programmed necrosis, such as necrosis, pyroptosis, and ferroptosis, are inherently more immunogenic than apoptosis. Programmed necrosis leads to the release of inflammatory cytokines, defined as danger-associated molecular patterns (DAMPs), resulting in a necroinflammatory response, which can drive the proinflammatory state under certain biological circumstances. Ferroptosis as a newly discovered non-apoptotic form of cell death, is characterized by excessive lipid peroxidation and overload iron, which occurs in cancer, neurodegeneration, immune and inflammatory diseases, as well as ischemia/reperfusion (I/R) injury. It is triggered by a surplus of reactive oxygen species (ROS) induced in an imbalanced redox reaction due to the decrease in glutathione synthesis and inaction of enzyme glutathione peroxidase 4 (GPX4). Ferroptosis is considered as a potential therapeutic and molecular target for the treatment of necroinflammatory disease, and further investigation into the underlying pathophysiological characteristics and molecular mechanisms implicated may lay the foundations for an interventional therapeutic strategy. This review aims to demonstrate the key roles of ferroptosis in the development of necroinflammatory diseases, the major regulatory mechanisms involved, and its potential as a therapeutic target.

Keywords: ferroptosis, necroinflammatory diseases, inflammatory response, immunogenicity, immune cell

OPEN ACCESS

Edited by:
Haichao Wang,
Feinstein Institute for Medical Research, United States

Reviewed by:
Jan Rossaint,
University of Münster, Germany
Jen-Tsan Ashley Chi,
Duke University, United States

***Correspondence:**
Ying-ping Tian
tianyingping999@163.com
Yong-ming Yao
c_ff@sina.com

Specialty section:
This article was submitted to Inflammation, a section of the journal Frontiers in Immunology

Received: *27 April 2021*
Accepted: *02 August 2021*
Published: *18 August 2021*

Citation:
Li J-y, Yao Y-m and Tian Y-p (2021) Ferroptosis: A Trigger of Proinflammatory State Progression to Immunogenicity in Necroinflammatory Disease. Front. Immunol. 12:701163. doi: 10.3389/fimmu.2021.701163

INTRODUCTION

Apoptosis, regarded to occur only in one form of programmed cell death, is deemed to play a part in homeostasis and host defense. This form yields cell death in a genetically regulated way that performs an induced impact on the adjacent cells. While another different form of necrosis, considered as a type of cell death in the setting of physicochemical stimulation, can be dictated by a

special molecular pathway that releases intracellular contents to induct inflammatory response (1). Compared to the formation of apoptotic bodies and membrane packaging during apoptosis, necrosis is characterized by cellular swelling, membrane permeabilization, and even release of cellular contents (2). Although conspicuous feature of these cell death processes may transform into differently immunogenical levels, impairment of scavenging function in apoptotic cells can result in necrosis, inducing the onset of inflammation (3). It is proved by accumulating evidences that cells indeed undergo programmed necrotic processed, such as necroptosis, pyroptosis, ferroptosis, and NET osis (**Figure 1**).

Necroinflammation, defined as the cascade connection of innate and adaptive immune responses to necroptotic cell death, might be regulated by particular signaling mechanisms such as necroptosis, ferroptosis, and pyroptosis. Cells suffering from oxidative stress may release immunogenic molecules, which trigger the systematic immune response against detrimental substances, ultimately leading to necrotic cell death in a physiological or pathophysiological state. Therefore, immune cell should be dependent on precisely discriminative mechanism to distinguish between the diverse forms of cell death, and concurrently detect signaling molecular transmitted by dying cells for activating immune system. As to date, evidences prove immune response to be affected *via* ferroptosis during programmed necroinflammatory process. A better understanding of ferroptosis as a form of necrosis, could lead to the pharmacological prevention in necroinflammatory disease.

Ferroptosis, characterized by iron-dependent lipid peroxidation, and triggered by a particular small-molecule inducer, is inducted by unique and precise mechanisms. In fact, superimposed lipid peroxidation has been confirmed to be the central part of ferroptosis. A long-chain-fatty-acidacetyl-coenzyme A synthase 4 (ACSL4) (4), which is an activator of the lipoxygenase-dependent signaling pathway, involves in ferroptosis initiation, and another antioxidant enzyme glutathione peroxidase 4 (GPX4) (5) subsequently triggers ferroptosis under the reduction/oxidation imbalanced status. The specific necrotic signaling pathway of ferroptosis may produce pathogenic cytokines peroxides that impair the immune response *via* activating immune cells. In addition, ferroptosis may upregulate subcellular structures such as hazardous peroxisomes on the surface of fractured organelles or ruptured mitochondria. More studies suggest that ferroptosis-related cell death has a potential link to necroinflammatory disease. Hence, further exploration in ferroptosis enhancing systematically proinflammatory state of the immune response might potentially target for novel mechanisms and therapies.

Abbreviations: ACSL4, long-chain-fatty-acidacetyl-Coenzyme A synthase 4; GPX4, glutathione peroxidase 4; ROS, reactive oxygen species; DAMPs, danger-associated molecular patterns; PCD, programmed cell death; NPCD, non-programmed cell death; GSH, glutathione; LOX, lipoxygenase; PAMPs, pathogen-associated molecular patterns; PRRs, pattern recognition receptors; AA, arachidonic acid; PTGS, prostaglandin-endoperoxide synthase; HPETE, hydroperoxyeicosatetraenotic acid; HETE, hydroxyeicosatetraenoic acid; PUFAs, polyunsaturated fatty acids; ILs, interleukins; TNF-α, tumor necrosis factor-α; LT, leukotriene; NF-κB, nuclear factor κB; I/R, ischemia/reperfusion; RSL3, Ras synthetic lethal 3; Fer-1, ferrostatin-1; COPD, chronic obstructive pulmonary disease; CS, cigarette smoke; HBE, human bronchial epithelial; IBD, inflammatory bowel disease; UC, ulcerative colitis; CD, Crohn's disease; IECs, intestinal epithelial cells; AKI, acute kidney injury; HMGB1, high mobility group box-1 protein. HSF, heat shock factor; HSPB1, heat shock factor1; SLC7A11, transmembrane protein transporter solute carrier family 7 member 11; SLC3A2, transmembrane regulatory protein solute carrier family 3 member 2; PE, phosphatidylethanolamine; AdA, adrenaline; Sp1, special protein 1; AIFM2/FSP1, apoptosis-inducing factor mitochondria-associated 2; CoQ, coenzyme Q; NADP, nicotinamide-adenine dinucleotide phosphate; NCOA4, nuclear receptor coactivator 4; IREB2, iron responsive element-binding protein 2; Atg5, autophagy-related 5; Atg7, autophagy-related 7; Nrf2, nuclear factor erythroid 2-related factor 2; Keap1, Kelch-like ECH-associated protein 1; HO-1, home oxygenase-1; FTH1, ferritin heavy chain; HSPs, heat shock proteins; LDH, lactate dehydrogenase; DFO, desferrioxamine; ccRCC, clear-cell renal cell carcinomas.

FERROPTOSIS AND REGULATORY MECHANISMS

Ferroptosis differs from other traditional forms of cell death in terms of initiative factor, dying cell morphology, regulatory pathway, as well as biological induction and inhibition (5, 6). It is notable that ferroptosis is a mitochondria-dependent type of cell death with the features in mitochondrial morphology including reduced mitochondrial volume, increased inner membrane density, rupture of the outer mitochondrial membrane and mitochondria cristae dysfunction (7). Moreover, the key mechanisms involved in ferroptosis depend on the metabolism of polyunsaturated fatty acid and the modulation of phospholipidome, especially the nonenzymatic lipoxygenase-mediated lipid peroxidation leading to the destruction of the lipid bilayer. Thus, ferroptosis occurs along with glutathione overconsumption, inhibition of glutathione synthesis and reduction of GPX4 activity when the redox reaction is disorganized. Up to date, as increasingly advanced understanding of ferroptosis in various domains, the signaling cascades including System Xc-, GPX4, MVA, and heat shock factor (HSF)1-HSPB1 (8) appear to be more clear. The major signaling pathways of ferroptosis are summarized in **Figure 2**.

Glutathione Metabolic Pathway

The activity of lipid repair enzyme called GPX4 which exerts an antioxidative effect on ferroptotic process depends on the biosynthesis of glutathione (GSH) (5), and is identified as a key regulatory factor in ferroptosis. Intracellular depletion of GSH leads to GPX4 inactivation and lipid peroxidation accumulation, eventually resulting in ferroptosis (9). In particular, GPX4 is specifically targeted by the endogenous ferroptosis-inducing agent of RSL3 (10), which catalyzes GSH-dependent reduction of hydroperoxides to lipid alcohols System Xc- composed of a transmembrane protein transporter solute carrier family 7 member 11 (SLC7A11) and a single-pass transmembrane regulatory protein solute carrier family 3 member 2 (SLC3A2), regulates ferroptosis together with glutathione metabolic pathway by exchanging glutamate and cystine at 1:1 ratio (11). Inhibition of system Xc- causes the depletion of intracellular cysteine, restricting the synthesis of glutathione, and triggering oxidative stress, and then the

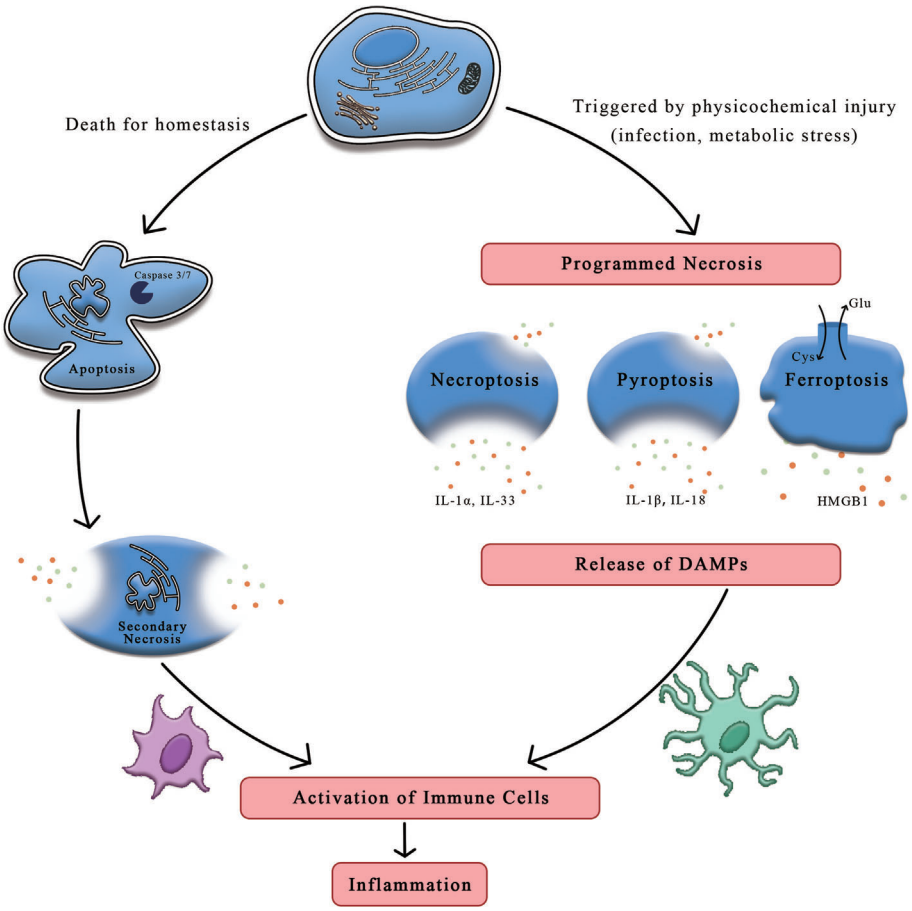

FIGURE 1 | The distinctions between apoptosis and necrosis. On account of the stimuli and context, cells can undergo apoptosis and necrosis. Apoptosis is thought to be programmed cell death relating to homeostasis while necrosis is induced by mechanical shear stress or other physicochemical factors including infection and oxidation, etc. Upon the stimulation of damaged signals, cells trigger programmed necrosis, such as necroptosis, pyroptosis and ferroptosis. Cells suffering from stress may release immunogenic molecules called DAMPs, which could initiate the systematic immune response against detrimental substances, ultimately leading to inflammation. HMGB1, high mobility group box-1 protein; DAMPs, danger-associated molecular patterns.

antioxidant enzyme GPX4 is impaired, which finally initiates ferroptosis. Moreover, increasing evidences support the hypothesis that trans-sulfuration as another regulator of ferroptosis, is the major source of compensatory for cysteine depletion and further inhibits erastin-induced ferroptosis (12). Therefore, GPX4 synthesis-related and system Xc- function-related pathway are essential in ferroptotic regulation.

Lipid Peroxidation Pathway

Researchers have discovered that ferroptosis is preferentially accompanies by lipid peroxidation including polyphosphorylated phosphatidylethanolamine (PE) containing polyunsaturated fatty acids (PUFAs) (13). ACSL4 is considered as the key enzyme to regulate lipid oxidative response and accelerate ferroptosis by generating oxidized PE in oxygenation localize, catalyzing adrenaline (AdA) to generate AdA acyl Co-A, which is esterified to AdA-PE (14). A mass of malondialdehydes is produced by AdA-PE oxidation and ultimately leads to ferroptosis. Expression of ACSL4 is regulated by certain molecules, such as special protein 1 (Sp1) (15), a transcription factor that upregulates ACSL4 transcription to promote ferroptosis. Inhibiting the activity of ACSL4 can block AdA esterificating into PE, which reduces susceptibility of mouse embryonic fibroblasts Pfa 1 cells to ferroptosis (13). These studies indicate that lipid peroxidation is the key step in ferroptosis.

NADPH-FSP1-CoQ10 Pathway

It has been demonstrated by Doll and colleagues that overexpression of apoptosis-inducing factor mitochondria-associated 2 (AIFM2, also named as FSP1) (16) is capable of reversing GPX4 suppression-induced ferroptosis, which proves FSP1 to be ferroptotic inhibitor independent on GPX4 mechanism. The N-terminus of FSP1 is representative for its structural domain called myristoylation with function of lipid modification, which promotes FSP1 locating on plasmalemma and reduces sensitivity of cells to ferroptosis (16). A previous

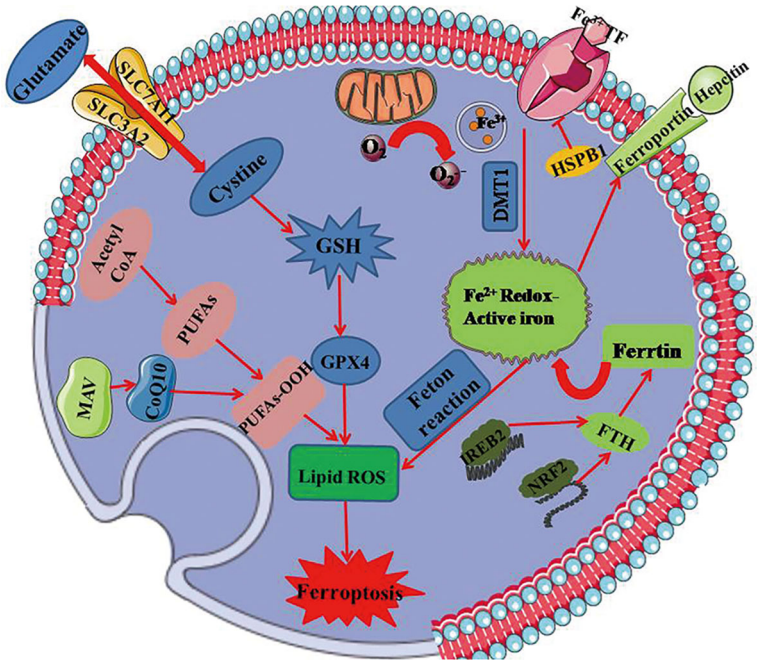

FIGURE 2 | The mainly regulated mechanism underlying ferroptosis. GPX4 regarded as the key regulator in ferroptosis relies on the biosynthesis of GSH. It produces an antioxidative effect on ferroptotic process, and is regulated by MAV signaling pathway. Xc- system that is composed of SLC7A11 and SLC3A2 regulates ferroptosis together with glutathione metabolic pathway by exchanging glutamate and cystine at 1:1 ratio. Ferroptosis is dependent on overload iron that ascribes to peroxides and divalent ferrous salts produced by fenton reaction. Iron can be transported from extracellular to intracellular in virtue of transferring protein. Mitochondria as the essential organ involving in ferroptosis, contains six ferroptosis-related genes and releases ferroptosis-induced lipid peroxides through the electron-transporting chain. PUFAs, polyunsaturated fatty acids; GSH, glutathione; GPX4, glutathione peroxidase 4; DMT1, divalent metal transporter 1; HSPB1, heat shock protein B1; FTH, ferritin heavy polypeptide; IREB2, iron response element binding protein 2; NRF2, nuclear factor erythroid-2-related factor 2; SLC7A11, transmembrane protein transporter vector family 7 member 11; SLC3A2, single-channel transmembrane regulatory protein solute carrier family 3 member2.

study verified FSP1 to be an nicotinamide-adenine dinucleotide phosphate- (NADP-) dependent coenzyme Q (CoQ) oxidoreductase, which is an electronic carrier and acts as lipidsoluble antioxidant (17). The recent studies demonstrate that FSP1 is paralleled with GPX4 to suppress ferroptosis by directly regulating the nonmitochondrial CoQ_{10} antioxidant system (18). Hence, inhibition of FSP1 combined with GPX4 might provide a more effectively targeting strategy for ferroptosis-associated diseases.

Iron Metabolism Pathway

Both process and development of ferroptosis relies on overload iron that ascribe to peroxides and divalent ferrous salts produced by fenton reaction. When intracellular iron homeostasis is disordered, nuclear receptor coactivator 4 (NCOA4) (19) mediated ferritinophagy leads to disfunction of transferrin, which ultimately enhances the production of oxygen centered free radicals to induce ferroptosis. The key encoder named iron responsive element-binding protein 2 (IREB2) (7) is responsible for regulating iron metabolism, and studies have revealed that silencing-expressed IREB2 might perform an impact on not only iron transportation but also genes expression of transferrins (5, 7, 8). Moreover, upregulation of autophagy-associated protein expression activates ferroptosis, and inhibition of autophagy-related 5 (Atg5) as well as autophagy-related 7 (Atg7) genes shows a suppressive activity on ferroptosis (20).

Other Molecular Related Signaling Pathway

In addition to the aforementioned signaling pathway, the nuclear factor erythroid 2-related factor 2 (Nrf2) (8, 21) involves in the regulation of ferroptosis due to its antioxidant function. When cells confront the normoxic setting, Nrf2 is united with Kelch-like ECH-associated protein 1 (Keap 1) to maintain an inactivated state by ubiquitylation in the proteasome, while Nrf2 is released from the conjugated Keap1 protein to transsituate to the nucleus under the oxidative stress (21). In 2016, Sun and his team demonstrated p62-Keap1-Nrf2 signaling pathway performed an antioxidative effect on the regulation of ferroptosis in hepatoma carcinoma cells, depended on the mechanism that p62 as an autophagy receptor could locate on cells to activate Nrf2 by devitalization of Keap1 (22). Nrf2-inhibited ferroptosis is also associated with the mediation of NQO1 (22), home oxygenase-1 (HO-1) (8), and ferritin heavy chain (FTH1) (5, 7), which shows a crosstalk between ferroptosis and autophagy. P53 is reported to mediate ferroptotic signaling pathway through down-regulating SLC7A11 expression to inhibit Xc-system. It is found that proliferation of ROS after activated P53 reduces antioxidant efficacy eventually contributing to ferroptosis, which is reversed by the treatment ferrostatin-1 (Fer-1) (23). Thus, P53 performs an essential impact on ROS-related metabolic signaling pathway of ferroptosis.

THE RELATIONSHIP BETWEEN FERROPTOSIS AND NECROINFLAMMATORY RESPONSE

Inflammation, generally in response to pathogen or tissue injury, is typically described as a complex biological response (24). The molecular mechanism of inflammation firstly proposed by Charles Janeway, states that the immune system can discriminate between self (healthy tissues) and non-self (invasivepathogens). Accordingly, pathogenic molecules, defined as pathogen-associated molecular patterns (PAMPs) are recognized by pattern recognition receptors (PRRs), which are responsible for identifying the existence of microorganisms and act as the first line of defense against infection and tissue injury (25). PRRs are widely expressed and located not only on various immune cells including macrophages and dendritic cells but also on nonprofessional immune cells, such as cells of the neurovascular unit as well as cerebral vasculature, and even on the abnormal tumor cells (26). These conservative microbial production, including lipopolysaccharide, lipoteichoic acid, bacterial lipopeptides, peptidoglycan, and bacterial DNA, are commonly referred to PAMPs, and then stimulate PRRs, which eventually result in the migration of immune cells to the site of infection (27). However, in addition to the recognition of pathogens, the immune system is capable of responding to cellular damage, including acute organ rejection, systemic autoimmune diseases, and inflammatory diseases. Afterwards, Matzinger proposed the notion of endogenous danger signals that can sense harmful stimuli by activating the immune response following stress-induced damage (28). This type of inflammation can be triggered by danger-associated molecular patterns (DAMPs) (28) in response to stress and cell death, which is discriminative to PAMPs (**Table 1**). DAMPs, such as high mobility group box-1 protein (HMGB1), heat shock proteins (HSPs), uric acid, thioredoxin, galectins and so on, are released during oxidative stress or tissue damage and subsequently initiate an inflammatory response (27, 28). Despite PRRs are applied to detect PAMPs in order to further identify DAMPs, DAMPs are still viewed as menacing microbes (**Table 2**). In fact, the processes and mechanisms implicated in the necroinflammatory response are extremely complex. Cells dying by necrotic mechanisms, whether in a controlled manner or by accident, are characterized by cytoplasmic membrane damage, releasing their intracellular contents (e.g., DAMPs), which can be recognized by the immune system through signaling pathways,

TABLE 2 | DAMPs and PRRs that recognize menacing microbes.

DAMP	PRR
HMGB1	RAGE, TLR2/4
Serum amyloid A	TLR1/2
Fatty acids	TLR4
Hyaluronic acid	TLR2/4
Uric acid	NOD1/2, NLRP3
ATP	NLRP3, P2XR, P2YR, NOD1/2
snRNPs	RIG-I, MDA5,TLR7/8
dsDNA	TLR9, DAI, AIM2
Histone	TLR2/4/9, NLRP3
IC	FcR, TLR9
HSPs	TLR2/4
Surfactant Protein A/D	TLR2/4
Oxidized LDL	TLR4
Defensins	TLR2/4
RNA	TLR7
LL37	RAGE, TLR7/9
S100 proteins	RAGE, NOD1/2, TLR4
Reg111a	TLR4
Lactoferrin	TLR4

TLR, Toll-like receptor; NOD, nucleotide-binding oligomerization domain-containing protein; NLRP, NLR family, pyrin domain containing; ATP, adenosine triphosphate; snRNAP, small nuclear ribonucleoproteins; RIG-I, retinoic acid-inducible gene I; MDA, melanoma differentiation associated protein; DAI (ZBP1), dnadependent activator of interferon-regulatory factors; AIM2, absent in melanoma 2; HMGB1, high mobility group box-1 protein; RAGE, receptor for advanced glycation endproducts; IC, immune complex; FcR, Fc receptor; HSP, heat shock protein; LDL, low-density lipoprotein; LL37, cathelicidin antimicrobial peptide.

TABLE 1 | Comparisons of PAMPs and DAMPs.

	PAMPs	DAMPs
Definitions	A particularly specific and highly conserved molecular structures owed by a certain types of microbial pathogens and their products, which can be recognized by nonspecific immune cells.	A type of molecular structures released into intercellular or blood circulation when the tissue or cells are suffering injury, hypoxia stress and then activated. It is the endogenous molecules released by organic cells.
Characteristics	(1) Specific to pathogenic microorganisms, but not produced by host cells.	(1) Activating innate immunity and adaptive immunity through variety of mechanisms.
	(2) Necessary for the survival or pathogenicity of microorganisms.	(2) Promoting the release of inflammatory mediators, regulating inflammatory response, and inducing the migration of immune cells to inflammatory sites.
	(3) As the molecular basis of extensively specific recognition of host innate immune cells.	(3) Increasing the ability of inflammatory cells to adhere and infiltrate.
Patterns	Lipopolysaccharide (LPS)	High mobility group box-1 protein (HMGB1)
	Lipoteichoic acid	Heat shock proteins (HSPs)
	Bacterial lipopeptides	S100 proteins
	Peptidoglycan	Uric acid
	Yeast and gram-positive bacteria	Adenosine and ATP
	Bacterial DNA	Galectins
	Flagellin	Thioredoxin
	Terminal mannose/fucose	IL-33/ST2

finally initiating a necroinflammatory process (29, 30). It has been hypothesized that the release of endogenous DAMPs can perform a vital function to evoke tissue inflammation and further excitation of regulatory cell death through autoamplification (31). Immune cells have the capability to detect various forms of hazardous cellular stresses and then transmit signals to elicit immune responses (32). Collectively, necroinflammation is associated with a persistent immune response and an inflammatory state, which induces the pathological process of human disease.

It is accepted that ferroptosis, as a type of necrotic death, is more immunogenic than apoptosis to induce the release of inflammatory mediators and DAMPs, thus rendering the cellular environment highly proinflammatory state. Despite the release and function of DAMPs in ferroptotic cells remains unclear to a large extent, DAMPs can impact on initiating and perpetuating a necroinflammation during ferroptosis. A recent study has provided evidence that HMGB1 is a specific DAMP released by ferroptotic cells in an autophagy-dependent manner (33). Ferroptosis-induced inflammatory response appears to be significantly attenuated by intervention of anti-HMHB1 neutralizing antibodies, which indicates targeting HMGB1 release can effectively inhibit an necroinflammation in ferroptosis. Notably, the relationship between ferroptosis and the necroinflammatory response is outlined in **Figure 3**.

REGULATION OF FERROPTOSIS IN NECROINFLAMMATORY RESPONSE

GPX4 Regulates Necroinflammation *via* Arachidonic Acid Metabolism During Ferroptosis

Iron-dependent peroxidized lipids and imbalanced metabolic arachidonic acid (AA) (13) are comprised in ferroptotic process, which exert regulatory effects on both occurrence and development of necroinflammatory diseases. However, in the early state of the ferroptotic-sensitization of cells, they might also play atypical roles in the mechanisms of over-activated autoimmune and innate immune system (34). Eicosanoids are derived from AA by the prostaglandin-endoperoxide synthase (PTGS) (35) or lipoxygenase (LOX) (36) enzymes, forming prostanoids, leukotrienes, respectively. Since these enzymes require lipid hydroperoxide for their activation, the overexpression of GPX4 results in a reduction in the cellular lipid hydroperoxide level, which effectively inactivates PTGS and LOX, eventually inhibiting eicosanoid synthesis (37–39). The antioxidative enzyme GPX4 alleviates inflammatory response through eliminating oxidative materials produced in AA metabolism, and regulates the inflammatory state by modulating LOX and PTGS activity for the duration of ferroptosis (40) (**Figure 4**). The activities of LOX and PTGS are determined by

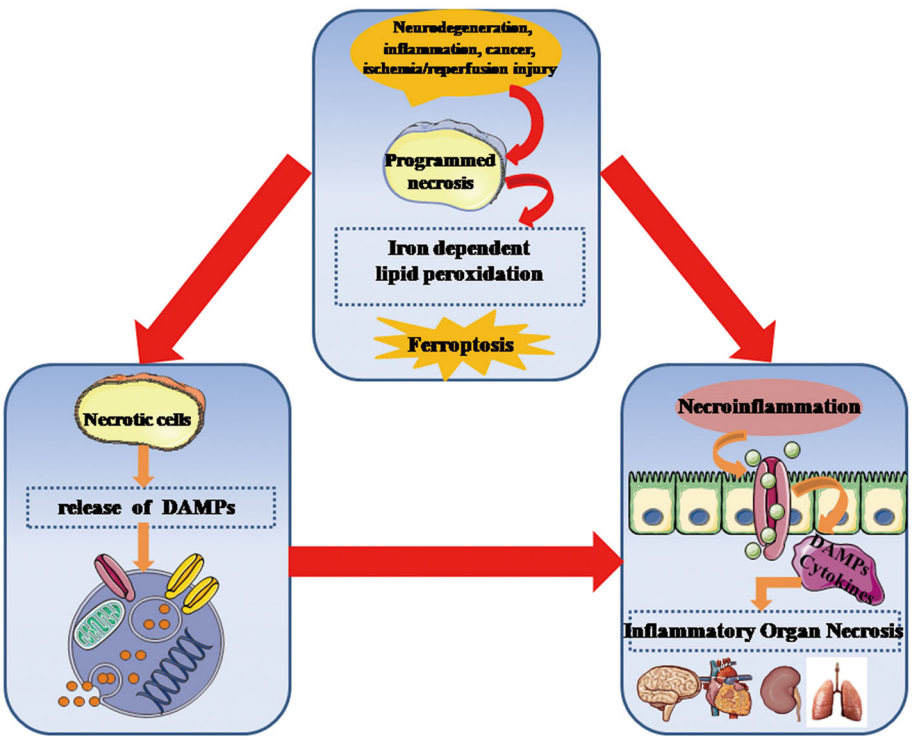

FIGURE 3 | Ferroptosis is critically involved in the development of necroinflammatory diseases. Genetically programmed necrosis is initiated by variously systematic stress including oxidation, immunogenic molecules, metabolic disturbance, and ischemia/reperfusion injury. In the setting of oxidative stress, ferroptosis-induced lipid peroxidation and ROS can promote the programmed necrotic cells to release DAMPs as well as inflammatory cytokines that stimulate innate immune cells to enhance necroinflammatory response. DAMPs, danger-associated molecular patterns; ROS, reactive oxygen species.

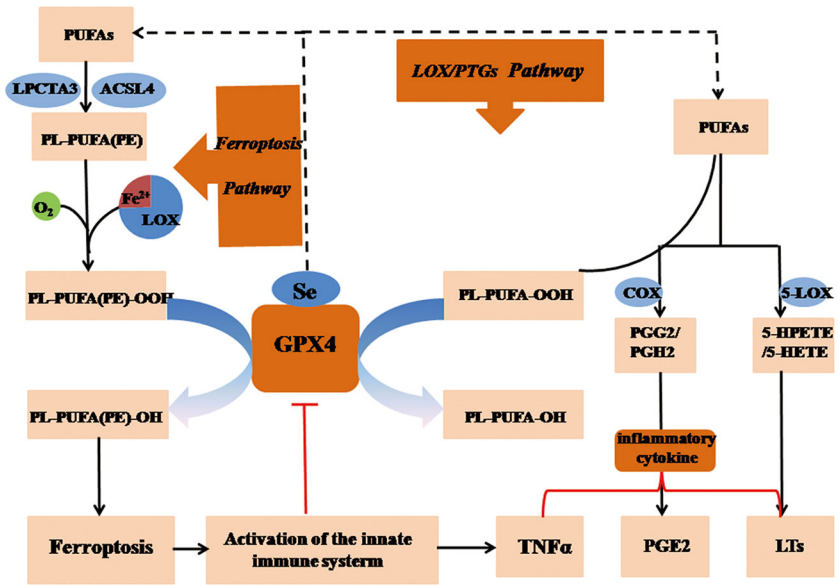

FIGURE 4 | GPX4 regulates necroinflammation *via* arachidonic acid metabolism in ferroptosis. Peroxidized lipids and imbalanced metabolic arachidonic acid (AA) are comprised in ferroptotic process, which exerts an regulatory impact on the process of necroinflammatory response. Upregulation of GPX4 might results in a reduction in the cellular lipid hydroperoxide level, which inactivates PTGS and LOX, eventually inhibiting eicosanoid synthesis. The antioxidative enzyme GPX4 alleviates inflammatory response through eliminating oxidative materials produced in AA metabolism, and regulates the inflammatory state by modulating LOX and PTGS activity in ferroptosis. GSH, reduced glutathione; GSSG, oxidized glutathione; LOX, lipoxygenase; GPX4, glutathione peroxidase 4; H_2O_2, hydrogen peroxide; PGG_2, prostaglandin G_2; PTGS, prostaglandin-endoperoxide synthase; HPETE, hydroperoxyeicosatetraenoic acid; (P)LOOH, (phospho) lipid hydroperoxide; PUFA, polyunsaturated fatty acid; AA, arachidonic acid.

the intracellular level of lipid peroxide for the reason that LOX consists of nonheme bound iron (Fe^{2+}) while PTGS contains hemoglobin (Fe^{3+}) in their corresponsive sites (41). Both LOX and PTGS are capable of promoting the catalysis of molecular oxygen during the oxidation of AA and other polyunsaturated fatty acids (PUFAs) (13) in a process. When suffering from oxidative stress, Fe^{2+} in LOX is oxidized to Fe^{3+}, whereas Fe^{3+} is oxidized to a ferryl-oxo species, which immediately oxidizes the Tyr385, producing a tyrosyl radical in the LOX oxygenase active site (42).

The LOX Mechanism During Ferroptosis

Previous study showed LOX inhibitor induces GSH depletion which is now defined as ferroptosis (43). In addition, Seiler's team reported that 12/15-LOX-defective cell was resistant to GSH depletion since tamoxifen-inducible GPX4 deficiency could be suppressed by 12/15-LOX specific inhibitors, and even result in cell death (44). They deduced that knockout of LOX family members could enhance ferroptosis, *via* cysteine/glutathione depletion and GPX inhibition. Overexpressing GPX4 in a neoplastic rat basophile cell line (RBL-2H3) strongly reduced the levels of leukotriene (LT) C4and LTB4, both products of the 5-LOX enzyme (44). This effect due to the reduction in 5-LOX activity instead of a drop in the rate of hydroperoxyeicosatetraenoic (HPETE) acid to hydroxyeicosatetraenoic (HETE) acid conversion (45).

LOX can regulate ferroptosis by generating LOX-derived proinflammatory metabolic products and stimulating the innate immune system. It seems reasonable that the function of GPX4 is impaired because of GSH depletion upon initial ferroptosis, which is the main cause of higher peroxidation in cells, and the eventual upregulation of LOX activity. On the basis of this mechanism, immune cells release proinflammatory mediators such as IL-6, γ-interferon, and tumor necrosis factor (TNF)-α, which might have an adverse influence on GPX4 activity (46). Ferroptotic cells not only trigger the immune response but can also release of DAMPs by means of self-degradation. Later, innate immune cells initiate LOX or PTGS enzymes, exacerbating inflammation by excreting LTs and hepoxilins. Taken together, activities of LOX and PTGS as well as DAMPs released by immune cells involve in ferroptotic mechanism in regulating necroinflammatory response.

The Role of PTGS in Ferroptosis

Expression of PTGS2 was found to be markedly upregulated in ferroptotic cells stimulated with Ras synthetic lethal 3 (RSL3) (7) or erastin, which confirmed the relationship between ferroptosis and necroinflammation (47). The PTGS2 inhibitor indomethacin, however, was incapable of preventing cells from undergoing ferroptosis, which was discovered in GPX4-defective cells (44, 48). Another study revealed that PTGS mRNA was similarly upregulated and prostaglandin E_2 was simultaneously generated in the skin epithelium of GPX4-knockout mice. Celecoxib, an inhibitor of PTGS, destroyed hair follicle during hair morphogenesis in GPX4-knockout mice (49). The reason behind PTGS2 upregulation in ferroptotic cells is proposed to be

linked to its role as a pharmacodynamic biomarker rather than the inhibitor of ferroptosis. Notably, PTGS inhibitors do not inhibit the occurrence of ferroptosis initiated by inducers or the genetic deletion of GPX4.

GPX4 Regulates Necroinflammation by Preventing TNF-α-Mediated Reaction of the NF-κB Pathway

TNF-α is a proinflammatory cytokine, triggering cells a life-and-death struggle under the inflammatory and oxidative stress, which plays a vital role in the immune response and metabolic homeostasis (50). TNF can be identified by two types of receptors that TNFR1 (51) expresses on immune and endothelial cells and TNFR2 (51) regulates cell survival and death by activating a key transcription factor named nuclear factor (NF)-κB (52, 53). It is accepted that NF-κB protein function on tissue regeneration, cellular metabolism, as well as immune modulation to affect cellular fate and inflammatory progression (54, 55), and high level of ROS can activate NF-κB signaling downstream of TNF-α (56). Importantly, NF-κB signal activation, as a downstream promoter element of TNF-α, is negatively suppressed in intracellular survival signaling (57) (**Figure 5**). Inversely, TNF-α-mediated NF-κB signaling can be markedly activated when ROS is producted in mitochondria (58). Another research coincide with the view that ROS-generation in mitochondria could be inhibited in T cells by vitamin E, a mitochondria-specific antioxidant (59). Park and colleagues discovered that TNF-α, as an upstream molecule, might precisely activate the NF-κB signaling pathway and enhance the expression of NF-κB (60).

The NF-κB signaling pathway plays a vital role in the regulation of immune and inflammatory processes *via* the transcription of target genes (61). More studies indicate that selenoprotein family member of GPX4 can counteract hydroperoxide-modulated events by directly driving hydrogen peroxidation during the activation of NF-κB (62, 63). Indeed, GPX4 expressed on mammals has been shown to prevent the activation of TNF-α-mediated NF-κB signaling (64). Therefore, GPX4 could attenuate the necroinflammatory response and suppress the inflammatory cytokines by reducing the reaction of TNF-α-mediated NF-κB signaling pathway (65).

FERROPTOSIS IN NECROINFLAMMATORY DISEASES

Increasing evidences substantiate the effect of ferroptosis on necroinflammatory diseases, such as neurodegeneration, I/R injury, inflammatory and immune diseases, transplant-related diseases as well as cancer. Theoretically, we speculate ferroptosis to be the potentially immunotherapeutic target in treatment of necroinflammatory diseases. Ferroptosis-induced tissues or organs on occurrence of necroinflammatory diseases are listed in **Table 3**.

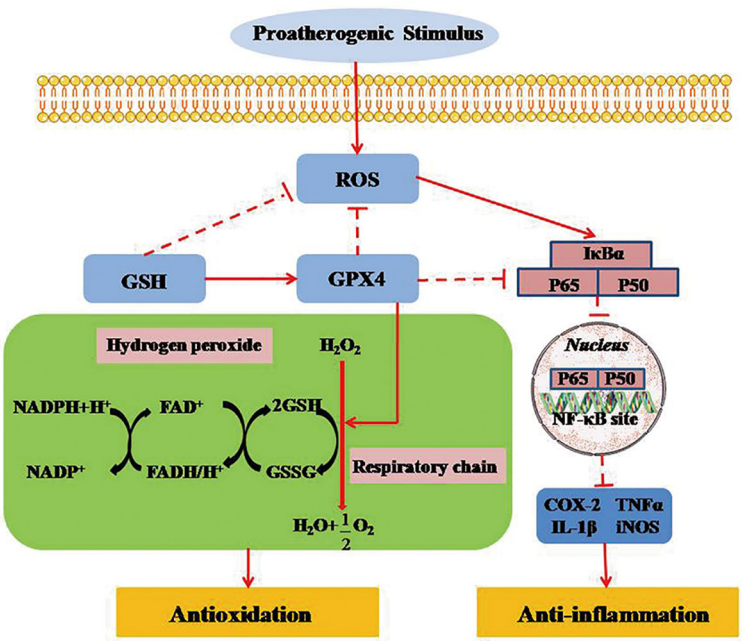

FIGURE 5 | GPX4 regulates necroinflammation by inhibiting TNF-α-mediated NF-κB signaling. TNF-α regulates cell survival and death by activating the key transcription factor of NF-κB. NF-κB signal activation, as a downstream promoter element of TNF-α, is negatively suppressed in intracellular survival signaling. Inversely, TNF-α-mediated NF-κB signaling can be markedly activated when ROS is produced in mitochondria. GPX4 can attenuate the necroinflammatory response and suppress the inflammatory cytokines by down-regulating TNF-α-mediated NF-κB signaling pathway. ROS, reactive oxygen species; GPX4, glutathione peroxidase 4; GSH, glutathione; GSSG, glutathione disulfide; FAD/FADH, flavin adenine dinucletide; NADP/NADPH, nicotinamide adenine dinucleotide phosphate; NF-KB, nuclear factor κB; IκBα, inhibitor of NF-κB α; TNF-α, tumor necrosis factor-α; LT, leukotriene; COX, cyclooxygenase; NOS, nitric oxide synthase.

TABLE 3 | Ferroptotic tissues and organs presenting necroinflammation.

System diseases	Type of diseases	Evidences	References
Nervous system disease	Alzheimer's disease	Deficiency of GPX4 resulted in reduction of neuron cells.	(66–68)
	Huntington's disease	Multiple consumption of cystathioe γ-lyse (an enzyme for cysteine biosynthesis)	(69)
	Parkinson's disease	Ferric sequestering agent showed protective effect.	(70–72)
Cardiovascular system disease	Ischemia/reperfusion (I/R) injury	GPX4 inhibited dysfunction of myocardial I/R area.	(73–77)
	Heart transplantation	Ferroptosis facilitated neutrophil recruitment in transplantation model.	(78)
Respiratory system disease	COPD induced by cigarette smoke (CS)	CS stimulated iron accumulation through NCOA4-mediated ferritinophagy.	(79, 80)
	Bronchial epithelial cell damage induced by Pseudomonas aeruginosa	Pseudomonas aeruginosa enhanced expression of pLoxA and oxidation.	(81, 82)
Digestive system disease	Inflammatory bowel disease (IBD)	Upregulating GPX4 and reversing NF-κB could relieve IBD.	(83–85)
	Nonalcoholic steatohepatitis	Hepatic ferroptosis initiated inflammation in steatohepatitis.	(86, 87)
Urinary system disease	Renal ischemia/reperfusion injury	I/R caused the release of proinflammatory mediators and aggravated cell death.	(88–92)
	Renal allograft rejection	Autoimmune and alloimmune kidney injury presented forms of necroinflammation and glomerulonephritis	(90)
	Acute kidney injury	Fer-1 prevented the necroinflammation of renal cells.	(93–95)
Integumentary system disease	Psoriasis	Downregulation of GPX4 resulted in ferroptosis and necroinflammation in psoriatic skin.	(96–98)
Genital system disease	Endometriosis	Dysregulated iron homeostasis induced endometriotic lesions with localized iron overload and inflammation.	(99–106)
	Male infertility	GPX4 variant led to impaired sperm development and male fertility.	(107–110)

Diseases of the Nervous System

Ferroptosis involves in the pathogenesis of neurodegenerative diseases including Parkinson's, Alzheimer's, Huntington's and neurodegeneration. In mouse models of the hippocampal region and the brain cortex, GPX4 knockout resulted in neuronal number reduction, lipid peroxidation, extracellular regulated protein kinase (ERK) activation, and inflammatory mediator release after administration with tamoxifen, which was enhanced by vitamin E deficiency whereas alleviated by the ferroptosis inhibitor of liproxstatin-1 (Lip-1) (66). The result revealed that cerebral cortex and hippocampus CA1 region seemed sensitive to ferroptosis. Interestingly, conditional GPX4 deficiency caused motor neuron degeneration, while GPX4 knockout resulted in a reduction of neuronal cells and inflammation of hippocampus (67, 68). Another model of Huntington showed cell death was suppressed by inhibiting lipid peroxidation when cells were pretreated with ferroptosis inhibitor of ferrostatin-1 (Fer-1) (111). Besides, cysteine synthetase depletion that caused necrotic cell death were detected in patients with Huntington's disease (69). In Parkinson's disease, it is demonstrated that protein kinase, defined as signal-regulated kinase-activating kinase (MEK), is independently activated by protein kinase Cα in extracellular, ultimately resulting in ferroptosis (70–72).

Diseases of the Cardiovascular System

In I/R injury *in vivo*, overload iron plays a critical role in the ferroptosis of myocardial cells. It seems Fe^{3+} molecule activators to be more liable to induce ferroptosis in cardiomyocytes than RSL3, which is inversely relieved by iron chelator of deferoxamine (73). Meanwhile, glutaminase inhibitor is able to decrease infarct size, and it proves glutaminolysis to be closely associated with the pathophysiology of ferroptosis (74). On the other hand, GPX4 regarded as a mitochondrial targeted mutant causes the cell membrane incomplete and the creatine kinase decreased, which distinctly inhibits mitochondrial lipid peroxidation and the injury of myocardial cell in the I/R area (75). Furthermore, iron chelation could not only decrease the myocardial infarct size by reducing the release of serum myocardial makers, but also enhance the survival of doxorubicin-induced cardiac dysfunction by suppressing lipid peroxidation and mitochondrial iron load (76). In a mouse model of coronary artery ligation-induced I/R injury, pretreatment with Fer-1 reduced the intermediate production of hydroperoxy-arachidonoyl-phosphatidylethanolamine, and subsequently decreased the myocardial cell mortality (77).

Diseases of the Respiratory System

Current studies on ferroptosis in pulmonary necroinflammatory disease mainly focus on chronic obstructive pulmonary disease (COPD) that is triggered by cigarette smoke (CS) and *Pseudomonas aeruginosa*-induced damage in bronchial epithelial cells. It was reported that CS not only induced necroptosis but also promoted the release of DAMPs in epithelial cells, thereby contributing to airway necroinflammation (79, 80). In the model of COPD established by exposure to CS, down-expression of GPX4 might ultimately induce iron accumulation and lipid peroxidation, which confirmed the key effect of ferroptosis on CS-induced COPD and further revealed the mechanism of iron accumulation inducing ferritinophagy mediated by NCOA4 in epithelial cells (81). As is revealed in human bronchial epithelial (HBE) cells invaded by pseudomonas aeruginosa, the feature of ferroptosis presented that polyunsaturated fatty acids was oxidized by pLoxA into 15-HOO-AA-PE (82).

Diseases of the Digestive System

Growing studies have indicated that ferroptotic mechanisms regulate necroinflammatory diseases of the digestive system

including Crohn's disease (CD), inflammatory bowel disease (IBD), ulcerative colitis (UC) and nonalcoholic steatohepatitis. IBD is an intestinal dysfunction induced by chronic inflammation, featured in the reduction of crypt, villus atrophy as well as inflammation of the intestinal mucosa and submucosal tissues induced by neutrophil accumulation (112–114). It generally occurs in the settings of gene mutation, oxidative stress, traumatic stress, relocation stress syndrome or environmental factors. Oxidative stress is considered as the main pathological process associated with ferroptosis, and is deemed to be the major factor in the prognosis of necroinflammation in IBD (115, 116). Emerging researches emphasis on the relationship between iron metabolism, intestinal microecological health, and intestinal inflammatory diseases. It has been proven that excessive iron induces IBD, triggering oxidative stress and even cell death (117). On account of the damage of intestinal integrity induced by excessive iron, oxidative reactions may destruct the physical barrier composed of intestinal mucosal epithelial cells leading to intestinal dysfunction (118). Accordingly, a novel inhibitor of inflammation and oxidation called pyrrolidine dithiocarbamate is demonstrated to be effective on improving IBD symptoms by upregulating GPX4 (83–85), which inversely suppressed NF-κB signaling (119). With respect to CD, GPX4 on epithelium is found to be down-expressed, which leads to intestinal function and even ferroptosis (120, 121). In order to further explore the function of GPX4 in intestinal epithelial cells, Sander et al. structured *Gpx4*$^{-/-}$ intestinal epithelial MODE-K cells with the specific GPX4^{-} small-interfering RNA (siGPX4) to silence GPX4 expression. It was resulted that intestinal epithelial cells with inactive GPX4 were more sensitive to ferroptosis, and multiple of necroinflammatory cytokines including IL-6, IL-12, IFN-γ and TNF-α were detected in supernatant (122, 123).

Recent studies indicate that ferroptosis-induced necroinflammation is relevant to nonalcoholic steatohepatitis by triggering cytokine release (86, 87). A research on nonalcoholic steatohepatitis in a murine model demonstrated that ferroptosis inhibitor effectively suppressed hepatic cell death through the inhibition of immune cell function and migration. Therefore, ferroptosis in hepatic cells might serve as a therapeutic target for the treatment of necroinflammation in nonalcoholic steatohepatitis.

Urinary System Diseases

Necroinflammation in renal I/R injury dependent on a transient insufficient blood supply finally results in critical damage in renal cells (124). Similarly, renal-necrosis is generally associated with autoimmune kidney injury, which is caused by various types of glomerulonephritis (88), interstitial nephritis (89), and allograft rejections (90). When renal tissue or cells undergo ischemic stress, endogenous DAMPs together with intracellular proinflammatory mediators, such as HSP, HMGB1, metabolites, and gene fragments, are largely release, stimulating immune cells to result in inflammatory cascade (91, 92). Immune cells including T cells and macrophages are rapidly activated to stimulate neutrophil aggregation, and release cytokines of IL-6, IL-12, IL-1α, and TNF-α to promote the migration of antigen presenting cells (e.g.dendritic cells) (125, 126). A continuous auto-amplification is formed when high level of mediators irritate cell death program. It follows that necrocytosis induces immunosuppression, and organ failure occurs (127).

Necroinflammation is regulated by ferroptosis in acute kidney injury. Preliminary studies indicated that Fer-1 could not only attenuate I/R injury-induced tubular injury but also decreased serum creatinine and urea nitrogen level (93). Pretreatment with Fer-1 was able to protect renal proximal tubular cells from necrosis in the renal ischemic tissue area by decreasing ROS levels (94). SLC7A11 is shown to be negatively regulated by the mutant cancer suppressor p53 (3KR) gene that down-regulates Xc- system to promote ferroptosis (95). Silencing p53 mutation results in SLC7A11 overactivation and protective effect on renal cells from ferroptotic injury. In accordance with the above studies, tubular cell with p53 deficiency is resistant to ferroptosis induced by acute kidney injury (128, 129). It is the reason that tubular cell with GPX4 deficiency is prone to suffering from ferroptotic necrosis and high mortality rates in mice (10).

Integumentary System Diseases

GPX4 knockout has been proved to induce ferroptosis-related necroinflammation in skin tissue (130–132). For the reason that ceramide analogs are testified to be an effective therapeutic in animal experiments, it is speculated that upregulating GPX4 might significantly relieve skin from ferroptosis-induced necroinflammatory injury (96, 97). In order to further investigate the interactive mechanism between GPX4 inactivation, ferroptosis and necroinflammation, Arbiser and colleagues collected data from healthy skin samples and psoriatic skin samples to analyze genetic sequences. They found necroinflammation in psoriatic skin samples, and treatment with ferroptosis inducer that inhibited Xc- system activity could decrease the level of Nrf2 (98). These findings provide a novel viewpoint on intrinsic connection between ferroptosis and necroinflammation in skin disease.

Diseases of the Reproductive System

Ferroptosis is reported to involve in reproductive necroinflammatory processes, such as endometriosis and male infertility (e.g., oligospermia). Selenium that is applied to the GPX4 synthesis plays an essential role in male fertility and sperm development (99, 100). GPX4 maintains sperm stability by acting as a major structural protein of the mitochondria capsule in the central part of mature spermatozoa. A recent clinical study demonstrated that approximately 30% oligoasthenozoospermia in infertile men showed a down-regulation of GPX4 when compared to healthy men with normal testes and spermatozoa (101). Another research revealed that sperm vitality obviously declined when GPX4 inactivated or dysfunctioned, which confirmed the key role in spermatogenesis and the process of embryo development in mice (102). Moreover, clinical investigations demonstrated Nrf2 was involved in the regulation of ferroptosis in oligospermia (103, 104). In comparison to the control group, Nrf2 suppressing

ferroptosis was notably down-regulated in mice with oligospermia (105, 106).

Studies on female reproductive system and endometriosis showed that overload iron was the major cause for endometriotic lesion (107–109). Ferroptosis inhibitor of deferoxamine cannot reverse pathological tissue damage, but improve iron metabolism, as well as reduce the proliferation of macrophages, which finally alleviates inflammatory response (110). Inversely, endometriotic lesion results in iron and ROS accumulation, which obstructs the normal growth of ectopic endometrial cells (133–135).

Transplantation-Related Diseases

Transplantation is currently becoming a life-saving straw for critical patients with organ function failure. However, graft rejection remains the mainly negative impact on the long-term prognosis due to an interaction between innate and adaptive immune responses. Increasing evidences document that necroinflammation is regarded as the essential pathological process in graft injury, and ferroptosis is pyramidally being proved to relate to transplantation-induced necroinflammatory response.

Previous studies reported that ferroptosis induced neutrophil migration and adhesion to the vascular endothelial cells by TLR4/Trif/type I IFN-dependent signaling pathway, in turn leading to heart transplantation-related injury (78). Accordingly, pretreatment of myocardial cells with Fer-1 could effectively inhibit neutrophil recruiting in the early stage of heart transplantation (78). These studies indicate that ferroptosis amplifies a cycle between sterile inflammation and immunological rejection, and aggravates graft injury. In the liver transplantation, inevitably hepatic I/R injury during the process of organ procurement may cause primary nonfiction and urgent rejective injury in the graft liver (136). Lipid peroxidation, upregulation of a ferroptotic biomarker Ptgs2 (136) as well as liver injury are shown in the mutine model of liver transplantation. High level of serum ferritin, a sign of iron load in ferroptosis, is also detected, which can be inhibited by Fer-1 (137). Moreover, a recent study on islet transplantation was consistent with the abovementioned viewpoint that ferroptosis involved in oxidative injury and necroinflammation after islet transplantation. The viability of transplanted islet was evaluated by lactate dehydrogenase (LDH), and outcomes revealed that pretreatment islet with ferroptosis inhibitors Fer-1 or desferrioxamine (DFO) improved graft injury in an immunodeficient mouse transplant model (138).

Cancer

Ferroptosis was first discovered in tumor cells when explored the death manner induced by lethal RAS-mutant gene, and it could be induced in most types of tumor by FINs erastin and RSL (5, 7). Erastin of 117 cancer cell lines from various tissues were detected to study RAS mutant mediated ferroptosis, and it was noted that kidney cancer cells showed the most sensitive to erastin (5). In the subsequent studies, they demonstrated that erastin, as ferroptosis inhibitor, contributed to improving pesticide effect of oncology chemotherapy, and was applied to test the sensitivity of cancer to ferroptosis (139).

On account of ROS being essential for existence and proliferation, cancer cells are invariably dependent on intracellular GSH. When authigenic cysteine is consumed to produce ROS, resulting in deficient for GSH synthesis, more extracellular cysteine need to be transferred by system Xc-. Therefore, disposition cancer cells with a recombinant cyste inase enzyme leading to exhaustion of cysteine, might selectively induce cell death in cancer cells (140). Of note, it is hypothesized that protein p53 possibly relates to system Xc- activity due to the cause that inase inhibitor sorafenib acting on system Xc- and regulated by p53 can induce ferroptosis (23).

Many studies have suggested that cancer cells with manifestation of treatment-resistant high-mesenchymal cell state greatly depend on lipid metabolic enzymes which are relevant to the ferroptotic signaling pathway. Thus, these cancer cells display more sensitive and vulnerable to ferroptosis in the setting of GPX4 inactivation. Similarly, a recent study supported this standpoint that the viability of clear-cell renal cell carcinomas (ccRCC) significantly decreased, which showed a hypersensitivity to GPX4 silencing and vulnerability to ferroptosis (141). Importantly, reduced fatty acid peroxidation owning to the inhibition of β-oxidation can effectively interdict ccRCC growth by suppressing ferroptosis. These results indicate that targeting ferroptosis contributes to exploring a novel therapy for overcoming drug resistance in cancer.

CONCLUSIONS

Ferroptosis is a novel-proposed regulated cell death process that relies on overload iron and glutathione metabolism, and plays a regulated role in necroinflammatory diseases. It is confirmed that ferroptosis involves in the pathologic process of various necroinflammatory diseases and regulates necrotic cell death. Recently, mechanism of ferroptosis in necroinflammatory diseases is being continually explored in infratest and many progresses have been made. However, certain limitations remain to be overcome. Firstly, comparing to our in-depth understanding of mechanisms involved in classical cell death programs, we know little about the mechanism of ferroptosis. Despite the roles of lipid peroxidation and inflammation are relatively well documented, more precise signaling pathways that may regulate the necroinflammatory response in relation to ferroptosis seem not clear. Second, potential ability of ferroptosis to activate the innate immune system to release inflammatory mediators and generate an immune response remains to be further explored. Third, most of the ferroptosis-related researches to date have depended on the established animal models, which have their own restrictions. Thus, conducting these hypotheses in clinical trials will be more reasonable. Furthermore, perspective researches should emphasize on the regulated mechanism of ferroptosis mediated by upstream and downstream signaling molecules as well as the intermolecular interactions. Hence, targeting ferroptosis might provide a potential therapy for necroinflammatory diseases in the future.

AUTHOR CONTRIBUTIONS

J-yL conducted the literature review and drafted the manuscript, which Y-mY and Y-pT conceptualized, supervised and revised. All authors contributed to the article and approved the submitted version.

FUNDING

This work was supported by grants from the National Natural Science Foundation of China (81730057, 81873946) and the National Key Research and Development Program of China (2017YFC1103302).

REFERENCES

1. Wallach D, Kang TB, Dillon CP, Green DR. Programmed Necrosis in Inflammation: Toward Identification of the Effector Molecules. *Science* (2016) 352:aaf2154. doi: 10.1126/science.aaf2154
2. Conrad M, Angeli JPF, Vandenabeele P, Stockwell BR. Regulated Necrosis: Disease Relevance and Therapeutic Opportunities. *Nat Rev Drug Discov* (2016) 15:348–66. doi: 10.1038/nrd.2015.6
3. Huang Z, Wu SQ, Liang YJ, Zhou XJ, Chen WZ, Li LS, et al. RIP1/RIP3 Binding to HSV-1 ICP6 Initiates Necroptosis to Restrict Virus Propagation in Mice. *Cell Host Microbe* (2015) 17:229–42. doi: 10.1016/j.chom.2015.01.002
4. Yang WS, Kim KJ, Gaschler MM, Patel M, Shchepinov MS, Stockwell BR. Peroxidation of Polyunsaturated Fatty Acids by Lipoxygenases Drives Ferroptosis. *Proc Natl Acad Sci USA* (2016) 113:E4966–75. doi: 10.1073/pnas.1603244113
5. Yang WS, Ramaratnam RS, Welsch ME, Shimada K, Skouta R, Viswanathan VS, et al. Regulation of Ferroptotic Cancer Cell Death by GPX4. *Cell* (2014) 156:317–31. doi: 10.1016/j.cell.2013.12.010
6. Kim EH, Wong SW, Martinez J. Programmed Necrosis and Disease: We Interrupt Your Regular Programming to Bring You Necroinflammation. *Cell Death Differ* (2019) 26:25–40. doi: 10.1038/s41418-018-0179-3
7. Dixon SJ, Lember KM, Lamprecht MR, Skouta R, Zaitsev EM, Gleason CE, et al. Ferroptosis: An Iron-Dependent Form of Nonapoptotic Cell Death. *Cell* (2012) 149:1067–72. doi: 10.1016/j.cell.2012.03.042
8. Xie Y, Hou W, Song X, Yu Y, Huang J, Kang R, et al. Ferroptosis: Process and Function. *Cell Death Differ* (2016) 23:369–79. doi: 10.1038/cdd.2015.158
9. Yang WS, Stockwell BR. Ferroptosis: Death by Lipid Peroxidation. *Trends Cell Biol* (2016) 26:165–76. doi: 10.1016/j.tcb.2015.10.014
10. Friedmann Angeli JP, Schneider M, Proneth B, Tyurina Y, Tyurin V, Hammond VJ, et al. Inactivation of the Ferroptosis Regulator Gpx4 Triggers Acute Renal Failure in Mice. *Nat Cell Biol* (2014) 16:1180–91. doi: 10.1038/ncb3064
11. Sato H, Tamba M, Ishii T, Bannai S. Cloning and Expression of a Plasma Membrane Cystine/Glutamate Exchange Transporter Composed of Two Distinct Proteins. *J Biol Chem* (1999) 274:11455–8. doi: 10.1074/jbc.274.17.11455
12. Hayano M, Yang WS, Corn CK, Pagano NC, Stockwell BR. Loss of cysteinyl-tRNA Synthetase (CARS) Induces the Transsulfuration Pathway and Inhibits Ferroptosis Induced by Cystine Deprivation. *Cell Death Differ* (2016) 23:270–8. doi: 10.1038/cdd.2015.93
13. Kagan VE, Mao G, Qu F, Angeli JP, Doll S, Croix CS, et al. Oxidized Arachidonic and Adrenic PEs Navigate Cells to Ferroptosis. *Nat Chem Biol* (2017) 13:81–90. doi: 10.1038/nchembio.2238
14. Anthonymuthu TS, Kenny EM, Shrivastava I, Tyurina YY, Hier ZE, Ting HC, et al. Empowerment of 15-Lipoxygenase Catalytic Competence in Selective Oxidation of Membrane ETE-PE to Ferroptotic Death Signals, HpETE-PE. *J Am Chem Soc* (2018) 140:17835–9. doi: 10.1021/jacs.8b09913
15. Li Y, Feng D, Wang Z, Zhao Y, Sun R, Tian D, et al. Ischemia Induced ACSL4 Activation Contributes to Ferroptosis-Mediated Tissue Injury in Intestinal Ischemia/Reperfusion. *Cell Death Differ* (2019) 26:2284–99. doi: 10.1038/s41418-019-0299-4
16. Bersuker K, Hendricks JM, Li ZP, Magtanong L, Ford B, Tang PH, et al. The CoQ Oxidoreductase FSP1 Acts Parallel to GPX4 to Inhibit Ferroptosis. *Nature* (2019) 575:688–92. doi: 10.1038/s41586-019-1705-2
17. Marshall KR, Gong M, Wodke L, Lamb JH, Jones DJL, Farmer PB, et al. The Human Apoptosis-Inducing Protein AMID Is an Oxidoreductase With a Modified Flavin Cofactor and DNA Binding Activity. *J Biol Chem* (2005) 280:30735–40. doi: 10.1074/jbc.M414018200
18. Doll S, Freitas FP, Shah R, Aldrovandi M, Costa da Silva M, Ingold I, et al. FSP1 Is a Glutathione-Independent Ferroptosis Suppressor. *Nature* (2019) 575:693–8. doi: 10.1038/s41586-019-1707-0
19. Mancias JD, Wang X, Gygi SP, Harper JW, Kimmelman AC. Quantitative Proteomics Identifies NCOA4 as the Cargo Receptor Mediating Ferritinophagy. *Nature* (2014) 509:105–9. doi: 10.1038/nature13148
20. Gao M, Monian P, Pan Q, Zhang W, Xiang J, Jiang X. Ferroptosis Is an Autophagic Cell Death Process. *Cell Res* (2016) 26:1021–32. doi: 10.1038/cr.2016.95
21. Reisman SA, Yeager RL, Yamamoto M, Klaassen CD. Increased Nrf2 Activation in Livers From Keap1-Knockdown Mice Increases Expression of Cytoprotective Genes That Detoxify Electrophiles More Than Those That Detoxify Reactive Oxygen Species. *Toxicol Sci* (2009) 108:35–47. doi: 10.1093/toxsci/kfn267
22. Sun X, Ou Z, Chen R, Niu X, Chen D, Kang R, et al. Activation of the P62-Keap1-NRF2 Pathway Protects Against Ferroptosis in Hepatocellular Carcinoma Cells. *Hepatology* (2016) 63:173–84. doi: 10.1002/hep.28251
23. Jiang L, Kon N, Li T, Wang SJ, Su T, Hibshoosh H, et al. Ferroptosis as a P53-Mediated Activity During Tumour Suppression. *Nature* (2015b) 520:57–62. doi: 10.1038/nature14344
24. Wallach D, Kang TB, Kovalenko A. Concepts of Tissue Injury and Cell Death in Inflammation: A Historical Perspective. *Nat Rev Immunol* (2014) 14:51–9. doi: 10.1038/nri3561
25. Akira S, Uematsu S, Takeuchi O. Pathogen Recognition and Innate Immunity. *Cell* (2006) 124:783–801. doi: 10.1016/j.cell.2006.02.015
26. Medzhitov R, Hurlburt PP, Janeway CA. A Human Homologue of the Drosophila Toll Protein Signals Activation of Adaptive Immunity. *Nature* (1997) 388:394–7. doi: 10.1038/41131
27. Zindel J, Kubes P. DAMPs, PAMPs, and LAMPs in Immunity and Sterile Inflammation. *Annu Rev Pathol* (2020) 15:493–518. doi: 10.1146/annurev-pathmechdis-012419-032847
28. Matzinger P. Tolerance, Danger, and the Extended Family. *Annu Rev Immunol* (1994) 12:991–1045. doi: 10.1038/41131
29. Chovatiya R, Medzhitov R. Stress, Inflammation, and Defense of Homeostasis. *Mol Cell* (2014) 54:281–8. doi: 10.1016/j.molcel.2014.03.030
30. Berghe TV, Linkermann A, Sandrine JL, Walczak H, Vandenabeele P. Regulated Necrosis: The Expanding Network of non-Apoptotic Cell Death Pathways. *Nat Rev Mol Cell Biol* (2014) 15:135–47. doi: 10.1038/nrm3737
31. Linkermann A, Stockwell BR, Krautwald S, Anders HJ. Regulated Cell Death and Inflammation: An Auto-Amplification Loop Causes Organ Failure. *Nat Rev Immunol* (2014) 14:759–67. doi: 10.1038/nri2545
32. Green DR, Ferguson T, Zitvogel L, Zitvogel L, Kroemer G. Immunogenic and Tolerogenic Cell Death. *Nat Rev Immunol* (2009) 9:353–63. doi: 10.1038/nri2545
33. Wen QR, Liu J, Kang R, Zhou BR, Tang DL. The Release and Activity of HMGB1 in Ferroptosis. *Biochem Biophys Res Commun* (2019) 510:278–83. doi: 10.1016/j.bbrc.2019.01.090
34. Wenzel SE, Tyurina YY, Zhao JM, St Croix CM, Dar HH, Mao G, et al. PEBP1 Wardens Ferroptosis by Enabling Lipoxygenase Generation of Lipid Death Signals. *Cell* (2017) 171:628–41. doi: 10.1016/j.cell.2017.09.044
35. Hemler ME, Cook HW, Lands WE. Prostaglandin Biosynthesis can be Triggered by Lipid Peroxides. *Arch Biochem Biophys* (1979) 193:340–5. doi: 10.1016/0003-9861(79)90038-9
36. Donnell VBO, Coles B, Lewis MJ, Crews BC, Matnett LJ, Freeman BA. Catalytic Consumption of Nitric Oxide by Prostaglandin H Synthase-1 Regulates Platelet Function. *J Biol Chem* (2000) 275:38239–44. doi: 10.1074/jbc.M001802200
37. Schnurr K, Belkner J, Ursini F, Schewe T, Kühn H. The Selenoenzyme Phospholipid Hydroperoxide Glutathione Peroxidase Controls the Activity

of the 15-Lipoxygenase With Complex Substrates and Preserves the Specificity of the Oxygenation Products. *J Biol Chem* (1996) 271:4653–8. doi: 10.1074/jbc.M001802200
38. Schnurr K, Borchert A, Kuhn H. Inverse Regulation of Lipid Peroxidizing and Hydroperoxyl Lipid-Reducing Enzymes by Interleukins 4 and 13. *FASEB J* (1999) 13:143–54. doi: 10.1096/fasebj.13.1.143
39. Huang HS, Chen CJ, Suzuki H, Yamamoto S, Chang WC. Inhibitory Effect of Phospholipid Hydroperoxide Glutathione Peroxidase on the Activity of Lipoxygenases and Cyclooxygenases. *Prostaglandins Other Lipid Mediat* (1999) 58:65–75. doi: 10.1016/s0090-6980(99)00017-9
40. Marinho HS, Antunes F, Pinto RE. Role of Glutathione Peroxidase and Phospholipid Hydroperoxide Glutathione Peroxidase in the Reduction of Lysophospholipid Hydroperoxides. *Free Radic Biol Med* (1997) 22:871–83. doi: 10.1016/s0891-5849(96)00468-6
41. Zafiriou MP, Deva R, Ciccoli R, Kapadai AS, Nigam S. Biological Role of Hepoxilins: Upregulation of Phospholipid Hydroperoxide Glutathione Peroxidase as a Cellular Response to Oxidative Stress? *Prostaglandins Leukot Essent Fatty Acids* (2007) 77:209–15. doi: 10.1016/j.plefa.2007.08.007
42. Chen CJ, Huang HS, Lin SB, Chang WC. Regulation of Cyclooxygenase and 12-Lipoxygenase Catalysis by Phospholipid Hydroperoxide Glutathione Peroxidase in A431 Cells. *Prostaglandins Leukot Essent Fatty Acids* (2000) 62:261–8. doi: 10.1054/plef.2000.0153
43. Li Y, Maher P, Schubert D. A Role for 12-Lipoxygenase in Nerve Cell Death Caused by Glutathione Depletion. *Neuron* (1997) 19:453–63. doi: 10.1016/s0896-6273(00)80953-8
44. Seiler A, Schneider M, Förster H, Roth S, Wirth EK, Culmsee C, et al. Glutathione Peroxidase 4 Senses and Translates Oxidative Stress Into 12/15-Lipoxygenase Dependent- and AIF-Mediated Cell Death. *Cell Metab* (2008) 8:237–48. doi: 10.1016/j.cmet.2008.07.005
45. Imai H, Narashima K, Arai M, Sakamoto H, Chiba N, Nakagawa Y. Suppression of Leukotriene Formation in RBL-2h3 Cells That Overexpressed Phospholipid Hydroperoxide Glutathione Peroxidase. *J Biol Chem* (1998) 273:1990–7. doi: 10.1074/jbc.273.4.1990
46. Latchoumycandane C, Marathe GK, Zhang R, McIntyre TM. Oxidatively Truncated Phospholipids Are Required Agents of TNF Alpha Induced Apoptosis. *J Biol Chem* (2012) 287:17693–705. doi: 10.1074/jbc.M111.300012
47. Stoyanovsky DA, Tyurina YY, Shrivastava I, Bahar I, Tyurin VA, Protchenko O, et al. Iron Catalysis of Lipid Peroxidation in Ferroptosis: Regulated Enzymatic or Random Free Radical Reaction? *Free Radic Biol Med* (2019) 133:153–61. doi: 10.1016/j.freeradbiomed
48. Schneider M, Wortmann M, Mandal KP, Arpornchayanon W, Jannasch K, Alves F, et al. Absence of Glutathione Peroxidase 4 Affects Tumor Angiogenesis Through Increased 12/15-Lipoxygenase Activity. *Neoplasia* (2010) 12:254–63. doi: 10.1593/neo.91782
49. Sengupta A, Lichti UF, Carlson BA, Christophe C, Ryscavage A, Mikulec C, et al. Targeted Disruption of Glutathione Peroxidase 4 in Mouse Skin Epithelial Cells Impairs Postnatal Hair Follicle Morphogenesis That Is Partially Rescued Through Inhibition of COX-2. *J Invest Dermatol* (2013) 133:1731–41. doi: 10.1038/jid.2013.52
50. Brenner D, Blaser H, Mak TW. Regulation of Tumour Necrosis Factor Signalling: Live or Let Die. *Nat Rev Immunol* (2015) 15:362–74. doi: 10.1038/nri3834
51. Grell M, Douni E, Wajant H, Löhden M, Clauss M, Maxeineret B, et al. The Transmembrane Form of Tumor Necrosis Factor Is the Prime Activating Ligand of the 80 kDa Tumor Necrosis Factor Receptor. *Cell* (1995) 83:793–802. doi: 10.1016/0092-8674(95)90192-2
52. Faustman D, Davis M. TNF Receptor 2 Pathway: Drug Target for Autoimmune Diseases. *Nat Rev Drug Discov* (2010) 9:482–93. doi: 10.1038/nrd3030
53. Fischer R, Maier O. Interrelation of Oxidative Stress and Inflammation in Neurodegenerative Disease: Role of TNF. *Oxid Med Cell Longev* (2015) 2015:610813. doi: 10.1155/2015/610813
54. Hayden MS, Ghosh S. Shared Principles in NF-kappaB Signaling. *Cell* (2008) 132:344–62. doi: 10.1016/j.cell.2008.01.020
55. Vallabhapurapu S, Karin M. Regulation and Function of NF-kappaB Transcription Factors in the Immune System. *Annu Rev Immunol* (2009) 27:693–733. doi: 10.1146/annurev.immunol.021908.132641
56. Nakajima S, Kitamura M. Bidirectional Regulation of NF-kappaB by Reactive Oxygen Species: A Role of Unfolded Protein Response. *Free Radic Biol Med* (2013) 65:162–74. doi: 10.1016/j.freeradbiomed.2013.06.020
57. Shen HM, Pervaiz S. TNF Receptor Superfamily Induced Cell Death: Redox-Dependent Execution. *FASEB J* (2006) 20:1589–98. doi: 10.1096/fj.05-5603rev
58. Morgan MJ, Liu ZG. Crosstalk of Reactive Oxygen Species and NF-kappaB Signaling. *Cell Res* (2011) 21:103–15. doi: 10.1038/cr.2010.178
59. Hughes G, Murphy MP, Ledgerwood EC. Mitochondrial Reactive Oxygen Species Regulate the Temporal Activation of Nuclear Factor kappaB to Modulate Tumour Necrosis Factor-Induced Apoptosis: Evidence From Mitochondria-Targeted Antioxidants. *Biochem J* (2005) 389:83–9. doi: 10.1042/BJ20050078
60. Park MH, Song HS, Kim KH, Son DJ, Lee SH, Yoon DY, et al. Cobrotoxin Inhibits NF-KappaB Activation and Target Gene Expression Through Reaction With NF-KappaB Signal Molecules. *Biochemistry* (2005) 44:8326. doi: 10.1021/bi050156h
61. Surh YJ, Chun KS, Cha HH, Han SS, Keum YS, Parket KK, et al. Molecular Mechanisms Underlying Chemopreventive Activities of Anti-Inflammatory Phytochemicals: Down-Regulation of COX-2 and iNOS Through Suppression of NF-κB Activation. *Mutat Res* (2001) 480:243–68. doi: 10.1016/s0027-5107(01)00183-x
62. Fialkow L, Wang YC, Downey GP. Reactive Oxygen and Nitrogen Species as Signaling Molecules Regulating Neutrophil Function. *Free Radic Biol Med* (2007) 42:153–64. doi: 10.1016/j.freeradbiomed.2006.09.030
63. Blaser H, Dostert C, Mak TW, Brenner D. TNF and ROS Crosstalk in Inflammation. *Trends Cell Biol* (2016) 26:249–61. doi: 10.1016/j.tcb.2015.12.002
64. Heirman I, Ginneverge D, Brigelius-Flohé R, Hendrickx N, Agostinis P, Brouckaert P, et al. Blocking Tumor Cell Eicosanoid Synthesis by GPx4 Impedes Tumor Growth and Malignancy. *Free Radic Biol Med* (2006) 40:285–94. doi: 10.1016/j.freeradbiomed.2005.08.033
65. Li C, Deng XB, Xie XW, Liu Y, Friedmann Angeli JP, Laet L. Activation of Glutathione Peroxidase 4 as a Novel Anti-Inflammatory Strategy. *Front Pharmacol* (2018) 9:1120. doi: 10.3389/fphar.2018.01120.eCollection 2018
66. Hambright WS, Fonseca RS, Chen L, Na R, Ran Q. Ablation of Ferroptosis Regulator Glutathione Peroxidase 4 in Forebrain Neurons Promotes Cognitive Impairment and Neurodegeneration. *Redox Biol* (2017) 12:8–17. doi: 10.1016/j.redox.2017.01.021
67. Chen L, Hambright WS, Na R, Ran Q. Ablation of the Ferroptosis Inhibitor Glutathione Peroxidase 4 in Neurons Results in Rapid Motor Neuron Degeneration and Paralysis. *J Biol Chem* (2015) 290:28097–106. doi: 10.1074/jbc.M115.680090
68. Yoo SE, Chen L, Na R, Liu Y, Rios C, Remmen HV, et al. Gpx4 Ablation in Adult Mice Results in a Lethal Phenotype Accompanied by Neuronal Loss in Brain. *Free Radic Biol Med* (2012) 52:1820–7. doi: 10.1016/j.freeradbiomed.2012.02.043
69. Paul BD, Sbodio JI, Xu R, Vandiver MS, Cha JY, Snowman AM, et al. Cystathionine γ-Lyase Deficiency Mediates Neurodegeneration in Huntington's Disease. *Nature* (2014) 509:96–100. doi: 10.1038/nature13136
70. Hare DJ, Double KL. Iron and Dopamine: A Toxic Couple. *Brain* (2016) 139:1026–35. doi: 10.1093/brain/aww022
71. Liu Z, Shen HC, Lian TH, Mao L, Tang SX, Sun L, et al. Iron Deposition in Substantia Nigra: Abnormal Iron Metabolism, Neuroinflammatory Mechanism and Clinical Relevance. *Sci Rep* (2017) 7:14973. doi: 10.1038/s41598-017-14721-1
72. Van BD, Gouel F, Jonneaux A, Timmerman K, Gelé P, Pétraultet M, et al. Ferroptosis, a Newly Characterized Form of Cell Death in Parkinson's Disease That Is Regulated by PKC. *Neurobiol Dis* (2016) 94:169–78. doi: 10.1016/j.nbd.2016.05.011
73. Baba Y, Higa JK, Shimada BK, Horiuchi KM, Suhara T, Kobayashi M, et al. Protective Effects of the Mechanistic Target of Rapamycin Against Excess Iron and Ferroptosis in Cardiomyocytes. *Am J Physiol Heart Circ Physiol* (2018) 314:H659–68. doi: 10.1152/ajpheart.00452.2017
74. Gao M, Monian P, Quadri N, Ramasamy R, Jiang XJ. Glutaminolysis and Transferrin Regulate Ferroptosis. *Mol Cell* (2015) 59:298–308. doi: 10.1016/j.molcel.2015.06.011

75. Dabkowski ER, Williamson CL, Hollander JM. Mitochondria-Specific Transgenic Overexpression of Phospholipid Hydroperoxide Glutathione Peroxidase (GPx4) Attenuates Ischemia/Reperfusion-Associated Cardiac Dysfunction. *Free Radic Biol Med* (2008) 45:855–65. doi: 10.1016/j.freeradbiomed.2008.06.021
76. Fang X, Wang H, Han D, Xie EJ, Wei JY, Gu SS, et al. Ferroptosis as a Target for Protection Against Cardiomyopathy. *Proc Natl Acad Sci USA* (2019) 116:2672–80. doi: 10.1016/j.freeradbiomed.2008.06.021
77. Li W, Feng GS, Gauthier JM, Lokshina I, Higashikubo R, Evans S, et al. Ferroptotic Cell Death and TLR4/Trifsignaling Initiate Neutrophil Recruitment After Heart Transplantation. *J Clin Invest* (2019) 129:2293–304. doi: 10.1172/JCI126428
78. Frye CC, Bery AI, Kreisel D, Kulkarni HS. Sterile Inflammation in Thoracic Transplantation. *Cell Mol Life Sci* (2021) 78:581–601. doi: 10.1007/s00018-020-03615-7
79. Comer DM, Kidney JC, Ennis M, Elborn JS. Airway Epithelial Cell Apoptosis and Inflammation in COPD, Smokers and Nonsmokers. *Eur Respir J* (2013) 41:1058–67. doi: 10.1183/09031936.00063112
80. Pouwels SD, Zijlstra GJ, Toorn MVD, Hesse L, Gras R, Ten Hacken NH, et al. Cigarette Smoke-Induced Necroptosis and DAMP Release Trigger Neutrophilic Airway Inflammation in Mice. *Am J Physiol Lung Cell Mol Physiol* (2016) 310:L377–86. doi: 10.1152/ajplung.00174.2015
81. Yoshida M, Minagawa S, Araya J, Sakamoto T, Hara H, Tsubouchi K, et al. Involvement of Cigarette Smoke-Induced Epithelial Cell Ferroptosis in COPD Pathogenesis. *Nat Commun* (2019) 10:3145. doi: 10.1038/s41467-019-10991-7
82. Haider HD, Tyurina YY, Ruminska KM, Shrivastava I, Ting HC, Tyurin VA, et al. Pseudomonas Aeruginosa Utilizes Host Polyunsaturated Phosphatidylethanolamines to Trigger Theft-Ferroptosis in Bronchial Epithelium. *J Clin Invest* (2018) 128:4639–53. doi: 10.1172/JCI99490
83. Zhai JX, Zhang ZX, Feng YJ, Ding SS, Wang XH, Zou LW, et al. PDTC Attenuate LPS-Induced Kidney Injury in Systemic Lupus Erythematosus-Prone MRL/lpr Mice. *Mol Biol Rep* (2012) 39:6763–71. doi: 10.1007/s11033-012-1501-7
84. Yucel M, Kucuk A, Bayraktar AC, Tosun M, Yalcinkaya S, Hatipoglu NK, et al. Protective Effects of the Nuclear Factor Kappa B Inhibitor Pyrrolidine Dithiocarbamate in Bladder Ischemia-Reperfusion Injury in Rats. *Mol Biol Rep* (2013) 40:5733–40. doi: 10.1007/s11033-013-2676-2
85. Sunil Y, Ramadori G, Raddatzc D. Influence of NFkappaB Inhibitors on IL-1beta-Induced Chemokine CXCL8 and -10 Expression Levels in Intestinal Epithelial Cell Lines: Glucocorticoid Ineffectiveness and Paradoxical Effect of PDTC. *Int J Colorectal Dis* (2010) 25:323–33. doi: 10.1007/s00384-009-0847-3
86. Tsurusaki S, Tsuchiya YC, Koumura T, Nakasone M, Sakamoto T, Matsuoka M, et al. Hepatic Ferroptosis Plays an Important Role as the Trigger for Initiating Inflammation in Nonalcoholic Steatohepatitis. *Cell Death Dis* (2019) 10:449. doi: 10.1038/s41419-019-1678-y
87. Afonso MB, Rodrigues PM, Carvalho T, Caridade M, Borralho P, Cortez-Pinto H, et al. Necroptosis Is a Key Pathogenic Event in Human and Experimental Murine Models of Non-Alcoholic Steatohepatitis. *Clin Sci* (2015) 129:721–39. doi: 10.1042/CS20140732
88. Patole PS, Pawar RD, Lichtnekert J, Lech M, Kulkarni OP, Ramanjaneyulu A, et al. Coactivation of Toll-Like Receptor-3 and -7 in Immune Complex Glomerulonephritis. *J Autoimmun* (2007) 29:52–9. doi: 10.1016/j.jaut.2007.04.004
89. Allam R, Anders HJ. The Role of Innate Immunity in Autoimmune Tissue Injury. *Curr Opin Rheumatol* (2008) 20:538–44. doi: 10.1097/BOR.0b013e3283025ed4
90. Kurts C, Panzer U, Anders HJ, Ress AJ. The Immune System and Kidney Disease: Basic Concepts and Clinical Implications. *Nat Rev Immunol* (2013) 13:738–53. doi: 10.1038/nri3523
91. Bianchi ME. DAMPs, PAMPs and Alarmins: All We Need to Know About Danger. *J Leukoc Biol* (2007) 81:1–5. doi: 10.1189/jlb.0306164
92. Bianchi ME, Manfredi AA. High-Mobility Group Box 1 (HMGB1) Protein at the Crossroads Between Innate and Adaptive Immunity. *Immunol Rev* (2007) 220:35–46. doi: 10.1111/j.1600-065X.2007.00574.x
93. Linkermann A, Chen GC, Dong G, Kunzendorf U, Krautwald S, Dong Z. Regulated Cell Death in AKI. *J Am Soc Nephrol* (2014) 25:2689–701. doi: 10.1681/ASN.2014030262
94. Nowak G, Soundararajan S, Mestril R. Protein Kinase C-Alpha Interaction With IHSP70 in Mitochondria Promotes Recovery of Mitochondrial Function After Injury in Renal Proximal Tubular Cells. *Am J Physiol Renal Physiol* (2013) 305:F764–776. doi: 10.1681/ASN.2014030262
95. Galluzzi L, Vitale I, Aaronson SA, Abrams JM, Adam D, Alnemri ES, et al. Essential Versus Accessory Aspects of Cell Death: Recommendations of the NCCD 2015. *Cell Death Differ* (2014) 22:58–73. doi: 10.1038/cdd.2014.137
96. Panee J, Stoytcheva ZR, Liu WY, Berry MJ. Selenoprotein H Is a Redox-Sensing High Mobility Group Family DNA-Binding Protein That Up-Regulates Genes Involved in Glutathione Synthesis and Phase II Detoxification. *J Biol Chem* (2007) 282:23759–65. doi: 10.1074/jbc.M702267200
97. Shin CS, Mishra P, Watrous JD, Carelli V, D'Aurelio M, Jainet M, et al. The Glutamate/Cystine xCT Antiporter Antagonizes Glutamine Metabolism and Reduces Nutrient Flexibility. *Nat Commun* (2017) 8:15074. doi: 10.1038/ncomms15074
98. Arbiser JL, Bonner MY, Ward N, Ward N, Elsey J, Rao S. Selenium Unmasks Protective Iron Armor: A Possible Defense Against Cutaneous Inflammation and Cancer. *Biochim Biophys Acta Gen Subj* (2018) 28:S0304–4165. doi: 10.1016/j.bbagen.2018.05.018
99. Wu SH, Oldfield JE, Whanger PH, Weswig PH. Effect of Selenium, Vitamin E, and Antioxidants on Testicular Function in Rat. *Biol Reprod* (1973) 8:625–9. doi: 10.1093/biolreprod/8.5.625
100. Ursini F, Heim S, Kiess M, Maiorino M, Roveri A, Wissing J, et al. Dual Function of the Selenoprotein PHGPx During Sperm Maturation. *Science* (1999) 285:1393–6. doi: 10.1126/science.285.5432.1393
101. Imai H, Suzuki K, Ichinose S, Oshima H, Okayasu I, Emoto K, et al. Failure of the Expression of Phospholipid Hydroperoxide Glutathione Peroxides in the Spermatozoa of Human Infertile Males. *Biol Reprod* (2001) 64:674–83. doi: 10.1095/biolreprod64.2.674
102. Imai H, Hakkaku N, Iwamoto R, Suzuki J, Suzuki T, Tajima Y, et al. Depletion of Selenoprotein Gpx4 in Spermatocytes Causes Male Infertility in Mice. *J Biol Chem* (2009) 284:32522–32. doi: 10.1074/jbc.M109.016139
103. Chen K, Mai ZX, Zhou YL, Gao XC, Yu B. Low Nrf2 mRNA Expression in Spermatozoa From Men With Low Sperm Motility. *Tohoku J Exp Med* (2012) 228:259–66. doi: 10.1620/tjem.228.259
104. Terai K, Horie S, Fukuhara S, Miyagawa Y, Kobayashi K, Tsujimura A. Combination Therapy With Antioxidants Improves Total Motile Sperm Counts: A Preliminary Study. *Reprod Med Biol* (2019) 19:89–94. doi: 10.1002/rmb2.12308.eCollection2020Jan
105. Gamage SMK, Lee KTW, Dissabandara DLO, King-Yin Lam A, Gopalan V. Dual Role Heme Iron in Cancer; Promotor of Carcinogenesis and an Inducer of Tumour Suppression. *Exp Mol Pathol* (2021) 120:104642. doi: 10.1016/j.yexmp.2021.104642
106. Shin D, Kim EH, Lee J, Roh JL. Nrf2 Inhibition Reverses Resistance to GPX4 Inhibitor-Induced Ferroptosis in Head and Neck Cancer. *Free Radic Biol Med* (2018) 129:454–62. doi: 10.1016/j.freeradbiomed.2018.10.426
107. Jiang QY, Wu RJ. Growth Mechanisms of Endometriotic Cells in Implanted Places: A Review. *Gynecol Endocrinol* (2012) 28:562–7. doi: 10.3109/09513590.2011.650662
108. Bullon P, Navarro JM. Inflammasome as a Key Pathogenic Mechanism in Endometriosis. *Curr Drug Targets* (2017) 18:997–1002. doi: 10.2174/1389450117666160709013850
109. Kobayashi H, Yamada Y, Kanayama S, Furukawa N, Noguchi T, Haruta S, et al. The Role of Iron in the Pathogenesis of Endometriosis. *Gynecol Endocrinol* (2009) 25:39–52. doi: 10.1080/09513590802366204
110. Defrère S, Langendonckt AV, Vaesen S, Jouret M, Ramos RG, Gonzalez D, et al. Ironoverload Enhances Epithelial Cell Proliferation in Endometriotic Lesions Induced in a Murine Model. *Hum Reprod* (2006) 21:2810–6. doi: 10.1093/humrep/del261
111. Skouta R, Dixon SJ, Wang JL, Dunn DE, Orman M, Shimada K, et al. Ferrostatins Inhibit Oxidative Lipid Damage and Cell Death in Diverse Disease Models. *J Am Chem Soc* (2014) 136:4551–6. doi: 10.1021/ja411006a
112. Molodecky NA, Soon IS, Rabi DM, Ghali WA, Ferris M, Chernoff G, et al. Increasing Incidence and Prevalence of the Inflammatory Bowel Diseases With Time, Based on Systematic Review. *Gastroenterology* (2012) 142:46–54. doi: 10.1053/j.gastro.2011.10.001

113. Naito Y, Takagi T, Yoshikawa T. Neutrophil-Dependent Oxidative Stress in Ulcerative Colitis. *J Clin Biochem Nutr* (2007) 41:18–26. doi: 10.3164/jcbn.2007003
114. Sann H, Erichsen JV, Hessmann M, Pahl A, Hoffmeyer A. Efficacy of Drugs Used in the Treatment of IBD and Combinations Thereof in Acute DSS-Induced Colitis in Mice. *Life Sci* (2013) 92:708–18. doi: 10.1016/j.lfs.2013.01.028
115. Liao GX, Detre C, Berger SB, Engel P, Malefyt RDW, Herzog RW, et al. Glucocorticoid-Induced Tumor Necrosis Factor Receptor Family-Related Protein Regulates CD4(+)T Cell-Mediated Colitis in Mice. *Gastroenterology* (2012) 142:582–91. doi: 10.1053/j.gastro.2011.11.031
116. Zanello G, Goethel A, Forster K, Geddes K, Philpott DJ, Croitoru K. Nod2 Activates NF-kB in $CD4^+$ T Cells But its Expression Is Dispensable for T Cell-Induced Colitis. *PloS One* (2013) 8:e82623. doi: 10.1371/journal.pone.0082623.eCollection2013
117. Maloy KJ, Powrie F. Intestinal Homeostasis and its Breakdown in Inflammatory Bowel Disease. *Nature* (2011) 474:298–306. doi: 10.1371/journal.pone.0082623.eCollection2013
118. Sina C, Kemper C, Derer S. The Intestinal Complement System in Inflammatory Bowel Disease: Shaping Intestinal Barrier Function. *Semin Immunol* (2018) 37:66–73. doi: 10.1016/j.smim.2018.02.008
119. Yin J, Wu M, Duan JL, Liu G, Cui ZJ, Zheng J, et al. Pyrrolidine Dithiocarbamate Inhibits NF-kappaB Activation and Upregulates the Expression of Gpx1, Gpx4, Occludin, and ZO-1 in DSS-Induced Colitis. *Appl Biochem Biotechnol* (2015) 177:1716–28. doi: 10.1007/s12010-015-1848-z
120. Pasparakis M, Vandenabeele P. Necroptosis and its Role in Inflammation. *Nature* (2015) 517:311–20. doi: 10.1016/j.smim.2018.02.008
121. Cummings RJ, Barbet G, Bongers G, Hartmann BM, Gettler K, Muniz L, et al. Different Tissue Phagocytes Sample Apoptotic Cells to Direct Distinct Homeostasis Programs. *Nature* (2016) 539:565–9. doi: 10.1038/nature20138
122. Sander JD, Joung JK. CRISPR-Cas Systems for Editing, Regulating and Targeting Genomes. *Nat Biotechnol* (2014) 32:347–55. doi: 10.1038/nbt.2842
123. Lisa M, Grabherr F, Schwärzler J, Reitmeier I, Sommer F, Gehmacher T, et al. Dietary Lipids Fuel GPX4-Restricted Enteritis Resembling Crohn's Disease. *Nat Commun* (2020) 11:1775–90. doi: 10.1038/s41467-020-15646-6
124. Mulay SR, Linkermann A, Anders HJ. Necroinflammation in Kidney Disease. *J Am Soc Nephrol* (2016) 27:27–39. doi: 10.1681/ASN.2015040405
125. Chadha R, Heidt S, Jones ND, Wood KJ. Th17: Contributors to Allograft Rejection and a Barrier to the Induction of Transplantation Tolerance? *Transplantation* (2011) 91:939–45. doi: 10.1097/TP.0b013e3182126eeb
126. Tesmer LA, Lundy SK, Sarkar S, Fox DA. Th17 Cells in Human Disease. *Immunol Rev* (2008) 223:87–113. doi: 10.1111/j.1600-065X.2008.00628.x
127. Bantel H, Osthoff KS. Cell Death in Sepsis: A Matter of How, When, and Where. *Crit Care* (2009) 13:173. doi: 10.1186/cc7966
128. Ying Y, Kim J, Westphal SN, Long KE, Padanilam BJ. Targeted Deletion of P53 in the Proximal Tubule Prevents Ischemic Renal Injury. *J Am Soc Nephrol* (2014) 25:2707–16. doi: 10.1681/ASN.2013121270.Epub2014May22
129. Zhou L, Fu P, Huang XR, Liu F, Lai KN, Lan HY. Activation of P53 Promotes Renal Injury in Acute Aristolochic Acid Nephropathy. *J Am Soc Nephrol* (2010) 21:31–41. doi: 10.1681/ASN.2008111133
130. Telorack M, Meyer M, Ingold I, Conrad M, Bloch W, Werner S. A Glutathione-Nrf2-Thioredoxin Cross-Talk Ensures Keratinocyte Survival and Efficient Wound Repair. *PloS Genet* (2016) 12:e1005800. doi: 10.1371/journal.pgen.1005800
131. Pinton J, Fridén H, Kettaneh-Wold N, Wold S, Dreno B, Richard A, et al. Clinical and Biological Effects of Balneotherapy With Selenium-Rich Spa Water in Patients With Psoriasis Vulgaris. *Br J Dermatol* (1995) 133:344–7. doi: 10.1111/j.1365-2133.1995.tb02657.x
132. Donadini A, Fiora C, Regazzini R, Perini D, Minoia C. Selenium Plasma Levels in Psoriasis. *Clin Exp Dermatol* (1992) 17:214–6. doi: 10.1111/j.1365-2230.1992.tb00212.x
133. Kao SH, Huang HC, Hsieh RH, Chen SC, Tsai MC, Tzeng CR. Oxidative Damage and Mitochondrial DNA Mutations With Endometriosis. *Ann N Y Acad Sci* (2005) 1042:186–94. doi: 10.1196/annals.1338.021
134. Murphy AA, Santanam N, Morales AJ, Parthasarathy S. Lysophosphatidyl Choline, a Chemotactic Factor for Monocytes/T-Lymphocytes Is Elevated in Endometriosis. *J Clin Endocrinol Metab* (1998) 83:2110–3. doi: 10.1210/jcem.83.6.4823
135. Scutiero G, Iannone P, Bernardi G, Bonaccorsi G, Spadaro S, Volta CA, et al. Oxidative Stress and Endometriosis: A Systematic Review of the Literature. *Oxid Med Cell Longev* (2017) 2017:7265238. doi: 10.1155/2017/7265238
136. Ploeg RJ, D'alessandro AM, Knechtle SJ, Stegall MD, Pirsch JD, Hoffmann RM, et al. Risk Factors for Primary Dysfunction After Liver Transplantation-A Multivariate Analysis. *Transplantation* (1993) 55:807–13. doi: 10.1097/00007890-199304000-00024
137. Yamada N, Karasawa T, Wakiya T, Sadatomo A, Ito H, Kamata R, et al. Iron Overload as a Risk Factor for Hepatic Ischemia-Reperfusion Injury in Liver Transplantation: Potential Role of Ferroptosis. *Am J Transplant* (2020) 20:1606–18. doi: 10.1111/ajt.15773
138. Bruni A, Pepper AR, Pawlick RL, Gala-Lopez B, Gamble AF, Kin T, et al. Ferroptosis-Inducing Agents Compromise In Vitro Human Islet Viability and Function. *Cell Death Dis* (2018) 9:595. doi: 10.1038/s41419-018-0506-0
139. Chen L, Li X, Liu L, Yu B, Xue Y, Liu Y. Erastin Sensitizes Glioblastoma Cells to Temozolomide by Restraining xCT and Cystathioninegamma-Lyase Function. *Oncol Rep* (2015) 33:1465–74. doi: 10.3892/or.2015.3712
140. Cramer SL, Saha A, Liu J, Tadi S, Tiziani S, Yan W, et al. Systemic Depletion of L-Cyst(E)Ine With Cyst(E)Inase Increases Reactive Oxygen Species and Suppresses Tumor Growth. *Nat Med* (2017) 23:120–7. doi: 10.1038/nm.4232
141. Miess H, Dankworth B, Gouw AM, Rosenfeldt M, Schmitz W, Jiang M, et al. The Glutathione Redox System Is Essential to Prevent Ferroptosis Caused by Impaired Lipid Metabolism in Clear Cell Renal Cell Carcinoma. *Oncogene* (2018) 37:5435–50. doi: 10.1038/s41388-018-0315-z

Conflict of Interest: The authors declare that the research was conducted in the absence of any commercial or financial relationships that could be construed as a potential conflict of interest.

Advantages of publishing in Frontiers

OPEN ACCESS
Articles are free to read for greatest visibility and readership

FAST PUBLICATION
Around 90 days from submission to decision

HIGH QUALITY PEER-REVIEW
Rigorous, collaborative, and constructive peer-review

TRANSPARENT PEER-REVIEW
Editors and reviewers acknowledged by name on published articles

Frontiers
Avenue du Tribunal-Fédéral 34
1005 Lausanne | Switzerland

Visit us: www.frontiersin.org
Contact us: frontiersin.org/about/contact

REPRODUCIBILITY OF RESEARCH
Support open data and methods to enhance research reproducibility

DIGITAL PUBLISHING
Articles designed for optimal readership across devices

FOLLOW US
@frontiersin

IMPACT METRICS
Advanced article metrics track visibility across digital media

EXTENSIVE PROMOTION
Marketing and promotion of impactful research

LOOP RESEARCH NETWORK
Our network increases your article's readership